5th Iran International Zeolite Conference

University of Tabriz, Tabriz, Iran

26-27 August 2018

By:

Faculty of Chemistry, University of Tabriz

In cooperation with the

Iranian Chemical Society

In cooperation with the

Islamic World Science Citation Center(ISC)

- Proceedings of 5th Iran International Zeolite Conference (**IIZC5**)
- By: Faculty of Chemistry, University of Tabriz
- Cover & Booklet Designer: Dr. Jamshid Rakhtshah

5th Iran International Zeolite Conference

University of Tabriz, Tabriz, Iran

26-27 August

Special Thanks to All Who Participated in Doing the 5th Iran International Zeolite Conference

and

Content

In the name of God

Dear Participant

On behalf of the Organizing Committee, I am delighted to welcome you to the 5th Iran International Zeolite Conference (IIZC5) in the University of Tabriz, Tabriz, Iran. Tabriz is one of the historical capitals of Iran which is regarded as "the capital of Islamic tourism" in 2018. It is famous for its handicrafts, including hand-woven rugs and jewelry. Tabriz contains many historical monuments, representing Iran's architectural transition throughout its deep history. Among these sites is the grand Bazaar of Tabriz which is one of the oldest bazaars in the Middle East and one of Iran's UNESCO World Heritage Sites.

Thirty years ago, I presented the research results of my M.Sc. thesis about the synthesis of zeolites and preparing of cracking catalysts by them in University of Tabriz. It was a beginning for research about zeolite chemistry in Iran and my academic work in this university. I am very pleased for development of this scientific field in Iran due to the possessing a lot of zeolite mines in this country. Now, this conference brings together scientists, researchers, academicians and R&D laboratories of industry around the world to share the latest developments on zeolite science and porous materials with the participants. The scientific program of conference covers various fields of zeolite science and technology including zeolite based nanotechnologies, synthesis and characterization of porous materials and applications of zeolites and porous materials.

The organizing committee of conference received more than 165 extended abstracts, in which 118 papers were accepted for presentation as orals and posters. The scientific program will feature 2 plenary lectures, 13 keynote lectures and 103 posters during 2 days.

I would like to thank the university of Tabriz and Faculty of chemistry for providing the opportunity to organize this conference. Also I want to thank the scientific and executive committee of conference. I would like offer a special thanks to all of the sponsoring organizations that supported us for this conference. Finally, I would like to thank all of the conference participants for their contributions which are the foundation of this conference.

Prof. Masoumeh khatamian
Chairman of 5th Iran International Zeolite Conference

Organizing Committee of IIZC5

Academic Staffs:

- Prof. Masoumeh Khatamian (Scientific Secretary)
- Dr. Seyed Abolfazl Hosseini-Yazdi (Executive Secretary)
- Prof. Mir Reza Majidi (Head of the Chemistry Faculty)
- Prof. Ali Akbar Khandar
- Dr. Mahtab Pirouzmand
- Dr. Behrouz Shaabani
- Dr. Abdolhossein Naseri
- Dr. Saeed Mohammad Sorureddin
- Dr. Mahmoud Zarei

And also with significant and valuable cooperation of

- Dr. Baharak Divband
- Dr. Maryam Saket Oskoui
- Dr. Azin Yavari
- Dr. Jamshid Rakhtshah (Postdoctoral fellowship in inorganic chemistry)
- Web administrator: Sara Fazli Shokouhi

- We acknowledge also the collaboration of following academics, PhD, MSc and BSc students (each group in alphabetical order) during the conference

PhD students

Chamani, Sanaz

Fazaeli, Monireh

Nikzad, Behnaz

MSc students

Fazli Shokoohi, Farzad

Hamooni, Taher

Marefat Izadi, Shahrzad

Maleki, Hossein

Norouzi, Amin

Novin, Amir

Nasiri, Taher

Noorbakhsh, Arash

Shahi, Robab

BSc students

Fazli Shokoohi, Ali

Fazli Shokoohi, Fatemeh

Scientific Committee of IIZC5 (in alphabetical order)

Hamid Reza **A**randiyan	University of Sydney, **Australia**
Darya **A**sheghali	University of Georgia, **USA**
Ali Akbar **B**abaluo	Sahand University of Technology, **Iran**
Eva **C**hmielewska	Comenius University in Bratislava, **Slovakia**
Giuseppe **C**ruciani	University of Ferrara, **Italy**
Baharak **D**ivband	University of Tabriz, **Iran**
Faezeh **F**arzaneh	Alzahra University, **Iran**
Bahram **G**hanbari	Sharif University of Technology, **Iran**
Semih **G**orduk	Yildiz Technical University, **Turkey**
Mohammad **H**aghighi	Sahand University of Technology, **Iran**
Hossein **K**azemian	University of Northern British Columbia, **Canada**
Ali **K**hademhosseini	University of California, Los Angeles, **USA**
Ali Akbar **K**handar	University of Tabriz, **Iran**
Masoumeh **K**hatamian	University of Tabriz, **Iran**
Alessio **L**angella	University del sannio, **Italy**
Roberto **M**illini	Eni. S. P. A. Development, Operations & Technology, **Italy**

Svetlana **M**intova	Université de Caen – CNRS, **France**
Masoud **M**irzaei	Ferdowsi University of Mashhad, **Iran**
Ali **M**orsali	Tarbiat Modares University, **Iran**
Mostafa **M**ohammadpour Amini	Shahid Beheshti University, **Iran**
Mahtab **P**irouzmand	University of Tabriz, **Iran**
Majid **P**oormoghaddam	The Deputy Minister Consultant in Mining Affairs and Mining Industry in Ministry of Industry, Mine and Trade
Zolfaghar **R**ezvani	Azarbaijan Shahid Madani University, **Iran**
Ufana **R**iaz	Jamia Millia Islamia, **India**
Sadegh **R**ostamnia	University of Maragheh, **Iran**
Maryam **S**aket	University of Tabriz, **Iran**
Mohammad **S**arrafzadeh	University of Tehran, **Iran**
Shabnam **S**ohrabnezhad	University of Guilan, **Iran**
Ali Akbar **T**arlani	Chemistry & Chemical Engineering Research Center of Iran, **Iran**
Valentin **V**altchev	Université de Caen – CNRS, **France**
Ajayan **V**inu	University of South Australia, **Australia**
Azin **Y**avari	University of Tabriz, **Iran**
Mojgan **Z**endehdel	University of Arak, **Iran**

The previous International Zeolite Conferences of Iran

1st	Tehran	2008	Dr. Hossein Kazemian	Amirkabir University of Tehran	
2nd	Tehran	2010	Dr. Hossein Kazemian Dr. Mozhgan Zendehdel	University of Tehran	
3rd	Arak	2012	Dr. Mozhgan Zendehdel	University of Arak	
4th	Golpayegan	2017	Dr. Mozhgan Zendehdel	University of Golpayegan	

IIZC 5 Time Schedule

Sunday August 26, 2018 (4 Shahrivar, 1397)	
08:30 – 10:00	Opening Ceremony
10:00 – 10:30	**Oral Presentation:** Dr. Majid Poor Moghadam **Title:** *Investigation and Studying the potentials of Meshkin-Shahr Zeolite zone* **Chairman:** *Dr. Mojgan Zendehdel - Dr. Bahram Ghanbari*
10:30 – 11:00	**Oral Presentation:** Dr. Giuseppe Cruciani **Title:** *Host-guest interactions and ferroelastic behavior in ZSM-5 zeolite* **Chairman:** *Dr. Mojgan Zendehdel - Dr. Bahram Ghanbari*
11:00 – 12:00	**Poster Session (Section A) & Coffee Break**
12:00 – 12:30	**Oral Presentation:** Dr. Soodabeh Davaran **Title:** *Synthesis and biomedical applications of magnetic mesoporous silica nanoparticles in drug delivery and tissue engineering* **Chairman:** *Dr. Shahin Ostan – Dr. Baharak Divband*
12:30 – 14:00	**Lunch Time**
14:00 – 14:30	**Oral Presentation:** Dr. Mostafa M. Amini **Title:** *Commercialization of Metal-Organic Frameworks: MOFs Moves to Market* **Chairman:** *Dr. Rahmatollah Rahimi – Dr. Mahtab Pirouzmand*
14:30 – 15:00	**Oral Presentation:** Dr. Bahram Ghanbari **Title:** *The motif of metal impregnation over low-Si/Al-ratio ZSM-5 catalyst in MTH process* **Chairman:** *Dr. Rahmatollah Rahimi – Dr. Mahtab Pirouzmand*
15:00 – 16:00 (Plenary lecture)	**Oral Presentation:** Dr. German Sastre **Title:** *Adsorption and diffusion of alkyl-aromatic molecules in a zeolite containing medium and large-pore micropores using computational chemistry methods* **Chairman:** *Dr. Giuseppe Cruciani - Dr. Mostafa M. Amini*
16:00 – 16:30	**Coffee Break**
16:30 – 17:00	**Oral Presentation:** Dr. Shahin Ostan **Title:** *Improving soil functions by zeolitic amendments in agricultural lands* **Chairman:** *Dr. Sadegh Rostamnia – Dr. Shabnam Sohrabnezhad*
17:00 – 19:00	**Workshop Time**

IIZC 5 Time Schedule

Monday August 27, 2018 (5 Shahrivar, 1397)	
08:30 – 09:00	**Oral Presentation:** Dr. Reza Behbahani **Title:** *Dehydrogenation of methanol to light olefins upon zeolite/alumina catalysts: Effect of reaction conditions, catalyst support and zeolite modification* **Chairman:** *Dr. German Sastre - Dr. Zahra Taheri*
09:00 – 09:40	**Oral Presentation:** Dr. Athanasios Godelitsas **Title:** *Transition Metal Complexes Supported on Natural Zeolites: New Composite Materials for Innovative Applications* **Chairman:** *Dr. German Sastre – Dr. Zahra Taheri*
09:40 – 10:40 (Plenary lecture)	**Oral Presentation:** Dr. Saim Ozkar **Title:** *Zeolite Confined Transition Metal Nanoclusters in Low Temperature Catalysis* **Chairman:** *Dr. German Sastre – Dr. Zahra Taheri*
10:50 – 11:40	**Poster Session (Section B) & Coffee Break**
11:40 – 12:10	**Oral Presentation:** Dr. Mojgan Zendehdel **Title:** *Micro-Mesostructured Zeolite* **Chairman:** *Dr. Masoud Mirzaei – Dr. Mahdi Niknam Shahrak*
12:10 – 12:40	**Oral Presentation:** Dr. Rahmatollah Rahimi **Title:** *Porphyrin/$ZnFe_2O_4$@polythiophene nanocomposite as adsorbent and photocatalyst for the removal of organic pollutants under visible light irradiation* **Chairman:** *Dr. Masoud Mirzaei – Dr. Mahdi Niknam Shahrak*
12:40 – 14:00	**Lunch Time**
14:00 – 14:30	**Oral Presentation:** Dr. Masoud Mirzaei **Title:** *Developing some POMs-templated MOFs: Crystal structure, magnetic and gas adsorption properties* **Chairman:** *Dr. Athanasios Godelitsas – Dr. Baharak Divband*
14:30 – 15:00	**Oral Presentation:** Dr. Sadegh Rostamnia **Title:** *Nano-pumice as reaction reactor: From microporous to mesoporous* **Chairman:**: *Dr. Athanasios Godelitsas – Dr. Baharak Divband*
15:00 – 16:00	**Oral Presentation:** Dr. Kalyanrao Mahadu Garadkar **Title:** *Zeolite Supported Metal Oxide Nanocomposites for Wastewater Treatment* **Chairman:** *Dr. Athanasios Godelitsas – Dr. Baharak Divband*
16:00 – 16:30	**Coffee Break**
16:30 – 18:30	**Workshop Time**

Opening Time of Restaurant

Breakfast	07:00 – 08:00
Lunch	12:30 – 14:00
Dinner	21:00 – 23:00

Workshops Time Schedule

Sunday August 26, 2018 (4 Shahrivar, 1397)		Organizer
17:00–19:00	Scanning Probe Microscopy (SPM)	Azar Kimia Khatam Co.
17:00–19:00	The device of chemical adsorption and desorption analysis and determination of specific surface area of materials (BET)	Azar Kimia Khatam Co.
Monday August 27, 2018 (5 Shahrivar, 1397)		
16:30 – 18:30	Molecular Docking	Dr. Zeinab Mirzaee
16:30 – 18:30	Characterization of materials by X-ray diffraction method	Dr. Ali Akbar Khandar
16:30 – 18:30	Scaffolds for tissue engineering	Azar Kimia Khatam Co.

Oral Presentations

Investigation and Studying the potentials of Meshkin-Shahr Zeolite zone

Majid Poor Moghadam
Researcher and mineral advisor of Ministry of Industry, Mine and Trade
**Email: Dr.poormoghadam@yahoo.com*

Abstract: According to the proposal of establishing the organization of the countries producing aluminum or OPEC aluminum by Russia (2017), and considering the low aluminum resources in the country, of 11 bauxite mines with a focus on Jajarm bauxite mine, and the existence of 16 thousand factories and workshops in Large, Medium and low sizes producing aluminum, and obtaining the 17th status in the world with production of 400 thousand tons per year, and 6 thousand direct employment and 250 thousand indirect employment and importing more than 250 thousand tons of aluminum . On the other hand, analcites with high percentage of aluminum oxide 23.16% which can play a role in the production of alumina, and regarding its potential in the north and northwest of Meshkin-Shahr as well as considerable improvements in the processing field of minerals, studying on Meshkin-shahr's analcites zone as a strategic mineral with special conditions of exploration, production, trade, export, valuation and employment, are of required competency to register an international brand and is considered as an Iranian product.

Keywords: aluminum, analcites, Meshkin-Shahr, minerals

Adsorption and diffusion of alkyl-aromatic molecules in a zeolite containing medium and large-pore micropores using computational chemistry methods

German Sastre
Instituto de Tecnologia Quimica UPV-CSIC. Universidad Politecnica de Valencia, Valencia (Spain)
e-mail: gsastre@itq.upv.es

A molecular dynamics study of the diffusion of trimethylbenzene (TMB) and xylene molecules involved in toluene and TMB transalkylation reaction (toluene+TMB→xylene+xylene) has been performed over 5 different zeolites, containing interconnected medium (10-ring) and large (12-ring) channels: BOG, MSE, IWR, SFS, and UWY. The shape selective properties of these frameworks were chosen through a screening among all zeolites, by defining criteria expected to maximize the selectivity to xylenes since all of them contain large channels, where bulky TMB (and of course the smaller toluene) should diffuse with little constraints, and also contain medium pore channels where xylene molecules (main reaction product) should diffuse preferentially. A wide range of 10-ring windows, between 4.6×5.3 Å(IWR) and 5.1×6.2 Å(UWY); as well as 12-ring windows, between 5.8×6.8 Å(IWR) and 6.1×7.9 Å(UWY), helps -but does not suffice- to explain the diffusional results of toluene, xylenes and TMBs in each zeolite [1,2]. Other factors, such as channel connectivity, sinusoidality, and presence of cavities will be invoked to draw the full picture that explains how selectivity to xylenes (the desired product) can be maximized.

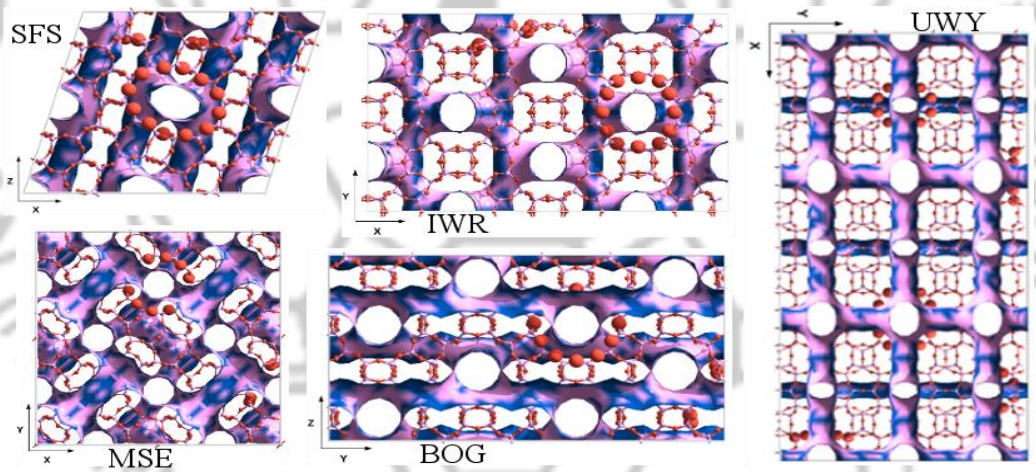

References:

[1] J. Toda, A. Corma, G. Sastre; "Diffusion of trimethylbenzenes and xylenes in zeolites with 12 and 10-ring channels as catalyst for toluene- trimethylbenzene transalkylation"; J. Phys. Chem. C 2016, 120, 16668-16680.

[2] J. Toda, G. Sastre; "Diffusion of Trimethylbenzenes, Toluene and Xylenes in UWY Zeolite as Catalyst for the Transalkylation of Trimethylbenzenes with Toluene"; J. Phys. Chem. C 2018, 122, 7885-7997.

Zeolite Confined Transition Metal Nanoclusters in Low Temperature Catalysis

Saim Özkar
Department of Chemistry, Middle East Technical University, 06800 Ankara, Turkey
E-mail: sozkar@metu.edu.tr

Although heterogeneous catalysis has many advantageous over the homogeneous one, the catalytic activity of bulk metals in heterogeneous catalysis is restricted because only a small fraction of atoms are on the surface of bulk metal. A promising way of increasing the surface area and, thus, the relative number of catalytically active sites is the use of metal nanoparticles with controllable size and size distribution. As a consequence of large fraction of atoms on the surface, the metal nanoparticles can provide much higher catalytic activity than the respective bulk metal counterparts in many catalytic reactions. In their catalytic application, however, one important problem is the aggregation of nanoclusters into clumps and ultimately to the bulk metal. The aggregation can be prevented by using stabilizers such as anions or polymers adsorbed on the nanoclusters surface, or by supporting them on materials with large surface area. Further enhancement in both catalytic activity and stability of transition metal(0) nanoclusters can be achieved by preparing them within the void spaces of zeolite. Zeolite-Y with highly ordered supercages of 1.3 nm size is an example of porous materials being a suitable host for transition metal(0) nanoclusters. It will be presented that intrazeolite metal nanoclusters of cobalt(0), nickel(0), ruthenium(0), rhodium(0) and iridium(0) can easily be prepared by a 2-step process at room temperature:

1. Ion exchanging the Na^+ cations of zeolite-Y with M^{q+} ions in the cavities

$$q\mathrm{Na}^+ - \mathrm{Y} + \mathrm{M}^{q+}(aq) \xrightarrow{ion\ exchange} \mathrm{M}^{q+} - \mathrm{Y} + q\mathrm{Na}^+(aq)$$

2. Reduction of metal ions within the cavities of zeolite-Y by $NaBH_4$ whereby Na^+ cations reoccupy their authentic cation sites, thus restoring the original zeolite composition.

$$M^{q+} - Y \xrightarrow{reduction\ by\ aqueous\ NaBH_4\ solution} M(0) - Y$$

The zeolite confined transition metal(0) nanoclusters, obtained in this way, were employed as catalyst in many important reactions such as hydrogenation, dehydrogenation, alcohol oxidation and coupling reactions as well as dehydrogenation of amine boranes. For example, the use of zeolite confined transition metal(0) nanoclusters as highly active and long-lived catalyst in hydrogen generation provides a safe way of controllable and fast generation of clean hydrogen for fuel cell applications.

Zeolite Supported Metal Oxide Nanocomposites for Wastewater Treatment

Kalyanrao Mahadu Garadkar
Nanomaterials Research Laboratory, Department of Chemistry
Shivaji University, Kolhapur, M. S. India
Kmg_chem@unishivaji.ac.in

Nanostructured materials have been received considerable attention due to their unique physicochemical properties and large number of unique applications. In particular semiconductor photocatalysis encompasses a number of diverse and related disciplines in Science and Engineering. It has been applied for mitigating environmental pollutants, wastewater treatment, generating solar cells and inhibition of bacteria, viruses etc. The most widely used semiconductor photocatalyst is TiO2 which become a ‘‘gold standard’’ in photocatalysis. Its popularity stems due to easy and inexpensive method of preparation, highly stable in aqueous medium, non-toxic and capable to degrade several classes of pollutants. Apart from this, nanoparticles of titania has certain limitations such as tendency of aggregation in suspension that rapidly lose their effective surface area, being a nonporous in nature, it exhibits low adsorption ability and low quantum degradation efficiency for pollutants. The photocatalytic activity of TiO2 is greatly influenced by crystal structure, particle size, porosity and surface area. Enhancement in the surface area of TiO2 is the most noticeable mean to improve the efficiency of photocatalytic oxidation reactions. Extensive efforts on research is underway the World over for the development of suitable high surface area photocatalyst. Therefore, several attempts were made to support fine particles of TiO2 on porous materials of large surface area using adsorbents like silica, alumina, clay, zeolite and activated carbon. Among these materials, great attention has been focused on zeolite due to its unique properties like uniform pores and channel sizes (3–8 Å). These studies have been built-in an effort to enhance the adsorption of reactant on the catalyst surface to improve the catalytic efficiency of photocatalysis. HZSM-5 Zeolite is crystalline inorganic microporous, aluminosilicate and material, consisting of a three-dimensional (3D) network. In the present study, we have accounted for the synthesis of TiO_2 supported on HZSM-5 by an energy efficient microwave method. Photocatalyst shows a maximum 96 % photodegradation of AG 25 (25 ppm) within 60 min under UV light irradiation at 0.1 g/dm.

We have also developed a biogenic method for the design of three different composite nanomaterials, CuxO/ZnO, Ag@CuxO/ZnO, and Au@CuxO/ZnO (x = I and II), with the surface plasmon resonance (SPR) effect and p−n heterojunction for photocatalysis. Ag@CuxO/ZnO and Au@CuxO/ZnO, exhibit much higher photocatalytic activity than ZnO and CuxO/ZnO for the degradation of industrial textile effluent and Methyl Orange under sunlight as well as UV light. The genotoxicity of TE prior to and past photodegradation was assessed. The effortlessness of the current method and considering the admirable photocatalytic performance of M@CuxO/ZnO NRs proposed its budding environmental cleaning function at an industrial scale. The degradation of TE prior to discharge in water bodies eliminates water pollution and provides clean accessible water.

Transition Metal Complexes Supported on Natural Zeolites: New Composite Materials for Innovative Applications

Athanasios Godelitsas
School of Science, National and Kapodistrian University of Athens, Zografou campus, 15784 Athens, Greece
E-mail: agodel@geol.uoa.gr

Zeolites constitute a major group of crystalline microporous -in fact nanoporous- materials including both natural (more than 50) and synthetic species (more than 100, also referred as molecular sieves). Their structure is characterized by a three-dimensional aluminosilicate framework adjusting the formation of intracrystalline micropores -channels- which normally host exchangeable cations (e.g. Ca^{2+}) and mobile H_2O-molecules. The size of the channels (generally <20 Å) regulating the sorptive properties of the materials, is related to the framework density (FD, in T_{sites}/1000 $Å^3$) and the cation exchange capacity (CEC, in meq/100 g) depends on the Si/Al ratio controlling the available negatively-charged extraframework sites. Similar synthetic microporous -nanoporous- materials known as zeotypes possess a relevant fundamental framework but with T-sites occupied by different elements (e.g. Al-P, Si-Ti), while the framework of the so-called porosils (silicalites) is built up exclusively by Si-tetrahedra. However, all natural zeolites are typical aluminosilicate solids exhibiting a higher FD in comparison to other tectosilicate phases such as feldspars, and are low-cost industrial minerals (mostly found in tuffs and basalts) with several commercial applications.

The zeolitic materials are not frequently used as synthesized or as obtained from the nature (unmodified), but their physicochemical properties are refined by chemical and/or thermal treatment. One of the novel procedures to obtain modified zeolites is the gradual loading of the crystals with transition metals and organic substances, which leads to complexes supported on the aluminosilicate zeolitic substrate. The coordination and organometallic compounds can either be encapsulated inside the micropores -nanopores- (intrazeolite complexes) or arranged on the surface of the crystals (surface complexes). The surface complexes are anchored by chemical bonds to active (Brønsted or Lewis) surface sites, whereas the intrazeolite ones are hosted into the channels allowing the zeolite to act as a "solid solvent". In the latter case, the guest complexes principally retain all of their properties and, being isolated in the micropores playing the role of "inorganic molecular-scale microreactors", are often more stable under dimerisation, auto-oxidation, clustering and thermal-degradation conditions. Moreover, in both cases the supported complexes are considered as "new" (not existing as individual chemical compounds) if oxygen-atoms of the zeolite lattice participate in the first coordination sphere. The above described solid systems constitute in fact an entirely new class of composite materials with great technological interest.

The existing literature [see e.g. 1-3] on synthetic zeolites (e.g. **FAU**-type) provides evidence for peculiar applications such as the shape/size-selective catalysis and even the biomimetic catalysis where the supported in the micropores „ship-in-a-bottle" complexes behave as the enzymes in the protein structure. These materials are the so-called zeozymes contributing to the establishment of the supramolecular solid-state science.

The relevant research [see e.g. 4-11] already performed using naturally occurring species is comparably limited and refers to **FAU**-type zeolites as well as to **HEU**-type zeolites (clinoptilolite/heulandite series, which are the most abundant zeolites on Earth). Different intrazeolite amd surface complexes (e.g. Ni^{2+}-pyridine and

Cu^{2+}-diethyldithiocarbamate; Fig. 1) have been investigated in respect of the above zeolites, whereas novel uses of the obtained composite solid materials have been pointed out, including the development of specific sorbents & catalysts, environment-friendly pesticides & insecticides, and modern pharmaceuticals & nutritients.

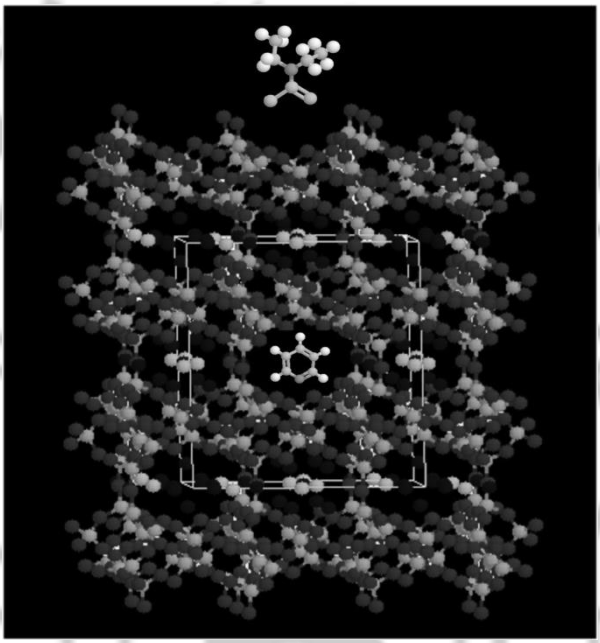

Figure 1. Examples of intrazeolite and surface complexes (e.g. Ni^{2+}-pyridine and Cu^{2+}-diethyldithiocarbamate) with regard to the structure of **HEU**-type zeolites.

References

[1] G. A. Ozin and C.Gil, Chem. Rev. 89 1749 (1989).

[2] P. C.H. Mitchell, Chem. & Ind.. 6 308 (1991).

[3] R. Parton et al., in Zeolite Micropor. Solids, E.G. Derouane et al. Eds. (1992) p. 555

[4] H. D. Simpson and H. Steinfink, J. Am. Chem. Soc. 91/23 6225 (1969).

[5] H.D. Simpson and H. Steinfink, J. Am. Chem. Soc. 91/23 6229 (1969).

[6] A. Godelitsas et al., Micropor. Mesopor. Materials 33 77 (1999).

[7] B. Concepción-Rosabal et al., Micropor. Mesopor. Materials 38 16 (2000).

[8] A. Godelitsas et al., Chem. Eur. J. 7 3705 (2001).

[9] Th. Armbruster et al., Micropor. Mesopor. Materials 57 121 (2003).

[10] A. Godelitsas et al., Micropor. Mesopor. Materials 61 69 (2003).

[11] A. Godelitsas and Th. Armbruster, Micropor. Mesopor. Materials 61 3 (2003).

Host-guest interactions and ferroelastic behavior in ZSM-5 zeolite

Matteo Ardit[a], Giada Beltrami[a], Annalisa Martucci[a], Luisa Pasti[b], Elisa Rodeghero[a], Giuseppe Cruciani[a*]
[a]*Department of Physics and Earth Sciences, University of Ferrara, Via Saragat, I-44122 Ferrara, Italy*
[b]*Department of Chemistry and Pharmaceutical Sciences, University of Ferrara, Via Borsari 46, I-44123 Ferrara, Italy*
**Corresponding author: cru@unife.it*

Abstract: The physical-chemical properties of guest molecules confined within a zeolite framework host are known to be strongly affected by the confinement effects exerted through non-covalent host-guest interactions. Based on synchrotron time-resolved powder diffraction measurements and the Landau theory of ferroelastic phase transitions, we provide in this work evidence for the strong coupling existing between the thermodynamic properties of organic molecules (toluene, 1,2-dichloroethane, methyl-tert-butyl-ether) adsorbed within the ZSM-5 zeolite and the lattice strain driving the monoclinic-to-orthorhombic (ferroelastic-to-paraelastic) phase transition which controls connectivity and diffusivity in the zeolite framework.

Keywords: ZSM-5, phase transition, host-guest interactions, ferroelastic behavior, Landau theory

Developing some POMs-templated MOFs: Crystal structure, magnetic and gas adsorption properties

Masoud Mirzaei Shahrabi
Department of Chemistry, Faculty of Science, Ferdowsi University of Mashhad, Mashhad, Iran
E-mail: mirzaeesh@um.ac.ir

In the past decades, great efforts have been devoted to the rational design and synthesis of inorganic-organic hybrid architectures and metal organic frameworks (MOFs). A common feature of such design approaches is to employ poly-functional organic ligands such as dicarboxylic acids and combine them with polyoxometallate (POMs) and N-donor co-ligands to prepare inorganic-organic hybrids and metal organic frameworks, respectively. These crystal structures have high structural stability and infinite variety of unique chemical, physical, and adsorption properties. Due to importance of this field, a novel series of inorganic-organic hybrid and MOFs architectures based on dicarboxylate/POMs and dicarboxylate/N-donor bases have been synthesized under mild, hydrothermal, and sonochemical conditions [1-4]. The objective of the present speech is to explore the effect of organic ligands, POMs charge density and synthetic conditions in final structures. The magnetic properties of some of these compounds have been investigated. Monte Carlo simulation has been employed for predicting the ability of some of these compounds to capture CH_4 and CO_2 and also to separate CH_4/H_2 and CO_2/N_2 mixtures.

References:

[1] M. Mirzaei, H. Eshtiagh-Hosseini, M. Alipour, A. Frontera, Coord. Chem. Rev., 2014, 275, 1.
[2] M. Mirzaei, H. Eshtiagh-Hosseini, N. Lotfian, A. Salimi, A. Bauza, R. Van Deun, R. Decadt, M. Barcelo-Oliver, A. Frontera, Dalton Trans., 2014, 43, 1906.
[3] A. Hassanpoor, M. Mirzaei, H. Eshtiagh-Hosseini, A. Majcher, CrystEngComm, 2018, DOI: 10.1039/c8ce00573g.
[4] A. Hassanpoor, M. Mirzaei, H. Eshtiagh-Hosseini, M. Niknam Shahrak, A. Majcher, Ultrason. Sonochem., 2018, submitted.

Dehydrogenation of methanol to light olefins upon zeolite/alumina catalysts: Effect of reaction conditions, catalyst support and zeolite modification

Reza Mosayebi Behbahani*, Saeed Hajimirzaei, Shahla Azarshin
Petroleum University of Technology Kut-Abdollah, Ahwaz, Iran
**Corresponding author: r_behbahani@yahoo.com*

The reaction of methanol to propene was studied in a fixed bed reactor using a pelleted zeolite in alumina matrix support catalyst. The effect of reaction conditions (temperature, pressure, space velocity, feed composition), as well as the effect of support to ZSM-5 zeolite ratio on the conversion of methanol to light olefins (C2 –C4) was studied. The best catalyst and optimum reaction conditions leading to a maximum yield of C2 –C4 were determined. Use of -alumina as support improved the catalyst selectivity to propene and light olefins. Zeolite/alumina catalyst with 25 wt.% ZSM-5 dispersed in a matrix containing 75% alumina led to highest selectivity to propene and light olefins. ZSM-5 zeolite was modified with phosphorus, Cs, Ca and Fe. The effect of their impregnation on the conversion of methanol and selectivity to light olefins was studied. Modification in all cases increased the shape-selectivity to light olefins. ZSM-5 zeolite ion exchanged by Cs led to highest selectivity to light olefins and particularly propene by changing the acid sites distribution.

Synthesis and biomedical applications of magnetic mesoporous silica nanoparticles in drug delivery and tissue engineering

Soodabeh Davaran
Faculty of Pharmacy, Tabriz University of Medical Sciences
Research Center for Pharmaceutical Nanotechnology, Tabriz University of Medical Sciences
E-mail: davaran@tbzmed.ac.ir

Research on nanotechnology, in particular, engineered nanomaterials, has received considerable attention. Recently, mesoporous silica nanoparticles (MSNs) have attracted increasing attention in such fields as drug delivery, diagnostic, medical imaging and tissue engineering. Mesoporous silica can deliver bioactive agents owing to the high loading efficiency in mesoporous channels. Magnetic analogues of mesoporous silica nanoparticles (MMSN), which contain the same beneficial characteristics of non-magnetic material, and feature of being responsive to magnetic field, are of particular interest. Magnetic mesoporous silica nanoparticles have been intensively studied as nanomaterials for biomedical applications due to large surface area (up to 1000 m2/g), tunable pore diameter (2–50 nm), narrow pore size distribution, high thermal stability, good biocompatibility and facial surface functionalization.

We have developed a magnetic mesoporous silica-based core/shell nanoparticles grafting a thermosensitive copolymer on their surface for nanomedicine applications, such as diagnostics, hyperthermia treatment, tissue engineering and stimuli-responsive targeted drug delivery. The nanoparticles can be loaded with a cargo (drug, cell, bioactive molecules) at low temperature. Then, at 37 °C the copolymer collapses closing the pore entrances and allowing the nanoparticles to carry the cargo at physiological conditions. These nanostructures are based on pH- and thermo-responsive N-isopropylacrylamide copolymers coated iron oxide magnetic mesoporous silica nanoparticles (MMSN@P(NIPAM-co-MAA) as a multifunctional platform for drug delivery with synergistic magnetic hyperthermia. We focus upon novel functions of magnetic mesoporous silica-based core/shell nanoparticles in anticancer drug release, and as tools to control the chemical and mechanical environment of stem cells.

Commercialization of Metal-Organic Frameworks: MOFs Moves to Market

Mostafa M. Amini*, Azar Soleymani
Faculty of Chemistry, Inorganic Chemistry and Catalysis Division, Shahid Beheshti University, G. C., Tehran 1983963113, Iran
**E-mail: m-pouramini@sbu.ac.ir*

Since the discovery and development of the first Metal-Organic Framework (MOF) by Kinoshita and co-workers in 1954 research into MOFs has gathered momentum due to their potential applications. In early 1990s Richard Robson at the University of Melbourne proposed the idea of nodes and spaces, almost four decades later, before exploring applications of MOFs. It was about late 1990s scientist began to synthesis MOFs for applications, and then rapidly this filed accelerated. Now, more than 20000 MOFs have been fabricated with some fascinating ligands and a wide range of transition, main group metals, lantanas and actinides with the surface area of 7000 m^2/g, to compare about 200 zeolites. To put that in context, other porous materials such as zeolites, mesoporous silica, and carbon their surface area max out at around 1000 m^2/g. Development of MOFs similar to the discovery of transistors could have an impact our lives in near future. MOFs can have a broad range of applications, including, as a vehicle to deliver medicines to certain organs in our body, storage of fuel such as hydrogen and methane, clean-up of contaminates from the environment, catalysis, and electronic [1]. However, big changes only happen if MOFs are demanded commercially. The big challenge exists now, is convincing industry and capital venture to invest for commercialization of MOFs. Probably the biggest challenge facing commercialization of MOFs, in spite of the state-of-art researches are conducted in academia, is the integration of MOFs into end-use products and development of market demand. One of the earliest efforts of the industry for commercialization of MOFs was hydrogen and methane storage and also was CO_2 capture [2]. Development of MOFs applications and their commercialization similar to any other commercialisations is a long-term issue and of course, depend on the global economy. For commercialization of MOFs, not only designing and scaling materials is needed but also engineering their integration into systems is highly required. A big challenge is obtaining finance for commercialization, and for granting finance; more industrial partners are needed to become interested in these materials. On the other hand, making the MOFs cheap is essential for commercialization; another solution is that the first MOF being commercialized soon, so that gives credibility to the field. If industry and government convinced that MOFs applications could be put in practice, more funding would be allocated for their development. In spite of many barriers, MOFs base products moving to the market. A new generation of MOFs that can have a chance to enter into niche markets with useful applications is emerging by a joint venture between academia and industry. Queen's University Belfast spin-off MOF Technologies in mid-2016 claimed to be the pioneer company in the world to start selling large volumes of MOFs by announcing that company is capable of making any MOFs by an efficient process [3]. One of the products among ten commercial products produce by MOFs Technologies is a MOF that used for fruit packaging. MOFs Technologies claimed can produce MOF in 100 Kg scale at production runs, including aluminium fumarate, MOF A520 [3].

BASF the German giant company is involved in research and development of MOFs more than a decade ago and mostly focused on the specialty chemical applications. This leading chemical company holds 2.5% of all MOFs patents worldwide more than any other organization [3]. BASF produces more than 100 MOFs at

laboratory scale in collaboration with Berkeley scientists and reported surface area of 10000 m^2/g for a laboratory sample, the largest observed surface area [3]. Now, BASF sells several MOFs in small scale through Merck Chemical Company, including Basolite C300 (HKUST-1) with the surface area of 1500-2100 m^2/g in price of $9,200 for 500 g (Fig. 2). This MOF has application in separation of C5 olefins from paraffin in steam creaking process. UOP is another large company which is active in research and development of MOFs and is a major patent holder. UOP MOFs patents mostly associated with fluid catalytic cracking applications.

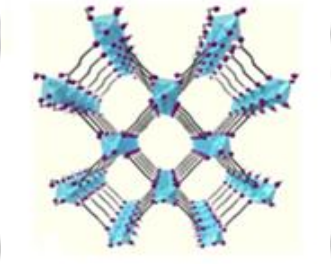

Fig. 1. Al-fumarate, Al MOF-520, a commercialized MOF [4].

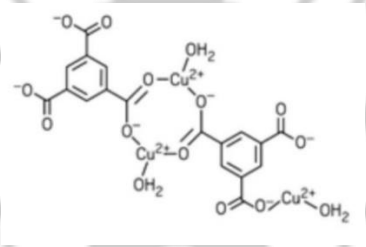

Fig. 2. Basolite C300 (HKUST-1) [3].

NuMat Technologies is another start-up company in Skokie in Chicago Illinois which established by a faculty in North Western University in the United States which commercializing MOF for semiconductor applications. NuMat Technologies goal is to bring down the high cost of storing toxic gases such as arsine, phosphine, and boron trifluoride which are used by the semiconductor industry. NuMat Technologies developed a technology in which the above toxic gasses can be stored in cylinders containing a MOF in much low pressure that the high-pressure cylinders presently used. Removing gas in such a low-pressure cylinder needs to apply vacuum which makes them safe in case leak. Such start-up companies for commercialization of MOFs in developed countries now are growing, and they realize that the MOF sector should be realistic and should be focused on top niche applications for near-term profits and success. Considering the drop in production cost and rising potential applications of MOFs, large volume opportunities just a couple years away. As a community, we're in a position now to push our idea and develop the applications of MOFs. People in the field should keep doing what they're doing because this is a field that has exploded. A number of exciting things have come out of the last few years. As long as we stay on the same trajectory, this field will be hard to beat.

References

[1] H. Furukawa, K.E. Cordova, M. O'Keeffe, O.M. Yaghi, Science **2013**, 341, 2013.
[2] O. Farha, B. Hernandez, Nature Chem. **2016**, 8, 990.
[3] A. Scott, Chem. Eng. New **2017**, 95, 18.
[4] M. Derakhshani, A.R. Hashamzadeh, M.M. Amini, Ceramic International, **2106**, 42, 17748.

Improving soil functions by zeolitic amendments in agricultural lands

Shahin Oustan
Soil Science Department, Faculty of Agriculture, University of Tabriz
oustan@hotmail.com

Over the years, natural zeolites (e.g. clinoptilolite, mordenite, phillipsite and chabazite) are expected to find promising applications in agriculture given their unique nano-porous structure, capability of adsorption, cation exchange as well as molecular sieving and eco-friendly nature for sustainable agriculture. These make them attractive for a variety of potential applications including use as soil conditioners (e.g. improving water retention in sandy soils and controlling runoff production and soil loss in steep slopes), nutrient retainers, slow-release fertilizers (N-P-K), zeoponic plant-growth substrates, carriers for pesticides and remediants in contaminated soils (particularly for blocking the movement of radionuclides and heavy metals). Besides, synthesis of high performance multifunctional zeolites (e.g. nano-zeolites with impregnated macro and micro-nutrients) or modification of existing zeolites (surface-modified zeolites for removal of heavy metals or nitrate or organo-zeolites) to obtain superior properties are recently under investigation. It is difficult to evaluate the performance of a particular application of a zeolite. This is because there are many factors (such as zeolite type, particle size, CEC and purity, and types of exchangeable cations and pre-treatments) that control its performance. Moreover, type of soil is a key factor in determining the effectiveness of zeolitic amendments to restore soil functions. Therefore, future works will need to address a number of questions with the use of zeolites in soils. Most benefits of soil-applied zeolite have been reported in course-textured acid or highly weathered soils. The addition of natural zeolites to soils increases both CEC and pH, which the latter is not suitable for alkaline soils. For this, acid zeolites with optimum Si:Al ratio containing high density of effective Bronsted acid sites may be good candidates for election. However, they must be fully characterized and tested before it can be used reliably. Eventually, very little (if any) is known about the long-term impact of zeolites on soil microbial community, which merits much more investigation in the future.

Nano-pumice as reaction reactor: From microporous to mesoporous

Sadegh Rostamnia
Organic and Nano Group (ONG), Department of Chemistry, University of Maragheh, P.O. Box 55181-83111, Tel (+98) 4212278001-108; Maragheh, Iran. E-mail: srostamnia@gmail.com; rostamnia@maragheh.ac.ir

Abstract: Nowadays, giant organic molecules have taken a great attention in nanoarchitecturing of nanoporous silica, metal-organic frameworks (MOFs) materials. Solid nanoporous (Nano-pumice) nanostructure binded dendrimers play a crucial role in the next-generation technologies within many fields such as medicine, drug delivery, sensors, catalysis, water treatment, etc. This paper discusses silica nanostructures which are arrayed by dendrimers and have been used for many applications such as drug delivery and catalysis. Also, this paper elaborates some possible pathways of binding a dendrimer to a silica surface. Synthesis of dendrimers on the surface of silica nanostructure is also discussed.

Keywords: Nano-pumice, microporous, mesoporous, catalysis.

Porphyrin/$ZnFe_2O_4$@polythiophene nanocomposite as adsorbent and photocatalyst for the removal of organic pollutants under visible light irradiation

Rahmatollah Rahimi[a]*, Parnian Kharazi[a], Mahboubeh Rabbani[a]
[a]*Department of Chemistry, Iran University of Science and Technology, Tehran 16846-13114, Iran*
**Corresponding author: rahimi_rah@iust.ac.ir*

Abstract: A new magnetically responsive three-component nanocomposite consisting of $ZnFe_2O_4$ (ZnFe), polythiophene (PTh) and porphyrin was successfully prepared by coating of $ZnFe_2O_4$ nanoparticles with polythiophene and subsequent sensitizing with tetrakis(4-carboxyphenyl)prophyrin (TCPP). In addition, photocatalytic–adsorption activities of prepared samples were carried out for removal of methyl orange (MO) and methylene blue (MB) under visible LED lamp light and sunlight irradiation. The results indicated that the synthesized nanocomposite not only shows excellent photocatalytic and adsorption activity for removal of MO and MB, respectively, but also can be separated easily by an external magnet and reused twice more.

Keywords: Porphyrin; $ZnFe_2O_4$; Polythiophene; Photocatalyst; Adsorption.

Micro-Mesostructured Zeolite

Mojgan Zendehdel
Department of Chemistry, Faculty of Science, Arak University, Arak 38156-8- 8349; Iran
**E-mail: m-zendehdel@araku.ac.ir, mojganzendehdel@yahoo.com*

Abstract: During the last decade significant efforts have been devoted to the preparation of micro–mesostructured zeolite materials. Micro–mesoporous materials are an important class of catalytic or absorbent materials, which has significant number of advantages with respect to both zeolites and mesoporous materials. As compared to zeolites, micro–mesoporous materials offer the following improvements:

- improved diffusion of reactants provided by mesoporous and therefore enhanced accessibility of the acid sites and higher effectiveness factors for catalytic transformations;
- shortened diffusion pass length and therefore reduced retention times of products in the micropores, which leads to lower probability of secondary reactions and hence improved selectivity to primary products;
- enhanced transport of coke precursors out of the catalyst and therefore improved resistance of the catalysts to the deactivation.

With respect to mesoporous materials the following advantages emerge:

- higher hydrothermal stability due to reinforcing of mesoporous walls by building of zeolite blocks, which allows for the repeated use of the catalyst in many reaction–regeneration cycles;
- high acidity of zeolite, which opens new horizons for application of mesoporous materials in the catalytic reactions demanding strong acidity.

Nanocrystalline zeolites which can be synthesized with two main methods, direct synthesis and solid templating are intercrystalline mesoporous material that results from the voids formed in between tiny zeolite crystals and the size and shape of the mesoporous.

Also another type of mesoporous zeolites includes ordinary zeolite single crystals perforated by irregular mesoporous which mesoporous can be introduced into zeolite crystals by post-synthesis treatments such as conventional dealumination and/or desilication procedures or with solid or supramolecular templating.

The next type of micro-mesoporous materials includes composite materials containing two phases, zeolite and mesoporous, interconnected with each other.

Another type of these materials is based on ordered mesoporous materials with tiny zeolite fragments in the walls. There are different synthetic strategies for the preparation of these materials such as dual templating, self-assembling of zeolite seeds, recrystallization or coating of mesoporous materials and recrystallization of zeolites.

The motif of metal impregnation over low-Si/Al-ratio ZSM-5 catalyst in MTH process

Bahram Ghanbari[a*], Fatemeh Kazemi Zangeneh[a], Zahra Taheri Rizi[b], Erfan Aghaei[b]
[a] *Department of Chemistry, Sharif University of Technology, Tehran, Iran*
[b] *Research Institute of Petroleum Industry, Tehran, Iran*
**Corresponding author: ghanbarir@sharif.edu*

Abstract: A series of metal-modified aluminum-rich-HZSM-5 (Si/Al = 11) zeolite catalysts were prepared in the absence and presence of the promotional effect of Zn, Fe, Mo and Cr in both alkaline and neural aqueous solutions and used in the conversion of methanol to aromatic hydrocarbons. The textural and surface properties of catalysts were characterized by using XRD, XRF, N_2 adsorption-desorption, NH_3-TPD, TGA, FT-IR, FE-SEM and FESEM/EDX techniques. Then, the aromatization of methanol over catalysts carried out in a fixed-bed tubular reactor at 375 °C and WHSV of 2 h^{-1} under ambient pressure. On the basis of GC and GC-MS results, [0.2Fe, 0.3Zn]-alk-HZSM-5 catalyst exhibited the selectivity for aromatic hydrocarbons, yielded up to >86% together with highly selectivity for xylenes (44.7 %) and very low content of benzene (0.1 %). Meanwhile, alkaline HZSM-5 catalyst produced aromatic compounds with xylenes selectivity 39.4% and the benzene selectivity (0.0 %). Moreover, 1-Mo-HZSM-5 catalyst displayed the selectivity for aromatic hydrocarbons (86%) as well as benzene (6.7%). Meanwhile, [0.4Fe, 0.6Zn]-HZSM-5 catalyst presented the maximum BTX (67.4%) and aromatics (88.1%).

Keywords: HZSM-5 zeolite; methanol to aromatics (MTA); alkaline treatment; metal impregnation.

Title, Presenter & Time of Posters

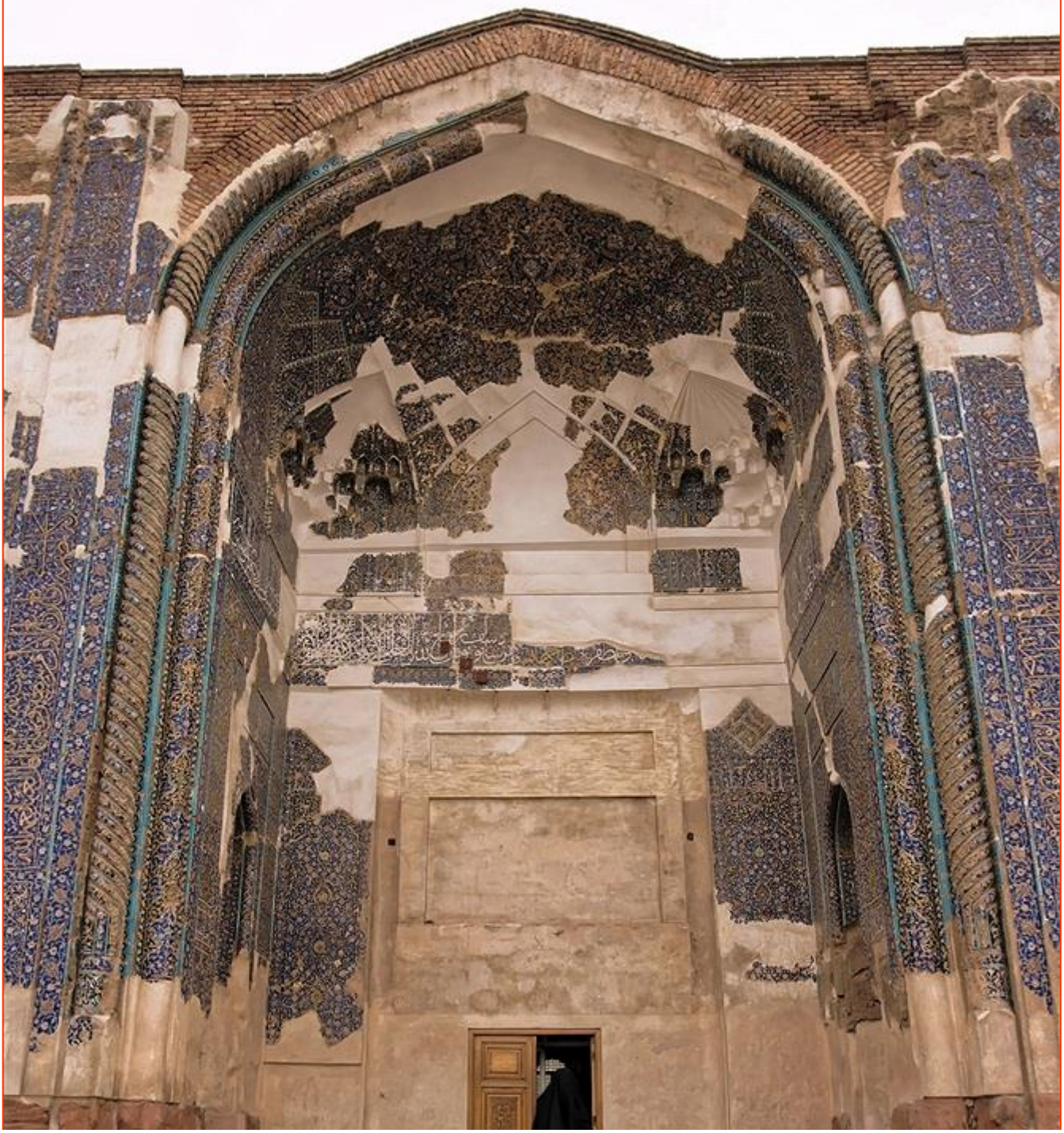

Title	Authors	Presenter	Num.
Sunday August 26, 2018, Section A		11.00 – 12.00	
Application of Zeolites			
A Comparative Study on Catalyst Deactivation of Platinum Incorporated Mesoporous Catalysts Modified by HZSM-5 for Removing Toluene as a Volatile Organic Compound	M. H. Peyrovi, N. Atashi, N. Parsafard	**Atashi, N**	**A1**
Kinetic Study for Catalytic Oxidation of Toluene as a Volatile Organic Compound Using Platinum Supported Catalysts	M. H. Peyrovi, N. Atashi, N. Parsafard	**Atashi, N**	**A2**
Investigation of Performance of Impregnated Zeolite Catalysts for Biodiesel Production	S. Mohebbi, M. Rostamizadeh	**Rostamizadeh, M**	**A3**
Performance Comparison of HZSM-5 and SAPO-34 Catalysts for Conversion of Methanol to Light olefins	L. Shirazi, K. Sharifi, Z. Taheri	**Shirazi, L**	**A4**
Catalytic Upgrading of Iranian Vacuum Residue on Alkali-treated ZSM-5 Zeolite: Viscosity Reduction	S. Safari, R. Karimzadeh	**Safari, S**	**A5**
Removal of Mixed Heavy Metal Ions in Ternary Aqueous Solution Using Functionalized MCM-41 Synthesized by Microwave Hydrothermal	S. Khademi, M. Hamadanian, B. Roozbehani	**Khademi, S**	**A6**
Hydrothermal Synthesis of H-ZSM-5 Catalysts Employing Mixed Template Method and its Application in Conversion of Methanol to Light Olefins	F. Gorzin, J. Towfighi Darian , F. Yaripour	**Gorzin, F**	**A7**
Zeolites as Supports for the Gadolinium and Iron Oxide Nanoparticles Based MRI Contrast Agents	N. Gharehaghajia , B. Divband	**Gharehaghaji, N**	**A8**
Effect of SiO_2/Al_2O_3 Ratios on the Activity of Fe-ZSM-5 Nano Catalysts in the Catalytic Oxidation of Toluene	A. Jodaei	**Jodaei, A**	**A9**
Effects of Calcination Temperature on Catalytic Activities of Ag/ZSM-5 Catalyst for Catalytic Oxidation of Toluene	A. Jodaei	**Jodaei, A**	**A10**
Zeolite as Antibacterial Agent for Active Packaging of Food	L. Rafiei, M. Azizi-lalabadi,	**Rafiei, L**	**A11**

	A. Ehsani, B. Divband		
The Effect of ZSM-5 Zeolite on Membrane Bioreactor Performance and Transmembrane Pressure	Z. Sajadian, H. Hazrati, M. Rostamizadeh	**Hazrati, H**	**A12**
Preparation of ZSM-5 Nanocrystals as a Green Acid Catalysis for the Synthesis of 2,3-dihydroquinazolin-4(1H)-ones	R. Teymuri, J. Safaei-Ghomi	**Teymuri, R**	**A13**
Synthesis of K-SAPO-34 and Ag-SAPO-34 Nano-catalysts for Methanol to Olefins (MTO) Process	M. Ghadiri, K. Mirza, M. Haghighi, A. Rahmati	**Ghadiri, M**	**A14**
Effect of Incorporating ZnO Nanoparticles into Orthodontic Composite Resins on Shear Bond Strength	M. Kachoei, B. Divband, M. Esmailzadeh, M. Rahbar, M. Ghanizadeh	**Esmailzadeh, M**	**A15**
The Study of Stability and Coke Deposition of Micro, Meso, and Micro/mesoporous supported Ni Catalysts for Toluene Hydrogenation	Z. Mohammadian , M. H. Peyrovi, N. Parsafard	**Mohammadian, Z**	**A16**
Removal of drug from aqueous solution using zeolitic imidazolate framework including Iron (Fe-ZIF-8)	S. Amani, M. Rostamizadeh	**Rostamizadeh, M.**	**A17**
Methanol to Highly Aromatic Gasoline Reaction over Ultrasound Assisted Co-impregnation Cu and Zn/HZSM-5 catalyst	Z. Taheri, E. Aghaei, L. Shirazi	**Taheri, Z**	**A18**
Heterogeneous Electro-Fenton and Electro-Fenton-like process catalyzed by promoted ZSM-5 zeolite: effect of promoter nature	S. Gharibian, M. Rostamizadeh, H. Hazrati	**Hazrati, H**	**A19**
Investigation on the Gross Teratopathogenic and Embryotoxic Effects of Nanozeolite on Chick Embryos in Ovo Environment	M. R. Amini, M. Hejazy, G. Akbari , M. Moradi	**Hejazy,M**	**A20**
Evaluation of Nanozeolite Administration on Viability and Development of Embryos Chicken Model	M. R. Amini, M. Hejazy, G. Akbari , B. Divband	**Hejazy,M**	**A21**
Removal of Abamectin from Wastewater by Iron-modified Bentonite	M. Moosavifar,	**Dibazar, M**	**A22**

	M. Dibazar, T. Sharifi		
Removal of Abamectin from wastewater by iron-modified kaolin	M. Moosavifar, M. Dibazar, T. Sharifi	**Sharifi, T**	**A23**
The efficiency of surfactant-modified zeolite ZSM-5 for oxidative desulfurization of dibenzothiophene	S. Shouhani, N. Rahemi, S. Allahyari	**Shouhani, S**	**A24**
Preparation of Solid hybrid catalyst (HY@NH_2@SO_3H) and its application in synthesis of coumarin	M. Zendehdel, F. Tavakoli	**Tavakoli, F**	**A25**
Effect of aging types on the purity and particle size of synthesized NaX via hydrothermal method	R. Javani, S. Darvishi Gilan, A. A. Babaluo	**Javani, R**	**A26**
A Temperature Programmed Desorption (TPD-CO_2) Investigation on NaY, DEA-NaY and Aminosilane-NaY	M. Tajbakhsh Jadidi, M. Fakhimi Abarghouei, H. Alinejad, K. Niknam	**Fakhimi Abarghouei, M**	**A27**
Investigation of Different Synthesized Zeolite Types with High Capacity of Moisture Absorption: A Review	A. Ranjbar Koh Farhadi, N. Rahemi, S. Allahyari, A. Beygi, S. Shouhani	**Ranjbar Koh Farhadi, A**	**A28**
Adsorption kinetics of Industrial Colors from Wastewater Using Surfactant-Modified Clinoptilolite	A. Froghirad, M. Ghaderzadeh, M. Moutab, K. Farhadi, A. Bahrami	**Froghirad, A**	**A29**
Preparation of ZSM-5 nanocrystals as a green acid catalyst for solvent-free synthesis of pyrimidinones	A. Bakhtiari, J. Safaei-Ghomi	**Bakhtiari, A**	**A30**
The Effect of Ag-Zn Zeolite on Antibacterial Properties and Setting Time of Dental Composite Resins	F. Dabaghi-Tabriz, B. Divband, M. Rahbar, M. Mahmoodabadi	**Dabaghi-Tabriz, F**	**A31**
Arsenic Removal from Wastewater Using a Low Cost Adsorbent Based on Natural Zeolite: Comparative Study	L. Sanaei, M. Tahmasebpoor, M.	**Tahmasebpoor, M**	**A32**

	Khatamian, B. Divband, A. Mokhtari		
Natural Zeolites			
Preparation of Zeolite A /Epoxy Nanocomposites by Ultrasonic Dispersion and Enhanced Thermal Properties	S. Khademi, M. Hamadaniana, B. Roozbehani	**Khademi, S**	A33
Chemical modification of bentonite with hydrochloric acid leaching under ultrasound radiation	R. Shahi, M. Khatamian, B. Divband	**Shahi, R**	A34
Use of Nano-Clays as a topical hemostatic agent in animal model	S. Javanmardi, M. Moradi Arzlou, B. Divband	**Moradi Arzlou, M**	A35
Introduce Nano Cu on Bentonite and Investigation of Antibacterial properties	P. Maleki, Z. Mortezaei, M. Zendehdel	**Maleki, P**	A36
Clinoptilolite vs Bentonite as Support of Silicotungstic Acid in Photodegradation of Wastewater	S. Rastegar, S. Allahyar, D. Kahforooshan, N. Rahemi	**Rastegar, S**	A37
Degradation of Methylene Blue using Mordenite Based Silicotungstic Acid Photocatalyst	S. Rastegar, S. Allahyar, D. Kahforooshan, N. Rahemi	**Rastegar, S**	A38
Molecular Sieves			
Adsorptive removal of tetracycline from aqueous solution using TiO2/MCM-41 nanocomposite	M. Khanmohammadi, F. Rahmani, J. Rahbar Shahrouzi	**Khanmohammadi, M**	A39
Shaping of Zeolite 4A by Binderless Process	M. Rezaie	**Rezaie, M**	A40
Shaping of Zeolite 4A by Binder Process	M. Rezaie	**Rezaie, M**	A41
LDH			
Synthesis of Nickel Tungstate /Nickel-Gallium-Layered Double Hydroxide Nanocomposites as Electrode Material in Supercapacitors	S. Sanati, Z. Rezvani	**Sanati, S**	A42

Graphene Quantum Dot/NiFe Layered Double-Hydroxide Composite as a Highly Efficient Electrocatalyst for Water Oxidation	L. Jafari Foruzin, Z. Rezvani. Habibi	**Jafari Foruzin, L**	**A43**
Photocatalytical Water Oxidation by TiO2/MMO Nanocomposites under Visible Light Irradiation	L. Jafari Foruzin, Z. Rezvani	**Jafari Foruzin, L**	**A44**
The effect of amines in the synthesis of layered double hydroxides	A. Mokhtari, Z. Kianinejad, M. Fazayeli	**Mokhtari, A**	**A45**
Computational Chemistry			
Preferential Siting of BEA, FAU, MOR, and MFI Zeolite Frameworks for Adsorbed Phenol: A Monte Carlo Study	F. Ektefa, S. Javadian	**Ektefa, F**	**A46**
Calculation of Heat Capacity of Clathrate Hydrate by Molecular Dynamics Simulations	H. Ghafari, H. Mohammadi-manesh	**Mohammadi-manesh, H**	**A47**
Molecular Dynamics Simulations of Hydrogen Bonding in sI Clathrate Hydrates with Ethylene oxide and Cyclopropane Guest Molecules	H. Ghafari, H. Mohammadi-manesh	**Mohammadi-manesh , H**	**A48**
Host-Guest chemistry of porous materials			
Novel Approach to the Synthesis of Polyhydroquinolines and Dihydropyridines Derivatives Using SBA-15/SO_3H Nanoreactor as a Highly Efficient and Reusable Catalyst	M. Dalili, S. Rostamnia	**Dalili, M**	**A49**
Pd@SBA-15/PrEn as an efficient, active and selective phosphine–free hybrid catalyst for the water medium Suzuki-Miyaura cross-coupling process	M. Dalili, H. Alamgholiloo, S. Rostamnia	**Dalili, M**	**A50**
A Review Study on photocatalytic activity of a series of modified zeolites in removal of dye contamination	M. Moosavifar	**Moosavifar, M**	**A51**
Monday August 27, 2018, Section B		**10:50 – 11:40**	
Zeolite based nanotechnologies			
Esterification of Oleic Acid for Biodiesel Production Catalyzed by Fe_3O_4@ZIF-8@TiO_2 Composite	A. Moatamed Sabzevar, M. Ghahramaninezhad, M. Niknam shahrak	**Niknam shahrak, M**	**B1**

Synthesis and Identification of Pd^{2+}/ZnO/HZSM-5 Nanocomposite and Study of its Photocatalytic Activity	B. Divband, M. Khatamian, R. Shahi	**Divband, B**	**B2**
Synthesis of γ-alumina from Nepheline syenite ore	S. Khadivi Derakhshan, N. Kamrani, B. Divband, M, Khatamian, H. Kakili	**Khadivi Derakhshan, S**	**B3**
Preparation and Characterization of Nano Mn_3O_4 and Mn_3O_4 /Zeolite A Composite	N. Kamrani, S. Khadivi Derakhshan, H. Kakili, M. Saket, M. Khatamian	**Kamrani, N**	**B4**
Synthesis and Characterization of Iron Hydroxide-Zeolite Nano Composites	S. Gholizadeh, M. Khatamian, M. Tahmasebpoor, B. Divband, A. Mokhtari	**Gholizadeh, S**	**B5**
Synthesis and Characterization of Zeolite Nano-Particles Impregnated Polyethersulfone Membranes by Electrospinning	F. Hossein Nouri, M. Zendehdel	**Hossein Nouri, F**	**B6**
Application of Nano Zeolite in Food Packaging	M. Azizi-lalabadi, L. Rafiei, A. Ehsani, B. Divband	**Azizi-lalabadi, M**	**B7**
Synthesis and Characterization of HY Zeolite @N-Cu	Z. Mortezaei, M. A. Bodaghi Fard, M. Zendehdel	**Mortezaei, Z**	**B8**
Synthesis and Characterization of Zeolite/Hydroxyapatite Nanocomposite, using in the Removal of Cr^{6+} from Aqueous Solution	A. Rezaei, M. Zendehdel	**Rezaei, A**	**B9**
Synthesis and Characterization of Aluminium-free MFI-type Cobaltosilicates using Hydrothermal Method	A. Mokhtari, M. Khatamian, Azin Yavari	**Mokhtari, A**	**B10**
Medical applications of zeolites	M. Moradi, S. Javanmardi, M. Ashrafizadeh,	**Moradi, M**	**B11**

	A. Faramarzpour		
Synthesize, Evaluation of Antibacterial and Antibiofilm behavior of Nano Silver Chloride on Acinetobacter baumannii	Z. Akhgari, A. Tanomand	**Akhgari, Z**	**B12**
Synthesis of AgCl nanoparticles functionalized on IL based SBA-15 as an effieint nanocatalyst for antibacterial and antibiofilm behavior on klebsiella pneumonia	Z. Akhgari, A. Tanomand	**Akhgari, Z**	**B13**
Synthesis and Characterization of Zeolite and Ionic Liquid Hybrid Material	S. Ganji, S. khaghani nezhad, M. Zendehdel	**Ganji, S**	**B14**
Preparation and characterization of graphene oxide / Mn_3O_4 nanocomposite and study of its photocatalytic properties	M. Khatamian, M. Saket, H. Kakili, N. Kamrani, S. Khadivi Derakhshan	**Kakili, H**	**B15**
Preparation and characterization of SAPO-34 zeolite nanocatalysts using diethyl amine (as template)	M. Ghadiri, K. Mirza, M. Haghighi, A. Rahmati, S. Abbaspour	**Ghadiri, M**	**B16**
Performance of natural zeolite for removal of lead: A review	F. Zare Pakzad, M. H. Sarrafzadeh, B. Divband	**Zare Pakzad, F**	**B17**

Synthesis of Mesoporous Materials

HFIP/SBA-15 as a Metal Free Catalyst for Synthesis of Rhodanines	H. Mohtasham, S. Rostamnia	**Mohtasham, H**	**B18**
Production of low cost and effective porous adsorbent from Iranian kaolin by sonication for recovery of wastewater contaminated by cationic dye	M. Foroughi, S. Hamedgolzar, A. Salem	**Foroughi, M**	**B19**
Electrodeposition of Mesoporous Nickel Film using Lyotropic Liquid Crystal Template	S. Barzegar, F. Nasirpouri	**Barzegar, S**	**B20**
Application of Porous Gd_2O_3 Nanoparticle as MRI Contrast Agent	N. Gharehaghaji, F. Bakhtiari Asl, B. Divband	**Bakhtiari Asl, F**	**B21**

Activity Evaluation of Mesosilicate Supported Nickel Catalysts in Vapor Phase Hydrogenation of Benzene	Z. Mohammadian, M. H. Peyrovi, N. Parsafard	**Mohammadian, Z**	**B22**
Synthesis of $NaHSO_4$ modified periodic mesoporous organosilica magnetic nanoparticles	M. Haghighat, M. Golshekan, F. Shirini	**Haghighat, M**	**B23**
Ag/AgCl/Zeolite (A) (LTA) Nanocomposite: A Highly Efficient and Stable Photo Catalyst Active under Visible Light	S. Hatef Tabar, M. R. Fakhri	**Fakhri, M R**	**B24**
Synthesis of Fe_3O_4@MCM-41@Zr Modified with Piperazine as a New Mesoporous Nanocomposite	R. Pourhasan-Kisomi, F. Shirini, M. Golshekan	**Pourhasan-Kisomi, R**	**B25**
Mesoporous Magnetic Graphene Oxide Nanocomposite as a Targeted Drug Carrier; Synthesis and Characterization	M. Pooresmaeil, H. Namazi	**Pooresmaeil, M**	**B26**
Loading Cobalt Phthalocyanine onto Graphene Oxide and Modified Graphene Oxide for Construction of Photoactive Catalyst	M. Ghaeini, M. A. Zanjanchi	**Ghaeini, M**	**B27**
Synthesis of Zeolite NaY from Rice Husk Ash with Ultrasound Aging and Conventional Aging	M. Askari, E. Aghaei, R. Karimzadeh	**Askari, M**	**B28**
Preparation of Mesoporous Nano-Silica (MNS) as Adsorbent	J. Rahimpour, M. H. Alibenhamid, A. Z. Aroguz	**Rahimpour, J**	**B29**
Synthesis of Mesoporous Superparamagnetic Ferrite Nanoparticles (Fe_3O_4) Using Lyotropic Liquid Crystal Phase Templates	S. Fallah, F. Nasirpouri	**Fallah, S**	**B30**
Synthesis of Zeolite from Coal Waste Ash by Hydrothermal Method using Alkaline Source	R. Gholinejad, E. Kamali, J. vahdati, S. Mollazadeh	**Gholinejad, R**	**B31**
Cooperative catalytic performance of SBA-15 and TFE in selective oxidation of sulfides	H. Mohtasham, A. Ahadi, S. Rostamnia	**Mohtasham, H**	**B32**
SBA-15/SO_3H nanoreactor and ultrasonic combination as a novel, ultra-fast, waste-free green catalytic system	A. Ahadi, S. Rostamnia	**Ahadi, A**	**B33**

MOF

The effects of incorporation of silver-zeolite on antibacterial efficacy, setting time and calcium release properties of mineral trioxide aggregate	F. Dabaghi-Tabriz, B. Divband, M. Rahbar, A. Bahramian, M. Esmailzadeh	**Rahbar, M**	**B34**
Stepwise Immobilization of Palladium Complex on to the Metal-organic Framework for Suzuki Cross-coupling Reaction	H. Alamgholiloo, M. Dalili, S. Rostamnia	**Alamgholiloo, H**	**B35**
Fe3O4-encapsulated ZIF-8 as a Novel Catalyst for Oxidative Desulfurization of a Model Fuel	H. Kargar, M. Ghahramaninezhad, M. Niknam Shahrak	**Niknam shahrak, M**	**B36**
IRMOF-3 as a heterogeneous nanocatalyst for Kabachnik–Fields three-component reaction	A. Ahadi, H. Mohtasham, S. Rostamnia	**Ahadi, A**	**B37**
Synthesis and Characterization of Iron-based Metal-Organic Framework MIL-53	R. Johnny, A. Ahmadpour, M. Ghahramaninezhad, T. Rohani Bastami	**Johnny, R**	**B38**
Metal Organic Frameworks As an Adsorbent For Water Contaminants	E. Z. Lotfi, M. R. Fakhri Heravi, A. Rostamiiranagh	**Fakhri, M. R.**	**B39**
Ethylenediamine Grafting on MIL-101(Cr) as an Efficient Catalyst for the Hantzsch Condensation Reaction	H. Alamgholiloo, S. Rostamnia	**Alamgholiloo, H**	**B40**
Combining of Catalytic Properties ZIF-8 and Fluorinated Alcohol Solvents (FAS) for N-formylation Reaction	M. Farajzhadeh, H. Alamgholiloo, R. Banaei, S. Rostamnia	**Farajzhadeh, M**	**B41**
Efficient adsorption and photocatalytic degradation of Congo Red by Zeolitic Imidazolate Framwork-8-encapsulated POM	F. Akbari , M. R. Mozdianfard,	**Niknam shahrak, M**	**B42**

	M. Niknam Shahrak, A. Ayati		
Metal-organic Frameworks: Synthesis and Application as a Drug Delivery System	M. Pooresmaeil, H. Namazi	**Pooresmaeil, M**	**B43**
Comparison of Congo red removal by a metal-organic framework in the presence of oxidizing agent & light	M. Rahim Soroush, A. Tarlani, R. Malek Mohammadi	**Rahim Soroush, M**	**B44**
Adsorptive Removal of Antibiotic Drugs from Contaminant Water by ZIF-8	R. Malek Mohammadi, M. Rahim Soroush, A. Tarlani	**Malek Mohammadi, R**	**B45**
Photodegradation of Methyl Orange Using ZIF-8 from Aqueous Solution	R. Malek Mohammadi, M. Rahim Soroush, A. Tarlani	**Malek Mohammadi, R**	**B46**
Adsorption Behavior of HKUST-1 for Methylene Blue Decoloration from Contaminated Water	M. Rahim Soroush, A. Tarlani, R. Malek mihammadi	**Rahim Soroush, M**	**B47**
Application of HKUST-1@GO Nanocomposite for the Removal of Lead from Wastewater	S. Alqaisi, A. Ahmadpour, M. Ghahremanine zhad, T. Rohani Bastami	**Alqaisi, S**	**B48**
MMMs			
Application of graphene quantum dots for drug delivery of anticancer	Z. Kianinejad	**Kianinjad, Z**	**B49**
Potential Application of Graphene Quantum Dots	Z. Kianinejad, A. Mokhtari	**Kianinjad, Z**	**B50**
Hierarchical and Hollow Zeolites			
Synthesize of Cu^0/Clinoptilolite and Investigation of Antibacterial properties	Z. Kalateh, Z. Mortezaei , P.	**Maleki, P**	**B51**

	Maleki, M. Zendehdel		
Removal Efficiency, Kinetic and Isotherms of dyes onto Natural Zeolite, Manisa, Turkey	J. Rahimpour, D. Lacin, F. Esenli, A. Z. Aroguz	**Rahimpour, J**	**B52**

Abstracts

5th Iran International Zeolite Conference

University of Tabriz, Tabriz, Iran

26-27 August 2018

A Comparative Study on Catalyst Deactivation of Platinum Incorporated Mesoporous Catalysts Modified by HZSM-5 for Removing Toluene as a Volatile Organic Compound

M. H. Peyrovi[a], N. Atashi[a], N. Parsafard[b]*

[a] *Faculty of Chemistry and Petroleum Sciences, Department of Petroleum Chemistry and Catalysis, University of Shahid Beheshti, Tehran,* 1983963113, *Iran*

[b] *Kosar University of Bojnord, Department of Applied Chemistry, North Khorasan,* 9415615458, *Iran*

* *Corresponding author: n-parsafard@kub.ac.ir*

Abstract: Volatile organic compounds are the main air pollutants emitted from petrochemical and allied industries especially due to the photochemical reaction in the atmosphere. Total oxidation of VOCs is one of the most promising techniques in order to operate at low temperatures. In this work, five weight percentages of Pt/HZSM5(x)-HMS catalysts were used for the oxidation of toluene. These catalysts were investigated for a period of time for the oxidation of toluene continuously at 350 °C for more than 60 h. The catalytic activity and selectivity were found to be a function of the time of feed stream. The results show that the decrease in catalytic activity was related to an increase in coke deposition over the catalytic surface. Among these prepared catalysts, Pt/HZSM5(30)-HMS has the low coke deposition than others.

Keywords: Toluene oxidation; Conversion; Selectivity; *meso*- Porous catalysts; Catalytic deactivation

1. Introduction

Volatile organic compounds (VOCs) are one of the major air pollutants supplies and their elimination by catalytic oxidation is one of the most promising ways among treatments. One of the advantages of this method is to direct the reaction to low temperatures (150-450 °C). In this way, two types of catalysts are usually applied: Noble-metal catalysts which possesses high activity but are very expensive and metal oxides which are cheaper but less active. It is well known that supports play an effective role in catalytic activities, particularly in oxidation reaction. Catalysts used for this reaction can be deactivated by coking. When a catalyst is deactivated, part of the VOC will remain unreacted and/or partially oxidized. So, both the activity and selectivity may change with time. This is important because the emission stream may contain products more toxic than the initial compound [1-4].

Since it is important to maintain the catalysts activity in a constant amount, especially to meet environmental regulations, the change of activity was investigated with time at a temperature, which the catalyst showed the best activity.

In the present work, the oxidation of toluene was carried out over Pt/HZSM5-HMS catalysts with various amounts of HZSM-5. Toluene is one of the aromatic VOCs that has high volatility devastating effects on the health and environment and very often

encountered in the work place environment [5,6]. This study reports the catalytic activity-time relationship of these catalysts used to oxidize toluene stream.

2. Experimental Part

Platinated catalysts were prepared by the impregnation method using $H_2PtCl_6.6H_2O$ as active phase solution according to our reported method [5,6]. The prepared composite catalysts were denoted as Pt/ZH-x that x shows the weight percent of HZSM-5 in these composite materials. In order to investigate the catalyst deactivation, catalytic combustion reactions were carried out in a continuous flow micro-reactor at 350 °C for more than 60 h. 300 mg of each fresh catalyst was placed at the fixed bed of the microreactor. Feed stream to the reactor was prepared by delivering liquid toluene with a syringe pump into dry air, which was metered using a mass flow controller. The temperature of the reactor was measured with a thermocouple and the effluent gases were analyzed on-line using two gas chromatographs (GC) for the quantitative determination of CO and CO_2.

After this, coke burning from the spent catalysts was carried out with a thermogravimetric analysis (TGA) released considerable amounts of coke.

3. Results and discussion

Figure 1 shows the conversion of toluene at a fixed temperature. The important observation is that the catalytic activity remains very stable for the used catalyst. However, the catalytic activity of these catalysts decreases smoothly with the reaction run times.

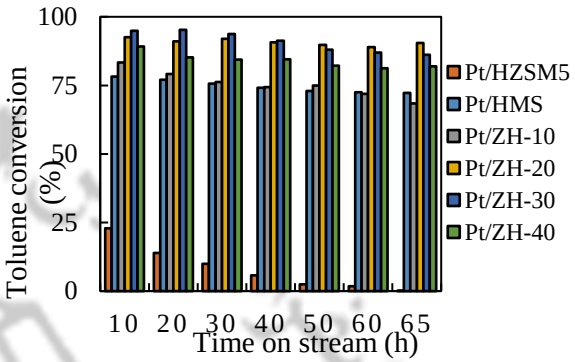

Figure 1. Toluene conversion as a function of reaction time.

During the same time period, the selectivity to carbon dioxide has almost not change as shown in Figures 2. The constant carbon monoxide selectivity in the effluent stream of the fixed bed reactor is also shown in Figures 3 for comparison purposes.

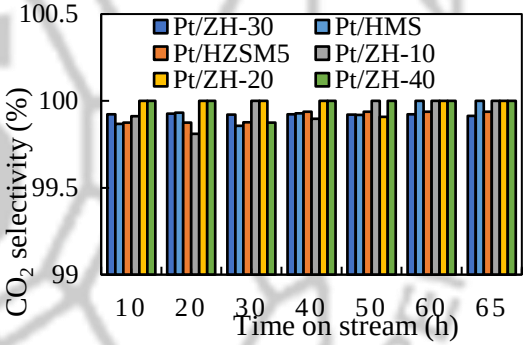

Figure 2. CO_2 selectivity as a function of reaction time.

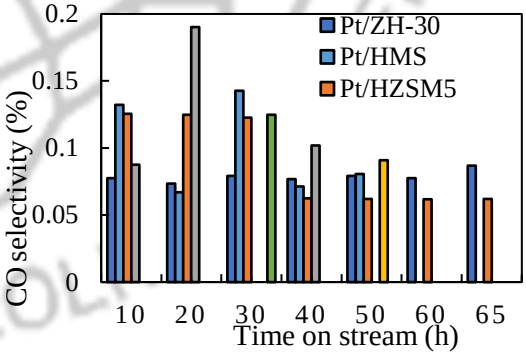

Figure 3. CO selectivity as a function of reaction time.

4. Conclusions

Coke burning from the spent catalysts by thermogravimetric analysis released considerable amounts of coke deposition. The results show that loading different HZSM-5 contents onto the similar catalytic supports would lead to the significant difference in coke formation (4-10 wt%). The greatest and the lowest amounts of coke formed on Pt/HZSM-5 (10 wt%) and Pt/ZH-30 (4 wt%), respectively. According to the results, it can be concluded that the best catalytic behavior was observed for Pt/ZH-30, with high toluene conversion (> 97%), the highest CO_2 selectivity (100%) and the low coke formation (4 wt%).

Acknowledgments

The authors greatly thank the financial support of the Iran National Science Foundation (project number 96003303). Grateful thanks also go to the Research Center of Shahid Beheshti University.

References

[1] Q. Dai, X. Wang, G. Lu, *Appl. Catal. B: Env.* 81 (2008) 192-202.

[2] J. Carpentier, J.F. Lamonier, S. Siffert, E.A. Zhilinskaya, A. Aboukaïs, *Appl. Catal. A: Gen.* 234 (2002) 91-101.

[3] P. Ge´lin, M. Primet, *Appl. Catal. B: Env.* 39 (2002) 1-37.

[4] S.C. Kim, *J. Hazard. Mater. B* 91 (2002) 285-299.

[5] N. Parsafard, M.H. Peyrovi, M.V. Shokoohi, *Iran. J. Chem. Chem. Eng.* Available Online from 20 December 2017, Articles in Press.

[6] M.H. Peyrovi, N. Parsafard, M. Rashidzadeh, *Micropor. Mesopor. Mat.* 200 (2014) 190-198.

Kinetic Study for Catalytic Oxidation of Toluene as a Volatile Organic Compound Using Platinum Supported Catalysts

M. H. Peyrovi [a], N. Atashi [a], N. Parsafard [b,*]

[a]*Faculty of Chemistry and Petroleum Sciences, Department of Petroleum Chemistry and Catalysis, University of Shahid Beheshti, Tehran, 1983963113, Iran*

[b]*Kosar University of Bojnord, Department of Applied Chemistry, North Khorasan, 9415615458, Iran*

** Corresponding author: n-parsafard@kub.ac.ir*

Abstract: The emission of volatile organic compounds to the air is a big concern due to their hazardous health and environmental effects. One of the best methods to eliminate these compounds is catalytic oxidation of VOCs to convert them into CO_2 and H_2O, which is the most efficient and cost-effective. In this research work, the catalytic total oxidation of toluene at 200-500 ˚C in air over Pt/HZSM5-HMS catalysts has been investigated. Several kinetic models have been selected and tested to investigate the kinetics of this reaction. The obtained results showed that the power law (PL) model and Langmuir-Hinshelwood (LH) model were not appropriate to get the kinetics of toluene combustion over the catalyst. On the contrary, the Mars-van Kreleven (MVK) mechanism represent a good fit ($R^2 = 1$) towards the experimental data and allowed to determine the kinetic parameters.

Keywords: Toluene oxidation; Kinetic modeling; Power law model; Langmuir-Hinshelwood; Mars-van Kreleven

1. Introduction

Volatile organic compounds (VOCs) are harmful for human health and environment. VOCs include alkanes, olefins, alcohols, ketones, aldehydes, aromatics, paraffins, and halogenated hydrocarbons. Toluene is one of the most common and toxic VOCs [1]. Catalytic oxidation is one of the several technologies for toluene gas-phase removal that offers some advantages including done at moderate operation temperature (165-450 °C), with high destruction efficiency, and no additional fuel or damaging by-products generated [2]. Toluene oxidation kinetics has been investigated recently over the various VOCs over several transition metal oxide catalysts [3]. In kinetic study, several models were used to describe the total oxidation of these compounds (VOCs) [3]. The first type is the power law model that has a mathematical foundation and not representing the chemistry of the reaction. A second model is based on two mechanisms involving either the reaction between the adsorbed oxygen and the reactant molecule adsorbed at the surface (Langmuir–Hinshelwood mechanism) or a reaction between adsorbed oxygen and the reactant in the gas phase (Eley-Rideal mechanism). These two mechanisms are based on the Langmuir model. The third type of

kinetic model is based on the Mars-van Krevelen mechanism that is one of the most common mechanisms in this field and is considered that the reaction occurs between the adsorbed VOCs and the lattice oxygen of the catalyst [4,5]. In this work, we investigate the oxidation of toluene focusing on kinetics of the reaction over Pt/HZSM5-HMS catalysts.

2. Experimental Part

Details of the materials used, synthesis procedure and characterization techniques are similar to our previous published work [5]. The prepared composite catalysts were denoted as Pt/ZH-x that x shows the weight percent of HZSM-5 in these composite materials.

Catalytic tests were performed in a continuous-flow fixed-bed microreactor. Toluene was supplied by a liquid-injection system, controlled by a liquid flow controller and mixed by air. The tests were performed at atmospheric pressure, reaction temperatures in the range of 200-500 ˚C, a varied flow rate of gaseous toluene from 1.5 to 3 ml h^{-1} and a varied O_2 flow rate of 12.6-50.4 ml min^{-1}. The catalytic activity was evaluated in terms of toluene conversion by on-line gas chromatography equipped with FID.

3. Results and discussion

To study the kinetics of this process, reaction rates were modeled to the below models. The power law equation is as follow:

$$r\left(\frac{\text{mol}}{\text{g.s}}\right) = kP_{O2}^{n}P_{Tu}^{m} \quad (1)$$

Where n and m are the partial orders of oxygen and toluene respectively, and k is the rate constant.

Table 1. Kinetic parameters at 350 °C for the toluene oxidation (n_{O2} and m_{Tu} are the partial reaction orders for oxygen and toluene, respectively).

Catalysts	n_{O2}	m_{Tu}	E_{app}^{act} *(kJ mol^{-1})*
Pt/HMS	-0.1	1.0	118.5
Pt/HZSM5	0.0	1.0	147.1
Pt/ZH-10	0.0	0.9	130.6
Pt/ZH-20	0.0	1.0	115.4
Pt/ZH-30	0.0	1.0	42.4
Pt/ZH-40	0.0	1.1	90.6

The rate equation 2 shows the Langmuir-Hinshelwood model:

$$-r = \frac{k \,.\, k_{Tu}.P_{Tu} \,.\, k_{O2}.P_{O2}}{(1+k_{Tu}.P_{Tu}+ k_{O2}.P_{O2})^2} \quad (2)$$

Where k_{O2} and k_{Tu} are the rate constants of O_2 and Tu adsorption, respectively.

According to Mars-van Krevelen mechanism, the rate of toluene oxidation can be expressed by below equation:

$$r = \frac{k_{O2}k_{Tu}P_{O2}P_{Tu}}{\gamma k_{Tu}P_{Tu}+k_{O2}P_{O2}} \quad (3)$$

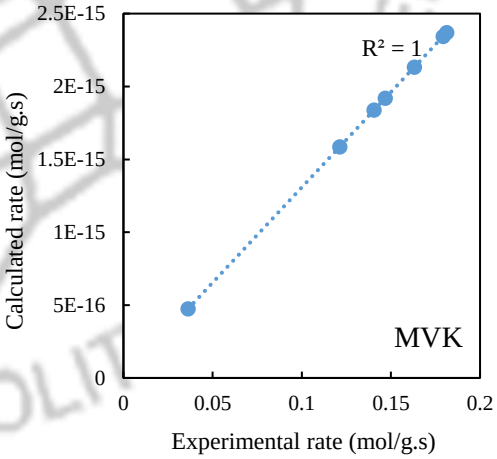

Figure 1. Estimated data by Mars-van Krevelen model for Pt/ZH-30.

ere, r: reaction rate ($\frac{\text{mol}}{\text{g.s}}$); P_{Tu}: partial pressure of toluene; P_{O2}: partial pressure of oxygen (Pa); k_{Tu}: rate constant of toluene oxidation (Pa); k_{O2}: rate constant of catalyst re-oxidation; γ is the stoichiometry coefficient of O_2 ($C_6H_5CH_3 + 9O_2 \rightarrow 7CO_2 + 4H_2O$) which is equal to 9.

4. Conclusions

The reaction orders obtained from power law model for toluene and oxygen on the prepared catalysts at a constant temperature were calculated 0.7-1.2 and -0.6 to 0.1, respectively. The lowest and highest calculated activation energies are 42.4 and 147.1 kJ mol^{-1} for Pt/ZH-30 and Pt/HZSM-5, respectively. The activation energies amount for Pt/ZH-30 is better than the reported value for complete combustion of hydrocarbons [5] that confirm the appropriate rate over these catalysts. Among the applied kinetic models, the Power-law (R^2 = 0.8) and Langmuir-Hinshelwood (R^2 = 0.7) models are unsuitable for this reaction as the predicted data were against the experimental data, and the Mars–van Krevelen model (R^2 = 1.0) can well predict the conversion behaviors of toluene oxidation.

Acknowledgments

The authors greatly thank the financial support of the Iran National Science Foundation (project number 96003303). Grateful thanks also go to the Research Center of Shahid Beheshti University.

References

[1] Y. Liu, J. Deng, S. Xie, Z. Wang, H. Dai, *Chin. J. Catal.* 37 (2016) 1193-1205.

[2] X. Liang, F. Qi, P. Liu, G. Wei, X. Su, L. Ma, H. He, X. Lin, Y. Xi, J. Zhu, R. Zhu, *Appl. Clay Sci.* 132 (2016) 96-104.

[3] S. Behar, N. A. Gómez-Mendoza, M. Á. Gómez-García, D. Świerczyński, F. Quignard, N. Tanchoux, *Appl. Catal. A: Gen.* 504 (2015) 203-210.

[4] N. Parsafard, M. H. Peyrovi, M. V. Shokoohi, *Iran. J. Chem. Chem. Eng.* Available Online from 20 December 2017, Articles in Press.

[5] M. H. Peyrovi, N. Parsafard, M. Rashidzadeh, *Micropor. Mesopor. Mat.* 200 (2014) 190-198.

Investigation of Performance of Impregnated Zeolite Catalysts for Biodiesel Production

S. Mohebbi[a,b], M. Rostamizadeh[a,b]*

[a] *Department of Chemical Engineering, Sahand University of Technology, Sahand New Town, East Azerbaijan, Iran*

[b] *Environmental Engineering Research Center, Department of Chemical Engineering, Sahand University of Technology, Sahand New Town, Iran*

**Corresponding author: Rostamizadeh@Sut.ac.ir*

Abstract: In this study, the production of biodiesel was investigated using the process of esterification of free fatty acids in the presence of methanol and ZSM-5 catalyst. ZSM-5 zeolite was synthesized using hydrothermal technique and the promoters were loaded by wet impregnation method in rotator evaporator. XRD and FT-IR analyzes were used to evaluate the structure and specifications of synthesized catalysts. All Experiments were tested in 4 hour, molar ratio of methanol to oil 10: 1, 160 °C, 10 wt% of catalyst, and mechanical stirring of 500 rpm. According to the results obtained from catalyst analysis, the molybdenum promoter with a conversion rate of 89% showed the best performance in the process of esterification.

Keywords: Esterification; FFA; ZSM-5; Promoter; Molybdenum

1. Introduction

With the modernization and industrialization of cities and countries, the need for high-speed energy is increasing. the development of alternative fuels, including biodiesel, which, given the availability of resources and as a sustainable resource, And renewable in recent years have been considered [1].

The use of heterogeneous alkali catalyst is a good idea to produce biodiesel, but this catalyst is not suitable for low-quality feeds that contain free fatty acids and water. Also, the use of homogeneous alkaline catalysts for low-quality feeds includes problems such as production of soap, increased viscosity of the product, the separation of product problems and the generation of high waste water [2]. Although homogeneous acid catalysts are suitable for high contain FFA and water-rich feeds, they still have problems such as non-reusability, corrosion of equipment and sewage production [3,4]. In contrast to homogeneous acid catalysts, heterogeneous acid catalysts have attracted a lot of attention due to the environmental friendly, easy to separation and the possibility of reuse [2, 3].

2. Experimental Part

2.1. Catalyst preparation

In this study, we used hydrothermal technique to synthesize of high silica ZSM-5 nanocatalyst catalyst (Si/Al=200) [5]. Catalysts wet impregnation with different promoters was performed in rotator evaporator device. The modified nanocatalysts included 30 wt% promoter based on the zeolite and

the modified catalysts named Mo/ZSM-5, Sn/ZSM-5 and Ni/ZSM-5.

2.2. Catalytic tests

In order to simulate the biodiesel production, the reaction was carried out in the presence of a mixture of free fatty acids and methanol in a stainless steel batch reactor at autogenously pressure with heating jacket. All experiments were tested with this reaction conditions: methanol/oleic acid molar ratio 10:1, catalyst amount 10 wt%, reaction temperature 160 °C, the stirring rate of 500 rpm and reaction time 4 h. the conversion rates of FFAs were calculated by Eq. (1). For this work, we use initial and final acid value of FFAs that was determined by titrametry following the procedure described by Ding et al. [6].

$$X = (S_i - S_f) / S_i \times 100\% \quad (1)$$

Where X is conversion rate of FFAs, S_i is initial acid value of FFAs, and S_f is final acid value of products at the end of reaction. Titrametry of each sample performed twice and averaged the results.

3. Results and discussion

3.1. Catalyst characterization

The catalysts include MFI-structure of ZSM-5 in consistent with standard ZSM-5 (JCPDS: 00-044-0002) (Fig. 1).

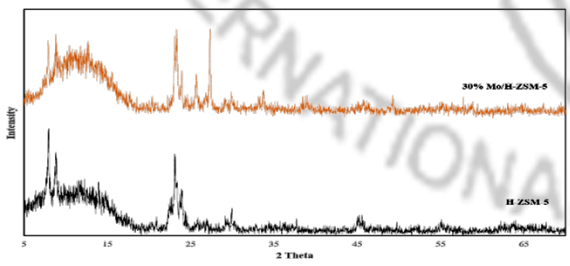

Figure 1. XRD pattern of the catalysts.

3.2. Catalyst performance

Effect of promoter was studied in order to understand catalytic activity in esterification process. The results showed that the conversion of esterification for Mo-ZSM-5 was highest in comparison with two other catalysts (Fig. 2). It may be due to surface activity such as higher amount of acid sites and surface area of Mo/H-ZSM-5 catalyst.

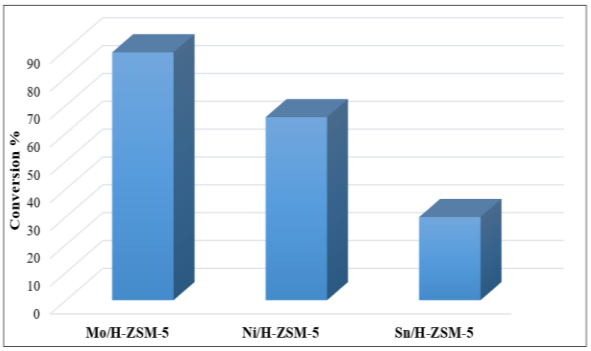

Figure 2. Conversion of different promoted nanocatalysts.

4. Conclusions

In this study, we concluded between the promoters that used, molybdenum loaded on ZSM-5 exhibited the best catalytic performance and enhanced the catalytic activity. When the esterification of FFA was carried out at batch reactor with methanol/oil=10/1, reaction temperature of 160 °C and reaction time of 4 hour with mechanical stirring for 500 rpm, the maximum FFA conversion of 89% was achieved.

References

[1] M. Hasan, M. Rahman, *Renew. Sust. Energ. Rev.* 74 (2017) 938-948.

[2] K. Sun, J. Lu, L. Ma, Y. Han, Z. Fu, J. Ding, *Fuel* 158 (2015) 848-854.

[3] K.Y. Nandiwale, S.K. Sonar, P.S. Niphadkar, P.N. Joshi and S.S. Deshpande, *Appl. Catal. A: Gen.* 460-461 (2013) 90-98.

[4] M. Kim, S. Yan, S.O. Salley, K.Y.S. Ng, *Catal. Comm.* 10(14) (2009) 1913-1919.

[5] M. Rostamizadeh, F. Yaripour, J. Taiwan Inst. Chem. Eng. 71 (2017) 454-463.

[6] J. Ding, B. He, J. Li, *Energies* 4 (12) (2011) 2212-2223.

Performance Comparison of HZSM-5 and SAPO-34 Catalysts for Conversion of Methanol to Light olefins

L. Shirazi*, K. Sharifi, Z. Taheri

Research Institute of Petroleum Industry, P.O. Box 14665-137, Tehran, Iran

**Corresponding author: shirazil@ripi.ir*

Abstract: In this study, the effect of two zeolites with different topologies (SAPO-34 and H-ZSM-5) in conversion of methanol to olefins (MTO) was comparatively investigated. The catalysts were hydrothermally synthesized and characterized by XRD, FTIR, SEM, BET, and TPD techniques. The performance of catalysts were carried out in a fixed bed reactor, at atmospheric pressure, 400 °C, WHSV of 2 h^{-1} and molar fraction of methanol in the feed is 0.3, which diluted with nitrogen. Due to the distribution of MTO reaction products, SAPO-34, small pore weak acid sites, showed the highest selectivity for light olefins such as ethene and propene, and no aromatics were detected, whereas H-ZSM-5, medium pore strong acid sites, indicated relatively high selectivity for light olefins like propene and butene, and high amount of aromatics were found. The study showed that the products distribution depends mainly upon the framework topology of the catalyst and olefin selectivity is found to be better when the catalyst has smaller particle size and larger pore volume. The high olefin selectivity is found in SAPO-34 about 96%, also high coke formation due to small pores of SAPO is observed that lead to rapid deactivation after 10 hours.

Keywords: HZSM-5; SAPO-34; Zeolite; Methanol to light olefins; Topology

1. Introduction

Methanol-to-olefins (MTO) conversion is a very important process for the production of light olefins, such as ethene and propene, from alternative and abundant resources of natural gas or coal [1]. Considerable effort has been done to the improvement of the catalyst performances and the process development. In parallel with the process development, numerous research works have been done to investigate the effect of different catalysts and illustrate the reaction mechanism of MTO conversion [2].

In the present study, methanol conversion was studied over H-ZSM-5 and SAPO-34 under the identical reaction conditions. Zeolites are interesting solid catalysts in chemical processes because of their specific molecular dimension, useful pore structure in shape selectivity, having medium acidity and good thermal stability.

2. Experimental Part

ZSM-5 zeolite with a Si/Al ratio of 80 was hydrothermally synthesized with TEOS as the Si source, aluminum isopropoxide as the Al source, and

TPAOH as the template. The crystallization was done at 180 ºC under static state for 24 h.

SAPO-34 zeolite was hydrothermally synthesized with the synthesis gels prepared from aluminum isopropoxide, orthophosphoric acid, fumed silica, TEAOH and water. The crystallization was carried out at 170 ºC under continuous stirring for 4 days. All the solid products were separated by centrifugation, washed with distilled water, and dried at 100 ºC overnight, followed by calcination at 550 ºC for 12 h to remove the organic template. To obtain the protonic form, the as-synthesized sample was further treated with 1.0 mol NH_4NO_3 solution, by refluxing twice at 85 ºC for 10 h, and then calcined at 550 ºC for 8 h to decompose the ammonium ions.

3. Results and discussion

The XRD and FTIR patterns of the synthesized catalysts of ZSM-5 and SAPO-34 are shown in figures 1 and 2. Peaks position of the samples is in accordance with standard pattern [3].

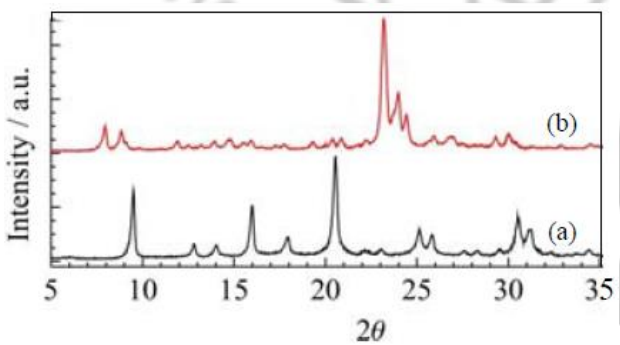

Figure 1. XRD patterns of (a) SAPO-34 and (b) ZSM-5.

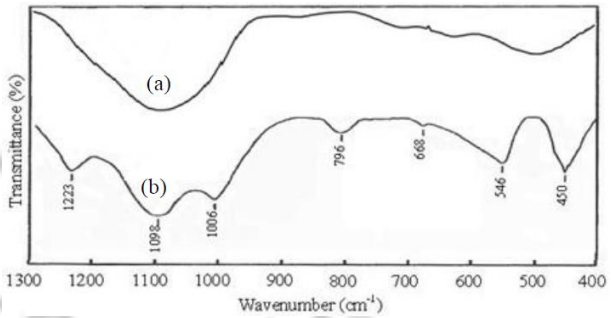

Figure 2. FTIR patterns of (a) SAPO-34 and (b) ZSM-5.

The SEM images of the two samples are given in figure 3. It can be seen that the particles morphology and size were different. For ZSM-5 sample, small particles were aggregated that caused larger particles formation.

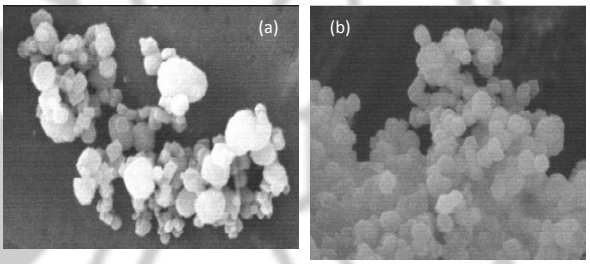

Figure 3. SEM images of samples: (a) SAPO-34, (b) ZSM-5.

Surface area and Pore volume of the samples are shown in table 1. ZSM-5 possessed the highest pore volume with a considerable fraction of mesopore volume formed due to small particles.

Table 1. Crystalline properties of the as-synthesized samples.

Zeolite	Surface Area (m^2g^{-1})	Pore Volume (m^3g^{-1})		
	Total	Total	Micropore	Mesopore
SAPO-34	503	0.32	0.25	0.07
ZSM-5	312	0.59	0.17	0.42

Significantly, MTO reaction was more effectively carried out only by Brönsted acid sites. NH_3-TPD data proved that SAPO-34 possesses a higher acidity than ZSM-5.

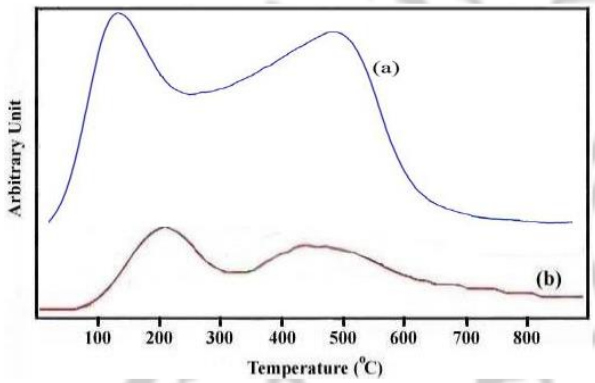

Figure 4. NH_3-TPD profiles of zeolite samples: (a) SAPO-34, (b) ZSM-5.

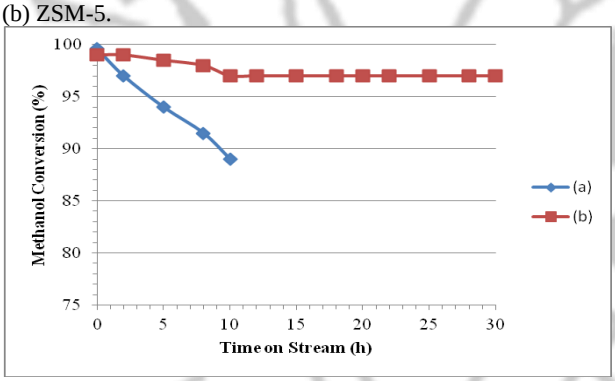

Figure 5. Methanol conversion as a function of time on stream over (a) SAPO-34, (b) ZSM-5.

As shown in figure 5, rapid deactivation is observed for SAPO-34 due to high coke formation in small pores.

Due to the product distribution for MTO in Table 2, SAPO-34 gives high selectivity to light olefins, especially to ethene, whereas ZSM-5 yields higher olefins like propene and butane.

Table 2. Methanol conversion and product distribution.

Zeolite	MeOH Conv. %	Selectivity, wt.%				
		Alkanes	Alkenes			Aromatics
			$C_2^=$	$C_3^=$	$C_4^=$	
SAPO-34	99.6	3.4	50.1	40.1	5.8	0.6
ZSM-5	99.0	7.0	17.5	48.4	24.7	2.4

4. Conclusions

The catalytic activity and selectivity of SAPO-34 and ZSM-5 were mostly determined by their pore structure and surface acidity. In the MTO reaction, the initial olefins selectivity and complete feed conversion can be observed on SAPO-34 catalysts while ZSM-5 showed excellent activity and competitive selectivity of olefins.

References

[1] R. Ahmadova, H. Ibrahimov, F. Babayeva, M. Rustamov, E. Kondratenko, *PPOR* 18 (2017) 171-187.

[2] L. Li, X. Cui, J. Li, J. Wang, J. Braz. *Chem. Soc.* 26 (2) (2015) 103-109.

[3] M. Rostamizadeh, F. Yaripour, H. Hazrati, *Polyolefins Journal* 5 (2018) 59-70.

Catalytic Upgrading of Iranian Vacuum Residue on Alkali-treated ZSM-5 Zeolite: Viscosity Reduction

S. Safari, R. Karimzadeh*

Department of Chemical Engineering, Faculty of Chemical Engineering, Tarbiat Modares University, Tehran, Iran

**Corresponding author: ramin@modares.ac.ir*

Abstract: ZSM-5 zeolite was alkali treated by NaOH solution in order to induce intracrystal mesoporosity via desilication. Prepared catalyst was tested in thermo-catalytic upgrading of vacuum residue (VR), a two-step process in which VR was thermally cracked at first stage then the pyrolysis vapors were in situ transferred to catalytic cracking step in a fixed bed reactor loaded with catalyst powder. Silica bead, microporous HZSM-5 and mesoporous HZSM-5 were tested in this process in order to investigate the effect of mesoporosity on attaining more valuable liquid product. The results showed that mesoporous catalyst reduced liquid product viscosity by 42.7% compared to product of thermal cracking of VR. This reduction was 23.8% and 8.9% for microporous HZSM-5 and silica bead, respectively.

Keywords: Vacuum residue; Upgrading; ZSM-5 zeolite; Mesoporosity; Viscosity

1. Introduction

Expanding demand for fuel-like distillates in one hand and decreasing amount of conventional oil sources on the other hand, have attracted attentions to heavy oil upgrading. Residues of vacuum and atmospheric distillation towers in refineries can be upgraded to more valuable products like light olefins and liquid fuels by different thermal and catalytic methods [1,2]. Catalytic upgrading of these heavy feeds has different challenges including mass transfer limitations due to the small size of zeolite micropores and large size of heavy hydrocarbon molecules, and rapid deactivation of catalyst due to the high amount of asphaltenes and heteroatoms present in the feed. In this research, mesoporosity was introduced to the zeolite structure via alkali treatment, as a promising method [3,4], to enhance the mass transfer in the zeolite. Also, upgrading process was conducted in two-step thermo-catalytic procedure in order to improve catalytic performance by separating the heavy and poisoning parts of feed in the first step and protecting the zeolite from rapid deactivation or pore blockage [5,6].

2. Experimental Part

As received ZSM-5 zeolite (SiO_2/Al_2O_3 = 40) was calcined at 550 ºC and then treated with 0.2 M NaOH solution at 80 ºC for 5 hours. The alkali treated and as received zeolite samples were ion exchanged with 1 M ammonium nitrate solution

and calcined at 550 ºC to form AT-HZSM-5 and HZSM-5 samples respectively.

30 g of Tehran refinery VR was thermally cracked at 450 ºC in a balloon shaped Pyrex glass reactor and produced vapors were directed to a S.S tube with a length 30 cm and ID 2 cm, loaded with 0.6 g catalyst diluted with 2.4 g silica bead at 450 ºC for 4 hours. The exiting vapors were condensed and liquid product was collected in a container placed in ice & water mixture and noncondensable gases were burned in the flare.

3. Results and discussion

Figure 1 shows the XRD patterns of ZSM-5 samples. The result shows that MFI crystalline phase was preserved in alkali treated sample, although crystallinity was reduced through desilication and partial dealumination of zeolite structure as could be predicted.

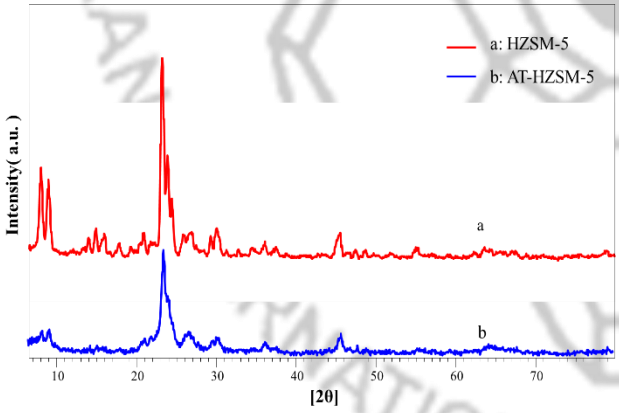

Figure 1. XRD patterns of AT-HZSM-5 and HZSM-5 samples.

Figure 2 represents the N_2 Adsorption/desorption isotherms of ZSM-5 samples. Alkali treated sample shows type IV isotherm with remarkable hysteresis loop indicating the presence of mesopores in AT-HZSM-5 structure.

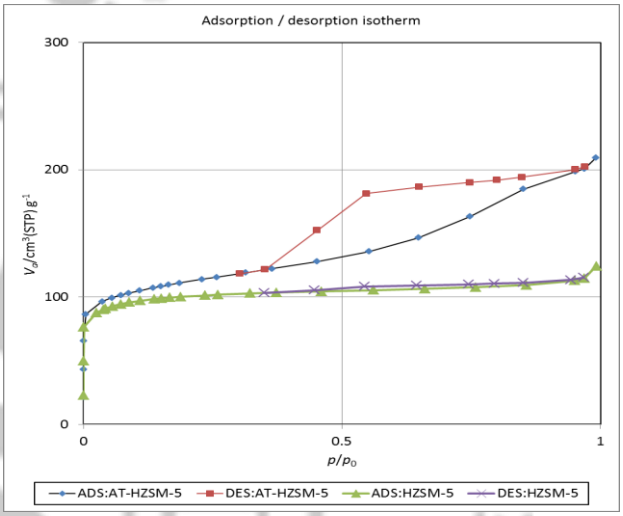

Figure 2. N_2-adsorption-desorption isotherms of AT-HZSM-5 and HZSM-5 samples.

Textural properties of samples are summarized in Table 1. S_{BET} and mesopore volume of zeolite are increased after alkali treatment.

Table 1. Textural properties of ZSM-5 samples.

Sample	S_{BET} [a] (m^2/g)	S_{ext} [b] (m^2/g)	V_{micro} [b] (ml/g)	V_{meso} [c] (ml/g)
HZSM-5	379.61	33.686	0.1390	0.051
AT-HZSM-5	406.58	144.3	0.1082	0.215

[a] From N_2 adsorption measurements (BET method).
[b] From N_2 adsorption measurements (t-plot).
[c] From N_2 adsorption measurements (BJH method)

Kinematic viscosity of the liquid product was determined by ASTM standard D445 for different experiments conducted: one step thermal cracking of VR, two-step thermo-catalytic cracking on silica bead, HZSM-5 and AT-HZSM-5. Results are presented in Table 2.

Table 2. Kinematic viscosity of liquid product for different conducted experiments.

Test	Liquid product yield (wt.%)	Kinematic viscosity at 40 °C (cSt)
Thermal Cracking	54.74	3.81
Silica	51.78	3.48
HZSM-5	47.59	2.90
AT-HZSM-5	35.37	2.18

Alkali treated ZSM-5 sample presents the lowest viscosity for liquid product among all the tests. This could be explained by accelerated diffusion of large hydrocarbon molecules into the zeolite pores, which contain acidic sites, due to the creation of mesopores with larger openings.

4. Conclusions

Catalytic upgrading of VR thermal cracking vapors results in viscosity reduction of liquid product. Comparing the performance of HZSM-5 and alkali treated HZSM-5 experiments results indicate that creation of mesopores in ZSM-5 structure reduces the mass transfer limitations and more heavy hydrocarbons crack to lighter ones resulting in lower viscosity of liquid product of VR upgrading process.

References

[1] R. Asgharzadeh Shishavan, M. Ghashghaee, R. Karimzadeh, *Fuel Process. Technol.* 92(2011) 2226-2234.

[2] B. Sarkar, W. Kwek, D. Verma, J. Kim, *Appl. Catal. A* 545 (2017) 148-158.

[3] S. Asadi, L. Vafi, R. Karimzadeh, *Micropor. Mesopor. Mater.* 255 (2018) 253-260.

[4] H. Mochizuki, T. Yokoi, H. Imai, S. Namba, J. N. Kondo, T. Tatsumi, *Appl. Catal. A* 449 (2012) 188-197.

[5] I.K. Basily, E. Ahmed, N.N. Ibraheam, *J. Anal. Appl. Pyrolysis* 32 (1995) 221-232.

[6] M. Artetxe, G. Lopez, M. Amutio, J. Bilbao, M. Olazar, *Chem. Eng. Sci.* 116 (2014) 635-644.

5th Iran International Zeolite Conference

University of Tabriz, Tabriz, Iran

26-27 August 2018

Removal of Mixed Heavy Metal Ions in Ternary Aqueous Solution Using Functionalized MCM-41 Synthesized by Microwave Hydrothermal

Sh. Khademi[a], M. Hamadanian[a] *, B. Roozbehani[b]

[a] *Institute of Nano Science and Nano Technology, University of Kashan, Kashan, Iran*

[b] *Fuel and Petrochemical Engineering Research Center, Abadan Institute of Technology, PUT, Abadan, Iran*

**Corresponding author: Hamadani@kashanu.ac.ir*

Abstract: Mesoporous silica (MS) has been one of the most versatile and successful adsorbents for the removal of environmental pollutants in recent years. N,N-Dimethylglycine functionalized MCM-41 silicas with uniform mesoporosity were prepared and employed for removing of heavy metal ions from ternary aqueous solution. The MCM-41 was synthesized by microwave hydrothermal method and reduced synthesis time by 100 times. We had studied the important parameters such as contact time and initial pH of the solution on the adsorption process. Scanning electron microscopy (SEM), X-ray powder diffraction (XRD), and N_2 adsorption-desorption isotherm techniques were used to characterize the obtained product.

Keywords: Mesoporous silica; Microwave Hydrothermal; Heavy Metal

1. Introduction

To synthesize improved adsorbents for the removal of toxic heavy metal ions from wastewater is a continuing research objective of environmental pollution control processes. Considerable efforts have been dedicated to the preparation of mesoporous silica-based adsorbents due to their unique large surface area, well-defined pore size and pore shape and well-modified surface properties. Most mesoporous materials themselves do not have specific binding sites for heavy metal ions. This application generally requires modification of the mesoporous surface [1]. Functional monolayers are chemically bonded to the surfaces of supports. The functionalized hybrid materials exhibit high adsorption capacity and specificity for metal ions [2]. Modified mesoporous adsorbents have prepared by grafting thiol ligands on the surface of the MCM-41 support, that are efficient in removing of mercury and other heavy metal ions. Morphological properties can be manipulated, widely acknowledged as major advantages of mesoporous silica over other adsorbents. The highly adaptable structure and surface chemistry, as well as the low production cost, are primary advantages of MS materials over other adsorbents with higher reported adsorption capacities for pollutants such as lead. The high degree of surface area relative to the overall mass of mesoporous silica materials means that there is the considerable room available for functionalization of the surface to occur [3].

2. Experimental Part

MCM-41 was synthesized by microwave hydrothermal method. A gel was prepared at 25 °C by dissolving a desired amount of CTAB in 20 ml of deionized water. Then, 15 ml tetraethyl orthosilicate (TEOS) and 0.05 g N,N-Dimethylglycine was added to a 40 ml of a solution containing 2.22 g NaOH within 1 h under stirring. The obtained gel heated to 100 °C by microwave irradiation under atmospheric pressure for 10 min. After cooling to room temperature, the solid product was separated by centrifugation, washed with deionized water and oven-dried at 80 °C.

In order to test the metal adsorption ability of the synthesized materials, a set of the mixed heavy metal ions solutions containing 100 mg l^{-1} of each of Cr^{3+} and Ni^{2+} ions were prepared by dissolving a weighed quantity of the respective nitrate salts in deionized water. Before mixing the adsorbate with the adsorbents, the initial pH of each solution (pH = 3 and 4) was adjusted to the required value by adding 0.1–10 M HNO_3 and 0.1–10 M NaOH solution**.** The set of adsorption experiments was carried out by stirring 20 mg of functionalized silica in 100 ml of a mixed metals solution at 25 °C. Adsorbent–solution mixtures were filtered through a PVDF the membrane of 0.45 µm to collect the final solutions. Metal concentrations, both in the initial and final solutions, were determined by an atomic absorption spectrometer.

3. Results and discussion

N_2 adsorption-desorption isotherm of the calcined sample is shown in Fig.1. Sample display type IV isotherms corresponding to conical or cylindrical mesoporous. BET surface areas and pore volumes are summarized in Table 1.

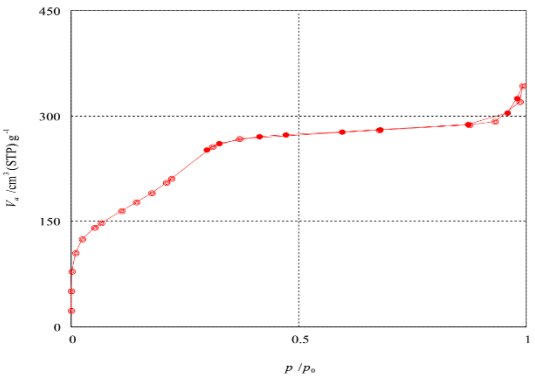

Figure 1. Nitrogen adsorption-desorption isotherms at 77 K of MCM-41-DMG.

Table 1. Surface properties of adsorbent.

Adsorbent	SBET (m^2/g)	d average (nm)	V total (cm^3/g)
MCM-41-DMG	810	3.3	1.124

The X-ray pattern of calcined powder of product is shown in Fig. 2. Fig. 2 shows four well defined peaks which can be indexed with 100, 110, 200 and 210 in hexagonal symmetry.

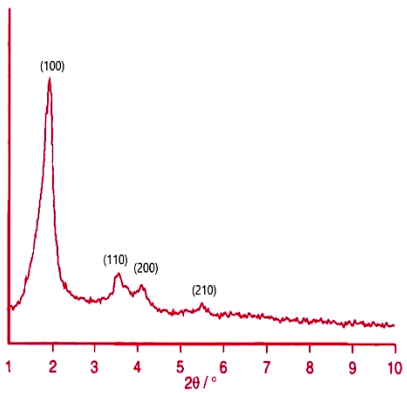

Figure 2. XRD pattern of MCM-41.

SEM image of the MCM-41 is presented in Fig. 3. The MCM-41 typically exhibits a Spherelike morphology.

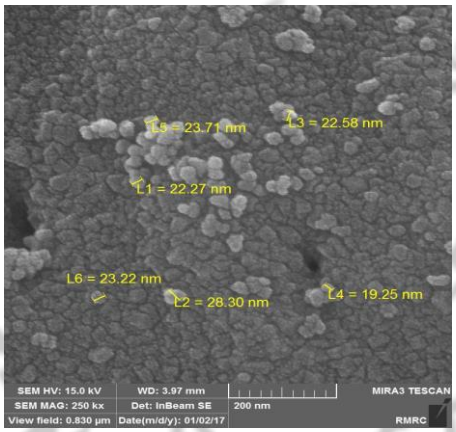

Figure 3. SEM image of MCM-41-DMG.

Effect of pH on the removal of Ni(II) and Cr(III) by MCM-41 and MCM-41-DMG (initial metal ion concentration for each of the metals: 100 mg l^{-1}, the mass of MCM-41 and MCM-41-DMG: 20 mg, shaking time: 30 min at 25 °C) is shown in Fig. 4.

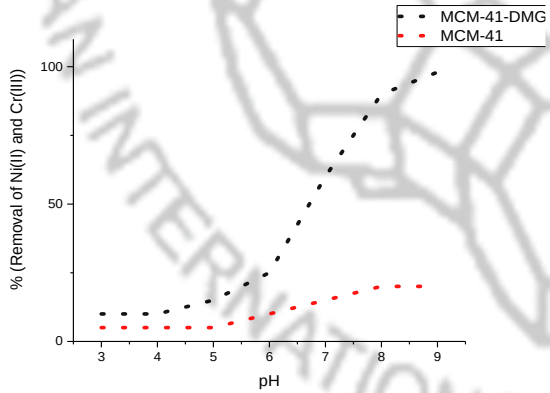

Figure 4. Adsorption of mixed heavy metal ions at different pH values.

Generally, the adsorption is a rapid process in the beginning due to availability of the active sites. By time, the adsorption centers were occupied and the process becomes slower. Shaking the samples is necessary to speed up the absorption process. The results of various shaking times (5-60 min) under previously specified optimum experimental conditions are displayed in Fig. 5.

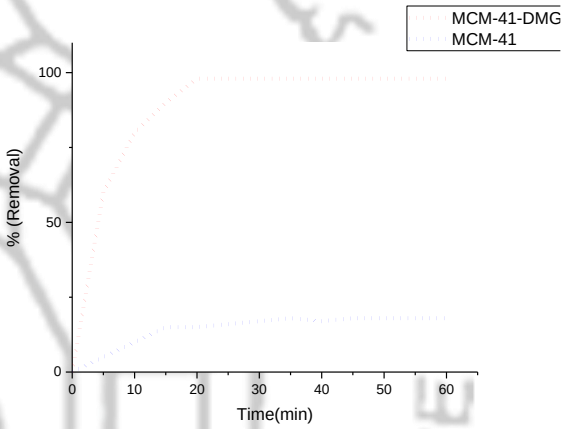

Figure 5. Removal percentage of Cr(III) and Ni(II) by MCM-41 and MCM-41-DMG at pH = 8.

4. Conclusions

The present study showed that the modified MCM-41 by DMG based adsorbents were effective in removing mixed heavy metal ions from aqueous solutions compared to the non-modified MCM-41.

References

[1] M. Anbia, K. Kargosha, S. Khoshbooei, *Chem. Eng. Sci.* 93 (2015) 779-788.

[2] A. Benhamou, M. Baudu, Z. Derriche, J.-P. Basly, *J. Hazard. Mater.* 171 (2009) 1001-1008.

[3] X. Chen, K.F. Lam, K.L. Yeung, *Chem. Eng.* 172 (2011) 728-734.

Hydrothermal Synthesis of H-ZSM-5 Catalysts Employing Mixed Template Method and its Application in Conversion of Methanol to Light Olefins

F. Gorzin[a]*, J. Towfighi Darian[a] , F. Yaripour [b]

[a] *Department of Chemical Engineering, Tarbiat Modares University, P.O. Box 14115-143, Tehran, Iran*

[b] *Catalysis Research Group, Petrochemical Research & Technology Company, National Iranian Petrochemical Company, P.O. Box: 1493, Tehran, Iran*

**Corresponding author: shirin.gorzin@gmail.com*

Abstract: The hydrothermal synthesis of H-ZSM-5 catalysts for application in methanol to olefin (MTO) reaction was performed by partial and total substitution of tetrapropyl ammonium hydroxide (TPAOH) with equivalent amount of the less expensive tetrapropyl ammonium bromide (TPABr) template. Five H-ZSM-5 zeolites were synthesized using silicic acid and sodium aluminate with various proportions of TPAOH and TPABr, constant TPA^+ concentration (0.04M) and initial gel pH (10.5). Increasing molar ratio of TPAOH in initial gel from 0.33 to 3 decreased the purity of H-ZSM-5, and affected its crystallinity and particle size. The catalytic performance tests were conducted in fixed-bed reactor at 480°C with a feed WHSV of $0.9h^{-1}$. All the catalysts exhibited approximately similar methanol conversion though their propylene selectivities and products distributions were dependent on the template composition. This work verified that despite providing the same TPA^+ and OH^- concentrations in the initial gel, the samples with different properties could form using diverse template combinations

Keywords: High silica H-ZSM-5; Methanol to light olefins (MTO); Mixed template; Hydrothermal synthesis; Selectivity

1. Introduction

Light olefins are widely used as raw materials in petrochemical industries. From the perspective of increasing oil prices methanol to olefins (MTO) process has recently attracted considerable attention [1]. H-ZSM-5 has more favorable properties because it gives high propylene yield with limited coke deposition. H-ZSM-5 catalyst can be synthesized with diverse templates including tetraalkyl ammonium ions, amines, and alcohols. Among these templates, TPAOH has been most commonly used for the synthesis of ZSM-5[2]. Using TPAOH as template, small particle size of ZSM-5 could be achieved [3]. However, TPAOH is an expensive material, and its high price limits its application in industrial scale. The cost of TPABr is much lower than TPAOH and it was successfully applied as a cheap template. Nevertheless, it results in large particle size, which affects the catalytic performance due to higher diffusion limitation. In this work, the H-ZSM-5 catalysts were synthesized hydrothermally

using a single template as well as mixed templates of TPAOH and TPABr. The effects of the molar ratio of TPAOH/TPABr on the catalytic performance of the catalysts in the MTO reaction were investigated in detail.

2. Experimental Part

High silica H-ZSM-5 catalysts (Si/Al= 200) were synthesized by the hydrothermal method. Solution A was prepared as a mixture of NaOH, $NaAlO_2$, template and water. Solution B was composed of silicic acid and distilled water. Templates were used according to Table 1. The solution A was added dropwise to solution B. The crystallization was carried out at 180 °C for 48 hours in autoclaves. The solid product was filtered, washed with deionized water until the neutral pH and then dried overnight at 105 °C. Finally, the catalyst samples were calcined at 530 °C for 12 h. The catalytic performance tests were conducted in fixed-bed reactor at 480°C with a feed WHSV of 0.9 h^{-1}.

3. Results and discussion

The effects of template type and combinations on the time-dependent products selectivity have been plotted in Figs. 1. The highest selectivities to light olefins ($C_2^=$–$C_4^=$) were observed for samples synthesized with a single template compared to co-templated samples. These results could be well explained by the acidity of the different catalysts. Strong acid sites on the H-ZSM-5 catalyst are active for the MTO reaction. As a consequence, samples S-3 to S-5 revealed lower activities. Figs. 1 (a) and 1 (b) illustrate the propylene selectivity and total light olefin compounds with time on stream for the different catalysts prepared with both single template and mixed templates. It is seen that combinations of TPAOH and TPABr templates do not enhance the propylene and total light olefin selectivities compared to this single template. The propylene selectivities by these catalysts were increased regularly (from 41.37 to 46.61%) with the molar ratios of TPAOH/TPABr. These results are principally because of increasing the TPAOH content in the mixed template leading to increase the strong acid sites density. Between the two catalysts prepared with a single template, sample S-2 obtained by TPABr template presented enhanced products selectivity. The superior catalytic performance of sample S-2 can be attributed to its higher surface area, smaller crystallite size, and higher number of strong acid sites in comparison with S-1, which has been associated with minimal side reactions.

4. Conclusions

Among the catalysts synthesized with mixed templates, the sample prepared with a 0.75:0.25 molar ratio of TPAOH/TPABr exhibited the best activity and the highest propylene selectivity. The catalyst prepared by single inexpensive template TPABr would be proposed for the MTO/MTP reaction.

Table 1. Gel compositions and experimental synthesis conditions for the different H-ZSM-5 catalysts prepared using single and mixed templates.

Sample	Molar ratios of templates		pH		Alkalinity ([OH⁻]) M × 10^{-4}
	TPAOH	TPABr	initial	Final	
S1	1(11.99 g)	0	13.4	11.4	25.12
S2	0	1 (5.77g)	13	10.5	3.16
S3	0.25 (2.8 g)	0.75 (4.33 g)	13.2	10.6	3.98
S4	0.50 (5.6 g)	0.50 (2.89 g)	13.4	11.1	12.59
S5	0.75 (8.4 g)	0.25 (1.44 g)	13.7	11.3	19.95

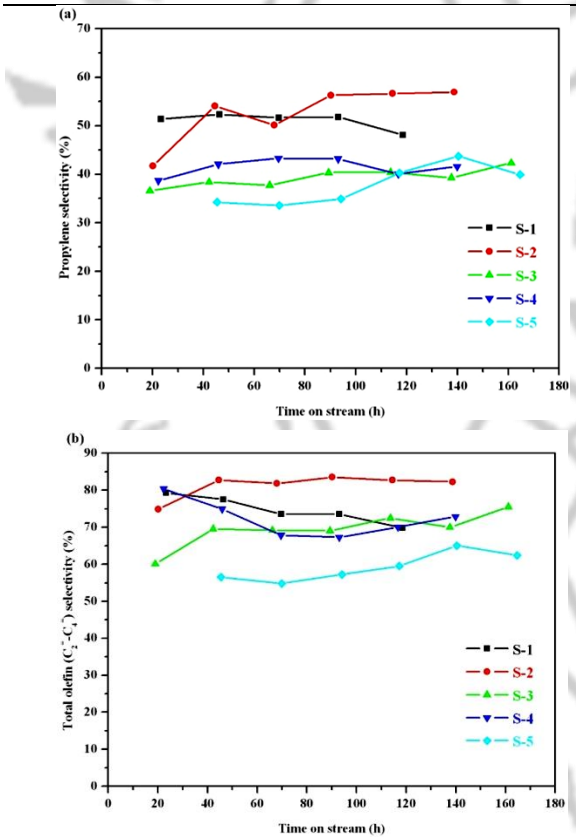

Figure 1. Product selectivity against time: (a) propylene and (b) total olefin ($C_2^=$–$C_4^=$) over different catalysts.

Acknowledgments

The authors would like to acknowledge Tarbiat Modares University (Tehran, Iran) for their financial supports of the research.

References

[1] W. Skistad, S. Teketel, F. Bleken, P. Beato and S. Bordiga et al., *Top. Catal.* 57 (2014)143-158.

[2] S. Sang, F. Chang, Z. Liu, C. He, Y. He, L. Xu, Catal. Today 93 (2004) 729-734.

[3] S. Schwarz, M. Kojima, C. O'Connor, *Appl. Catal. A* 73 (1991) 313-330.

Zeolites as Supports for the Gadolinium and Iron Oxide Nanoparticles Based MRI Contrast Agents

N. Gharehaghaji[a], B. Divband[b, c]*

[a] *Radiology Department, Paramedical Faculty, Tabriz University of Medical Sciences, Tabriz, Iran*

[b] *Stem Cell Research Center, Tabriz University of Medical Sciences, Tabriz, Iran*

[c] *Infectious and Tropical Diseases Research Center, Tabriz University of Medical Sciences, Tabriz, Iran*

**Corresponding author: baharakdivband@yahoo.com*

Abstract: The aim of this study is to review the zeolites capability to use as support for magnetic resonance imaging (MRI) contrast agents. Additionally, different biomedical applications of the magnetic zeolites are reviewed.

Keywords: Zeolite; Gadolinium; Iron oxide; MRI contrast agent

1. Introduction:

MRI as a powerful medical imaging modality provides detection of soft tissue lesions. MRI contrast agents have an important role in better diagnosis of diseases. These agents are included paramagnetic (usually gadolinium (Gd)) or superparamagnetic (iron oxide nanoparticles) materials, which can decrease T1 and T2 relaxation times of the accumulated regions. Ability of a contrast agent to improve the contrast of MR images is considered as relaxivity [1].

Zeolites are aluminosilicate microporous materials with well-defined pores and channels [2]. These special structures provide a good area for placement of the MRI contrast agents. Hydrophilicity of the zeolites depends on the Si/Al ratio. Lower Si/Al ratio leads to more hydrophilicity, which is important for MR imaging.

Gd-zeolite, at the first study, was used as oral MRI contrast agent to evaluate gastrointestinal system in adult volunteers. No significant adverse reactions were seen with Gd-zeolite in this study [3].

Study of the relationship between the structure of the Gd-NaY and Gd-NaA zeolites and the resulted relaxivity showed much lower relaxivity for Gd-NaA zeolite because of its smaller pore size. Additionally, a partial dealumination of the zeolites led to a much higher relaxivity than the non-dealuminated materials [4]. Increasing of Si/Al ratio of zeolites leads to decreasing of the residence time of water protons in both of the inner sphere and in the interior of zeolites, which causes increasing of r1 relaxivity [5]. Evaluation of potential application of Gd-doped zeolite NaY nanoparticles as an MRI contrast agent showed immobilization of Gd ions in the interior of the zeolite and limitation of the relaxivity due to slow

diffusion of water protons from the pores of the NaY zeolite channels into the bulk water [6].

Some studies have been conducted using Fe_3O_4 nanoparticles with ZSM-5 and NaA zeolites. The resulted nanocomposites showed high r2 relaxivity and were introduced as strong MRI T2 agents [1,7]. However, NaA zeolite showed higher relaxivity at the similar iron oxide content due to the differences in the zeolites structures. Furthermore, r1 relaxivity of the Fe_3O_4/4A zeolite was higher than that of Fe_3O_4/ZSM-5 for the same reason [8].

The result of one study showed that using of different synthesis method can affect on medical application of Fe_3O_4/ZSM-5 nanocomposite. Synthesis of the nanocomposite with ion exchange method leads to a lower presence of the iron oxide nanoparticles on the nanocomposite surface, which provides a good efficiency to drug loading for drug delivery purposes [9]. On the other hand, with hydrothermal synthesis method, the resulted Fe_3O_4/ZSM-5 nanocomposite is a good agent for enhancement of MRI contrast [1].

Zeolites are good supports not only for magnetic Gd and iron oxide nanoparticles but also for optical materials. Therefore, bimodal MR and optical imaging is possible. Such bimodal probe was reported using LTL nanozeolite with deposition of Gd and Eu in the large and small cavities, respectively [10].

2. Conclusions

Zeolites have a high potential to serve as supports for Gd and iron oxide nanoparticles. Magnetic zeolites can be used for contrast enhancement MRI, drug delivery and bimodal imaging.

Acknowledgments

This study was financially supported by Tabriz University of Medical Sciences - Iran.

References

[1] Z. Atashi, B. Divband, A. Keshtkar, M. Khatamian, F. Farahmand-Zahed, A. Kiani Nazarlo, N. Gharehaghaji, *J. Magn. Magn. Mater*. 438 (2017) 46-51.

[2] P. Payra, P.K. Dutta, S.M. Auerbach, K.A. Carrado, P.K. Dutta, *Handbook of Zeolite Science and Technology*, 2004, CRC Press, New York.

[3] S.W. Young, F. Qing, D. Rubin, K.J. Balkus, J.S. Engel, J. Lang, *JMRI* 5 (1995) 499-508.

[4] É. Csajbók, I. Bányai, L. Vander Elst, RN. Muller, W. Zhou, J.A. Peters, *Chem. Eur. J*. 11 (2005) 4799-807.

[5] M. Norek, I.C. Neves, J.A. Peters, *Inorg. chem.* 46 (2007) 6190-6.

[6] C. Platas-Iglesias, L. Vander Elst, W. Zhou, R.N. Muller, C.F. Geraldes, T. Maschmeyer, *Chem. Eur. J*. 8 (2002) 5121-31.

[7] N. Gharehaghaji, B. Divband, L. Zareei, *J. Magn. Magn. Mater*. 456 (2018) 136-41.

[8] N. Gharehaghaji, B. Divband, Z. Atashi, L. Zareei, Fe_3O_4/zeolite nanocomposites: effect of zeolite support type on MRI Longitudinal relaxivity. Second Nanomedicine & Nanosafety Conference, Tehran, Iran. November 29-30, 2017.

[9] N. Gharehaghaji, B. Divband, *Nanomedicine* 5 (2018) 15-8.

[10] F. Mayer, W. Zhang, T. Brichart, O. Tillement, C.S. Bonnet, É. Tóth, *Chem. Eur. J*. 20 (2014) 3358-64.

Effect of SiO_2/Al_2O_3 Ratios on the Activity of Fe-ZSM-5 Nano Catalysts in the Catalytic Oxidation of Toluene

A. Jodaei*

Department of Chemistry, Islamic Azad University, Sofian Branch, Sofian, Iran

**Corresponding author*: *az.jodaei@gmail.com*

Abstract: The objective of this work is to study the effects of SiO_2/Al_2O_3 ratios in HZSM-5 and Fe-ZSM-5 catalysts on the catalytic oxidation of toluene. Catalytic tests were carried out inside a U-shaped fixed bed reactor under atmospheric pressure and different temperatures. The results showed that, with an increase in the SiO_2/Al_2O_3 (from 14 to 400, molar ratio), the catalytic activity decreases especially in HZSM-5 catalysts. The catalysts were characterized by X-ray diffraction (XRD) and scanning electron microscopy (SEM).

Keywords: HZSM-5; SiO_2/Al_2O_3; Toluene; Catalytic oxidation

1. Introduction

Volatile organic compounds (VOCs) are the major contributor to air pollution due to their toxic and fusty nature, concern in global warming, smog formation, etc. Many industrial processes and transportation activities lead to the accumulation of VOCs in the atmosphere [1], and hence control of VOCs is the key challenge within the research area of environmental catalysis. Several methods are employed for the removal of VOCs, including thermal/catalytic oxidation, plasma-catalysis, biological degradation, photo catalysis and adsorption processes [2]. Among these methods, catalytic oxidation is the promising process for the removal of VOCs, which converts the harmful VOCs into harmless CO_2 and H_2O. In catalytic oxidation, the most important factor is the selection of the catalysts, catalyst precursor, support, preparation method [3] and metal loading [4]. Due to its unique channel structure, thermal stability, highly hydrophobic and shape-selective property, ZSM-5 zeolite has been widely used in adsorption, separation and catalytic processes in industry. Moreover, the $SiO_2/A1_2O_3$ ratio can significantly affect the acidity and selectivity of ZSM-5 zeolites [5].

Therefore, the objective of this work is to find a way to increase the catalyst activity with varying $SiO_2/A1_2O_3$ ratio.

2. Experimental Part

ZSM-5 (14, 40, 50, 100 and 400) samples were supplied in sodium-form. The latter were converted into H-form (HZSM-5) and Fe-ZSM-5 by

impregnation method and converted into pellet using a hydraulic pellet making press. Catalytic oxidation reactions of organic compounds were carried out under atmospheric pressure according to the procedure described in our previous works [6].

3. Results and discussion

Figurer 1 shows the XRD pattern of the HZSM-5 zeolites with various $SiO_2/A1_2O_3$ ratios. It is observed that the XRD patterns of these samples all agree well with the XRD patterns in the Ref. [34] and the positions of the characteristic peaks for these samples are the same with those of the standard samples.

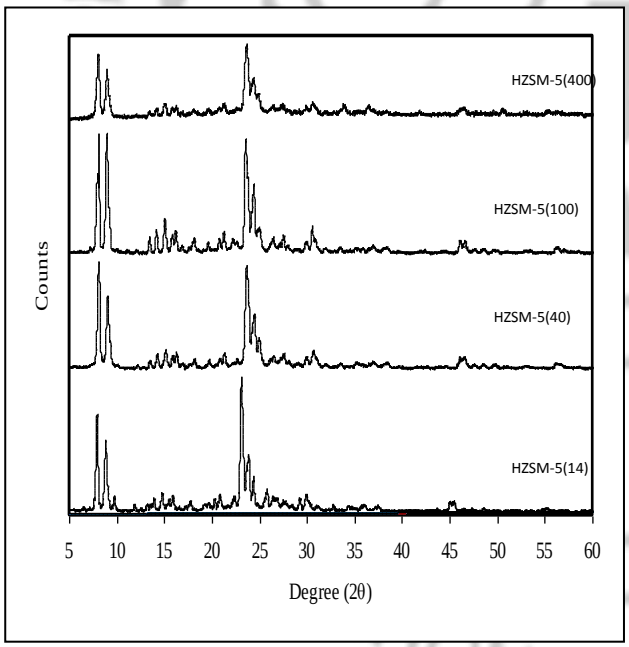

Figure 1. The XRD patterns of HZSM-5 zeolites with various SiO_2/Al_2O_3 ratios.

The combustion of toluene over HZSM-5 zeolites with various SiO_2/Al_2O_3 ratios is present in Figure 2. The sequence of catalytic activity was as follows: HZSM-5(14)> HZSM-5(40)> HZSM-5(100)> HZSM-5(400).

It is known that when the Si/Al ratio increases, the acidity of HZSM-5 decreases, because increases the bronsted acid sites to lewis acid sites.

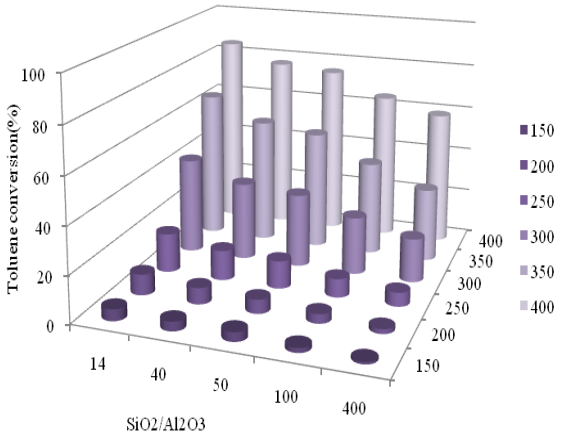

Figure 2. Toluene conversion as a function of temperature over H-ZSM-5 catalysts with various SiO_2/Al_2O_3 ratios.

In order to further improve the performance of the HZSM-5 zeolites, iron was loaded on HZSM-5 zeolites. Comparing to HZSM-5 zeolites, 99% of toluene conversion occur at lower temperatures over Fe-ZSM-5 catalysts (Figure 3). In other word, catalytic activity of Fe-ZSM-5 catalyst is higher than HZSM-5 zeolite, revealing that iron plays an important catalytic role in conversion of organic compounds.

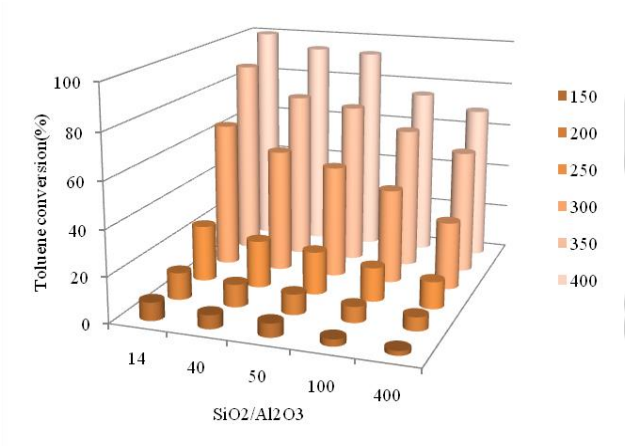

Figure 3. Toluene conversion as a function of temperature over Fe-ZSM-5 catalysts with various SiO_2/Al_2O_3 ratios.

4. Conclusions

Oxidation of toluene on four ZSM-5 zeolite catalysts with different SiO_2/Al_2O_3 ratios are investigated experimentally. It is found that with increasing SiO_2/Al_2O_3 ratio from 14 to 400, the catalytic activity of Fe-ZSM-5 nanocatalysts decreases.

References

[1] S.S.T. Bastos, S.A.C. Carabineiro, *Catal. Today* 180 (2012) 148-154

[2] H. Huang, J. Chen, *Chem. Eng. J.* 264 (2015) 24-31.

[3] M.P. Rosynek, C.A. Polanky, *Appl. Catal.* 73 (1991) 97-112.

[4] S. Vetrivel, A. Pandurangan, *Appl. Catal. A: Gen.* 264 (2004) 243-252.

[5] W. Fei, W. Wenchuan, H. Shiping, T. Jiawei, X. Zaiku, *Chin. J. Chern. Eng.* 5(3) (2007) 376-386.

[6] A. Jodaei, D. Salari, A. Niaei, M. Khatamian, A. Hosseini, *Environ. Techno*. 32 (2011) 3-4.

Effects of Calcination Temperature on Catalytic Activities of Ag/ZSM-5 Catalyst for Catalytic Oxidation of Toluene

A. Jodaei*

Department of Chemistry, Islamic Azad University, Sofian Branch, Sofian, Iran

**Corresponding author*: *az.jodaei@gmail.com*

Abstract: A series of Ag/ZSM-5 catalysts for the selective catalytic oxidation of toluene was prepared by precipitation method at different calcination temperature. SEM images explore the effects of calcination temperature on the physical and chemical properties of Ag/ZSM-5 catalysts. The catalytic activity test indicated that the Ag/ZSM-5 catalyst calcined at 600 °C demonstrated the best performance for toluene removal.

Keywords: Calcination temperature; Ag/ZSM-5; Nano catalyst; Catalytic oxidation

1. Introduction

VOCs are a kind of the main sources for the formation of ozone and photo-chemical smog in urban area, and it was found long-term exposure to VOCs, even at the ppm level, can result in the harmful effects on human health [1]. Until now, a number of methods have been developed for the removal of VOCs. Among the strategies, catalytic combustion is one of the most effective methods to decompose VOCs. Previous studies have shown that VOCs can be completely oxidized into CO_2 and H_2O over noble metals (Pt, Pd, and Au) and transition metal oxides (Co_3O_4, FeO_x, MnO_x, NiO, ZnO and CuO) [2].

One of the parameters can affect the activity of catalyst, is calcination temperature. When the calcination temperature is too low, the metal salts decompose incomplete which would decrease the amount of active component. However, when it is too high, the phenomenon of sintering may take place in catalyst, and lead to serious decrease of the specific surface area of catalyst and the dispersion of active component. Particularly, the calcination temperature is believed to be related to crystallinity, specific surface area and the final oxidation states of metal oxide. The present work is devoted to a systematic study of the effects of calcination temperatures on Ag/ZSM-5 catalysts.

2. Experimental Part

Herein, a series of Ag/ZSM-5 catalysts was synthesized through a conventional precipitation method and the calcination temperatures were varied in the range from 200 °C to 700 °C. Catalytic oxidation reactions of organic compounds were carried out under atmospheric pressure according to the procedure described in our previous works [4].

3. Results and discussion

One of the factors that can affect the activity of catalysts is the calcination temperature.

Thus, Ag-ZSM-5 catalysts with a 5 wt% silver content were calcined at 300, 400, 500, 600 and 700 °C, respectively.

Figure 1 shows the conversion efficiency of toluene as a function of temperature for complete oxidation on Ag-ZSM-5 catalysts.

As can be seen, with increasing calcination temperature up to 600 °C, catalyst activity increases, but, with a further increase in the calcination temperature, the catalyst activity decreases again.

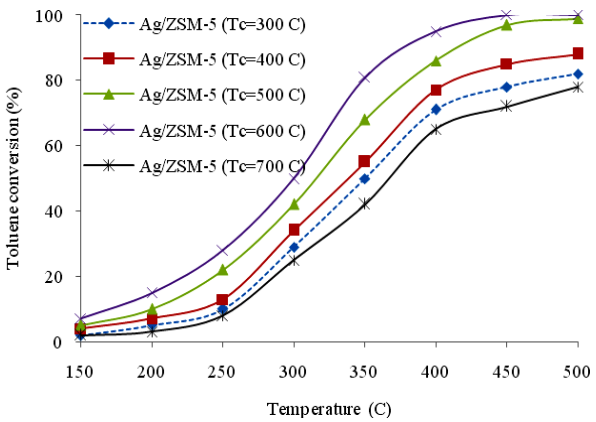

Figue 1. Toluene oxidation on Ag-ZSM-5 catalysts as a function of temperature.

With increasing calcination temperature, the salt content of the metals is gradually removed from the catalyst surface and particle size has decreased in the zeolite level, also, it causes the surface particles to become larger in the catalysts.

The excessive increase in temperature may cause the catalyst to be sintering, in other words, blockage of internal pores, which leads to restrictions on the transfer of mass.

In addition, the excessive increase in temperature causes the growth of the particle size of metal on zeolite. It leads to a reduction of the specific surface area and reduction of active metal phases on zeolite.

SEM images in Figure 2 show and confirm this.

The sequence of activity of catalysts at different temperatures of calcination can be shown as follows:

Ag-ZSM-5(T_c=600°C) > Ag-ZSM-5(T_c=500°C) > Ag-ZSM-5(T_c=400°C) > Ag-ZSM-5(T_c=300°C) > Ag-ZSM-(T_c=700°C)

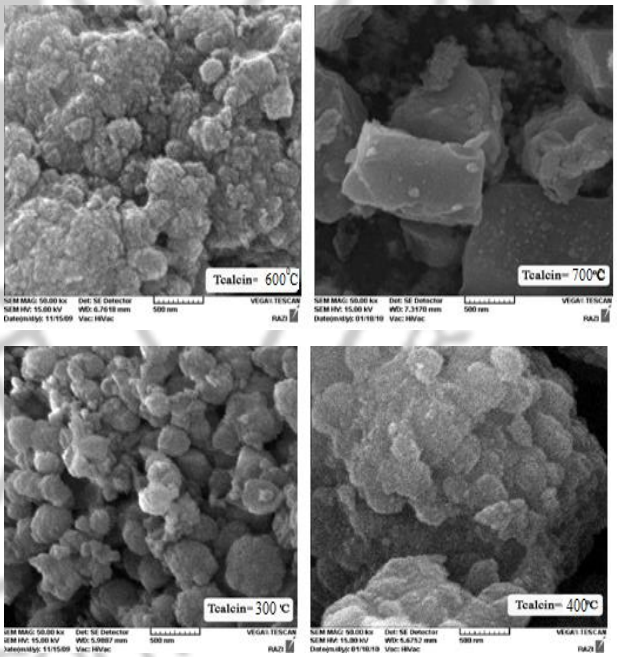

Figure 2. SEM images of Ag-ZSM-5 catalysts.

4. Conclusions

As described above, it can be found that the catalytic performance and the physicochemical properties of Ag/ZSM-5, such as the specific surface area and catalytic ability were affected significantly by the calcination temperatures.

References

[1] Y. Wang, D. Yang, L. Shaozhong, *Micropor. Mesopor. Mater.* 258 (2018) 1725.

[2] J. Kaspar, P. Fornasiero, N. Hichkey, *Catal. Today* 77 (2003) 419-449.

[3] L. Xiaorong, L. Pengfei, L. Jun, H. Kai, *Appl. Surf. Sci.* 307 (2014) 382-387.

[4] A. Jodaei, D. Salari, A. Niaei, M. Khatamian, A. Hosseini, *Environ. Techno*. 32 (2011) 3-4.

Zeolite as Antibacterial Agent for Active Packaging of Food

L. Rafiei[a]*, M. Azizi-lalabadi[b], A. Ehsani[b], Baharak Divband[c,d]

[a] *Department of Food Sciences and Technology, Urmia University, Urmia, Iran*

[b] *Department of Food Sciences and Technology, Tabriz University of Medical Sciences, Tabriz, Iran*

[c] *Stem Cell Research Center, Tabriz University of Medical Sciences, Tabriz, Iran*

[d] *Infection and Tropical Disease Research Center. Tabriz University of Medical Sciences, Tabriz, Iran*

**Corresponding author: leilarafiei199@yahoo.com*

Mini review

The food package is an important factor on food preservation and quality. Microbial growth has been motivating the development of innovations for inhibition of microbial contaminants in foods. Active packaging can be used with the purpose to extend product's shelf life. The inclusion of antimicrobial substances in plastic films has the purpose of their gradual release on the surface of the food, inhibiting the growth of microorganisms, increasing the shelf life and safety of the product [1]. The antimicrobial activity of silver containing zeolites on different microorganisms has been studied elsewhere, drawing commercial and industrial interest, mainly on health and food applications. This study aimed at the preparation of antimicrobial films based on silver (Ag) exchanged zeolite. Silver exchanged zeolite showed antimicrobial activity on E. coli were those prepared with 5% zeolite containing 5% silver, showing the potential application of such films in food preservation and safety [1-2].

The importance of packaging has been increasingly receiving much importance due to the new consumer's behavior (internet shopping, consumption of fast meals, frozen meals, demands for frozen meals packed in individual portions, etc.), which arises a new market for food. These new markets demand distribution for longer distances, and thus require increased food shelf life [1–3].

The use of an active packaging can increase safety and quality of the food, by interaction of the active principle contained in the packaging material with the food or the microorganisms. These technologies may increase the shelf life and reduce the risk of contamination by pathogens [4].

The inclusion of antimicrobial substances in plastic films has the purpose of their gradual release on the surface of the food, inhibiting the growth of microorganisms, increasing the shelf life and safety of the product. The antimicrobial agent interacts with the headspace between the package film. The proposed or tested antimicrobial compounds for food packaging applications include organic acids/anhydrides, fungicides, bactericides, enzymes, ceramic materials with Ag ions, plant extracts, and inorganic gases [5, 6].

Several investigations have been carried out concerning the use of synthetic and natural (clinoptilolite) zeolites: A, X, Y, Z, and clinoptilolite

supporting metal ions (Ag, Cu, Zn, Hg, Sn, Pb, Bi, Cd, Cr, and Ti) as antibacterial agent's antimicrobial properties. The antibacterial zeolite was produced commercially and approved by the Food and Drug Administration (FDA) and the Environmental Protection Agency (EPA) [7].

The antimicrobial potential is increased since both sides of the films are active, and also the diffusion rate of Ag out of the material is slower, when contrasted to loading the silver ions directly into the polymer matrix. This may increase the potential application in long-term antimicrobial behavior and safety for food applications, since smaller amounts of silver are released in the food that is in contact with package. Studies could be found, concerning the application of silver containing zeolites on polymer films, like polypropylene, polyurethane and polylactide. Plastics such as polypropylene, polyethylene, polyamides, polyethyleneterephthalate, polyvinylidene chloride copolymers, etc., and paper, paperboard, and aluminum foils have been used as food-packaging materials [6-8].

Among the natural biopolymers, starch has been considered as the most promising raw material to develop new environmentally friendly materials especially for packaging and disposable applications because of its low density, its renewable character and its complete biodegradability, and its availability worldwide under different shapes at relatively low cost. The main disadvantages of biodegradable starch based films, compared to conventional polymers, are their hydrophilic character and their poor mechanical properties which lead to low stability [9]. Many research works have focused on improving the physical properties of natural polymer based-films by decreasing the hydrophobicity and increasing and stabilizing the mechanical properties [10]. The incorporation of nano-sized fillers into natural polymer-based matrices, to produce nanocomposite materials, can be a powerful solution to improve these properties. [9,11]. Zeolites are currently used in industry; the three main uses being ion exchange, gas separation and catalysis. Enhanced mechanical performances of polymers can be achieved through the incorporation of inorganic materials into the polymer matrix and zeolites are shown to be alternative inorganic fillers for this purpose.

In Conclusions the results obtained in this review showed that the zeolite impregnated with metal ions can use as antimicrobial agent for application in food packages, aiming at increasing food safety and shelf-life.

References

[1] L. Vermeiren, F. Devlieghere, M. Van Beest, N. De Kruijf, J. Debevere, *Trends Food Sci. Technol.* 10 (1999) 77-86.

[2] K. Sonneveld, *Packag. Technol. Sci.* 13 (2000) 29-35.

[3] P. Suppakul, J. Miltz, K. Sonneveld, S.W. Bigger, *J. Food Sci.* 68 (2003) 408-420.

[4] D.S. Cha, M.S. Chinnan, *Rev. Food Sci. Nutr.* 44 (2004) 223-237.

[5] P. Appendini, J.H. Hotchkiss, *Innov. Food Sci. Emerg. Technol.* 3 (2002) 113-126.

[6] A.R.F. Moraes, L.E.R. Gouveia, N.F.F. Soares, M.M.S. Santos, M.P.J.C. Gonçalves, *Cienc. Tecnol. Aliment* 27 (2007) 33-36.

[7] B. Kwakye-Awuah, C. Williams, M.A. Kenward, I. Radecka, J. Appl. Microbial. 104(5) (2008) 1516-1524.

[8] H. Pehlivan, D. Balkse, S. Ülkü, F. Tihminlioglu, *Compos. Sci. Technol.* 65 (2005) 2049-2058.

[9] H. Liua, D. Chaudharya, S.-I. Yusa, M.O. Tade, *Carbohyd. Polym.* 83 (2011) 1591-1597.

[10] J.-W. Rhim, J.-H. Lee, H.-S. Kwak, *Food Sci. Biotechnol.* 14 (1) (2005) 112-116.

[11] H. Almasi, B. Ghanbarzadeh, A.A. Entezami, *Int. J. Biol. Macromol.* 46 (2010) 1-5.

The Effect of ZSM-5 Zeolite on Membrane Bioreactor Performance and Transmembrane Pressure

Z. Sajadian[a,b], H. Hazrati[a,b]*, M. Rostamizadeh[a,b]

[a] *Department of Chemical Engineering, Sahand University of Technology, Sahand New Town, East Azerbaijan, Iran*

[b] *Environmental Engineering Research Center, Department of Chemical Engineering, Sahand University of Technology, Sahand New Town, East Azerbaijan, Iran*

** Corresponding author: H.Hazrati@sut.ac.ir*

Abstract: In this work, the influence of adding ZSM-5 zeolite into the membrane bioreactor for fouling reduction of membrane and chemical oxygen demand (COD) removal was studied. We used a 60cm×22cm×5.6cm micro filtration PVDF membrane. Adding ZSM-5 zeolite to system reduced transmembrane pressure (TMP) by 25% and COD removal efficiency in system with ZSM-5 was about 11.82 % higher than system without zeolite. Furthermore, the soluble microbial product (SMP) concentration in the sludge decreased in the system with ZSM-5 zeolite.

Keywords: MBR; ZSM-5; TMP; COD removal efficiency

1. Introduction

In the past few years, using membrane bioreactor for treating water and wastewater become very common due to its advantages upon traditional water treatment methods like active sludge method. MBRs are the high quality of treated water due to producing a small amount of sludge and its process flexibility for different conditions. However, one of the major drawbacks for using the technology is fouling the pores of the membrane during the treating process [1]. For an economical and long term MBR process, control and reduction of membrane fouling is necessary. One of the ways for reaching this goal is the addition of additives to MBR [2]. These additives like activated carbon and zeolites are known as bio-fouling reducers and cause changes in wastewater properties, improvement of filtration process and reduce fouling. In this research, we use ZSM-5 zeolite as Bio fouling reducer (BFR).

2. Experimental Part

2.1 Setup

Experimental setup consists of 60 cm × 22 cm × 6.5 cm bioreactor which can carry 7 liter inside. Membrane used for this setup is microfiltration membrane with effective area of 0.1 m^2, nominal diameter of 0.4 µm and made by Sinap Company in China. Material used for making this membrane is PVDF.

2.2 Aerobic Sludge

Initial sludge for reactor is from aeration tank in Tabriz petrochemical complex. The composition of

reactor feed is C_2H_5OH, CH_4N_2O, K_2HPO_4, KH_2PO_4, $CaCl_2.2H_2O$, $FeCl_3$, $MgSO_4.7H_2O$ and molasses.

2.3 Experiment

Experiments were conducted in two 30th days period; one without zeolite (BFR0) and one with zeolite (BFR1). Air entering the reactor is about 8 to 9 lit/min and HRT and SRT are 8 hours and 15 days respectively. Temperature is 30 to 33 °C and pH is 7 to 8. 4 g/lit zeolite was used for experiment.

2.4 Analysis

Mixed liquor suspended solid (MLSS), Mixed liquor volatile suspended solid (MLVSS), soluble microbial products (SMP) and chemical oxygen demand (COD) are measured according to standard methods. TMP was measured by vacuum gauge 972B MKS, and for determining adsorbent value in the COD and SMP test was used UV Shimadzu-1280.

3. Results and discussion

3.1. Influence of adding zeolite on COD removal

The difference of COD on influent and permeate was calculated as organic removals performance of the MBR. Figure 1 shows that both MBR systems reach about 80% of COD removal in 30 days period. COD removal in system without ZSM-5 has an increasing trend because reactor conditions become steady state. COD removal in system with ZSM-5 has an increasing trend too but it decreases in last week and it is probably because of decreasing the amount of ZSM-5 in the last week of experiment.

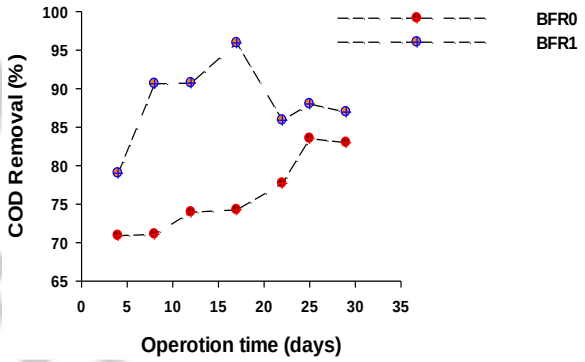

Figure1. Influence of ZSM-5 on COD removal.

COD removal in system with ZSM-5 was about 11.82% higher than system without zeolite and it is because of adsorption ability of ZSM-5

3.2. Influence of ZSM-5 on TMP

TMP is regarded as transmembrane pressure, which is the pressure difference between two sides of membrane [3]. It is used as a criterion to represent the amount of fouling in a membrane. TMP in both systems increased after 30 days. In system with ZSM-5, TMP increases step by step but in day 8 until day 20 is fixed and after that it increases again. This is because of adsorption EPS/SMP by ZSM-5 during the process. Increasing in TMP rate after day 20 is maybe because of reduction of zeolite adding amount to the system in the last days of experiment. In system without ZSM-5, TMP increases during the experiment period. ZSM-5 decreases TMP 25% overall in these experiments.

3.3. Influence of ZSM-5 on MLSS

Initial value for MLSS was 3000 mg/L because both systems use the same sludge at beginning. Results

show that both systems have same trend and in both systems, MLSS increased but not so much and it is because of short residence time of sludge. Average value for MLSS in 30 days period for both systems is 3700 mg/L. This means ZSM-5 has no significant influence on MLSS.

3.4. The effect of ZSM-5 on SMP

As the fouling process is complicated and depends on numerous factors and addition of ozone to the reactor will cause numerous and complicated reaction, different studies have reported different results and ozone addition did not induce a specific trend in these parameters [3]. The results show that total SMP, SMPp (protein fraction) and SMPc (carbohydrate fraction) decreased in system with ZSM-5 (Table 1).

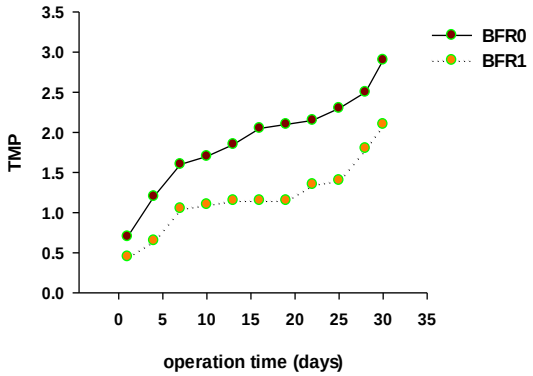

Figure 2. Influence of ZSM-5 on TMP.

The reason could be the presence of ZSM-5 in the system; SMP can adhere to the adsorbent through functional groups like OH in zeolite structure and therefore leave the system with excess sludge [4].

Table 1. Total SMP, SMP_p , SMP_c value for both condition.

MBR	SMP (mg/L)		
	SMP_p	SMP_c	Total SMP
BFR0	82	168	250
BFR1	17	147	164

4. Conclusions

The TMP value for system with ZSM-5 was decreased by 25% in comparison with the case with no adsorbent. Also make COD reduction 83%. Adding zeolite is a good way for fouling reduction of membrane and this make MBR processes more economical and common.

References

[1] H. Hazrati, M. Jahanbakhshi, M. Rostamizadeh, *J. Membr. Sci*. 555 (2018) 455-462.

[2] A. Yuniarto, Z.Z. Noor, Z. Ujang, G. Olsson, A. Aris, *Desalination*, 316 (2013) 146-153.

[3] L. Malaeb, P. Le-Clech, J.S. Vrouwenvelder, G.M. Ayoub, P.E. Saikaly, *Water Res*. 47 (15) (2017) 5447-5463.

[4] O.T. Iorhemen, R.A. Hamza, J.H. Tay, *Biores. Technol.* 240 (2014) 9-24.

Preparation of ZSM-5 Nanocrystals as a Green Acid Catalysis for the Synthesis of 2,3-dihydroquinazolin-4(1*H*)-ones

R. Teymuri, J. Safaei-Ghomi*

Department of Organic Chemistry, Faculty of Chemistry, University of Kashan, Kashan, P.O. Box 87317-51167, Iran

**Corresponding author: safaei@kashanu.ac.ir*

Abstract: ZSM-5 zeolite as a great catalyst system has been prepared and tested their catalytic activity in aqueous-mediated greener synthesis of 2,3-dihydroquinazolin-4(1*H*)-one derivatives in higher yield with shorter reaction time. Recyclability of novel catalyst system was also studied which resulted in no loss of their catalytic activity up to five cycles makes the whole system industrially viable.

Keywords: ZSM-5, Zeolite, Multi-component, Dihydroquinazolinone, Nanocatalyst

1. Introduction

Multicomponent reactions (MCRs) have emerged as a mostly popular synthetic tool for the prompt and favourable access of diverse heterocycles [1]. Noteworthy, one of this fused-heterocycle is 2,3-dihydroquinazolinone (DHQZ-1) which contains wide pharmacological properties including anti-inflammatory, antibacterial, antitumor, and anticonvulsant [2]. Having looked at this importance, there are many methods for the synthesis of 2,3-dihydroquinazolinone moiety preparation. In addition, various catalysts were employed including, $KAl(SO_4)_2.12H_2O$ [3], aluminum methanesulfonate [4], ZnO nanoparticles [5]. Whereas the majority of these procedures have noticeable negative aspects such as long reaction times, low yields, harsh reaction conditions, and use of expensive and toxic catalysts. Therefore, to avoid these limitations, the exploration of an efficient, easily available catalyst with high catalytic activity and short reaction times for the preparation of dihydroquinazolins is still favored.

Development of heterogeneous catalytic processes for fine and specialty chemicals is an important inter-disciplinary research objective for industrialists and academicians. Zeolites, glasses, carbons, and oxides are members of a large group of porous materials known as molecular sieves. Among these, zeolites are the most attractive candidates for industrial applications because of their unusual features. The exchangeable cations in zeolites can be substituted by protons, which behave as strong Brønsted acid sites [6].

Consequently, the development a favourable approach for the preparation of 2,3-dihydroquinazolin-4(1*H*)-ones via the condensation reaction of isatoic anhydride, aldehydes, and primary amine or ammonium acetate using ZSM-5 nanocrystals as a reusable and efficient catalyst.

2. Experimental Part

2.1. Preparation of ZSM-5 nanocrystals

ZSM-5 zeolite was synthesized hydrothermally. The template (0–1.2 ml) and TEOS (4.15 ml) were mixed with distilled water (4 ml), and was stirred for 1 h (I). NaOH (0.18 g) was also added with distilled water (8 ml). Aluminum isopropoxide (AIP) (0.18 g) was added to distilled water (8 ml) and stirred for 1 h. The resulting mixture (II) was added dropwise to mixture (I) with stirring, and the resulting gel was stirred for 120 min. Subsequently, the obtained hydrogel had the following molar ratio: $1Al_2O_3$:$46SiO_2$:4TPAOH:$5Na_2O$:$2500H_2O$. Then the gel was transferred to a stainless-steel autoclave for 3 days in oven at 165 °C. The autoclave was quenched with water, and the solid product was filtered, washed with distilled water and dried at 110 °C overnight. To produce the final product, the obtained material was calcined at 550 °C for 8 h.

2.2. General procedure for the preparation of 2,3-dihydroquinazolin-4(1*H*)-ones

ZSM-5 nanocrystals as an efficient catalyst was added to an ethanol/H_2O solution of isatoic anhydride (1 mmol), primary aromatic amine (1.1 mmol) and aldehyde (1.0 mmol) was heated for the desired times. As soon as the complete disappearance of the starting material, as checked by TLC; the catalyst was removed by filtration. 10 ml ice water was added and the precipitated product was filtered. At the end of the process, the

residue was recrystallized from ethanol to obtain the crude product

3. Results and discussion

Nano-ZSM exhibited MFI framework structure with high phase purity, which was conirmed by XRD (Fig. 1). XRD pattern of Nano-ZSM-5 was broad when compared to ZSM-5, which conirms that the material is nanocrystalline in nature.

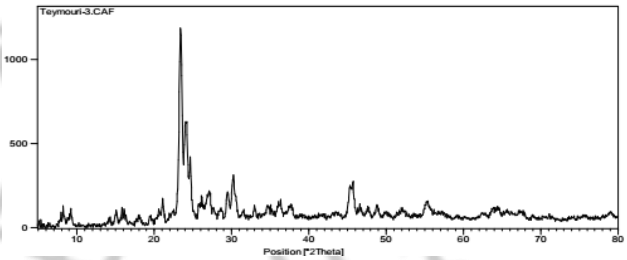

Figure 1. XRD pattern of Nano-ZSM-5.

The morphology of nano-ZSM-5 was observed with scanning electron microscope (SEM) and the representative image is shown in Fig. 2.

In continues, the current reaction are proceed by 5 mol% of ZSM-5 as nanocatalyst and some of synthesized compounds are represented in Table 1.

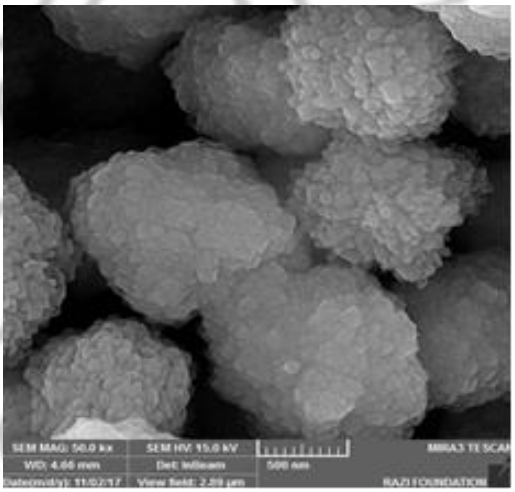

Figure 2. SEM image of Nano-ZSM-5.

Table 1. Synthesis of disubstituted 2,3-dihydroquinazoline 4(1*H*)-ones using ZSM-5 nanocrystals.

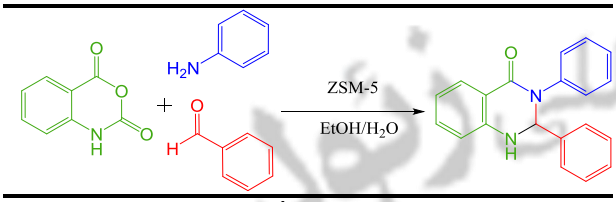

name	aldehydes[b]	Time (min)	Yield
4k	benzaldehyde	25	94
4l	4-nitrobenzaldehyde	28	96
4m	4-cholorobenzaldehyde	25	95
4n	4-methylebenzaldehyde	27	93
4o	2-nitrobenzaldehyde	27	90

4. Conclusions

To recapitulate briefly, we have reported a green and efficient method for the synthesis of 2,3-dihydroquinazolin-4(1*H*)-ones derivatives via three-component one-pot condensation of isatoic anhydride, aromatic aldehyde and primary amines using ZSM-5 nanocrystals as new catalyst at 80 °C. The current method provides obvious positive points such as environmental friendliness, significantly shorter reaction time, markedly excellent yields and simple workup procedure.

References

[1] A. Rahmati, Z. Khalesi, *Tetrahedron* 68 (2012) 8472-8479.

[2] Y. Hu, E.A. Ehli, J.J. Hudziak, G.E. Davies, *Pharmacogenomics J*. 12 (2012) 372-378.

[3] M. Dabiri, P. Salehi, S. Otokesh, M. Baghbanzadeh, Gh. Kozehgary A.A. Mohammadi, *Tetrahedron Lett*. 46 (2005) 6123-6126.

[4] Z. Song, L. Liu, Y. Wang, X. Sun, *Res. Chem. Intermed.* 38 (2012) 1091.

[5] I. Yavari, S. Beheshti, *J. Iran. Chem. Soc.* 8 (2011) 1030-1035.

[6] D.P. Serrano, J. Aguado, G. Morales, J.M. Rodriguez, A. Peral, M. Thommes, J.D. Epping, B.F. Chmelka, *Chem. Mater.* 21 (2009) 641-654.

Synthesis of K-SAPO-34 and Ag-SAPO-34 Nano-catalysts for Methanol to Olefins (MTO) Process

M. Ghadiri[a]*, K. Mirza[b], M. Haghighi[c], A. Rahmati[a]

[a] *Chemical Engineering Department, Urmia University of Technology, P. O. Box 57155-419, Urmia, Iran.*

[b] *Department of Chemical engineering, Faculty of engineering, Soran University, Soran, Erbil, Iraq*

[c] *Chemical Engineering Department, Sahand University of Technology, P.O. Box 51335-1996, Sahand New Town, Tabriz, Iran.*

**Corresponding author: m.ghadiri@uut.ac.ir*

Abstract: SAPO-34 nanostructured catalyst was hydrothermally synthesized and Ag-SAPO-34 and K-SAPO-34 catalysts were prepared by ion exchange of SAPO-34 catalyst with $AgNO_3$ and KNO_3 solutions, respectively. The samples were characterized by X-ray diffraction (XRD), field emission scanning electron microscopy (FESEM), and ammonia temperature programmed desorption (NH_3-TPD) techniques. Prepared samples were examined in methanol to olefins (MTO) process. It was found that Incorporation of K^+ and Ag^+ in SAPO-34 structure, leads to increase selectivity of ethylene and propylene.

Keywords: Nano-Catalyst; Olefins; K-SAPO-34; Selectivity; Ag-SAPO-34

1. Introduction

In industry, light olefins mainly are produced from thermal cracking of naphtha. In recent years, catalytic process of Methanol to Olefins (MTO) has been considered to be a conceivable replacement for thermal cracking of naphtha. SAPO-34 has been proved to be very potential catalyst in this reaction. Metals incorporation to SAPO-34 framework to produce Me-SAPO-34, is the most common way to increase its selectivity and lifetime. It can affect on catalytic properties such as acid sites concentration and strength that leaded to reduce the deactivation rate of catalyst [1-3].

2. Experimental Part

2.1. Materials

Aluminium chloride ($AlCl_3.6H_2O$, Fluka, 99%), phosphoric acid (H_3PO_4, Merck, 85%), fumed silica (SiO_2, Aldrich, 100%), potassium nitrate (KNO_3, Kian Kaveh, 99%) and silver nitrate ($AgNO_3$, Merck, 99.8%) were used as Al, P, Si, K, and Ag sources, respectively. Diethyl amine (DEA, Aldrich, 99%) was used as the structure directing agent.

2.2. Catalyst Preparation

For catalyst preparation at first, aluminium chloride was added to 16.5 ml of deionized water and stirred for 50 minutes at room temperature. During the stirring, H_3PO_4 was added dropwise to this mixture. After mixing the solution for 30 minutes, fumed silica was added to the mixture. In the next step,

DEA was slowly added and precursor mixture was stirred for 3 hours. The molar ratio of the synthesis gel was $1Al_2O_3$:$1P_2O_5$:$0.6SiO_2$:9DEA:$110H_2O$. In the second step, the obtained colloidal solution was transferred into a stainless steel autoclave and was kept at room temperature for 24 hours in a continuous stirring manner. The obtained gel then was heated at 200 °C for 46 hours. Then, as-synthesized catalyst was dried at 110 °C and calcined at 550 °C for 12 hours.

To obtain K-SAPO-34 and Ag-SAPO-34 samples, K and Ag was introduced to SAPO-34 zeolite by ion exchange between a solution of KNO_3 and $AgNO_3$ in water (0.01 M) and the zeolite at room temperature for 1 hour. In the first ion exchange, modified SAPO-34 catalysts designed as K-SAPO-34 (1) and Ag-SAPO-34(1). Then, K and Ag were introduced into the K-SAPO-34 (1) and Ag-SAPO-34(1) zeolites by ion exchange between a solution of KNO_3 and $AgNO_3$ in water (0.01 M) and the zeolite at room temperature for 1 hour. Modified catalysts designed as K-SAPO-34 (2) and Ag-SAPO-34(2). Four samples were dried at 110 °C for 12 hours and were calcined at 550 °C for four hours.

2.4. Catalytic Performance Test

Methanol to olefins reaction was tested at 300- 500 ºC using a laboratory-scale reactor that includes a gas feeding unit, a fixed bed reactor and an analytical section operating at atmospheric pressure. A mixture containing methanol and water (30 mol% methanol, 70 mol% H_2O) was prepared in a saturator at 8.9 ºC. 1 g of catalyst with quartz was put in reactor and was calcined under argon flow at 550 ºC for 1 hour. Argon gas was used to reactor as carrier gas of the reactants and the products of gas chromatograph were equipped with a Plot-U column and a flame-ionization detector (FID). The reaction was performed with a gaseous hourly space velocity (GHSV) of the methanol at 4200 cm^3/g.h. The stability test was performed at constant feed composition, reaction temperature, and gas hourly space velocity.

3. Results and discussion

3.1. XRD Analysis

Figure 1 shows the X-ray diffraction patterns of the SAPO-34, Ag-SAPO-34(2) and K-SAPO-34(2) nanostructured catalysts. It can be observed that all of these structures are the same and have the peak positions at 2θ = 9.5, 12.9, 16.0, 17.7, 20.6, 24.9, 25.9, 30.6, and 31.0°. Therefore, all of catalysts have structure corresponding to chabazite phase of SAPO-34 (JCPDS: 01-087-1527, Rhombohedral) which indicates high purity of catalysts [2].

The relative crystallinity of the catalysts was calculated using sum of the intensity of the more important peaks at 2θ = 9.5, 12.9, 20.6° on the basis of the best prepared sample. The crystallinity of the K-SAPO-34(2) catalyst was higher than the other catalysts. This is taken as the reference when determining the crystallinity of the other samples. It was found that relative crystallinity of all catalysts related to the formation of SAPO-34 phase decreased in the following order:

K-SAPO-34(2) > SAPO-34 > Ag-SAPO-34(2)

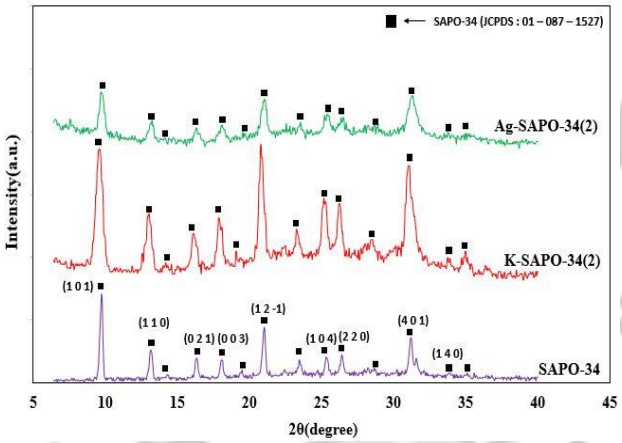

Figure 1. XRD patterns of nanostructured catalysts K- SAPO-34(2), Ag-SAPO-34(2), and SAPO-34.

3.2. FESEM Analysis

The FESEM image of the SAPO-34 catalysts is shown in Figure 2. The catalyst particles of catalyst have cubic morphology. This morphology is similar to the CHA-structure. As it is shown in this very figure, there are crevices on the surface of SAPO-34 particles that may decrease attrition resistant of the catalyst particles.

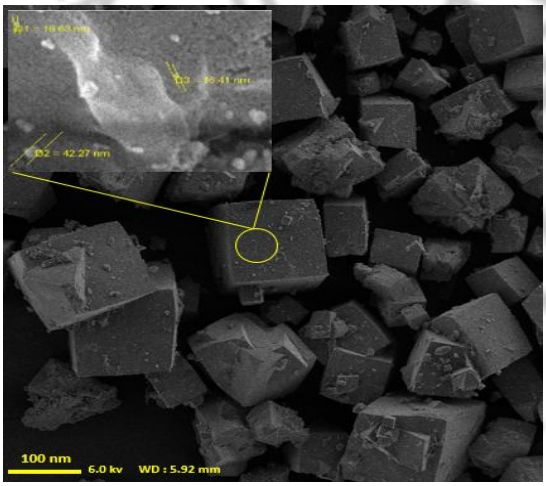

Figure 2. FESEM image of SAPO-34 nano-catalyst.

3.3. NH_3-TPD Analysis

NH_3-TPD analyses determine the acid concentration and strength distribution of acid sites of catalysts, the results of which are presented in Figure 3. Increasing NH_3 desorption temperatures means stronger bonds and hence stronger acidic sites. For SAPO-34 and Ag-SAPO-34(2) was observed that by Ag^+ ion exchange, acid strength of weaker and stronger acid sites increased from 182 to 287 °C and 413 to 616 °C, respectively. K^+ ion exchange can reduce the acid strength of strong acid sites and acid amount of weak acid sites. The results of NH_3-TPD analysis confirm that the strength of the weak acid sites in the K-SAPO-34(2) is lower than that in Ag-SAPO-34(2) and higher than in SAPO-34. The results of the reactor tests also confirmed that the K-SAPO-34(2) has the largest selectivity of olefins.

3.4. Catalytic performance study toward MTO process

The selectivity to ethylene over SAPO-34, K-SAPO-34(2) and Ag-SAPO-34(2) catalysts at different reaction temperatures (300 to 500 °C) is shown in Figure 4.

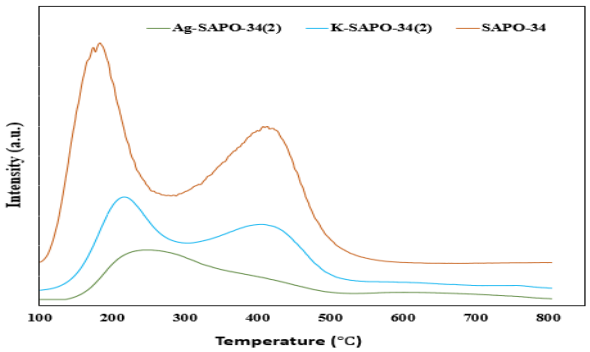

Figure 3. NH_3-TPD analysis of Ag-SAPO-34(2), K-SAPO-34(2) and SAPO-34 catalysts.

As it is shown in Figure 4, ethylene production over SAPO-34 and K-SAPO-34(2) catalysts has increased by cracking of propylene and butylenes. Moreover, K-SAPO-34(2) catalyst has indicated higher ethylene selectivity than SAPO-34 catalyst at the temperatures higher than 400 °C. Coking can lead to catalytic deactivation at high temperatures. K-SAPO-34(2) catalyst, compared with all other catalysts, provides more propylene at the temperatures ranging from 350 °C to 500 °C.

Ethylene selectivity increases to 70% in line with an increase in the temperature up to 450 °C in the presence of Ag-SAPO-34(2) catalyst, but it decreases beyond this temperature. Compared with SAPO-34 and K-SAPO-34(2) catalysts, Ag-SAPO-34(2) zeolite is more selective toward ethylene production at 350-450 °C. It was found that the catalytic performance of K-SAPO-34(2) and Ag-SAPO-34(2) is better than K-SAPO-34(1) and Ag-SAPO-34(1).

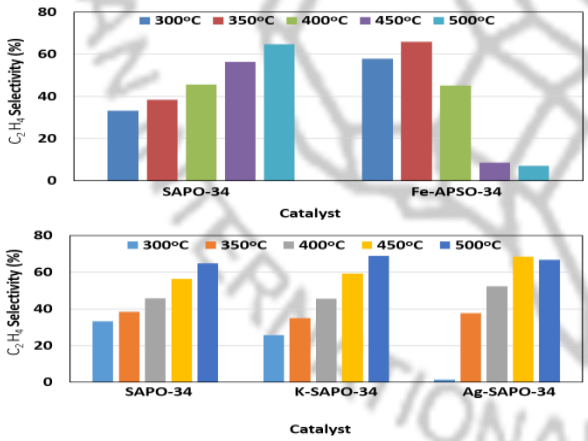

Figure 4. Ethylene selectivity vs. temperature over SAPO-34, K-SAPO-34, and Ag-SAPO-34 catalysts.

4. Conclusions

Ag-SAPO-34 and K-SAPO-34 catalysts were prepared by ion exchange of SAPO-34 catalyst with $AgNO_3$ and KNO_3 solutions, respectively. It was found that potassium ion exchange could increase the strength of the weak acid sites. Selectivity of olefins for K-SAPO-34 and Ag-SAPO-34 catalysts was more than that of SAPO-34 catalyst.

References

[1] P. Sadeghpour, M. Haghighi, *Particuology* 19 (2015) 69-81.

[2] Kh. Mirza, M. Ghadiri, M. Haghighi, A. Afghan, *Micropor. Mesopor. Mater.* 260 (2018) 155-165.

[3] M. Charghand, M. Haghighi, *Adv. Powder Technol.* 25 (2014) 1728-1736.

Effect of Incorporating ZnO Nanoparticles into Orthodontic Composite Resins on Shear Bond Strength

M. Kachoei[a], B. Divband[b], M. Esmailzadeh[e]*, M. Rahbar[c], M. Ghanizadeh[d],

[a] *Department of Orthodontics, Faculty of Dentistry, Tabriz University of Medical Sciences, Tabriz, Iran*

[b] *Department of Chemistry, University of Tabriz, Tabriz, Iran*

[c] *Operative and Esthetic Department, Dental and Periodontal Research center, Faculty of Dentistry, Tabriz University of Medical Sciences, Tabriz, Iran.*

[d] *Department of Oral and Maxillofacial Surgery, Faculty of Dentistry, Tabriz University of Medical Sciences, Tabriz, Iran*

[e] *Dentistry student, Faculty of Dentistry, Tabriz University of Medical Sciences, Tabriz, Iran*

**Corresponding author: mahdieh_es@yahoo.com*

Abstract: Fixed orthodontic treatment with the aim of modifying the patient's functional and esthetic problems, beside to satisfaction of the majority of such patients, might have complications for these patients, including debonding of brackets and tooth discoloration around brackets. On this basis, the present study was undertaken to evaluate the effect of incorporating ZnO and Ag/ZnO nanoparticles into orthodontic composite resins on shear bond strength of these composite resins.

Keywords: Ag/ZnO; CompositeResins; Nanoparticles; Shear Bond Strength

1. Introduction

Orthodontic treatment is very advantages to patients with functional and esthetic problems and results in satisfaction of the majority of such patients. However, such treatment might have complications for these patients, including demineralization, caries and tooth discoloration around brackets and the bonded areas in the form of white spot lesions (WSL), which are considered a major challenge for clinicians and a major challenge and a factor for dissatisfaction of patients. This problem makes the patients susceptible to more widespread caries, especially in patients with poor oral hygiene. In this context, patients receiving a full fixed treatment plan are more susceptible to caries and exhibit a significant increase in *S. mutans* counts in their plaque and saliva [1]. In the presence of an increased count of cariogenic bacteria in the saliva and plaque and also poor oral hygiene, decalcification and carious lesions can occur in less than 4 weeks [2].

Fluoride-containing materials, especially fluoride varnishes, are widely used to prevent caries but they have two problems: first, they need regular patient cooperation and second, they have a moderate effect on prevention of WSL and caries [3]. Fluoride-containing bonding agents, too, have the problem of rapid release during the first 24 hours, with a decrease in release over time [1].

ZnO and ZnO-containing materials have significant antibacterial activity and are used in different ways for the treatment of traumatic injuries, foot injuries and burns [4]. Dental materials, including endodontic sealers and adhesive cements, use this property of ZnO for bonding of fixed restorations. The antibacterial mechanism of ZnO involves its activity as an activator for enzymes. It is toxic to bacteria at a concentration of 0.5 ppm and concentrations of 4,6 and 16 ppm can inhibit bacterial growth [5].

Ahn et al., too, improved the antibacterial properties of orthodontic composite resins as adhesive agents by adding silver nanoparticles to their structure. However, there was no significant difference between these experimental composite resins and the conventional composite resin in shear bond strength [6]. Although silver nanoparticles induce favorable antibacterial properties, they might result in a dark color in composite resin, creating esthetic problems. Ag/ZnO nanoparticles are white in color and incorporating them into composite resins with the same color does not lead to esthetic problems. On the other hand, it is expected that use of these nanoparticles, which contain both silver and zinc oxide, will increase their antibacterial properties.

Considering the properties mentioned for Ag/ZnO nanoparticles and the unfavorable properties of silver nanoparticles alone and since fixed orthodontic treatment requires a material with suitable mechanical properties, the present study was undertaken for the first time to evaluate the effect of incorporating ZnO and Ag/ZnO nanoparticles into orthodontic composite resins on the shear bond strength of these composite resins.

2. Experimental Part

In this study, 120 extracted sound human second premolar teeth were collected for the evaluation of shear bond strength. The teeth were randomly divided into 4 groups (n=30). In group 1, composite resin without nanoparticles (O) was used for bonding of brackets. In groups 2 to 4, composite resin with ZnO nanoparticles (Z), composite resin with ZnO nanoparticles and silver ions (A&Z) and composite resin with Ag/ZnO nanoparticles synthesized using optical precipitation (AZ) were used for bonding of brackets, respectively. After the shear bond strength test, data were analyzed with SPSS 21. Statistical significance was set at $P<0.05$.

3. Results and discussion

In this study, 4 different types of orthodontic composite resin were evaluated. In group 1, conventional composite resin (O) was used, and in the other 3 groups, composite resins with ZnO nanoparticles (Z), ZnO and silver nanoparticle solution (A&Z) and Ag/ZnO nanoparticles (AZ) synthesized with optical precipitation was used.

Table 1 presents the descriptive data of shear bond strength tests in each study group separately. Based on Table 1, the mean shear bond strength value in the A&Z group was lower than that in other groups, with the highest shear bond strength in the AZ group (Graph 1).

Kolmogorov-Smirnov test showed normal distribution of data in the present study (P>0.05). In addition, Levene's test showed that the variances of the groups were the same (P>0.05). Therefore, one-way ANOVA was used to compare the mean shear bond strength values between the study groups, which reveled significant differences in mean shear bond strength values between the different study groups (P=0.0001).

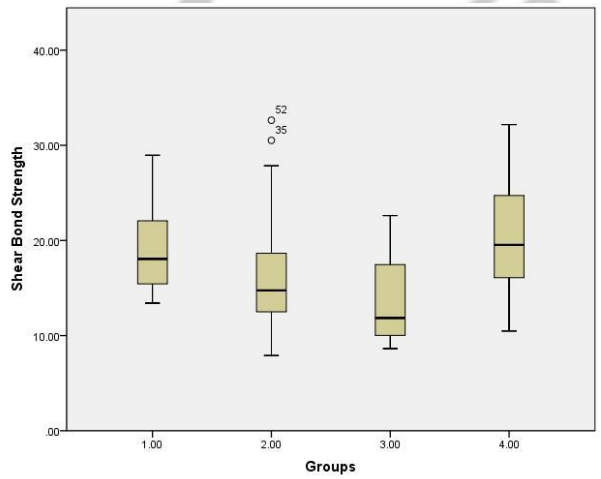

Graph 1. Comparison of shear bond strength in each study group.

Table 1. The descriptive data of shear bond strength in each study group.

Group	NO.	Mean of Shear Bond/Strength (MPa)	Std. Deviation	Min.	Max.
A(O)	30	19.03	4.12	13.42	28.95
B(Z)	30	16.35	1.11	7.90	32.63
C(A&Z)	30	13.61	0.73	8.64	22.61
D(AZ)	30	20.49	1.03	10.48	32.17
Total	120	17.37	0.51	7.90	32.63

Tukey test showed that the mean shear bond strength of A&Z composite resin was significantly less than that of conventional composite resin (P<0.05). In addition, the mean shear bond strength of AZ composite resin was significantly higher than those of Z and A&Z composite resins. There was no significant difference in the shear bond strength between the AZ and conventional (O) composite resins (P=0.15).

Patients' cooperation to observe the oral hygiene has always been a challenge during orthodontic treatment. Therefore, many clinicians prefer methods that do not require patient cooperation [7]. Although fluoride-releasing materials are appropriate for patients susceptible to caries, they are predominantly used in the dental office and there are also limitations in relation to the number of times they can be used [8].

In another study, Ahn et al. concluded that composite resin adhesives containing silver nanoparticles and silica nano-fibers prevent demineralization of enamel around orthodontic brackets without compromising their mechanical properties [6].

The results of a study by Tavassoli et al. on the effect of adding ZnO nanoparticles to flowable composite resins on their antibacterial and physical properties and strength showed that an increase in these nanoparticles resulted in a significant increase in their antibacterial activity. In addition, they showed that incorporation of nanoparticles into composite resins resulted in a significant increase in the compressive strength and shear bond strength of composite resins, with no changes in their flexural

strength. In the present study, too, although the shear bond strength of Ag/ZnO nanoparticle-containing composite resins, synthesized using optical precipitation, was higher than that in the control group, the difference was not significant statistically. Therefore, incorporation of nanoparticles to orthodontic composite resins does not result in a change in the mechanical properties of these composite resins.

Contreras et al. evaluated the effect of incorporating titanium nanoparticles into glass-ionomer and concluded that incorporation of these particles increases the compressive and flexural strengths of glass-ionomers, in addition to conferring antibacterial properties. In the present study, too, no changes were detected in the shear bond strength to enamel [9]. Pousti et al. showed in another study that incorporation of titanium nanoparticles into orthodontic composite resins confers antibacterial properties, with no changes in the shear bond strength. In a study by Cheng et al. in 2012, incorporation of silver nanoparticles into composite resins improved the mechanical properties of these composite resins and they exhibited antibacterial properties. In a different study by Argueta-Figueroa et al. in 2015, the shear bond strength of orthodontic adhesives, containing copper nanoparticles, was reported to be higher than that in the control group, with no changes in color and other properties.

4. Conclusions

Incorporation of Ag/ZnO nanoparticles synthesized using optical precipitation intoorthodontic composite resins did not change mechanical properties; however, incorporation of ZnO nanoparticles containing silver ions decreased the shear bond strength.

References

[1] T.A. Al-Musallam, C.A. Evans, J.L. Drummond, C. Matasa, C.D. Wu, *Am. J. Orthod. Dentofac.* 129 (2) (2006) 245-251.

[2] L. Gorelick, A.M. Geiger, A.J. Gwinnett, *Am. J. Orthod. Dentofac.* 81 (2) (1982) 93-98.

[3] D.C. Chan, E.J. Swift Jr., S.E. Bishara, *J. Dent. Res.* 69 (9) (1990) 1576-1579.

[4] D.P. Lookingbill, S.H. Miller, R.C. Knowles, *Arch. Dermatol*. 114 (12) (1978)1765-1768.

[5] D.G. Bates, J.M. Navia, *Arch. Oral Biol*. 24 (10-11) (1979) 799-805.

[6] S.J. Ahn, S.J. Lee, J.K. Kook, B.S. Lim, *Dent. Mater.* 25 (2) (2009) 206-213.

[7] E. Paschos, T. Kleinschrodt, T. Clementino-Luedemann, K.C. Huth, R. Hickel, K.H. Kunzelmann, I. Rudzki-Janson, *Am. J. Orthod. Dentofacial Orthop.* 135 (2009) 603-612.

[8] N. Farhadian, A. Miresmaeili, B. Eslami, S. Mehrabi, *Am. J. Orthod. Dentofacial Orthop.* 133 (2008) 95-98.

[9] R. Garcia-Contreras, R.J. Scougall-Vilchis, R. Contreras-Bulnes, H. Sakagami, R.A. Morales-Luckie, H. Nakajima, *J. Appl. oral sci.* 23 (3) (2015) 321-328.

The Study of Stability and Coke Deposition of Micro, Meso, and Micro/mesoporous supported Ni Catalysts for Toluene Hydrogenation

Z. Mohammadian [1], M. H. Peyrovi [1] and N. Parsafard [2,*]

[1]*Faculty of Chemistry and Petroleum Sciences, Department of Petroleum Chemistry and Catalysis, University of Shahid Beheshti, Tehran,* 1983963113, *Iran*

[2]*Kosar University of Bojnord, Department of Applied Chemistry, North Khorasan,* 9415615458, *Iran*

** Corresponding author: n-parsafard@kub.ac.ir (N. Parsafard)*

Abstract: The hydrogenation of C=C bonds is one of the most low-cost methods to reduce the carcinogenic effect of VOCs. In this work, a series of micro, meso, and micro/mesoporous Ni supported catalysts were used for toluene hydrogenation. Physicochemical properties of these catalysts were characterized by techniques as XRD, FT-IR, XRF, IR-Py, NH_3-TPD, N_2 adsorption-desorption. The stability and selectivity of the prepared powders were investigated at 423 K and atmospheric pressure. The results indicate that the best performance obtains for the Ni/HMS catalyst after 12 h.

Keywords: Toluene hydrogenation; VOCs; Conversion; Selectivity; Coke deposition.

1. Introduction

Unsaturated compounds have highly toxic and carcinogenic effects. Also, according to the environmental laws, their concentrations in fuels should be reduced. Toluene is also one of the aromatic volatile compounds (VOCs) that has been widely studied in researches to reduce or eliminate it [1, 2]. The hydrogenation reaction is one of the most commonly used methods for eliminating unsaturated compounds. So in this project, we have been focused on this issue. The toluene hydrogenation has been done in the three-phase system (liquid feed, solid catalyst and hydrogen gas). We used various catalysts such as metal oxides, mesoporous, zeolites, and carbon materials for this catalytic hydrogenation. The hexagonal mesoporous silica (HMS) attracted the attention of researchers over recent years, due to the sponge-like structure and the formation of spherical pores with a two-dimensional hexagonal arrangement. One of the advantage of HMS is easy preparation by sol-gel method using inexpensive alkyl amine as a template at room temperature. In addition, HMS template walls are thicker than other meso materials. As a matter of fact, several metal nanoparticles (NPs) have been used extensively, however, Pt and Pd NPs are interested because of their significant conversion, but nickel NPs considered as a wise choice due to their cost-available and same functional in comparison with them [3-5]. The main objective of this study is to prepare a series of green, low-cost and efficient catalyst for toluene hydrogenation, which interestingly have been observed acceptable activity and coke-resistance over 12 h on stream.

2. Experimental Part

The catalytic behaviors of 25 wt% Ni supported catalysts were taken into account for the toluene hydrogenation reaction. A solution of $Ni(NO_3)_2.6H_2O$ (Merck) with appropriate concentration for 25 wt% loading of nickel was used for the impregnation of Al_2O_3, SiO_2, HMS, HZSM-5 and HZSM5/HMS (as ZH) supports [3,4]. The catalysts were mixed with this solution at room temperature. After evaporation of the solvent, these catalysts were dried in a static air at 110 ^oC overnight and calcined at 300 ^oC for 4 h.

The hydrogenation of toluene (Tu) to methyl cyclohexane was performed in a continuous fixed-bed micro reactor at a constant (atmospheric) pressure and 150 ^oC. This process was conducted over 0.5 g of each loaded catalyst with Tu and H_2 as feed. Before the catalytic test, the catalysts were reduced under H_2 flow with 40 mL min^{-1} rate in 400 ^oC for 2 h. The obtained results of each catalytic performance were recorded by online gas chromatograph. To investigate the stability of catalysts versus the effective factors in the deactivation of catalysts as coke deposition, all catalysts were tested for 12 h on feed stream.

Table 1. Physico-chemical properties of calcined catalysts.

3. Results and discussion

Catalysts	S_{BET} (m^2/g)	V_p ($cm^3.g^{-1}$)	d_p (nm)	AC (µmol/g)
Ni/HMS	763	0.74	3.9	65
Ni/ZH-40	674	0.58	3.4	237
Ni/HZSM-5	406	0.21	2.1	223
Ni/SiO_2	310	0.67	8.6	69
Ni/Al_2O_3	158	0.64	16.2	296

The catalysts that calcined were characterized by different analysis in order to identify their structural and surface properties. Their features are summarized in the Table 1.

The FT-IR spectra (not shown here) show the wide band in 3440-3600 cm^{-1} and 1625 cm^{-1} is related to Si-OH stretching vibrations and asymmetry stretching and bending mode of hydroxyl group. The peaks around 464, 1085 and 1230 cm^{-1} represent the asymmetric stretching and bending vibrations of ≡Si–O–Si≡ group in Ni/HMS catalyst. The symmetric and asymmetric stretching vibrations of Si-O-Si band around 802 and 1024 cm^{-1} reflect the zeolite structure. The peak at 1107 cm^{-1} is characterized for silica. The peaks at 845 and 812 cm^{-1} are regarded as stretching vibrations of Si–O that its bending mode is observed at 473 cm^{-1}. The weak bands at 570 and 730 cm^{-1} are related to γ-Al_2O_3 phase [3].

The XRD spectra (not shown here) show the main peaks at 37.2°, 43.2°, 62.7°, 75.2° and 79.4° indexed as the Ni phase. The low intensity peaks at 2θ of 37.6°, 46° and 68° are related to γ–Al_2O_3. The peaks at 2θ =1°–2°, 2.3° and 2.7° are attributed to 100, 110 and 200 planes of silica. Also this pattern exhibits a broad peak that characterized the amorphous silica at 2θ =23° [3].

The resistance of catalysts to poisoning by some factors such as hydrocarbons and sulfur compounds which are cause to changing the activity and selectivity of catalysts. To this aim, powders was stayed under stream for 12 h at 423 K. As can be seen in Figure 1, the maximum changes in the performance of the catalyst takes place in the first

two hours of experiment. The results showed that the conversion of all catalysts declined by increasing TOS and this reduction for Ni/ZH-40 catalysts is higher than others. Also, the highest conversion and selectivity are related to Ni/HMS catalyst (47%), respectively. According to the selectivity of catalysts, the best selectivity after 12 h is related to the Ni/HMS. Conforming to the occurred changes in the catalysts activities and the amount of coke deposition, Ni/HZSM5 catalyst showed better stability than other catalysts in this reaction without coke content.

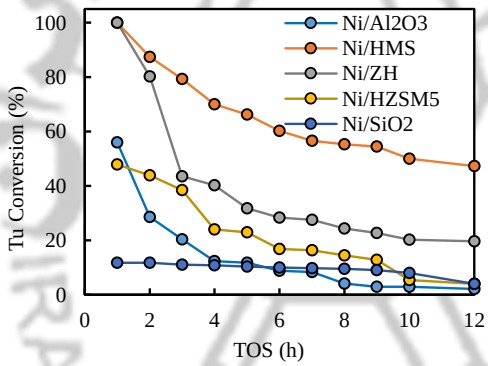

Figure 1. The effect of reaction time on toluene conversion over impregnated catalysts.

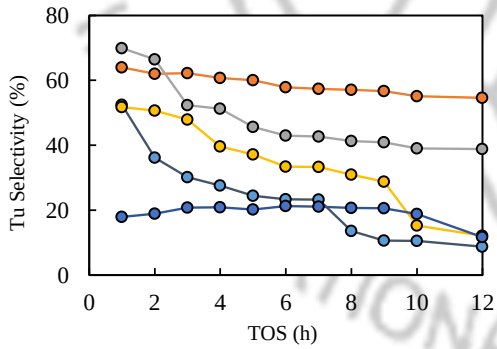

Figure 2. The effect of time on stream on toluene selectivity at 423 K for 12 h.

4. Conclusions

In summary, the various supports were prepared and their stability and coke deposition were evaluated at 423 K and atmospheric pressure in toluene hydrogenation. The results indicated that the maximum toluene conversion (>47%) and selectivity (>50%) were achieved over Ni/HMS.

References

[1] B. Chen, U. Dingerdissen, *Appl. Catal. A: Gen.* 280 (2005) 17-46.
[2] S.C. Qi, X.Y. Wei, Z.M. Zong, Y.K. Wang, *RSC Adv.* 3 (2013) 14219-14232.
[3] M. H. Peyrovi, N. Parsafard, Z. Mohammadian. *Chin. J. Chem. Eng.* 26 (2017) 521-528.
[4] N. Parsafard, M. H. Peyrovi, M. Rashidzadeh, *Micropor. Mesopor. Mat.* 200 (2014) 190-198.

5th Iran International Zeolite Conference

University of Tabriz, Tabriz, Iran

26-27 August 2018

Removal of drug from aqueous solution using zeolitic imidazolate framework including Iron (Fe-ZIF-8)

S. Amani[a,b], M. Rostamizadeh[a,b*]

[a] *Department of Chemical Engineering, Sahand University of Technology, Sahand New Town, East Azerbaijan, Iran*

[b] *Environmental Engineering Research Center, Department of Chemical Engineering, Sahand University of Technology, Sahand New Town, Iran*

**Corresponding author: Rostamizadeh@Sut.ac.ir*

Abstract: The purpose of this study is to investigate catalytic performance of heterogeneous zeolite catalyst (Fe-ZIF-8) for removing drug from the aqueous wastewater through Electro-Fenton (EF) process. Fe-ZIF-8 was synthesized at ambient temperature and characterized by X-ray diffraction (XRD) and acidimetric-alkalimetric titration method. The catalyst was able to remove 91% of the drug from the solution over a period of 60 min. The performance of the synthesized heterogeneous catalyst was investigated in neutral pH. The results showed that Fe-ZIF-8 had the great potential to remove drug from wastewater in neutral pH level.

Keywords: Electro-Fenton; Heterogeneous; Zeolite; ZIF.

1. Introduction

Toxicity, biodegradability and drug resistance have led to the use term "pseudo-polluting pollutants" for pharmaceutical compounds in the environment. These compounds can create potential hazards for aquatic and terrestrial organisms by entering the environment and natural water resources and humans in contact with them. Therefore, development of suitable, inexpensive, fast and recyclable wastewater treatment technologies is essential. One of these hazardous drug combinations is PHP with the chemical formula of $C_{11}H_{11}N_5 \cdot HCl$ [1]. EF process is a suitable method for treatment of wastewaters containing pharmaceutical compounds because, unlike other wastewater treatment methods such as membrane separation or adsorption, it does not only transfer pollution from one phase to another, but it is capable of completely eliminating the organic pollutions. In this study, zeolite based nanocatalyst with organic-metallic network (Fe-ZIF-8) is synthesized and its catalytic performance for removing pollutants at different pH levels is evaluated.

2. Experimental Part

Fe-ZIF-8 was synthesized by hydrothermal method [2]. XRD pattern of Fe-ZIF-8 were recorded by (D8 Advance Bruker AXS). Acidimetric-alkalimetric titration method determined point of zero charge (pH_{pzc}) for the nanocatalyst [3]. To measure PHP removal, the experiments were carried out in a 100 ml bubble reactor. Graphite electrodes, connected to

a DC power supply are attached to the edge of the beaker and partially immersed in 50 ml of aqueous synthetic wastewater solution containing 10 ppm of PHP, 0.05 M Na_2SO_4 as electrolyte and specified amount of catalyst. After connecting current between electrodes, 4 ml of the solution is taken up and centrifuged, every 15 minutes. After centrifuging, concentration of the sample is measured by UV-Vis spectrophotometer (2100, UNICO, USA) at 431 nm. PHP removal is calculated according to Eq.1:

$$\%\ PHP\ removal = \frac{C0-Ct}{C0} \times 100 \qquad (1)$$

3. Results and discussion

3.1. Catalyst characterization

Fig.1 shows the XRD pattern of Fe-ZIF-8. pH_{PZC} of Fe-ZIF-8 is equal to 8. Surface of Fe-ZIF-8 particles attain positive charge (excess of protons) at pH < pH_{pzc} and negative charge (lack of protons) at pH > pH_{pzc} which influences adsorption capacity of the nanocatalyst at different pH levels.

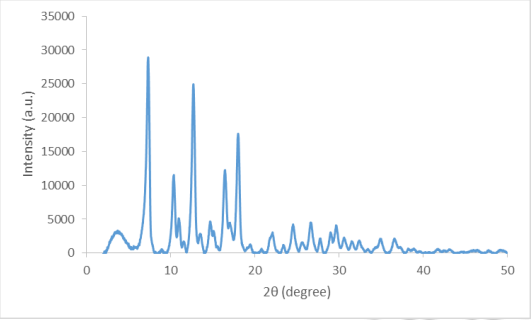

Figure 1. The XRD pattern of Fe-ZIF-8

3.2. Effect of pH

Solution pH is an effective factor due to dependency of hydroxyl radical OH° production on pH level and the sedimentation of Fe^{2+} as iron sludge in neutral pH levels. The highest activity of the EF is achieved near pH=3.5. This is due to reduced oxidation ability of OH radicals near the neutral pH levels and more stability at pH in 2~4 [4]. Moreover, the increase in alkalinity leads to reduced H_2O_2 stability [5]. Therefore, the strict acidic pH control is considered as a drawback of EF system. By comparing catalytic performance of Fe-ZIF-8 at pH 3-7 (Fig.2), it is clear that pH=3 results in the highest PHP removal. However, at pH=7, along with sharp reduction of OH oxidation ability and conversion of H_2O_2 to water, sharp reduction in the efficiency of EF for PHP removal is expected. Due to the enhanced adsorption of PHP molecules onto Fe-ZIF-8 particles as a result of electro-static forces generated between the positively charged Fe-ZIF-8 particles (pH_{PZC}=8) and the negatively charged PHP molecules (pKa=5.15), heterogeneous EF system catalyzed by Fe-ZIF-8 results in negligible drop in PHP removal at pH=7.

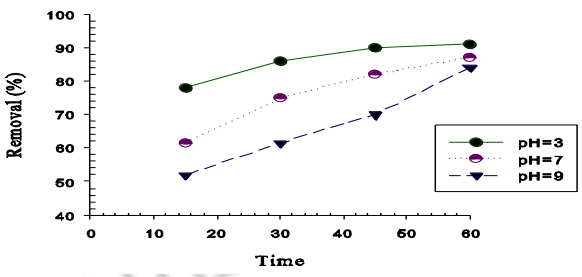

Figure 2. PHP removal efficiency using Fe-ZIF-8 at pH= 3 and7.

4. Conclusions

EF is a high-performance method for the removal of pharmaceutical compounds. Hydrothermally synthesized Fe-ZIF-8 was used as heterogeneous catalyst for PHP removal from aqueous solution in EF process. The degradation efficiency of PHP remained almost unchanged at neutral pH level, comparing with acidic pH level. The potential drawbacks of EF system such as catalyst separation after reaction and strict acidic pH control could be addressed through application of Fe-ZIF-8 as heterogeneous catalyst.

References

[1] A.R. Abbasi, S. Hatami, *J. Inorg. Organomet. P.* 27 (2017) 1941-1949.

[2] M. Thi Thanh, T. Vinh Thien, V. Thi Thanh Chau, P. Dinh Du, N. Phi Hung, D. Quang Khieu, *J. Chem.* 2017 (2017).

[3] R. Davarnejad, A. Sahraei, *Desalin. Water Treat.* 57 (2016) 9622-9634.

[4] B. Hou, H. Han, S. Jia, H. Zhuang, P. Xu, D. Wang, *J Taiwan Inst Chem E.* 56 (2015) 138-147.

5th Iran International Zeolite Conference

University of Tabriz, Tabriz, Iran

26-27 August 2018

Methanol to Highly Aromatic Gasoline Reaction over Ultrasound Assisted Co-impregnation Cu and Zn/HZSM-5 catalyst

Z. Taheri[a,*], E.Aghaei[b], L.Shirazi [a]

[a] *Research Institute of Petroleum Industry (RIPI), P.O.Box 14665-1998, Tehran, Iran*

[b] *Young Researchers and Elite Club, Kermanshah Branch, Islamic Azad University, Kermanshah,Iran*

**Corresponding author: taheriz@ripi.ir*

Abstract: To achieve the proper efficiency in the methanol to gasoline process, ZSM-5 was modified by metal doping with the aid of ultrasound. Type of metals impregnation (conventional method or by aid of ultrasound) had strong effects on phsico-chemical properties and catalytic performance. The XRD analysis showed crystallinity reduction by metals doping especially in the presence of ultrasound. The catalytic performance of catalysts were evaluated by conducting experiments at 375 ºC, WHSV 5.5 h-1 in a fixed bed reactor. The major products were aromatics hydrocarbons. In the impregnated samples by aid of ultrasound benzene formation strongly reduced relative to conventional impregnated sample. Based on the obtained results can be concluded that metal impregnation by aid of ultrasound, improve aromatic gasoline yield and reduce benzene formation. It is suggested that the ultrasound enhanced the synergetic effect of metals and acid sites, which was confirmed with low benzene production and high aromatic gasoline yield.

Keywords: Cu and Zn/HZSM-5; Ultrasound; Methanol; Methanol to Gasoline(MTG).

1. Introduction

The limited fossil fuel resources as well as political and environmental concerns have motivated the exploration of new sources for transportation fuels worldwide [1]. However, the proven reserves of fossil oil are expected to last only about a few more decades at the present rate of consumption. Therefore, searching for future energy sources as alternatives to crude oil is one of the most important issues [2].

Methanol can be produced from synthesis gas, which could be gained from many resources such as coal, natural gas or even biomass and industrial wastes. The MTG technologies mainly known as methanol-to-gasoline were regarded as new routes to convert methanol or renewable resources into high-octane gasoline [3].

Over the last few years, great attention has been paid to the use of ultrasound energy in material chemistry and considered a very interesting technique to prepare novel supported materials and catalysts [4].

According to the fact that catalytic process is a surface phenomenon, a sufficiently high dispersion of active metals is required. Among introduced methods, ultrasound-assisted synthesis seems an effective way.

2. Experimental Part

In order to produce HZSM-5, NH_4ZSM-5 was calcinated. Then, Cu and Zn metals were co-impregnated over HZSM-5 by aid of ultrasound or using conventional method. HZSM-5 was suspended in a beaker under stirring conditions and then, certain amount of zinc nitrate and copper nitrate were added. Then, ultrasound radiation applied to the solution and finally filtration, drying and calcination have been carried out.

3. Results and discussion

The XRD patterns of the synthesized catalysts and standard peaks of ZSM-5 (JCPDS number= 00-046-0751) are shown in figure 1. Peaks position of all the samples even metals co-impregnated sample with ultrasound power are in accordance with standard pattern of MFI framework. Co-impregnation of metals with conventional method and in the presence of ultrasonic caused peaks intensity reduction. This is due to interaction of metals with surface and crystals destruction in the presence of ultrasound.

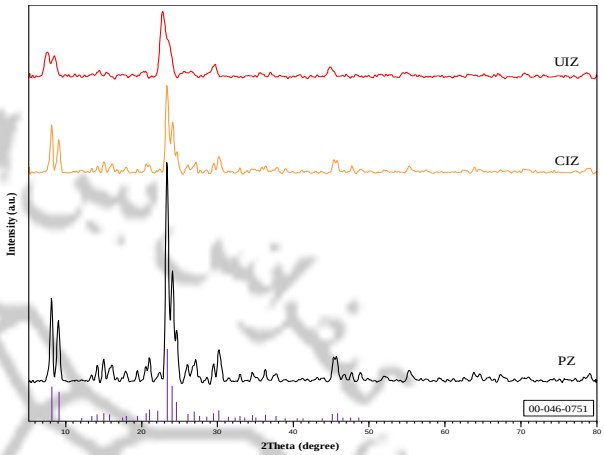

Figure 1. XRD patterns of parent HZSM-5 (PZ) and Cu-Zn/HZSM-5 synthesized with conventional impregnation method (CIZ) and ultrasound impregnated method (UIZ).

The FESEM images of the different samples are given in figure 2. It can be seen that the particles morphology were more irregular after Cu and Zn co-impregnation. For CIZ sample, small particles formation. In the presence of ultrasound, particles were aggregated that caused larger particles composed of irregular fine and rough surface particles ranged from 50 to 500 nm.

Aromatics and benzene selectivity with TOS over synthesized samples are shown in figure 3. The impregnated sample in the presence of ultrasound have higher aromatics selectivity and lower benzene formation compared with impregnated sample by conventional impregnation method.

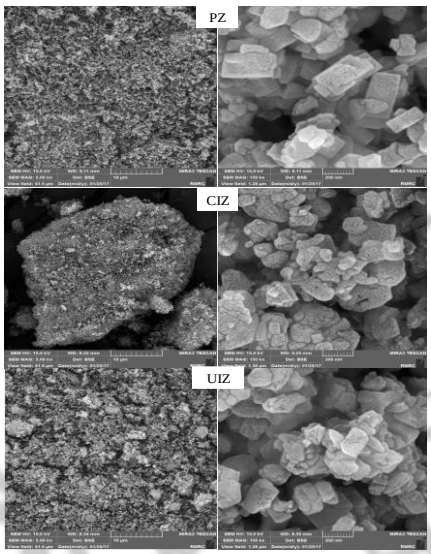

Figure 2. FESEM images of parent HZSM-5 (PZ) and Cu-Zn/HZSM-5 synthesized with conventional impregnation method (CIZ) and ultrasound impregnated method (UIZ).

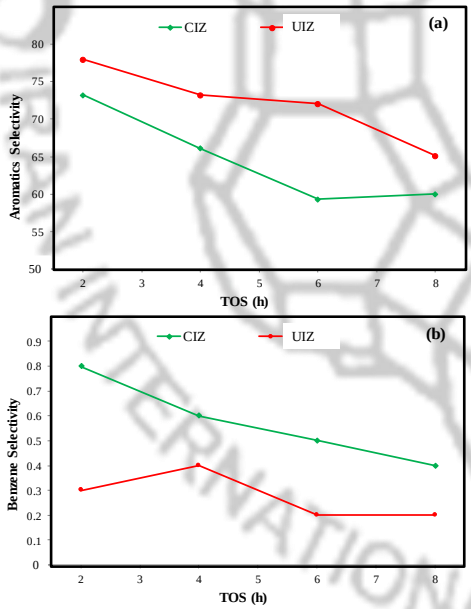

Figure 3. Aromatics and benzene selectivity with TOS over CIZ and UIZ.

4. Conclusions

Using ultrasound power for metals impregnation reduced crystallinity and produces small particles. Ultrasound radiation prevented aggregation of small particles. Using ultrasound due to well metal dispersion caused high aromatics selectivity and low benzene production.

References

[1] M. Li, Y. Huang, I.N. Oduro, Y. Fang, *Fuel Process. Technol.*, 149 (2016) 1-6.
[2] Y. Ni, A. Sun, X. Wu, G. Hai, J. Hu, T. Li, G. Li, , *J. Nat. Gas Chem.* 20 (2011) 237-242.
[3] M. Ghavipour, R.M. Behbahani, G.R. Moradi, A. Soleimanimehr, *Fuel*, 113 (2013) 310-317.
[4] R. Khoshbin, R. Karimzadeh, *Adv Powder Technol*. 28 (2017) 973-982.

5th Iran International Zeolite Conference

University of Tabriz, Tabriz, Iran

26-27 August 2018

Heterogeneous Electro-Fenton and Electro-Fenton-like process catalyzed by promoted ZSM-5 zeolite: effect of promoter nature

S. Gharibian[a,b], M. Rostamizadeh[a,b], H. Hazrati[a,b]*

[a] *Department of Chemical Engineering, Sahand University of Technology, Sahand New Town, East Azerbaijan, Iran*

[b] *Environmental Engineering Research Center, Department of Chemical Engineering, Sahand University of Technology, Sahand New Town, Iran*

** Corresponding author: H.Hazrati@sut.ac.ir*

Abstract: In this study we aim to evaluate effect of Fe and Mn impregnation on the ZSM-5 catalyst performance in removal of Methylene Blue (MB) through Electro-Fenton (EF) from aqueous wastewater. The zeolite catalyst was synthesized by hydrothermal method. The catalysts were characterized using X-ray diffraction (XRD) and acidimetric-alkalimetric titration method and N_2 adsorption-desorption. Impregnation of promoters modified the textural properties of catalysts. The results showed that Fe resulted in the higher MB removal compared with Mn.

Keywords: Advanced Oxidation Processes (AOPs); electro-Fenton; heterogeneous; Zeolite; transition metals

1. Introduction

Recently, EF process as a promising AOPs, due to, bio-compatibility, cost-effectiveness and high efficiency has been significantly improved. Potential drawbacks of homogenous EF, including, strict acidic condition control and inability to recycle catalyst could be addressed through utilization of heterogeneous catalyst [1]. Zeolites due to crystal cage-like structure and high specific surface area possess great potential as substrate for heterogeneous EF catalyst. Fe, as conventional catalyst of Fenton system could be included in zeolite particles structure through different methods, such as impregnation [2]. However, in order to fully understand mechanism of EF process, nature of promoter included in zeolite structure must be evaluated [3].

2. Experimental Part

The parent ZSM-5 was synthesized hydrothermally. Complete synthesize procedure is described in details, in our previous study [2]. Wet impregnation of parent catalyst resulted in bimetallic catalyst including 0.1%wt. metal promoter. After impregnation, catalyst was dried for overnight at 105 ^oC which followed by calcination at 530 ^oC (with a rate of 3 $^oC\ min^{-1}$) for 12 h under air flow. XRD experiments were carried out with a D8 Advance Bruker AXS X-ray diffractometer with Ni-filtered Cu Kα radiation (λ=0.15418 nm) at 40 kV. Acidity of catalysts were measured by Temperature

Programmed Desorption of Ammonia (NH_3-TPD, Micromeritics, USA). Specific surface area was measured using the N_2 adsorption–desorption technique at -196.2 °C (Quantachrome, USA). EF and EF-like processes were carried out in a bubble reactor using graphite as electrode. MB removal was determined using UV-Vis spectroscopy method (UNICO model UV-2100 spectrophotometer, USA) according Eq.1:

$$\%MB\ removal = \frac{C_0 - C_t}{C_0} \times 100 \qquad (1)$$

where C_0 and C_t are the MB concentration in initial wastewater and sample, respectively.

3. Results and discussion

The catalysts include MFI-structure of ZSM-5 in consistent with standard ZSM-5 (JCPDS: 00-044-0002) (Figure 1). The relative crystallinity of catalysts is the ratio of the peak area located at 2θ=22.5-24.5° in compare with the parent catalyst (ZSM-5).

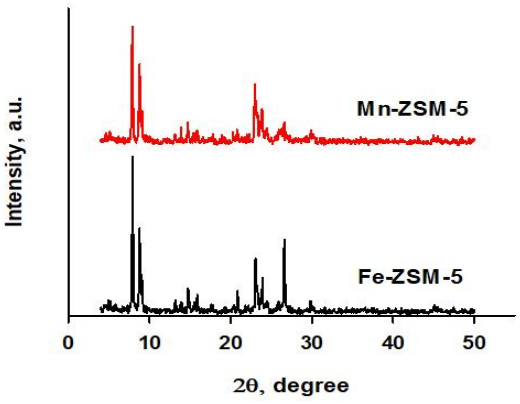

Figure 2. The XRD patterns of the catalysts

The reduction of BET surface area and pore volume for the bimetallic catalyst attribute to slightly micropore damage or pore blockages. The impregnation reduces the acidity of catalysts owing to the interaction of Fe species with zeolite framework.

Table 1. Relative crystallinity and textural data

Sample	Crystallinity (%)	S_{BET} (m^2g^{-1})	Acidity (mmol NH_3 g^{-1})		
			weak	Strong	total
ZSM-5	100.00	321.10	0.52	0.52	1.04
Fe-ZSM-5	72.41	294.40	0.41	0.52	0.93
Mn-ZSM-5	92.89	317.70	0.4	0.4	0.8

3.1. Catalytic performance

Effect of promoter nature was studied in order to fully understand mechanism of EF and EF-like process. Fe-ZSM-5 resulted in 91% MB removal in compare to 85% MB removal for Mn-ZSM-5. Better performance of Fe in MB removal could be explained by higher activation of MB molecules via complexion but, Mn affinity to absorb electrons is higher than Fe, due to higher redox potential ($E^0_{(Fe^{3+}/Fe^{2+})} = 0.77V, E^0_{(Mn^{3+}/Mn^{2+})} = 1.50V$) and this leads to faster regeneration of Mn[4]. This is clear from the results that difference between removal efficiencies of Fe and Mn decreases over time. These results, agree with results of Irmak et. al for degradation of 4-chloro-2-methlphenol by EF process replacing Fe with Mn[5].

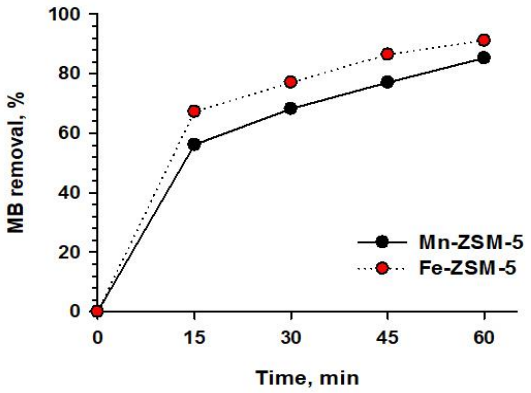

Figure 3. MB removal efficiency using ZSM-5 zeolite promoted by Fe and Mn.

4. Conclusions

In order to fully understand mechanism of EF and EF-like systems, effect of nature of ZSM-5 zeolite promoter was investigated by comparison between Fe and Mn active sites. It was determined that redox couple of metal plays in important role in catalytic performance of promoter. Thus, new method for improving efficiency of EF system for more efficient removal of pollutant is proposed in this study.

References

[1] P. Nidheesh, *RSC Adv.*, 51 (2015) 40552-40577.

[2] M. Rostamizadeh, A. Jafarizad, and S. Gharibian, *Sep. Technol*, 192 (2018) 340-347.

[3] N. Oturan, M. Zhou, and M.A. Oturan, *J. Phys. Chem. A*,. 39 (2010) 10605-10611.

[4] M. Pimentel et al., *Appl Catal B: Environ*. 83 (2008) 140-149.

[5] S. Irmak, H.I. Yavuz, and O. Erbatur, *Appl Catal B: Environmental*,. 63 (2006) 243-248.

Investigation on the Gross Teratopathogenic and Embryotoxic Effects of Nanozeolite on Chick Embryos in Ovo Environment

M.R. Amini[a], M. Hejazy*[b], Gh. Akbari [b], M. Moradi[c]

[a]*Faculty of veterinary medicine, university of Tabriz*

[b]*Basic science department, Faculty of veterinary medicine, university of Tabriz*

[c]*Pathobiologic department, Faculty of veterinary medicine, university of Tabriz*

**Corresponding Author: mhejazy@ut.ac.ir*

Abstract: In veterinary medicine, zeolites are used as animal feed additives, ammonia purification of fish and aquatic pools, animal smell and moisture control, harmful heavy metals and mycotoxins, and as a toxin binder. This study was designed to investigate the possible effects of nanozeolitis to investigate the development of embryonic chicken anomalies, tetratogenic and embryotoxic effects of nanozeolite. Eggs (120) were prepared from Ross breeder chickens and randomly divided into 4 groups of 30 (one control group and three experimental groups). In the control group, 0.3 ml of the physiologic serum was injected, and in the experimental groups, 0.3 ml of the solution of nanozeolitis (5, 50, 100 mg / L) injected into egg albumin, then the eggs were incubated for 19 days. Teratogenic effects were including deformity of legs and wings and liver and heart failure.

Keywords Nanoparticles; Embryotoxic; Teratogenic.

1. Introduction

Zeolites are crystalline aluminosilicate structures that have a porous structure and have the ability to absorb and release fluids and molecules that have a good diameter. Also, cationic exchanges are not subject to structural changes in the characteristics of zeolites [1]. The special physical and chemical properties of zeolites have made them suitable for industry, agriculture, veterinary and environmental applications. In animal medicine, animal feed additive, ammonia purification of fish and aquatic pools, control of the smell and moisture of pets (animal beds such as dogs and others), the absorption of harmful heavy metals and mycotoxins and is used as toxin binder [2].

Pregnancy is a critical period due to the organization of the molecular and cellular level and the high sensitivity of the embryo to environmental toxins. So that the formation of the organism is sensitive to any material that causes changes, and the embryo is sensitive to the effects of xenobiotic due to the lack of development of biotechnological pathways [3].

Chick embryo model is a convenient, simple and accessible model used in toxicological and toxicological studies to evaluate the toxic and teratogenic effects of the substance. Furthermore, the independence of the fetus from the mother and the rate of growth of the fetus can allow the immediate evaluation of the direct effects of nanomaterials on the fetus in a short time [4]. The aim of this study

was to evaluate the effects of embryotoxic and teratogenic nanoosolitis on chick embryos in ovo environment.

2. Experimental Part

The nanosoliths used in this research in sizes 80 to 100 nanometers were prepared by the Faculty of Chemistry of the University of Tabriz and its physical properties were evaluated by the Faculty of Chemistry. Broiler eggs (120) from the Ross breeder from the Incubation Company. the eggs were weighed and randomly divided into 4 groups of 30 (one control group and three experimental groups). In the control group, only 0.3 ml of physiologic serum will be injected. In the test groups, 0.3 ml of nano-soolitis solution (5, 50, 100 mg / L) to egg albumin (two-thirds of egg height). Chicken from a rounded end was injected using a 20 milliliter sterile syringe. The injection hole was covered with paraffin sterilized alcohol and incubated eggs at 37.5 ° C and 60% humidity. At end of incubation, the teratogenic effects of nanozeolite were investigated.

3. Results and discussion

In the administration of nano-zeolite, the embryo's eggs were smaller and significant morphological and anomalous changes were observed.19-day evaluations showed that the administration of nanozolite at doses of 5 and 50 mg /L resulted in rigid large yolk sac which not absorbed by the chick. Teratogenic effects were including deformity of legs and wings and liver and heart failure. The comparison between the three experimental groups shows that increasing the dose of zeolite increases toxic effects on the development of the fetus.

4. Conclusions

The study of fetal toxicity and its effects on the development of the fetus is very important because of the possibility of their passage from the dams.Nanoparticles can also cross the blood-brain barrier of the fetus and cause neurobehavioral neurobehavirol in the fetus and infants.The penetration of nanoparticles into different tissues and organs and blood flow and their effects on their longevity or their final effects should be studied in order to optimize their use and minimize adverse effects. More studies are needed to develop appropriate strategies to protect against the cytotoxic effects of nanoparticles. These strategies may include covering or other changes in the surface of the nanoparticles to enhance their safety. So far, a limited number of tests have been carried out in different models, so the possibility of comparisons is limited, and studies are required to address the toxic effects of the species. Because animal-dependent differences

in the toxicity of similar nano-particles have been observed in different species. In this case, chick embryos appear to be more resistant to exposure to nanoparticles. But dose dependent toxicity and tetratogenicity was observed in chicks.

References

[1] S. Salvestrini, P. Sagliano, P. Iovino, S. Capasso, C. Colella, *Appl. Clay Sci.* 49 (2010) 330-335.
[2] X. Karamanlis, P. Fortomaris, G. Arsenos, I. Dosis, D. Papaioannou, C. Batzios, A. Kamarianos, *Asian-Aust J. Anim. Sci.* 21 (2008) 1642-1650.
[3] U. Taylor, A. Barchanski, W. Kues, S. Barcikowski, D. Rath, *Reprod. Domest. Anim.* 47 (2012) 359-368.
[4] H. Rashidi, V. Sottile, *Bioessays* 31 (2009) 459-465.

Evaluation of Nanozeolite Administration on Viability and Development of Embryos Chicken Model

M. R. Amini[a], M. Hejazy*[b], Gh. Akbari [b], B. Divband[c]

[a]*Faculty of veterinary medicine, university of Tabriz*

[b]*Basic science department, Faculty of veterinary medicine, university of Tabriz*

[c]*Department of Inorganic Chemistry, Faculty of Chemistry, university of Tabriz*

**Corresponding Author: mhejazy@ut.ac.ir*

Abstract: The applications of nanoparticles in medicine, industry, and other branches related to humans, living organisms and the environment are very significant in light of the advancement of nanotechnology. The purpose of this paper is to investigate the effects of various nano-materials, in particular their toxic effects on fetal development, and the study of studies in this field. Accordingly, different protective strategies will be taken against the likely adverse effects. Broiler eggs (n=120) was purchased from the Ross breeder from the hatchery. The eggs were randomly divided into 4 groups of 30 (one control group and three experimental groups). In the control group, only 0.3 ml of physiological saline was injected, 0.3 ml of zeolite solution was injected into egg albumin in the test groups. Then the eggs were incubated for 19 days. At the end of the day, 20 incubations of live embryos were sacrificed and the embryos and organs (brain, heart, liver, spleen) were weighed.

Keywords: nanoparticles; Toxic effects; Fetal development.

1. Introduction

Given the small size of the nanoparticles, the surface area of the particles and their activity in unit weight will increase. The increasing expansion of nanotechnology has led to the use of nanoparticles in various medical and veterinary products and pharmaceutical and experimental products. A few nanoparticles with a diameter of 2-10 nm are used for imaging in evolutionary processes. However, there are still many uncertainties regarding the clinical aspects of the use of nanoparticles in clinical trials. Research has shown that nanoparticles can cause toxicity and oxidative stress in cell lines, in mammals and in aquatic animals [1-2]. The toxic effects of nanoparticles in addition to the chemical composition are caused by the size, shape and surface of the particles and combined with different materials. the independence of the fetus from the mother and the rate of growth of the fetus can allow the immediate evaluation of the direct effects of nano-materials on the fetus in a short time [3-4].

2. Experimental Part

Nano-zeolite used in this research in sizes of 15 to 30 nanometers was made by the Faculty of Chemistry of Tabriz University. Broiler eggs (n=120) from the Ross breeder from the Incubation Company. After 4 days, the eggs are weighed and randomly divided into 4 groups of 30 (one control group and three experimental groups). In the control group, only 0.3 ml of the physiologic serum will be injected, 0.3 ml of zeolite solution to egg albumin (two thirds of the egg height from the rounded end), using syringe Sterile 27 gauge will be injected 20 millimeters. The injection hole will be covered with sterile alcohol and will be covered with paraffin. Then the eggs are incubated at 37.5 ° C and 60% humidity and displaced once a day for 19 days. At the end of the day, 20 incubations will examine the growth rate of embryos inside the egg and their survival. Then, live embryos were sacrificed and the embryos and organs (brain, heart, liver, spleen, bursa of the fabercius) were weighed.

3. Results and discussion

The administration of nano-zeolite in the stages of development and development of chick embryos as a model for evaluating human embryonic damage has shown that an increase in the dose of nano-zeolite is associated with an increase in the mortality rate of embryos in different stages of growth and complications. 19-day evaluations showed that the administration of nano-zolite at doses of 5 and 50 mg / L resulted in increased viability and reduced side effects and increased the fetal mortality rate by 66% at a dose of 100 mg / l. The results showed that nanozeolite decreased significantly the spleen weight dose dependently ($P<0.05$). Nanozeolite also increased the embryos weight significantly at the dose of 5mg/L but at the higher doses the weight decreased significantly($P<0.05$). It also decreased the liver weight at the dose of 5mg/L, but at the higher doses the liver weight decreased. Nanozeolite have elevated the brain weight at the dose of 5 mg/L($P<0.05$). The weight changes of burs of fabersious and heart was not significant in treated groups. The comparison between the three experimental groups shows that increasing the dose of zeolite increases toxic effects on the development of the fetus.

4. Conclusions

The penetration of nanoparticles into different tissues and organs and blood flow and their effects on their longevity or their final effects should be studied in order to optimize their use and minimize adverse effects. It should be noted that not only the chemical composition but also the physical parameters will affect the final

toxicity, but the way of administration and the way of entering organisms varies among different species, which will affect the toxicity of nanoparticles in that species. Several questions have been raised about the safety of nanoparticles that have become unresponsive, which should be addressed promptly in light of the increasing use of nanoparticles in medicine and veterinary medicine.

References

[1] Y. Baratli, A.-L. Charles, V. Wolff, L. Ben Tahar, L. Smiri, J. Bouitbir, J. Zoll, M. Sakly, C. Auger, T. Vogel, *BioMed research international* 2014 (2014).
[2] N. von Moos, V.I. Slaveykova, *Nanotoxicology* 8 (2014) 605-630.
[3] C.M. Coleman, *Birth Defects Res. C. Embryo Today Rev.* 84 (2008) 245-256.
[4] H. Rashidi, V. Sottile, *Bioessays* 31 (2009) 459-465.

Removal of Abamectin from Wastewater by Iron-modified Bentonite

M. Moosavifar,* M. Dibazar, T. Sharifi

[a]*Department of Chemistry, Faculty of Science, University of Maragheh, P.O. Box 55181-83111, Maragheh, Iran*

**Corresponding author: m.moosavifar90@gmail.com*

Abstract: This paper aims to investigate the effect of modified bentonites removal of Abamectin from wastewater. In this paper, modified kaolin with Fe^{2+} was prepared and the physicochemical property was studied by FT-IR, XRF, XRD, FESEM and EDS technique. The effect of several parameters including concentration of pesticides, contact time, H_2O_2 concentration and pH effect were also studied. Mineralization of organic compound was verified by measuring of COD in the beginning and at the end of reaction. Conclusion: As a result, the application of this method is recommended for removing toxins from aqueous environments.

Keywords: Pesticides; Hydrogen peroxide; COD.

1. Introduction

Today, the importance of water as a living fluid in dry and developing countries is more and more understandable [1]. Limitation of water resources, lack of rainfall, the risk of a water crisis in the country and the importance of water reuse on the one hand and increased pollution of surface water and underground water. Agricultural activities, on the other hand, need to find suitable solutions for removing or reducing pollutants from wastewater and water resources [2].

2. Experimental Part

This experimental study was applied to provide an academic system for the removal of abacomycin from aqueous solution using Fenton process on a laboratory scale in a UV-based reactor. The chemicals used in this study were abamectin, bentonite, sodium chloride, iron chloride, and oxygenated water from Merc Co. Spectrophotometer (uv) was used at ambient temperature of 258 nm to measure the concentration of abacomycin. The pH meter has been used to determine the pH of the solutions.

3. Results and discussion

Advanced oxidation process under laboratory conditions is an effective method for removing abatmetic pesticide from solutions. One of the most important criteria for choosing this method is economics and some of the green methods.

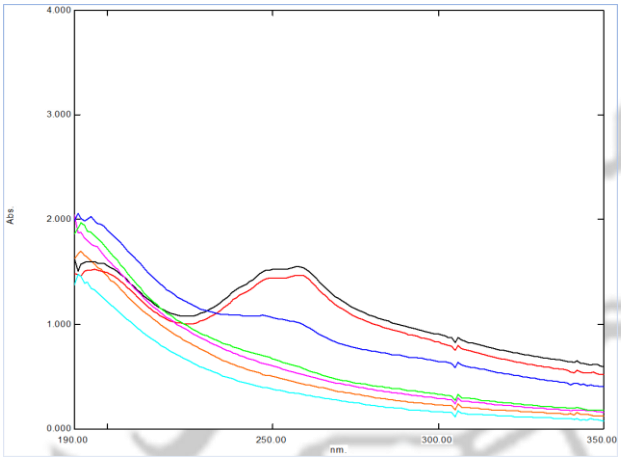

Figure 1. Effect of Contact Time on the Effectiveness of Abamectin Removal 100ppm and pH = 7

Descriptions of tables should be placed just above of each table.

Table 1. Abamectin absorption at different pH

Sample	pH	Absorb
1	7	0.33
2	2	0.25
3	12	0.4

4. Conclusions

The results of this study showed that bentonite is capable of removing toxins from aqueous media with high efficiency.

References

[1] M. Vagı, A. Petsas, *Advanced Oxidation Processes for the Removal of Pesticides from Wastewater: Recent Review and Trends,* 15th International Conference on Environmental Science and Technology. CEST2017, Rhodes, Greece, 2017.

[2] S. Brand, M.P. Schlüsener, D. Albrecht, U. Kunkel, C. Strobel, T. Grummt, T.A. Ternes, *Water Res.* 136 (2018) 207-219.

Removal of Abamectin from wastewater by iron-modified kaolin

M. Moosavifar*, T. Sharifi, M. Dibazar

aDepartment of Chemistry, Faculty of Science, University of Maragheh, P.O. Box 55181-83111, Maragheh, Iran

**Corresponding author: E-mail: m.moosavifar90@gmail.com*

Abstract: The development of new photochemical methods for the decontamination of wastewater containing significant concentrations of aromatic pesticides is described. The chemical method which used in this work is based on the Fenton process. In this paper, kaolin was modified by Fe^{2+} ion exchange. The obtained catalyst characterized by XRD, FT-IR, FESEM and EDX technique. The catalytic activity of catalyst investigated in the removal of abamectin. The effect of several parameters, including pesticide contamination concentration, pH, catalyst amount and H_2O_2 concentration was studied in the removal of contamination. COD analysis proved the mineralization of abamectin. Pseudo-first order kinetic suggested for the degradation of pesticide. The results of degradation showed the modified catalyst is an effective photocatalyst for removal of abamectin from wastewater.

Keywords: Wastewater, Photocatalyst, abamectin, Modified kaolin

1. Introduction

A vast variety of pesticides are used for agricultural pests in our country. The release of these persistent organic pollutants [1]. into water supplies leaves adverse effects on both the environment and public health. Advanced oxidaon processes have been used recently for pesticide removal [2]. In this research, the combined UV/H_2O_2 process has been investigated for the removal of abamectin by modified kaolin. In this survey, samples have been prepared with different amounts such as: concentrations, PH, H_2O_2 and photocatalyst.

Residual concentrations were determined using UV spectrum. Based on the results, increasing pH reduced pesticide concentration and increased contact time had a direct effect on enhancing removal efficiency. The combined UV/H_2O_2 process was found to have a high efficiency in degrading abamectin based on our results, this method may be suggested for the removal of pesticides from aqueous solutions.

2. Experimental Part

2.1. Materials and apparatus

All reagents and chemicals were supplied by Merck and Sigma Aldrich Company (American) and were used without any further purification Phosalone pesticide was purchased from gol sam Company

(Iran). All the solutions were prepared, using deionized water and their concentrations were analyzed and using a UV–Vis spectrophotometry.

3. Results and discussion

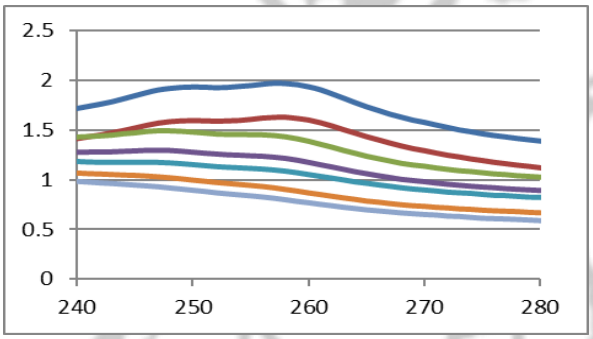

Figure1. Effect of varios amount of photocatalyst 4-NP:100 ppm, pH =8, contact time = 180 min.

Table 1. Example of absorbance of modified kaolin.

Sample	photocatalyst	Amount of absorb
1	0.02	0.79
2	0.04	0.82
3	0.06	0.43
4	0.08	0.45
5	0.1	0.62

4. Conclusions

Considering the results, the optimum process was chosen. The increase in photocatalyst and concentration significantly increases and subsequently leads to a decrease in efficiency. A significant percentage of abamectin is decomposed early in the reaction. The results of this study show The Fenton process with iron modified kaolin has a good effect on abamectin removal and can be selected as an appropriate method.

References

[1] E. H. Hicham, J. Bakouri Morillo, A. Ouassini, *J. of Hydrology*, 353 (2008) 335- 342.

[2] F. J. Benitz, J. L. Acero, F. J. Real, *J. of Hazardous Materials*, 89 (2002b) 51-65.

The efficiency of surfactant-modified zeolite ZSM-5 for oxidative desulfurization of dibenzothiophene

S. Shouhani[1,2], N. Rahemi[1,2], S. Allahyari[1,2]

1- Chemical Engineering Faculty, Sahand University of Technology, Sahand New Town, Tabriz, Iran.

2- Environmental Engineering Research Centre, Sahand University of Technology, Sahand New Town, Tabriz, Iran

**Corresponding author: Sepid.anjello@yahoo.com*

Abstract: In this study, the ability of surfactant-modified zeolite (SMZ) to remove Dibenzothiophene (DBT) from oil model was investigated. Zeolite was modified with four different natural surfactants including Ziziphus Spina Christi, Liquorice, Rosemary, and Tragacanth. The zeolite bed that was modified at 1 g Rosemary concentration showed good performance in removing DBT. In fact, our research has been using a different surfactant to prepare various ZSM-5 based heterogeneous catalysts to produce low-sulfur fuels combining liquid-liquid extraction and oxidative processes.

Keywords: Zeolite; Surfactant; ODS; ZSM-5; Nano-Catalyst

1. Introduction

With the rapid expansion of the global industry and the growing trend of means of transportation, the consumption of hydrocarbons worldwide has increased dramatically. The problem facing the refining industry today is an increase in demand for the production of very low and high-quality sulfur fuels in the transportation industry such as gasoline, diesel and jet fuel, which are a major part of energy supply, responsible for Sulfur compounds and can be considered undesirable in petroleum fuels and cause many problems, both economically and environmentally. In recent years, there have been a lot of changes in environmental regulations to protect the health and prevent the threat of contaminants from the combustion of fuel [1]. Various processes have been used to reduce the sulfur content of fuels, some of which are catalytic and some non-catalytic so that in recent years, zeolite catalysts have been used for more desulfurization. The porous structure of zeolites, the density of acid sites, high strength, distribution of acid sites, and the interaction between the base and the metals are factors that influence the activity, selectivity, and stability of zeolite catalysts [2]. In fact, zeolites are acid catalysts capable of defeating the hydrogen bond, and therefore, these types of catalysts, which are formed from intermediate metal sulfide on zeolites, can be used for deep desulfurization processes [3].

2. Experimental Part

2.1. Synthesis of ZSM-5

The synthesis of ZSM-5 nanostructures was carried out by mixing 0.018 g $NaAlO_2$, 0.113 g NaOH and 1.7 ml water with magnetic stirring for 15 minutes. Subsequently, 1 g of natural surfactant was added to the mixture (Solution 1). Then, 2.7 g SiO_2, 0.113 g NaOH and 7 ml water together solved (Solution 2). Solution 1 slowly was added to Solution 2 and the resulting mixture was stirred for 1 h. The mixture was maintained at 180 ˚C in an autoclave for 48 h on the oven.

The mixture was filtered, washed with distilled water to remove the impurities, followed by drying at 100 ˚C for 12 hours. Finally, the product was calcined under static air at 540 ˚C for 24 hours.

2.2. Catalyst preparation

For the preparation of the catalysts, 1.7 g concentrated ZSM-5 and 0.3 g Phosphotungstic acid was dispersed in 40 mL of distillate water under stirring at 60 ˚C. Then, drying of the mentioned catalysts at 60 ˚C for 24 hours was performed.

2.3. ODS Process

In a typical reaction, 0.2 g of each catalyst were separately added to a solution containing 500 ppm dibenzothiophene (DBT) in n-hexane and the mixture was stirred at 60 ˚C for deferent time. The oxidation of model oil into the corresponding sulfone or sulfoxide using H_2O_2 as the oxidant was performed. After the required time (30, 45, 60 and 75) the mixture was cooled rapidly to room temperature, transferred to a separating funnel and the upper phase (model oil) was withdrawn. The ODS studies were carried out in a biphasic system using model diesel/extraction solvent (Acetonitrile) ratios 1:1.

The extracted sample was analyzed by UV_{328} to determine the concentration of sulfur in the model oil. Then % removal of sulfur was calculated by the following equation:

$$Conversion.(\%) = \frac{[DBT]_i - [DBT]_f}{[DBT]_i} \times 100$$

Where $[DBT]_i$ is the blank sample (without catalyst), and $[DBT]_f$, is the catalytically oxidized DBT [4].

3. Results and discussion

The effect of reaction temperature on desulfurization was studied. Fig. 5 showed the removal content of DBT with reaction time over various catalysts. In the case of zeolite modified with Ziziphus Spina Christi and Tragacanth, there is no significant removal percentage and we can observe the alternate process of elimination. The zeolite that has been modified with Liquorice has reduced by increasing the reaction time. Rosemary modified zeolite has also been increasing and decreasing frequency, however, it has the highest absorption percentage. Maximum removal of DBT was observed at 75 min with the zeolite modified with rosemary surfactant are shown in Fig 1.

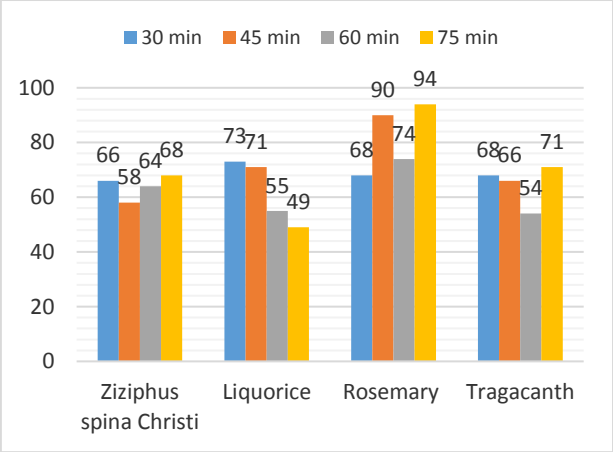

Figure 1. Percentage of DBT removal based on the type of surfactant at different time

4. Conclusions

It was established that the total removal of DBT can be achieved by performing the reaction at optimized conditions of 60 ˚C for 75 minutes with rosemary as a surfactant.

References

[1]. I. Shimoyama ،Y. Baba, *J. Carbon* (2016) 115-125.

[2]. F. Yu, C. Liu, B. Yuan, P. Xie, C. Xie, S. Yu, *J.* Fuel 177 (2016) 39–45.

[۳] خشایار شریفی، سید جاوید روئیایی، رویین حلاج، امیر اتابک اسدی،" مروری بر کاتالیست های مورد استفاده در گوگرد زدایی از خوراک نفتا پالایشگاه"، سومین کنفرانس بین المللی دستاوردهای نوین پژوهشی در شیمی و مهندسی شیمی، مهر ماه ۱۳۹۵، تهران

[4]. W. Abdul-Kadhim, M. Asyrak-Deraman, Efficient and Reusable Iron-Zinc Oxide Catalyst for Oxidative Desulfurization of Model Fuel, page 8, 2017.

Preparation of Solid hybrid catalyst (HY@NH_2@SO_3H) and its application in synthesis of coumarin

M. Zendehdel [a], F. Tavakoli [a] *

[a] *Department of Chemistry, Faculty of Science, University of Arak, Arak 38156-8- 8349, Iran*

**Email: F.Tavakoli20@yahoo.com*

Abstract:

Solid hybrid catalysts, are regarded as an important class of catalysts. In this work, HY zeolite has been functionalized by trimethoxysilyl propyl amine. Then, the amine group has been sulfonated by chloro sulfonic acid. All steps have been characterized by FT-IR, XRD, SEM analysis. After the characterization of the (Z-HY@NH_2@SO_3H) catalyst, its catalytic activity was evaluated for the synthesis of Coumarin.

Keywords: Zeolite HY, Hybrid catalyst, Functionalize, Sulfamic acid, Coumarin.

1. Introduction

In the synthesis of complex organic molecules like natural products, protection of functional groups plays a critical role. Functionalized Zeolites usage as useful heterogeneous catalysts in organic synthesis have been in the center of attention due to their unique physical and chemical features namely acidic and basic nature, shape selectivity, micro porosity and thermal stability [1,2].

Coumarin and its derivatives form an elite class of compounds; they represent the ring systems of several important groups of natural products [3]. They have been used as anticoagulants [4,5], additives in food and cosmetics, and in the preparation of insecticides, optical brighteners and dispersed fluorescent and laser dyes [6].

2. Experimental Part

Preparation of HY Zeolite

2 gr of NaY Zeolite was added to NH_4Cl solution (0.002 M) and stirred for 24 hours. The solid filtered and washed with water. Then, the powder was calcinated in 300 ˚C for 5 h.

Preparation of HY/NH_2/SO_3H

To a mixture of HY zeolite in toluene, trimethoxysilyl propylamine was added and stirred for 24 hours in reflux condition. Then zeolite was filtered and dried at 60 ˚C. For solfonation, chlorosolfonic acid and triethylamine was added to a mixture of functionalized zeolite (1 gr) in toluene (20

mL) and stirred at reflux condition for 24 hours. Then, solfonated zeolite was filtrated and dried.

3. Results and discussion

Zeolites have been used as heterogeneous catalyst in many organic reactions. In this work we first Preparation HY zeolite then, HY zeolite has been functionalized by trimethoxysilyl propyl amine. Then, the amine group has been sulfonated by chloro sulfonic acid. All steps have been characterized by FT-IR, XRD, SEM. All analysis confirmed that the catalyst has been synthesized successfully. The FT-IR spectra of (Z-HY@ NH_2@SO_3H) shown in **Fig. 1**, that indicate an intense band about ca.1056 cm^{-1} attributable to the asymmetric stretching of Al–O–Si chain of zeolite, and also symmetric stretching and bending frequency bands of Al–O–Si framework of zeolite appear at ca.782 and 463 cm^{-1}, respectively. S=O stretching appeared at 1161 cm^{-1}, and O–H group appeared at 3400–3500 and 797 cm^{-1}.

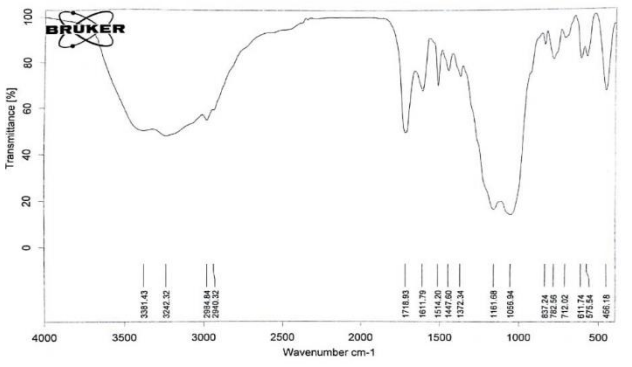

Figure 1. The FTIR of Z-HY@NH_2@SO_3H

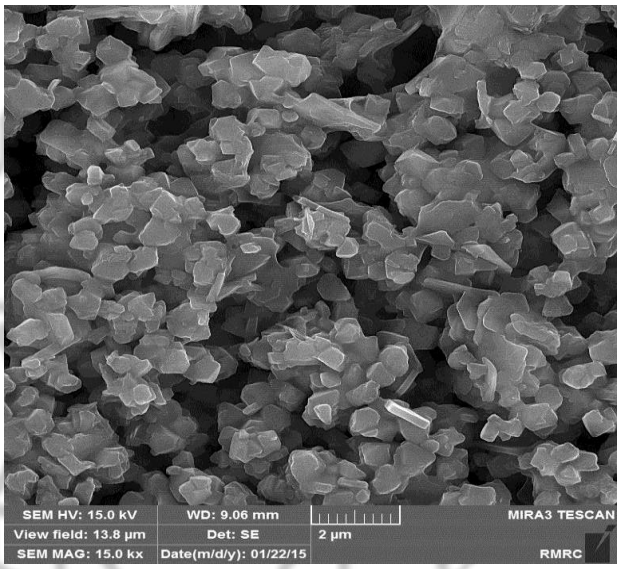

Figure 2. The SEM image of Z-HY@NH_2@SO_3H

In Fig.2, we have seen the FESEM micrographs of the (Z-HY@NH_2@ SO_3H) catalyst. The particle sizes are around 200 nm and this decrease of size for modified zeolite is due to the complex formation on the support [7]. According to similar studies, in the XRD patterns of zeolite HY and (Z-HY@NH_2@SO_3H) in the present study no changes were detected in the crystalline structure and morphology of zeolite during the immobilization procedures, also the percentage of amorphous phase is small [8,9].

4. Conclusions

We modified and tested Solid hybrid catalysts (HY@NH_2@SO_3H) as a new, heterogeneous, highly

efficientand environment-tally friendly catalyst for synthesis of coumarin.

Acknowledgments

The authors thank Arak University for the scientific and instrumental support.

References

[1] A. Corma, *Chem. Rev*. 95 (1995) 559–614.

[2] C.M.B. Line, G.J. Kearley, *Chem. Phys*. 234 (1998) 207–222.

[3] M.M. Heravi, M. Khorasani, F. Derikvand, *Catalysis Communications*, 12 (2007) 1886-1890.

[4] A.K. Mitra, A. De, N. Karchaudhuri, S.K. Misra, A.K. Mukopadhyay, *J. Indian Chem. Soc*, 75 (1998) 666.

[5] G. Cravotto, G.M. Nano, G. Palmisano, S. Tagliapietra, *Tetrahedron*: *Asymmetr.*, 12 (2001) 707.

[6] (a) G. Jones, *Org. React*, 1967 (15) 204;

(b) F. Bigi, L. Chesini, R. Maggi, G. Sartori, *J. Org. Chem*, 64 (1967) 1033.

[7] L. Ma'mani, M. Sheykhan, A. Heydari, M. Faraji, Y. Yamini, *Appl. Catal. A*, 377 (2010) 64–69.

[8] X.N. Zhao, H.C. Hu, F.J. Zhang, Z.H. Zhang, *Appl. Catal. A: Gen.*, 482 (2014) 258–265.

[9] S. Mandal, D. Roy, R. V. Chaudhari, and M. Sastry, *Chem. Mater*, 16 (2004) 3714-3724.

Effect of aging types on the purity and particle size of synthesized NaX via hydrothermal method

R. Javani[a,b] , S. Darvishi Gilan[a,b] , A. A. Babaluo[a,b]*

[a] *Chemical Engineering Department, Sahand University of Technology, Tabriz, Iran*

[b] *Nanostructure Materials Research Center(NMRC), Sahand University of Technology, Tabriz, Iran*

**Corresponding author: a.babaluo@sut.ac.ir*

Abstract: NaX zeolite particles were synthesized by in situ hydrothermal method and effects of static and rotary aging type on the synthesis was investigated. The SEM images showed the synthesized zeolite particles under the rotary aging condition have better crystals intergrown rather than the synthesized under the static aging condition. Also, these images depicted the LTA phase formation under static aging condition. Furthermore, size of NaX zeolite particles was measured by PSA. The results showed the synthesized zeolite particles under the rotary aging condition with the maximum particles size distribution of 616 nm are smaller than the synthesized zeolite particles under the static aging condition with the maximum particles size distribution of 862 nm.

Keywords: NaX zeolite, aging time, rotary condition, static condition

1. Introduction

The NaX zeolite with the specific framework composed of linking sodalite cavity through double six-rings which create a large super cage cavity, among various types of zeolites offers a large pore diameter (0.74nm). Because of its well-defined structure, large pore volume, and appropriate ion exchange capability. This zeolite is widely employed as ion-exchanger, absorbent and catalyst [4-6]. Most applications of zeolites are closely related to their framework, shape and particulate properties. Recently, many attempts are shown that the crystallization and aging time of reaction mixture had very important effects on the zeolite synthesis [7].

Shafiei et al. have reported successful synthesis of X zeolite with 2 h rotating aging with synthesis time of 8 h at the temperature of 95°C with the molar composition of Al_2O_3:5SiO_2:50Na_2O:1000H_2O [8]. Zhu et al. studied the effects of temperature and aging on the X zeolite synthesis with the composition of 65Na_2O:1Al_2O_3:10SiO_2:2000H_2O [7]. For this purpose, the temperature of aging time ranging from 30 to 60°C and the time in the range of 0-24 h were examined. Studies showed that the increase of aging time for each aging temperature decreases the formation of LTA phase. Also, the higher applied temperatures, i.e., 50 and 60 °C, were more desirable to reduce the formation of another phases [3]. As shown, aging time can cause the synthesis with high

purity which can also be explained by the accelerated crystallization [9]. Up to now, among various studies, there is no report on the effects of rotary and static aging time on the X-type zeolite synthesis. Static aging time can cause the inhomogeneous reaction pool resulting in the as-synthesized phases synthesis.

In this study, effect of various aging type, rotary and static aging, on the purity and particle size of synthesized NaX zeolites prepared via hydrothermal method was investigated.

2. Experimental

The NaX zeolite particles were synthesized using the hydrothermal method. The clear solutions, with the molar compositions of $65Na_2O:1Al_2O_3:10SiO_2:2000H_2O$ were prepared by dropwise adding aluminate solution into silicate solution. Two synthesis solutions with above compositions under rotary and static aging time were aged at ambient temperature for 24 h, respectively. For each condition, the synthesis solution was poured into a Teflon holder in the conventional autoclave. Then hydrothermal synthesis condition began by applying the temperature of 100 °C for 5 h.

The zeolite particles were characterized by scanning electron microscopy (SEM) and particle size analyzer.

3. Results and discussion

3.1. Aging type effect on the synthesis purity

Figures 1 and 2 show the SEM images of the synthesized particles at different aging types.

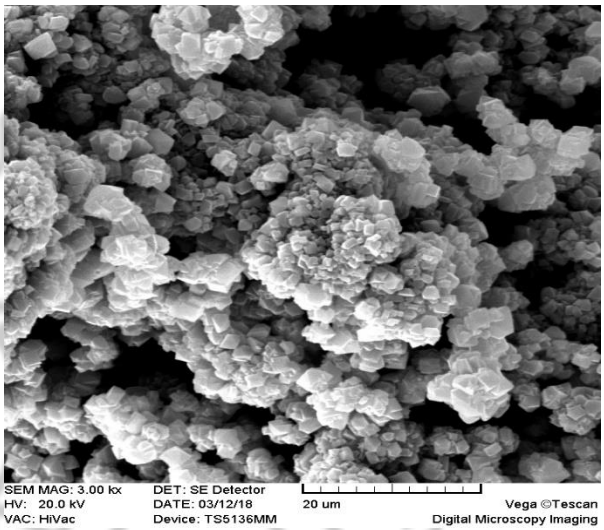

Figure 1. SEM image of the synthesized particles under rotary aging condition, 25°C

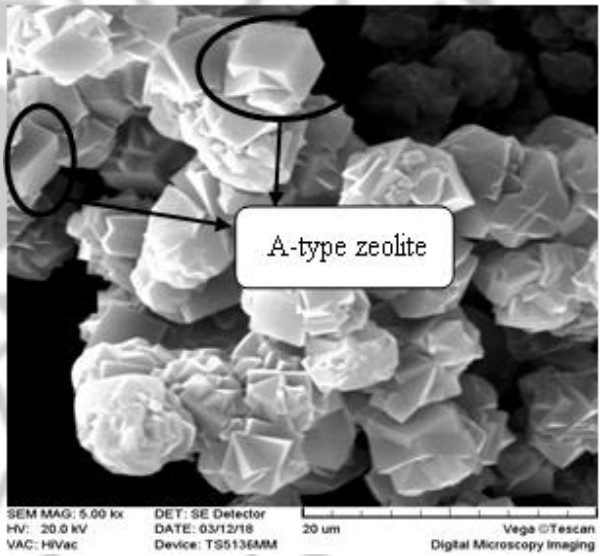

Figure 2. SEM image of the synthesized particles under static aging condition, 25°C

As shown, the synthesized zeolite particles under the rotary aging condition have better crystals intergrown and purity rather than the synthesized

particles under the static aging condition. These images depict the LTA phase formation under static aging condition that is due to lack of suitable stirring.

3.2. Aging type effect on the synthesized particles size

The results of PSA showed the synthesized zeolite particles under the rotary aging condition with the maximum particles size distribution of 616 nm that are smaller than the synthesized zeolite particles under the static aging condition with the maximum particles size distribution of 862 nm. This smaller particles size distribution is due to the appropriate aging condition that by accelerating the crystallization rate and the control of the number of nuclei can be achieved.

4. Conclusions

The synthesized zeolite particles under static aging contain LTA phase, whereas rotary aging could effectively overcome the formation of LTA phase. The better crystals intergrown and purity of the synthesized particles under the rotary aging condition is due to the homogeneous reaction pool with the suitable stirring. Also, the smaller particles size distribution of the synthesized zeolite particles under the rotary aging condition is achieved by accelerating the crystallization rate and the control of the number of nuclei.

References

[1] X. Zhang, D. Tang, M. Zhang, R. Yang, *Powder Technol.* 235 (2013) 322–328.

[2] H. Kazemian, H. Modarress, M. Kazemi, F. Farhadi, *Powder Technol.* 196 (2009) 22–25.

[3] Y. Yan, T. Bein, J. Am. Chem. Soc. 117 (1995) 9990–9994.

[4] M. Ansari, A. Aroujalian, A. Raisi, B. Dabir, M. Fathizadeh, *Adv. Powder Technol.* 25 (2014) 722–727.

[5] L. Tosheva, V.P. Valtchev, *Chem. Mater.* 17 (2005) 2494–2513.

[6] C.S. Cundy, P.A. Cox, *Chem. Rev.* 103 (2003) 663–701.

[7] G. Zhu, Y. Li, H. Chen, J. Liu, W. Yang, *J. Mater. Sci.* 43 (2008) 3279–3288

[8] K. Shafiei, S. G. Pakdehi, M. Kazemi Moghaddama, T. Mohammadi, *Separ. Sci. Technol.* 50 (2015) 136-140.

[9] A. van Niekerk, J. Zah, J.C. Breytenbach, H.M. Krieg, *J. Membrane Sci.* 300 (2007) 156-164.

5th Iran International Zeolite Conference

University of Tabriz, Tabriz, Iran

26-27 August 2018

A Temperature Programmed Desorption (TPD-CO_2) Investigation on NaY, DEA-NaY and Aminosilane-NaY

M. Tajbakhsh Jadidi*, M. Fakhimi Abarghouei, H. Alinejad, K. Niknam

Department of Organic Chemistry, Faculty of Chemistry, University of Mazandaran, Babolsar, Iran

**Corresponding author: tajbaksh@umz.ac.ir*

Abstract: In this Study, a new synthesized Y-type zeolite (NaY) was modified with diethanolamine and 3-aminopropyltrimetoxysilane, in order to probe the influence of the modification of the adsorbent's surface on CO_2 desorption. The surface nature of NaY was changed after modification, which causes a significant increase in the CO_2 adsorption capacity. The CO_2 adsorption capacity of the modified NaY increased with temperature. The adsorbents were characterized by TPD-CO_2 Technique. These results showed that functionalized NaY zeolites have excellent potential for CO_2 adsorption at high temperatures.

Keywords: CO_2 desorption; TPD-CO_2; Y-Type Zeolite; Diethanolamine, 3-aminopropyltrimetoxysilane.

1. Introduction

CO_2 is the major Greenhouse Gas (GHG), which may cause undesired consequences to the environment, such as global warming.CO_2 behaves like a blanket, entraps the infrared radiations coming from the earth's atmosphere, and results in an increase in the earth's surface temperature [1]. The concentration of CO_2 has increased from about 280 ppm to the current amount of 380 ppm. The development of CO_2 capture and separation technologies is the solution to overcome this global problem [2].

2. Experimental Part

This work explores the modification of the surface of a new synthesized Y-type zeolite by DEA and 3-Aminopropyltrimetoxysilane has been selected as modification materials for NaY zeolite. The objectives of this study are to explore the adsorption capacity of the modified zeolites using TPD-CO_2 Technique between 50-510 ºC.

3. Results and discussion

The specific surface area of zeolites measured by the standard method of Brunauer, Emmett and Teller (BET).

Table 1. specific surface area of zeolites.

Adsorbent	BET Surface Area (m^2/g)
NaY Zeolite	810.64
DEA-NaY	5.45
Aminosilane-NaY	157.08

To determine the amount of zeolite adsorption thermal program desorption technique is suitable. The TPD-CO_2 technique was used for this study.

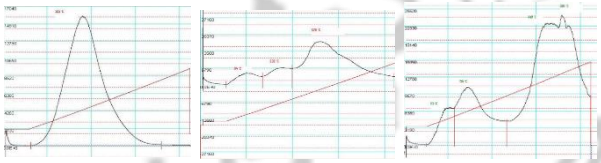

a **b** **c**

Figure 1. TPD-Co_2 NaY(a), DEA-NaY(b) and Aminosilane-NaY(C).

Table 2. CO_2 dessorbtion of zeolite.

Adsorbent	CO_2 adsorption capacity(mmol/g)		
NaY	202 ^{0}C		
	2.174		
DEA-NaY	94 ^{0}C	202 ^{0}C	320 ^{0}C
	0.353	0.509	2.899
Aminosilane-Nay	113 ^{0}C	176 ^{0}C	449-506 ^{0}C
	0.366	1.218	4.076

4. Conclusions

In this study, NaY Zeolite has been impregnated with DEA, Aminosilane. The samples are characterized by BET, TPD-CO2. The BET surface area of NaY decreases. The nitrogen adsorption isotherm becomes an even line and the volume adsorbed decreases. This phenomenon suggests the occupation of the pores by amine and aminosilane. The modified adsorbents have also been evaluated for their CO_2 adsorption capacities and it has been observed that the modified zeolites desorb less than the pristine material at low temperatures, but their CO_2 uptake increases with a rise in the temperature.

Acknowledgments

The authors are thankful to Mazandaran University and Persian Gulf University for their financial support in this project.

References

[1] M. Babaei, M. Anbia, M. Kazemipour, *J. Adv. Environ. Health Res.* 5(2) (2017) 70-7.

[2] R. Chatti, A.K. Bansiwal, J.A. Thote, V. Kumar, P. Jadhav and S.K. Lokhande, et al. *Micropor. Mesopor. Mater.* 121(1) (2009) 84-9.

5th Iran International Zeolite Conference

University of Tabriz, Tabriz, Iran

26-27 August 2018

Investigation of Different Synthesized Zeolite Types with High Capacity of Moisture Absorption: A Review

A. Ranjbar Koh Farhadi[a,b]*, N. Rahemi[a,b], S. Allahyari[a,b], A. Beygi[a,b], S. Shouhani[a,b]

[a] *Chemical Engineering Faculty, Sahand University of Technology, Sahand New Town, Tabriz, Iran.*

[b] *Environmental Engineering Research Centre, Sahand University of Technology, Sahand New Town, Tabriz, Iran.*

**Corresponding author: asma_farhadii@yahoo.com*

Abstract: Today, the removal of moisture in industrial factories, which is the product of wear and tear, has become a big problem. For this reason, we try to select an appropriate adsorbent for high moisture absorption. In this paper, we intend to study the effect of pressure on the absorption rate in previous studies. According to past experiments and the results obtained, they have the potential to absorb zeolites under pressure. By studying different zeolites and comparing their performance, we concluded that 3A zeolites absorption capability High humidity.

Keywords: Zeolite; Synthesized; High Capacity; Absorption; Moisture

1. Introduction

1.1 Zeolites

The term zeolite is derived from the Greek words: "Zeo" and "lithos" meaning "to boil" and "a stone". So, Zeolite = boiling stone, the ability of these materials to absorb water and release it upon heating. Zeolites are porous crystalline framework materials containing pores of molecular size (5–12Å or 0.5–1.2 nm). Zeolites are Microporous materials [9].

1.2. Zeolite Names and Framework Type Code

The first synthetic zeolite was made from Na, Si, and Al at Linde's laboratories in Tonawanda, NY. It was termed zeolite A. Sometime later, Linde synthesized zeolites X and Y. The major difference between X and Y are their SiO_2/Al_2O_3 ratios in their framework. For X, this was 2–3; for Y, it was 3.5–5.5, which conferred greater hydrothermal stability, which was important in applying it to catalytic cracking.

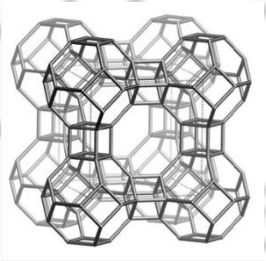

Figure 1. The 4MR rings of the sodalite units, which is, Type A zeolite.

1.3. Importance of moisture absorption

In various industrial processes, many of the exhaust gases contain water vapor. For example, in petrochemical processes such as steam cracking, steam vaporization, and gas-water change reaction, water is injected during the reaction. Exhaust gases

from iron/steel processing, coal gas, olefin/paraffin processing, etc., also include water vapor. In particular, natural gas is typically saturated with steam under natural conditions of production. In the separation of gas, water vapor is the most common undesirable impurity that is eliminated from the desired components of the exhaust gas mix. In addition, the removal of water from the air dryer and the process of air separation is very important. Accordingly, the dehydration process usually takes place in a pre-treated unit to prevent unexpected complications during further processing. Removing water from the gas stream reduces the ability of adverse effects, such as corrosion in the presence of acid contamination, hydrate formation, the reaction of hydrolysis with the liquids itself and the density or freezing of moisture. Removing water from the gas stream reduces the ability of adverse effects, such as corrosion in the presence of acid contamination, hydrate formation, the reaction of hydrolysis with the liquids itself and the density or freezing of moisture [1,2]. Therefore, various methods of dehydrogenation in the industry, such as adsorption, adsorption, and compression, are used. Among them, the attraction is known as the most efficient method. [1,2,3] Since absorption is merely a surface phenomenon and absorption is a function of temperature and pressure, the equilibrium of water vapor absorption is essential in selecting the suitable absorber and designing an essential absorption process [4,5].

1.4. Different thermosynthetic theories for absorbing moisture

With the study, the most experimental data obtained with the models by the Aranovich and Donohue (A-D) and n-layer BET [7] Frenkel Halsey-Hill [6] have been corrected using Langmuir, Toth, UNILAN, and Sips [6-8] isotherms.

The AD equation is as follows:

$$q = f(P)/(1 - P/P_S)^d$$

Given the equation f (P), the capacity of the monolayer, q_m, can be determined as f (P_s), since f (P_s) is related to the maximum absorption of the single layer. By placing f (P) with the Langmuir, Toth, UNILAN, or Sips equations, experimental results can be obtained .For example, the graph below illustrates the empirical and correlated isotherms for water vapor adsorption on zeolite 13X at different temperatures [10], which gives the exact equation with SIPS isotherm the most accurate results [6-8].

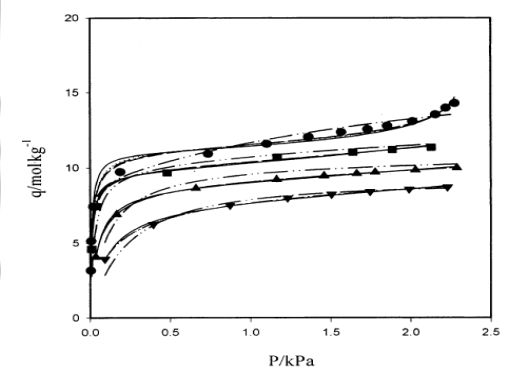

Figure 2. Experimental and correlated isotherms for water vapor adsorption onto Zeocarbon at various temperatures- Langmuir equation,- - - Toth equation, … UNILAN equation -.- Sips equation [7].

1.5. Types of zeolite with high absorbance

The absorption capacity of Y zeolites is greater than that of X zeolite. The water absorption capacity was a 13X zeolite, zero carbon, and Al_2O_3 except in 293.2 K and in the high-pressure zone. In addition, zeolite 13X and zeocarbon isotherms were more desirable than aluminum Al_2O_3.

The absorption capacity of zeolite 4A from all solvents is clearly lower than the water vapor absorption capacity. As found for zeolite 3A, methanol and ethanol have a water absorption capacity significantly higher than water vapor absorption.

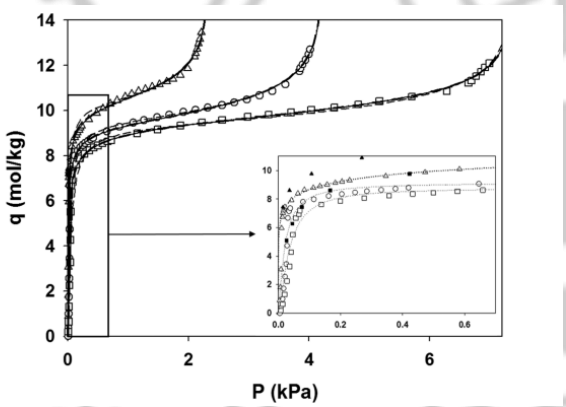

Figure 3. Equilibrium data of water vapor on zeolite 3A in pellet form with binder [6].

2. Conclusions

By observing the graphs, which are drawn up by increasing pressure on different zeolites, it can be concluded that the adsorption rate of adsorbent 3A is higher at lower pressures.

References

[1] T. Kudra, A.S. Mujumdar, *Advanced drying technologies*, 2009, CRC Press, Cleveland.

[2] P. Gandhidasan, A.A. Al-Farayedhi, A.A. Al-Mubarak, *Energy* 26 (2001) 855-868.

[3] F. Štepánek, M. Kubíček, M. Marek, *Ind. Eng. Chem. Res.* 37 (1998) 1435-1443.

[4] H. Ahn, C.H. Lee, Adsorption dynamics of water in layered bed for air-drying TSA process. *AIChE J.* 49 (2003) 1601-1609.

[5] K. Yang, *Gas separation by adsorption process*, 1987, Butterworths, Boston, MA.

[6] K.-M. Kim, H.-T. Oh, S.-J. Lim, K. Ho, Y. Park, C.-H. Lee, *J. Chem. Eng. Data* 61(4) (2016) 1547-1554.

[7] J.-H. Kim, C.-H. Lee, W.-S. Kim, J.-S. Lee, J.-T. Kim, J.-K. Suh, J.-M. Lee, *J. Chem. Eng. Data* 48 (1) (2003) 137-141.

[8] A. Gorbach, M. Stegmaier, G. Eigenberger. *Adsorption* 10 (1) (2004) 29-46.

[9] I. Petrov, T, Michalev, *Synthesis of Zeolite A: A Review*, 51 (2012) 30-35.

Adsorption kinetics of Industrial Colors from Wastewater Using Surfactant-Modified Clinoptilolite

A. Froghi[1*], M. Ghaderzadeh [2], M. Moutab [1], K. Farhadi[2], A. Bahrami[1]

[1]*Department of Mining Engineering, Faculty of Engineering, Urmia University, Urmia, Iran*

[2]*Department of Chemistry, Faculty of Science, Urmia University, Urmia, Iran*

**Corresponding author: mehranforughirad1@gmail.com*

Abstract: One of the applications of Clinoptilolite zeolite is the adsorption of impurities and paint residues from paint factories. In order to investigate this characteristic of clinoptilolite, the present study is accomplished on clinoptilolites of Shahindezh, West Azerbaijan province. For this purpose, the clinoptilolite sample was first crushed with jaw crusher and then grounded using ball mill and then classified into three size fractions of -500+250, -250+106 and -106. Then, in order to remove the water present in the mineral structure, one sample from each fraction was heated to 160 ° C for 6 hours. After drying, each fraction was analyzed for the amount of adsorption of waste dyes in the paint. In order to investigate the effect of modification on adsorption rate, one sample was modified with anionic surfactants. According to experiment results, modified zeolite has the ability to absorb many cationic colors such as methylene blue and green malachite with a very high adsorption rate. Non-modified zeolite was able to adsorb anionic color such as methyl orange and alizarin red with a lesser adsorption rate. Besides, the effect of pH an adsorption value was investigated. The results showed that pH value increases with an increase in pH value.

Keywords: Natural and Modified zeolite; Removal; Wastewater; Clinoptilolite; Surfactant

1. Introduction

The mineral Clinoptilolite, is a member of zeolite family (zeolites are relatively diverse due to their physical and chemical properties) and one of the most useful types of natural zeolites. Clinoptilolite is from the silicates group and the sub-group of tectosilicates (chemistry: aluminum calcium potassium sodium hydrate silicate,). Clinoptilolite is commonly used as a chemical filter, chemical absorbent and water purifier [1]. These compounds have a quadrilateral structure (four oxygen atoms around a silicon atom), in which there are cavities and channels with diameter of 3-10 angstroms. These cavities contain 10-20% water. This structure has led to a cation exchange with a capacity of 2.16-4.73 meq/gr in clinoptilolites. The ionic exchange and absorption capability enables these structures to eliminate many cationic constituents from solutions. Zeolites have few tendencies to exchange anionic compounds [2]. Zeolites of Shahindezh City are of clinoptilolite type. Containing impurities are minerals of iron, calcite, chlorite and minerals of the Montmorillonite group.

Available phases include: quartz 20%, shard 20% to 25%, total quartz and feldspar, 15% microporous, Impurities in a few hundred percent (3)

2. Experimental procedure

The clinoptilolite sample was first crushed with jaw crusher and then ground using ball mill and then classified into three size fractions of -500+250, -250+106 and -106. After each, the range was 200 grams.

Natural zeolites are initially protonated and then generated by [Na] + positive Chargeon the surface. The goal is to modify zeolite to absorb methyl orange and alizarin red. The second mode of surfactant [SDS] - is mounted on protonated zeolite, thus reacting polar heads with protons, and long chains at modified zeolite levels will have the ability to exchange anion with colors like methylene and green malachite.

3. Results and discussion

In all previous studies, the effect of operational parameters including initial pH, adsorbent dosage, contact time, initial dye concentration and temperature were investigated in batch adsorption experiments. The experimental equilibrium data were tested by two widely used isotherm models namely, Langmuir and Freundlich.

Adsorbent concentration was in the range of 10–500 mg L^{-1} in the adsorption profile of dyes versus adsorbent concentration. It is observed that the percentage of dye removal increases with increase in adsorbent dosage. Then, the effect of pH on the removal efficiency of tested dyes was studied at different pH values ranging from 2.0 to 10.0. The maximum removal efficiency of cationic dyes such as malachite green and anionic dyes such as methyl orange was achieved at mild alkaline and neutral pH values respectively. The uptake of dyes as a function of contact time showed fast adsorption rate and more than 90% of dyes were removed during 20 min through attachment-controlled process. The effect of different initial dye concentrations on SDS modified zeolite was subsequently studied. In all experiments, the removal percentage of cationic and anionic dyes increased with increase in initial dye concentration and showed little increase at higher concentrations. Typical figure regarding malachite green was shown in Figure 1.

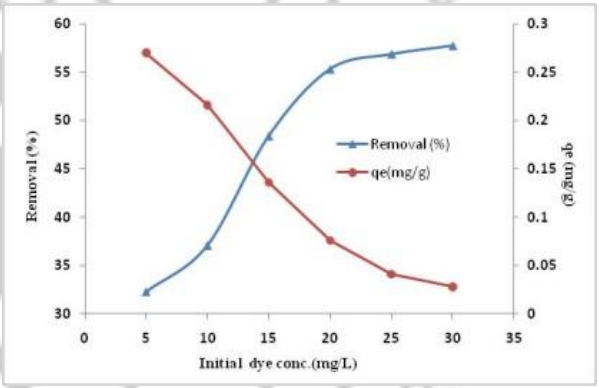

Figure 1. Effect of initial dye concentration on percentage removal of malachite green by zeolite

The Langmuir and Freundlich isotherms for the dye-SDS modified zeolite system were used for determination of constants. The obtained results showed that Langmuir model yields a much better fit than the Freundlich model.

In order to investigate the mechanism of adsorption and potential rate controlling steps such as chemical reaction, diffusion control and mass transport

processes, kinetic models have been used to test experimental data. Adsorption kinetics follows preferably the pseudo second-order kinetics that showed the best correlation of the data in most cases.

4. Conclusions

• Natural zeolite in West Azerbaijan Province with high cation exchange capacity and high potential for water and wastewater purification has been used to remove the anionic methyl orange and alizarin red colors with high absorption capacity using this rich and inexpensive absorber.

• Modified zeolite with high anion exchange capacity has the ability to remove methylene blue and green malachite colors to a very high standard.

References

[1] S. Ghadiri, R. Nabizadeh, A. Mahvi, S. Nasseri, H. Kazemian, A. Mesdaghinia, et al. *Iranian J Environ Health Sci Engin.*, 7 (2010) 241.

[2] F. Ouadjenia-Marouf, R. Marouf, J. Schott, A. Yahiaoui. *Arabian J. Chem.*, 4 (2013) 401-406.

[3] A. Bahrami, National Design, Understanding the Functional Capabilities of Iran's Zeolites in Industries, 2004

Preparation of ZSM-5 nanocrystals as a green acid catalyst for solvent-free synthesis of pyrimidinones

A. Bakhtiari, J. Safaei-Ghomi*

Department of Organic Chemistry, Faculty of Chemistry, University of Kashan, Kashan, P.O. Box 87317-51167, I. R. Iran

**Corresponding author: safaei@kashanu.ac.ir*

Abstract: synthesis of pyrimidines derivatives was catalyzed by ZSM-5 zeolite as a great catalyst system. Its catalytic activity leads to improvement of the progress of Biginelli-like reaction to produce in high yield. Reusability of novel catalyst system was also studied which resulted in no loss of their catalytic activity up to five cycles makes the whole system industrially viable.

Keywords: ZSM-5, Zeolite, Multi-component, pyrimidinones, Nanocatalyst

1. Introduction

Recently, the synthetic organic chemists have been interested in multicomponent reaction because of procedural simplicity and synthetic efficiency. Pyrimidines synthesized from Biginelli reaction have attracted a lot of attention in natural and synthetic organic chemistry, due to their wide range of biological activities and pharmaceutical properties. The development of simple synthetic routes for the synthesis of these compounds is one of the great interests for organic chemists. A number of methods have been reported for the synthesis of pyrimidines in the presence of some catalysts such as sodium acetate and pyridine [1], $Bi(NO_3)_3.5H_2O$ [2], NaOH [3], CuO microspheres [4] and K_2CO_3 [5,6]. In spite of the availability of these methods, there remains enough scope for the use of an efficient and reusable catalyst to synthesize these organic compounds. The simple recycling of catalyst makes the workup procedures easier and eliminates harsh conditions for the reaction.

Development of heterogeneous catalytic processes for fine and specialty chemicals is an important inter-disciplinary research objective for industrialists and academicians. Zeolites, glasses, carbons, and oxides are members of a large group of porous materials known as molecular sieves. Among these, zeolites are the most attractive candidates for industrial applications because of their unusual features. The exchangeable cations in zeolites can be substituted by protons, which can behave as strong Brønsted acid sites [7].

In this study, we report the use of ZSM-5 nanocrystals as an efficient catalyst for the

preparation of pyrimidine derivatives by one-pot reaction of aromatic aldehydes, guanidine hydrochloride and dialkyl malonate.

2. Experimental Part

2.1. Preparation of ZSM-5 nanocrystals:

ZSM-5 zeolite was generated hydrothermally. At the first TEOS (4.15 ml) and the template (0–1.2 were mixed with distilled water (4 ml), and 1 h was stirred (I). Afterwards, NaOH (0.18 g) was also added with distilled water (8 ml). Aluminum isopropoxide (AIP) (0.18 g) was added to distilled water (8 ml) and stirred for 1 h. The resulting mixture (II) was added dropwise to mixture (I) with stirring, and the resulting gel was stirred for 120 min. Subsequently, the obtained hydrogel had the following molar ratio: $1Al_2O_3$: $46SiO_2$: 4TPAOH: $5Na_2O$: $2500H_2O$. Then, the gel was transferred to a stainless-steel autoclave for 3 days in oven at 165˚C. The autoclave was quenched with water, and the solid product was filtered, washed with distilled water and dried at 110 °C overnight. To produce the final product, the obtained material was calcined at 550 °C for 8 h.

2.2. General procedure for the preparation of pyrimidines:

A mixture of aldehydes (1 mmol), dialkyl malonate (1 mmol), guanidine hydrochloride (1 mmol) in water and ethanol mixture (1:1) was reflaxed for the desired times. The reaction was catalyzed by ZSM-5 nanocrystals as an efficient catalyst that was added to an ethanol/H_2O mixture and monitored by TLC. After the completion of reaction, the catalyst was removed by filtration. 10 mL ice water was added and the precipitated product was filtered. At the end of the process, the residue was recrystallized from ethanol to obtain the crude product

3. Results and discussion

Nano-ZSM exhibited MFI framework structure with high phase purity, which was confirmed by XRD (Fig. 1). XRD pattern of Nano-ZSM-5 was broad when compared to ZSM-5, which confirms that the material is nanocrystalline in nature.

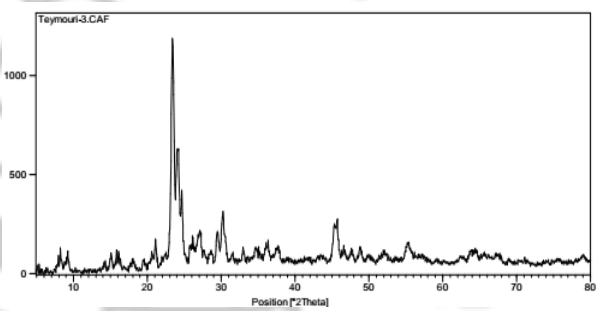

Figure 1. XRD of Nano-ZSM-5

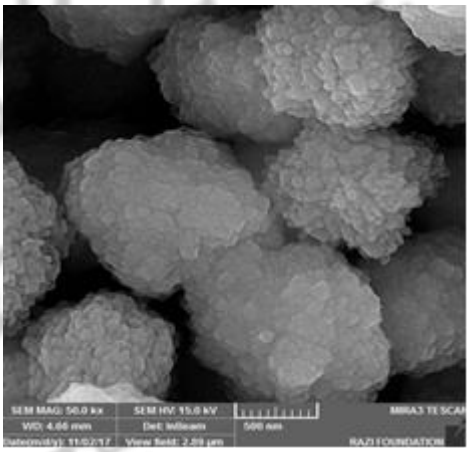

Figure 2. SEM of Nano-ZSM-5

The morphologies of nano-ZSM-5 was observed with scanning electron microscope (SEM) and the representative image are shown in Fig. 2.

In continues, the current reaction is preceded by 5 mol% of ZSM-5 as nanocatalyst and some of obtained compounds are represented in Table 1.

Table 1. Synthesis of pyrimidines using ZSM-5 nanocrystals.

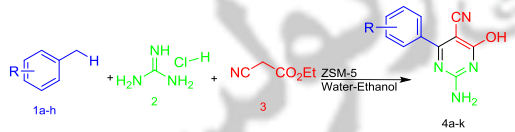

name	aldehydes[b]	Time (h)	Yield
4a	4-Me-C_6H_4	2	94
4b	4-Cl-C_6H_4	1	93
4c	4-OH-C_6H_4	1	91
4d	3-NO_2-C_6H4	2	93
4f	2,3-di-Cl-C_6H_3	2	90

Spectral data for some selected 5-pyrimidinecarbonitriles 2-Amino-4-hydroxy-6-(4-methylphenyl pyrimidine-5-carbonitrile 4a:

M.p: 324-325°C; IR (KBr): 3400, 3138, 2208, 1645, 1570, 1485, 1408, 1250 cm^{-1}, ^1H NMR (DMSO-d_6, 400 MHz): δ (ppm)= d = 2.38 (s, 3H, CH3), 3.32 (br. s, 1H, OH) [exchanged with water of DMSO] 7.38 (d, 2H, J=8Hz, Ar-H), 7.93(d, 2H, J=8Hz, Ar-H), 8.28 (br. s, 2H, NH_2), ^{13}C NMR (DMSO-d_6, 100 MHz): δ (ppm) = 22.1, 86.4, 120.1, 130.6, 131.3, 135.6, 141.8, 157.2, 162.6, 172.1; Anal. For $C_{12}H_{10}N_4O$ = C, 63.71; H, 4.46; N, 24.76 %. Found: C, 63.14; H, 4.47; N, 24.36 %

2-Amino-6-hydroxy-4-(4-chlorophenyl) pyrimidine-5-carbonitrile 4b:

M.p: 347–348 °C, IR (KBr): 3400, 3135, 2210, 1638, 1574, 1482, 1410, 1248 cm^{-1}. ^1H NMR (DMSO-d_6, 400 MHz): δ (ppm)= 7.169 (br. s, 1H, OH), 7.216 (br. s, 2H, NH_2); 7.536 (d, 2H, J=8Hz, Ar-H); 7.80 (d, 2H, J=8Hz, Ar-H). ^{13}C NMR (DMSO-d_6, 100 MHz): δ (ppm)= 84.9; 117.1; 128.4; 130.1; 135.3; 135.7; 156.5; 161.7; 170.3. Anal. For $C_{11}H_7N_4OCl$ = C 53.78, H 3.28, N 23.51%; found C 53.65, H 3.20, N 23.45%.

4. Conclusions

To recapitulate briefly, we have reported a green and efficient method for the synthesis of pyrimidines *via* three-component one-pot condensation of of aromatic aldehydes, guanidine hydrochloride and dialkyl malonate using ZSM-5 nanocrystals as new catalyst at 80°C. The current method provides obvious positive points such as environmental friendliness, significantly shorter reaction time, markedly excellent yields and simple workup procedure.

References

[1] M.J. Waring, D.J. Baker, S.N. Bennett, A.G. Dossetter, M. Fenwick, R. Garcia, J. Georgsson, S.D. Groombridge, S. Loxham, P.A. MacFaul, *MedChemComm*, 6 (2015) 1024.

[۲] J. Evenäs, F. Edfeldt, M. Lepistö, N. Svitacheva, A. Synnergren, B. Lundquist, M. Gränse, A. Rönnholm, M. Varga, J. Wright, Bioorg. *Med. Chem. Lett.*, 24 (2014) 1315.

[3] M. Zahedifar, H. Sheibani, *Res. Chem. Intermed.*, 41 (2015) 105.

[4] M. Deshmukh, S. Salunkhe, D. Patil, P. Anbhule, *Eur. J. Med. Chem.*, 44 (2009) 2651.

[5] S.J. Ahmadi, S. Sadjadi, M. Hosseinpour, *Monatsh. Chem.*, 142 (2011) 1163.

[6] H.I. El Diwani, H.T. Abdel-Mohsen, I. Salama, F.A.-F. Ragab, M.M. Ramla, S.A. Galal, M.M. Abdalla, A. Abdel-Wahab, M.A. El Demellawy, *Chem. Pharm. Bull.*, 62 (2014) 856.

[7] D.P. Serrano, J. Aguado, G. Morales, J.M. Rodriguez, A. Peral; M.Thommes, J.D. Epping, B.F. Chmelka, *Chem. Mater.* 21 (2009) 641.

The Effect of Ag-Zn Zeolite on Antibacterial Properties and Setting Time of Dental Composite Resins

F. Dabaghi-Tabriz[a], B. Divband[b], M. Rahbar[a]*, M. Mahmoodabadi[c]

[a] *Operative and Esthetic Dentistry Department, Faculty of Dentistry, Tabriz University of Medical Sciences, Tabriz, Iran*

[b] *Department of Inorganic Chemistry, Faculty of Chemistry, University of Tabriz, Tabriz, Iran*

[c] *Dentistry Student, Faculty of Dentistry, Tabriz University of Medical Sciences, Tabriz, Iran*

**Corresponding Author: mahdirhbr@gmail.com*

Keywords: Ag-Zn Zeolite; Antibacterial properties; Composite resin

1. Introduction

Leakage of oral fluid caused by the poor sealing ability of either temporary or permanent filling materials may result in bacterial contamination of a tooth cavity or prepared tooth surfaces, possibly leading to pulp irritation or more serious pulpal reactions [1]. Therefore, an effort to prevent bacterial while the final restoration is being constructed, contamination of the prepared cavity surfaces, is believed to be one of the key factors to obtaining a successful long-term cast restoration.

Among metallic elements or their salts, silver powder is known to possess antibacterial properties [2]. Silver is one of the common metallic elements used in dentistry that is less toxic to host tissues compared to other commonly used elements for making metallic restorative materials, such as mercury or copper [3]. In 1989, Hagiwara successfully developed a zeolite, which incorporated silver and zinc ions. A zeolite was used as a carrier for silver and zinc ions because this material has the ability for loading ions in its molecular structure for the ions to exchange assessments and clinical research in the ambient environment. This material was expected to have long-lasting antibacterial activity from the continuous release of these ions. On the basis of this development, the authors initiated studies to develop a temporary filling material which provides antibacterial activity and ease of manipulation. In a previous study, incorporating zeolite powders with Ag (3-5%) and Zn (8%) ions (Ag-Zn-Zeolite) into light-cured temporary filling materials revealed prominent antibacterial activity, possibly due to the release of Ag and/or Zn [4]. These results led to further biological of Ag-Zn-Zeolite to dental composite resin.

2. Experimental Part

Particles of zeolite with an average diameter of 1 mm, which contained both silver and zinc ions and silica (SiO2) submicrofiller, were incorporated into the resin matrix. In all the materials used, the resin matrix content was kept at 40 wt% and each material contained a different amount of Ag-Zn-Zeolite. The

cavity sealing ability of the experimental materials was evaluated according to the method used in a previous study [4]. A cylindrical butt joint cavity (2 mm in diameter and 2 mm deep) was prepared in a mica- containing machinable glass ceramic using a specially designed diamond-coated drill (2 mm dia., 2 mm long) driven by an air- turbine handpiece. The experimental dental composite resin was inserted and polymerized with visible light for 60 s. The surface of the glass ceramic, excluding the cavity margin, was then covered with nail enamel. Subsequently, the specimen was immersed in an aqueous solution of 2% basic fuchsin at 37 °C for one week. After 1 week, the temporary filling material was mechanically removed with a dental probe. The margins of the cavity were observed under a stereomicroscope (40*3 magnification). Six specimens were prepared for each group. The degree of dye penetration into the cavity walls at the location where it had penetrated the deepest. The results were statistically analyzed using a ridit analysis at $\alpha = 0.05$ [5-6].

The bacterial growth inhibition of the experimental temporary materials was examined according to the method reported in a previous study [4]. The bacterial strains used in the present study comprised Streptococcus mutans ATCC 25175, Streptococcus mitis ATCC 33399.

The amounts of silver and zinc ions released from these materials were measured by atomic absorption spectrophotometry.

3. Results and discussion

The results indicated that the occurrence of marginal leakage was low in all of these materials. These materials exhibited prominent in-vitro antibacterial activity against S. mutans and S. mitis. The Ag-Zn-Zeolite in these materials was able to release very small but detectable amounts of Ag and Zn even 4 weeks after the immersion started. The larger the amounts of Ag-Zn-Zeolite that were incorporated, the greater the release of silver and zinc. However, it appears that increasing antibacterial activity is not promoted by the higher ratio of Ag-Zn-Zeolite.

4. Conclusions

The release of large amounts of both silver and zinc are probably not needed to produce antibacterial activity. There is considerable interest in combining a small amount of Ag-Zn-Zeolite, which promotes antibacterial activity. It can be assumed that incorporating a small amount of Ag-Zn-Zeolite into temporary filling materials was sufficient for clinical application.

References

[1] M. Brannstrom, K.J. Nordenvall, *J. Dent. Res.* 57 (1978) 3-10.

[2] H. Horiguchi, *Chemistry of Antibacterial and Anti mildew*, (1991) Sankyo Press Ltd, 46-59, Tokyo, Japan.

[3] J. Leirskar, Scand. *J. Dent. Res.* 82 (1974) 74-81.

[4] B.M. Hotta, C. Minami, S. Ohashi, D. Taguchi, *Jap. J. Conserv. Dent.* 38 (1995) 23-26.

[5] I.D.J. Bross, *Biometrics* 14 (1958) 18-38.

Arsenic Removal from Wastewater Using a Low Cost Adsorbent Based on Natural Zeolite: Comparative Study

L. Sanaei[a], M. Tahmasebpoor[a]*, M. Khatamian[b], B. Divband[b], A. Mokhtari[b]

[a] *Faculty of Chemical & Petroleum Engineering, University of Tabriz, Tabriz, Iran*

[b] *Department of Inorganic Laboratory, Faculty of Chemistry, University of Tabriz, Tabriz, Iran*

**Corresponding author: tahmasebpoor@tabrizu.ac.ir*

Abstract: It has been found that zeolite based nanocomposites exhibit a high arsenic removal efficiency. In this study, natural zeolite of clinoptilolite was modified with Fe_3O_4 nanoparticles, and then this nanocomposite was converted to granules using ionic gelation method. Based on the results, 0.1 and 0.7 g/l of adsorbents dose were chosen as optimal values for the powders and granules to reach the maximum arsenic removal, respectively, which are considerably lower than those reported for the adsorbents in the literature. This suggests that newly prepared low cost Fe_3O_4 coated clinoptilolite can be considered as a potential adsorbent in the remediation of aqueous waste contaminated with arsenic.

Keywords: Arsenic; Zeolite; Water-treatment; Nanocomposite; Granule

1. Introduction

Arsenic (As) is a semi-metallic element, which is present in some water sources in varying amounts of soluble forms [1]. Use of As contaminated water may cause numerous diseases of the skin and internal organs. Recently, extensive research to develop cost-effective methods for As removal has been carried out. Adsorption technique is generally considered as a promising method due to easy separation of sorbent from aqueous media after treatment. Sorption of As on natural zeolites has been studied extensively in recent years due to their low cost and availability in nature [2]. In the present work, a new innovative modified zeolite is synthesized as both powders and granules to achieve superior adsorption capacity of As from aqueous solution. Then the obtained results are compared with the results of other researches in which the removal of As is achieved by applying other sorbents.

2. Experimental Part

The natural zeolite (clinoptilolite), was modified by iron oxide nanoparticles to prepare the nanocomposite powders; (Fe_3O_4 coated clinoptilolite), using precipitation method and then the ionic gelation method was used to convert the powders to the composite granules.

3. Results and discussion

In order to evaluate the adsorbent efficiency of Fe_3O_4 coated clinoptilolite, both in the shape of powders and granules, firstly, the As removal values of the previous works were presented in Figure 1. Zhang et al. [3] investigated iron(III) oxide loaded melted slag

(IOLMS) as an adsorbent for As removal from aqueous system. As it is obvious, 40 g of IOLMS could only remove 75% of As(III) from the solution with initial As concentration of 200 mg/l. Çiftçi et al. [4] investigated a novel adsorbent named nickel/nickel boride nanoparticles coated resin for the removal of As(III) from water. As can be seen, beyond the adsorbent dose of 3.0 g/l, the As(III) removal efficiency was more than 91% for the initial As concentration of 100 µg/l. At 7.0 g/l adsorbent dose, 99.5% As removal efficiency was obtained and 10.0 g/l adsorbent dose was chosen as optimal value. Bibi et al. [5] investigated Hydrated Cement, Marble Powder and Brick Powder as adsorbents for As removal from water. As shown, percent removal of As increased by increasing adsorbent dose up to 30 g/l with sorption efficiency of 98.8% for Hydrated Cement, 96.4% for Bricks Powder and 95.3% for Marble Powder. Further increase in adsorbent dosage up to 40 g/l caused no effect on the percent removal of As. On the basis of above mentioned results, 30 g/l was found as optimum for As adsorption.

The effect of adsorbent dose on the As removal by prepared Fe_3O_4 coated clinoptilolite as both powders and granules was also investigated in Figure. 2. This figure indicated that the removal efficiency of As increased as the adsorbent dose increased, but above a specific clinoptilolite dosage, the increase in As removal was negligible. 0.1 and 0.7 g/l of adsorbents dose were chosen as optimal for the powders and granules, respectively. The higher required amount of granules rather than powders to reach the same adsorption efficiency is mainly attributed to the more surface area available in the case of powders.

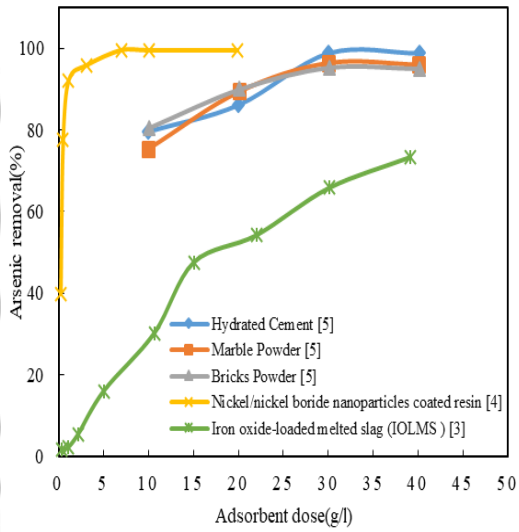

Figure 1. The effect of adsorbent dosage on As adsorption efficiency (initial concentration of As was 200 mg/l [3], 100 μg/l [4] and 100 μg/l [5])

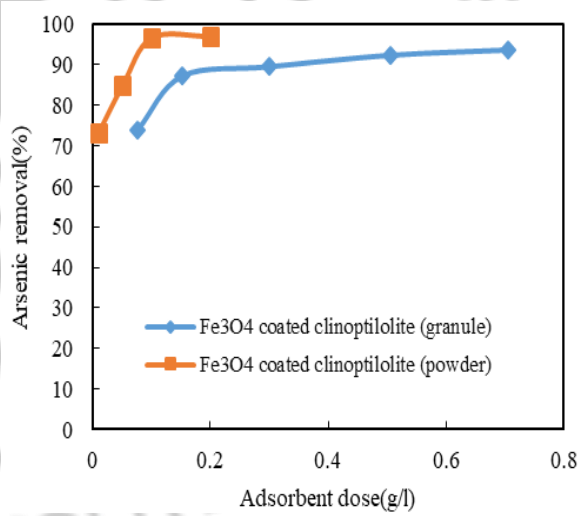

Figure 2. As removal by powder and granule Fe_3O_4 coated clinoptilolite (initial concentration of As was 200 μg/l)

The results of our study suggests that newly prepared low cost Fe_3O_4 coated clinoptilolite adsorbent can be considered as a promising and potential adsorbent in the remediation of aqueous waste contaminated with As. Because the optimal Fe_3O_4 coated clinoptilolite adsorbent dose required to reach more that 90% As removal is considerably lower compared to those investigated in the literature.

4. Conclusions

The natural clinoptilolite modified with iron-oxide; both in the case of powder and granule, was successfully employed for the removal of As from water. The results showed that the granulation did not cause a significant decrease in the percentage uptake. Also, the optimal Fe_3O_4 coated clinoptilolite adsorbent dose required to reach more that 90% As removal was considerably lower compared to those investigated in the literature.

References

[1] M.B. Baskan, A. Pala, *Desalination*, 281 (2011) 396.
[2] P. Chutia, S. Kato, T. Kojima, S. Satokawa, *J. Hazard. Mater.* 162 (2009) 204-211.
[3] F.-S. Zhang, H. Itoh, *Chemosphere*, 60 (2005) 319.
[4] T.D. Çiftçi, E. Henden, *Powder Technol.* 269 (2015) 470.
[5] S. Bibi, A. Farooqi, K. Hussain, N. Haider, *J. Clean. Prod.* 87 (2015) 882.

Preparation of Zeolite A /Epoxy Nanocomposites by Ultrasonic Dispersion and Enhanced Thermal Properties

S. Khademi[a], M. Hamadanian[a] *, B. Roozbehani[b]

[a] *Institute of Nano Science and Nano Technology, University of Kashan, Kashan, Iran*

[b] *Fuel and Petrochemical Engineering Research Center, Abadan Institute of Technology, PUT, Abadan, Iran*

**Corresponding author: Hamadani@kashanu.ac.ir*

Abstract: Epoxy-based nanocomposite films were synthesized by incorporating of zeolite A nanoparticle. In this study the epoxy/ zeolite A nanocomposite films are prepared by a facile route using ultrasonic mixing and spin coating. The synthesized nanocomposites film was characterized by scanning electron microscopy (SEM), thermal gravity analysis (TGA), and FTIR spectroscopy.

Keywords: Nanocomposites; Ultrasonic Dispersion; Zeolite A

1. Introduction

Nanocomposites enable completely new possibilities for the design of new materials. By the insertion of nanoparticles into a polymer matrix, the strength, and toughness can be enhanced simultaneously, that is not possible to the same degree for composites with microscale reinforcements [1].

The dispersion of the nanofillers in the polymer matrix leading to a big particle-matrix interface, which is indispensable for the improvement of the materials properties, remains a big challenge. In the last years, ultra-sonication proofed to be an adequate alternative technique for the dispersion of nanoparticles [2].

However, most studies were carried out in aqueous solutions, and there are only very few experiences for the ultrasonic dispersion of particles in high viscosity liquids such as epoxy resin.

Chatterjee and Islam found out that the optimum sonication time of nanoscale TiO_2 in the epoxy resin is 30 min. Also, Rodgers et al. used this same ultrasonic processing time to disperse SiC nanoparticles [3].

In this study, zeolite A (LTA) nanoparticles were inserted in epoxy resins and dispersed by means of ultrasonic processing. nanocomposite samples with particle content were manufactured to perform thermal stability tests.

2. Experimental Part

As matrix material, the commercially available bisphenol-A epoxy resin Epilox A Epiran-01 provided by the company Khozestan Petrochemical. Zeolite A nanoparticles from Sigma Aldrich prepared and were added to the liquid epoxy resin (20% (w/w)) and 20 min sonicate for dispersion.

Finally, 2% by weight of amine hardener is added to the mixture.

3. Results and discussion

Fig. 1. shows a typical FESEM image of zeolite A/epoxy composites. As can be clearly seen, the epoxy surface was well decorated by zeolite A nanoparticles sparsely and evenly.

The FT-IR spectra of zeolite A/epoxy nanocomposite and zeolite A are given in Fig. 2. The peaks at 990 cm^{-1} and 462 cm^{-1} correspond to the asymmetric stretching vibration of inner tetrahedral and the bending vibration modes of T–O bonds in TO_4 tetrahedral of zeolite structure (where T = Si or Al), respectively.

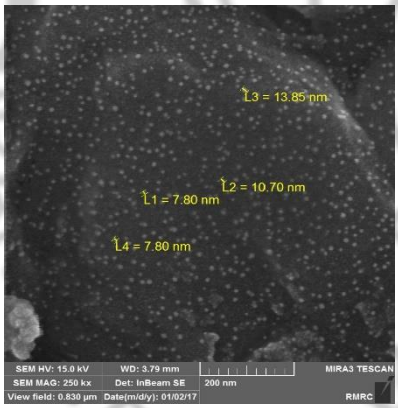

Figure 1. SEM image of the nanocomposite with 20% (w/w) zeolite A in epoxy resin.

Fig. 2a shows the infrared spectrum of nanocomposite zeolite A/ epoxy. The peaks at 1731 and 3440 cm^{-1} are attributed to the carboxylic C=O and O–H stretching vibration, respectively.

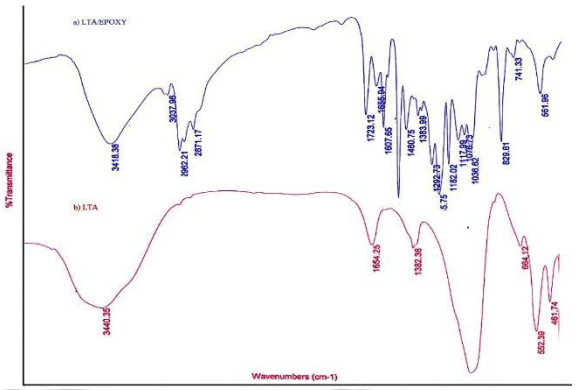

Figure 2. FT-IR spectra of (a) nanocomposite zeolite A/epoxy (b) zeolite A

The thermal degradation of nanocomposite zeolite A/epoxy and pure epoxy was performed up to 800 ^{0}C Fig. 3. exhibited that 85% of zeolite A/epoxy nanocomposite remained stable up to 600 ^{0}C, however, pure epoxy presented 98% weight loss around 200 ^{0}C. For zeolite A/epoxy, the major weight loss of approximately 15% was observed around 400 ^{0}C which may be attributed to the disintegration of the epoxy chains attached to zeolite A surface.

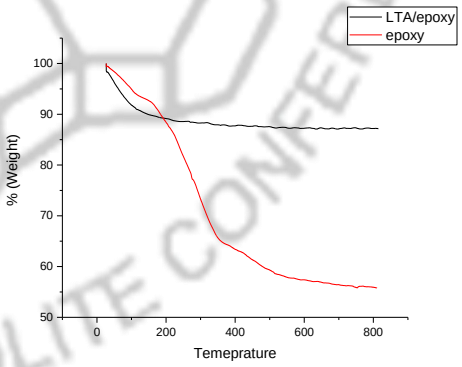

Figure 3. TGA analysis of pristine pure epoxy, and anocomposite zeolite A/epoxy

4. Conclusions

In this study, zeolite nanoparticles could be successfully dispersed in epoxy resin by means of ultrasound and the resulting nanocomposites showed an enhanced performance over the neat polymer. Nanocomposite samples manufactured after sonication showed an enhanced thermal stability.

References

[1] M. Huskić, S. Bolka, A. Vesel, M. Mozetič, A. Anžlovar, A. Vizintin, E. Žagar, *Eur. Polym. J.* 101 (2018) 211-217.

[2] M. Martin-Gallego, V. Yuste-Sanchez, R. Sanchez-Hidalgo, R. Verdejo, M.A. Lopez-Manchado, *Chem.Rec.* (2018).

[3] M. Goyat, S. Rana, S. Halder, P. Ghosh, *Ultrason. Sonochem.* 40 (2018) 861-873.

Chemical modification of bentonite with hydrochloric acid leaching under ultrasound radiation

R. Shahi*, M. Khatamian, B. Divband

[a] *Department of Inorganic Chemistry, Faculty of Chemistry, University of Tabriz, Tabriz, Iran*

**Corresponding author: RShahiii@yahoo.com*

Abstract: The prominent and functional features of clay minerals along with their accessibility and affordability, have led to the use of these minerals in various industries. The clay is found in nature abundantly and can be used in its natural form or modified according to its application before use. This will improve their catalytic properties. Bentonite is a type of clay with a layer structure that is classified in this group. In the present project, a sample of bentonite of Iran, a mineral in East Azarbaijan province, was chemically modified with hydrochloric acid at room temperature. The bentonite structure changes caused by acid modification were determined by XRD patterns and SEM images. Studies have shown that when the clay is in contact with strong inorganic acids for some minutes, its surface and its adsorption activity increase.

Keywords: Bentonite; Hydrochloric acid; Modification; Surface area

1. Introduction

Bentonite is a set of clay minerals, which are swollen minerals, and mostly contains montmorillonite. This clay is found in nature abundantly and has a high adsorption potential. The interlayer cations of this material can be replaced with other organic and inorganic cations. In order to increase the efficiency of bentonite, this mineral is subject to chemical modification. In the process of chemical modification with acid, bentonite is washed by inorganic acids in optimal conditions. This action causes an increase in the adsorption of bentonite and removal of some mineral impurities. The ratio of acid to soil, contact time and contact temperature of acid and soil are important parameters in the acid leaching of clay minerals [1-3].

2. Experimental Part

For chemical modification of bentonite, 5 g of raw bentonite was poured in 15 mL of hydrochloric acid with different concentrations and the mixture was stirred by a magnetic stirrer for one day to homogenize the prepared mixture. The homogenous mixture was then placed in an ultrasound bath for 4 hours and finally the suspension was centrifuged and it was washed with distilled water to adjust the neutral pH. The modified bentonite was dried in oven at 100˚C for 12 hours. Bentonite powder was identified by SEM and XRD techniques.

3. Results and discussion

Figure 1 shows XRD pattern of bentonite before and after acid leaching. The index peaks of the bentonite XRD pattern has been appeared at 2θ = 7.26°, 19.75° and 21.88°. In the XRD pattern of bentonite modified with acid, shift of the strong peak of 2θ =7.26° related to montmorillonite of raw bentonite to angles lower than 2θ, could be due to the increase of distance between layers as a result of acid leaching. This distance is variable and increases as a result of chemical modifications between layers. It can also be seen that the specified peaks for some of the associated minerals, such as quartz and illite, appear after moderate chemical modification. Figure 2 shows the SEM image of raw bentonite. In this figure, bentonite is composed of several sheets and is in the form of accumulated agglomerates. The layer structure and different particle sizes are some of characteristics, which are clearly observed in this image.

Figure 3 shows SEM images of bentonite modified with hydrochloric acid (a) 1 M and (b) 2 M. By comparing the images (a) and (b), it can be found that the modification of bentonite with acid 1 M has no considerable influence on bentonite sheets, and clay particles can be more separated by increasing acid concentration. In the process of acid leaching, the migration of H^+ ions into bentonite layers causes the opening of sheets of these minerals, and the cation exchange creates a gap between the particles and decreases the size [1].

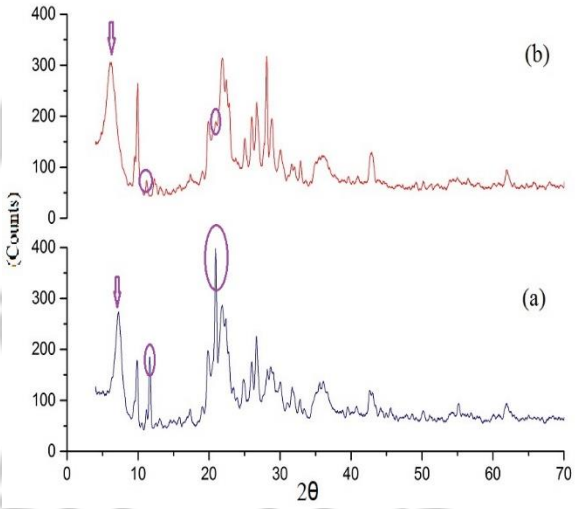

Figure 1. XRD patterns of the raw bentonite (a) and modified bentonite (b)

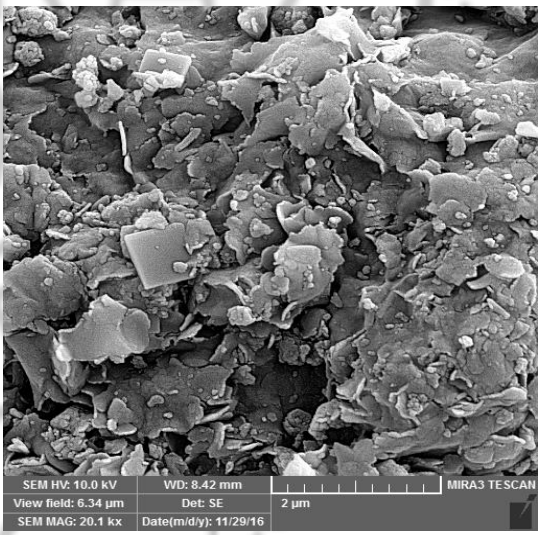

Figure 2. SEM image of raw bentonite

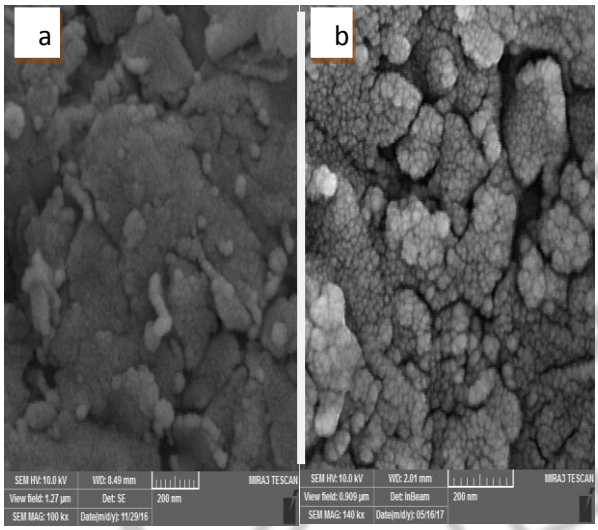

Figure 3. SEM images of bentonite modified with hydrochloric acid 1 M (a) and 2 M (b).

4. Conclusions

When the clay contacts a strong inorganic acid for 24h, its specific surface area and its adsorption activity increases, so that the exchangeable metal cations in the clay layer are separated and H^+ is replaced by them. As a result of acid leaching, the clay particles are separated and some mineral impurities are removed or the intensity of the peaks decreases, so that its catalytic properties and adsorption increase. As concentration of acid increases, the peak intensity and crystallinity decreases as a result of the attack of hydronium cations into bentonite layers.

References

[1] S. Bendou, M. Amrani, *Journal of Minerals and Materials Characterization and Engineering* 2 (2014) 404.

[2] A.K. Panda, B.G. Mishra, D.K. Mishra, R.K. Singh, *Colloids Surf. Physicochem. Eng. Aspects* 363 (2010) 98-104.

[3] I. Daou, O. Zegaoui, A. Amachrouq, *Water Sci. Technol.* 75 (2016) 1098-1117.

Use of Nano-Clays as a topical hemostatic agent in animal model

S. Javanmardi[a], M. Moradi Arzlou*[b], B. Divband[c]

[a] Department of Clinical Sciences, Faculty of Veterinary Medicine, University of Tabriz, Tabriz, Iran.
bDepartment of Pathobiology, Faculty of Veterinary Medicine, University of Tabriz, Tabriz, Iran.
[c]Department of Inorganic Chemistry, Faculty of Chemistry, University of Tabriz, Tabriz, Iran
**Corresponding author: ma.moradi@Tabrizu.ac.ir*

Abstract: Severe blood loss due to trauma is life threatening for the wounded in battle fields, civilian victims of vehicle accidents, street violence, wilderness accidents and construction incidents. Rapid hemostasis is crucial not only for decreasing mortality in these conditions, but also for optimal recovery. In this study, combination of different Nano-clays (NCs) is used as a topical hemostatic agent in a lethal rabbit model of complex groin injury. The mortality in the NSc group (25.0%) is significantly less than that in the control group (56. %). When NCs comes into contact with blood, it rapidly adsorbs water from the blood and holds the water molecules in the pores by hydrogen bonds. Additionally, the negative charge surface provides key surface chemistry, rapidly activating the coagulation process and promoted local hemostasis.

Keywords: Nano-clay, local, hemostatic agent, rabbit

1. Introduction

Hemorrhage is the leading cause of preventable death after a traumatic injury. Commercial hemostatic agents exist, but have various disadvantages including high cost, short shelf-lives, or secondary tissue damage. Hemorrhage is also a primary cause of death on the battlefield, contributing to the 90% of military deaths that occur before medical care is reached. More than half of these deaths occur prior to the victim receiving hospital care**.** These deaths are most prevalent in the emergency medical or military. Sometimes hemorrhage occurs in locations where direct pressure could not stop the bleeding**.** A reduction in the time in which traumatic injuries causing major blood loss receive treatment would save lives and increase the productivity of our communities. In this situation, topical hemostatic agents have been proposed to facilitate hemostasis in severe bleeding preferred.

Clay is a porous agent that is offering a large surface area and acting as a molecular sieve, in-expensive and biocompatible. In this study, combination of different Nano-clays (NCs) is used as a topical hemostatic agent in an external wound model in rabbits.

2. Experimental Part

The objective of our study was to evaluate the hemostatic efficiency Nano-clays. In a lethal rabbit model of complex groin injury using medical gauze as the reference. All research was conducted in compliance with the Animal Welfare. The environment temperature was regulated between 26 °C and 34 °C. The rabbit was first fixed on the operating table and anesthetized with combination of Acepromazine 1%, Xylazine 2% and Ketamine 5%.

A complex groin injury was created in 20 rabbits to produce an uncontrolled hemorrhage. This injury included transection of the proximal thigh soft tissue, complete division of the left groin artery, vein, muscle and nerve just below the groin. This was achieved by cutting these structures with medical scissors. An exposure and cut about 1 cm deep and 4 cm long in the groin was performed to produce the injury. All animals were randomized to be treated with the medical gauze (control group) or NCs+medical gauze immediately. NCs were directly poured into the wound over the vascular injury site, covered with three pieces of gauze, followed by application of direct pressure with the hands (Fig.2).

Fig. 1) Clay Fig.2) NCs were directly poured into the wound over the injury site in the NCs and Control group

In all groups, the compression was maintained for 3 min. After that, the gauze was carefully removed and the hemostasis was evaluated. No additional treatment would be applied, even if the resumption of bleeding was observed. The hemostasis was judged to be complete if there was no oozing of any kind after 20 s of visual observation by two separate laboratory assistants. Mortality was monitored for 3 h after the cut was produced. If the animals began to hemorrhage from the wound site during this course, no additional treatment would be applied. After 3 h, if the animals were still alive the incision, the incision was closed with stitches.

3. Results and discussion

There are significant differences for the hemostatic efficiency between the groups in the animal experiment. Only 6% of the animals achieve hemostasis after gauze treatment (control), while all animals in the CNs group achieve hemostasis (Fig.3). The complex groin injury causes 65% mortality in the control (medical gauze) group. The application of Nano-clays decreases the mortality to 25%. These results demonstrate that the Nano-clays have significant effects in bleeding stop and decreasing the mortality in the lethal rabbit model as a topical agent. When NCs comes into contact with blood, it rapidly adsorbs water from the blood and holds the water molecules in the pores and formed a physical barrier. Additionally, the negative charge surface provides key surface chemistry, rapidly activating the coagulation process and promoted local hemostasis.

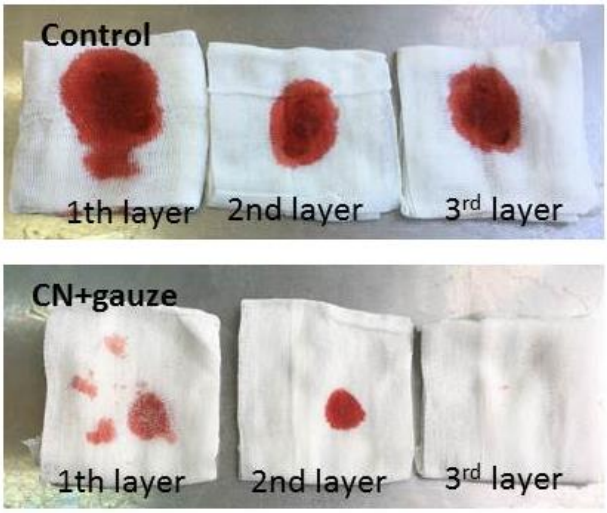

Figure3. The optical image of the first, second and third layer of the medical gauze used

4. Conclusions

In conclusion, the application of Nano-clay in the lethal rabbit model of groin injury significantly decreased the mortality due to hemorrhage. Moreover, their low cost, bio-compatibility, make them an excellent topical hemostatic agent for external wounds.

References

[1] S. E. Baker, A. M. Sawvel, N. Zheng and G. D. Stucky *Chem. Mater.* 19 (2007) 4390–4392

[2] S. Kheirabadi, J.E. Mace and B. TerrazasI., *J. Trauma Inj. Infect. Crit. Care*, 68 (2010) 269–277.

[3] H.B. Alam, Z. Chen, A. Jaskille and R. Querol *J. Trauma Inj. Infect. Crit. Care*, 56 (2004) 974–983.

[4] M.B. Rahmany, R. Hantgan, M. Van Dyke, *Biomaterials*, 34 (2013) 2492–2500.

5th Iran International Zeolite Conference

University of Tabriz, Tabriz, Iran

26-27 August 2018

Introduce Nano Cu on Bentonite and Investigation of Antibacterial properties

P. Maleki*[a], Z. Mortezaei [b], M. Zendehdel[b]

[a]*Department of Biology, Faculty of Science, Arak University, Arak 38156-8- 8349, Iran*

[b]*Department of Chemistry, Faculty of Science, Arak University, Arak 38156-8- 8349, Iran*

**Corresponding author: P-Maleki @araku.ac.ir*

Abstract: In this work Cu^0–Bentonite compound was prepared and characterized by using FT-IR, XRD, SEM techniques. Then their antibacterial properties against different bacteria (gram-positive and gram negative bacteria) was investigated.

Keywords: Nano Cu, Bentonite, Antibacterial properties

1. Introduction

Microorganisms are part of the organic matter in the wastewater. These organic materials can affect human health and are commonly found in wastewater because they are present in fecal material. The removal or inactivation of pathogenic microorganisms is the last step in the treatment of wastewater. Some chemical and physical agents, such as chlorine, ultraviolet light, reverse osmosis, and silver catalyst are well developed [1–3]. The bactericide activity of Copper ions has been known for a long time. Copper is an essential mineral perceived by the public today as being of "exceptional biologic and public health importance", especially regarding prenatal and postnatal development [4]. In the last few years, several investigations were carried out using synthetic and natural zeolites that combined with silver ions to obtain disinfection agents for the treatment by microbiologically polluted water.

2. Experimental Part

Synthesis of Cu^0-Bentonite

At first, $CuCl_2.2H_2O$ solution was added to Bentonite and stirred for 48 h at room temperature. Then Cu^{2+} was introduced to it and the solid compound (Cu^0-Bentonite) was synthesized by adding $NaBH_4$ solution. The product was heated and dried at 120 ºC for 3h in oven.

3. Results and discussion

The Cu^0–Bentonite compound synthesized successfully and characterized using FT-IR, XRD, SEM techniques.

The FT-IR spectrum of Cu^0-Bentonite indicate an intense band about ca.1080 cm^{-1} attributable to the asymmetric stretching of Al–O–Si chain of zeolite. The symmetric stretching and bending frequency bands of Al–O–Si framework of zeolite appear at ca.795 and 469 cm^{-1}, respectively.

X-ray diffraction pattern of Cu^0-Bentonite is shown in Fig.2. A, some diffraction peaks in range 2θ = 0-80 ˚ can be indexed as the Cu and Bentonite. The

peak from Cu which introduce to the zeolite structure can clearly be seen 2θ= 5.3°. The result in Fig. 3 showed that the synthesized Cu^0-Bentonite powder were particle Shape with the diameter of 11-17 nm and were made.

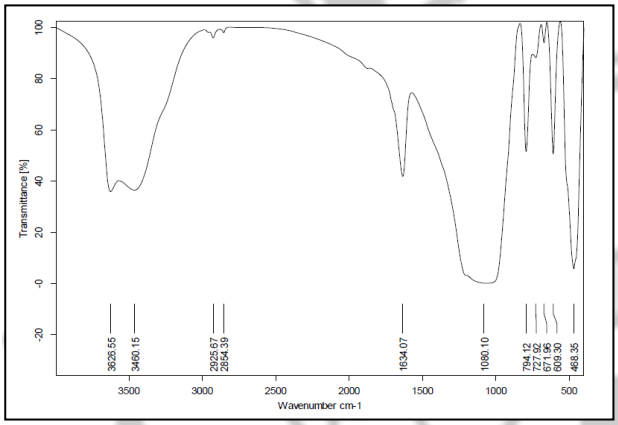

Figure 1. The FT-IR of Cu^0-Bentonite

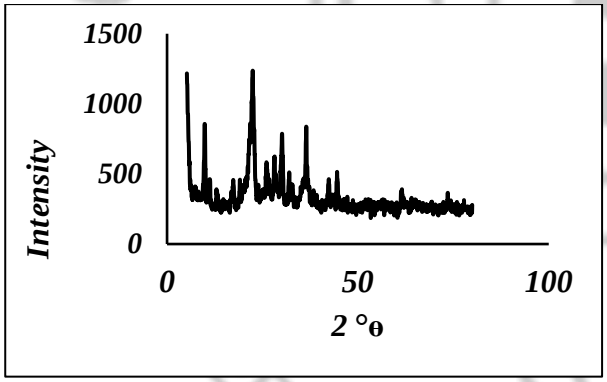

Figure 2. The XRD pattern of Cu^0-Bentonite

Antibacterial activity study

The in vitro antibacterial activity of the investigated compounds was tested against pathogenic Gram-negative bacteria's such as P. aeruginosa and E. coli and Gram-positive bacteria's such as B. subtilis and S. aureus using the paper disc diffusion method according to the procedure described by Hwang and Ma [5]. This method is a way to measuring efficiency of an antibacterial agent against the mentioned bacterial growth. Mueller Hinton broth was used for preparing culture media for the bioassay of the organisms. A lawn culture from 0.5 Mac Farland suspension of each strain was prepared on Mueller Hinton agar. The agar medium was sterilized in autoclave, cooled to room temperature, and then poured into sterilized Petri dishes. The bacteria of interest are swabbed uniformly across a culture plate, while the Petri dishes are cooled over 24 h. Discs of samples were placed on the surface of the medium and finally, all Petri dishes containing bacteria and antibacterial reagents were incubated and maintained at 37 C for 24 h. After this period, the diameters of the inhibition zones formed around each disc were determined and presented in mm.

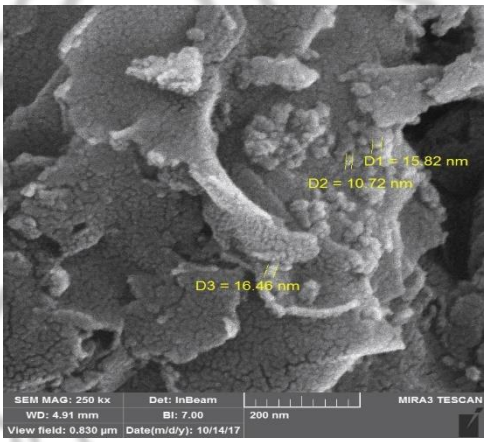

Figure 3. The SEM image of Cu^0-Bentonite

4. Conclusions

The in vitro antibacterial activity of Cu^0-Bentonite was evaluated against Bacillus subtilis and Staphylococcus aureus (as Gram-positive bacteria), Pseudomonas aeruginosa and Escherichia coli (as Gram-negative bacteria), and compared with standard drugs. The results show that Cu^0-Bentonite has more inhibition on bacterial growth.

References

[1] G. Finch, E. Black, L. Gyurek, *Water quality technology conference, AWWA* (1994) 1303-1309.

[2] W. Gujer, U. von Gunten, *Water Res.* 37 (2003) 1667-1677.

[3] E. Hassinger, A.D. Thomas, B.B. Paul, *Reverse osmosis units water facts*, 1994.

[4] K.M. Hambidge, N.F. Krebs, *J. Nutr.* 137 (2007) 1101-1105.

[5] J.-J. Hwang, T.-W. Ma, *Mater. Chem. Phys.* 136 (2012) 613-623.

Clinoptilolite vs Bentonite as Support of Silicotungstic Acid in Photodegradation of Wastewater

S. Rastegar[a], S. Allahyari*[a], D. Kahforooshan[a], N. Rahemi[a]

a Chemical Engineering Faculty, Sahand University of Technology, Tabriz, Iran.

**Corresponding author: Allahyari@sut.ac.ir*

Abstract: In this study, silicotungstic acid (HSiW) was impregnated on natural zeolites of clinoptilolite (HSiW/Clin) and bentonite (HSiW/Bent). SEM analysis indicated while both samples had homogeneous distribution and nano scale particles, but particles of HSiW/Clin were smaller with no agglomeration. Optical studies with DRS showed that HSiW/Clin had more light absorption both in visible and UV regions and its band gap was lower. While HSiW/Clin as a photocatalyst degraded 92% of methylene blue, HSiW/Bent barely could degrade 40%. Study on effect of HSiW/Clin loading indicated that there was an optimum amount of 0.2 g in which the highest MB degradation took place.

Keywords: Photocatalyst; Wastewater; Natural zeolite; Clinoptilolite; Bentonite.

1. Introduction

Nowadays water sources are exposed to various microbial and chemical contaminations. Colors are among the most dangerous chemical compounds found in industrial wastewater. Photocatalytic oxidation has the ability to remove organic pollutants and microorganisms[1]. In this research, the goal was selecting a proper support among natural zeolites or clays for photocatalyst of silicotungstic acid to remove organic pollutants like methylene blue from wastewater. Silicotungstic acid as a polyoxometalate is able to remove organic pollutants after absorbing UV light as a strong oxidizing agent [2]. The simplicity of the procedure, low cost, non-toxicity, abundance and environmentally benign nature are the advantages of using natural zeolites and clays.

2. Experimental Part

HSiW was added to ion exchanged and acid washed supports of clinoptilolite and bentonite. The slurry was stirred at 70°C for 4h. Then the powder was dried in an oven for 12 h at 80°C.

3. Results and discussion

According to SEM analysis shown in Fig.1, both samples of HSiW/Clin and HSiW/Bent have a spherical and homogeneous morphology in nano range. The average particle size in HSiW/Clin and HSiW/Bent photocatalysts was 7.9 nm and 11.08

nm, respectively. Agglomerations in irregular shape was founded in HSiW/Bent photocatalyst.

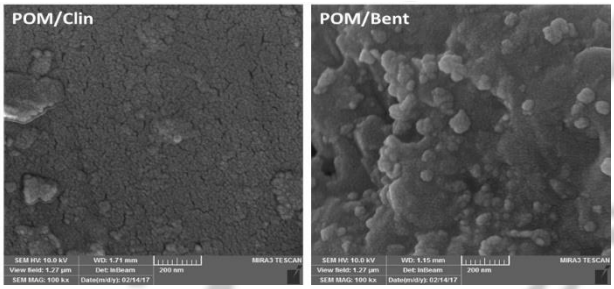

Figure 1. SEM pictures of HSiW/Clin and HSiW/Bent

DRS analysis indicated in Fig.2 showed stronger photo activity of studied photocatalysts in UV light (200-400 nm) and weaker in visible light (> 400 nm wavelength) [3]. Comparing DRS of photocatalysts showed that HSiW/Clin in both regions of UV and visible has higher photo activity which means more capability of electron-hole formation. Calculated band gap from Tauc plots showed 3.1 and 3.22 eV band gap for HSiW/Clin and HSiW/Bent respectively. Lower band gap of photocatalyst with clinoptilolite leads to easier electron-hole formation as first step of photolysis. The photocatalytic removal of

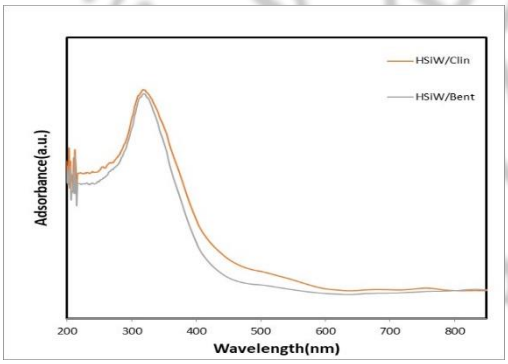

Figure 2. DRS analysis of HSiW/ Clin and HSiW/Bent

methylene blue was carried out and the results in Fig.3 revealed that HSiW/Clin is capable of removing 92% of initial methylene blue after 90 min of UV irradiation while HSiW/Bent just degraded almost 40%.

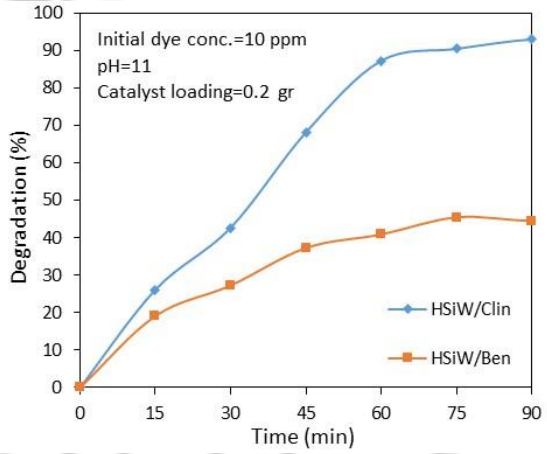

Figure 3. photodegradation of MB over HSiW/Clin and HSiW/Bent

Uniform and agglomeration free morphology, small particle size and more production of electron-hole in HSiW/Clin are the reasons of higher photocatalytic activity. Moreover, XRD and FTIR (not shown) indicated that HSiW/Clin has smaller crystallites of HSiW with more crystallinty and also stronger interaction between HSiW and support in the case of HSiW/Clin photocatalyst. Figure 4 shows the effect of HSiW/Clin loading in methylene blue photodegradation. The photolysis just removed 10% of methylene blue. Introducing HSiW/Clin to the reactor increased the MB degradation because now besides photolysis free radicals produced from electron- holes can proceed the degradation.

Enhancing the photocatalyst loading increased the MB degradation but adding more catalyst than 0.2 g declined the performance probably due to light scattering and mass transfer limitations.

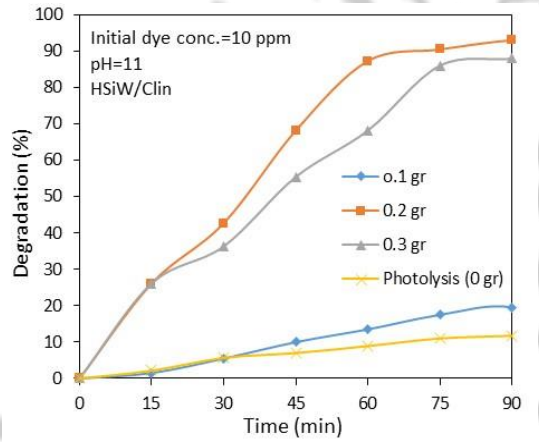

Figure 4. Effect of HSiW/Clin loading on MB degradation

4. Conclusions

In this research, it was shown that support in photocatalysts has a great role. Comparing natural minerals of clinoptilolite and bentonite as support of silicotungstic acid showed clinoptilolite due to possessing uniform morphology, stronger interaction with HSiW, smaller particles, and more light absorption in all range of wavelengths has higher capability of MB photodegradation.

References

[1] M.N. Chong, B. Jin, C.W. Chow, C. Saint, Water Res. 44 (2010) 2997-3027.
[2] T. Fotiou, T.M. Triantis, T. Kaloudis, E. Papaconstantinou, A. Hiskia, J. Photochem. Photobiol. A: Chem. 286 (2014) 1-9.
[3] W. Zhou, M. Cao, S. Su, N. Li, X. Zhao, J. Wang, X. Li, C. Hu, J. Mol. Catal. A: Chem. 371 (2013) 70-76.

Degradation of Methylene Blue using Mordenite Based Silicotungstic Acid Photocatalyst

S. Rastegar[a], S. Allahyari*[a], D. Kahforooshan[a], N. Rahemi[a]

[a] *Chemical Engineering Faculty, Sahand University of Technology, Tabriz, Iran.*

**Corresponding author: Allahyari@sut.ac.ir*

Abstract: In this research, methylene blue photocatalytic degradation was carried out using photocatalyst of silicotungstic acid on natural zeolite of mordenite as support. This photocatalyst was characterization by XRD, FESEM and DRS analyses and the results showed that silicotungstic acid/mordenite (HSiW/Mord) has a uniform, agglomeration free distribution with average size of 9.7 nm. This catalyst indicated almost sharp peaks of HSiW and no peaks of mordenite in XRD pattern. DRS confirmed 3.17 eV for band gap of HSiW/Mord photocatalyst which is reduced compared to HSiW. The evaluation of photocatalytic activity showed that HSiW/Mord in the concentration of methylene blue of 10 ppm and pH=11 is almost 60% of initial value.

Keywords: Photocatalyst; Wastewater; Natural zeolite; Mordenite; Silicotungstic acid

1. Introduction

The colorful wastewater from textile industries is one of the major sources of environmental pollution. Among the colored materials, azo dyes have many uses [1]. Knowing the limitation in water resources and increasing need for optimal utilization of refined wastewater, makes the introducing novel treatment methods important. The use of heterogeneous photocatalytic processes to remove pollutants from wastewater is an effective and efficient method [2]. Polyoxometalates are homogenous effective photocatalysts which are suffering from difficult separation after use. Impregnation of these materials on porous supports can solve the problem. Therefore, in this study, natural zeolite of mordenite which is inexpensive and abundant was studied as support of silicotungstic acid.

2. Experimental Part

HSiW was impregnated on ion exchanged and acid washed support of mordenite. The slurry was stirred at 70 °C or 4h. Then the powder was dried for 12 h at 80 °C.

3. Results and discussion

FESEM picture in Fig. 1 shows the uniform morphology of HSiW/Mord without any agglomeration. Particle size distribution indicated average particle size of 9.7 nm for this catalyst. HSiW/Mord has particles with sizes barely exceeded from 30 nm.

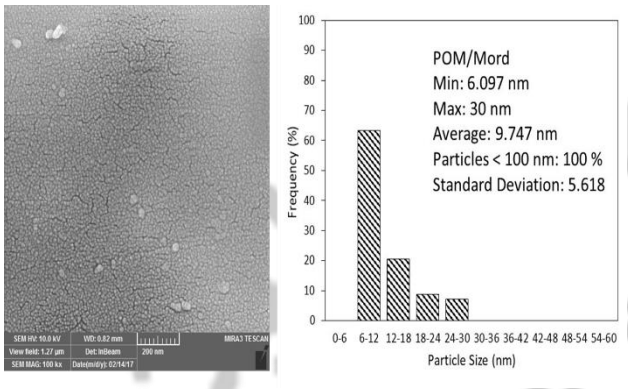

Figure 1. FESEM picture of HSiW/mordenite

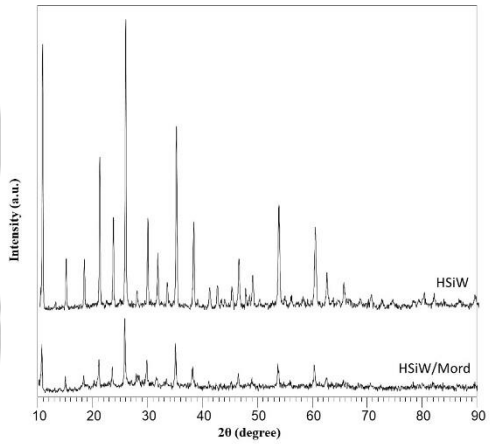

Figure 2. XRD pattern of HSiW/mordenite

The XRD pattern of pure HSiW and HSiW/Mord has been indicated in Fig. 2. Pure HSiW is strongly crystalline but HSiW/Mord has lower crystalline degree. The peaks attributed to mordenite are absent which confirms amorphous nature of this zeolite or very small crystallites. The small particles confirmed from FESEM and XRD resulted in strong interaction between HSiW and mordenite.

According to the result of DRS analysis given in Fig. 3, the HSiW/Mord photocatalyst has the potential for photocatalyst activity both in visible and ultraviolet regions. According to literature, Keggin type polyoxometalates, including silicotungstic acid only has light absorption in UV region [3] and no photoactivity for mordenite has been reported. The photo activity of HSiW/Mord in UV and visible wavelengths observed in this paper shows positive effect of natural zeolite of mordenite in formation of visible light driven photocatalysts probably due to trapping electrons.

Mordenite similar to other zeolites has a negative surface charge that results in electron donation to HSiW. The HSiW/Mord photocatalyst has 3.17 eV ban gap according to Tauc calculations while the band gap of HSiW has been reported to be 3.4 eV [4]. This reduction in band gap reveals the effect of mordenite in shifting the photo activity of the catalyst to visible region.

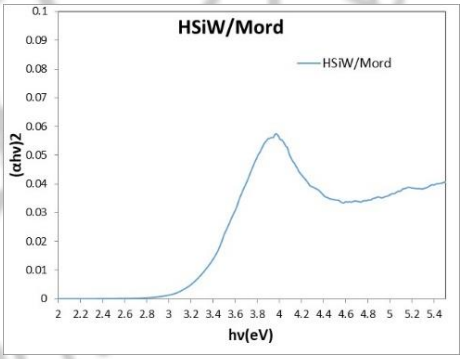

Figure 3. DRS pattern of HSiW/mordenite

The results of photocatalytic methylene blue removal have been indicated in Fig. 4. The HSiW/Mord photocatalyst, could remove 60% of the MB after 105 minutes.

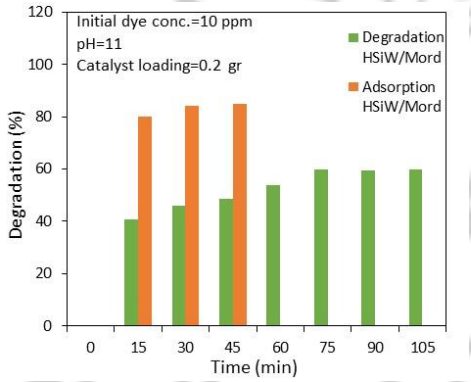

Figure 4. Adsorption and degradation of MB by HSiW/Mordenite

4. Conclusions

In this study HSiW/Mord photocatalyst was introduced and its physical and chemical properties were investigated. The efficiency of this photocatalyst in MB degradation was almost 60%. HSiW/Mord due to uniform morphology, small particle size, crystalline degree, photoactivity in both UV and visible regions has the ability to decompose methylene blue in water.

References

[1] A. Khataee, M. Zarei, R. Ordikhani-Seyedlar, *J. Mol. Catal. A: Chem.* 338 (2011) 84-91.

[2] O.M. Rodriguez-Narvaez, J.M. Peralta-Hernandez, A. Goonetilleke, E.R. Bandala, *Chem. Eng. J.* 323 (2017) 361-380.

[3] W. Zhou, M. Cao, S. Su, N. Li, X. Zhao, J. Wang, X. Li, C. Hu, *J. Mol. Catal. A: Chem.* 371 (2013) 70-76.

[4] K.-J. Kim, O.-B. Yang, *J. Photochem. Photobiol. A: Chem.* 173 (2005) 56-63.

Adsorptive removal of tetracycline from aqueous solution using TiO_2/MCM-41 nanocomposite

M. Khanmohammadi[a], F. Rahmani[b*], J. Rahbar Shahrouzi [a]

[a] *Faculty of chemical engineering, Sahand University of Technology, Sahand new town, Tabriz, Iran*

[b] *Department of engineering, chemical engineering group, University of Kurdistan, sanandaj, Iran*

**Corresponding author: farhad.rahmanichiyane@gmail.com*

Abstract: In this study, TiO_2/MCM-41 nanocomposite was prepared by loading 10 wt.% titania onto the mesopores structure of hydrothermally synthesized MCM-41 molecular sieve via impregnation method and was used to remove Tetracycline by adsorption process. The XRD and EDX results revealed that the nanocomposite adsorbent was successfully synthesized. Using BET N_2-adsorption technique, the specific surface area of TiO_2/MCM-41 was found to be 870 m^2/gr. The experimental results demonstrated that TiO_2 and neat MCM-41 exhibit very less pollutant adsorption compared to TiO_2/MCM-41. It was also found that the nanocomposite adsorbent has excellent adsorptive potential, giving 92 % removal at 50 mg/L Tetracycline concentration and ambient temperature after 5 hrs. From kinetic studies, the adsorption of Tetracycline on TiO_2/MCM-41 was found to follow the pseudo-second-order kinetics.

Keywords: Adsorption; TiO_2/MCM-41; Tetracycline; Kinetics studies.

1. Introduction

Pharmaceutical antibiotics have been applied worldwide in human therapy and the farming industry. Thus, antibiotics especially tetracycline (TC) antibiotics have attracted many people's attentions, recently. TC has been considered to be a class of potential pollutants. Little amount of TCs can cause serious environmental pollution. The continuous release of TC into aquatic environment increases the potential for antibiotic resistance among microbial populations, and the degradation by-products have been proven even more toxic than the parents [1].

Adsorption of various pollutants from aqueous solution has proven to be an excellent way to treat effluent. According to the literature, numerous low cost materials have been successfully applied in the removal of pollutants from aqueous solution, some of which are coal, fly ash, wood, silica, shale oil ash, Fuller's earths, zeolite, perlite and etc [2].

Mesoporous materials with ordered pore structure and large surface area have shown promise for applications ranging from air to water purification. These materials are considered to have good potential for adsorption/separation applications because of regular hexagonal structure, uniform pore distribution, large surface area and large pore volume. Untreated or functionalized mesoporous silica has been applied in different pollutants adsorption. For example, the MCM-41 was used to

remove nitrobenzene, phenol, o-chlorophenol and divalent metal cations from aqueous solution [1]. Based on the literature assignments [3], TiO_2 loading over MCM-41 significantly enhance adsorption capacity of adsorbent in the adsorptive removal of Cr(VI) in aqueous state. To the best of our knowledge, there is no literature about the TiO_2-loaded MCM-41 molecular sieve as adsorbent for the TC removal.

The objective of this research is to study the removal efficiency of TC using MCM-41/TiO_2. Also, kinetic data have been evaluated.

2. Experimental Part

The pristine MCM-41 was prepared by hydrothermal method reported in literature [4] and the TiO_2/MCM-41 samples were prepared by post synthesis method. The required amount of the titanium (IV) tetraisopropoxide, corresponding to 10 wt.% TiO_2 in the final product, was added to the MCM-41-suspended isopropanol solution and the mixture was mixed. The impregnation lasted until isopropanol evaporated. After dried, the impregnated sample was calcined at 500 °C for 3 hr.

The batch experiments were carried out in 250 mL reactor equipped with an external water-cooling bath by agitating 0.1 g of TiO_2/MCM-41 adsorbent with 200 mL of the aqueous TC solution (50 mg/L) for a predetermined period at 300 K on a magnetic stirring in dark condition. After the adsorption, the concentration of TC in the solution was determined by UV–vis spectroscopy (UV-6700 Series, Jenway, UK, $\lambda = 360$ nm).

3. Results and discussion

As shown in Fig. 1, the percentage adsorption of TC increased with increase in contact time and reached the equilibrium after 5 hours. The removal of TC happened immediately at first due to the enough reactive sites available on the surface of TiO_2/MCM-41. After 5 hr when most of reactive sites were occupied, TC adsorption proceeded with very slow speed. Also, the obtained results were evident that the percentage adsorption of TC decreased from 81% in TiO_2/MCM-41 to 20 % and 8 % in neat MCM-41 and TiO_2 at initial TC concentration of 50 mg/L after 2 hr, respectively.

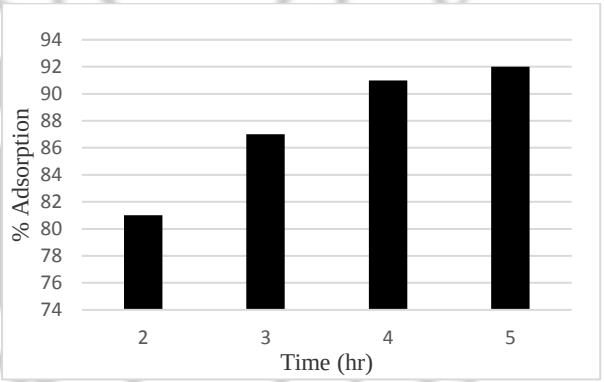

Figure 1. Percentage adsorption of TC on TiO_2/MCM-41 at different time.

The pseudo-second-order model is represented as Eq. (1):

$$\frac{1}{q} = -\left(\frac{1}{k_2 q_e^2}\right)\left(\frac{1}{t}\right) + \frac{1}{q_e} \quad (1)$$

Where k_2 is the rate constant of the second-order adsorption (g mg^{-1} min^{-1}) and q and q_e are the transient and equilibrium amount of adsorbate adsorbed [5]. In Fig. 2, plot 1/q versus 1/t was used for obtaining the rate parameters .The Kinetic

parameters for the adsorption of TC presented in Table 1.

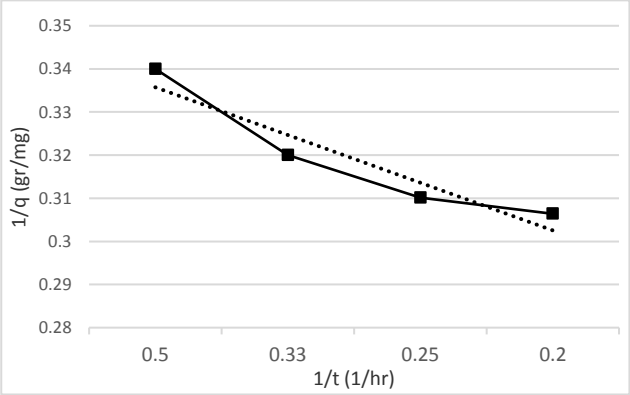

Figure 2. Pseudo-second order kinetic model for removal of TC by MCM-41/TiO_2

Table 1. The kinetic parameters for adsorption of TC

Concentration (mg/L)	k_2	q_e (mg/g)	R^2
50	10.86	2.88	0.9017

4. Conclusions

The data indicates that MCM-41/TiO_2 composite system is an effective adsorbent for treatment of tetracycline in contaminated water. The maximum adsorption of TC by MCM-41/TiO_2 can reach 92%. The kinetics of TC adsorption was well described *pseudo*-second order model.

Reference

[1] M. Liu, L. an Hou, S. Yu, B. Xi, Y. Zhao, and X. Xia, *Chem. Eng. J.* 223 (2013) 678–687.

[2] E. Bulut, M. Özacar, and I. A. Şengil, *J. Hazard. Mater.* 154 (2008) 613–622.

[3] K. Parida, K. G. Mishra, and S. K. Dash, *J. Hazard. Mater.* 241-242 (2012) 395–403.

[4] E. Asghari, M. Haghighi, and F. Rahmani, *J. Mol. Catal. A Chem.* 418-419 (2016) 115–124.

[5] L. Zhang, X. Song, X. Liu, L. Yang, F. Pan, and J. Lv, *Chem. Eng. J.* 178 (2011) 26–33.

5th Iran International Zeolite Conference

University of Tabriz, Tabriz, Iran

26-27 August 2018

Shaping of Zeolite 4A by Binderless Process

M. Rezaie*

Behdash Chemical Company, LIA Industrial Park. Bouein Zahra Rd, Qazvin, Iran

**Corresponding author:Rezaie.marzi@gmail.com*

Abstract: For many commercial uses of molecular sieves, it is more desirable to have a larger molecular sieves body or agglomerate rather than the small crystals in order to achieve the highest possible volumetric adsorption capacity as well as to facilitate handling of the adsorbent. At the same time, it is desirable that this agglomerate have not only such characteristics as relatively high attrition resistance and crush strength, but also that it maintain substantially all the adsorption capacity, adsorption selectivity, and thermal stability characteristics exhibited by the finely-divided crystalline material. In this paper binderless process for shaping of zeolite 4A is proposed.

Keywords: Zeolite 4A powder; Binderless; Binder; Kaolin

1. Introduction

In 1862, the first synthesis of zeolite was reported by St. Claire-Deville [1]. However, the pioneer work of Barrer on zeolite in 1948 concluded that a wide range of zeolites could be synthesized from aluminosilicate gels [2,3], which has brought to the new advancement of zeolite from various sources of alumina and silica. Gougazeh and Buhl [4] emphasized the importance of synthesizing zeolite in the form that suits to the industrial application. Also, Meng et al. [5] is just concern about green routes for synthesizing zeolites, distinctively concentrating on significant reduction of organic templates and possible elimination of solvent by employing templates recycling approach with the use of nontoxic templates. Zeolite A is the type of synthetic zeolite which has special properties such as large ion exchange capacity, mechanical strength and particular crystal shape. Besides, it is environmentally safe with almost zero loading of harmful effects on the environment [6]. Since the formation of zeolite 4A is a very important factor in their industrial uses, in this paper binderless method for shaping of zeolite 4A was summarized. Ultrafine to fine cohesive solid powders are often shaped by mixing a powder with the solid binder to initiate agglomeration. The added liquid binder or mixture, is then solidified by thermal drying or crystallization on cooling following super-saturation, forming so-called ‘solid binder bridges’ between the primary particles. The binder content, the binding mechanism and the shaping process in itself, basically affect the physical and chemical properties of the final shapes [7].

2. Process of zeolite shaping

Many methods such as spheres, beads, etc., are known for making agglomerates from molecular sieve powder. An appropriate binder material such as a clay (bentonite, kaolin or attapulgite), an organic and inorganic compound is utilized for this purpose. Large-scale production with acceptable results have been achieved by these processes. However, they are relatively complicated and need careful control to insure consistent properties in the agglomerated product [8]. There are two general processes for the formation of zeolites: 1- Use of permanent binders that remain in the structure, 2- Use of temporary binders that are converted to zeolite during reaction (binderless structure).

3. Forming of zeolite 4A by binderless process

Usually, in this process kaolin consider as temporary binder and for better performance, it turns into reactive kaolin by thermal process. Then reactive kaolin and distilled water were mixed with desired weight of NaA zeolite powder that produced according to the literature and stirred gently till a thick slurry was prepared. The slurry was set aside to release the extra water and form a paste. This paste were formed by tumbling and dried till the moisture decreased. Next digestion and crystallization process was performed continually [8,9]. Kaolin type materials having SiO_2/Al_2O_3 ratio in the range of about 1.2 to nearly 2.3 may be used in this process. Analysis of typical kaolin-type materials is shown in Table 1.

Table 1. Analysis of typical kaolin-type materials.

Oxide	Georgia Kaolinite A		Georgia Kaolinite B		North Carolina Kaolinite C		Utah Halloysite	
	Percent by wt.	Moles	Percent by wt.	Moles	Percent by wt.	Moles	Percent by wt.	Moles
Na_2O	0.2		0.4		0.82		<0.1	
K_2O	<0.1		0.43					
Al_2O_3	40.2	1.0	37.2	1.00	37.2	1.0	37.3	1.00
SiO_2	45.0	1.9	44.82	2.04	48.2	2.20	41.6	1.89
Ign. Loss (as H_2O)	9.4	1.33	14.68	2.23	13.1	1.99	20.0	3.04
TiO_2	2.5		1.26					
Other	1.4		1.31		0.78			
	98.8		100.1		100.1		98.9	

According to this patent the mixture of 20% 4A powder and 80% reactive kaolin were desirable for forming of 4A (Table 2).

Table 2. Production of 4A preforms from 4A powder, Reactive kaolin and Included Caustic.

Composition of Mixture Before Shaping		Digestion Condition					Product Purity Percent 4A	Capacity Factor
				Reactant Comp.				
Wt. Percent 4A Powder	Wt. Percent Reactive Kaolin	Time, Hr.	Temp., °C	Na_2O/SiO_2	SiO_2/Al_2O_3	H_2O/Na_2O		
10	90	0					78	0.64
		4	R.T.	0.8	2.0	40	84	0.68
		2	45	0.8	2.0	20	91	0.70
		4	45	0.8	2.0	20	92	0.72
15	85	4	R.T.	0.8	2.0	20	92	0.71
20	80	0					81	0.62
		4	R.T.	0.8	2.0	20	90	0.68
		16	R.T.	0.8	2.0	20	94	
		4	45	0.8	2.0	20	92	0.72
		16	45	0.8	2.0	20	95	0.74
		24	45	0.8	2.0	20	92	0.72
25	75	0					82	0.66
		4	R.T.	0.8	2.0	20	92	0.70
30	70	4	45	0.8	2.0	20	90	0.73

4. Conclusion

In this paper, formation of zeolites was explained by binderless process as green method. This method has advantages and disadvantages that rely on the binder structure and method of work, thus the adsorption rate of a molecular sieve product is not only dependent on the size of the formed zeolite particles, but also the type and characteristics of binder blended with the zeolite.

Acknowledgments

The author is thankful to Research Council of Behdash Chemical Company for financial support to this study.

References

[1] T. B. Reed, D. Breck, *J. Amer. Chem. Soc.* 78 (1956) 5972-5977.

[2] R. Szostak, *Molecular Sieves Principles of Synthesis and Identification*, 1989, Blackie Academic and Professional, London.

[3] D.W. Breck, *Zeolite molecular sieves: structure, chemistry and use*, 1974, New York.

[4] M. Gougazeh, J.-C. Buhl, *J. Assoc. Arab Univ. Basic Appl. Sci.* 15 (2014) 35-42.

[5] X. Meng, L. Wang, F.-S. Xiao, *Sustainable Routes for Zeolite Synthesis*, in *Zeolites in Sustainable Chemistry*, 2016, Springer.

[6] K. Hui, C.Y.H. Chao, *J. Hazard. Mater.* 137 (2006) 401-409.

[7] W.B. Pietsch, *Agglomeration processes: phenomena, technologies, equipment*, 2008, John Wiley & Sons.

[8] L.T. Le Roy, G.L. Ribaud, *Process for producing molecular sieve bodies*, 1964, Google Patents.

[9] K. Shams, S. Mirmohammadi, *Micropor. Mesopor. Mater.* 106 (2007) 268-277.

.

5th Iran International Zeolite Conference

University of Tabriz, Tabriz, Iran

26-27 August 2018

Shaping of Zeolite 4A by Binder Process

M. Rezaie*

Behdash Chemical Company, LIA Industrial Park. Bouein Zahra Rd, Qazvin, Iran

**Corresponding author:Rezaie.marzi@gmail.com*

Abstract: In commercial processes, the porous powders are processed to produce structured bodies by a variety of shaping methods. A larger molecular sieves body or agglomerate rather than the small crystals has the highest possible volumetric adsorption capacity as well as to facilitate handling of the adsorbent. It is desirable that these shapes show crush strength, attrition resistance, thermal stability and high adsorption capacity and selectivity. In this paper binder process for shaping of zeolite 4A is investigated.

Keywords: Zeolite 4A powder; Binder; Binderless; Kaolin; Attapulgite

1. Introduction

Zeolites are crystalline aluminumsilicates with molecule sized pores or pore channels and high specific surface areas. The ordered zeolite pores (typically 2.5–10 Å) enable the separation of gases and catalytic transformations of small molecules [1,2]. The inorganic crystalline structures of zeolites are highly stable to temperature variations, and their catalytic and adsorption features render them desirable in various household and industrial applications. Powder processing routes to produce structured adsorbents and catalysts have much in common with ceramic processing. The main processing steps involve: (i) mixing the porous powder with inorganic and organic additives, (ii) shaping the powders into the desired engineering shape, and (iii) removing temporal additives and creating a mechanically robust structure by thermal treatment. The porous powders are processed to produce structured bodies by a variety of shaping processes. The subsequent thermal treatment is primarily performed to increase the bonding in the shaped powder body but may be combined with a burn-out step for the removal of organic additives used to facilitate the shaping process. Inorganic binder such as clays and silica are commonly added to impart the desired mechanical strength [3]. The binder content, the binding mechanism and the shaping process in itself, fundamentally influence the physical and chemical properties of the resulting shapes [4]. Zeolite A is the type of synthetic zeolite, which has special properties such as large ion exchange capacity, mechanical strength and particular crystal shape. Besides, it is environmentally safe with almost zero loading of harmful effect on the environment. Since the

formation of zeolite 4A is a very important factor in their industrial uses, in this paper methods for shaping of zeolite 4A were summarized.

2. Process of zeolite shaping

There are two general processes for the formation of zeolites: 1- Use of permanent binders that remain in the structure, 2- Use of temporary binders that are converted to zeolite during the reaction (binderless structure). A variety of shaping processes such as spheres, beads, etc., from molecular sieve powder are known. Such methods involve the use of a suitable binder material such as a clay (bentonite, kaolin or attapulgite), an inorganic compound or an organic compound. These methods, several of which have been adapted to large-scale production with satisfactory results, however, these are relatively complicated and require careful control to insure consistent properties in the agglomerated product.

3. Forming of zeolite 4A by binder process

Usually, in this process kaolin, attapulgite and highly dispersed attapulgite clay consider as permanent binder. Attapulgite is a magnesium aluminum phyllosilicate with formula $(Mg,Al)_2Si_4O_{10}(OH)\cdot 4(H_2O)$. In common, process clay (kaolin or attapulgite) is mixed with zeolite and shaped. The formation of this zeolite body is caused to decrease the surface area and adsorption capability of body. So highly dispersed attapulgite clay applies as the binder that is blended with the zeolite powder. This binder has a large surface area and therefore increases the adsorption capacity of preforms thus the adsorption rate of a molecular sieve product is not only rely on the size of the formed zeolite particles, but also the type and features of the binder mixed with the zeolite. The same type and quantity of zeolite when blended with different binder produces zeolite blends, which exhibit distinct characteristics depending on the binder that is utilized. This process is done as follows [5]:

1- Making a zeolite powder, 2- Preparing the binder, 3- Blending the zeolite with clay (kaolin, attapulgite and highly dispersed attapulgite) as binder and water to produce a mixture, 4- Forming a molecular sieve body from the mixture, 5- Calcination the body to form the molecular sieve adsorbent blend product.

According to this patent, the amount of highly dispersed attapulgite binder that is utilized can range from 5 to about 30% by weight, and most preferably in the range of about 10% of the mixture. Common attapulgite clay binder applies about 20% or more. A pore forming agent may be combined to the zeolite/attapulgite clay mixture during the mixing step to enhance the total pore volume of the end product (Table 1).

Table 1. Comparative results between highly dispersed attapulgite and attapulgite binder.

Comparative Results of a Conventional 5A Molecular Sieve and a Molecular Sieve Produced with 15% Highly Dispersed Attapulgite Clay as a Beneficiated Attapulgite Binder		
	Reference Material (20% Conventional Dense Attapulgite Binder)	According to Invention (15% Highly Dispersed Attapulgite Clay)
Bead Size [mm]	2-3	2-3
Crush Strength [N]	57	41
Attrition [%]	0.03	0.01
Bulk Density [g/l]	729	710
Water Mass Transfer Zone [mm]	137	106
Water Adsorption Kinetic at p/p_0 (after 120 min.) [%]	15.0	17.2

4. Conclusion

In this paper, binder process as general method for the formation of zeolites was explained. This method has advantages and disadvantages that depend on the binder structure and method of work, thus the adsorption rate of a molecular sieve product is not only dependent on the size of the formed zeolite particles, but also the type and characteristics of binder blended with the zeolite.

Acknowledgments

The author is thankful to Research Council of Behdash Chemical Company for financial support to this study.

References

[1] N. Hedin, L. Chen, A. Laaksonen, *Nanoscale*, 2 (2010) 1819-1841.

[2] J. Pérez-Ramírez, C.H. Christensen, K. Egeblad, C.H. Christensen, J.C. Groen, *Chem. Soc. Rev.* 37 (2008) 2530-2542.

[3] N. Gordina, V.Y. Prokof'ev, A. Il'in, *Glass Ceram.* 62 (2005) 282-286.

[4] W.B. Pietsch, *Agglomeration processes: phenomena, technologies, equipment*, 2008, John Wiley & Sons.

[5] A. Pfenninger, S. Odolo-Hitz, K. Weston, B. Kleeb, D. Jaussaud, *Process for production of molecular sieve adsorbent blends*, 2005, Google Patents.

Synthesis of Nickel Tungstate /Nickel-Gallium-Layered Double Hydroxide Nanocomposites as Electrode Material in Supercapacitors

S. Sanati, Z. Rezvani*

Department of Chemistry, Faculty of Basic Sciences, Azarbaijan Shahid Madani University, Tabriz, Iran

**Corresponding author: zrezvani@azaruniv.ac.ir*

Abstract: Amorphous $NiWO_4$ nanostructure is suggested to exert a synergistic impact on the efficiency of the NiGa-layered double hydroxide (NiGa-LDH) as a supercapacitor electrode material. $NiWO_4$/ NiGa-LDH nanocomposites were synthesized under mild conditions and at room temperature by using of deionized water as a solvent. The synthesized nanocomposites were characterized by Powder X-ray diffraction (PXRD). Electrochemical tests of nanocomposites were considered by using of cyclic voltammetry (CV), galvanostatic charge-discharge and electrochemical impedance spectroscopy (EIS) techniques. The results reveal that the $NiWO_4$/NiGa-layered double hydroxide nanocomposite has higher specific capacitance in pseudocapacitors.

Keywords: Layered double hydroxide; Nanocomposite; Electrode material; Supercapacitor

1. Introduction

Energy is one of the biggest challenges for the 21st century and there has been a gradually increasing demand for environmental friendly high-power energy storage devices. Among all of the energy storage devices, supercapacitors, which are also known as electrochemical capacitors, have received considerable amount of attention in recent years due to their high capacitance and power characteristics. Supercapacitors have been significantly figured out by their increasing applications in large industrial equipments, renewable energy power plants, hybrid electric vehicles, and memory back-up devices [1].

Currently, pseudocapacitive positive electrode materials made of nanoplate-shaped transition-metal compounds, such as metal oxides/hydroxides and layered double hydroxides (LDHs), have been shown to hold great potential for advanced supercapacitors. LDHs have been reported as an electrode material for supercapacitors because of their unique structural anisotropy, low cost, high specific capacitance, environmentally friendly nature and effective utilization of transition metal atoms.

Layered double hydroxides (LDHs) as a family of inorganic two-dimensional layered materials, have

found various applications in many fields of science over the past few years such as catalysis, molecule and drug delivery, adsorption, separation, energy storage, hydrogen and oxygen evolution reactions, owing to their low cost, capability to ion exchange, chemical multifunctionality, versatility to composites, and easily tailored properties [2].

2. Experimental Part

A co-precipitation method was employed to synthesize NiGa-LDH. Dissolution of $Ni(NO_3)_2.6H_2O$ (3 mmol, 0.872 g), $Ga(NO_3)_3.X\ H_2O$ (1mmol, 0.254 g) in to deionized water (20 ml) was performed. After that, a NaOH solution (1 M) was used to control the precipitation pH at 8.5. At room temperature for 24 hours, LDH sample was aged with continuous stirring. Using distilled water, LDH slurry was washed 3 times and dried.

3. Results and discussion

XRD patterns of the produced samples are represented in Fig.1 Based on the XRD images, the low intensity and broad nature of $NiWO_4$ diffraction peak can be attributed to the nanoscale and/or amorphous state of the as-synthesized $NiWO_4$ [3]. Three diffraction peaks at 2θ = 11.68°, 23.6° and 35.1° were observed for pristine LDH presents (003), (006) and (009), respectively. This shows that the product is an LDH-type material characteristic basal reflection [4].

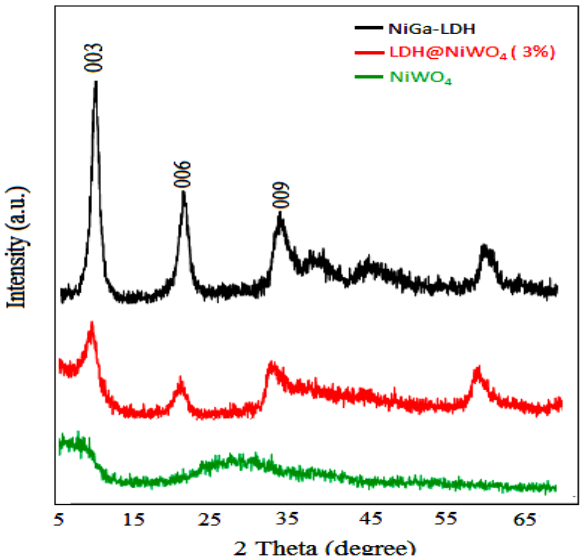

Figure 1. XRD patterns of pristine LDH, LDH/$NiWO_4$ (3%), and $NiWO_4$ samples.

Under a system with three electrodes, we evaluated the nanocomposites electrochemical characteristics. Cyclic voltammetry (CV) is an essential technique used to get qualitative information on the electrochemical procedure occurring in materials. Fig. 2 represents cyclic voltammograms of LDH, LDH/$NiWO_4$ (5%), $NiWO_4$ that characterized in a 6 M KOH solution at a 50 mVs^{-1} rate of scan. Obviously, in all of the CV curves, one pair of the redox peaks is visible in the range of 0-0.6 V (vs. SCE). Faradaic reactions of redox associated with Ni^{2+}/Ni^{3+} redox couples are mostly responsible for the emergence of these peaks, which might be mediated by alkaline electrolyte's OH^- ions [5].

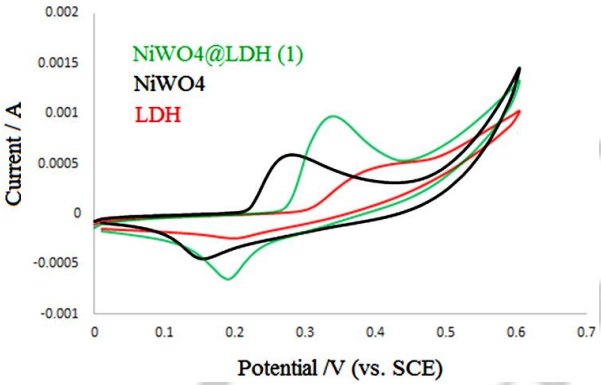

Figure 2. CV curves of pristine LDH, $NiWO_4$ and LDH/ $NiWO_4$ composites at a scan rate of 50 $mV.s^{-1}$.

4. Conclusions

In conclusion**,** a co-precipitation approach was used to synthesize NiGa-LDH/$NiWO_4$ composites with different weight ratios of the $NiWO_4$ to NiGa-LDH as electrode materials in supercapacitors. Investigation of the structures was done. In order to show their potential as electrode materials for supercapacitors, electrochemical measurements were done.

Acknowledgments

We are grateful for the support from Azarbaijan Shahid Madani University.

References

[1] W. Tian, Q. Gao, W. Qian, *ACS Sustainable Chem. Eng.* 5 **(**2017**)** 1297-1305.

[2] P. Huang, C. Cao, Y. Sun, S. Yang, F. Wei, W. Song**,** *J. Mater. Chem. A,* 3 (2015) 10858-10863.

[3] F. Zhang, L. Hao, L. Zhang X. Zhang, *Int. J. Electrochem. Sci*. 6 (2011) 2943-2954.

[4] L.J. Zhang, K.N. Hui, K.S. Hui, X. Chen, R. Chen, H. Lee, *Int. J. Hydrogen Energy* 41 (2016) 9443-9453.

[5] K. Yuan, Y.Z. Xu, J. Uihlein, G. Brunklaus, L. Shi, R. Heiderhoff, M.M. Que, M. Forster, T. Chassé, T. Pichler, T. Riedl, Y.W. Chen, U. Sche, *Adv. Mater.* 27 (2015) 6714-6721.

Graphene Quantum Dot/NiFe Layered Double-Hydroxide Composite as a Highly Efficient Electrocatalyst for Water Oxidation

L. Jafari Foruzin[a], Z. Rezvani[a]*, B. Habibi[b]*

[a]*Inorganic Chemistry Laboratory, Department of Chemistry, Faculty of Sciences, Azarbaijan Shahid Madani University, Tabriz 53714-161, Iran.*

[b]*Electroanalytical Chemistry Laboratory, Department of Chemistry, Faculty of Sciences, Azarbaijan Shahid Madani University, Tabriz 53714-161, Iran.*

**Corresponding authors: B.Habibi@azaruniv.ac.ir ; zrezvani @azaruniv.ac.ir*

Abstract: Here, the Graphene Quantum Dot /nickel -iron layered double hydroxide (GQD/NiFe-LDH) was synthesized by the hydrotermal method and investigated by X-ray. According to the results obtained from XRD, GQD/NiFe-LDH is nano size with high crystalline quality of the crystals. The resulting GQDs /NiFe-LDH complex exhibits high electrocatalytic activity (with a onset potential of ~0.90 V vs saturated calomel electrode, in a neutral media) and stability for oxygen evolution, and was comparable to those of the most active perovskite-based catalyst.

Keywords: Graphene quantum dots; NiFe-LDH; Water oxidation.

1. Introduction

Layered double hydroxides (LDHs), as a family of layered anionic materials, have attracted considerable attention and have been exploited as a fruitful source of materials for application in electrochemistry [1,2]. In particular, NiFe-LDH possesses a layered and relatively open structure, which makes the rapid diffusion of reactants and products and even the fast proton-coupled electron transfer process in the water oxidation reaction much easier [3], but the poor electrical conductivity restricts its widespread application in electrocatalysis [4, 5]. With the aim to increase the electrical conductivity of LDHs, we report the structural and electrochemical investigation of GQD/NiFe-LDH composite catalysts and use of GQD/NiFe-LDH for the oxygen evolution reaction (OER) in neutral electrolytes. We can conclude that the GQD/NiFe-LDH composite is a better OER catalyst than either the pristine NiFe-LDH.

2. Experimental Part

2.1. Preparation of GQDs

The GQDs was directly synthesized by pyrolyzing of the citric acid. In a typical route, 2.0 g citric acid was put into autoclave and heated to 180 ^{0}C. About 30 min later, the citric acid molecules were pyrolyzed,

cross-linked, and finally converted into carbon nanoparticles as a pale yellow liquid. Pyrolysis process continues as temperatures increase by more heating and the color of solution in reaction flask changes from yellow to orange as a result of formation of GQDs.

2.2 Preparation of GQDs/NiFe-LDH nanocomposite

The GQDs/NiFe-LDH nanocomposite was prepared by the ultrasonic method. Typically, an aqueous solution containing Ni $(NO_3)_2.6H_2O$ and Al $(NO_3)_3.9H_2O$, was prepared and added dropwise into a 20 ml solution containing the sonicated GQDs, under vigorous stirring conditions. During the addition of the metal ions solutions, the pH of the reaction mixture was maintained at 10.0 using 2 M NaOH solution. The obtained product was aged for 24h at 60 ^{0}C in autoclave.

3. Results and discussion

3.1. Physicochemical characterization

3.1.1. XRD characterization

Fig. 1 shows XRD patterns of the synthesized GQDs and prepared GQDs/NiFe-LDH nanocomposite. Fig. 1 (a) displays the XRD pattern of GQDs/NiFe-LDH. Symmetric reflections for (003), (006), (009), and (110) are exposed by the NiFe-LDH sample while representing a hexagonal lattice of R3m symmetry [6, 7]. The XRD pattern of synthesized GQDs (Fig. 1b.) exhibits a broad peak, belonging to the (002) plane of graphene with a relatively low intensity.

3.2 Electrocatalytic characterizations of GQDs/NiFe-LDH

Fig. 2 suggests that the GQDs/NiFe-LDH composite was a novel electrocatalyst material with high OER activity in neutral solutions, and we deduce that the strong electrocatalytic performance is mainly attributed to the formation of the NiFe-LDH phase. Strong association of the LDH with GQDs further facilitated charge transport and improved catalyst activity. The CQD/NiFe-LDH catalyst showed an onset potential of OER at ~0.9 V versus the SCE while the onset potential at NiFe-LDH which synthesized by hydrothermal and co-precipitation was 1 and 1.05 V. SCE respectively.

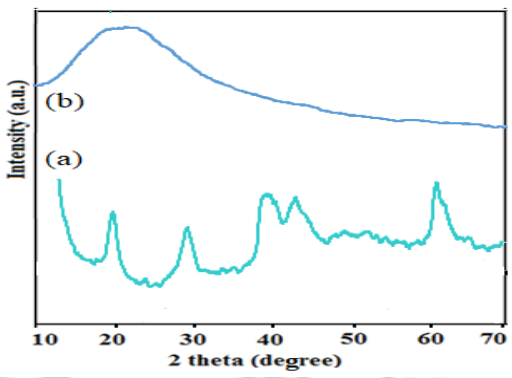

Figure 1. XRD patterns of the (a) GQDs/NiFe-LDH (b), GQDs

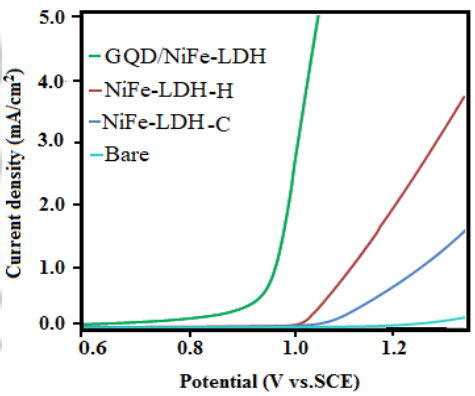

Figure 2. LSV curves of the GQDs/NiFe-LDH and NiFe-LDH

4. Conclusions

In summary, we report that an advanced GQD/NiFe-LDH nanocomposite catalyst can be synthesized by a plain precipitation−Hydrothermal route. This inexpensive, earthabundant, and easily constructed catalyst exhibited excellent OER electrochemical activity with small onset potentials of ~900 mV in neutral solution. Our studies provide new insight into designing and fabricating effective OER electrocatalysts by synergistic coupling of nonprecious functional materials with GQDs, which are strongly required for energy conversion and storage technologies.

Acknowledgments

We are grateful to Azarbijan Shahid Madani University for financial supports.

References

[1] S. Cho, J. W. Jang, K. j. Kong, et al. *Adv. Funct. Mater.* 23 (2013) 2348-2356

[2] F. Song, X. Hu, *J. Am. Chem. Soc.* 136 (2014) 6481−16484.

[3] L. J. Zhou, X. Huang, H. Chen et al. *Dalton Trans.* 44 (2015)11592-11600

[4] D. ch. Xia, L. Zhou, Sh. Qiao, et al. *Mater. Res. Bull.* 74 (2016) 441–446.

[5] M. Gong, Y. Li, H. Wang, Y. Liang, et al, *J. Am. Chem. Soc.* 135 (2013) 8452-8455.

[6] L. J. Foruzin, Z. Rezvani, Y. H. Shishavan, et al, *Int. J. Hydrogen energy* 43 (2018)150-160

[7] Y. Dou, X. Liu, M. Shao et al. *J. Mat. Chem.* 1 (2013) 4786-4792.

5th Iran International Zeolite Conference

University of Tabriz, Tabriz, Iran

26-27 August 2018

Photocatalytical Water Oxidation by TiO_2/MMO Nanocomposites under Visible Light Irradiation

L. Jafari Foruzin, Z. Rezvani*

Inorganic Chemistry Laboratory, Department of Chemistry, Faculty of Sciences, Azarbaijan Shahid Madani University, Tabriz 53714-161, Iran.

** Corresponding author: zrezvani @azaruniv.ac.ir*

Abstract: Titanium dioxide/ZnAl-layered double hydroxide nanocomposites (TiO_2/ZnAl-LDH) were prepared by using the co-precipitation method. Then, the TiO_2/ metal mixed oxides (TiO_2/MMOs) were roduced by annealing TiO_2/ZnAl-LDH at 430 °C. The obtained materials were characterized by X-ray diffraction (XRD). In the next step, we investigated the photocatalytic activity of the TiO_2/MMOs nanocomposites toward O_2 generation from the aqueous solution, under visible light. The photocatalytic activity of the TiO_2/MMO is better than that of TiO_2/ZnAl-LDH. The TiO_2/MMO nanocomposite could produce 371 $\mu molh^{-1}g^{-1}$ of O_2 using 20 mg of the photocatalyst.

Keywords: Water oxidation; Photocatalyst; TiO_2/MMO.

1. Introduction

Nowadays, the need for cheap, clean, and renewable energy resources using solar energy has become a universal problem [1,2]. One of the simple solar energy conversion systems is direct water oxidation, which uses the semiconductor photocatalyst. Owing to the advantages of photocatalytic water oxidation, such as its low pollution level, reduced energy consumption, and low cost, many recent studies have focused on O_2 production by using semiconductor photocatalysts [3].

Two-D, inorganic, solid semiconductors with a large surface area and high photocatalytic efficiency is an efficacious strategy for enhancing the performance of the water oxidation catalysts[4].

The purpose of this study is to design photocatalytic water oxidation by visible-light-responsive semiconductors with favorable features, such as low production cost, good visible light absorption, and high efficiency for O_2 evolution at neutral pH and room temperature.

2. Experimental Part

2.1. Preparation of TiO_2/ZnAl-LDH

The TiO_2/ZnAl-LDH was synthesized by the co-precipitation method at the controlled pH. Drop by drop, 10 mL of a solution containing 8.91 g (0.03

mol) of $Zn(NO_3)_2.6H_2O$ was added into a three-necked, round-bottom flask containing 11.26 g (0.03 mol) of the $Al(NO_3)_3.9H_2O$ solution. The pH was maintained constant at about 9–9.5 with adding the base solution (0.67 M Na_2CO_3 and 2.25 M NaOH); after five minutes, 4.80 g (0.06 mol) of TiO_2 was added (the molar ratio of TiO_2: Zn: Al is 2: 1: 1). The suspension was stirred for 18 hours at 40 °C in an oil bath. The solid was centrifuged, washed with deionized water, and dried at 30 °C for 24 hours to obtain TiO_2/ZnAl-LDH.

3. Results and discussion

3.1. Physicochemical characterization

3.1.1. XRD characterization

The X-ray diffraction patterns of TiO_2/ZnAl-LDH and TiO_2/MMO are presented in Figure 1 (a) and (b). Fig. 1(a) displays the XRD pattern of TiO_2/ZnAl-LDH. Symmetric reflections for (003), (006), (009), and (110) are exposed by the ZnAl-LDH sample while representing a hexagonal lattice of R3m symmetry [5]. The X-ray diffraction pattern in Figure 2 (b) indicates that after the heat treatment of TiO_2/ZnAl-LDH, the peaks of ZnAl-LDH disappeared completely and some new peaks emerged as ZnO (JCPDS No. 89–1397).

3.2 Evaluating the photocatalytic activity

To measure the amount of O_2, the researchers used an HQ40d portable dissolved O_2 meter connected to an O_2 monitor with a digital readout.

As shown in Figure 2, TiO_2/ZnAl-LDH and TiO_2/MMO display O_2 generation rates of 254.5 and 371 $\mu molh^{-1}g^{-1}$ respectively. It can be seen from Figure 8 that TiO_2/MMO have high photocatalytic activity. Moreover, the physical mixture of the ZnAl-LDH and TiO_2 samples, which annealed at 430 °C, has a relatively weak O_2 generation ability (85 $\mu molh^{-1}g^{-1}$) because of the high charge recombination. On the other hand, the TiO_2 showed a very small photocatalytic activity because the TiO_2 can not absorb any light in the visible light range.

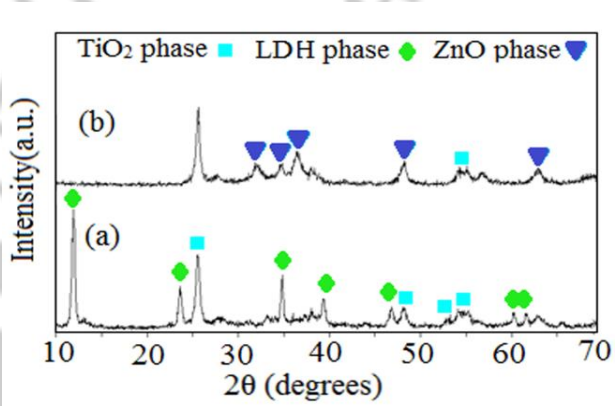

Figure 1. XRD spectra of (a) TiO_2/ZnAl-LDH and (b) TiO_2/MMO

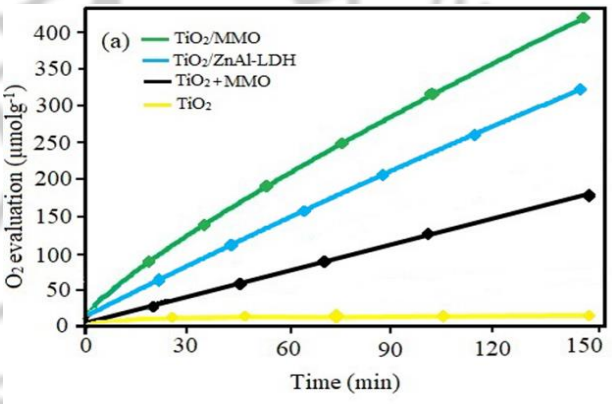

Figure 2. Photocatalytic O_2 generation over TiO_2/ZnAlLDH, TiO_2/MMO, TiO_2, and TiO_2 + MMO which physically mixed

4. Conclusions

To summarize, a TiO_2/MMO nanocomposite was synthesized from the TiO_2/ZnAl-LDH, which was annealed. The TiO_2/MMO has the higher photocatalytic behaviour in photocatalytic water oxidation than TiO_2/ZnAl-LDH for water oxidation under visible light irradiation at room temperature and neutral pH. Our results show that by using 200 mg of the photocatalyst and 1 mmol of $AgNO_3$ as a sacrificial agent, TiO_2/MMO produces 371 $\mu molh^{-1}g^{-1}$ of O_2, while TiO_2/ZnAl-LDH produce 254.5 $\mu molh^{-1}g^{-1}$ of O_2. On the other hand, TiO_2 and MMO, which were mixed physically and were annealed, generated a small amount of O_2. The TiO_2/MMO shows significantly enhanced efficiency and better photocatalytic activity.

Acknowledgments

We are grateful to Azarbijan Shahid Madani University for financial supports.

References

[1] F. Meng, J. Li, S. K. Cushing, et al *ACS Catal.* 3 (2013) 6481−16484.

[2] M. T. Nguyen, S. Piccinin, N. Seriani, et al. *ACS Catal.* 5 (2015) 715-721.

[3] H. Katsumata, H. Ando, T. Suzuki, et al. *Ind. Eng. Chem. Res.* 54 (2015) 3532-3535.

[4] A. Tanaka, K. Nakanishi, R. Hamada, et al. *ACS Catal.* 3 (2013) 1886-1891.

[5] Y. Dou, X. Liu, M. Shao et al *J. Mat. Chem.* 1 (2013) 4786-4792.

5th Iran International Zeolite Conference

University of Tabriz, Tabriz, Iran

26-27 August 2018

The effect of amines in the synthesis of layered double hydroxides

A. Mokhtari[a]*, Z. Kianinejad[a]

a Department of Inorganic Chemistry, Faculty of Chemistry, University of Tabriz, Tabriz, Iran

**Corresponding author: Azmokhtari6302@gmail.com*

Abstract: Layered double hydroxides (LDH) which are one type of layered materials and are also known as anionic clays, are promising layered materials due to some of their interesting properties, such as ease of synthesis, unique structure and high chemical and thermal stability [1]. Layered double hydroxides (LDHs), with nitrate as the charge balancing anion in the interlayer space, were synthesized by precipitation from homogeneous solution containing different amines [e.g., hexamethylenetetraamine (HMTA), diethylenediamine (DEDA), trimethylamine (TMA) and dimethylamine (DMA)]. This study investigates the use of different amines instead of nitrogen atmosphere in synthesis of nitrate containing LDHs.

Keywords: Layered double hydroxides, amine, Coprecipitation, crystallinity

1. Introduction

1.1. LDH

Metal hydroxide with hierarchical nanostructures has emerged as one of the most promising materials for their unique and attractive properties and feasibility of applications in various fields [2]. These materials are described according to the standard formula; $[M^{II}_{1-x}M^{III}x(OH)_2]^{x+}[X^{m-}_{x/m}\cdot nH_2O]^{x-}$, abbreviated as $[M^{II}$-M^{III}-X], where M^{II} and M^{III} are divalent and trivalent metal ions, respectively and X^{m-} the interlayer anion with x being dened as the $M^{II}/(M^{II} + M^{III})$ ratio. A variety of layered materials have been synthesized by different methods [3]. The structure of LDH is presented in Figure 1. Different routes to synthesis of layered double hydroxides (LDH) in the past few years have been reported. The main route, which is most frequently followed, is coprecipitation route (direct method). A method of hydrothermal crystallization is presented for synthesizing the pure and highly crystalline NO_3 LDH samples. LDHs M^{II}-M^{III} were synthesized with nitrate, instead of carbonate, as the interlayer anions in the presence of different types of amines without a N_2 atmosphere [4,5].

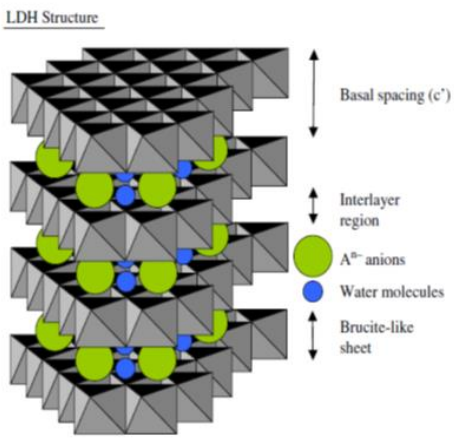

Figyre 1. Schematic diagram of LDH

1.2. Proposed Mechanism for the Concomitant Synthesis of Highly Crystalline LDH in the presence of amine

Based on the work by Dutta et al., [6] a tentative mechanism of formation of Zn-Al LDH in homogeneous solution using different amines outlined by reactions (1)–(9). Reactions 1 and 2 show that the firstly hydrolysis of amines occurred, which produces ammonia and formaldehyde. Therefore, the reaction solution was alkaline. In alkaline condition, Al salt can change to form $Al(OH)_3$ or $Al(OH)_4^-$ species (pH=6–7), as shown in reactions 3 and 4 [7] and also Zn^{2+} ions can convert to the partially soluble such as $Zn(OH)_2$ and $Zn(OH)_4^{2-}$ or $Zn(NH_3)_4^{2+}$ (reactions 4–6) [8]. The reaction among $Al(OH)_4^-$ with either of the above gives rise to Zn-Al LDH phase via the reaction 8, which is thermodynamically favored [4]. So it can be concluded that the use of amines as a source of ammonia might keep the reaction solution buffered at near neutral pH, which is considered a key determinant for the over-all nucleation and crystal growth process of LDH.

$$C_2N_2H_6 + 2H_2O \rightarrow 2NH_3 + 2HCHO \quad (1)$$

$$NH_3 + H_2O \rightarrow NH_4^+ + OH^- \quad (2)$$

$$Al^{3+} + 4OH^- \rightarrow Al(OH)_4^- \quad (3)$$

$$Al(OH)_4^- \rightarrow Al(OH)_3 + OH^- \quad (4)$$

$$Zn^{2+} + 2OH^- \rightarrow Zn(OH)_2 \quad (5)$$

$$Zn(OH)_2 + 2OH^- \rightarrow Zn(OH)_4^{2-} \quad (6)$$

$$Zn^{2+} + 4NH_3 \rightarrow Zn(NH_3)_4^{2+} \quad (7)$$

$$Zn(OH)_2 + NH_3 \rightarrow Zn(NH_3)_4^{2+} + 2OH^- \quad (8)$$

$$Al(OH)_3/Al(OH)_4^- + Zn(OH)_4^{2-}/Zn(NH_3)_4^{2+} + OH^- + NO^{3-} + H_2O \rightarrow \text{Zn-Al LDH} \quad (9)$$

In order to confirm the occurrence of the above mechanism, the synthesis of Zn-Al-NO_3 LDH was also performed by using ammonium nitrate and potassium nitrate salts instead of amine. The XRD patterns reveal that the potassium nitrate salt is not suitable for the synthesis of Zn-Al-NO_3 LDH, because of formation of the Zinc oxide. However, the ammonium nitrate salt is suitable for this synthesis, since, the ZnAl-NO_3 LDH is formed with a better phase purity, while, the crystallinity of sample is lower than that of the amine-assisted route. Figure 2 shows the XRD patterns of the as-prepared samples.

2. Conclusions

In this mini review, it has been shown that it is possible to synthesize M^{II}-M^{III} layered double hydroxides using nitrate instead of carbonate in the interlayer space, without using nitrogen atmosphere and making use of different amines. The mechanism for concomitant synthesis of highly crystalline LDH has been discussed. Also,

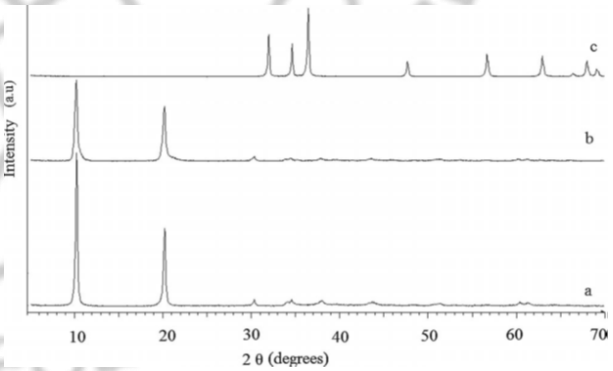

Figure 2. PXRD patterns of Zn-Al-NO_3 LDH prepared in the presence of (a) TMA, (b) ammonium nitrate salt and (c) potassium nitrate salts [4].

to evaluate the current method, the synthesis of LDH was performed with ammonium nitrate and potassium nitrate salts and the results confirmed the proposed mechanism. Hence, we speculate that this method will be a general, facile and low cost method for preparing a uniform LDH.

Acknowledgments

We would like to thank the University of Tabriz and Iranian Nanotechnology Initiative Council for the financial support of this project.

References

[1] G. Mishra, B. Dash, S. Pandey, *Appl. Clay Sci*. 153 (2018) 172-186

[2] K. Dutta, S. Das, A. Pramanik, *J. Colloid Interface Sci*. 366 (2012) 28–36.

[3] L. Gao, Y. Tang, Q. Xue, Y. Liu, Y. Lu, *Energy Fuels* 23 (2009) 624–630.

[4] Z. Rezavani, F. Khodam, A. Mokhtari, K. Nejati, K. Z. Anorg. *Allg. Chem.* 640 (2014) 2203-2207.

[5] K. Nejati, A. Mokhtari, F. Khodam, and Z. Rezvani, *Can. J. Chem.* 1 (2016) 66-71.

[6] K. Dutta, S. Das, A. Pramanik, *J. Colloid Interface Sci.* 366 (2012) 28–36.

[7] G. Cui, D. G. Evans, D. Li, *Polym. Degrad. Stab* 95 (2010) 2082– 2087.

[8] X. Hu, Y. Masuda, T. Ohji, K. Kato, *Langmuir* 24 (2008) 7614– 7617.

Preferential Siting of BEA, FAU, MOR, and MFI Zeolite Frameworks for Adsorbed Phenol: A Monte Carlo Study

F. Ektefa*, S. Javadian

Department of Physical Chemistry, Faculty of Science, Tarbiat Modares University, Tehran, Iran

**Corresponding author: fatemehektefa@yahoo.com*

Abstract: The adsorption through zeolite is an efficient way of phenol removal from water. The adsorption performance of all-silica zeolites including BEA (Beta), FAU (Faujasite), MFI (silicalite-1), and MOR (Mordenite) to adsorb phenol from phenol/water vapor mixture was predicted and compared through Grand Canonical Monte Carlo (GCMC) simulation. The preferential siting of zeolite is suggested by GCMC simulation. Phenol species display preferred siting in the middle of spacious intersections and bulky channels. The adsorbed water molecules are positioned preferentially around the phenols in the zeolite intersection. Hydrogen bonding and dispersion can improve the formation of clusters of organic compounds in the intersection and middle channel of zeolite. Our calculations may be helpful to elucidate and select a promising adsorbent targeting the phenol removal from water.

Keywords: Zeolite; Monte Carlo; Adsorption

1. Introduction

Phenol is considered as one of the most serious organic pollutants regarding its damages to human health and aquatic life due to high toxicity even at low concentration [1]. Adsorption is an effective process to treat the wastewaters containing phenol [2]. Zeolites have been considered as efficient adsorbents for removal of phenol from waste effluents. Their framework consists tetrahedral TO_4 (T = Si and Al) linked by shared oxygen atoms [3,4].

Deep understanding of the preferential siting and adsorption energy distribution is of a great deal of importance to consider the performance of zeolites. The comparative adsorption of mixture of phenol/water over Beta, FAU, MFI, and MOR zeolites is investigated by Monte Carlo technique. Deconvolution of adsorption energy distribution functions into separate gaussian peaks is presented for the first time in this work.

2. Computational methods and models

All-silica and defect-free framework of BEA, FAU, MOR, and MFI zeolites are mainly focused in this work. The coordinate of the zeolite framework was taken from XRD patterns based on International Zeolite Association database. Simulation boxes of BEA, FAU, and MFI zeolites are represented by supercells consisting 8 unit cells, 2×2×2. Also, MOR supercell contains 16 unit cells, 2×2×4. All

adsorption simulations were carried out by Accelrys_Materials Studio 4.3 software package [5].

3. Results and discussion

The simulation offers valuable information about the adsorbate preferential siting in zeolite framework. Figure 1 shows the snapshots of water and phenol species obtained from GCMC simulations. From the snapshots, the water molecules can homogeneously distribute throughout the channels over the intersections of zeolites due to their small size. Contrarily, the phenol species have restricted motions through small pores and cages and display preferred siting in the middle of spacious intersections and bulky channels. As can be easily seen in Figure 1, the adsorbed water molecules are positioned preferentially around the phenols in the zeolite intersection. Several attractions like hydrogen bonding and dispersion can improve the formation of clusters in the intersection and middle channel of zeolites. Water and phenol molecules can be placed in all FAU positions (Figure 1b) and the supercages are not assumed as the preferential adsorption sites. This finding will be confirmed by the adsorption energy distribution obtained from MC as well as XRD data of FAU showing there is only one type of adsorption site (T1) in framework.

Figure 2 shows the adsorption energy distribution of phenol on four studied zeolites at 378 K and is close to a Gaussian function. The curves were fitted to overlap peaks and deconvolute of gaussian peaks into separate distributions for phenol adsorption to gain insight about the distribution of phenol through the zeolite channels as follows: i) there are three peaks observed at on the BEA related to these circumstances that may exist three separate adsorption sites, two main channels and intersection channel. ii) FAU possesses supercages, which adsorb phenol in the same sites since it has one tetrahedral center and a negligible peak that maybe due to improper situation of phenol. iii) two discrete peaks were found in the energy distribution of phenol on the MFI related to these positions the zigzag channels and channel intersections are the preferred sites of adsorption. iv) there are two obvious peaks in MOR diagram which can be explained structurally. MOR has 12-membered ring channel interconnected by 8-membered ring channels. As can be seen from snapshots as shown in Figure 1, phenol molecules distribute in the 12-membered ring channel. Based on XRD data, there are four types of tetrahedral centers in MOR in which T1, T2, and T4 are located in the 12-membered ring channel and T3 placed in 8-membered ring channels. It is predicted that T1, T2, and T4 are preferred than T3 toward adsorption.

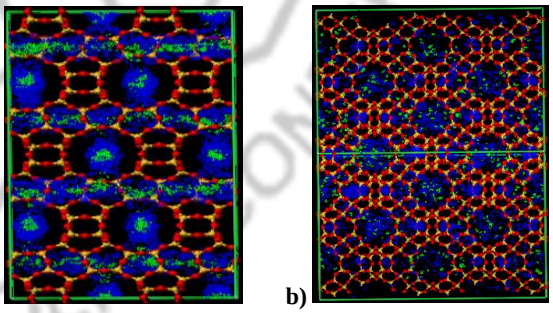

a) **b)**

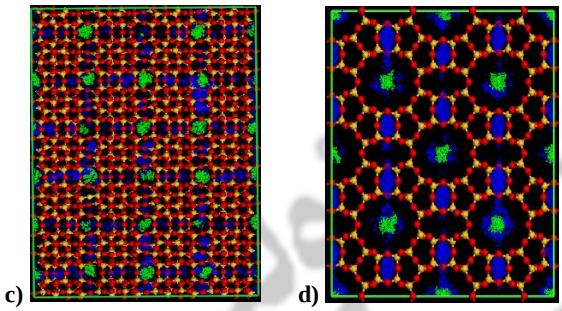

Figure 1. Density field for phenol (green) and water (blue) in a) BEA b) FAU c) MFI d) MOR computed by GCMC.

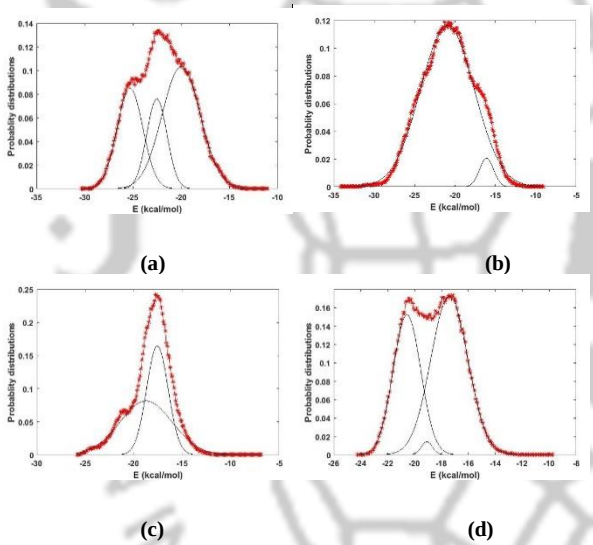

Figure 2. Energy distributions of phenol in a) BEA, b) FAU, c) MFI, and d) MOR.

4. Conclusions

Phenol adsorption on four zeolites namely FAU, MOR, BEA, and MFI zeolite substrates was studied in aqueous medium as an environmental challenge. The adsorbate preferential siting and adsorption energy distribution of phenol on four studied zeolites obtained from GCMC simulations and explained structurally, as well.

References

[1] K. Sunil, K. Jayant, *Adsorption* 1 (2013) 88-96.

[2] S. Lin, R. Juang, *J. Environ. Manage.* 90 (2009) 1336-1349.

[3] G. Busca, S. Berardinelli, C. Resini, L. Arrighi. *J. Hazard. Mater.* 160 (2008) 265-288.

[4] M. Ahmaruzzaman, *Adv. Colloid Interfac.* 143 (2008) 48-67.

[5] http://accelrys.com

5th Iran International Zeolite Conference

University of Tabriz, Tabriz, Iran

26-27 August 2018

Calculation of Heat Capacity of Clathrate Hydrate by Molecular Dynamics Simulations

H. Ghafari[a], H. Mohammadi-manesh[a,*]

[a]*Department of Chemistry, faculty of science, Yazd University, Yazd, Iran*

**Corresponding author: mohammadimanesh@yazd.ac.ir*

Abstract: In this work, molecular dynamics simulation (MD) was conducted using the combination of two force fields (GAFF and TIP4P/ice) to evaluate the constant-volume heat capacity and constant-pressure heat capacity of Trimethylene oxide (TMO), Ethylene oxide (EO) and Formaldehyde (FA) in structure I clathrate hydrate at temperature range 50-250 K. Temperature dependent of enthalpy (E_{NPT}) and total internal energy (E_{NVT}) were obtained for TMO, EO and FA in sI hydrate from MD simulation using NPT and NVT ensembles. The heat capacity of EO hydrate compared with the corresponding experimental values. The guest molecules are different in size, nature and ability formation of guest-host hydrogen bonding. These computational results show that there is a meaning relation between guest-host interaction and specific heat capacity.

Keywords: Constant-volume heat capacity, Constant-pressure heat capacity, Molecular dynamic simulation, clathrate hydrate

1. Introduction

The specific heat capacity is the most important property, it determines how much heat can be stored in a certain amount of substance. Clathrate hydrates are abundant in nature and a topic of great interest today. The thermodynamic conditions for formation of clathrate hydrate have been difficult to measure thermodynamic properties such as heat capacity. The heat capacity of sI ethylene oxide clathrate hydrate, the pure and KOH-doped argon and tetrahydrofuran clathrate hydrates and structure I hydrate of trimethylene oxide has been measured by experimental methods [1-4]. The heat capacity Xe hydrate have been calculated by using molecular dynamics simulation [5] and for $Kr(H_2O)_{20}$ cluster Parallel-tempering isothermal-isobaric Monte Carlo simulations [6]. In this paper, we are estimated the heat capacities at constant volume (C_V) and constant pressure (C_P) for Trimethylene oxide (TMO), Ethylene oxide (EO) and Formaldehyde (FA) sI clathrate hydrate from MD simulations in *NVT* and *NPT* ensembles respectively and under increasing temperature from 50 K to 250 K.

2. Computational details

In the simulations, 3 × 3 × 3 replica of the sI clathrate hydrate unit cell with 46 water molecules is used. The large cage guest molecules (TMO, EO and FA) were modeled with the general AMBER force field (GAFF) [7] and the Murad–Gubbins potential [8] were chosen for methane molecule. The water

molecules in the clathrate were modeled using TIP4P/ice four-charge model [9]. Columbic Long-range interactions were calculated using the Ewald summation method and all interatomic interactions in the simulation box were calculated within a cutoff distance of R_{cutoff}=15 Å. Simulations in *NVT* and *NPT* ensembles for each clathrate hydrate by 270 ps with an equilibration time of 70 ps are performed.

3. Results and discussion

By MD simulations in *NVT* and *NPT* ensembles, the heat capacities at constant-volume (C_V) and at constant-pressure (C_P) for binary clathrate hydrate are calculated between 50–250 K and 1 bar respectively. In order to calculation C_p and C_V, we obtained the fourth degree polynomial fit of E_{NPT} (enthalpy of system) and E_{NVT} (total internal energy of system) as a function of temperature (see 1 and 2 Figures), respectively and we used from 1 and 2 equations and differentiate the fitted function to obtain heat capacity.

$$C_V = \left(\frac{\partial E_{NVT}}{\partial T}\right)_V \quad (1)$$

$$C_P = \left(\frac{\partial E_{NPT}}{\partial T}\right)_P \quad (2)$$

The constant-pressure heat capacity of TMO, EO and FA guest molecules in sI clathrate hydrate as a function of temperature at 1 bar fitted to a line as follows:

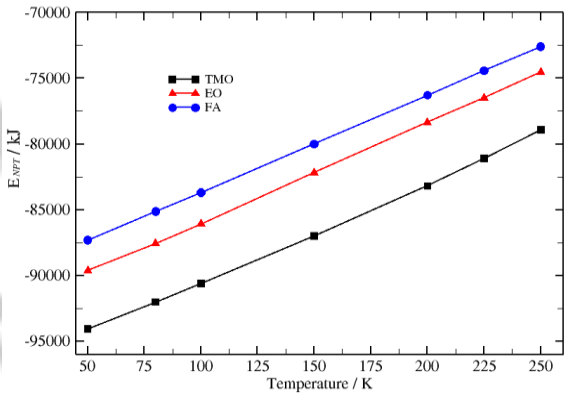

Figure 1. Temperature dependent of enthalpy (E_{NPT}) of structure I hydrate for TMO, EO and FA by TIP4P/ice water model.

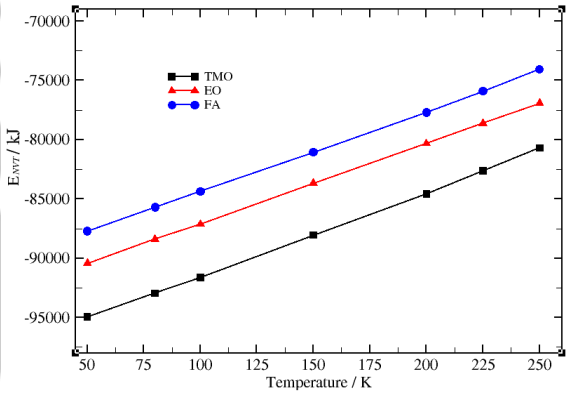

Figure 2. Temperatures dependent of total internal energy (E_{NVT}) of structure I hydrate for TMO, EO and FA by TIP4P/ice water model.

$$C_P\,(\mathrm{TMO}) = 56.639 + 0.28492\ T - 0.00195597\ T^2 + 5.5024\times10^{-6}\ T^3 \quad (3)$$

$$C_P\,(\mathrm{FA}) = 74.652 - 0.07065\ T + 0.00072849\ T^2 - 1.89168\times10^{-6}\ T^3 \quad (4)$$

$$C_P\,(\mathrm{EO}) = 21.506 + 1.12016\ T - 0.0071208\ T^2 + 1.43228\times10^{-5}\ T^3 \quad (5)$$

The calculated C_P ($J.kg^{-1}.K^{-1}$) of guest molecules in sI clathrate hydrate are given in Table 1.

Table 1. The specific constant-pressure heat capacity of TMO, EO and FA in sI clathrate hydrates at 1 bar and different temperatures.

Temperature (K)	TMO	EO	FA	EO (exp.) [10]
50	2044.5	2026.6	2589.1	-
80	2137.9	2401.4	2588.8	-
100	2179.1	2525.3	2599.0	-
150	2266.9	2558.7	2637.5	1247
200	2434.5	2480.8	2654.1	1488
225	2587.7	2510.7	2638.5	1630
250	2808.3	2645.6	2598.4	1804

The constant-volume heat capacity of TMO, EO and FA guest molecules in sI clathrate hydrate as a function of temperature at 1 bar fitted to a line as follows:

C_V(TMO) = 42.95 + 0.5692 T - 0.0039762 T^2 + 9.36×10^{-6} T^3

C_V (EO) = 63.36 + 0.0875 T - 0.00056889 T^2 + 1.18996×10^{-7} T^3

C_V (FA) = 68.27 + 0.0188 T - 0.00066537 T^2 + 2.95884×10^{-6} T^3

The calculated C_V ($J.kg^{-1}.K^{-1}$) of guest molecules in sI clathrate hydrate are given in Table 2.

Table 2. The specific constant-volume heat capacity of TMO, EO and FA in sI clathrate hydrates at 1 bar and different temperatures.

Temperature (K)	TMO	EO	FA
50	1920.6	2189.9	2418.6
80	2079.8	2218.5	2387.0
100	2129.9	2227.8	2366.5
150	2160.3	2230.8	2353.9
200	2226.7	2228.3	2460.0
225	2340.7	2234.2	2582.2
250	2544.5	2249.7	2763.7

4. Conclusions

As expected, the constant-pressure heat capacity of variety guest molecules is larger than corresponding to the constant-volume heat capacity. The calculated C_P ($J.kg^{-1}.K^{-1}$) for the EO molecule with experimental measurements is much less than the C_P calculated in this paper which may be due to the difficulty of compressing clathrate hydrate and therefore, the micro-pores and residual gas may greatly lower the experimental values of the specific heat capacity of clathrate hydrate. The smaller value of heat capacity of TMO molecule compared with EO and FA can be interpreted by the smaller enthalpy of guest-host hydrogen bond formation for TMO than the other guest molecules. For TMO molecule with increasing temperature, the heat capacities increase extremely. This behavior may be related to probability of formation of guest-host

hydrogen bonding for this guest is greater than the other guest molecules.

References

[1] O Yamamuro, Y Handa, M Oguni, H Suga, *J Incl Phenom Macrocycl Chem* 8 (1990) 45-58.
[2] O Yamamuro, M Oguni, T Matsuo, H Suga, *J Incl Phenom Macrocycl Chem* 6 (1988) 307-18.
[3] O Yamamuro, M Oguni, T Matsuo, H Suga, *Solid State Commun* 62 (1987) 289-92.
[4] J Comper, A Quesnel, C Fyfe, R Boyd. *Can J Chem* 61 (1983) 92-6.
[5] W Cheng, H Zhou, S Ren, *Chin Sci Bull* 50 (2005) 822-5.
[6] D Arismendi-Arrieta, A Vítek, R Prosmiti, *J Phys Chem C*. 120 (2016) 26093-102.
[7] W Cornell, P Cieplak, C Bayly, I Gould, K Merz, D Ferguson, *J Am Chem Soc* 117 (1995) 5179-97.
[8] S Murad, K Gubbins. In Computer Modeling of Matter, 1978 (Ed: Lykos P), American Chemical Society, 62, Washington, DC.
[9]. J Abascal, E Sanz, R Fernández, C Vega, *J Chem Phys* 122 (2005) 234511.
[10] D Leaist, J Murray, M Post, D Davldson, *J Phys Chem.* 86 (1982) 4175-4178.

5th Iran International Zeolite Conference

University of Tabriz, Tabriz, Iran

26-27 August 2018

Molecular Dynamics Simulations of Hydrogen Bonding in sI Clathrate Hydrates with Ethylene oxide and Cyclopropane Guest Molecules

H. Ghafari[a]*, H. Mohammadi-manesh[a]

[a] *Department of Physical-Chemistry, Faculty of Chemistry, University of Yazd, Yazd, Iran*

**Corresponding author: ghafari.hakime@gmail.com*

Abstract: Molecular dynamics simulations are used to study structure and guest dynamic properties of Ethylene oxide (EO) sI clathrate hydrate with ability formation of guest-host hydrogen bonding and compared to cyclopropane sI clathrate hydrate with inability formation guest-host hydrogen bonding. To illustrate the formation of guest-host hydrogen bonding, radial distribution function (RDFs) are plotted for Ethylene oxide and Cyclopropane. The velocity autocorrelation function (VACF) and Fourier transform of VACF for EO and Cyclopropane molecules calculated in order to investigate the effect of guest-host hydrogen bonding on the dynamics of guest motions.

Keywords: Guest-host hydrogen bond, Molecular dynamics simulation, Ethylene oxide sI clathrate hydrate, Radial distribution function, Dynamics properties

1. Introduction

Clathrates are inclusion compounds that forms in different pressure and temperature environments involving different guest-host. Moderately high temperature and low pressure clathrates such as zeolites. Normal temperature and pressure clathrates like clathrin. Low temperature and high pressure clathrates such as clathrate hydrate. High temperature and high pressure clathrates, such as fullerenes [1]. Clathrate hydrates are non-stoichiometric crystalline inclusion compounds in which a water host lattice encages small guest atoms or molecules in cavities. Ethylene oxide forms a typical structure I hydrate and has been studied by experimental measurements [2, 3] Measuring such properties is also rather time-consuming, difficult and costly by experimental methods. Molecular dynamics simulation were performed for considering formation guest-host hydrogen bonding for variety guest molecules such as ethanol sI clathrate hydrate, 1-propanol sII clathrate hydrate, *tert*-butylamine (tBA) sII clathrate [4-6]. However, the effect of guest-host interactions on macroscopic properties is still far from complete for this guest. The clathrate hydrate structure relevant to this work are cubic structure I (sI or CS-I) which contains two small 12-sided cages (pentagonal dodecahedral, D; 5^{12}), six large 14-sided cages (tetrakaidecahedral, T; $5^{12}6^2$) and 46 water molecules per unit cell. The unit cell of the sI phase is shown in Figure 1. Herein, we study structural (radial distribution function) and dynamical such as velocity autocorrelation function

of Ethylene oxide (EO) and Cyclobutane in large cage sI clathrate and methane help gas in small cage sI clathrate hydrate.

2. Computational details

Constant pressure/temperature *NPT* molecular dynamics simulations on periodic simulation cells were performed using the DL_POLY software program version 2.18 [7] with pressure and temperature regulated using the modified Nosé−Hoover thermostat-barostat algorithm [8, 9] and thermostat and barostat relaxation times of 0.1 and 1.0 ps, respectively. Columbic Long-range interactions were calculated using the Ewald summation method and all interatomic interactions in the simulation box were calculated within a cutoff distance of R_{cutoff}=15 Å. Final *NPT*

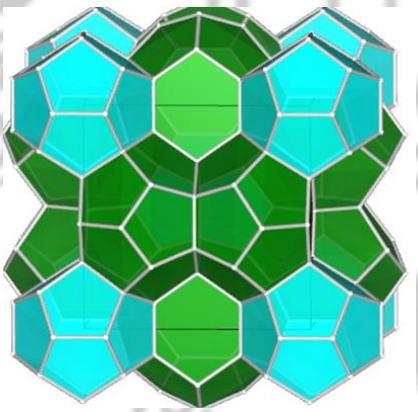

Figure 1. The structure I clathrate hydrate unit cell. The green cages are the 14-sided T cages and the blue cages are the 12-sided D cages. Corners represent the position of water molecules in the lattice and edges represent the hydrogen bonding between water molecules in the lattice. The guest molecules reside inside the cages.

Configurations are used for *NVE* dynamics calculations at each temperature. The *NVE* simulations for the dynamics were performed for a total time of 250 ps with the first 50 ps used for equilibration.

3. Results and discussion

The formation of guest–host hydrogen bonds is evident from the OS–HW radial distribution function (RDF) plots for EO sI clathrate shown in Figure by 2(a) SPC/E and 2(b) TIP4P/ice water model. The RDFs for the analogous carbon atom of Cyclopropane are also shown with dashed line in Figure 2(a) by SPC/E and 2(b) TIP4P/ice water model. As seen in Figure 2, the RDF plot of EO clathrate hydrate has a peak at range of hydrogen bond (~2 Å) that this peak for TIP4P/ice is clearer than SPC/E water model. The absence of such peak in the RDF plot for Cyclopropane show that this molecule has not any interaction with cage water.

The velocity autocorrelation function (VACF) for oxygen atom of EO and a selected carbon of Cyclopropane molecules are calculated for study of the dynamics of the guest motions and are shown by SPC/E and TIP4P/ice water model in Figure 3(a) and 3(c), respectively. The velocity autocorrelation function (VACF) is defined by,

$$C(t) = \frac{\langle v_i(t) \cdot v_i(0) \rangle}{\langle v_i(0) \cdot v_i(0) \rangle}$$

Where $v_i(t)$ is velocity of atom i at time t.

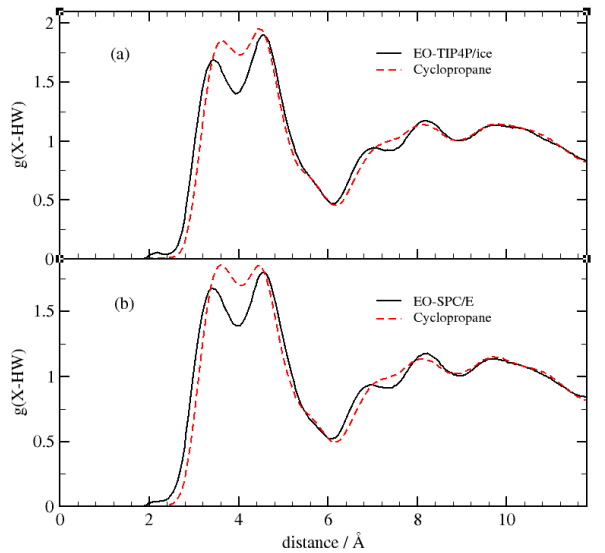

Figure 2. The X-HW RDF plot with (a) TIP4P/ice and (b) SPC/E water potential at 250 K which X for EO is Oxygen atom (OS) and for Cyclopropane is carbon selected atom.

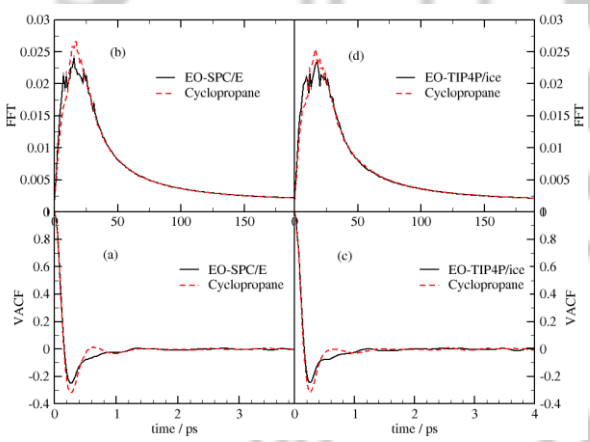

Figure 3. The velocity autocorrelation function for the oxygen atoms for EO and carbon selected atoms for Cyclopropane using (a) SPC/E and (c) TIP4P/ice water potential. The Fourier transform of VACF for EO and Cyclopropane with simulation using (b) SPC/E and (d) TIP4P/ice water potential at 250 K and ambient pressure.

The VACF of Cyclopropane decays to zero randomizes more rapidly than the VACF of EO molecule. After the minimum, the VACFs decay to zero which is called the velocity randomization time. The VACF for the EO guest decays to zero slower than the VACF for Cyclopropane that the formation hydrogen bond between oxygen atom of EO and hydrogen atom of water lattice may contribute to the slower decay VACF plots. The Fourier transform of the VACFs are shown by SPC/E and TIP4P/ice water model in Figure 3(b) and 3(d), respectively.

4. Conclusions

We performed molecular dynamics simulations of guest-host hydrogen bonding in the large cage sI clathrate hydrate with the guest molecules ethylene oxide and cyclopropane with the TIP4P/ice and SPC/E water potentials. The hydrogen bonding tethers guest molecules to the cage wall and affects the dynamics of the guest in the large cages. The velocity autocorrelation function and Fourier transform of VACF are used to investigate guest dynamical properties. These quantities give a general indication of the rattling motion of the guests in the large cages. We have studied the sI clathrates with the cyclic guest molecules, Cyclopropane and Ethylene oxide. According to the RDF plots the ether oxygen atom of the polar EO molecule form guest-host hydrogen bonds with one sI large cage water molecule. The EO hydrogen bonding is predicted to be stronger for TIP4P/ice than the SPC/E simulation and generally the range of hydrogen bonding

distances predicted by the SPC/E potential is broader.

References

[1] S. Vaidya, *Resonance* 2004 (9) 18-31.

[2] R. K. McMullan, G. A. Jeffrey, *J. Chem. Phys.* 42 (1965) 2725.

[3] D. W. Davidson, G. J. Wilson, *Can. J. Chem.* 41 (1963) 1424.

[4] S. Alavi, R. Ohmura, J. A. Ripmeester, *J. Chem. Phys.* 134 (2011) 05472.

[5] K. Udachin, S. Alavi, J. A. Ripmeester, *J. Chem. Phys.* 134 (2011) 121104.

[6] S. Alavi, K. Udachin, J. A. Ripmeester, *Chem. Eur. J.* 16 (2010) 1017-1025.

[7] Smith, W.; Forester, T.; Todorov, I. *The DL_POLY molecular simulation package*, 2007 V. 2.18. Daresbury Laboratory: Daresbury, UK.

[8] S. A. Nosé, *J. Chem. phys.* 81 (1984) 511-519.

[9] W. G. Hoover, *Phys. Rev. A* 31 (1985) 1695.

5th Iran International Zeolite Conference

University of Tabriz, Tabriz, Iran

26-27 August 2018

Novel Approach to the Synthesis of Polyhydroquinolines and Dihydropyridines Derivatives Using SBA-15/SO_3H Nanoreactor as a Highly Efficient and Reusable Catalyst

M. Dalili, S. Rostamnia*

Organic and Nano Group, Department of Chemistry, Faculty of Science, University of Maragheh, PO BOX 55181-8311, Maragheh, Iran

**Corresponding author: srostamnia@gmail.com*

Abstract: An efficient and simple route for preparation of polyhydroquinolines and dihydropyridines derivatives via SBA-15/SO_3H catalyzed ring opening of diketene in four component Hantzch-type reactions are presented. Dihydropyridines derivatives based on neat adduct of diketene, alcohols and aldehydes using SBA-15 sulfonic acid modified mesoporous substrates, a green and reusable catalyst are also synthesized. In this paper, the present method includes some advantages such as simple procedure, waste-free, green, using small amount of catalyst, high yield of products and short reaction time.

Keywords: Diketene; SBA-15/SO_3H; Polyhydroquinoline; Dihydropyridines; Nanoreactor

1. Introduction

Fabrication of the ordered porous nanomaterials such as SBA-15 exposed an extreme interest since their high surface area, high thermal and mechanical stability as a result of small nanoparticles pore sizes [1]. Incorporating the organic-inorganic hybrid SBA-15 family with organic ligands in the pores of the silica wall not-only make the materials hydrothermal stable and hydrophobic, but also provide the materials with improved catalytic activity during applications for organic process [2].

Polyhydroquinoline and dihydropyridines have attracted much attention due to their pharmacological properties as a wide spectrum of biological activates [3]. Consequently, a number of many different protocols for producing them via using solvents and heavy metals, which are not in the context of green catalysts, have been reported. As a result, in the present work we tried to expand a waste-free and effective green pathway with high yield.

2. Experimental Part

After hydrothermal preparation of SBA-15, a mixture of calcined SBA-15 (1 g) and (3-mercaptopropyl) trimethoxysilane (1.75 g) in dry toluene (13 ml) was refluxed for 24 h. The product was filtered, and then dried under vacuum. Then

the solid product was oxidized with H_2O_2 (30%, excess) and two drop of H_2SO_4 in methanol (20 ml) for 20 h. Then the mixture was filtered and washed with H_2O and dried in vacuum (Scheme 1).

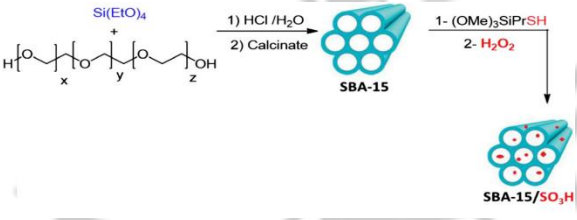

Scheme 1. Stepwise synthetic scheme for the synthesis of SBA-15/SO_3H.

3. Results and discussion

Here, we fabricated covalently bonded sulfonic acid/SBA-15 silica porous nanoreactor based on our previous reports. Finally, we investigated these catalysts in the preparation of Polyhydroquinoline and dihydropyridines in terms of both reactivity and efficiency based on green chemistry desires.

Table 1. SBA-15/SO_3H catalyzed the neat four-component synthesis of polyhydroquinolines derivatives.

Entry	Ar	Time (min)	Yield (%)
1	C_6H_5	25	90
2	2-Cl-C_6H_4	30	85
3	4-OMe-C_6H_4	20	90

Table 2. The neat four-component synthesis of dihydropyridines derivatives.

Entry	Ar	R	Yield (%)
1	3-Cl-C_6H_4	Me	91
2	2-Cl-C_6H_4	Me	80
3	4-NO_2-C_6H_4	Me	93

The SBA-15/SO_3H heterogeneous nanocatalyst was synthesized by grafting of –SO_3H onto the SBA-15 by refluxing a mixture of calcinated SBA-15 in dry toluene. Then the resulting solid product was oxidized with H_2O_2.

Then as a method reaction, the mixture of enamine, aldehydes, diketene and methanol as reactant and solvent were prepared in the presence of SBA-15/SO_3H and after 16 min, the reaction was completed with high yield of product. After completion of the reaction, the catalyst was separated by simply centrifuging, and then washed with hot EtOH and water, supporting the use of the modified catalyst in the reaction method for at least 5 times.

The neat reaction of diketene, aldehydes 1, alcohols 2, with ammonium acetate in the presence of the SBA-15/SO_3H catalyst was found to generally afford the 1,4-dihydropyridines (DHPs) 3 in good yields (Table 2).

4. Conclusions

In conclusion, we demonstrated that covalently bonded sulfonic acid SBA-15 is an efficient solid catalyst for the synthesis of Polyhydroquinoline

and dihydropyridines derivatives based on the diketene ring-opening reaction under neat conditions and short reaction times. Simple separation, easy recovery and reusability of the catalyst make it a highly efficient and convenient catalyst.

References

[1] X. J. Feng, M. Yan, X. Zhang, M. Bao, *Chin. Chem. Lett.* 22 (2011) 643–646.

[2] S. Rostamnia, T. Rahmani, *Appl. Organometal. Chem.* 29 (2015) 471–474.

[3] F. Matloubi Moghaddam, H. Saeidian, Z. Mirjafary, A. Sadeghi, *Iran. Chem. Soc.* 6 (2009) 317-324.

Pd@SBA-15/PrEn as an efficient, active and selective phosphine–free hybrid catalyst for the water medium Suzuki-Miyaura cross-coupling process

M. Dalili, H. Alamgholiloo, S. Rostamnia*

Organic and Nano Group, Department of Chemistry, Faculty of Science, University of Maragheh, PO BOX 55181-8311, Maragheh, Iran.

Email.srostamnia@gmail.com; Dalili.mrm@gmail.com

Abstract: In this present work the amine ligands embedded into the ordered silica mesoporous (PdX_2@SBA-15/Y, Y=1,2) as solid support for palladium complexes was designed. Among all of them, the covalently bonded $Pd(OAc)_2$/ethylenediamine complex into SBA-15 shows superior activity and selectivity toward Suzuki-Miyaura cross-coupling in aerobic condition with excellent yields. The as synthesized catalyst could be separated easily from reaction products and used for at least 10 times.

Keywords: Mesoporous, Suzuki reaction, Pd@SBA-15/PrEn, transition-metal complex.

1. Introduction

Nanoreactors are very small nanoscale enclosures that have a great potential for improving chemical transformation by protecting catalysts against environmental influences and encapsulating them in a small place for a long time [1]. There are different kinds of nanoreactors that have been developed till now such as metal-organic frameworks (MOF), zeolites, meso porous silica, and carbon nanotube (CNT) [2]. Among them, mesoporous silica, especially SBA-15, have been extremely considered because of their significant properties such as large surface areas, tunable structure and modifiable functional groups on surface of channels provide them with improved catalytic properties in applications for organic synthesis [3].

The aim of transition metal-catalysed organic synthesis is carbon-carbon (C-C) bond formation. In this respect, Pd complexes as an important transition metal catalysts are the best choice for catalyzing of the Suzuki reactions [4].

In this work, we investigated the activity and efficiency of a series of palladium-supported

functionalized mesoporous nanoreactors as a green and waste-free catalysts for synthesis of biaryls.

2. Experimental

After hydrothermal preparation of the SBA-15, the calcinated SBA-15 (1 g) will react with 2 mmol (433 µL) of $(MeO)_3SiPrNH(CH)_2NH_2$ in dried toluene under reflux condition for 24 h. After that, the solid SBA-15/PrEn product was filtered, and then dried under vacuum. In next step, the SBA-15/PrEn (1 g) will react with 100 mL of 0.055 M solution of $Pd(OAc)_2$ in toluene for 8 h at room temperature. After sonication (2× 3 min) the $Pd(OAc)_2$@SBA-15/PrEn product was filtered, and then dried at 60 ºC (Scheme 1).

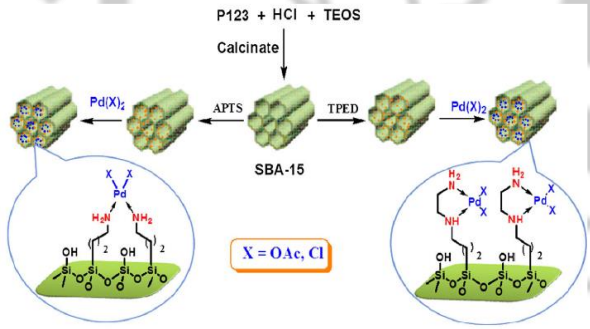

Scheme 1: Synthesis of Pd@SBA-15/PrEn.

3. Results and discussion

We fabricated SBA-15 silica mesoporous and after incorporating a series of the covalently bonded organic ligands into the SBA-15 mesoporous silicas and preparation of the various Pd pre-catalyst, we investigated these catalysts in Suzuki reaction.

Table 1. Different catalysts in the model reaction of Suzuki coupling

Entry	catalysts	%Pd leaching	%Yield
1	$PdCl_2$@SBA-15/$PrNH_2$	0.41	91
2	$Pd(OAc)_2$@SBA-15/$PrNH_2$	0.35	93
3	**$Pd(OAc)_2$@SBA-15/$PrNHEtNH_2$**	**0.07**	**96**

Performing the reaction in the presence of $Pd(OAc)_2$@SBA-15/$PrNHEtNH_2$ resulted in the production of **3** in 96% yield. These results clearly indicate the efficiency of the $Pd(OAc)_2$@SBA-15/$PrNHEtNH_2$ catalyst in both stability and activity.

After the selection of the best catalyst (Table 1, catalyst **3**), in order to optimize the reaction conditions, the effect of various parameters on the yield of 3 was examined. For this purpose, the model reaction was performed using different bases, solvents, time and Pd mol% in the presence of $Pd(OAc)_2$@SBA-15/$PrNHEtNH_2$pre-catalyst. As can be seen in Table 2, the best results were obtained using DMF–H_2O (1:1, 2 ml) as the solvent, using K_2CO_3 as base with 0.5 mol% Pd for 0.5 h.

Table 2. Optimization of model reaction over catalyst **3** pre-catalyst

Base	Solvent	Time (h)	Yield (%)
NaOH	H_2O	1	76
K_2CO_3	**DMF:H_2O**	**0.5**	**96**
Na_2CO_3	DMF:H_2O	1	86

4. Conclusions

Various Pd sources were incorporated into SBA-15 containing propyl amine ($PrNH_2$) and propyl ethylenediamine (PrEn). In a systematic study among these engineering porous nanomaterials, the $Pd(OAc)_2$@SBA-15/PrEn acts as aphosphine-free, highly efficient and low Pd leached pre-catalyst for Suzuki reaction.

References

[1] F.h. Lin, R.a. Doong, *J. Phys. Chem. C;* 121 (2017) 7844-7853.

[2] A. Botos, J. Biskupek, T.W. Chamberlain, G.A. Rance, C.T. Stoppiello, J. Sloan, Z. Liu, K. Suenaga, U. Kaiser, A.N. Khlobystov, *J. Am. Chem. Soc;* 138 (2016) 8175-8183.

[3] S. Rostamnia, T. Rahmani, *Appl. Organometal. Chem;* 29 (2015) 471-474.

[4] S. Rostamnia, H. Alamgholiloo, X. Liu, *J. Colloid Interface Sci;* 469 (2016) 310-317.

A Review Study on photocatalytic activity of a series of modified zeolites in removal of dye contamination

M. Moosavifar*

[a] *Department of Chemistry, Faculty of science, University of maragheh, Maragheh, Iran*

**Corresponding author: m.moosavifar90@gmail.com*

Abstract: A new class of supported photocatalysts is introduced with high activity under UV irradiation for the removal of dye contaminations. The composition comprises silicoaluminates (zeolite) as the support, TiO_2 or Ti derivatives as the semiconductor, metal ion or metallocomplexes as the promoter of reaction or photosensitizer was used in the photocatalytic performance. From photocatalyst preparation point of view, the synthesis consists of the impregnation, isomorphous replacement and template synthesis method. The objective is to investigate two classes of the zeolites namely Na–Y and beta zeolite which have emerged as suitable supports for photocatalytic application which functionalized by metal ion or metallcomplexes to improve photocatalytic activity. The efficiency of catalysts was determined based on the amount of degradation of dye contamination. The effect of several parameters was investigated in the removal of dye. The kinetic of degradation suggested being pseudo-first order. Mineralization of wastewater was obtained by using COD analysis. All of catalysts showed a good efficiency in the removal and degradation of pollution.

Keywords: metallocomplexes, isomorphous substitution, photocatalyst, degradation, wastewater.

1. Introduction

The industrial wastewater containing the various dyes is responsible for water pollution, due to their carcinogenic behavior [1,2]. Traditional methods to remove organic chemicals from effluents include the use of adsorbents, thermal destruction, biodegradation and oxidation process. However, advanced oxidation processes (AOPs) have become important because the AOPs can convert a wide range of harmful dyes into non-toxic products, CO_2 and water at ambient temperature. For now, many approaches have also been performed for modification of TiO_2. On the other hand, the

combination of TiO_2 and phoetosensitizer and various support materials such as porous siliceous materials is intensively studied for designing the unique composites with specific functions with modified photocatalytic performances [3].

Here, we reported new catalytic systems by simple and rapid methods with synergistic effect which provided by metal oxide, Ti derivatives and support and exhibited high photoactivity in the decolorization of methyl orange and 4-nitrophenol.

2. Experimental

At first, NaY zeolite was prepared in accordance to the reported procedure [4]. Modification of Y zeolite was performed by inclusion of metallocomplexes into zeolite supercage or isomorphous substitution. The modified catalysts were investigated in the photodegradation of 4-nitrophenol.

3. Results and discussion

The modified catalysts were prepared by template synthesis, impregnation and post synthesis method. The XRD pattern of the photocatalysts indicated that the catalysts have crystallinity almost identical to that of the parent NaY zeolite. This improved the modification of zeolite by ion metal or metallocomplexes not impact on zeolite structure. However, the presence of peaks in the region in accordance with TiO_2 confirmed the insertion of TiO_2 in zeolite cages.

FESEM-EDX spectrum of further showed the presence of component of photocatalyst. It proved the formation of metallocomplexes into zeolite cages (Fig. 2). However, the presence of some ripples on nano scale can be related to substituted species on external zeolite surface.

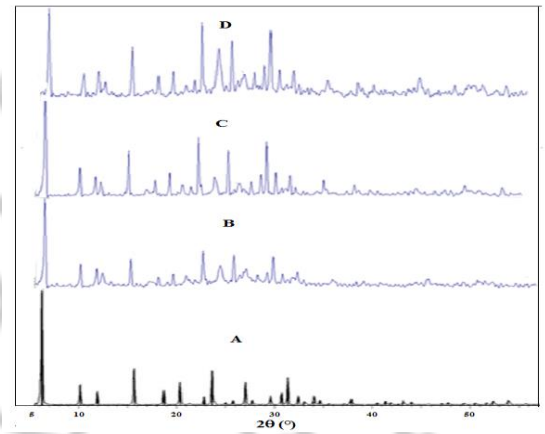

Fig. 1.XRD patterns of a) NaY, b) CeTPP/TiO_2/NaY, c) FeTPP/ NaY d) Ce-Fe/HY

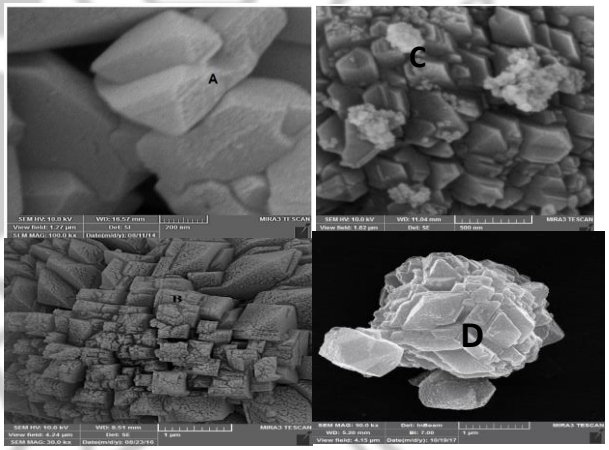

Fig. 2. FESEM micrograph of a) NaY, b) FeTPP/ NaY, c) CeTPP/NaY/ TiO_2 and d) Fe-Ce/NaY

The photocatlytic activity of catalysts were investigated in the photodegradation of 4-NP. The results showed based on functionalizing of zeolite with metallo-complex, TiO_2 or substitutaion

isomorphous, the photocatalytic activity of systems increases. It can be concluded they have synergetic effect which increased the photocatalytic activity.

Table 1 showed the catalytic activity of three catalysts. As it is clear, in the entry 2, 3, Fe act as semiconductor as well as TiO_2 and can be accelerate AOP's process (Fenton reagent). The results indicated in all of systems, mineralization was occurd. Therefore, these systems are suitable and efficient catalysts for removal of wastewater.

Table1. The results of COD analysis and removal percentage

	Catalyst	COD	Removal Efficiency (Time120 min)
1	CeTPP/TiO_2/ NaY	53.2%	80%
2	FeTPP/ NaY	74%	90%
3	Ce-Fe/HY	72.80%	100%

4. Conclusions

In this study, the preparation of catalysts was performed using impregnation and template synthesis method and post-synthesis treatment. The catalysts displayed efficient photoactivity in the phodegradation of 4-NP. The results indicated all of catalysts can be degraded 4-NP in the presence of H_2O_2 and UV irradiation. In this experiments 4-NP were degraded to simple materials based on COD analysis results.

References

[1] A. Sivakumar, B. Murugesana, A. Loganathan, P. Sivakumar., *J. Taiwan Inst. Chem. Eng.* 45 (2014) 2300–2306.

[2] M.R. Hoffmann, S.T. Martin, W. Choi, D.W. Bahnemann, *Chem. Rev*. 1995, 95, 69–96.

[3] C. Lavanya, R. dhankar, S. chhikara, S. sheora, *Int. J. Curr. Microbiol. App. Sci* (2014)3(6), 189-199

[4] M. Moghadam, S. Tangestaninejad, V. Mirkhani, I. Mohammadpoor-Baltork, M. Moosavifar, *J. Mol. Catal. A: Chem., (*2009), 302, 68-75.

[5] M. Moosavifar, A. Alemi, M.R. Marefat, N. Nouruzi, H. Mahmoodi, *J. Iran. Chem. Soc.*, 11 (2014), 1561-1567.

5th Iran International Zeolite Conference

University of Tabriz, Tabriz, Iran

26-27 August 2018

Esterification of Oleic Acid for Biodiesel Production Catalyzed by Fe_3O_4@ZIF-8@TiO_2 Composite

A. Moatamed Sabzevar, M. Ghahramaninezhad, M. Niknam shahrak*

Department of Chemical Engneering, Quchan University of Technology, Quchan, Iran

**Corresponding author: m.niknam.sh@qiet.ac.ir*

Abstract: In this paper, a nano-structured Fe_3O_4@ZIF-8@TiO_2 catalyst was prepared via a versatile recipe and then characterized by the Fourier transform infrared spectroscopy (FT-IR) and x-ray diffraction (XRD) analyses. Afterward, the as-synthesized Fe_3O_4@ZIF-8@TiO_2 catalyst utilized for the esterification reaction of oleic acid to produce biodiesel in a batch reactor system. The obtained results revealed that the process efficiency can be achieved to a good conversion of 78% after only 1 h under mild condition of 50 °C temperature along with only 0.125 g Fe_3O_4@ZIF-8@TiO_2 catalyst. Furthermore, effect of various operational parameters on the process efficiency including ethanol/oil molar ratio (10:1, 20:1, and 30:1) and time (5 to 120 min) was investigated to achieve the highest biodiesel production efficiency.

Keywords: Magnetic ZIF-8; Biodiesel; Fe_3O_4@ZIF-8@TiO_2 composite; Esterification

1. Introduction

Controlling and reducing the huge emissions of toxic and harmful gases from exhaust of vehicles due to fossil fuel combustion, has become one of the most significant challenges in the world. So, major consideration has been devoted to the usage of biodiesel all over the world as a promising alternative for fossil fuels because of its much lower emission of sulfur, carbon monoxide and smoke within the combustion [1]. One of the most common procedures to produce biodiesel is established based on heterogeneous catalysts. A lot of heterogeneous solid catalysts were investigated for trans-esterification reaction of oil to produce biodiesel so far [2]. Among of the different types of solid catalysts used for biodiesel production process, metal-organic Frameworks (MOFs) owing to high chemical stability, high contact levels and selectivity are known as one of the best candidate. In this research, a novel hybrid catalyst based on ZIF-8 powered by TiO_2 nano-particles (Fe_3O_4@ZIF-8@TiO_2), has been synthesized and its application for esterification reaction has been considered.

2. Experimental Part

All chemical materials and agents for synthesis of Fe_3O_4 nano particles, ZIF-8 and TiO_2 were supplied from Merck and used as received. Synthesis of Fe_3O_4 nano-particles (MNPs) were carried out based on available procedures in the literature [4]. After

successful preparation of Fe_3O_4 nano-particles, magnetic ZIF-8 was synthesized using encapsulation of Fe_3O_4 nanoparticles inside ZIF-8 where encapsulation reaction was executed under sonication bath at 160 °C [5]. Finally for synthesis of TiO_2-coated Fe_3O_4@ZIF-8 (Fe_3O_4@ZIF-8@TiO_2), 0.6 ml acetic acid and 10 ml ethanol solution were added to 14 ml $Ti(OBU)_4$ and 1.0 g ZIF-8 were added to the solution and mixed for 2 h. 0.16 ml acetic acid and 11.6 ml deionized water were then added to 15 ml ethanol and the pH was adjusted by acetic acid to 13. Afterward, second solution was added to first solution slowly. The titanium sol/ Fe_3O_4@ZIF-8 changed to titanium gel/ Fe_3O_4@ZIF-8 after aging for 2 h and were dried at 160 °C in oven. Finally, the powder was calcined at 300 °C [6]. In all experiments, the conversion of oleic acid was determined by titration using NaOH and phenolphthalein solution as indicator.

3. Results and discussion

Successful synthesis of novel magnetic catalyst was confirmed using the x-ray diffraction (XRD) and Fourier transform infrared spectroscopy (FT-IR) analyses as demonstrated in Fig. 1 and Fig. 2, respectively. In Fig. 1, XRD pattern for the as-synthesized Fe_3O_4@ZIF-8@TiO_2 are reported. The important peaks of TiO_2 nano- particles (TNP) are revealed at $2\theta = 35.30°$. As shown in XRD pattern of TNP, other crystal peaks are appeared at 2θ of 29.10°, 42.01°, 54.34°, 62.71 which is consistent with anatase phase of TiO_2 [6].

The FT-IR spectrum of Fe_3O_4@ZIF-8@TiO_2 catalysts are illustrated in Fig 2. In the spectra, all the samples showed the important bands in the range of 500–700 cm^{-1}, which were determined to characteristic of an O–Ti–O lattice.

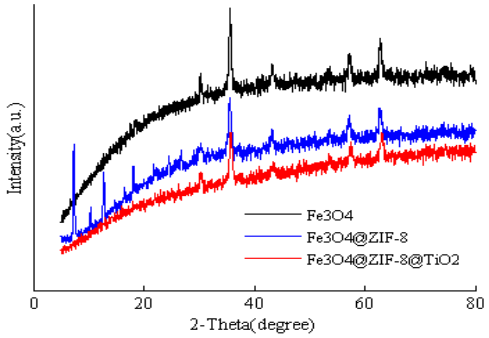

Figure 1. Experimental XRD patterns of the as-synthesized Fe_3O_4, Fe_3O_4@ZIF-8 and Fe_3O_4@ZIF-8@TiO_2.

The peak around 1400 cm^{-1} was allocated to bending vibrations of O–H. The peaks appeared surrounding 1630 cm^{-1} were determined to the bending vibration of the adsorbed H_2O. The broad peaks above 3000 cm^{-1} were because of O–H stretching vibration of water and Ti–OH.

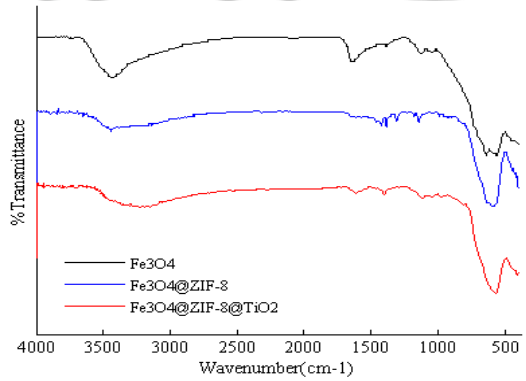

Figure 2. FT-IR spectra of the as-synthesized Fe_3O_4, Fe_3O_4@ZIF-8 and Fe_3O_4@ZIF-8@TiO_2.

After successful synthesis of novel Fe_3O_4@ZIF-8@TiO_2 catalyst, its application for esterification of oleic acid (OA) with ethanol was investigated. The

catalytic performance of the prepared Fe_3O_4@ZIF-8@TiO_2 catalysts for the esterification of oleic acid with ethanol was fulfilled where in a typical reaction, 0.125 g catalyst, 0.05 mol OA, and a molar ratio of EtOH to OA from 30:1, 20:1 and 10:1 at different reaction time were used. Influences of EtOH/OA molar ratio on process efficiency are shown in Fig. 3. As it is indicated, with increase in EtOH/OA molar ratio, process efficiency increases. In other words, the conversion of OA increased with increasing in the ethanol concentration in the reactant. According to Fig. 3, the conversion of oleic acid to ethyl ester (biodiesel) at 50 °C for 1 h in EtOH/OA molar ratio of 30: 1 is higher than that EtOH/OA molar ratio of 20:1 and 10:1.

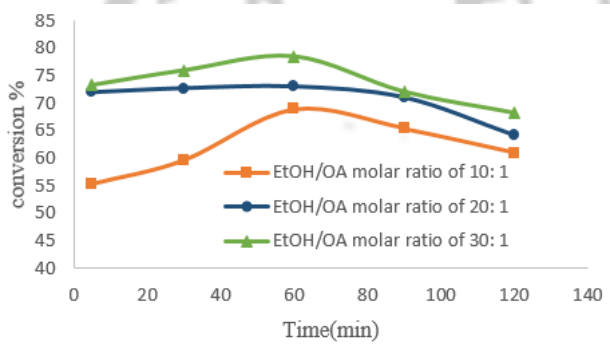

Figure 3. Effect of EtOH/OA molar ratio on the conversion of OA to ethyl ester over (50 °C; 0.125 g catalyst).

4. Conclusions

In the present work, esterification of oleic acid using a novel Fe_3O_4@ZIF-8@TiO_2 catalyst was performed. The as-prepared composite shows high activities for esterification of oleic acid with ethanol. As the EtOH/OA molar ratio increases, the conversion increases. Furthermore, the catalyst can be separated by magnet and reused.

References

[1] M. Saeedi, R. Fazaeli, H. Aliyan, *J. Sol-Gel Sci. Technol.* 77 (2016) 405-415.

[2] S. Sandesh, P. Kumar, R. Kristachar, P. Manjunathan, A.B. Halgeri, G. Shanbhag, *Appl. Catal. A: Gen.* 523 (2016) 1-11.

[3] K. Zhou, S. Chaemchuen, *International Journal of Environmental Science and Development* 8 (2017) 251-254.

[4] Y.R. Yao, W.Z. Huang, H. Zhou, X. Cui, Y.F. Zheng, X.C. Song, *J. Nanopart. Res.* 16 (2014) 1-10.

[5] C. Yim, H. Lee, S. Lee, S. Jeon, *RSC Adv.* 7 (2017) 1418-1422.

[6] G. Li, R. Haddad, H. Jiang, D. Li, T. Liao, L. Yuan, *Water sci. Technol.* 17 (2017) 1730-1739.

Synthesis and Identification of Pd^{2+}/ZnO/HZSM-5 Nanocomposite and Study of its Photocatalytic Activity

B. Divband*, M. Khatamian, R. Shahi

Department of Inorganic Chemistry, Faculty of Chemistry, University of Tabriz, Tabriz, Iran

**Corresponding author: RShahiii@yahoo.com*

Abstract: Zeolites are a large family of minerals that due to their large surface area and the high adsorption property, they can act as the substrate beds along with semiconductors form effective composites. Based on this, a triple Pd^{2+}/ZnO/HZSM-5 composite was prepared using acrylamide monomer with a gel degradation method. This nanocomposite was identified with XRD, SEM, and EDX techniques. In the study of photocatalytic activity on the prepared sample, this composite was able to adsorb 4-nitrophenol and degrade it.

Keywords: Pd^{2+}/ZnO/HZSM-5 nanocomposite; Destruction of gel; Photocatalytic activity

1. Introduction

Zeolites are crystalline aluminosilicates, consisting of structural units of AlO_4 and SiO_4 (tetrahedral). These tetrahedrals are connected by oxygen bridges and form network of channels and cavities with different sizes and shapes [1]. ZnO, as a relatively inexpensive and environmentally friendly photocatalyst with band gap of 3.37 eV, has a good effect in the photocatalytic degradation of phenols and nitrofenols through supporting on zeolite [2]. Introducing the cation of intermediate elements through the chemical mechanism such as doping is a strategy to reduce the band gap of ZnO and shift of the semiconductor adsorption wavelength to the visible region for replacement of the UV source with a solar radiation and visible source to provide the energy needed for the photogradiation process of pollutants. Metal ions can act as a load separating center on the ZnO surface and also facilitate the process of transporting generated e^- and h^+ to the pollutant, and thereby increasing the ZnO catalytic activity and degradation efficiency of the pollutant. 4-nitrophenol (4-NPh) is an important member of the nitrophenol group that is the most common pollutants in many Chemical industry and pharmacy wastewaters; therefore, it is important to remove this compound from wastewaters before safe disposal into the surface waters. [3-4].

2. Experimental Part

ZnO/HZSM-5 composite was prepared using zinc acetate, nitric acid, citric acid and zeolite. Then, 0.2 g of composite was added to 20 ml of water inside a crucible, and the mixture was stirred for 1 hour and then, was placed in an ultrasound bath for 1 hour. 0.3

g of monomer acrylamide was added to the mixture and stirred for 20 minutes. Then, the $PdCl_2$ was added to the mixture and stirred. The crucible was then placed in a water bath at 80 ˚C. In order to dry the obtained transparent porous polymer gel, it was placed in an oven at 100 ˚C for 12 hours. The dried and hard polymer was heated to 300 ˚C for 10 hours to burn the organic material completely; then, it was calcined for 5 hours at 550 ˚C. Also, the photocatalytic activity of the as-prepared catalyst is tested for degradation of 4- NPh.

3. Results and discussion

Figure1 shows XRD pattern of Pd^{2+}/ZnO/HZSM-5 nanocomposite. Considering the appearance of intensive peak of HZSM-5 in the sample, it is shown that zeolite support is stable during the process of degradation of acrylamide gel and calcination, and is not subject to alteration. The appearance of ZnO peaks can be also observed, but no additional peak associated with the Pd^{2+} ion is observed that is due to the very small amounts of this ion inside the holes and channels of HZSM-5. Figure 2 shows the SEM images and EDS analysis of the Pd/ZnO/HZSM-5 nanocomposite. It is probable that the presence of small bright particles is related with ZnO particles. EDS analysis also showed the presence of small amount of Zn and Pd, which confirms the presence of ZnO and Pd cations in the composite. The efficiency of nanocomposite prepared for degradation of 4-NPh was investigated. As shown in figure 3, this nanocomposite can destroy 98% of paranitrophenol, which is related to the adsorption and availability of active sites for degradation.

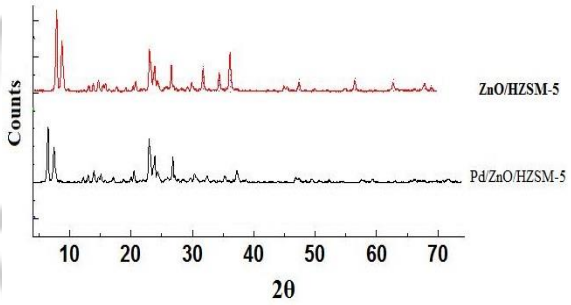

Figure 1. XRD pattern of the ZnO/ HZSM-5 and Pd^{2+}/ZnO/HZSM-5 nanocomposite.

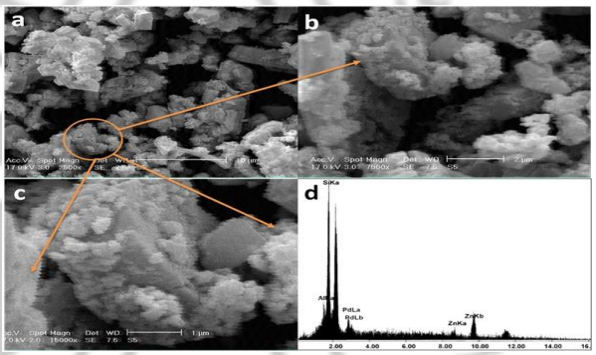

Figure 2. SEM images and EDS analysis of the Pd/ZnO/HZSM-5 nanocomposite.

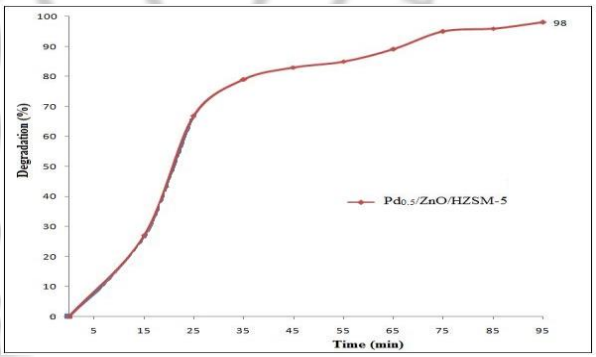

Figure 3. Percentage of 4-NPh degradation by Pd/ZnO/HZSM-5 nanocomposite.

4. Conclusions

To prepare this triple nanocomposite, intermediate element such as Pd was doped through the acrylamide gel degradation method. The nanocomposite by various techniques was identified and it was observed that doping Pd had no effect on the structure and location of the peaks in the XRD pattern of zeolite and ZnO, only the peak intensity was reduced slightly. According to SEM images, particle size was in the range of nanometer scale. The composite was able to remove 98% of 4-nitrophenol over a period of 95 min.

References

[1] Ch. Rhodes, *Annu. Rep. Prog. Chem.* 103 (2007) 287-325.

[2] K.M. Parida, S.S. Dash, D.P. Das, *J. Colloid Interfac. Sci.* 298 (2006) 787-793.

[3] A. Maleki, B. Shahmoradi, *Water Sci. Technol.* 11 (2012) 1923-19288.

Synthesis of γ-alumina from Nepheline syenite ore

S. Khadivi derakhshan[a]*, N. Kamrani[a], B. Divband[a], M, Khatamian[a], H. Kakili

[a] *Department of Inorganic Chemistry, Faculty of Chemistry, University of Tabriz, Tabriz, Iran)*

**Corresponding author: s.khadividerakhshan@yahoo.com*

Abstract: We reported a new method for the synthesis of γ-alumina. Nanosized γ-alumina was synthesized successfully by a simple method using Nepheline syenite ore and Lime by leaching. X-ray diffraction, FTIR spectroscopy were used to characterize the structure and morphology of synthesized powder.

Keywords: γ-Alumina, Nanostructure, Nepheline Syenite, X-ray diffraction.

1. Introduction

In the past few years, the field of nano-crystalline oxide materials has attracted more attention. Nepheline syenite is an igneous rock. The formula of Nepheline syenite is $Na_3KAl_4Si_4O_{16}$ and the alumina content of Nepheline syenite approximately is 25% [1]. It is also used in ceramics and as industrial filler. Aluminum oxide is used extensively because of its high melting point, uniform channels, high surface area, uniform pore size distribution and high heat resistance and is used as a adsorbents, catalysts, planting, biological basis or catalyst support. Alumina exists in a variety of metastable structures including γ-, η-, δ-, θ-, κ- and χ-alumina, as well as its stable α-alumina phase [1]. Among these transitions, γ-alumina is one kind of extremely important nanosized materials. It is extensively used as catalyst, catalytic supports and adsorbents. Chemical routes for production of aluminum oxide include sol-gel, hydrothermal processing and control precipitation of aluminum salts, alkoxides, metallic powders [3], spray pyrolysis and combustion synthesis [4]. It is worth noting that the Chemical materials such as aluminum alkoxide, aluminum nitrate economical due to their high price, but mineral materials such as Kaolin and Nepheline syenite are suitable because of easy access, inexpensive price and providing easy method for the preparation of alumina.

2. Experimental Part

The raw powders of Nepheline syenite were obtained from Azarshahr, Iran.

The mineral concentrate is sintered with limestone and following alkali tube digestion and further processing, the resulting liquor is autoclaved and the resulting filter cake calcined to produce alumina. The residue from tube digestion is fed to a cement kiln, while the liquor from alumina filtration is also processed to yield high purity potassium and sodium carbonates. The pH of the solute was decreased to 10

by adding HNO_3 solution with the magnetic stirring until the alumina was precipitated completely. Then the reaction mixture was placed in a Parr-Teflon lined stainless steel vessel. It was sealed and heated at 200°C for 24 h.The precipitate was collected by centrifuge and washed with ethanol. Finally, the as-synthesized samples were calcined at 750 °C for 3 h.

3. Results and discussion

The XRD pattern confirmed the cubic structure of alumina. Fig.1 shows the XRD pattern of nano γ-alumina and five index peaks of γ-alumina were observed at 32.57, 36.54, 39.56, 45.52 and 66.99°. From Debye-Scherrer formula the average crystalline size of produced nanocrystals was calculated as about 17 nm.

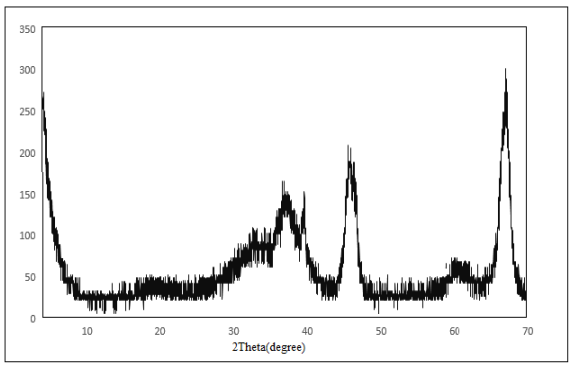

Figure 1. The XRD pattern of prepared nano γ-alumina at 750 °C.

The FT-IR analysis of the synthesized γ-alumina is shown in Fig. 2. According to the infrared spectrum, four peaks are observed. The peaks in the region of 400-1,000 cm^{-1} were generally associated with the stretching vibration of Al-O bonds. Peaks in the region of 1,400 cm^{-1} to 1,600cm^{-1} are associated with the formation of alumina. The peaks around 3,500cm^{-1} and 1,630 cm^{-1} were assigned to stretching and bending modes of adsorbed water.

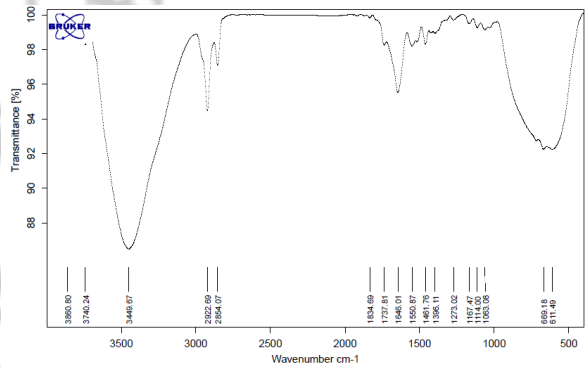

Figure 2. FTIR spectra of γ-alumina.

4. Conclusions

The nano γ-alumina in the cubic crystal structure with the average crystalline size of 42nm was prepared successfully from Nepheline syenite ore.

Acknowledgments

We especially thank the Tabriz University, Tabriz for financial support.

References

[1] M. Chitan, S.A. Hosseini, D. Salari, A. Niaei, H. Mehrizadeh, *Korean J. Chem. Eng.* 34 (2017) 66-72.

[2] E. Jorjani, M. Amirhosseini, *Alumina Production Process from Nepheline Ore in Razgah (Iran),*111-115.

[3] M. Tabatabaee, N. Saberi, *Int. J. Bio-Inorg. Hybd. Nanomat* 1 (2012) 253-256.

[4] K. Varatharajan, S. Dash, A. Arunkumar, R. Nithya, A. Tyagi, B. Raj, *Mater. Res. Bull.* 38 (2003) 577-583.

5th Iran International Zeolite Conference

University of Tabriz, Tabriz, Iran

26-27 August 2018

Preparation and Characterization of Nano Mn_3O_4 and Mn_3O_4 /Zeolite A Composite

N. Kamrani *, S. Khadivi derakhshan, H. Kakili, M. Saket, M. Khatamian

Department of Inorganic Chemistry, Faculty of Chemistry, University of Tabriz, Tabriz, Iran

**Corresponding author: n.kamrani30@gmail.com*

Abstract: Mn_3O_4 nanoparticles and Mn_3O_4/ zeolite A composite were prepared by a simple precipitation method using cetyltrimethylammonium bromide (CTAB) as a template agent. The prepared samples were characterized by X-ray powder diffraction (XRD) and scanning electron microscopy (SEM).

Keywords: Mn_3O_4; Zeolite A; Composite; Nanoparticle; XRD; SEM

1. Introduction

Hausmannite (Mn_3O_4) is a material with normal spinel structure possessing tetrahedral [1]. Manganese oxides are widely used as electrode materials [2], catalysts [3], and soft magnetic materials [4] .Various methods have been reported for the synthesis of Mn_3O_4 nanoparticles. Among these methods, the most common one can be regarded as the calcination of oxides, hydroxides, hydroxyoxides, oxysalts, carbonates, nitrates or sulfates of manganese in air at about 1000 ˚C [5].

Zeolite A is a crystalline material that can be applied in the field of catalysis, separation, ion exchange, and adsorption.

Here, we reported a simple low-temperature process for synthesizing of Mn_3O_4 nanoparticles as well as the composite of Mn_3O_4/zeolite A.

2. Experimental Part

The synthesis of Mn_3O_4 nanoparticles was performed at room temperature, using the precipitation route. A proper amount of $MnCl_2.4H_2O$ was added to an aqueous solution of NaOH. Then 0.025 g cetyltrimethylammonium bromide (CTAB) was dispersed and homogenized under slowly magnetic stirring during 24 hours. The precipitate was filtered and carefully washed with distilled water for several times. The resulting product was dried in the oven at 80 ˚C for 24 hours.

The synthesis of Mn_3O_4/zeolite A composite was performed at room temperature, too. A proper amount of $MnCl_2.4H_2O$ was added to an aqueous solution of NaOH. Then 0.025 g CTAB was loaded into a beaker, which was then put into an ordinary ultrasonic for 30 minutes till $MnCl_2$ was completely dissolved and form a clear brown solution , then 4.5 g of commercial zeolite A was added into the solution and ultrasound irradiation was continued for one more hour. In the next step, the resulting mixture was dispersed and homogenized under slowly magnetic stirring during 24 hours. After filtering the precipitate, it was washed with distilled water for several times. The resulting product was dried in the oven at 80 ˚C for 24 hours.

3. Results and discussion

3.1. X-ray diffraction

Figure 1 shows XRD patterns of as-prepared Mn_3O_4 nanoparticles. The diffraction peaks correspond to the tetragonal Mn_3O_4 single phase (JCPDS Card 00-008-0017).

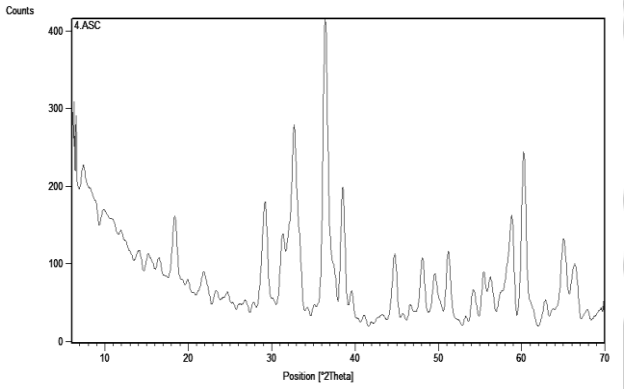

Figure 1. XRD Pattern of product after heating.

Figure 2 and Figure 3 show XRD patterns of commercial Zeolite A and as-synthesized Mn_3O_4/4A zeolite composite, respectively.

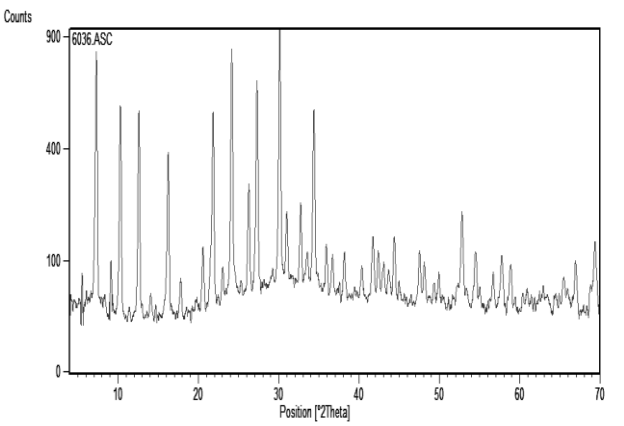

Figure 2. XRD Pattern of commercial zeolite A.

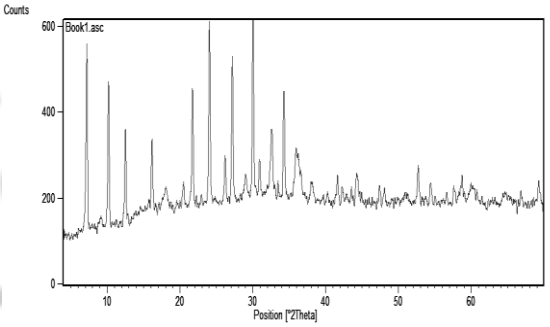

Figure 3. XRD Pattern of as-prepared Mn_3O_4/zeolite A composite.

3.2. SEM analysis

The microstructure and morphology of the Mn_3O_4 nanoparticles was studied by SEM. It can be seen that the materials were composed of uniform and mono-dispersed spherical nanoparticles.

Based on Fig. 4, the primary particle size can be estimated as equal to 20 nm.

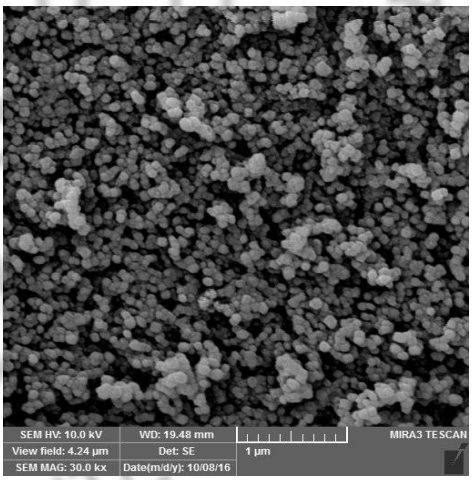

Figure 4. SEM image of as-synthesized Mn_3O_4.

4. Conclusions

Mn_3O_4 nanoparticles were successfully prepared by using the precipitation method at room temperature in the presence of CTAB, as a template agent. X-ray structural analyses confirmed that Mn_3O_4 nanoparticles crystallize in a tetragonal crystal system.

According to the XRD results (Figure 2 and 3), the synthesis of Mn_3O_4/ zeolite A composite was performed successfully.

Acknowledgments

The authors are thankful to University of Tabriz for supporting this study.

References

[1] R. Ribeiro, S. de Lazaro, S. Pianaro, *J. Magn. Magn. Mater.* 391 (2015) 166-71.

[2] A.R. Armstrong, P.G. Bruce, *Nature*, 381 (1996) 499-500.

[3] Y.C. Son, V.D. Makwana, A.R. Howell, S.L. Suib, *Angew. Chem. Int. Edit.* 40 (2001) 4280-4283.

[4] W.S. Seo, H.H. Jo, K. Lee, B. Kim, S.J. Oh, J.T. Park, *Angew. Chem. Int. Editi.* 43 (2004) 1115-1117.

[5] J. Du, Y. Gao, L. Chai, G. Zou, Y. Li, Y. Qian, *Nanotechnology* 17 (2006) 4923-4928.

Synthesis and Characterization of Iron Hydroxide-Zeolite Nano Composites

S. Gholizadeh[a]*, M. Khatamian[a], M. Tahmasebpoor[b], B. Divband[a], A. mokhtari[a]

[a] *Department of Inorganic Chemistry, Faculty of Chemistry, University of Tabriz, Tabriz, Iran*

[b]*Department of chemical engineering, Faculty of Chemistry, University of Tabriz, Tabriz, Iran*

**Corresponding author: shahingholizadeh1370@yahoo.com*

Abstract: Iron oxy hydroxides can be used as model systems for the study of fundamental colloid and surface properties of metal oxides. In current study Nano composite has been synthesized by co-precipitation and Sono chemistry methods. The prepared nano composites were characterized using x-ray diffraction (XRD) and scanning electron microscope (SEM).

Keywords: Iron hydroxide; Nano composites; Zeolite; Clinoptilolite

1. Introduction

Iron hydroxide [Am-$Fe(OH)_3$] exists in a large class of inorganic compounds and applied in various areas of industry, in particular in the preparation of magnetic materials, catalysts, inorganic pigments and sorbents [1].

Zeolites are porous aluminosilicates with a crystal structure, containing a system of channels and chambers. Their structure provides them with unique surface properties; such as ion-exchange, adsorption, molecular-sieves and catalytic capabilities [2]. In addition, zeolites can be used as substrates for different nanoparticles because they can improve the properties of these particles and enhance their performances in various applications.

Therefore, in this work iron hydroxide-zeolite nano composites were synthesized and characterized.

2. Experimental Part

Nano composites were prepared by the addition of 1.62 g of clinoptilolite to 1.665 g of analytical grade $Fe(SO_4)_3$ dissolved in 200 ml of distilled water. Then 25 ml of 1 M NaOH was added to suspension and immersed for 2 h in an ultrasonic bath. The resultant precipitate was washed several times with distilled water and dried at room temperature.

3. Results and discussion

The XRD patterns of pure $Fe(OH)_3$ and nano composite are shown in Fig. 1. The XRD pattern of pure $Fe(OH)_3$ (Fig. 1a) shows typical pattern of amorphous 2-line ferrihydrite, with the two broad bands at approximately d = 2.56 Å and 1.48 Å (2θ = 35 ° and 62.8 ° with Cu-K_α radiation) [3]. The XRD pattern of prepared composite indicated the

characteristic peaks of both Clinoptilolite and $Fe(OH)_3$, which shows the crystal structure of Clinoptilolite is not destroyed during the synthesis of $Fe(OH)_3$. No characteristic peaks of other impurities were detected in the pattern [4].

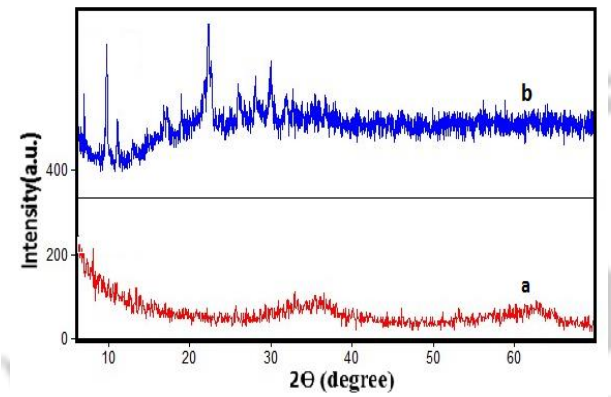

Figure 1. X-ray diffraction patterns of $Fe(OH)_3$ (a) and iron hydroxide- clinoptilolite (b).

The size and morphology of the clinoptiloite are illustrated in Fig. 2. The morphology of clinoptiloite is approximately plate-like and the size distribution of particles is not uniform.

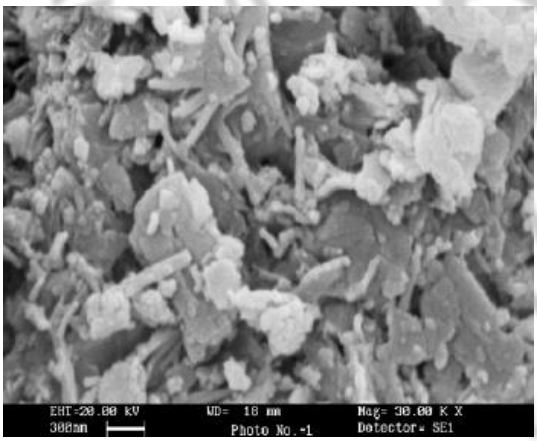

Figure 2. SEM image of clinoptilolite.

4. Conclusions

The XRD results confirmed that the synthesis of nano-$Fe(OH)_3$/zeolite composite was achieved successfully by using the co-precipitation and sono chemistry methods.

Acknowledgments

We would like to thank the University of Tabriz and Iranian Nanotechnology Initiative Council for the financial support of this project.

References

[1] V.V. Popov, A.I. Gorbunov, *Inorg. Mater.* 42 (2006) 275-281.

[2] L. Bandura, R. Panek, W. Franus, International scientific conference "Modern technologies of zeolite tuff usage in industry" 2014.

[3] N. Papassiopi, F. Pinakidou, M. Katsikini, G.S. Antipa, C. Christou, A. Xenidis, E.C. Paloura, *Chemosphere* 111 (2014) 169-176.

[4] M. Khatamian, S. Hashemian, A. Yavari, M. Saket, *Mater. Sci. Eng.: B* 177 (2012) 1623-1627.

5th Iran International Zeolite Conference

University of Tabriz, Tabriz, Iran

26-27 August 2018

Synthesis and Characterization of Zeolite Nano-Particles Impregnated Polyethersulfone Membranes by Electrospinning

F. Hossein Nouri, M. Zendehdel*

Department of Chemistry, Faculty of Science, Arak University, Arak 38156-8- 8349, Iran

** Corresponding author: m-zendehdel@araku.ac.ir*

Abstract: The aim of this study was electrospinning of Zeolite nanoparticles impregnated poly (ether sulfone) and evaluation of the filtration efficiency. The produced membranes were characterized by SEM for morphology.

Key words: Polyether sulfone; Zeolite; Electrospinning

1. Introduction

Polymeric membranes, as important separation tools, are used in various industries. These membranes are porous or dense and are categorized as symmetric or asymmetric membranes. In these devices, the separation process is based on the size or structure of substrates. Nowadays, although different methods are used to fabricate separation membranes, the use of nanofibers has attracted the researcher attention considerably [1-3].

Electrospinning is one of the versatile techniques with the ability to produce cost-effective, large production, highly porous nanofibers (about 80%), highly interconnected pores and the large ratio of surface area to volume is the characteristics of these membranes. On the other hand, polyethersulfone (PES) is a polymer with special properties including heat and chemical resistance, as well as biocompatibility. In these membranes, the selections of appropriate ratio zeolite nanoparticles, process, and environmental conditions are overviews on the electrospinning process of polyethersulfone membrane for nano filter membrane application [1-3].

2. Experimental Part

At first, PES was dissolved in DMF mixture at 60 °C for 24 h until it becomes a homogenous solution [2]. Four different concentration (i.e. 23, 20, 17 and 14.5 w/w%) of PES solution were prepared, then the resulting material was reacted with 0.1 g nano clinoptilolite zeolite in 60 °C for 12 h.

The spinning solution was loaded in a syringe as the spinneret and was extruded to the spinneret with a needle. For a generation of direct-current voltages, the spinneret was connected to high voltage. A syringe pump was used to squeeze out the polymer solution at the flow rate of 0.5 ml/h. Different voltages of 18 and 17 kV were applied between the syringe and collector. The distance between the collector and the spinneret was 15 cm and kept constant during the experiment. All PES

solution was electrospun onto aluminum foil or non-woven support with bigger pore size than the samples do not affect the results.

3. Results and discussion

The morphology of electrospun PES membranes prepared from different concentrations was investigated using SEM (Fig. 1). Particles show a wide range of shapes and sizes. The SEM images indicate the presented of well-defined nano zeolite presence on its external surface. The mixed bead-fiber morphology was seen from the membrane fabricated by the 20 wt% PES/DMF/zeolite solution.

In contrast, the uniform fiber morphology was found in membranes from 20 to 14.5 wt% PES/DMF/Zeolite solution. The average fiber diameter increased from 250 nm to 800 nm as the solution concentration was increased from 23 wt% to 14.5 wt%.

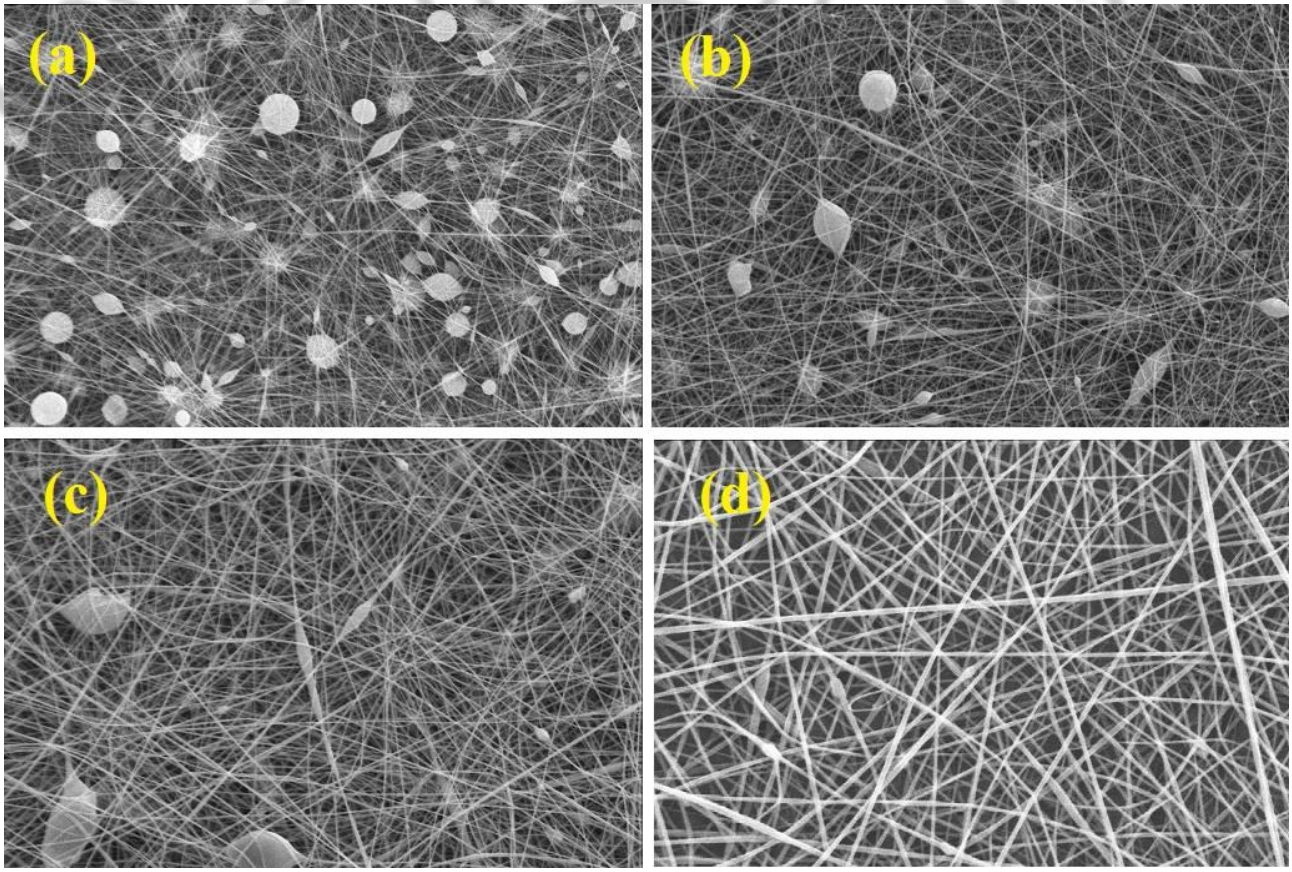

Figure 1. SEM images of electrospun PES/nano zeolite membranes from different PES/DMF concentrations: (a) 14.5 wt%, (b) 17 wt%, (c) 20 wt%, (d) 23 wt%, (the scale bar is 6 µm).

4. Conclusions

High-quality electrospun polyethersulfone (PES) membranes could be fabricated by using DMF as solvent. Uniform fiber morphology (diameter: 250–800 nm) was obtained at PES concentrations from 23 to 14.5 wt% in DMF. With the addition of nano zeolite, the average fiber diameter was slightly increased and zeolite nanoparticles trap in polyethersulfone fibers.

Acknowledgments

This paper was funded by Arak university therefore, acknowledge technical and financial support of Arak university.

References

[1] S. Khezli, M. Zandi, J. Barzin, *J. Polymerization*, 5 (2015) 4-15.

[2] K. Yoon, B. Hsiao, B. Chu, J. *Polymer*, 50 (2009) 2893-2899.

[3] Z. Yaakobb, M. Ghasemic, D. Khademe, *J. Defect and Diffusion Forum*. 312-315 (2011) 607-612.

Application of Nano Zeolite in Food Packaging

M. Azizi-lalabadi[a,d*], L. Rafiei[b], A. Ehsani[a], B. Divband[c,e]

[a] *Department of Food Sciences and Technology, Tabriz University of Medical Sciences, Tabriz, Iran*

[b] *Department of Food Sciences and Technology, Urmia University, Urmia, Iran*

[c] *Stem Cell Research Center, Tabriz University of Medical Sciences, Tabriz, Iran*

[d] *Students' Research Committee, Department of Food Sciences and Technology, Tabriz University of Medical Sciences, Tabriz, Iran*

[e] *Infection and Tropical Disease Research Center. Tabriz University of Medical Sciences, Tabriz, Iran*

**Corresponding author: marymazizi766@gmail.com*

Mini Review

Nowadays there are several research topics on the properties of nanoparticles, which can affect their chemical, optical, electrical, and biological characteristics. Nanoparticles are known as potent antimicrobial agents with various techniques on determining the antimicrobial mechanism of nanoparticles [1,2]. Zeolites are crystalline low-density aluminosilicates, which are called "molecular sieves" with a microporous three-dimensional structure. Pore sizes are in the range of 0.3–2 nm. These pores are usually full with water molecules or alkali or alkali-earth cations. These compounds have wide usage because of physicochemical properties of large surface area, pore compositional, framework flexibilities, physical, thermal and hydrothermal stabilities, high adsorption capacity, non-toxicity, ion exchange ability, selectivity and their economic benefits. Hence, they offer great advantages in comparison with non-porous solids. Zeolites have a TO4 tetrahedral structure (T is Si or Al in a natural zeolite), which are linked to other atoms by sharing corner oxygen atoms. Altering the ratio of Si/Al and replacing another atom such as P, B, Ga, Fe, and Ti, into T atom situation, several compositions and structures of zeolites and zeolite-like materials can be synthesized for instance Y-type, A-type, X-type, ZSM-5-type, BEA-type, P-type or mordenite [2]. Y and X are the most generally used zeolites, because of their market availability, variety, micro porosity and well-defined composition.

Natural zeolites have powerful repulsive force toward anions because of their skeleton structure with negative charges. Their complicated structural arrangement is further responsible for the high specific surface area of these materials, which create a large structure (exceeding 700 m^2/g). And this is the key factor for the outstanding adsorption and catalytic properties of these materials [2,3]. Recent

studies have revealed that the addition of different types of nano-sized materials into natural polymers, in order to yield nanocomposite, can be a well-organized solution to improve these characteristic such as reducing permeability to water vapor, increasing thermal stability and improving physical, mechanical and gas barrier properties. These are attributed to the strong interfacial interaction of polymer matrix and filler with the formation of tortuous pathway of gas diffusion. The essential technology for the production of nanoparticle-included bio nanocomposites is the control of particle size and their monotonous distribution inward the polymer [4,5].

The use of thin films zeolite varies based on two main factors including structure and composition and the orientation of zeolites, which have affected not only their molecular sieving abilities but also their optical and electronic characteristics. Zeolites can be normally synthesized in highly viscous colloidal suspensions when they are formed of thin films. In general, for food applications, zeolites are among the most widely used materials to incorporate silver as antimicrobial agent. For example, silver-zeolite nanoparticle framework, at concentrations of 1, 2 and 5 g/100 g zeolite, showed positive antibacterial activity against gram-negative and gram-positive bacteria such as E. coli, Shigella dysentriae and Staphylococcus aureus respectively [6]. In the USA, technologies with the basis of zeolites are listed under the US FDA Inventory of Effective Food Contact Substance Notifications (EFCSN) for being used in food-contact polymers. In Europe, the European Food Service Authority (EFSA) also disclosed a positive idea about the use of two zeolites having silver ions in food contact surfaces; in these zeolites, migration of silver into the food matrices was limited to 50 g of silver per kg of food. In recent years, different zeolites containing Ag, Cu or Zn have been applied for antibacterial purposes. Scientists have evaluated Ag-zeolites fungicidal effect on citrus and they obtained the best result with large pores and high Si/Al ratio of zeolite. The antifungal activity of silver zeolites depended on Si/Al ratio, the amount of silver and the topology of the zeolites. In general, higher silver content resulted in better antifungal activity and unfortunately obvious phytotoxicity on the fruit surface [6,7].

These features enable discrimination among molecules based on their size and shape, their passage control through porous system and their reactions to active sites.

In conclusion, based on the results, the application of nano zeolite in food packaging, for fixing nano particles in polymeric matrix can be a good approach to create active food package and increase the shelf life of the components.

References

[1] E. Koohsaryan, M. Anbia, *Chinese J. Catal.* 37 (4) (2016) 447-467.

[2] S. Mintova, J. Grand, V. Valtchev, *Comptes Rendus Chimie* 19 (1) (2016) 183-191.

[3] S. Mandal, H.L. Williams, H.K. Hunt, *Micropor. Mesopor. Mater.* 203 (2015) 245-258.

[4] G. Ciobanu, G. Carja, O. Ciobanu, *Mater. Sci. . Eng.: C* 27 (5) (2007) 1138-1140.

[5] D. Wang, J. An, Q. Luo, X. Li, M. Li, *J. Appl. Polym. Sci.* 110 (5) (2008) 3038-3046.

[6] S.H. Othman, N.R. Abd Salam, N. Zainal, R. Kadir Basha, R.A. Talib, *Int. J. Photoenergy* 2014 (2014) 1-6.

[7] E. Ye, X.J. Loh, *Australian J. Chem.* 66 (9) (2013) 997-1007.

5th Iran International Zeolite Conference

University of Tabriz, Tabriz, Iran

26-27 August 2018

Synthesis and Characterization of HY Zeolite @N-Cu

Z. Mortezaeia, M. A. Bodaghi Farda, M. Zendehdel*[a]

[a] *Department of Chemistry, Faculty of Science, Arak University, Arak 38156-8- 8349; Iran*

**Email:m-zendehdel@araku.ac.ir*

Abstract: The main goal of this work was Synthesis of complex with copper on HY zeolite as a simple and low–cost substrate. Then the modified HY zeolite characterized using FT-IR, XRD and SEM techniques.

Keywords: Synthesis; copper; HY zeolite

1. Introduction

According to the International Union of Pure and Applied Chemistry (IUPAC), a microporous and mesoporous material are defined as a porous material with pore diameters lower than 2 nm and between 2 and 50 nm, respectively [1, 2]. Various natural and synthetic porous materials such as MCM-41, SBA-15 and zeolite with high surface area, chemical inertness, high resistanceandsuitable channels have the ability of functionalization transition metal complexes. Functionalizing the metal complexes on porous materials created an easy separation of the solid antibacterial agent by simple filtration, and these materials can be reused multiple times without significant loss in activity, thereby decreasing cost [3].

2. Experimental Part

The preparation method of HY zeolite has been reported in the literature [3].

In the first step, 3-chloropropylmethoxysilane was reacted with 2-aminopyridine for 30 h under nitrogen atmosphere and dry toluene solvent. Then the resulting material was reacted with HY zeolite, refluxed for 24 h under nitrogen atmosphere. Finally, the solid product was filtered, dried at 100 ◦C for 24 h [4]. In the second step, 0.5 g of it was added to dry toluene and homogenized with ultrasonic. Then, Cu^{+2} solution was added to it and refluxed at 100 ◦C for 24 h under nitrogen atmosphere. In the final step, the product was filtered, washed and dried.

3. Results and discussion

HY@N-Cuwas successfully synthesized and characterized using FT-IR, XRD and SEM techniques.

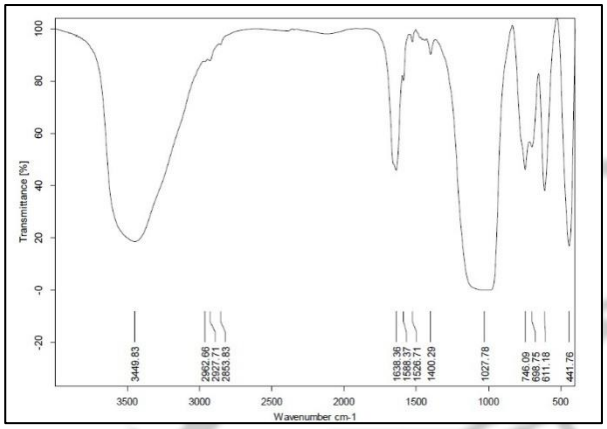

Figure 1. The FT-IR spectrum of HY@NH

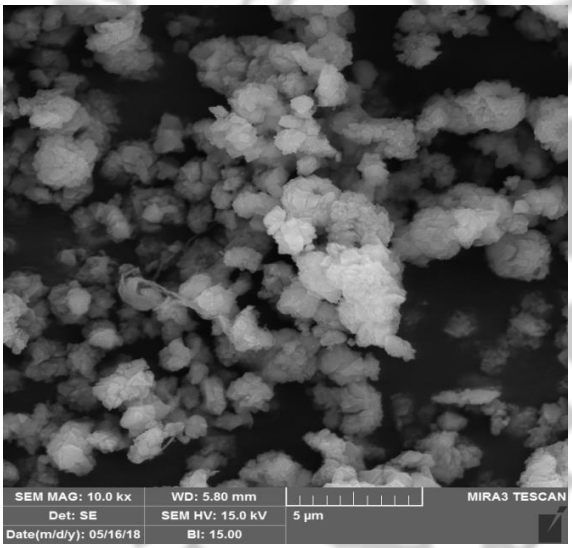

Figure 2. The SEM image of HY@N-Cu

In Fig.1 the FT-IR spectrumof HY@NHshowed an intense band about ca. 1028 cm^{-1} attributable to the asymmetric stretching of Al–O–Si chain of zeolite. The symmetric stretching and bending frequency bands of Al–O–Si framework of zeolite appear at ca.746 and 442 cm^{-1}, respectively.

In Fig.2 the SEM graph showed the morphology and structural features ofHY@N-Cu. In the case of pure HY zeolite, the particle size is around200 nm, this decreasing in size may be due to the functionalization process on the surface.

Fig .3 represents the X-raydiffract gram of HY@N-Cu. The results show that no changes were detected in the crystalline structure and morphology of zeolite during the immobilization procedures.

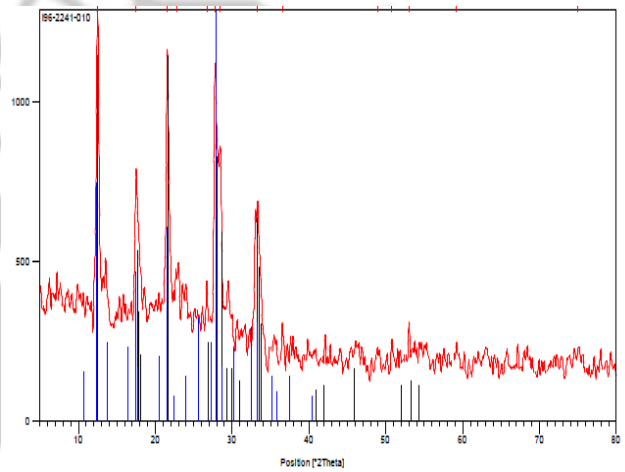

Figure 3. The XRD pattern of HY@N-Cu

200 nm, this decreasing in size may be due to the functionalization process on the surface.

Fig .3 represents the X-raydiffract gram of HY@N-Cu. The results show that no changes were detected in the crystalline structure and morphology of zeolite during the immobilization procedures.

4. Conclusions

The HY@N-Cu compound has been prepared and and characterized using FT-IR, XRD and SEM techniques.

Acknowledgments

Thanks are due to the Research Council of Arak University of Technology and Centerof Excellence in the Chemistry Department of Arak University of Technology for supporting of this work.

References

[1] A.F. Moreira, D.R. Dias, I.J. Correia, *Microporous Mesoporous Mater.* 236 (2016) 141-157.

[2] L. Wang, W. Ding, Y. Sun, *Mater. Res. Bull.* 83 (2016) 230-249.

[3] M. Zendehdel, M.A. Bodaghifard, H. Behyar, Z. Mortezaei, *Microporous Mesoporous Mater.* 266 (2018) 83-89.

[4] S. Rostamnia, H. Xin, *J. Mol. Liq.* 195 (2014) 30-34.

5th Iran International Zeolite Conference

University of Tabriz, Tabriz, Iran

26-27 August 2018

Synthesis and Characterization of Zeolite/Hydroxyapatite Nanocomposite, using in the Removal of Cr^{6+} from Aqueous Solution

A. Rezaei, M. Zendehdel*

Department of Chemistry, Faculty of Science, Arak University, Arak 38156-8- 8349, Iran

**Corresponding author: m-zendehdel@araku.ac.ir*

Abstract: Chromium is one of the most dangerous inorganic water pollutants with two oxidation states (Cr (VI) and Cr (IV)). Cr (VI) is more toxic and known to have cytotoxicity, mutagenicity and carcinogenicity. In this study, the removal behavior of a composite of zeolite with respect to Cr (VI) has been studied. The structural characteristics of Hydroxyapatite–Zeolite were investigated by SEM, FT-IR and XRD techniques. The impact of various operating parameters, including pH (5–11), concentrations of modified zeolite (0.5–5.0 g), initial concentration of Cr (VI) and contact time (10–360 min), was investigated on the removal of Cr (VI) from water through different experimental runs in the batch system. These results show that natural zeolites hold great potential to remove cationic heavy metal species from industrial wastewater.

Keywords: Zeolite; Hydroxyapatite; Removal Chromium (VI)

1. Introduction

Heavy metal contamination is an important problem because these elements have non degradable nature and accumulate in living organism resulting in heavy metal poisoning. The Cr(VI) state is of particular concern because of its toxicity. The mordenite has suitable mineralogical properties that enable them to be used for ion exchange processes. This includes total cation exchange capacity. More recently, much attention has focused on surface functionalization of nanostructured absorbentsby using glycine [1], chitosan [2,3], gum Arabic, glutaraldehyde, polyethylenimine, polymer, EDTA, aminogroups, 3-mercaptopropionic acid, citric acid, poly(acrylic acid), and humic acid. Several processes are utilized to eliminate dissolved heavy metal including precipitation, ion exchange, and electroanalysis, and reverse osmosis, ultrafiltration and phytoextraction. Among the processes, adsorption is easy to handle and has a good removal efficiency. However, the modified composite natural zeolite/HA was used as an adsorbent for the removal of Cr (VI) from aqueous solution. Natural zeolites are crystalline microporous aluminosilicates with very well defined structures that consist of a framework formed by tetrahedra of SiO_4 and AlO_4. Hydroxyapatite belongs to the apatites group with the formula $Ca_{10}(PO_4)_6(OH)_2$, have biocompatibility, anion-exchange properties, and great adsorption properties.

The adsorption of the Cr(VI) from an aqueous solution on HA/ZE was studied in this work as well as the effect of the pH and temperature on the

adsorption capacity, and the reversibility of the adsorption process was also investigated.

2. Experimental Part

The synthesis of pure CaHAp nanoparticles was carried out in aqueous medium using the hydrothermal method. Amount of potassium dihydrogen phosphate solution was mixed at stirring with calcium nitrate solution. The pH of the mixture was maintained at 11 by the addition of ammonium hydroxide solution (NH_4OH) under nitrogen gas and zeolite was added to solution. The resulting mixture was treated in an autoclave with temperature program.

3. Results and discussion

Fig. 1 shows the FTIR spectrum of the HA/ZE composite in the range 400–4000 cm^{-1}.

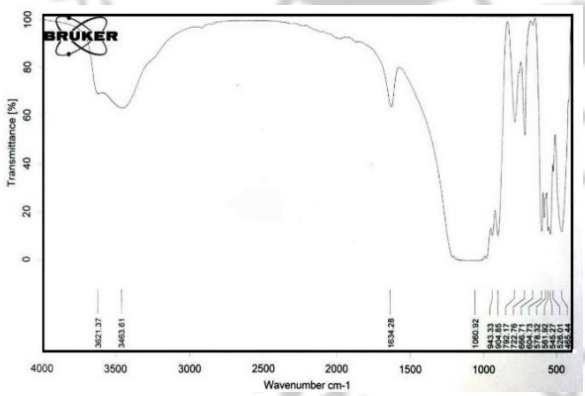

Figure 1. TheFT-IR spectrum of the HA/ ZE.

The X-ray diffractometer of HA/ZEin (Fig. 2) showed that the crystalline structures and a single phase of HAP with a hexagonal structure.

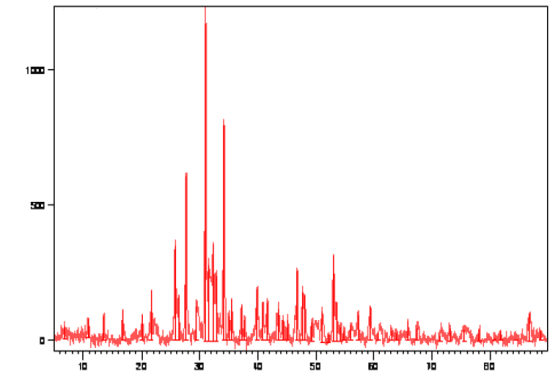

Figure 2. The XRD pattern of the HA/ ZE.

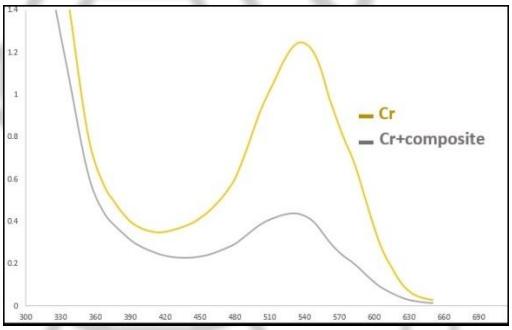

Figure 3. UV–visible spectra, the effect of composite in Cr solution.

The SEM image showed the morphology and structural features of HA/ZE nanocomposite (Fig. 4).

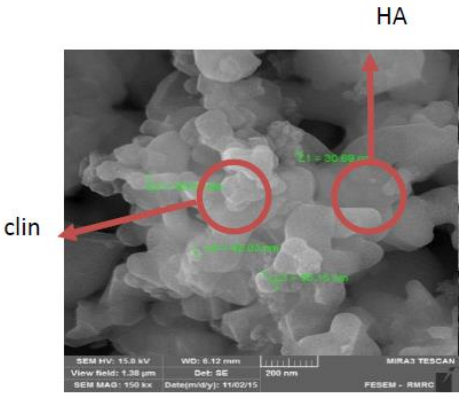

Figure 4. The SEM image of the HA/ZE.

4. Conclusions

The result shows that HA/ZE nanocomposite is an effective adsorbent for the removal of Cr (VI). Influence of various variables including solution pH, concentration of zeolite, and concentration of contaminant, and adsorption time on removal of chromium ion was evaluated. Also, the results from this study will be useful for the development of modified hydroxyapatite-based composite materials for various applications.

References

[1] Z.Z. Zhang, M.Y. Li, W. Chen, S.Z. Zhu, N.N. Liu, L.Y. Zhu, *Environ. Pollut*. 158 (2010) 514-519.

[2] S.J. Kang, K. Egashira, A. Yoshida, *Appl. Clay. Sci.* 13 (1998)117-135.

[3] M. Dakiky, M. Khamis, A. Manassra, M. Mer'eb, *Adv. Environ. Res.* 6 (2002) 533-540.

5th Iran International Zeolite Conference

University of Tabriz, Tabriz, Iran

26-27 August 2018

Synthesis and Characterization of Aluminium-free MFI-type Cobaltosilicates using Hydrothermal Method

A. Mokhtari[a]*, M. Khatamian[a]

a Department of Inorganic Chemistry, Faculty of Chemistry, University of Tabriz, Tabriz, Iran

**Corresponding author: Azmokhtari6302@gmail.com*

Abstract: MFI-type Cobaltosilicate zeolites with different Si/Co ratio were synthesized by hydrothermal method using silicic acid and sodium tetraborate decahydrate as starting materials. A highly crystalline MFI zeolite structure was formed under pH=13 in several days. The effect of several parameters including gel composition and pH on the crystallization of zeolites was systematically studied. Direct evidence of the incorporation of Co in the zeolite framework sites was observed by performing structure parameter refinements, and supported by data collected from other characterization techniques such as: X-ray diffraction (XRD), scanning electron microscopy (SEM), and Fourier transform infrared spectroscopy (FT-IR). The experimental results show that [Co]-MFI molecular sieves were successfully synthesized.

Keywords: Hydrothermal synthesis; Isomorphous substitution; Cobaltosilicate; MFI-zeolite

1. Introduction

Zeolites, crystalline microporous aluminosilicates, have been widely used as solid acid catalysts in the petrochemical industry and as sorbents in the field of water and wastewater treatment due to their large surface area and unique thermal, hydrothermal and chemical stability [1]. The synthesis of new micro- and mesoporous materials is interesting for both practical and fundamental reasons. The size distribution and topology of micropores in materials of similar compositions can be very different, depending on the method of synthesis [2]. Several transition metals have been substituted into crystalline silica or aluminophosphate frameworks to yield the corresponding metallosilicates or metalloaluminophosphate molecular sieves. Under controlled synthesis conditions, the metal can enter into the framework with the same coordination geometry as the parent element, which is tetrahedral coordination in these systems [3]. In our previous works, we have synthesized different MFI-type zeolites such as ferrisilicate [4], chromosilicate [5], borosilicate [6] and manganosilicate [7] with efficient and applicable methods. Therefor, in this work, we report the effect of gel composition and pH on the crystallization and morphology of MFI-type cobaltosilicate ([Co]-MFI) zeolites.

2. Experimental Part

[Co]-MFI zeolites with different Si/Co ratios were prepared in a non-stirred autoclave by hydrothermal

procedure using silicic acid (Merck), as a source of Si, Cobalt (III) nitrate (Merck), as the source of chromium, tetrapropylammonium bromide (TPABr, Merck) as template and sodium carbonate (Panreac, 99.8%). The pH of mixture was adjusted to the desired amount using diluted NaOH and crystallization was carried out at 160 °C. Finally, the products were calcined at 500 °C in air for 3 h and designated as Y[Co]-MFI(x), which x stands for pH value and Y=Co/Si (molar ratio).

3. Results and discussion

The XRD patterns of [Co]-MFI zeolites synthesized at different pH values are shown in Figure 1. It can be seen from XRD patterns that all samples show the characteristic peaks of the MFI structure in the range of 2θ = 7- 9° and 2θ = 23- 25°. No additional peaks due to the presence of crystalline impurities are observed in these patterns. On the other hand, it was revealed that the highly crystalline cobaltosilicate zeolites can be obtained at relatively high pH values (pH= 13) using the starting materials and synthesis conditions described here. However, there are variations in the intensities of some lines between these samples and MFI zeolite (which has been prepared in our laboratory). The XRD pattern of [Co]-MFI zeolites with different Co/Si ratio values are shown in Figure 2. With increasing the concentration of cobalt in the synthesis gel, the crystallinity of the final product was found to be decreased.

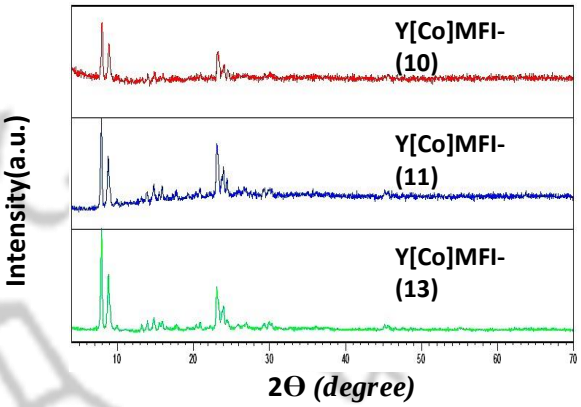

Figure 1. The XRD pattern of [B]-MFI zeolites in different pH in Y=0.03

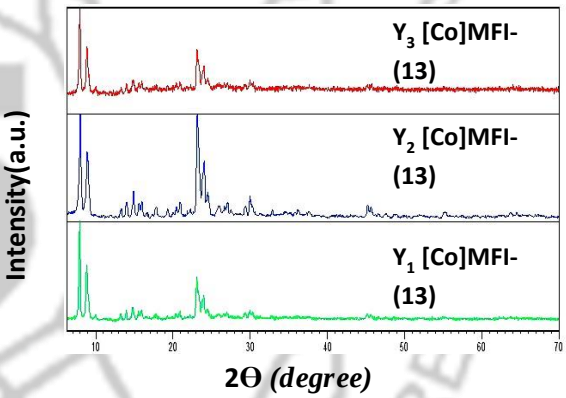

Figure 2. The XRD pattern of [B]-MFI zeolites with different Co/Si ratios Y_1=0.03, Y_2=0.05, Y_3=0.07

SEM was used to investigate the morphology of the samples. SEM images of [Co]-MFI sample after calcination in air appears cubic particle and its particle size ranges from 2 to 3 µm. The SEM image of the sample shows that the growth of crystal grains is well.

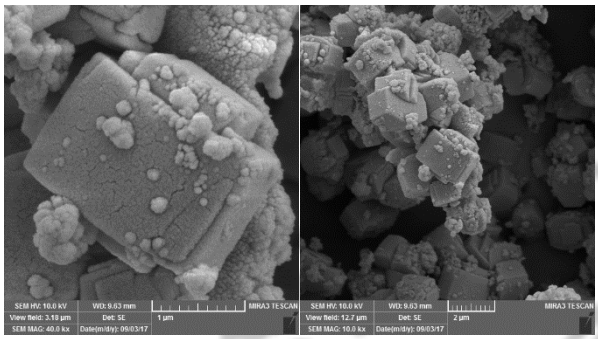

Figure 3. SEM images of [Co]-MFI(13)

4. Conclusions

The [Co]-MFI zeolites was synthesized by hydrothermal method at different pH values and different Co/Si ratios. In the synthesis of Y[Co]MFI zeolites, a pure MFI phase was obtained with a relatively low concentration of cobalt in the synthesis gel. For highest cobalt concentration, in the synthesis gel the final product was found to be impure. The SEM images proved the morphology and particle size of zeolites.

Acknowledgments

We would like to thank the University of Tabriz and Iranian Nanotechnology Initiative Council for the financial support of this project.

References

[1] P. Pal, J.K. Das, N. Das, S. Bandyopadhyay, *Ultrason. Sonochem.* 20 (2013) 314-321.

[2] S.A. Johnson, E.S. Brigham, P.J. Ollivier, T.E. Mallouk, *Chem. Mater.* 9 (1997) 2448–2458.

[3] A.M. Prakash, L. Kevan, *J. Am. Chem. Soc.* 120 (1998) 13148–13155.

[4] M. Khatamian, A.A. Khandar, M. Haghighi, M. Ghadiri, M. Darbandi, *Powder Technol.* 203 (2010) 503–509.

[5] M. Khatamian, M. Saket Oskoui, M. Darbandi, *Micropor. Mesopor. Mat.* 182 (2013) 50–61.

[6] M. Khatamian, A. Yavari, A. Akbarzadeh, E. Alizadeh, Materials Science & Engineering C, 78 (2017), 1212-1221

[7] Maasoumeh Khatamian, Sima Heidari, Mohammad Mahdi Najafpour, International Journal of Hydrogen Energy 42 (2017) 7938-7950.

5th Iran International Zeolite Conference

University of Tabriz, Tabriz, Iran

26-27 August 2018

Medical applications of zeolites

M. Moradi*[a], S. Javanmardi[b], M. Ashrafizadeh[c], A. Faramarzpour

[a] *Department of Pathobiology, Faculty of Veterinary Medicine, University of Tabriz, Tabriz, Iran.*
[b]*Department of Clinical Sciences, Faculty of Veterinary Medicine, University of Tabriz, Tabriz, Iran.*
[c]*Underraduated student of Veterinary Medicine, University of Tabriz, Tabriz, Iran*
**Corresponding author: ma.moradi@Tabrizu.ac.ir*

Abstract: Zeolites are porous tectosilicates which emanate from natural or are synthetic. The crystallization process is one of the methods that we can use to produce these important materials in the laboratory. The zeolites are agents that be applied in different fields and that is the reason that scientists call them as "magic stones". They have various uses such as catalysts and molecular screeners, separating different molecules, air purification and eliminating radioactive pollutions. The porous identity, ability for high absorption and ion exchange characteristics are appropriate features that cause the wide range use of zeolites. Zeolites are appropriate tools for protection of environment, eliminating and removing harmful agents from animal and human organisms, ameliorating the condition of nutrition, controlled drug delivery and separating biomolecules. In this review, we will report the important features of zeolites and their applications in the biotechnology and medicine, in according to the recent findings.

Key word: Zeolite, Medicine, Biotechnology, Drug Delivery

Introduction:

Zeolites are hydrated tectosilicates that are found in the form of minerals in the nature. These materials can be produced in the laboratory. The crystallization process of zeolites is performed by hydrothermal reaction. The zeolites can be used in industry and biomedicine and that is why the zeolites have been called "magic stones". The porous nature and ion exchange features are properties that cause the wide use of zeolites. The dimensions and the size of pore of zeolite are factors which regulate the rate of absorption by zeolites. Zeolites are used in the petrochemical industry as accelerators, as molecular screeners for segregating and sorting based on their dimensions, as absorbent for water and soil, for eliminating radioactive pollutions and for

absorbing the solar heat energy and hindering the waste of heat [1].

In this review, we will investigate the uses of zeolites in the medicine and biotechnology. These applications include living environment support (absorbing harmful materials from soil, water and air), detoxification of living organisms, uses in agriculture and veterinary medicine, biomolecules and cell types separation, drug delivery that are just a few of applications of these important materials.

1. Protection of Environment by Zeolites

The water and soil can be protected by applications of zeolites and air purification and radioactivity decontamination are other uses. As we mentioned, these uses are based on the high absorption and ion change feature of zeolites. For these uses, the most important zeolite that has been extensively used, is clinoptilolite; For instance, a surfactant (hexadecyl trimethylammonium) modified clinoptilolite and also pure clinoptilolite was applied for eliminating ammonium and nitrates from wastewater. Bentonite and goethite are zeolites that are used for soil purification [2].

2. The Applications of Zeolites in Organism Detoxification

Removing harmful agents from animal and human organisms can be performed by using zeolites. It has been proven that after exposing mice to the clinoptilolite, those disorders remarkably decreased [3].

3. Veterinary Medicine and Zeolites

Improving the morphology, function and microbial flora of digestive tract, delivery of important ions, elevating the nutrition condition, healing the immunity and detoxification of food are areas that the zeolites can be applied in the veterinary medicine.

4. Separating biomolecules and zeolites

The process of purification of proteins and detaching the components of cell such as proteins and nucleic acids can be performed by using zeolites. For instance, with moderate radical nitroxide exchange reactions, the movement of different proteins can be inhibited on the surface of zeolite L crystals [4].

5. Drug Delivery and Zeolites

The anti-inflammatory, anticancer (such as rapamycin) and antimicrobial drugs can be delivered by using zeolites. For instance, the clinoptilite has been suggested for oral delivery of aspirin in a pH-dependent manner [5].

Table 1: The applications of zeolite in different fields

Fields / Applications	Environmental protection	Construction	Agriculture	Medicine/Hygiene	Gas treatment
1	Water Decontamination	Concrete additive	Desodoration	Pharmaceuticals	Drying of gases
2	Heavy metal absorption	Water softening	Carrierforagrochemicals	Cosmetic products	Air decomposition
3			Bio Fuels (Biogas)	Detergents	Solvent recovery

Conclusion:

The zeolites have opened a new filed of research. Zeolites are natural or synthetic agents that are useful in the wide spectrum of applications such as biotechnology and medicine. In recent years, the promising improvements have been performed in the field of zeolites and in according to the various applications of these important materials in the different sciences, it hopes that the use rate of them increases during the next years.

References:

[1] D.I. Tchernev, *Rev. Mineral. Geochem.* 45 (2001) 589-617. REV MINERAL GEOCHEM

[2] A. Z. Molla, S. Ioannou, E. Mollas Skoufogianni, A. Dimirkou, *Bull. Environ. Contam. Toxicol.* 98 (2017) 347-350.

[3] Beltcheva, M., Metcheva, R., Popov, N. et al. *Biol. Trace Elem. Res.* 147 (2012) 180.

[4] M. Becker, L. De Cola and A. Studer, *Chem. Commun. (Camb.)* 47 (2011) 3392.

[5] M. Tondar, M. J. Parsa, Y. Yousefpour, A. M. Sharifi and S. V. Shetab-Boushehri, *Acta Chim. Slov.* 61 (2014) 688.

5th Iran International Zeolite Conference

University of Tabriz, Tabriz, Iran

26-27 August 2018

Synthesize, Evaluation of Antibacterial and Antibiofilm behavior of Nano Silver Chloride on *Acinetobacter baumannii*

Z. Akhgari[a], A.Tanomand[b]*

[a] *Microbiology Department, Islamic Azad University, Qom branch, Qom, Iran*

[b] *Microbiology Department, Maragheh Faculty of Medical Science, Maragheh University of Medical Sciences, Maragheh, Iran*

[*] *Corresponding author: Tanomanda@tbzmed.ac.ir*

Abstract: Due to the resistance of bacteria to antibiotics and usual antimicrobial agents, a lot of researches have done to find new types of effective antimicrobial agents. With development of Nanotechnology, Silver is being used increasingly against all gram negative bacteria and gram positive bacteria in the form of nanoparticles with high antimicrobial activity and low prices. The nano silver with approximate diameter of 20 nm from Pishtazan Inc. Mashad, Iran and 5 nm from the Department of Chemistry in Maragheh University were prepared. Its concentration was determined by spectroscopy method in University of Tabriz (Chemistry Department). Antimicrobial effects were determined by minimum Inhibitory Concentration (MIC) and Minimum Bactericidal Concentration (MBC) by micro-broth-dilution method, disc diffusion and well diffusion methods. The results of the MIC, MBC against *Acinetobacter baumannii* on average was 156/25 ppm, 312/5 ppm. Effect of silver nanoparticles on inhibiting the growth of *Acinetobacter Baumannii* and biofilm arising from it, in a standard form is examined.

Keywords: Silver nanoparticles, Acinetobacter baumannii, biofilm, MIC, MBC

1. Introduction

Acinetobacter Baumannii is an opportunistic pathogen bacterium and is one of the most important factors for nosocomial infection. These bacteria produce extracellular polysaccharide, which is known as biofilm. Because of high drug resistance in the bacteria, Nowaday the use of silver nanoparticles is also recommended to combat with bacteria. During this study, effect of silver nanoparticles on inhibiting the growth of *Acinetobacter Baumannii* and biofilm arising from it, in a standard form is examined [1].

2. Experimental Part

In this study, we determined the MIC and MBC silver nanoparticles for expected bacteria with broth dilution method. Also bacteria sensitivity was studied using disk diffusion and well diffusion method. Also biofilm tests and the effect of silver nanoparticles on biofilms of *Acinetobacter Baumannii* were performed using microtiter plate assay and fuchsin staining.

3. Results and discussion

Results demonstrated that colloidal silver nanoparticles can be prevented biofilm formation

of bacteria. [2]. The results of the MIC, MBC in bacteria (standard) on average was 156/25 ppm, 312/5 ppm. Also the results of disk diffusion and well diffusion methods showed that with increasing concentrations of silver nanoparticles, the diameter halo of lack of growth bacteria increases [3]. According to the results, whenever the concentration of silver nanoparticles was great and their size was small, the antibacterial effect will be better.

Figure 1. Effect of silver nanoparticles on *Acinetobacter baumanni* with well diffusion method.

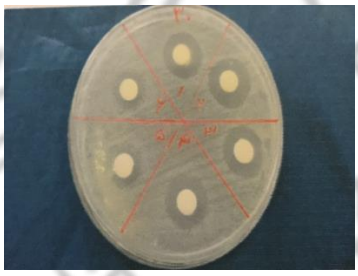

Figure 2. Effect of silver nanoparticles on *Acinetobacter baumanni* with disk diffusion method

4. Conclusions

Overall results showed that colloidal silver nanoparticles have antibacterial and antibiofilm properties on *Acinetobacter baumannii*.

References

[1] M. Niakan, S. Niakan, S. Hesaraki, M. R. Nejadmoghaddam, M. Moradi, M. Hanafiabdar, R. Allamezadeh, and M. Sabouri, 5 (2013) 8347.
[2] V. Ravishankar Rai, A. Jamuna Bai, A Méndez-Vilas A, editor. Mysore: Formatex. 2011.
[3] Pal, S., Tak, Y. K., & Song, J. M. 73 (2007) 1712-1720.

5th Iran International Zeolite Conference

University of Tabriz, Tabriz, Iran

26-27 August 2018

Synthesis of AgCl nanoparticles functionalized on IL based SBA-15 as an effieint nanocatalyst for antibacterial and antibiofilm behavior on *klebsiella pneumonia*

Z. Akhgari[a], A. Tanomand[b*]

[a] *Microbiology Department, Islamic Azad University, Qom branch, Qom, Iran*

[b] *Microbiology Department, Maragheh Faculty of Medical Sciences, Maragheh University of Medical Sciences, Maragheh, Iran*

[*] *Corresponding author: Tanomanda@tbzmed.ac.ir*

Abstract: Silver chloride nanoparticles functionalized on IL based SBA-15 was established to be efficient nanocatalyst for antibacterial and antibiofilm behavior on *klebsiella pnemonia*. Antimicrobial effects were determined by Minimum Inhibitory Concentration (MIC) and Minimum Bactericidal Concentration (MBC) by micro-broth-dilution method, disc diffusion and well diffusion methods. Effect of silver NPs on inhibiting the growth of *Klebsiella pneumonia* and biofilm arising from it, in a standard form is examined.

Keywords: *Klebsiella pneumoniae*, IL(SO_3)/AgCl@SBA-15, MIC and MBC, Biofilm

1. Introduction

Multi-drug resistance is a growing problem in the treatment of infectious diseases and the widespread use of broad-spectrum antibiotics has produced antibiotic resistance for many human bacterial pathogens. Advances in nanotechnology have open new horizons in nanomedicine, allowing the synthesis of nanoparticles (NPs) that can be assembled into complex architectures [1].

In most clinics, one of the major problems of antimicrobial resistance is occured in nosocomial pathogens leading to the increase of hospital costs [2]. Among the *Klebsiella pneumoniae* resistant isolates is shown most resistance to amoxicillin, cefixime and cephalothin antibiotics [2]. Because of high drug resistance in this group of bacteria, problems in the treatment of infections caused by these bacteria has been created [1-2]. The effects of silver NPs and its antimicrobial activity are attracted the special interest of researcher.

2. Experimental Part

Synthesis of SBA-15 was performed according to previous method which is described in elsewhere [3-4]. The as-synthesized IL(SO_3)/ SBA-15 was added to a 30 mL mixture of CTAB, imidazole and 1,2-oxathiolane 2,2-dioxide in the presence of dispersed SBA-15 (1 g) and allowed to stir for 1h reflux condition. Then, 0.1 gr of $AgNO_3$ and KCl was added to the mixture

and allowed to ultrasonic wave 2h and to obtain IL(SO_3)/AgCl@SBA-15 (Scheme 1).

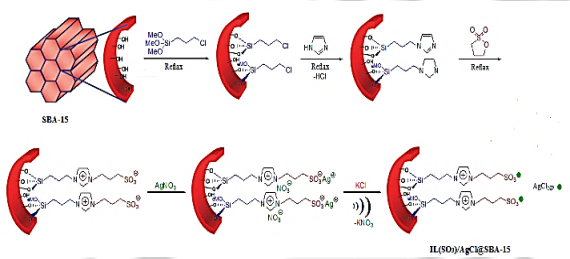

Scheme 1. Schematic illustration for the preparation of (IL(SO_3)/AgCl@SBA-15)

3. Results and discussion

In this research, the antimicrobial and anti-biofilm effect of AgCl loaded on SBA-15 were investigated on inhibit the growth of bacteria *Klebsiella pneumonia* [1]. For the purpose of determining the MIC and MBC of the catalyst for the desired bacteria, the broth dilution method was used. Also bacteria sensitivity was studied using disk diffusion and well diffusion method [2].

The crystallinity and purity of IL(SO_3)/AgCl@SBA-15 were checked by powder X-ray diffraction (PXRD) measurement. The results demonstrate that the peak positions matched well with that of the simulated diffraction pattern (Figure 1).

The results of disk diffusion and well diffusion method indicated that with increasing concentrations of catalyst, the diameter of lack growth bacterial zone increases. The results of the MIC, MBC against *Klebsiella pneumonia* on average was 1250 ppm and 2500 ppm. Results of biofilm created by the bacterium *Klebsiella pneumoniae* showed that with increasing concentrations of catalyst, effect of anti-biofilm increase. The result of broth dilution method showed low concentration catalyst has also the ability to inhibit the growth of *Klebsiella pneumonia*. Moreover, it is noteworthy that the drug resistance mechanism in bacteria does not have any interference on effect of AgCl loaded on IL-SBA-15.

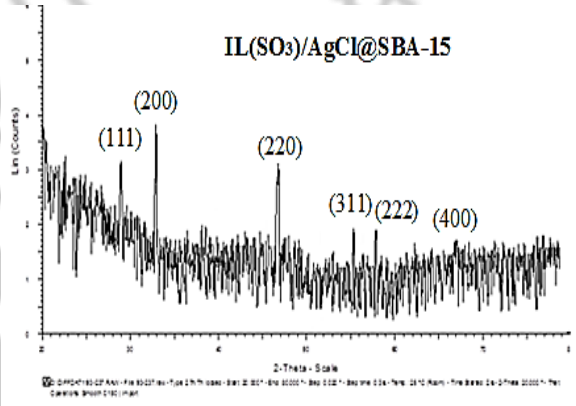

Figure 2. XRD template related to IL(SO_3)/AgCl@SBA-15

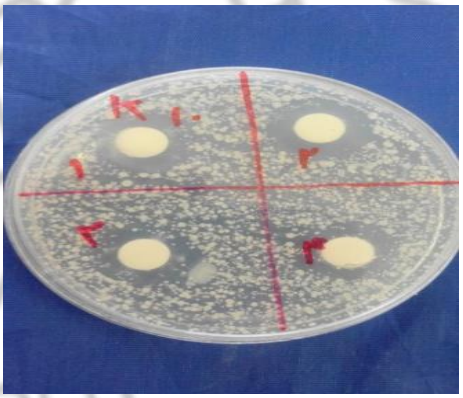

Figure 3. sensitive of *Klebsiella pneumoniae* to colloidal silver nanoparticles

4. Conclusions

Overall results showed that colloidal silver composite materials, antibacterial and antibiofilm properties are on *Klebsiella pneumoniae*.

References

[1] A. Kishen, Z. Shi, A. Shrestha, *Journal of Endodontics*, 12 (2008) 1515-1520.
[2] S. Kittler, C. Greulich, J. Diendorf, M. Koller, *Chem. Mater.*, 16 (2010) 4548-4554.
[3] S. Rostamnia, A. Hassankhani, H.G. Hossieni, B. Gholipour, H. Xin, *J. Mol. Catal. A: Chem.* 395 (2014) 463-469.
[4] S. Rostamnia, E. Doustkhah, *RSC Adv.* 4 (2014) 28238-28248.

5th Iran International Zeolite Conference

University of Tabriz, Tabriz, Iran

26-27 August 2018

Synthesis and Characterization of Zeolite and Ionic Liquid Hybrid Material

S. Ganji[a], S. khaghani nezhad[a], M. Zendehdel[a]*

[a] *Department of Chemistry, Faculty of Science, Arak University, Arak 38156-8- 8349; Iran*

**Email: m-zendehdel@araku.ac.ir*

Abstract: In this study ionic liquid functionalized on zeolite and characterized by some different method such as: FT-IR, XRD, SEM, EDX.

Key words: Inorganic-organic hybrid, Zeolite, Ionic liquid

1. Introduction

Recently, one of the most important material which uses in the catalytic reactions are Ionic liquids. The ionic liquid plays the dual role of solvent and acid catalyst. Also, a large volume of studies has been published describing the role of heterogeneous catalysis in organic reaction. Zeolite is a special type of ordered microporous support with unique and significant properties which development preparation of cleaner and efficient catalyst. [1-4].

2. Experimental Part

At first, 3-chloropropyltrimethoxysilan was reacted with an Ionic liquid (1-Methylimidazole), then the resulting material was introduced to HY zeolite and refluxed under nitrogen atmosphere. Finally, the solid product was filtered, drying at 100 ◦C for 24 h [5] and characterized.

3. Results and discussion

The FT-IR spectrum of Ionic liquid which introduced to/HY zeolite show an intense band about ca. 1016 cm^{-1} attribute to the asymmetric stretching of Al–O–Si chain of zeolite (Fig.1). The symmetric stretching and bending bands of Al–O–Si framework of zeolite appear at ca.748 and 438 cm^{-1}, respectively. The C-H and N-H vibration bands show in the 2800-3500 and 1500-1650 cm^{-1} regions.

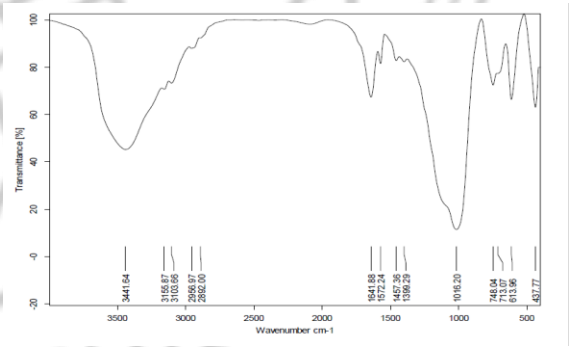

Figure 1. The FT-IR spectrum of Ionic liquid/HY zeolite

Fig .2 represented material the X-ray diffraction of Ionic liquid /HY zeolite hybrid, that confirmed no changes were detected in the crystalline structure and morphology of zeolite during the immobilization procedures.

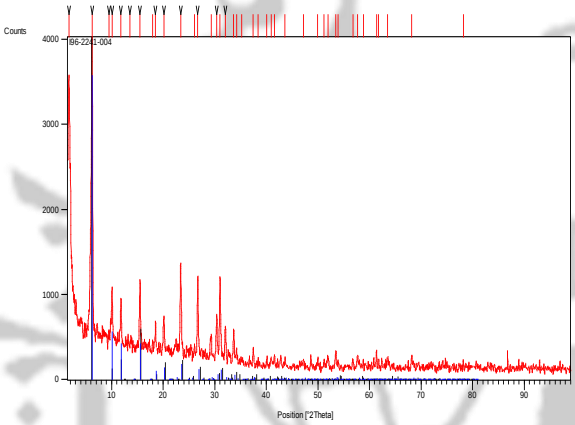

Figure 2. The XRD pattern of Ionic liquid /HY zeolite

We have seen the FESEM micrographs of Ionic liquid /HY zeolite hybrid (Fig. 3) with a wide range of sizes. It indicates the presence of well-defined HY zeolite crystals with some shadow of modification presence on its external surface. The particle sizes are around 160 nm and this decrease of size for modified zeolite is due to the complex formation on the support.

Fig .4 represented the EDAX of Ionic liquid /HY zeolite that shows the elemental percent on the surface it.

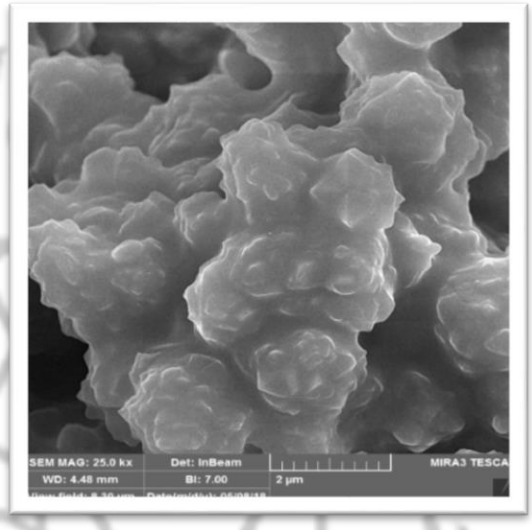

Fig 3. FESEM micrograph of Ionic liquid /HY zeolite

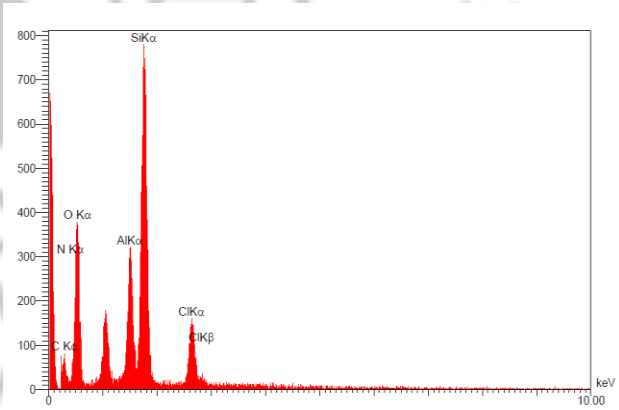

Fig .4 The EDAX of Ionic liquid /HY zeolite

4. Conclusions

In Summary, the result show that ionic liquid functionalizes on the surface of zeolite. The make a green research in this area for future environmentally friendly development of ionic liquid.

Acknowledgments

This paper was funded by Arak University therefore; acknowledge technical and financial support of Arak University.

References

[1] C. Yue, D. Fang, L. Liu, T. F. Yi, *J.mol.liq*, 163 (2011) 99-21.
[2] L. Yling, Gu. D., X. Xiaping, *Chinese journal of chem*. 27 (2009)1558-1562.
[3] M. K. Potdar, M. S. Rasalkar, M. M. Salunkhe, *J. Mol. Catl. A: Chem*. 235 (2005) 249-252.
[4] Q. Liu, M. H. A. Janssen, F. Van Rantwijk, R. A. Sheldon, *Green Chem*. 7 (2005) 39-42.
[5] S. Rostamnia, H. Xin, *J. Mol. Liq*. 2014 (195) 30-34.

5th Iran International Zeolite Conference

University of Tabriz, Tabriz, Iran

26-27 August 2018

Preparation and characterization of graphene oxide / Mn_3O_4 nanocomposite and study of its photocatalytic properties

M. Khatamian[a], M. Saket[a], H. Kakili[a*], N. Kamrani[a], S. Khadivi Derakhshan[a]

Departmentof Inorganic Chemistry, Faculty of Chemistry, University of Tabriz, Tabriz, Iran

**Corresponding author:Hiroo.k.mahabad@gmail.com*

Abstract: Hausmannite (Mn_3O_4) is one of the most stable manganese oxides which can be used as an efficient catalyst for oxidative degradation of organic dyes [1]. Graphene oxide / Mn_3O_4 nanocomposite was synthesized using a reflux method at a temperature of 80 ° C. To identify the structure and morphology, XRD pattern and SEM images of the sample were investigated. The XRD pattern shows the presence of nano sheets of graphene oxide besides the particles of Mn_3O_4 with a tetragonal crystalline form. The photocatalytic efficiency of the sample was evaluated using a Methyl Orange solution with a concentration of 20ppm. Removal percentage graph of methyl Orange shows the ability of the sample to degrade88.46% of the mentioned dye.

Keywords: Hausmannite, Nanocomposite, Graphene oxide.

1. Introduction

Metal oxide nanoparticles have better optical, magnetic and electrical properties than their bulk form [2]. Recently, manganese oxides have been widely used in science and technology due to their magnetic and electrical properties [3].

Mn_3O_4 is known as an effective and inexpensive catalyst to limit NO_x and CO emissions it can also be used as an electrode for lithium ion batteries and super capacitors [4].

Graphene-based nanocomposites are a new class of nanoparticles with a high potential for degradation of water contaminants. A variety of metal oxide nanoparticles, such as Cu_2O, SnO_2, MnO_x, TiO_2 and FeO_x can form composites with graphene. The photocatalytic performance of the mentioned nanocomposites is improved compared to the pure metal oxide nanoparticles. For example, a TiO_2-graphene nanocomposite has been reported to have a much higher photocatalytic activity and a greater stability in benzene degradation than the pure form of TiO nanoparticles[5].There are several methods for the synthesis of nanoparticles,such as Co-precipitation method[6]and the hydrothermal process[7]. In this paper, synthesis ofMn_3O_4 nanoparticle was carried out using a precipitation method.

2. Experimental Part

Graphene oxide was synthesized using the Homer method. Mn_3O_4 nanoparticles have been synthesized using the method of precipitation with ultrasound. For this purpose, the proper amounts of sodium hydroxide and cethyltherimethyl ammonium bromide and manganese(II)chloride 4 hydrate were dissolved in 100ml of deionized water under ultrasound. After 24 hours, the deposits were washed several times with deionized water.

They were calcined at 500°C after drying for 2 hours. To prepare the composite, reflux method was used in which 0.1g of graphene oxide and 0.1g of nanoparticles Mn_3O_4 were dissolved under ultrasound in deionized water and the reaction mixture was heated for 8 hours at a temperature of 80°C under reflux. Finally, the deposits were washed several times with deionized water and dried at 60°C.

To investigate and characterize the structure of the sample, a X-ray diffractometer device D500 Siemens was used. The morphology of the sample was studied using a scanning electron microscope (Central Laboratory of Tabriz University) Photocatalytic properties of the synthesized sample was investigated using a methyl orange solution irradiated with visible light LED lamp power 9W.

3. Results and discussion

Figure1 shows the XRD pattern of the nanocomposite of GO/Mn_3O_4.Small peak in 2θ of 9.299 is related to the GO. Also, the peaks in 2θs of 18.15,32.51,36.29and58.68 which assigned respectively to the crystalline planes of Mn_3O_4 with Miller indices of(101),(103),(211),(321), respectively can confirm the presence of Mn_3O_4 nanoparticles in the mentioned composite.

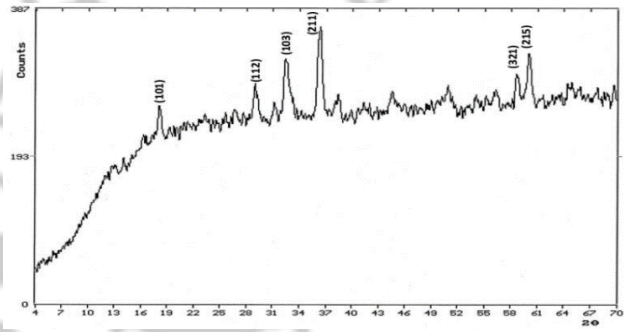

Figure 1 XRD pattern of nanocomposite (GO / Mn_3O_4)$_r$

The SEM image of nanocomposite (GO / Mn_3O_4)$_r$ is shown in Fig. 2. The formation of nanoparticles of Mn_3O_4 on graphene layers can be detected clearly, which is distributed unevenly on graphene layers. Layers of graphene oxide are also visible in the image.

Figure 3 shows the photocatalytic activity of (GO / Mn_3O_4)$_r$ nanoparticles in the removal of methyl orange dye at a concentration of 20ppm under visible light exposure for 5 hours. Graphene with a zero-energy gap acts as a conductor for electron transport during photocatalytic process andcan also enhance the effective adsorption of organic pollutants. The photocatalytic degradation efficiency of Mn_3O_4

nanoparticles can beimproved to 88.46 percent in the case of forming composite with garaphene oxide.

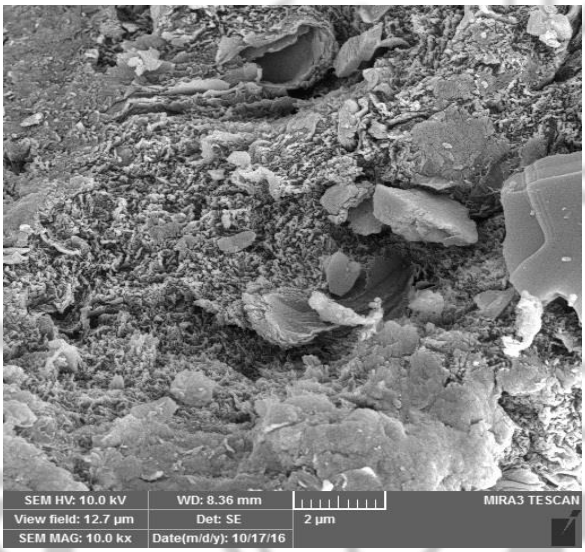

Figure 2.SEM image of nanocomposite (GO / Mn_3O_4)**r**

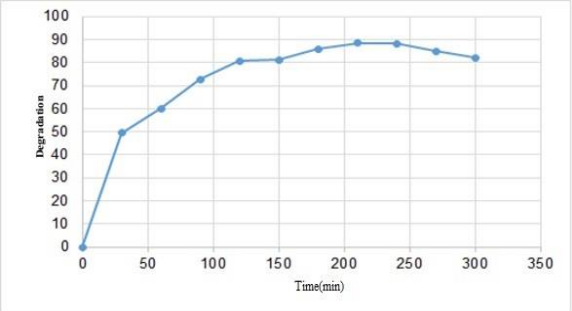

Figure 3. Photocatalytic activity of (GO/Mn_3O_4)**r** nanoparticles in removal of methyl orange

4. Conclusions

The nanocomposite of Mn_3O_4/GO was prepared using reflux method. The XRD pattern shows the dominant phase of Mn_3O_4according to its preferred crystalline plane with Miller indice of (211), as well as the presence of graphene oxide sheets. The SEM image of this nanocomposite confirms the presence of nanoparticles on the graphene oxide sheets. The results obtained from the study of photocatalytic properties show the degradation of 88.46% of methyl orange after 5 hours irradiation under visible light.

References

[1] M. Baldi, E. Finocchio, F. Milella, G. Busca, Appl. Catal. B. Environ. 16 (1998) 43-51.

[2] Y. Koseoglu, F.F. Yildiz, G.S. Alvarez, M. Toprak, M. Muhammed, B. Aktas, *Phys. Status Solidi (b)* 42 (2005) 1712.

[3] A. Olmos, R. Redon, G. Gattorno, M. Zamora, F. Leal, A. Osorio, J. Saniger, *J. Colloid Sci.* 291(2005) 175.

[4]B. Chen, G. Rao, S. Wang, Y. Lan, L. Pan, *Mater. Lett.* 154 (2015) 160-162.

[5] L. Duan, Z. Wang, Y. Hou, Z. Wang, G. Gao, W. Chen, P.J. Alvarez, *Water Res.* 103 (2016) 101-108.

[6] X. Zhang, Z. Xing, Y. Yu, Q. Li, K. Tang, T. Huang, Y. Zhu, Y. Qian, D. Chen, CrystEngComm 14 (2012) 1485-1489.

[7] J.-H. Park, B. Kwon, S.-G. Oh, Chem. Lett. 41 (2012) 1317-1318

5th Iran International Zeolite Conference

University of Tabriz, Tabriz, Iran

26-27 August 2018

Preparation and characterization of SAPO-34 zeolite nanocatalysts using diethyl amine (as template)

M. Ghadiri[a*], K. Mirza[a], M. Haghighi[b], A. Rahmati[a], S. Abbaspour[c]

[a]*Chemical Engineering Department, Urmia University of Technology, P.O. Box 57155-419, Urmia, Iran.*

[b]*Department of Chemical engineering, Faculty of engineering, Soran University, Soran, Erbil, Iraq*

[c]*Chemical Engineering Department, Sahand University of Technology, P.O. Box 51335-1996, Sahand New Town, Tabriz, Iran.*

[d]*Faculty of Medicine, Ilam University of Medical Sciences, Ilam, Iran.*

Abstract: In this study SAPO-34 zeolite nanocatalysts were synthesized successfully from silicic acid and using aluminium chloride as Si and Al sources, respectively via hydrothermal procedure, at different pH and hydrothermal temperatures, in the presence of diethyl amine (DEA) as a template. Effect of different parameters like pH and hydrothermal temperatures were investigated. Prepared samples have been characterized by XRD, TEM, EDAX and FTIR analysis. FTIR spectra confirm the production of ZSM-5 type SAPO-34 zeolite. The TEM images confirm the particle size of the samples in the range of 7–20 nm. XRD patterns showed middle alkali precursor and 180 °C hydrothermal temperature lead to production crystalline phase of SAPO-34 material.

Keywords: Zeolite, SAPO-34, Diethyl amine, ZSM-5, Aluminium chloride

1. Introduction

Silicoaluminophosphate (SAPO-n) molecular sieves such as SAPO-34, as acidic catalyst with Chabazite framework, have been widely used in many chemical processes such as methanol to olefins (MTO). These catalysts have cages with 8 membered rings and size of 0.43 – 0.50 nm, high thermal stability, moderate acidity and shape selectivity [1]. SAPO-34 is produced with Si incorporation to aluminophosphate (AlPO4-n) framework that leads to the formation of Brønsted acidic sites and catalytic property [2]. Therefore, the template plays effective role in the synthesis of SAPO-34. These materials were able to act as the space filling, governing the distribution of Si in the framework, charge compensating and structure-directing agent towards a Chabazite structure. There are a number of studies reported on investigation of effect of template type on SAPO-34 properties such as particle size, morphology and crystallinity. It was found that the physicochemical

properties of SAPO-34 changes in the presence of different templates [3].

The most commonly used template for the crystallization of SAPO-34 zeolites is TEAOH, because catalyst synthesized by TEAOH showed good catalytic performance in the industrial processes. However, its relatively high cost may be a serious obstacle for industrial applications. According to previous reports, DEA with less cost can produce SAPO-34 catalyst with high crystallinity and purity [4].

In the present paper we have demonstrated the hydrothermally synthesis of SAPO-34 catalyst using DEA as a template, in the presence of aluminum chloride as Al source. The physicochemical properties of the synthesized samples were assessed by different characterization techniques including X-ray diffraction (XRD), transmission electron microscope (TEM) and Fourier transform infrared (FT-IR) spectroscopy.

2. Materials and Methods

2.1 Materials

Fumed silica (SiO_2, Aldrich, 100%), phosphoric acid (H_3PO_4, Merck, 85%) and aluminum chloride ($AlCl_3.6H_2O$, Fluka, 99%) were used as Si, P and Al sources, respectively. Diethyl amine (DEA, Aldrich, 99%) was used as structure directing agent.

2.2 Catalyst Preparation and Procedures

Samples were synthesized based on the hydrothermal method. The molar ratio of the synthesis gel of samples were $1Al_2O_3:1P_2O_5:0.6SiO_2:9DEA:110H_2O$. For preparation, in the stage (a) aluminum chloride was added to deionized water. After mixing for 50 min, specific amount of H_3PO_4 was added dropwise to mixture. Then, fumed silica was added and stirred until homogeneous mixture was obtained. In the next step, DEA was slowly added to precursor mixture and kept at room temperature for 3h with stirring. According to (b) stage, the precursor solution was transferred into a stainless steel autoclave where it was heated at 200°C. In (c) stage, the resulting solids was centrifuged and washed three times with deionized water and then dried at 110°C for 12 h. The organic template and the water molecules trapped within the pores of samples were removed by calcination at 550°C.

2.3 Catalyst Characterization Techniques

The crystallographic properties of samples such as crystal phases and crystallite size were analysed by X-ray diffraction technique. XRD patterns were recorded on a Bruker D8 advance diffractometer with Cu Kα radiation (λ = 1.54178Å). The surface functional groups of synthesized catalysts were measured using FTIR spectroscopy. FTIR spectra of the samples was recorded in the range of 380–4000 cm^{-1} by UNICAM 4600 instrument. TEM studies, combined with EDAX were carried out on a 208F 100KW Philips instrument.

3. Results and discussion

3.1 XRD Analysis

Figure 1 shows the XRD patterns of synthesized samples with different pH of initial gel. As shown in figure 1 (a), it is clear that the acidic precursor mixture prevents SAPO-34 crystallization, because hydrolysis of aluminum chloride leads to produce the hydrochloric acid (HCl). The samples perpared at alkali initial gel have the complete structure of chabazite without any impurity (JCPDS: 01-087-1527, Rhombohedral) as indicated by peaks position at 2θ = 9.8, 12.9, 15.9, 17.7, 20.6, 24.9, 25.9, 30.6, 31.08° [5]. The results indicated that higher pH range of 9-10 cause to neutralize the hydrochloric acid and formation of SAPO-34 structure.

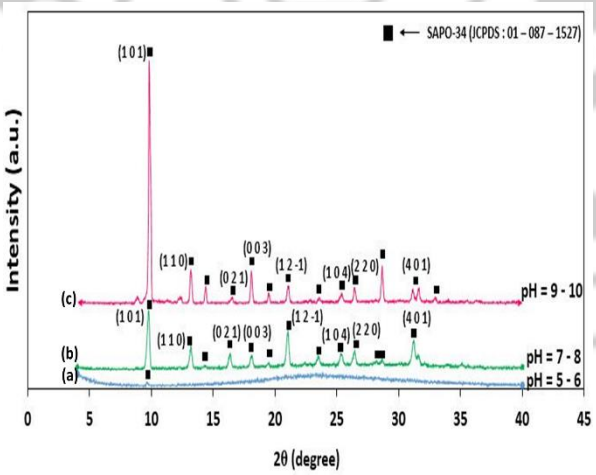

Figure 1. XRD patterns of samples obtained from different pH of initial gel.

Figure 2 clearly shows that the crystallization of SAPO-34 was completed at 180 °C, in comparison to the X-ray patterns of the sample prepared at 200 °C. The samples obtained in the lower temperatures (150 °C) were amorphous. Researches have shown that high temperatures accelerate nucleation and crystallization rates thus favored its formation [6].

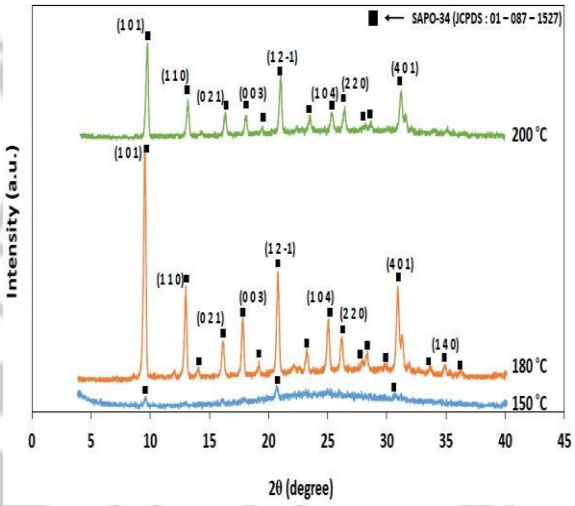

Figure 2. XRD patterns of samples obtained from different hydrothermal temparatures.

3.2 FT-IR Analysis

FTIR spectra of nanostructured SAPO-34 catalysts compared with standard sample is shown in Figure 3. The absorption peak at wavenumber of 466.84 cm^{-1} can be assigned to SiO_4 and the peak at 630.28 cm^{-1} can be attributed to the D6-ring formation of SAPO-34 structure. Presence of these peaks is according to structure of SAPO-34 crystals which have been confirmed by XRD. The band at 1079.24 cm^{-1}, well documented in the literature, was assigned to the asymmetric stretch vibration of O-P-O. The absorption

peaks at 2492.47 and 2949.57 cm^{-1} can be corresponded to physical adsorption of CO_2 from the surrounding. Moreover, the peak at 1654.23 cm^{-1} attributes the vibration of hydroxyl groups from adsorbed water (physical adsorption) on sample. In addition, the absorption bound at 3370.98 cm^{-1} showed stretching vibration of hydroxyl group, which are assigned to Si-OH–Al groups [7]. Existence of hydroxyl groups on samples surface indicates the acid sites and catalytic properties.

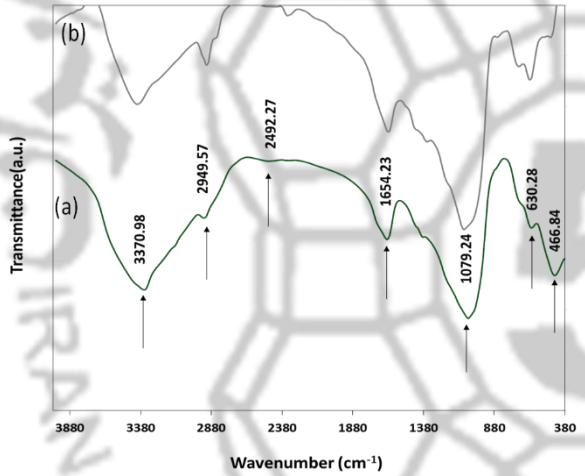

Figure 3. FT-IR analysis of (a) nanostructured SAPO-34 catalysts compared with (b) standard sample.

3.3 TEM Analysis

The TEM images of the SAPO-34 catalysts are shown in Fig. 4. It can be observed that all of these structures are the same and size distribution of synthesized SAPO-34 ranged from 7 to 20 nm.

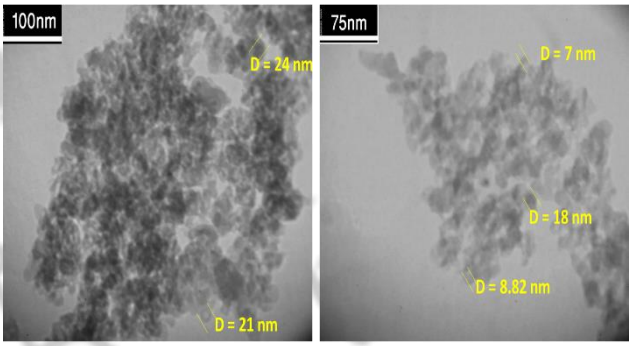

Figure 4. TEM images of SAPO-34 sample.

4. Conclusions

It was shown that the DEA template has a significant effect on the physiochemical characteristics of the synthesized samples. XRD patterns showed low amount of template and acidic condition prohibits the formation of CHA structure. Also, crystal size and crystallinity of SAPO-34 catalyst increases by increasing hydrothermal time.

Acknowledgments

The authors gratefully acknowledge Urmia University of Technology and Sahand University of Technology for financial support.

References

[1] S. Aghamohammadi, M. Haghighi, M. Charghand, *Mater. Res. Bull* 50 (2014) 462-475.

[2] T. Álvaro-Muñoz, C. Márquez-Álvarez, E. Sastre, *Catal. Today*, 213 (2013) 219-225.

[3] T. Álvaro-Muñoz, C. Márquez-Álvarez, E. Sastre, *Catal. Today* 179 (2012) 27-34.

[4] Kh. Mirza, M. Ghadiri, M. Haghighi, A. Afghan, *Microporous Mesoporous Mater.* 260 (2018) 155-165.

[5] M. Charghand, M. Haghighi, S. Saedy, S. Aghamohammadi, Adv. *Powder Technol.* 25 (*2014)* 1728–1736.

[6] H. Feng, C. Li, H. Shan, *Appl. Clay Sci*. 42 (2009) 439-445.

[7] S. Aghamohammadi, M. Haghighi, *Chem. Eng. J*, 264 (2015) 359-375.

5th Iran International Zeolite Conference

University of Tabriz, Tabriz, Iran

26-27 August 2018

Performance of natural zeolite for removal of lead: A review

F. Zare Pakzad[a], M. H. Sarrafzadeh[b], B. Divband[c]

[a]*UNESCO chair on water reuse, School of chemical engineering, Collage of chemical engineering, University of Tehran, Tehran, Iran*

[b] *UNESCO chair on water reuse, School of chemical engineering, Collage of chemical engineering, University of Tehran, Tehran, Iran*

[c] *Department of Inorganic Chemistry, Faculty of Chemistry, University of Tabriz, Tabriz, Iran*

faranak.pakzad@ut.ac.ir

Abstract: The presence of heavy metals in industrial wastewater, because of their capability to aggregation has many health risks to human beings. Lead metal is placed in a category of heavy metals that has harmful effects on human health, thus it is necessary to be removed from water sources and industrial effluents. Among various methods of removing cations from wastewater, adsorption by zeolites has many advantages over conventional methods. Due to the abundance of natural zeolites and their low cost, ionic exchange by natural zeolites is a more appropriate method and even in some cases, zeolites can be recovered. In this review, the adsorption of lead ions from aqueous solutions with cilinoptilolite (Iranian natural zeolite) and modified sample of this zeolite was studied. The removal efficiency of lead was increased in treated mode.

Keywords: Natural Zeolite; Cilinoptilolite**;** lead removal; surface modification;

1 Introduction

Industrial wastewater is one of the most important sources of environmental pollution that is mainly related to tannery, textile, metal mixing and melting industries, metal industries and etc [1].

Heavy metals do not have toxic effect in element mode. They can be dangerous where as a cation they are connected to a chain of carbon atoms.

Lead has high toxicity and its proximity damages the nervous system, kidneys and etc. The main sources of lead generation are greenhouse gas emissions, lead melting, gasoline and coal burning, mines, electronics, metallurgy and alloy and steel production. Chemical precipitation, oxidation, ultrafiltration, reverse osmosis, adsorption on active carbon and reverse ion exchange are the main

techniques for treatment of contaminated wastewater containing heavy metals. Adsorption with several advantages over other methods such as low cost, flexibility and design simplicity, easy operation, non-susceptibility to toxic contaminants and the lack of secondary production and harmful substances is a good method to treat wastewater and remove heavy metals. Zeolites are hydrated aluminosilicate crystals that contain cations of alkaline and alkaline earth metals. They are characterized by cation exchange and having a reversible capability to adsorb and desorb of water without causing major changes in their molecular structure. Among the natural zeolites, cilinoptilolite has been selected for its greater selectivity properties with cations, high ion exchanging capacity, resistance to environmental conditions and more abundance [2].

2 Removal of lead from wastewater via adsorption

Zeolites exhibit high selectivity for removing various types of heavy metals and are considered suitable for the removal of precious and semi-precious metals as well as the heavy metals from industrial and processing wastewaters [3].

In 2014, Afshari et al. [1] investigated the capability of the modified cilinoptilolite for the removal of lead from synthetic metal wastes. They modified the cilinoptilolite with Fe_3O_4 and TiO_2 nanoparticles and studied the effect of several parameters including pH, temperature, and the amount of adsorbent etc. on the removal efficiency. Their results revealed that the modified cilinoptilolite has high capability in lead removal where the maximum efficiency was 92% at pH=4 and T=313K.

In 2013, Saadani et al [2] in another work studied the adsorption isotherm and kinetics of lead from waste latex with natural zeolites. The modified zeolite with hexadecyl trimethyl ammonium bromide possessed more potential for the removal of lead from waste latex compared to natural zeolite.

In 2018, Javanmardi et al [4] studied the performance of natural zeolite (cilinoptilolite) in lead removal from Aqueous solutions and definition of kinetics and isotherm adsorption. Different pH, particle contact time and concentration of adsorbents have applied to the experiments and optimal results reported at pH equals 8, concentration adsorbent equals 5 [g/Lit] with 45 minutes of particle contact time. Finally, the results showed that the best removal efficiency was 89.6%.

3 Summary and Conclusions

Most industrial wastewaters contain heavy metals that are harmful for human beings and should be removed. There is various treatment methods for wastewater in which adsorption by zeolites gave more promising results. The control of contaminants of natural zeolites depends primarily on their ion-exchange capabilities. Natural zeolites like cilinoptilolite showed limited capability in metal

removal from wastewater; hence, modifying its surface improved the removal efficiency significantly

4. References

[1] N. Afshari, M. Nikazar, V. Kiarostami, *JARC*, 3 (2014) 75-86

[2] M. Saadani, M. Gholami, S. K. Ghadiri, E. Shojaee, E. A. Mehrizi, *J. Health Syst. Res. 5* (2013) 1094-1107.

[3] S. Kesraoui-Ouki, C. R. Cheeseman, R. Perry, *J. Chem. Biotechnol.* 59 (1994) 121-126.

[4] P. Javanmardi, A. Takdastan, R. Jalilzadeh yengejeh, *Journal of water and wastewater*, 29 (2018) 108-114.

5th Iran International Zeolite Conference

University of Tabriz, Tabriz, Iran

26-27 August 2018

HFIP/SBA-15 as a Metal Free Catalyst for Synthesis of Rhodanines

H. Mohtasham, S. Rostamnia*

Organic and Nano Group (ONG), Department of Chemistry, Faculty of Science, University of Maragheh, PO BOX 55181-83111, Maragheh, Iran.

**Corresponding author: srostamnia@gmail.com*

Abstract: Hexafluoroisopropanol dispersed catalytically amount of SBA-15 (HFIP/SBA-15) with organic substrate was found to be an efficient, ultra-fast and waste-free approach for the synthesis of the biologically and pharmaceutically interesting alkyl rhodanines. The advantages of the present method are low catalyst loading, simple procedure, waste-free and direct synthetic entry to excellent yield of rhodanines, high reusability of the catalyst, and short reaction time. Also, the reaction can be performed without activation and modification of the substrates under the neutral conditions. The solid SBA-15 and HFIP could be recovered and reused for recycling.

Keywords: Fluorinated alcohol; Hexafluoroisopropanol; SBA-15; Thioxo-thiophenecarboxylate

1. Introduction

The strategy of using unfunctionalized SBA-15 as catalyst, which has advantage of porous mesochannels as nanoreactor, is typically easier than functionalization or modification of SBA-15 to RX@SBA-15 while it needs fewer synthetic steps [1]. On the other hand, fluorinated alcohols (RfOH) demonstrate their unique properties as solvents/co-solvents or additives in the organic synthesis [2-3].

Following to our recent success in applying the TFE/SBA-15 nanoreactor in the imidazole preparation [1] an active and recyclable HFIP medium (1,1,1,3,3,3-hexafluoro-2-propanol or hexafluoroisopropanol) catalyst was applied in the present research for synthesis of alkyl rhodanines under mild reaction conditions. While this approach showed reusability for both HFIP and SBA-15, it minimized the wastes and side products.

2. Experimental Part

In this work, SBA-15 nanoreactor was synthesized by the procedure reported by Zhao et al. [3]. Schematic representation of the synthetic procedure for SBA-15 and HFIP/SBA-15 adduct as a combined catalyst was shown in Fig. 1.

3. Results and discussion

The SEM and TEM images as morphological and channels study of SBA-15 mesoporous material are presented in the same figure 2.

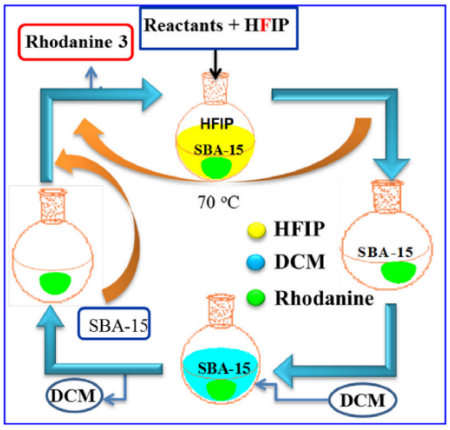

Figure 1. Schematic representation of the SBA-15 and HFIP recycling.

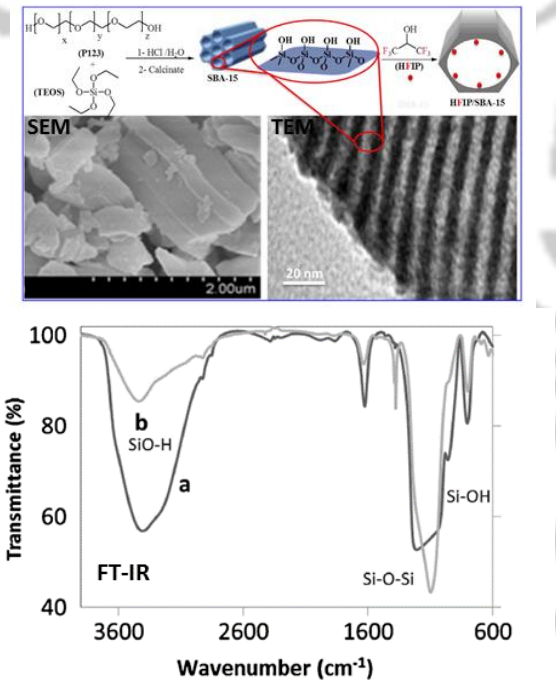

Figure 2. Schematic representation of the synthetic procedure for SBA-15 mesoporous and its SEM and TEM images and FT-IR [a) newly prepared; b) used 10 times] spectra of SBA-15.

Table 1. Optimization of reaction conditions for the synthesis of rhodanine.[a]

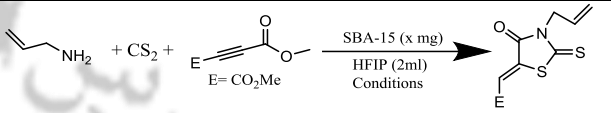

Entry	SBA-15 (mg)	Solvent	Time (min)	Temp. (ºC)	Yield (%)[b]
1	10	THF	5	r.t.	24
2	10	CyHex[b]	10	r.t.	23
3	20	CyHex[b]	5	r.t.	31
4	10	H_2O	5	r.t.	26
5	10	EtOH	5	r.t.	33
6	10	TFE	5	r.t.	71
7	10	TFE	10	r.t.	88
8	10	^{i}PrOH	5	r.t.	37
9	10	^{i}PrOH	10	r.t.	45
10	10	HFIP	5	r.t.	73
11	10	HFIP	10	r.t.	95
12	10	HFIP	10	40	94
13	15	HFIP	10	r.t.	94
14	20	HFIP	10	r.t.	93
15	10	HFIP	15	r.t.	93

[a] Reaction condition: allyamine (1 mmol), CS_2 (1 mmol), and DMAD (1 mmol) was added SBA-15 in 2 ml solvent.
[b] Cyclohexane.

In the FT-IR spectrum of SBA-15, the bands from 807 and 1100 cm^{-1} are assigned to the vibrations of (Si–O–Si) bond, and the band at about 960 cm^{-1} is assigned of (Si–OH) bond and the SiO–H groups are appeared by the very broad IR absorption band in the 3100–3700 cm^{-1} region (Fig. 2).

In order to investigate the catalytic activity and application of SBA-15 (mesochannels of SBA-15 as reaction vessel or reactor in nano-scale) in the multicomponent synthesis of rhodanine, we examined

its efficiency in the model reaction. Due to the fact that the solvent may play an important role in this process, different solvents were screened. The model reaction was examined in cyclohexane, EtOH, TFE, ^{i}PrOH, H_2O, and HFIP using SBA-15 (Table 1).

In this condition, the nanochannels of the SBA-15 provide a synergistic means to input the reactants and also drive out the products for next recycles.

4. Conclusions

In conclusion, an efficient protocol for the one step preparation of alkyl rhodanines from the three-component condensation reaction of amines, carbon disulfide, and electron deficient acetylenes using a reusable HFIP/SBA-15 adduct was described. The reactions were carried out under mild condition with short reaction time and facile work-up. Fluorinated alcohol-mediated procedure, also produced the corresponding products in good yields without any CS_2 waste. The SBA-15 (also HFIP) could be successfully recovered and reused at least for ten runs.

References

[1] S. Rostamnia, A. Zabardasti, *J. Fluorine Chem.* 144 (2012) 69-72.

[2] L. Eberson, M.P. Hartshorn, O. Persson, F. Radner, *Chem. Commun.* (1996) 2105-2112.

[3] For the synthesis of high surface area SBA-15 see: D. Zhao, J. Feng, Q. Huo, N. Melosh, G.H. Fredrickson, B.F. Chmelka, G.D. Stucky, *Science,* 279 (1998) 548-552.

5th Iran International Zeolite Conference

University of Tabriz, Tabriz, Iran

26-27 August 2018

Production of low cost and effective porous adsorbent from Iranian kaolin by sonication for recovery of wastewater contaminated by cationic dye

M. Foroughi[a], S. Hamedgolzar[a], A. Salem[a]*

[a] *Chemical Engineering Department, Faculty of Chemical Engineering, Sahand University of Technology, Tabriz, Iran*

**Corresponding author: salem@sut.ac.ir*

Abstract: The discharge of industrial wastewaters contaminated by cationic dyes caused to serious environmental problem for soil, surface and ground water. The present study was aimed to produce low cost porous adsorbent from Iranian kaolins which contains high level of quartz. In the first step, the two processed kaolins were mixed with different content of sodium hydroxide and treated by heating at 700 °C. Secondly, the obtained materials was quenched into the water to prepared porous adsorbents with sonication. The removal efficiency of produced adsorbents is fundamentally depends on raw material composition and sodium hydroxide content. The presence of illite and pyrophillite in kaolin cause to decrease the sodium hydroxide content and achieve an appropriate amorphous adsorbent whilst, the ultrasound- assisted technique should be applied to provide a suitable adsorbent when the kaolinite is the predominant phase in clay. Moreover, the alkali ratio should be increased to 2.3. The employed technique can be easily applied to produce an effective adsorbent for removal of cationic dye from textile wastewaters.

Keywords: Kaolin; Porous adsorbent; Cationic dye; Sonication; Wastewater.

1. Introduction

Among the several pollutants of soil, surface and ground water, the dyes are well known as priority sources of pollutions even at low level of content. In recent years, several physico-chemical treatments have been proposed to produce effective adsorbents for removal of dyes from wastewater of textile plants. However, there is an increase interest for fabrication of low cost and effective adsorbents that retain the toxic species [1]. The aim of present study is to produce an effective amorphous adsorbent from Iranian kaolins for cationic dye removal. The relationship existing between the sonication and dye removal efficiency can help to identify the microstructure of adsorbent which is the most promising for dye removal from wastewaters [2, 3].

2. Experimental Part

Two types of processed Iranian kaolins were selected and named as KH and ZN. The mentioned materials were mixed with sodium hydroxide in which the alkali

ratio was changed from 1.3 to 2.3 and then calcined at 700 °C for 2 h. The heat treated materials were quenched in water in normal and ultrasound-assisted conditions. The obtained suspensions were filtrated and washed with distilled water for several times. The resultant powders were dried at 100 °C for 24 h and used as the adsorbents for the removal of cationic dye, methylene blue, from wastewater. Batch adsorption studies were conducted by addition of 10 mg of adsorbents into 20 ml dye solution. The dye concentration analysis of centrifuged solution was immediately measured with UV-vis spectrophotometer (Jenway, 6705, UK). The produced powders were characterized by X-ray diffraction (XRD; Model D-5000, Siemens, Germany) with mono-chromated CuKα radiation. The morphology and size of the powders were observed by scanning electron microscopy (SEM; Model 440I EOL, UK).

3. Results and discussion

The kaolinite, illite and pyrophillite are the predominated clay minerals obtained in KH while ZN contains kaolinite and calcite was found as impurity. Both of used raw materials contain high level of quartz which prevents to produce an effective adsorption. Fig. 1 shows the adsorption efficiency of dye as a function of alkali ratio. With the increase in alkali ratio from 1.3 to 2.0 the dye adsorption increased slowly in which the complete removal of dye was achieved by adsorbent produced by KH. The quantity of dye removed from aqueous solution by adsorbent fabricated from KH is higher than that produced by ZN. Also, it is possible to completely remove dye by preparation of adsorbent with sonication in which ZN is used as starting material.

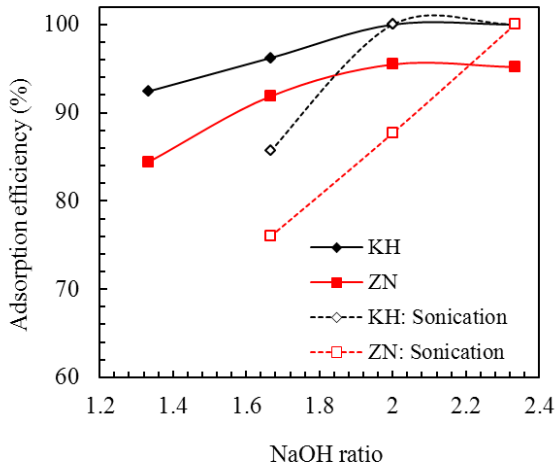

Figure 1. Dye removal as a function of alkali ratio.

Fig. 2 shows the XRD patterns of fabricated adsorbents produced in optimal conditions. Both of powders were identified as amorphous phase in which quartz remained partially unreacted as a peak appeared at diffraction angle of 26.8°. Meanwhile, the XRD patterns reveal other phases than quartz as hydrosodalite.

The flaky pieces of clay minerals broke easily under the vigorous stirring in the alkali-etching process, leading to the generation of small fragments as observed in Fig. 3. After alkali treatment, the kaolinite layers have randomly arranged pores, leading to further increase in

surface area. ZN seems to save the random structure and the particles undergo little change in shape after leaching but the porosity increases, remarkably.

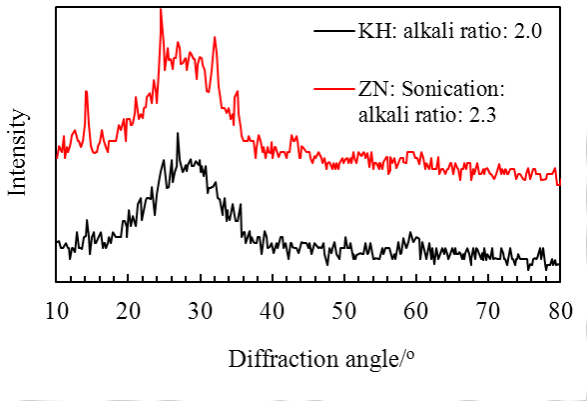

Figure 2. XRD patterns of optimal adsorbents.

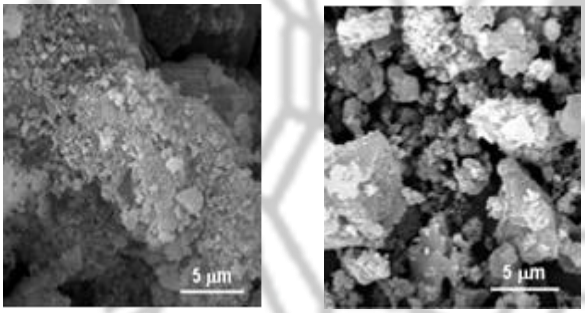

(a) (b)

Fig. 3. SEM images of adsorbents fabricated from (a) KH and (b) ZN with sonication.

4. Conclusions

Alkali treatment of Iranian kaolins in strong conditions is a promising method for the obtaining porous adsorbent for removal of cationic dye from wastewaters. The number of available sites increases with the application of ultrasound technique therefore, results in the increase in the amount of adsorbed dye cations. In order to obtain the optimal adsorbent from kaolin containing high level of kaolinite, the higher content of NaOH should be employed during the heat treatment with sonication.

References

[1] Zh. Shu, T. Li, J. Zhou, Y. Chen, Z. Sheng, Y. Wang, X. Yuan, *Appl. Clay Sci.* 123 (2016) 76-82.

[2] Zh. Shu, T. Li, J. Zhou, Y. Chen, D. Yu, X. Yuan, Y. Wang, *Appl. Clay Sci.* 107 (2015) 182-187.

[3] S. Kumar, M.M. Malik, R. Purohit, *Mater Today-Proc.* 4 (2017) 350-357.

5th Iran International Zeolite Conference

University of Tabriz, Tabriz, Iran

26-27 August 2018

Electrodeposition of Mesoporous Nickel Film using Lyotropic Liquid Crystal Template

S. Barzegar, F. Nasirpouri*

Department of Materials Engineering, Sahand University of Technology, Sahand New Town, Tabriz, Iran

**Corresponding author: f.Nasirpouri@yahoo.com*

Abstract: In recent years, mesoporous materials owing to their high surface area, high surface to volume ratio and porosity are of interest in fuel cells and catalaysis. In this research, mesoporous Ni films were electrodeposited galvanostatically through lyotropic liquid crystal template of cetyltrimethylammoniumbromid (CTAB) cationic surfactant, Ni sulfate hexahydrate and boric acid solution. Mesoporous Ni films characterized using low angle X-ray diffraction, field emission scanning electron microscopy and electrochemical methods. Low angle X-ray diffraction pattern of mesoporous Ni film electrodeposited from LLC phase containing 30 Wt% of surfactant at 2 $mAcm^{-2}$ showed d-spacing and pore to pore distance respectively 83.16 and 96.13 Å. This film had the highest surface area among other current densities and surfactant concentrations.

Keywords: Electrodeposition; Mesoporous; Lyotropic liquid crystal; CTAB; Ni

1. Introduction

Lyotropic liquid crystal phases with periodic long range order and nanometer size lattice parameter are a useful route for producing nanomaterials [1]. In this research, electrodeposition of mesoporous Ni films from LLC phases containing different concentrations of Cetyl trimethyl ammonium bromide (CTAB) cationic surfactant is studied for the first time, and the effect of CTAB concentration on the mesopore structure is investigated.

2. Experimental Part

Aqueous solution containing 0.1 M $NiSO_4.8H_2O$ and 0.2 M boric acid is used as the precursor. LLC phase is formed by adding different concentrations of CTAB cationic surfactant to the solution from 10 to 30 Wt%. The solution is stirred and kept at 30 ˚C for 45 minutes. Electrodeposition carried out galvanostatically on 1 Cm^2 Cu substrate and 2 Cm^2 Pt anode at 2 $mACm^{-2}$ constant current. After electrodepostion, mesoporous Ni films were rinsed with deionized water and held in 50% ethanol and deionized water solution for about 12 hours in order to remove LLC template. Characterisation of mesoporous films carried out using FESEM to study surface morphology, low angle XRD

to investigate the structure of mesopores and electrochemical surface area measurement.

3. Results and Discussion

Morphological investigation of electrodeposited mesoporous Ni films showed that mesoporous Ni films are composed of mesoporous spherical grains that are connected together and formed the texture of the films (Figure 1). By increasing the concentration of surfactant from 10 to 30 Wt% the spherical grains get smaller that is because of the completion of a compact hexagonal structure of LLC template. By increasing the concentration of surfactant that results in an increase in the number of micells and also the order of micells in the template [1], the spherical grains that are growing between micells get smaller and smaller. While in lower concentration of CTAB, micells stand in higher distance and larger grains growin the space among them.

Low angle diffraction pattern of mesoporous Ni film that is electrodeposited from 30 Wt% of CTAB LLC phase depicted that a mesoporous structure is formed.

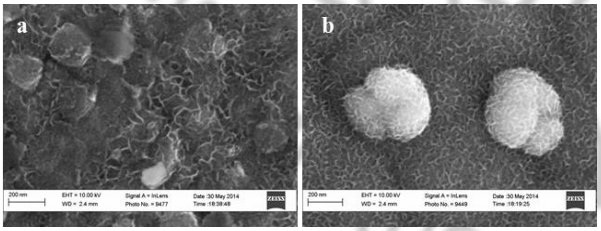

Figure 1. FESEM images of mesoporous Ni films electrodeposited from a)10 and b)30 Wt% surfactant.

According to figure 2 diffraction pattern showed a strong peak at 2Θ equal to 1.06° that is related to (100) diffraction plane of hexagonal pore structure. Interplanar distance is calculated about 83.16 Å. Moreover pore to pore distance in hexagonal structure of mesopores can be calculated, that is 96.13 Å for mesoporous Ni film electrodeposited from LLC phase containing 30 Wt%of CTAB surfactant [2]. This distance is the sum of pore diameter and pore wall. It is obvious that X-Ray diffraction pattern of mesoporous Ni films did not show a particular peak of Ni because of that Bragg diffraction condition did not confirm. Higher intensity of diffraction peak at 30 Wt% CATB in comparition to 10 Wt% verified more order of the pores in more surfactant concentration.

Electrochemical surface area of mesoporous Ni films can be calculated considering the surface below Ni oxidation peak in current-time curve that is equal to the charge associated with oxidation of surface of Ni film to $Ni(OH)_2$. Knowing that the charge associated with the formation of a monolayer of α-$Ni(OH)_2$ on Ni electrode is approximately 514 $C.cm^{-2}$, the electrochemical surface area of mesoporous Ni film can be calculated [3]. Investigation of mesoporous Ni films elctrodeposited from different concentrations of CTAB showed that mesoporous Ni film electrodeposited from 30 Wt% of CTAB had the largest surface area among all, that is because of the ordered array of micells that completed the hexagonal structure and resulted in mesoporous film with more ordered pores and higher surface area.

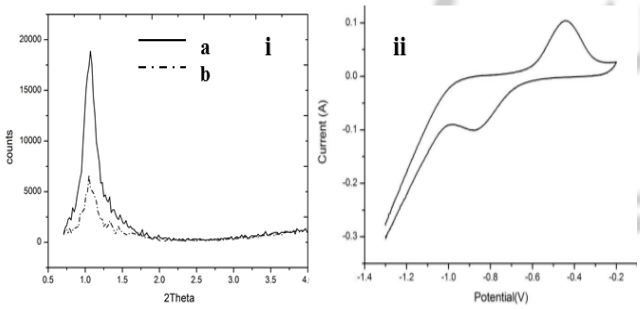

Figure 2. i) Low angle X-ray diffraction pattern of mesoporous Ni films electrodeposited from a)30 and b)10 Wt% CTAB ii) Cyclic voltamogram of mesoporous Ni film electrodeposited from 30 Wt% CTAB in 0.2 M NaOH solution with i = 2 $mACm^{-1}$.

4. Conclusions

LLC phase of CTAB surfactant can be used as a template for electrodeposition of mesoporous metal films with different structures depend on the tempereture and concentration of CTAB. Ni film electrodeposited from LLC phase containing 30 Wt% CTAB showed an ordered mesoporous structure with pore to pore distance of 96.13 Å and electrochemical surface area of 400 Cm^2 per geometric surface area that is the highest among other films and depicts that this film is a good candidate for utilizing in catalysis, fuel cell and also supercapasitor applications.

Refrences

[1] Y. Yamauchi, K. Kuroda, *chem. Asian J.* 3(4) (2008) 664-676.

[2] P.N. Bartlett, P.N. Birkin, M.A. Ghanem, P. de Groot, M. Sawicki, *J. Electrochem. Soc.* 148 (2001) C119-C123.

[3] I.J. Brown, S. Sotiropoulos. *Electrochimica Acta* 46(17) (2001) 2711-2720.

[4] P.N. Bartlett, D. Pletcher, T.F. Esterle, C.T. John Low, *J. Electroanal. Chem.* 688 (2013) 232-236.

5th Iran International Zeolite Conference

University of Tabriz, Tabriz, Iran

26-27 August 2018

Application of Porous Gd_2O_3 Nanoparticle as MRI Contrast Agent

N. Gharehaghaji[a], F. Bakhtiari Asl[b]*, B. Divband[c, d]

[a] *Radiology Department, Paramedical Faculty, Tabriz University of Medical Sciences, Tabriz, Iran*

[b] *Medical Physics Department, Medical Faculty, Tabriz University of Medical Sciences, Tabriz, Iran*

[c] *Stem Cell Research Center, Tabriz University of Medical Sciences, Tabriz, Iran*

[d] *Infectious and Tropical Diseases Research Center, Tabriz University of Medical Sciences, Tabriz, Iran*

** Corresponding author: fatemehbaxtiari@gmail.com*

Abstract: Porous gadolinium oxide (Gd_2O_3) nanoparticles were synthesized using sol-gel method and images of different concentrations of the nanoparticles were prepared. MRI was performed by a 1.5 Tesla instrument. The curves of the T1 and T2 relaxation times acquired from MRI experiments. According to the relationship between relaxation rates and concentration, porous Gd_2O_3 nanoparticles are good MRI T1 contrast agent.

Keywords: Porous gadolinium oxide nanoparticles; Contrast agent; Magnetic resonance imaging

1. Introduction

Magnetic resonance imaging (MRI) is a powerful modality for diagnosing many diseases because of its high spatial resolution. MRI sensitivity can be improved using contrast agents (CAs) which affect relaxation rates of water proton. T2 CAs produced a dark region in the MR images while T1 agents lead to a bright region [1].

Among different nanoparticles (NPs), gadolinium oxide (Gd_2O_3) has a good potential for the effective CA because of the seven unpaired electrons for Gd^{3+}. Gd_2O_3 nanoparticles have been introduced as T1 CA in many studies [2]. For example, in a study, PVP-modified Gd_2O_3 NPs were prepared for the in vivo MRI of the tumor-bearing mice, and a significant signal enhancement was observed [3]. The study of Faucher et al. showed that PEG-Gd_2O_3 NPs offer high positive contrast enhancement in the T1-weighted images [4].

2. Experimental Part

Porous Gd_2O_3 NPs were prepared by sol-gel method. Different concentrations of the Gd_2O_3 NPs in aqueous solution were prepared and used for MR imaging and analysis. The T1 and T2 weighted MR imaging was performed by a 1.5 Tesla Avanto Siemens machine. The T1 and T2 weighted images were prepared with different TR and TE amounts, respectively, and signal intensity were measured for each concentration. Then, the relationship between relaxation rates and concentration was considered.

3. Results and discussion

The curves of the T1 and T2 relaxation times obtained from MRI experiments are shown in the figures 1 and 2. In the T1 relaxation curve, signal intensity was exponentially improved with TR increasing. An exponentially decay was shown in the T2 relaxation curve with TE increasing. The relationship between relaxation rates and concentration of the porous Gd_2O_3 showed that the NPs act as t1 CA. This finding is similar to the prior studies on the other Gd_2O_3 NPs [1,4,5].

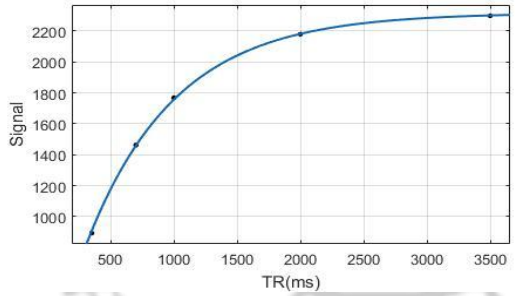

Figure 1. T1 relaxation time curve.

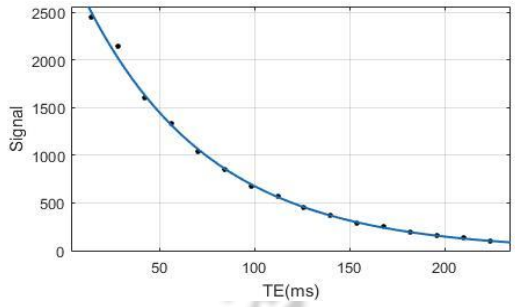

Figure 2. T2 relaxation time curve.

4. Conclusions

In summary, porous Gd_2O_3 NPs were successfully synthesized by sol-gel method. MR results demonstrated that porous Gd_2O_3 NPs have great potential to use as T1 CA for MR imaging.

Acknowledgments

This study was financially supported by Tabriz University of Medical Sciences - Iran.

References

N. Luo, X. Tian, J. Xiao, W. Hu, C. Yang, L. Li, D. n, *J. Appl. Phys.* 113 (2013) 164306.

[2] J.Y. Park, M.J. Baek, E.S. Choi, S. Woo, J. H. Kim, T.J. Kim, J.C. Jung, K.S. Chae, Y. Chang, G.H. Lee, *ACS nano* 3 (2009) 3663-3669.

[3] J. Fang, P. Chandrasekharan, X.-L. Liu, Y. Yang, Y.-B. Lv, C.-T. Yang, J. Ding, *Biomaterials* 25 (2014) 1636-1642.

[4] L. Faucher, Y. Gossuin, A. Hocq, M.-A. Fortin, *Nanotechnology* 22 (2011) 295103.

[5] M. Cho, R. Sethi, A. narayanan, S. Lee, N. Benoit, N. Taheri, P. Decuzzib, L. Colvin, *Nanoscale* 6 (2014) 13637-13645.

5th Iran International Zeolite Conference

University of Tabriz, Tabriz, Iran

26-27 August 2018

Activity Evaluation of Mesosilicate Supported Nickel Catalysts in Vapor Phase Hydrogenation of Benzene

Z. Mohammadian [1], M. H. Peyrovi [1], N. Parsafard [2,*]

[1]*Faculty of Chemistry and Petroleum Sciences, Department of Petroleum Chemistry and Catalysis, University of Shahid Beheshti, Tehran,* 1983963113, *Iran*

[2]*Kosar University of Bojnord, Department of Applied Chemistry, North Khorasan,* 9415615458, *Iran*

** Corresponding author: n_dastmoozeh@sbu.ac.ir (N. Parsafard)*

Abstract: Partial hydrogenation of benzene is one of the most cost-effective approaches to producing chemical materials that are used as intermediates. In this work, a series of Ni supported catalysts were used which prepared by impregnation method and evaluated for the hydrogenation reaction of benzene. Physicochemical properties of these catalysts were characterized by techniques as XRD, FT-IR, XRF, IR-Py, NH_3-TPD, N_2 adsorption-desorption. The Performance and selectivity of the prepared powders were investigated in the temperature range of 403-463 K and atmospheric pressure. The results indicate that the best performance obtains for the Ni/SiO_2 catalyst at 423 K.

Keywords: Benzene hydrogenation; Conversion; Selectivity; Vapor phase.

1. Introduction

The removal of aromatic compounds due to carcinogenic effects is one of the most important issues in the petrochemical industry and environmental protection. In order to reduce the destructive effects of these compounds, there are two common methods: hydrogenation and catalytic oxidation. Researchers' attention was attracted to the catalytic hydrogenation reaction as a reduction method with higher yields (>40%). To increase the efficiency of the above method, many efforts have been made to expand mesoporous catalysts. Among the metals that are used in this process, nickel is easy to access and cost-effective compared to other precious metals, therefore has attracted the petrochemical industry's tendency.

Variables such as reaction temperature, residence time, catalyst preparation method, nickel loading amount, and the partial pressure of hydrogen and benzene affect the activity and stability of the catalyst in the reaction of benzene hydrogenation. In this research, we have provided a series of silicate supported catalysts for the selective hydrogenation of benzene in a mixture of aromatics and finding the best one [1,2].

2. Experimental Part

A solution of Ni $(NO_3)_2.6H_2O$ (Merck) with appropriate concentration for 25 wt% loading of nickel was used for the impregnation of SBA-15, SiO_2, HMS and MCF supports [3-5]. The catalysts were mixed with this solution at room temperature and evaporated at 353 K. The impregnated materials were dried at 383 K and calcined in air atmosphere up to 573 K for 4 h.

To study the activity and selectivity of catalysts in the process of hydrogenation of benzene, a fixed-bed micro reactor was used at atmospheric pressure. Prior to this measurement, 0.5 g of each catalyst was placed in the reactor at 673 K for two hours in the presence of helium to clean the catalysts. For each test, the feed was mixed with a specific stream of air and volatile organic compounds and passed through the catalyst.

3. Results and discussion

Some of the surface properties of the prepared catalysts have been reported in Table 1. As it is clear, according to the pore size diameters and also the IUPAC division, the prepared nickel catalysts classified in the mesoporous materials group. Also, it should be noted that according to mentioned division, materials with less than 2 nm in pore size, such as zeolites, are classified in the microporous substances, and macropores are labeled for powders that these pore sizes are more than 50 nm. The catalytic performance was investigated over the nickel catalysts at 403-463 K and atmospheric pressure. This reaction was done in the presence of H_2 to saturate the benzene. The effect of reaction temperature on the activity of catalysts is shown in Figure 1. According to the thermodynamics and Gibbs free energy of the reaction, cyclohexane is the main and expected product. As can be seen in this figure, the highest conversion of benzene to cyclohexane is achieved for all catalysts at 423 K. The maximum conversion in benzene hydrogenation (>99%) was achieved for Ni/HMS at 423 K, while the lowest conversion is for this catalyst at 463 K (<22%). Figure 2 shows the dependences of the catalysts selectivity to cyclohexane on reaction temperature in benzene (Bz) hydrogenation.

Table. 1. Surface properties of Ni catalysts.

alysts	$_{BET}$(m^2/g)	(cm^3/g)	d_p(nm)
SiO2	310	0.67	8.6
MCF	428	0.91	, $d_{windows}$=3.8
SBA-15	565	0.64	6.9
HMS	763	0.74	3.9

The results show that Ni/SiO_2 catalyst has the best selectivity (75% at 403 K) toward cyclohexane. This implies that Ni/SiO_2 catalyst has a tendency to preferably hydrogenate benzene.

In order to determine the catalyst with the best performance (activity and selectivity), cyclohexane yield was calculated (Figure 3) and the results indicated that the Ni/SiO_2 has the best performance at 423 K.

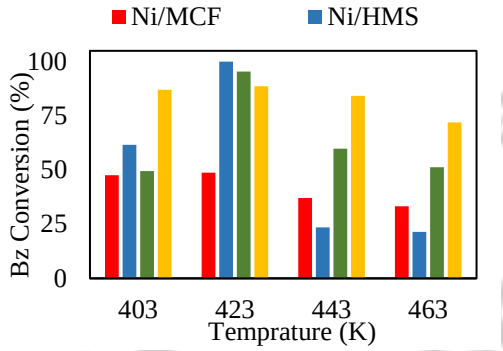

Figure 1. Temperature dependence of Bz conversion over impregnated catalysts.

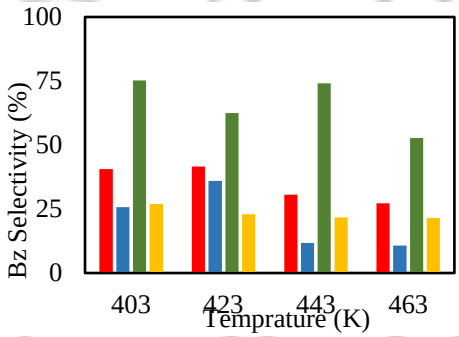

Figure 2. Effect of reaction temperature on cyclohexane selectivity over nickel catalysts.

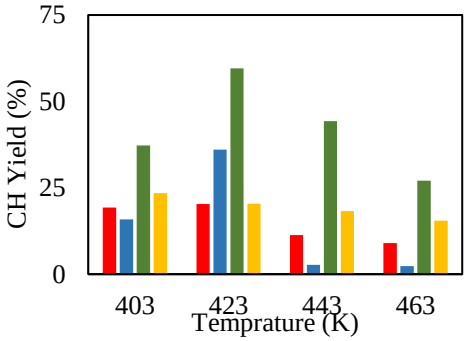

Figure 3. Calculation of cyclohexane (CH) yield as a function of temperature over powders.

4. Conclusions

In summary, the mesoporous supports were successfully synthesized and their physicochemical properties were characterized by various techniques. The catalytic study was carried out for the benzene hydrogenation reaction. The results indicated that the maximum benzene conversion (>99%) was achieved over Ni/HMS at 403 K. Also the best CH selectivity (above 75% at 403 K) and CH yield (60%) is related to Ni/SiO_2 catalyst at 423 K.

References

[1] H. Liu, R. Fang, Z. Li, Y. Li, *Chem. Eng. Sci.*, 122 (2015) 350–359.
[2] X. Liu, C. Meng, Y. Han, *Nanoscale* 4 (2012) 2288-2295.
[3] M. H. Peyrovi, N. Parsafard, Z. Mohammadian, *Chin. J. Chem. Eng.* 26 (2017) 521-528.
[4] N. Parsafard, M. H. Peyrovi, M. Rashidzadeh, *Micropor. Mesopor. Mater.* 200 (2014) 190-198.
[5] J. Zhu, T. Wang, X. Xu, P. Xiao, J. Li, *Appl. Catal., B: Env.* 130 (2013) 197-217.

5th Iran International Zeolite Conference

University of Tabriz, Tabriz, Iran

26-27 August 2018

Synthesis of $NaHSO_4$ modified periodic mesoporous organosilica magnetic nanoparticles

M. Haghighat[a], M. Golshekan[b], F. Shirini[a]*

[a] *Department of Chemistry, College of Science, University of Guilan, Rasht, Iran.*

[b] *Institute of Medical Advanced Technologies, Guilan University of Medical Science, Rasht, Iran*

**Corresponding author: shirini@guilan.ac.ir*

Abstract: Immobilized $NaHSO_4$ on core/shell phenylene bridged periodic mesoporous organosilica magnetic nanoparticles (Fe_3O_4@Ph-PMO-$NaHSO_4$) was successfully prepared in three steps: (i) preparation of Fe_3O_4 nanoparticles by a precipitation method, (ii) synthesis of an organic-inorganic periodic mesoporous organosilica structure with phenyl groups on the surface of Fe_3O_4 magnetic nanoparticles (MNPs) and (iii) finally adsorption of $NaHSO_4$ on periodic mesoporous organosilica (PMO) network. The results of N_2 adsorption-desorption isotherms, XRD and TEM showed formation of the Periodic mesoporous organosilica magnetic nanocomposite with the uniform size up to 15 nm.

Keywords: PMO, nanocatalyst, Fe_3O_4@Ph-PMO-$NaHSO_4$.

1. Introduction

In recent years, porous materials have played a very important role in science and industry so that billion dollars are spent annually in the use of these materials in various fields. Some of these important fields are ionic exchange, separation, catalysis, preparation of batteries, fuel cells, sensors and many others. Among these materials, mesoporous silica has attracted considerable attention in the field of adsorption and catalysis because of its uniform pore size, large pore volume and high surface area [1]. Periodic mesoporous organosilica materials as a member of this family are a class of hybrid materials which organic groups are distributed in uniformly inside the framework, causing properties including mechanical and hydrothermal stability, diffusion of guest molecule and lack of pore blocking and they are more hydrophobic and stable in water than pure organized silicas (MCM-41 or SBA-15). This feature expands the range of applications in, for example, optical gas sensing, catalysis, chromatography, separation and nanotechnology [2-3]. For the preparation of this kind of materials, a common method included the hydrolysis and condensation of a bridged organosilane precursor of the type $(R`O)_3$ Si-R-$Si(OR`)_3$ (R` is methyl or ethyl and R is an organic group) in the presence of a structure directing agent can

be used. Based on this, one-pot synthesis was used as a method for the preparation of periodic mesoporous organosilica magnetic nanocomposite which is possible by the co-condensation of magnetic nanoparticles and tetraethyl orthosilicate (TEOS) with a bridged organosilane precursor of the type $(R`O)_3$ Si-R-Si$(OR`)_3$ in the presence of a surfactant.

2. Experimental Part

2.1 Preparation of Fe_3O_4@Ph-PMO nanocomposite

For the synthesis of Fe_3O_4@Ph-PMO, Pluronic p123 (Mn = 5800 g/mol) was dissolved in a mixture of Fe_3O_4 and concentrated HCl in distilled water under argon gas protection at room temperature. Then, 1,4-bis (triethoxysilyl) benzene and tetraethoxysilane were added simultaneously to the mixture dropwise and stirred for 2 hours at 40 ˚C. At the end of this process, the magnetic composite was kept at 100 ˚C for 24 h under static conditions. The resultant solid was filtered, and the template was removed by solvent extraction. For this purpose, the magnetic nanocomposite was dispersed in acetone and refluxed at 56 ˚C for 10 h, then washed with distilled water and hot ethanol. This procedure was repeated twice to be sure of removing of the surfactant.

2.2 Preparation of Fe_3O_4@ Ph-PMO-$NaHSO_4$ nanocatalyst

Fe_3O_4@Ph-PMO-$NaHSO_4$ was prepared by adding the synthesized mesoporous Fe_3O_4@Ph-PMO nanoparticles to an aqueous solution of $NaHSO_4 \cdot H_2O$ and the mixture was sonicated at 25 °C for 1 min. In continue, the mixture was stirred for 30 min. Finally, water was removed by decanting and the powder was dried in an oven at 90 ˚C for 2 h. A brown solid acid formulated as Fe_3O_4@ph-PMO-$NaHSO_4$ was obtained.

3. Results and discussion

3.1 BET analysis

The results of N_2 adsorption-desorption isotherms of Fe_3O_4@Ph-PMO and Fe_3O_4@Ph-PMO-$NaHSO_4$ were shown in Figure 1. From N_2 adsorption-desorption analysis of samples, a type IV BET isotherm for both samples was obtained, which is attributed to mesoporous structures. The Brunauer-Emmet-Teller (BET) surface areas and total pore volume of Fe_3O_4@Ph-PMO were 357.83 $m^2.g^{-1}$ and 0.5154 $cm^3.g$, respectively. The BET surface area and total pore volume of Fe_3O_4@Ph-PMO-$NaHSO_4$ decreased to 163.5 $m^2.g^{-1}$ and 0.3093 $cm^3.g$ which proves the adsorption of $NaHSO_4$ on the surface and successful synthesis of the nanocatalyst.

TEM analysis

Figure 2 shows TEM image of the synthesized Fe_3O_4@Ph-PMO-$NaHSO_4$. The TEM image revealed that all samples were spherical-like particles. Based on the TEM images, analysis of the Fe_3O_4@Ph-PMO-$NaHSO_4$ surface morphology demonstrated that the aggregation of the particles is uniform and the size of them is up to 15 nm**.**

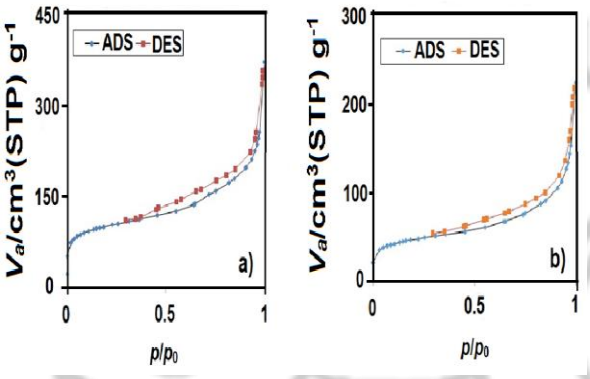

Figure 1. N_2 adsorption-desorption of Fe_3O_4@Ph-PMO (a), and Fe_3O_4@Ph-PMO-$NaHSO_4$ (b).

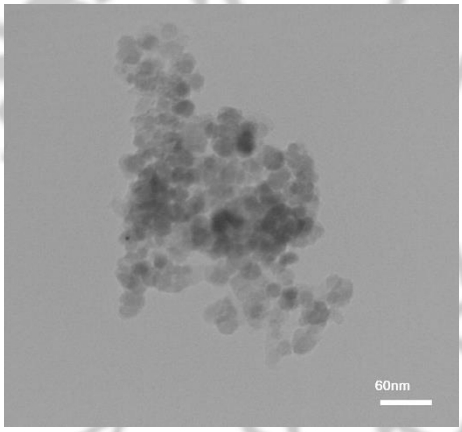

Figure 2. The TEM image of Fe_3O_4@Ph-PMO-$NaHSO_4$.

4. Conclusions

In conclusion, $NaHSO_4$ modified periodic mesoporous organosilica magnetic nanoparticles with the uniform size up to 15 nm successfully was synthesized *via* one-pot synthesis method. This method is based on the co-condensation of magnetic nanoparticles and tetraethyl orthosilicate (TEOS) with a bridged organosilane precursor of the type $(R`O)_3$ Si-R-Si$(OR`)_3$ in the presence of a surfactant.

Acknowledgments

We are thankful to the Research Council of the University of Guilan for the partial support of this research.

References

[1] S. S. Park, M.S. Moorthy, C. H, *Korean J. Chem. Eng*. 31 (2014) 1707-1719.

[2] F. Goethals, B. Meeus, A. Verberckmoes, P. Van der Voort, *J. Mater. Chem.* 20 (2010) 1709-1716.

[3] N. Mizoshita, T. Tani, S Inagaki, *Chem. Soc. Rev.* 40 (2011) 789-800.

[4] C. P. Moura, C. B. Vidal, A. L. Barros, L. S. Costa, L. C.G. Vasconcellos, F. S. Dias, R. F. Nascimento, *J. Colloid Interface Sci.* 363 (2011) 626-634.

5th Iran International Zeolite Conference

University of Tabriz, Tabriz, Iran

26-27 August 2018

Ag/AgCl/Zeolite (A) (LTA) Nanocomposite: A Highly Efficient and Stable Photo Catalyst Active under Visible Light

S. Hatef Tabar[a], M. R. Fakhri[b]*

[a] *Chemical Expert, East Azarbaijan Water & Wastewater Co, Tabriz, Iran*

[b] *Water quality control manager, East Azarbaijan Water & Wastewater Co, Tabriz, Iran*

**Corresponding author: somayehatef@yahoo.com*

Abstract: Ag/AgCl/Zeolite (A) nanocomposite was fabricated via a facile microwave hydrothermal method followed by a precipitation–photo-reduction method. The photocatalytic activity of the obtained product was evaluated by the photodegradation of methyl orange (MO) under visible light irradiation, and it was found, interestingly, that Ag/AgCl/Zeolite (A) nanocomposite exhibits high visible light photocatalytic activity and good stability. The characterization results showed the Ag/AgCl/Zeolite (A) particles were cubic and crystalline Ag/AgCl was deposited on the surface of the Zeolite (A). Scanning electron microscopy (SEM), X-ray powder diffraction (XRD) and UV-vis diffuse reflectance spectra were used to characterize the obtained product.

Keywords: Visible light degradation; Microwave synthesis; Nanocomposite; Ag/AgCl/Zeolite (A).

1. Introduction

Since the discovery of the photocatalytic splitting of water on TiO_2 electrodes by Fujishima and Honda in 1972, the semiconductor-mediated photocatalytic degradation of organic contaminations has attracted much attention [1].

Combining adsorbents (e.g., zeolites and mesoporous silica's) and semiconductor photo catalysts make it possible to create advanced photocatalytic systems with improved adsorption and condensation properties—for example, reduction of air and water pollution using solar light, as well as photo oxygenation of hydrocarbons, de-NOx processes, and other photochemical processes of concern in environmental sciences [2].

As well as we can use of noble metals nanoparticles as a photocatalyst because noble metals nanoparticles can significantly absorb visible light due to their localized surface plasmon resonance (LSPR) [3]. Silver halides are photosensitive materials broadly used as source materials in photographic films. On absorbing a photon, a silver halide particle generates an electron and a hole, and subsequently, the photogenerated electron combines with an Ag^+ ion to form an Ag^0 atom.

Although the intrinsic light response of AgCl locates in the UV region, once it absorbs a photon an electron–hole pair will be generated in the silver chloride particle, and subsequently the photogenerated electron combines with an Ag^+ ion to form an Ag^0 atom. Finally, a cluster of silver atoms is formed on the surface of the AgCl particle upon absorption of photons, which could extend the light response of AgCl into the visible light region [4].

2. Experimental Part

The Zeolite (A) prepared with sodium silicate solution, sodium aluminate and sodium hydroxide chemicals. Firstly, the chemicals were mixed in deionized water and the gel formed. The gel was crystallized by microwave heating at 100°C in only 10 min. The molar ratio of the synthesis mixture was 1 SiO_2: 0.5 Al_2O_3: 1.5 Na_2O: 96.5 H_20. Than Zeolite (A) (1g) was mixed in the 100ml $AgNO_3$ solution by intensive mechanical. Subsequently, saturated NaCl solution was poured into AgNO3/Zeolite (A) solution and the mixture solution was vigorously stirred to form AgCl/Zeolite (A) solution. The solution was illuminated using 300 W Xe arc lamp with the UV filter for 30 min under the nitrogen atmospheric condition. Ag nanoparticles were generated on the surface of AgCl/Zeolite (A) by the photo-reduction method. Then the product was centrifuged and washed several time with deionized water. Eventually, the product dried at room temperature. Photocatalytic activity of Ag/AgCl/Zeolite (A) nanocomposite was evaluated by the degradation of MO solution under visible light irradiation. Each time, 0.05 g photocatalyst was dispersed into 40 ml MO aqueous solution with a concentration of 10 mg/l. MO concentration analysed using the UV–Vis spectrometer.

3. Results and discussion

The crystal structure of the obtained Zeolite (A) and Ag/AgCl Zeolite (A) nanocomposite product was examined by means of X-ray diffraction (XRD) are shown in Fig.1. Fig.1a shows the XRD patterns of pure zeolite (A) obtained by a microwave hydrothermal reaction process with JCPDS card number of (43-142). The XRD pattern of Ag/AgCl/Zeolite (A) shows several additional peaks, which are indexed to the AgCl (JCPDS file: 31-1238) and metal silver (JCPDS file: 65-2871) Fig.1b.

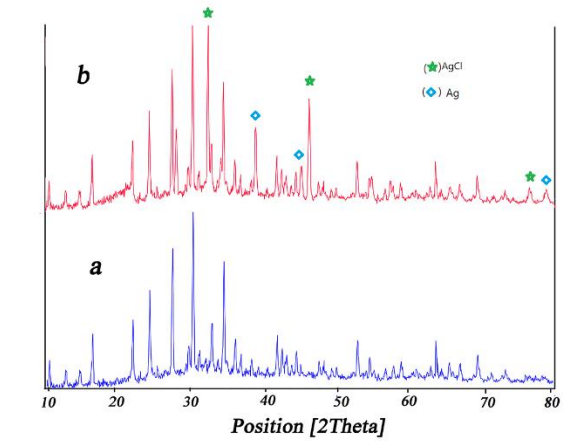

Figure 1. XRD patterns of (a) Zeolite (A) (LTA), (b) Ag/AgCl/Zeolite (A) nanocomposites.

UV-visible diffuse reflectance spectroscopy (DRS) was used to characterize the electronic states of the obtained product. Fig. 2 displays a typical UV-visible diffuse reflectance spectrum of the obtained Ag/AgCl/Zeolite (A) nanocomposite photo catalyst. It is found that the Zeolite (A) is an insulator and Ag/AgCl/Zeolite (A), has strong absorption both in the UV and visible light regions.

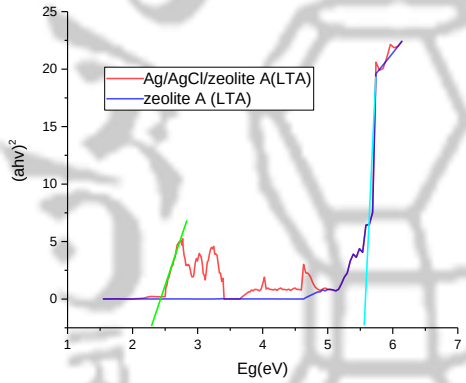

Figure 2. UV–Vis spectrum (DRS) (calculated band gap for Zeolite (A) and Ag/AgCl/Zeolite (A) nanocomposites.

Fig. 3 presents typical SEM images of the as-prepared Ag/AgCl/Zeolite (A) photo catalyst. As shown in Fig. 3, the Ag/AgCl/Zeolite (A) photo catalyst has a cube-like morphology, with sizes of 50–400 nm.

The photocatalytic activity of the obtained Ag/AgCl/Zeolite (A) photo catalyst was evaluated by measuring the photodegradation of MO dye under visible light irradiation. Fig. 4 shows the photodegradation curves of MO dye. The MO dye is almost completely decomposed after only 10 min under visible light irradiation in the presence of the obtained Ag/AgCl/Zeolite (A) photo catalyst.

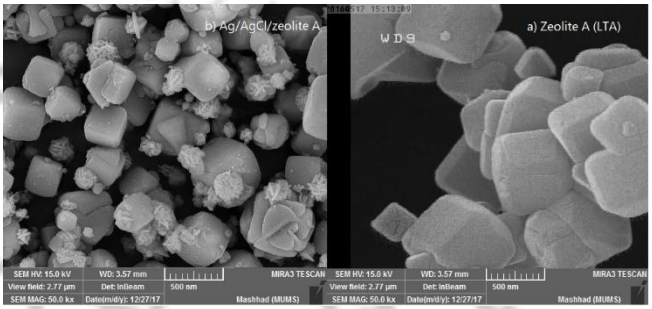

Figure 3. SEM images of (a) Zeolite (A), (b) Ag/AgCl/Zeolite (A) (LTA) nanocomposites.

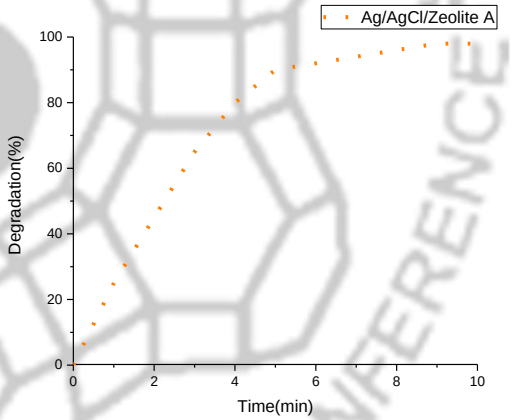

Fig.4. Photodegradation of methyl orange (MO) using Ag/AgCl/ Zeolite (A) (LTA) nanocomposites under visible irradiation.

4. Conclusions

We successfully synthesized the plasmonic photo catalyst Ag/AgCl/Zeolite (A), with cube-like morphology, through a simple microwave hydrothermal process followed by the precipitation-photo-reduction method. The as-synthesized Ag/AgCl/Zeolite (A) photo catalyst exhibits high photocatalytic activity under visible light irradiation and MO dye can be decomposed by more than 98% within 10 min. Zeolite (A) causing the enhanced adsorption property of MO dye.

References

[1] Z. Ambrus, N. Balázs, T. Alapi, G. Wittmann, P. Sipos, A. Dombi and K. Mogyorósi, *Catal. B* 81 (2008) 27-37.

[2] C. Tabor, R. Murali, M. Mahmoud and M. A. El-Sayed, the J. Phys. *Chem. A*. 113 (2008) 1946-1953.

[3] Y. Kuwahara, J. Aoyama, K. Miyakubo, T. Eguchi, T. Kamegawa, K. Mori and H. Yamashita, *A. Appl. Catal*. 285(2012) 223-234.

[4] a) C. An, S. Peng and Y. Sun, *Adv. Mater*. 22(2010) 2570-2574.

5th Iran International Zeolite Conference

University of Tabriz, Tabriz, Iran

26-27 August 2018

Synthesis of Fe_3O_4@MCM-41@Zr Modified with Piperazine as a New Mesoporous Nanocomposite

R. Pourhasan-Kisomi [a], F. Shirini [a]*, M. Golshekan [b]

[a] *Department of Chemistry, college of Science, University of Guilan, Rasht, Iran*

[b] *Institute of Medical Advanced Technologies, Guilan University of Medical Science, Rasht, Iran*

**Corresponding author: Shirini@guilan.ac.ir*

Abstract: In this study, due to the unique properties of mesoporous compounds and their wide range of applications in chemistry, we have introduced Fe_3O_4@MCM-41@Zr modified with piperazine as an effective mesoporous nanocomposite which is magnetically separable using an external magnetic field. The synthesis and characterization of the mentioned mesoporous nanocomposite were considered and verification of the synthesized nanocomposite structure was done using different analyses like BET, TEM and XRD.

Keywords: Fe_3O_4@MCM-41@Zr-piperazine; mesoporous; magnetic; nanocomposite.

1. Introduction

Silica mesoporous compounds are defined as natural and artificial compounds having a pore size of 2-50 nm, classified between the two micro and macroporous classes. The reason for the focus of many studies by researchers and scientists on silica mesoporous materials like MCM-41 is their exclusive characteristics such as high surface area (~1000 $m^2.g^{-1}$), large pore size (2-50 nm), narrow pore size distribution, high thermal stability and the feasibility of using them in a broad variety of applications such as catalization, sensors, photocatalysis, isolation, absorption, etc [1]. To increase the efficiency of the mesoporous specious, immobilization of metal nanoparticles like Zr on mesoporous compounds due to their intrinsic chemical and optical properties, is particularly effective [2]. And also another way to increase the efficiency of the mesoporous species for different applications is modifying their surface by creating functional groups to change the acidic or basic properties of their surface. In this line, functionalization by organic amine groups like piperazine as a basic functional group seems to be a good idea [3].

On the other hand, in order to protect the environment and to prevent the attainment of filtration and refinement these nanocomposites the modification of methods that can develop and reuse such compounds at low concentrations in complex matrices will be strongly

needed. To do this, by synthesizing the mesoporous nanocomposite in the form of magnetic nanoparticles, it can be recovered using an external magnetic field and increased the performance of the nanocomposite in subsequent reuses [4]. Accordingly, we have introduced and identified "piperazine -functionalized Fe_3O_4@MCM-41@Zr-MNPs" as a stable and highly active superparamagnetic mesoporous nanocomposite. which can be used for diverse applications like catalyzing the organic transformations and absorption of heavy metals from water.

2. Experimental Part

2.1. The synthesis of Fe_3O_4@MCM-41@Zr-MNPs

For this pupose, appropriate amount of cetyltrimethylammonium bromide (CTAB), NaCl and the synthesized Fe_3O_4-MNPs (which was accomplished according to our previous method with minor modification [5]) were mixed in H_2O at room temperature, with further adding $ZrOCl_2.8H_2O$ which stirred vigorously for 1 h, followed by the addition of tetraethyl orthosilicate (TEOS) which stirring for 1 day. then mixture was transferred to an autoclave at 100 °C for 24 h. The solid product was separated using an external magnetic field, washed with distilled water, and dried at 120 °C for 5 h. Finally, the template was removed from the as-synthesized Fe_3O_4@MCM-41@Zr-MNPs by calcination of the synthesized particles at 550 °C for 6 h.

2.2. The synthesis of piperazine-functionalized Fe_3O_4@MCM-41@Zr-MNPs

In this step, appropriate amount of piperazine was dissolved in methanol, and calcined Fe_3O_4@MCM-41@Zr-MNPs was added to the solution. The suspension was stirred at room temperature for 5 h and then dried at 70 °C for the removal of solvent, followed by further drying at 100 °C for 1 h.

3. Results and discussion

The synthesized mesoporous nanocomposite was characterized by a variety of techniques in which TEM, XRD are explained here.

3.1. TEM analysis

The TEM images of the prepared functionalized Fe_3O_4@MCM-41@Zr-MNPs are shown in Fig. 1. The TEM images disclosed the spherical-like particles of all samples including agglomeration of dark MNPs cores surrounded by lighter amorphous silica shells bearing metals nanoparticles with the size up to 23 nm.

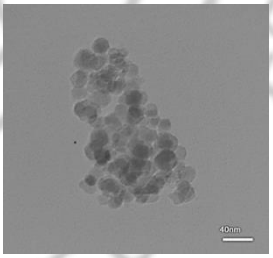

Figure 1. The TEM images of Fe_3O_4@MCM-41@Zr-piperazine-MNPs

3.2. XRD analysis

The XRD patterns of Fe_3O_4@MCM-41@Zr-MNPs before and after modification with piperazine are shown in Fig. 2. in which the peaks with 2Θ at 29.72°, 35.57°, 43.17°, 57.15° and 62.77° are characteristic peaks of Fe_3O_4 and the three peaks with 2Θ at 1.5°–10° are the characteristic peaks of MCM-41 [5]. The obvious diffraction (100) peak around 0.8°-1°, and one poorly resolved diffraction (110) peak around 2°-4°, indicates the presence of ordered mesostructure and the incorporation of Zr^{4+} in the framework of MCM-41 as a sufficient evidence. With loading of piperazine, there is decrease of peak intensity as well as a shift of the (100) peak for Fe_3O_4@MCM-41@Zr-MNPs to the low angle degree for Fe_3O_4@MCM-41@Zr-piperazine-MNPs which is an evidence of successful loading of piperazine on a well-organized mesoporous nanocomposite.

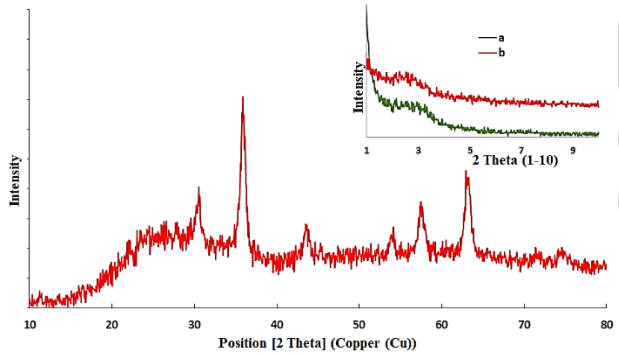

Figure 2 The XRD patterns of a) Fe_3O_4@MCM-41@Zr-MNPs and b) Fe_3O_4@MCM-41@Zr-piperazine-MNPs.

4. Conclusions

In conclusion, we have synthesized an efficiently improved mesoporous nanocomposite via introducing functionalized Zr nanoparticles in the mesoporous structure in the form of magnetic nanoparticle. The obtained results of different analyses validate the structural correctness and justify the accurate performance of the mesoporous nanocomposite**.**

References

[1] V. Polshettiwar, R.S. Varma, Green Chem. 12 (2010) 743-754.

[2] Z.-H. Zhang, T.-S. Li, Curr. Org. Chem. 13 (2009) 1-30.

[3] K.L. Levine, J.O. Iroh, P.B. Kosel, Appl. Surf. Sci. 230 (2004) 24-33.

[4] Y. Kobayashi, M. Horie, M. Konno, B. Rodríguez-González, L.M. Liz-Marzán, *J. Phys. Chem. B*, 107 (2003) 7420-7425.

[5] N. Saadatjoo, M. Golshekan, S. Shariati, H. Kefayati, P. Azizi, J. Mol. Catal. A: Chem. 377 (2013) 173-179.

5th Iran International Zeolite Conference

University of Tabriz, Tabriz, Iran

26-27 August 2018

Mesoporous Magnetic Graphene Oxide Nanocomposite as a Targeted Drug Carrier; Synthesis and Characterization

M. Pooresmaeil[a], H. Namazi[a,b]*

[a] *Research Laboratory of Dendrimers and Nanopolymers, Faculty of Chemistry, University of Tabriz, P.O. Box 51666, Tabriz, Iran. Tel.: +98 4133933121, Fax: +98 4133340191,*

[b]*Research Center for Pharmaceutical Nanotechnology (RCPN), Tabriz University of Medical Science, Tabriz, Iran.*

**Corresponding author: namazi@tabrizu.ac.ir*

Abstract: This work, presents the preparation and characterization of a drug carrier based on mesoporous silica-coated magnetic graphene oxide (MG@$mSiO_2$). Ibuprofen (IBU) as an anti-inflammatory drug was loaded in the MG@$mSiO_2$. Prepared nanocomposite was characterized by Fourier transform infrared spectroscopy (FT-IR), and N_2 adsorption/desorption analysis. Drug loading and releasing results showed that the prepared nanocomposite has a good potential as a drug carrier.

Keywords: Magnetite; Graphene oxide; Mesoporous; Targeted drug delivery.

1. Introduction

GO has a two-dimensional (2D) honeycomb lattice structure with abundant oxygen-containing functional groups. In the recent years, GO has become a good candidate for drug delivery. The combination of GO with other nanoparticles such as Fe_3O_4 leads to the formation of GO with new surface properties [1]. The decoration of Fe_3O_4 nanoparticles (MNPs) on the GO induces magnetic properties to it consequently, drug release could be done in a targeted way [2]. One of the limitations of magnetic nanoparticles is the tends to the aggregation. Research suggested which combining of MNPs and mesoporous silica or GO, could overcome the MNPs agglomeration [3].

Mesoporous compounds have high drug loading capacity due to the properties such as large surface area and several pores in its structure [4]. From the above contents, it is clear that the combination of GO, magnetite, and $mSiO_2$ (MG@$mSiO_2$) could be a suitable candidate for drug delivery [5]. The main aim of the current study was to design a new nanocomposite and evaluate its ability for the targeted IBU delivery.

2. Experimental Part

2.1. Materials and Characterization

All materials were purchased from Merck.

The Fourier transform infrared spectra were recorded on an FT-IR spectrometer (Bruker Instruments). N_2 adsorption/desorption isotherm measurement was performed at -196 °C.

2.2. Preparation of MG@mSiO$_2$

GO nanosheets were prepared according to the Hummers' method [6]. In the next step, GO (0.1 g) was sonicated in the water (150 ml), then $FeCl_2.4H_2O$ (0.6 g) and $FeCl_3.6H_2O$ (1.6 g) were added to it. The mixture was added dropwise into a balloon which containing 30% ammonia solution (25 ml) reaction was continued at 80-85 °C. After one hour the reaction was finished. MG precipitate was separated, washed with deionized water and ethanol then dried. In the next step, MG (100 mg) was dispersed in the 100 ml of deionized water contains CTAB (1 g). Next deionized water (800 ml) and NaOH (100 ml, 0.01 M) were added to it. The reaction mixture was sonicated for 10 min then, the temperature was adjusted to 60 °C for 30 min. In the following step, TEOS/ethanol solution was added dropwise to the mixture over 12 h at 60 °C. The MG@mSiO$_2$ was separated, washed and then dried. For removing of the CTAB from pores, MG@mSiO$_2$ was refluxed at ammonium nitrate solution.

2.3. Ibuprofen load and releasing

MGO@mSiO$_2$ (0.1 g) was added to IBU solution (0.1 g in 14 ml n-hexane). The mixture was shaken for 48 h then, nanocarrier was separated from the drug solution. The amount of loaded IBU was determined about (15.7%). Drug release study was done at PBS solution (pH=7.4).

3. Results and discussion

Fig. 1 shows the FT-IR spectra for the GO (a), MG (b), and MG@mSiO$_2$ (c). GO shows the intense and wide peak at 3418 cm^{-1} which related to the O–H stretching vibrations. The peaks at 1724 cm^{-1}, 1620 cm^{-1}, 1363 cm^{-1}, and 1055 cm^{-1} are assigned to the C=O stretching, C=C bond, C–OH stretching bond and C–O stretching peak, respectively. In the MG spectrum, there is one main peak at 576 cm^{-1} which results from the Fe-O vibration. The spectrum of MG@mSiO$_2$ shows three new peaks compared with MG, which related to the asymmetric stretching, symmetric stretching vibration and bending vibration of Si–O–Si.

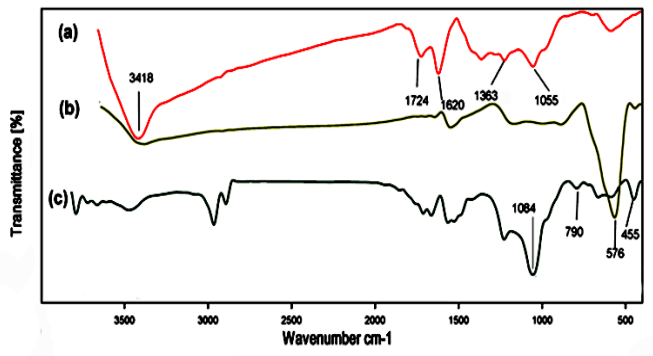

Figure 1. The FT-IR spectra of GO (a), MG (b), MG@mSiO$_2$ (c).

We studied the mesoporosity of MG@mSiO$_2$ using N_2 adsorption and desorption technique.

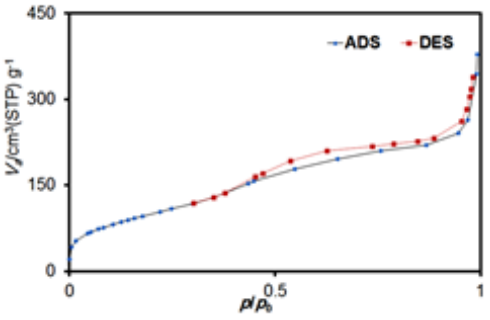

Figure 2. N_2 isotherm for MG@mSiO_2 at -196 ˚C.

The nitrogen adsorption-desorption pattern shows typical IV isotherm pattern that is an evidence for mesoporous materials. Also, using the BET results, average pore size was calculated about 5.7 nm. Total pore volume and BET surface area were calculated about 0.53 cm^3/g and 375.62 m^2/g, respectively.

Fig. 3 shows the drug release results for the MG@mSiO_2 in the simulated intestinal fluid conditions (pH 7.4, 37 °C). The amount of released drug was calculated using below equation. From the Fig. 3 it is clear that MG@SiO_2-IBU has the ability to release the loaded drug within two hours.

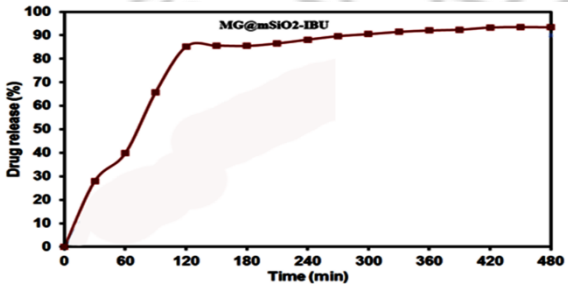

Figure 3. Drug release behavior for MG@SiO_2-IBU.

Drug release (%)=(the amount of released drug)/(the amount of loaded drug)×100

4. Conclusions

The purpose of this work was the preparation and characterization of new targeted drug carrier based on the MG. MG@mSiO_2 Nanocomposite was characterized using FT-IR and BET technique. Drug release results show that the prepared nanocomposite could be a good drug carrier for the targeted IBU delivery.

Acknowledgments

Authors gratefully acknowledge the University of Tabriz and RCPN of the Tabriz University of Medical Science for the financial supports for this research.

References

[1]. D.P. Singh, C.E. Herrera, B. Singh, S. Singh, R.K. Singh, R. Kumar, *Mater. Sci. Eng. C*, 86 (2018) 173-197.

[2]. A. Pourjavadi, Z.M. Tehrani, A. Shakerpoor, *Supramol. Chem.* 28 (2016) 624-633.

[3]. N. Alegret, A. Criado, M. Prato, *Curr. Med. Chem.* 24 (2017) 529-536.

[4]. F. Gu, M. Liang, D. Han, Z. Wang, *RSC Adv.* 5 (2015) 39964-39972.

[5]. H. Wan, Y. Zhang, Z. Liu, G. Xu, G. Huang, Y. Ji, Z. Xiong, Q. Zhang, J. Dong, W. Zhang, *Nanoscale* 6 (2014) 8743-8753.

[6]. X. Sun, Z. Liu, K. Welsher, J.T. Robinson, A. Goodwin, S. Zaric, H. Dai, *Nano research* 1 (2008) 203-212.

5th Iran International Zeolite Conference

University of Tabriz, Tabriz, Iran

26-27 August 2018

Loading Cobalt Phthalocyanine onto Graphene Oxide and Modified Graphene Oxide for Construction of Photoactive Catalyst

M. Ghaeini, M. A. Zanjanchi*

Department of Chemistry, Faculty of Science, University of Guilan

**Corresponding author: Zanjanchi@guilan.ac.ir*

Abstract: A conventional method for the preparation of graphene oxide (GO) was used. This method describes as modified Hummers' method ($KMnO_4$, $NaNO_3$, H_2SO_4) which is most common method used for preparing graphene oxide. Nitrogen-doped graphene (NG) sheets were also prepared by thermal annealing graphite oxide using melamine as source of nitrogen. Reduced graphene oxide (RG) was also synthesized by hydrazine hydrate. The products were characterized by XRD, UV-Vis, EDX, SEM, Elemental Maps Analysis and FTIR. It was shown that parts of the cobalt phthalocyanine (CoPc) immobilized onto (GO), (NG) and (RG) layers. The photocatalytic activity of the CoPc/GO, CoPc/NG and CoPc/RG were evaluated. The degradation efficiency of the produced photocatalysis dichlrophenol DCP were tested under visible light irradiation. CoPc/NG showed the best efficiency and nearly complete degradation of DCP occurs with 135 min.

Keywords: Cobalt phthalocyanine (CoPc); Graphene oxide (GO); Nitrogen doped graphene oxide (NG); Photocatalytic; Reduced graphene oxide (RG)

1. Introduction

Nowadays emission of harmful and dangerous substances which is released from various chemical industries are major concern. Dichlorophenol (DCP), which is commonly used as herbicide, biocide and wood preservative is an extremely dangerous pollutant due to its high toxicity towards all organisms.

Over the past decades, different techniques for the treatment of organic-contaminated wastewaters have been applied including photocatalysis. Recently, cobalt phthalocyanine (CoPc), a two-dimensional 18-π electron aromatic macrocycle with a Co atom located at the central cavity, has been intensively studied as an effective catalyst. CoPc is thermally and chemically stable, and cost-effective. Nitrogen doping has been an impressive way to modified the properties of graphene. Three prevalent bond in configurations are obtained when doping nitrogen on to the graphene (NG) pyridinic N, pyrrolic N and graphitic N. (CoPC) and NG sheets can be subsidized with arranged optoelectronic properties. The interaction between phthalocyanine. Reduced graphene oxide (RG), obtained by reduction of graphene oxide (GO), displays unique electrical and electrochemical properties that make it an ideal host for

CoPc complexes. Exfoliated GO is an atomically thin sheet of covalently bonded carbon decorated with oxygen containing functional groups (hydroxyl, epoxide, carbonyl and carboxyl). Compared with GO, RG and NG shows some impressive properties that make it an amazing support for improvement of disparate surface of CoPc catalyst. In this work CoPc will be loaded on to GO, NG and RG activity for degradation of dichlorophenol (DCP) as an organic pollutant will be studied under light visible.

2. Experimental Part

Graphene oxide was prepared by the modified Hummer's method by the oxidation of natural graphite flakes.

Annealing mixture of GO: melamine was carried out in a homemade tube furnace in the vicinity of inert gas to prepare NG.

RG was prepared by reduction of GO with hydrazine hydrate was added to GO aqueous suspension (3 mg/mL). it was heated in an oil bath at 80 °C for 10h. The RG precipitate was filtration and washed several times with water and methanol, after that dried in an oven at 60 °C.

For preparing CoPc/GO, CoPc/RG and CoPc/NG nanocomposite: designated amount of CoPc was added into the mixed solvent containing 2 g $AlCl_3$ and 100 mL acetone and then the mixture was stirred for 2 h after that adding of 1 g GO. The stirring mixture was then stirred at 60 °C until the solvent was evaporated. The powder obtained was washed with water.

3. Results and discussion

The XRD patterns of GO and the NG are shown in Fig. 1. A characteristic diffraction peak of GO was observed at 2θ=11.4, corresponding to an interlayer distance of 0.76 nm. On the other hand, the basal reflection peak of GO disappeared in the XRD pattern of the NG due to the exfoliation of graphene sheets during the thermal annealing process. Interestingly, the basal reflection peak of GO shifted to 2θ=25.3 in the NG.

The existence of Co in our composite can be confirmed by the EDX spectra, as shown in Table 1. The SEM images of CoPc/NG compound exhibit the typical silklike wrinkled flakes, thin and random NG sheets; the nanosheets are twisted and crumpled in an agglomerated phase as shown in Fig. 2. All these results clearly indicate the successful synthesis of CoPc/GO and CoPc/NG.

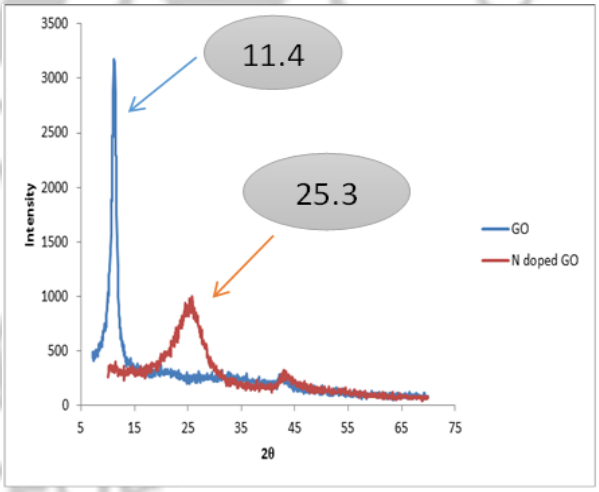

Figure 1. XRD patterns of NG and GO

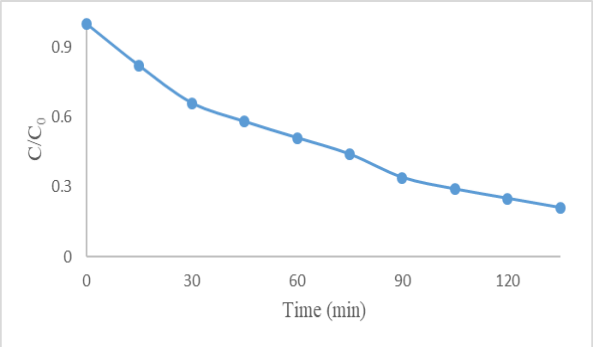

Figure 3. Degradation of DCF under visible light irradiation with CoPc/NG

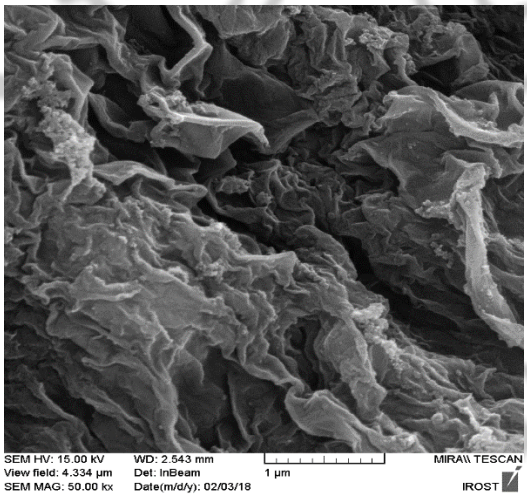

Figure 2. SEM image of CoPc/NG

To optimize the content of CoPc in NG different amount was used. The bare CoPc/NG nanocomposites were evaluated by the degradation of DCP in water under visible light. as shown in Fig. 3.

Table 1. Elemental analysis

	CoPc/GO		CoPc/NG	
Element	%W	%A	%W	%A
C	27.67	34.07	60.48	66.25
O	66.69	61.66	15.83	13.02
N	3.55	3.74	21.57	20.26
Co	2.10	0.53	2.13	0.48

.

Conclusions

The Photocatalytic activity of CoPc/NG was evaluated. The degradation efficiency of dichlrophenol DCP under visible light irradiation was about 80% within 135 min using CoPc/NG

Acknowledgments

We gratefully acknowledge the Research Department of University of Guilan for supporting this work.

References

[1] M. Mukherjee, U.K. Ghorai and et al. *Appl. Surf. Sci.* 418 (2017) 156-162.

[2] Q. Wang, H. Li and et al. *Appl. Catal. B. Environ.* 192 (2016) 182-192.

[3] P. Kumar, A. Kumar and et al. *Chem. Eur. J.* 20 (2014) 1-9.

[4] H. Wang, T. Maiyalagan, X. Wang, *ACS Catal.* 2 (2012),781-794.

[5] Z. Sheng, L. Shao, J. Chen, W. Bao, F. Wang, and X. Xia, *Am. Chem. Soc*. 5 (2011) ,4350–4358.

5th Iran International Zeolite Conference

University of Tabriz, Tabriz, Iran

26-27 August 2018

Synthesis of Zeolite NaY from Rice Husk Ash with Ultrasound Aging and Conventional Aging

M. askari[a], E. Aghaei[a], R. Karimzadeh[a]*

[a] *Department of chemical engineering, Faculty of chemical engineering, Tarbiat Modares University, Tehran, Iran*

**Corresponding author: ramin@modares.ac.ir*

Abstract: In this research, zeolite NaY was synthesized using extracted silica from rice husk ash as silica source and hydrothermal method. The synthesis of this type of zeolite was done by hydrothermal and ultrasound pretreatment prior hydrothermal methods. The properties of the synthesized zeolites were determined using XRD, FESEM analysis and their performance was investigated in the catalytic cracking of heavy hydrocarbon in a fixed bed reactor. The products properties were determined using SIMDIS analysis and also density, viscosity and refractive index of the products were ascertained. The results showed that the synthesized zeolite by ultrasound pretreatment prior hydrothermal method had approximately better catalytic performance because of the effect of these irradiations on the zeolite crystallinity and particles surface grooving. According to XRD results, the crystallinity of the synthesized zeolite by ultrasound pretreatment prior hydrothermal method was 21% greater than prepared sample using conventional hydrothermal method.

Keywords: Zeolite NaY; Rice Husk Ash; Ultrasound pretreatment.

1. Introduction

Rice husk ash (RHA) contains 87-97% of silica in a hydrate amorphous form which is good precursor for chemical synthesis involving silicate sources. Further, RHA can be used as an alternative source for active silica production. Zeolite NaY commonly applied as catalyst and adsorbents and play important role in petroleum and petrochemical industries[1]. Ultrasonic (UTS) energy can initiate reactions more easily[2]. UTS has been applied in crystallization because of its significant influence on the induction periods and nucleation[3].

2. Experimental Part

Rice husk was collected from a local rice mil and other chemicals were commercially available sodium hydroxide (Merck), sodium aluminate (BDH), Ammonium nitrate (Merck), Hydrochloric acid (Mojjalali).

RHA in amorphous phase was prepared by leaching rice husk with HCl acid and calcination. NaY zeolites were synthesized with two steps method shown in figure1.

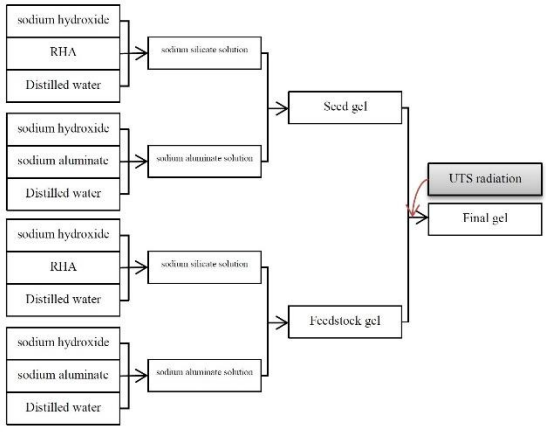

Figure 1. two step synthesis method

The sample crystallized at 102 °C for 24 hours. The final obtained product was filtered, washed and dried at 100 °C in an oven. The difference between two NaY zeolites preparation is in using ultrasound radiation. The delivered power of ultrasound waves was 250 W. Ion exchange was done with Ammonium nitrate for three times.

Catalytic performance of the synthesized zeolites were examined in the catalytic cracking of heavy hydrocarbon process in a fixed bed reactor.

3. Results and discussion

The products from both routes were characterized by XRD compared with the pattern of standard NaY. As shown in figure 2, all peaks in both routes were similar to those of the standard NaY. Thus, products contained NaY in pure phase. As shown in figure 2, NaY zeolite that synthesized with ultrasond radiation has sharper peaks than the other one. The synthesized sample by conventional hydrothermal method has lower crystallinity.

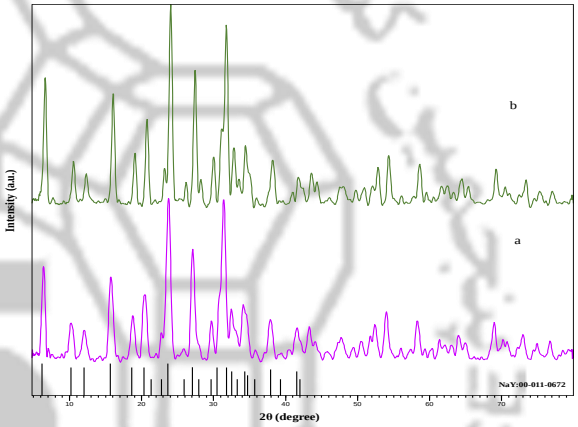

Figure 2. XRD pattern of synthesized zeolites in hydrothermal(a) and hydrothermal using UTS methods(b)

The FESEM images of both synthesized NaY is shown Figure 3. As shown in Figure 3, the particle size distribution is approximately the same. Apparently, some of the crystals have been intermixed and created agglomerated particles, which can indicate the growth of the crystal layer on each other. There are more grooves on the surface of synthesized zeolite using UTS radiation that can increase feed molecules availability to catalytic active sites. Results of the SIMDIS analysis, Boiling points, Density, Viscosity and Refractive Index are shown in table 1. Regarding the results of these

analyses it can be said that the C12 and lower values are related to the gasoline range. The gasoline cut is 27.346% for feed and in the products which obtained from catalytic cracking process in the presence of hydrothermal using UTS and hydrothermal synthesized zeolites are 49.378% and 50.552% respectively.

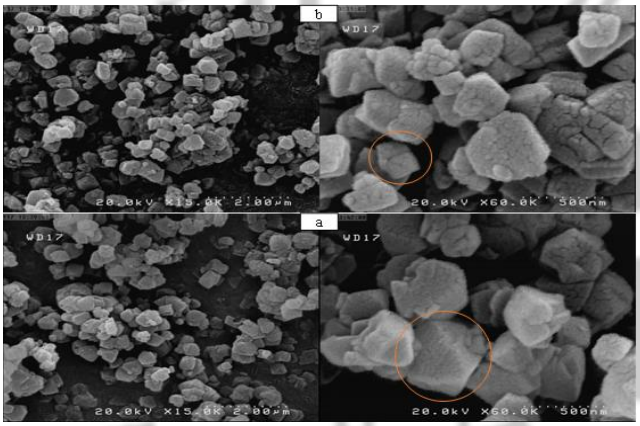

Figure 3. FESEM pattern of synthesized zeolites in hydrothermal(a) and hydrothermal using UTS methods(b)

Table 1. SIMDIS, Boiling point, Viscosity, Density and Refractive Index in hydrothermal(a) and hydrothermal using UTS methods(b)

	feed	Product obtained from type a zeolite	Product obtained from type b zeolite
Boiling Point □C	115.7	29.2	29.6
C12 %	27.364	50.552	49.378
Density (gr/ml)	0.86886	0.8508	0.85005
Viscosity (cst)	1.85	1.13	1.08
Refractive Index	1.479	1.483	1.481

4. Conclusions

RHA used as a silica source for the synthesis of NaY zeolite. The NaY in pure phase was obtained in two hydrothermal and hydrothermal using UTS radiation routes. Their performance were examined in the process of catalytic cracking of heavy hydrocarbon in a fixed bed reactor. The crystallinity of the synthesized zeolite by hydrothermal using ultrasonic method was 21% greater than hydrothermal synthesized zeolite crystallinity.

References

[1] W. Tan, S.Yap, A. Matsumoto. *Adsorption*, 17 (2011) 863-868.

[2] S.S. Bukhari, S. Rohani, H. Kazemian, *Ultrason. Sonochem.* 28 (2016) 47-53.

[3] S. Askari, S. Alipour, R. Halladj, *J. Porous Mat.* 20 (2013) 285-302.

5th Iran International Zeolite Conference

University of Tabriz, Tabriz, Iran

26-27 August 2018

Preparation of Mesoporous Nano-Silica (MNS) as Adsorbent

J. Rahimpour*, M. H. Alibenhamid, A. Z. Aroguz

Department of Chemistry, Faculty of Engineering, İstanbul University, Avcilar, İstanbul, Turkey

**Corresponding author: jenipiano76@yahoo.com*

Abstract: There is big potential of the applications of Mesoporous Nano-Silica (MNS) materials on the adsorption process. In current study, Mesoporous Nano-Silica (MNS) has been successfully synthesized and used as adsorbent to remove dye from aqueous solution by adsorption process. The effect of the initial concentration of the solute, amount of the adsorbent and solution pH wasinvestigated. The pseudo-first-order and second-order-kinetic models were applied to the experimental data in order to investigate the adsorption kinetic. Langmuir, Freundlich, Temkin isotherm models were used to investigate the nature of the adsorption. The results indicated that the multilayer adsorption has been achieved. The structure of the mesoporus adsorbent was analyzed using SEM and FTIR.

Keywords: Mesoporous Nano-Silica; Adsorption; Isotherm; Kinetic; Dye

1. Introduction

Over the last decade many researches were studied on mesoporous materials due to their wide range of applications as adsorbent. Because their controlled structure has excellent properties such as adjustable nanopore sizes, high specific surface areas, large pore volume, and hydrophilic surface feature [1]. Studies on the synthesis of novel controlled mesoporous materials and investigation of reaction mechanisms have gained great attention [2].

With the increase in industrialization, the production of new materials has also revealed new environmental pollution with huge amount of wastes. These wastes cause very serious environmental pollution. Discharging of dyes from these industries to the aquatic medium is also responsible for this environmental pollution. In addition to their toxic nature and the resistivity properties, dyes damage the liver and nervous system when breathing as well as irritate the skin and the eyes [3]. They prevent sunlight from reaching into water. As a result of this, photosynthesis in aquatic medium does not occur.

For all these reasons, it is necessary to remove dyes before or after released into the environment. Adsorption technique is one of the best methods to remove dyes from aqueous solution.

2. Experimental Part

Mesoporous Nano-Silica (MNS) adsorbent with high pore size and high surface area was simply synthesized by stirring TritonX-100 and Tween 80 in distilled water at 40 °C until to get a clear solution of the mixtures. First TEOS, then sodium fluoride was added to the solution drop by drop. The resulting products were recovered by filtration, then washed repeatedly with water and dried overnight at room temperature. The materials were calcined at 450 °C for 5 h at a heating rate of 1 °C/min. [3,4]

The calcined products were used as adsorbent. The efficiency of swelling properties of the substances prepared in this work was measured by tea bag procedure. The maximum swelling was obtained 6-8 times more comparing with the dry sample after 90 minutes. 50, 100, 150, 200 ppm methyl blue dye solutions prepared and their adsorptive capacities on the MNS were researched. The adsorption was followed by using UV-VIS spectrophotometer at 600 nm wavelength.

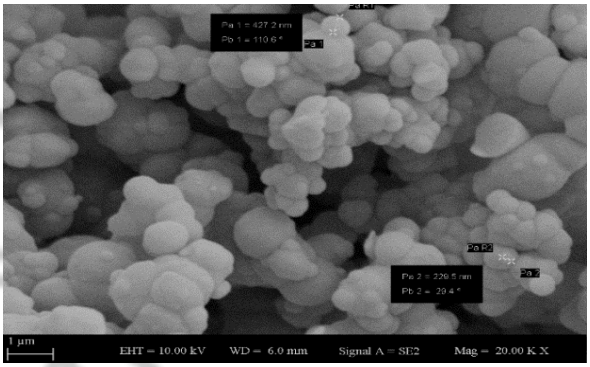

Figure 1. SEM results of TWN80 before calcination.

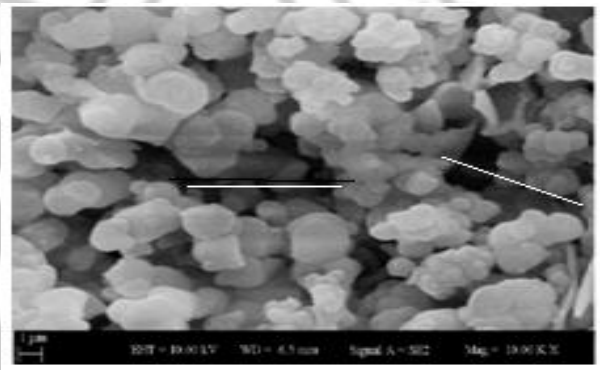

Figure 2. SEM results of TWN80 after calcination.

3. Results and discussion

The morphologies of the mesoporous adsorbent before and after calcination process are shown in Fig. 1 and Fig. 2.

SEM results of TWN80 show that porous size after calcination become bigger and related to the mesoporous particles size. FTIR results of the samples are shown in Fig.3 and Fig4.The results show that the calcination procedure did not destroy the samples but it was helpful to obtain mesoporous structure.

The maximum percentage of adsorption was found to be 81.5% for 200 ppm concentration. The percentage of adsorption increases as the concentration of the dye increases (Fig.5). The adsorption took place very quickly in the first two hours and then reached equilibrium. The increasing of the initial concentration of solute in the solution causes to increase the number of collisions between the adsorbent and the dye molecules.

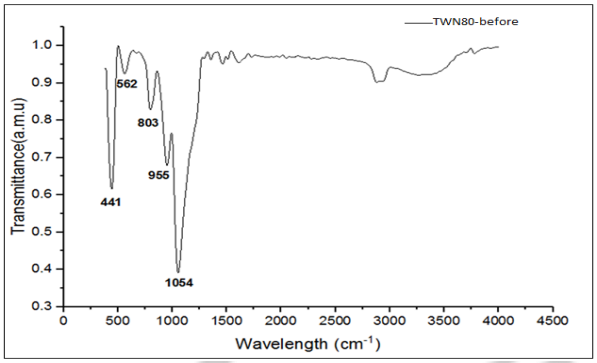

Figure 3. FT-IR of TWN80 Before calcination.

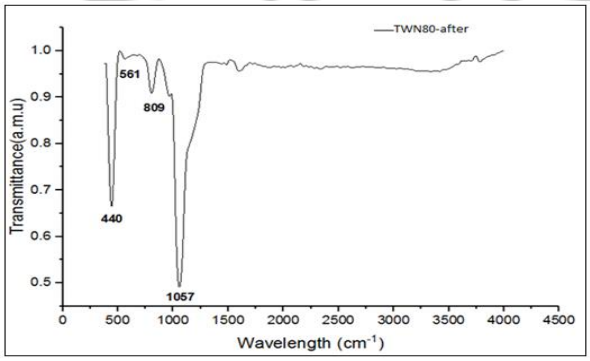

Figure 4. FT-IR of TWN80After calcination.

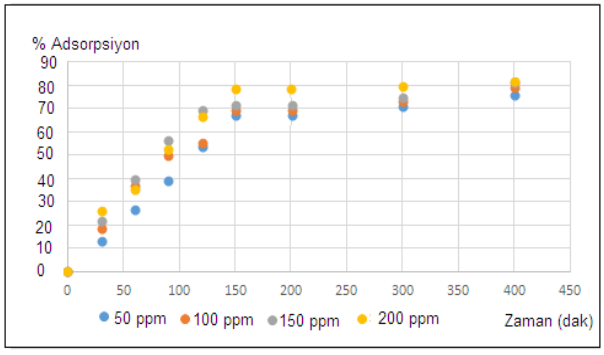

Figure 5. The uptake percentage of dye.

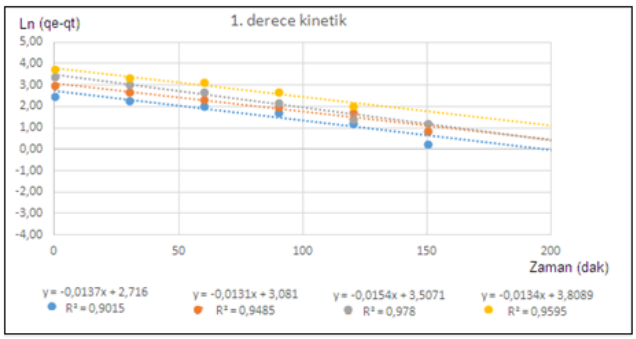

Figure 6. Lagergren first order kinetic.

From the R^2 values it can be concluded that the adsorption followed first order kinetic. The experimental and theoretical q_e values also support these results. Fig. 6 Indicates the first order kinetic is suitable for the adsorption process.

4. Conclusions

Mesoporous Nano-Silica (MNS) has been successfully synthesized as an adsorbent for dye adsorption. The suitability of Langmuir and Freundlich isotherm models for adsorption was investigated using data obtained from adsorption of methyl blue dye. It has been seen that adsorption is multi-layer and follows first order kinetic model. It was found that the mesoporous materials prepared in this study can be used effectively in the adsorption process.

Acknowledgments

This work was supported by the Research Fund of the Istanbul University. Project number: BAP 55992.

References

[1] R. Saeedirad, S. TaghvaeiGanjali, M. Bazmi, A.M. Rashidi, *J. Taiwan Inst. Chem. E* 82 (2018) 10-22.

[2] P.N.E. Diagboya, E.D. Dikio, *Micropor. Mesopor. Mater.* 266 (2018) 252-267.

[3] Y. He, L. Luo, S. Liang, M. Long, H. Xu, *J Colloid Interfac. Sci*. 525 (2018) 126-135.

[4] A.Z. Aroguz, *J. Hazard. Mater.* 135 (2006) 100-105.

5th Iran International Zeolite Conference

University of Tabriz, Tabriz, Iran

26-27 August 2018

Synthesis of Mesoporous Superparamagnetic Ferrite Nanoparticles (Fe_3O_4) Using Lyotropic Liquid Crystal Phase Templates

S. Fallah [a], F. Nasirpouri [a,*]

[a] *Faculty of Materials Engineering, Sahand University of Technology, Tabriz, Iran*

**Corresponding author: nasirpouri@sut.ac.ir*

Abstract: Mesoporous ferrite nanoparticles were synthesized by ultra-sonic assisted co-precipitation of iron chloride salts dissolved in aqueous domains of lyotropic liquid crystalline phases of cetyltrimethylammonium bromide (CTAB) surfactant. Microstructure, morphology, size distribution, porosity and magnetic behaviour of synthesized nanoparticles in deferent concentrations of the surfactant were studied. The liquid crystalline templates and the superparamagnetic mesoporous ferrite nanocrystals were characterized by X-ray diffraction (XRD) and field emission scanning electron microscopy (FESEM). Barrett-Joyner-Halenda (BJH) method analysis was used to indicate the pore width and Brunauer-Emmett-Teller (BET) helped to indicate the specific surface area of mesoporous ferrite nanoparticles (Fe_3O_4) exhibiting a surface area up to 105 m^2/gr giving rise to an average pore size of 14 nm. Rietveld refinement results show 75 % of synthesized powder is Fe_3O_4 and the rest about 25 % is ϒ-Fe_2O_3.

Keywords: “Superparamagnetic”; “mesoporous”; “ferrite”; “nanoparticles”

1. Introduction

Nanoscale mesoporous magnetic materials are a new class of advanced materials that receive much attention for different applications such as pollution abatement, drug delivery and targeting and sensing. The properties of these materials are extremely dependent on the shape, size, and structure of mesoporous.

Auvray et al. [1] and Luigi [2] have studied different lyotropic crystalline phase of CTAB. Above a critical micellar concentration (CMC), micelles begin to form. By increasing the surfactant concentration, the micelles transition from the spherical shape into rod-like, and then hexagonal (H1), monoclinic, cubic with symmetry Ia3d, layer I and layer II. Micelles were formed below the 20% CTAB; hexagonal shapes between 20 to 77% and other structures are possible above 77%.

2. Experimental Part

Mesoporous ferrite powder was obtained by mixing Iron (II & III) chlorides ($FeCl_3.6H_2O$, 97%, Mw = 270.29 gr/mol; FeCl2, 99%, Mw = 129.7 g/mol) in

ethanol (ration Fe^{2+}/Fe^{3+} = 2) at 70℃. CTAB (Mw = 364.46 g/mol, Sigma–Aldrich) solution was prepared by dissolving different fractions of CTAB in 180 mL ethanol and deionized water at 70℃ including 0, 3 and 15%. While mixing, 2M NaOH (95%, M=40.00 gr/mol) solution was added drop-wisely. Suspension's color changed to black. Then, the suspension was sonicated for 3h. Finally, synthesized nanoparticles were centrifuged, filtered and washed several times with deionized water.

Fourier-transform infrared spectroscopy (FTIR) spectra were taken with a TENSOR 27 (Brucker) FT/IR-4000 apparatus XRD. XRD patterns of the prepared samples were acquired with a Bruker D8-ADVANCE X-ray diffractometer using CuK, radiation (40 kV, 300 mA). XRD patterns were refined by Maud. Nitrogen adsorption/desorption measurements at liquid nitrogen temperature (77K) were taken with a BEL BELSORP MINI II apparatus. Prior to the measurements, the samples were degassed for 3 hours at 150℃ with BEL PREP VAC II.

Table 1. BET surface area and BJH size distribution

Sample	CTAB %	a_{BET} (m^2/gr)	r_{BJH} (nm)	Calcination time (hr.)
1	0	15.92	25	0
2	3	105.93	14	24
3	15	78	1.72	24

BET isotherms and BJH pore size distributions are shown in Fig. 1.

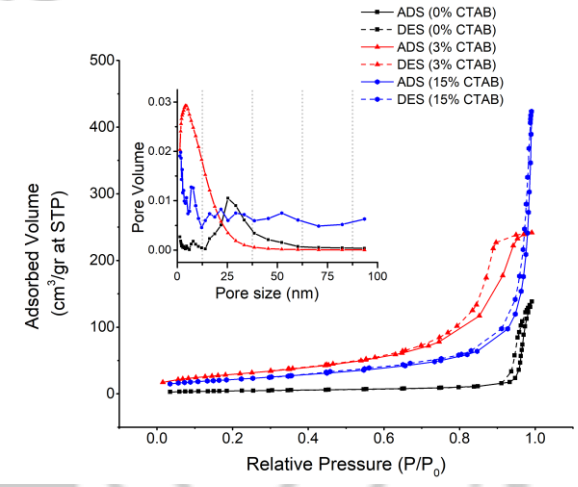

Figure 1. Nitrogen adsorption/desorption isotherms for synthesized Fe_3O_4 with 0, 3 & 15% CTAB and BJH pore distribution.

FESEN images of prepared Fe_3O_4 is shown in Fig. 2.

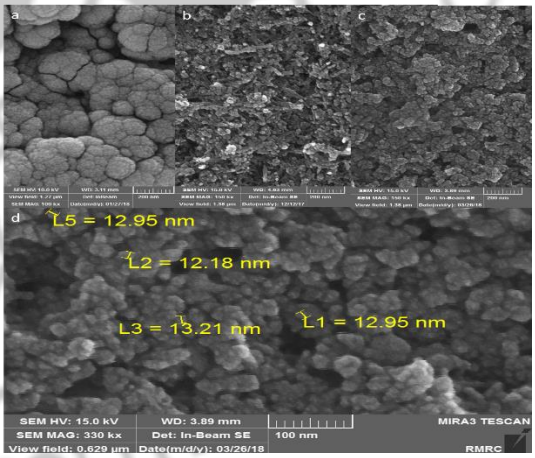

Figure 2. FESEM images of synthesized ferrite with a: 0 %CTAB, b: 15 % CTAB and c, d: 3 % CTAB.

3. Results and discussion

Isotherm shows in Figure 4 is a typical type IV adsorption-desorption isotherm with H1 hysteresis. That shows mesoporosity with cylindrical pores. BET results are summarized in Table 1. As you see the surface area in sample 3 is less than sample 2 with 3% CTAB, we think it's because of incomplete extraction.

As you see in Fig. 2d average particle size of prepared powder is 13 nm.

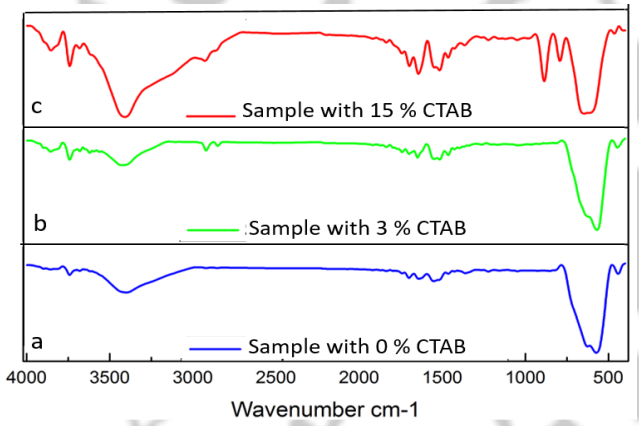

Figure 3. FT/IR spectra of Fe sample: (a) 0% CTAB, (b) 3 %CTAB (c) 15 % CTAB.

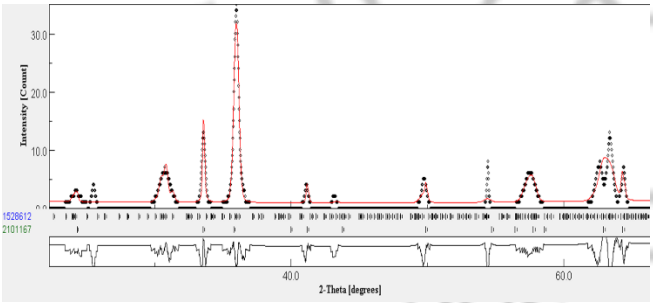

Figure 4. Rietveld refined XRD pattern of as-prepared iron oxide powder. Major reflections from Fe_3O_4, γ-Fe_2O_3 and phases are indexed.

FTIR spectra of the sample with 15 % CTAB shows wide hydrogen band indicating that CTAB extraction is not complete.

In Figure 4 it can be seen that about 75 % of the XRD sample is Fe_3O_4 and the other 25 % is Υ-Fe_2O_3 (magnetite).

4. Conclusions

The sonochemical method for the preparation of Fe_3O_4 has been reported. The iron oxide has good magnetic properties. The surface area of the material has been found to be higher after extraction of surfactant with deionized water. The extracted iron oxide has shown excellent catalytic properties.

References

[1] X. Auvray, C. Petipas, R. Anthore, I. Rico, A. Lattes, *J. Phys. Chem.*, 93 (1989) 7458–7464.

[2] L. Coppola, R. Gianferri, I. Nicotera, and C. Oliviero, *Phys.Chem.*, 6 (2004) 2364–2372.

5th Iran International Zeolite Conference

University of Tabriz, Tabriz, Iran

26-27 August 2018

Synthesis of Zeolite from Coal Waste Ash by Hydrothermal Method using Alkaline Source

R. Gholinejad, E. Kamali*, J. vahdati, S. Mollazadeh

Department of Metallurgical and Materials Engineering, Faculty of Engineering, Ferdowsi University of Mashhad, Mashhad, Iran

**Corresponding author: elhamkamali@um.ac.ir*

Abstract: Coal mines and coal-fired plants produce huge amounts of waste and ash, which can be a serious threat to the environment. In this research, Coal waste from Agh Darband Coal Mine was converted to zeolite. For this purpose, the coal waste was first burnt at 1100 oC to produce ash. Then a hydrothermal method was applied to synthesize zeolite from coal waste ash. The hydrothermal treatment was carried out at 140 °C for different durations of 12, 18 and 24 hours in an aqueous NaOH solution. The chemical and structural properties of the synthesized material as well as its surface area was investigated using X ray florescence (XRF), X ray diffraction (XRD) and BET techniques. The results confirmed the successful synthesis of zeolite, which mainly consisted of Na-P type and ANA (Analcime) type zeolites. The BET studies revealed a considerable increase in the surface area from 1.25 $m^2 g^{-1}$ for coal waste ash to 55.73 $m^2 g^{-1}$ for the produced zeolite synthesized at optimum conditions.

Keywords: Zeolite; Ash coal; Analcime; Na-P; Hydrothermal

1. Introduction

In many countries, the power plants are dependent on the coal combustion energy, which results in enormous amounts of residual ash, not only occupying vast areas of the land but also scattering in the atmosphere [1-3]. Nowadays, different strategies are applied not only to reduce the environmental impacts of coal wastes and ash, but also to make an economic profit out of them [4]. Its conversion to novel nanomaterial such as zeolites is also another strategy that has gained enormous attention in the last decades [3]. Owing to their microporous structure as well as ion exchange capability, Zeolites are good candidates in applications such as catalysis, absorbent materials, molecular sieves and ion exchange materials [5]. Alumina silicate in coal ash is an ideal source of Si and Al for the synthesis of zeolites. One of the main methods for synthesizing zeolite is the hydrothermal method, which, along with the source of coal and burning conditions, determines the type of zeolite produced [6].

2. Experimental Part

The as received coal waste was first dried and then milled in a low energy ball mill for 1h in with ball to powder ratio of 10. The milled powder was sieved to particle size range of 53 to 74 microns. Finally, the ash was prepared by heating the coal powder at 1100 °C for 4 hours in air atmosphere. A facile one pot hydrothermal method was used to synthesize zeolites from coal ash. First, 3g of the prepared ash was added to a 1.5 M NaOH aqueous solution and kept under vigorous stirring for 2 hours at room temperature. The mixture was then transferred into a Teflon lined stainless steel autoclave and heated at 140 °C for different durations of 12, 18 and 24 h.

3. Results and Discussion

The two exothermic peaks at the temperature ranges of 450-600 °C and 900 °C are the consequence of decomposition of carbon and volatile content, respectively.

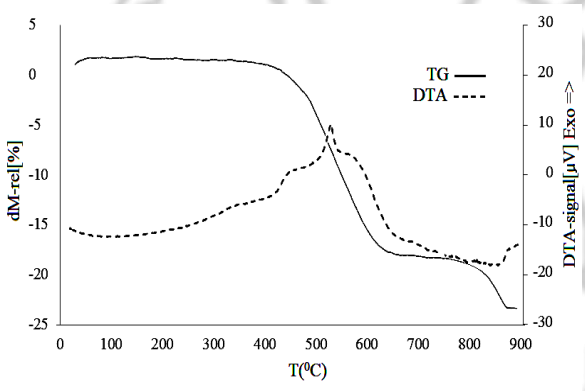

Figure 1. TG- DTA data curves of coal waste.

The chemical composition of the prepared ash was measured using XRF and is shown in Table 2. The results show that our ash prepared from waste coal has a chemical composition very similar to the coal driven fly ashes reported in the literature.

XRD pattern of the prepared ash is shown in Fig. 2 a. The peaks are mainly related to quartz and mullite crystalline phases. 12 h of hydrothermal treatment resulted in disappearance of the mullite and quartz crystalline phase peaks, while an amorphous background was observed along with relatively weak crystalline peaks. (Fig. 2b) were characteristics of Na-P type zeolites. Corresponding to ANA type zeolite (analcime).

Table 1. BET test for: Ash, Z12h (synthesized zeolite 12h, 1.5M), Z18h (synthesized zeolite 18h, 1.5M), Z24h (synthesized zeolite 24h, 1.5M).

sample	S_{BET} /(m^2g^{-1})	Pore V/(cm^3g^{-1})	V_m /(m^3g^{-1})
Ash	1.25	0.0067	0.28
Z12h	26.67	0.06	6.14
Z18h	55.73	0.17	1280
Z24h	19.68	0.09	4.52

Increasing the hydrothermal time to 18 h, resulted in higher crystallinity of the XRD patterns (Fig. 2c), with sharper peaks of both Na-P and ANA type zeolites. Finally, the long duration of 24 h, led to a fully crystalline zeolite, with mainly ANA type crystal structure. According to the XRD studies, it can be concluded that, during the hydrothermal treatment in

NaOH solution, the Mullite and Quarts crystalline phases in the ash, dissolved and re-nucleated by making Al-O-Si bonds. Furthermore, the Na^+ ions, also occupied the octa/tetrahedral spaces, resulting in a neutral zeoliteic material. The surface area, pore volume and mean pore size of the prepared ash, and synthesized zeolites, were also measured using BET and the results are presented in table 1. The BET measurements showed that the prepared ash had a very small specific surface area of 1.25 $m^2.g^{-1}$ while the hydrothermal treatment could successfully increase this surface area for 15 to 45 fold. The powders synthesized at 12, 18 and 24 h had specific surface areas of 26.7 and 55.7 and 19.68 m^2g^{-1} respectively. The pore volume also increased from 0.007 in ash to 0.06, 0.17 and 0.09 cm3g-1 after 12, 18 and 24 h respectively. These findings, suggest that 18h is the optimum hydrothermal durations.

Table 2. The Chemical composition of the prepared ash.

Comp.	Wt%	Comp.	Wt%
SiO_2	54.92	MnO	0.11
Al_2O_3	27.73	CaO	4.85
Na_2O	0.76	P_2O_5	0.15
MgO	0.88	Fe_2O_3	8.24
K_2O	1.02	SO_3	0.05
TiO_2	0.88	LOI	0.24

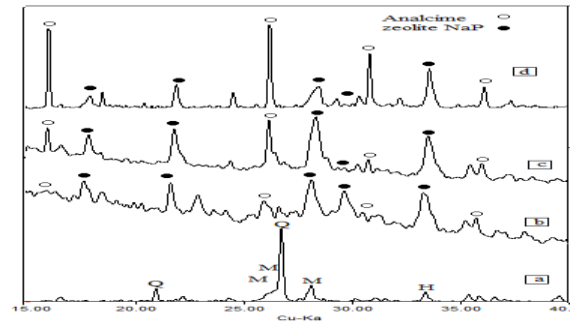

Figure 2. XRD patterns of (a) the prepared ash; and the synthesized products at different hydrothermal durations of (b) 12h, c)18h, d)24h; (Q: quartz; H: Hematite; M: Mullite).

4. Conclusions

In this paper, zeolite was directly synthesized from coal waste ash with a simple hydrothermal treatment. According to XRD studies, the hydrothermal treatment led to formation of Na-P and ANA type zeolites and an increase in the synthesis duration at NaOH concentration of 1.5 M, resulted in a decrease in Na-P and an increase in ANA type zeolites. The BET measurements showed that the synthesized zeolite at duration of 18h had the highest surface area of 55.7 m^2g^{-1}, which was 45 times higher than the starting ash.

References

[1] V.K. Jha, M. Nagae, M. Matsuda, M. Miyake, *J. Environ. Manage.* 90 (2009) 2507-2514.

[2] S.S. Rayalu, A.K. Bansiwal, S.U. Meshram, N. Labhsetwar, S. Devotta, *Catal. Surv. Asia* 10 (2006) 74-78.

[3] P. Solanki, V. Gupta, R. Kulshrestha, *J. Chem.* 7 (2010) 1200-1205.

[4] A. Modarres, M. Rahmanzadeh, *Constr. Build. Mater.* 66 (2014) 476-483.

[5] S. Malamis, E. Katsou, *J. hazard. Mater.* 252 (2013) 428-461.

[6] O.B. Kotova, I.N. Shabalin, D.A. Shushkov, L.S. Kocheva, *Adv. Appl. Ceram.* 115 (2016) 152-157.

5th Iran International Zeolite Conference

University of Tabriz, Tabriz, Iran

26-27 August 2018

Cooperative catalytic performance of SBA-15 and TFE in selective oxidation of sulfides

H. Mohtasham, A. Ahadi, S. Rostamnia *

Organic and Nano Group (ONG), Department of Chemistry, Faculty of Science, University of Maragheh, PO BOX 55181-83111, Maragheh, Iran. Email:srostamnia@gmail.com;

Hamed Mohtasham1372@gmail.com;

Abstract: In this paper, trifluoroethanol (TFE) was confined into SBA-15 and compared with its similar non-fluorous systems in the metal-free oxidation of sulfides to sulfoxides in the presence of H_2O_2. This catalytic system successfully performed the oxidation and also showed superior activity to the other non-fluorous versions.

Keywords: Trifluoroethanol (TFE), SBA-15, Hydrogen peroxide, Oxidation, Sulfoxide.

1. Introduction

Fluorine atom on the organic compounds can influence the physicochemical properties [1]. Fluorine on the alcohols can denote a different feature which can be utilized for many applications such as the catalyst and solvent [2]. In our previous developed synthetic methods for the synthesis of organic polar molecules using SBA-15 family catalysts [3]. The big challenge was the mass transfer of organic substrates into the SBA-15 pores as a catalyst center [5]. Hence we aimed to examine the catalytic activity of trifluoroethanol (TFE) confined SBA-15 nanoreactor in the oxidation reaction of sulfides to sulfoxides owing to cooperative catalytic activity of SBA-15 with TFE. Sulfoxides are pharmaceutically active and valuable intermediates in the synthesis of bioactive compounds [6]. However, our proposed catalytic system for the oxidation of sulfides has surpassed these methods and these drawbacks are resolved.

2. Experimental Part

For the synthesis of SBA-15 [4–6], triblock copolymer surfactant of P123 as a template (4.0 g) was dissolved in H_2O (30 mL) and 2 M HCl (120 g). Then, tetraethyl orthosilicate (TEOS, 9 g) was added to mixture, which was stirred for 8 h at 40 ℃. The resulting mixture was transferred into a Teflon-lined stainless steel autoclave and kept at 100 °C for 20 h. After cooling, to room temperature, the product was filtered, washed with water and dried overnight at 70 °C in air. The sample was then raised to a temperature of 500 °C in the rate of 2 °C/min to remove the template by calcination method.

3. Results and discussion

When TFE was confined into the pores of SBA15, a remarkable change happens in the FT-IR spectrum of SBA-15 away from related bands of own TFE. According to this observation, a remarkable interaction between TFE and SBA-15 is predictable (Scheme 1).

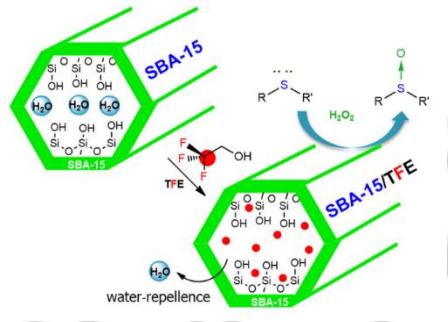

Scheme 1. Schematic illustration for the preparation of SBA-15/TFE.

Diffraction peaks at below 28 corresponding to the (100), (110), and (200) are readily recognized from the XRD pattern of SBA-15 (Fig. 2). The observed diffraction peaks agree with the 2D hexagonal SBA-15. The stability and integrity of the SBA-15/TFE under the reaction conditions and after reuse were also investigated. The XRD patterns of both the fresh and reused catalysts (Fig.1 a and b) indicate that just a small change occurred for SBA-15 in its mesoscopic structure during the reaction and the recycling stages. Fortunately, the progress of reaction that is not affected by this small distortion recyclability of the catalyst is still reinforced. SEM and TEM images of the catalyst indicate its mesostructured and surface morphology which demonstrate the structure of SBA-15/TFE (Fig. 1).

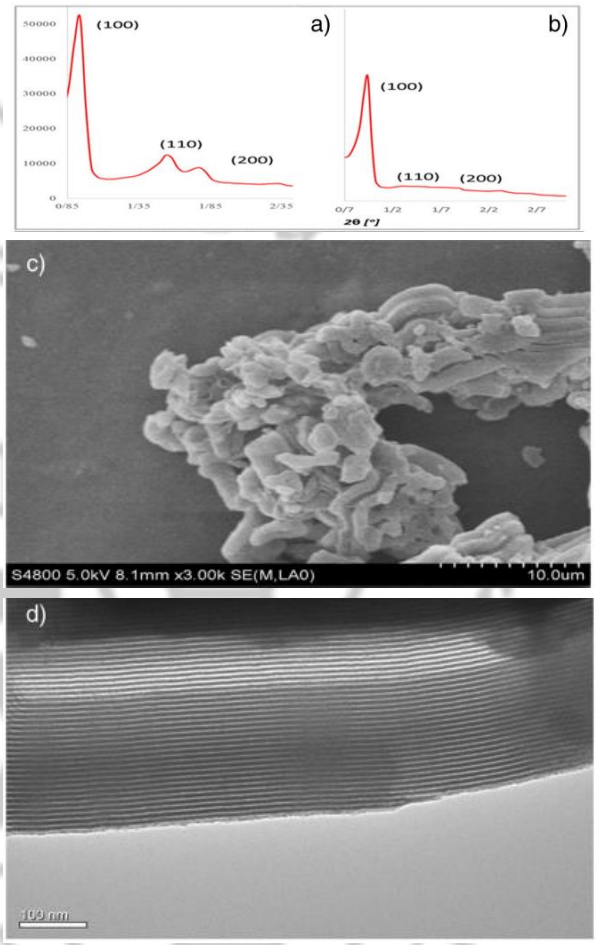

Figure 1. Characterization of SBA-15/TFE for its (a, b) low angle XRD pattern - newly prepared, and after 10 runs, respectively, (c, d) TEM and SEM images, respectively.

Thus, after sufficient studies for the optimization of the selective oxidation of sulfides to sulfoxides, it was extended to the other derivatives of sulfides and results obtained from the derivatives are depicted in Table 1. The optimized conditions in this work assigned room

temperature with 0.02 g of SBA-15 and 3 mL TFE in each mmol of sulfide. The best ratio for the amount of H_2O_2 was also 4 eq (30% wt) for each equivalent of sulfide.

Table 1. Optimization reaction conditions for the oxidation of sulfides. [a]

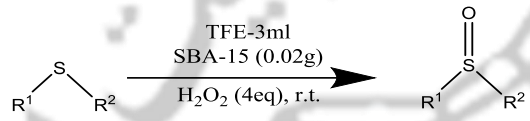

Entry	R^1	R^2	Time (min)	Yield (%)[b]
1	Ph	$PhCH_2$	50	98
2	Ph	Ph	60	85
3	4-Br-C_4H_4	$phCH_2$	30	95
4	Ph	Me	35	98
5	Ph	2-Py	30	98
6	3-MeO-C_4H_4	3-NO_2-C_4H_4	30	95
7	Ph	3-MeO-C_4H_4	40	95
8	3-MeO-C_4H_4	3-MeO-C4H4	60	90
9	$PhCH_2$	$PhCH_2$	20	98
10	4-Br-C_4H_4	4-MeO-C_4H_4	30	95

[a] Reaction condition: sulfide (1 mmol), H_2O_2 (4 mmol), TFE (3 ml).
[b] Yields based on GC analysis.

In order to study the recyclability of combined catalytic system, both SBA-15 and TFE were separated from reaction mixture and reused for the next runs.

4. Conclusions

In summary, a facile catalytic system was proposed by our studies in this work for the oxidation of sulfides. Moreover, we found that the confinement of TFE into the SBA-15 pores caused an increase in the rate of mass transfer through activation by removal of water. SBA-15/TFE can also as an acidic media to accelerate the oxidation reaction. Ease of work-up, recyclability, and chemoselectivity towards sulfoxides were also the other scopes of this catalytic system.

References

[1] B.E. Smart, *J. Fluor. Chem.* 109 (2001) 3–11.

[2] A. Dandia, R. Singh, J. Joshi, S. Kumari, *J. Fluor. Chem.* 156 (2013) 283–289.

[3] S. Rostamnia, H. Xin, *Appl. Organomet. Chem.* 27 (2013) 348–352.

[4] S. Rostamnia, H. Xin, X. Liu, K. Lamei, *J. Mol. Catal. A Chem.* 374–375 (2013) 85–93.

[5] S. Rostamnia, E. Doustkhah, A. Nuri, *J. Fluor. Chem.* 153 (2013) 1–6.

[6] M.C. Carreno, *Chem. Rev.* 95 (1995) 1717–1760.

5th Iran International Zeolite Conference

University of Tabriz, Tabriz, Iran

26-27 August 2018

SBA-15/SO_3H nanoreactor and ultrasonic combination as a novel, ultra-fast, waste-free green catalytic system

A. Ahadi, S. Rostamnia *

Organic and Nano Group (ONG), Department of Chemistry, Faculty of Science, University of Maragheh, PO BOX 55181-83111, Maragheh, Iran. Email:srostamnia@gmail.com; arefehahadi@yahoo.com;

Abstract: Sonicated catalytically amount of the SBA-15/SO_3H nanoreactor with organic substrate was found to be an efficient, ultra-fast and waste-free green approach for the synthesis of the α-amino phosphonates as models of organic reactions. The advantages of present combined method are the use of a low scale catalyst, simple procedure with an easy filterable work-up method, waste-free, green and direct synthetic entry to excellent yield of products in a high reusability and a short reaction time.

Keywords: Combined catalytic system (US/SBA-15), Ultrasonic irradiation, SBA-15/SO_3H, Green chemistry.

1. Introduction

Functionalized mesoporous silica with their nano-channels has shown catalytic performance because of their high surface area, low densities, high thermal and mechanical stability as a result of small nanoparticle sizes [1-2]. Incorporating the covalently bonded Bronsted sulfonic acid functionality into the SBA-15 mesoporous silicas (SBA-15/SO_3H) are of particular interest in organic synthesis, environmental chemistry and industry because of its high selectivity and high yielding abilities, and also heterogeneity and reusability capacities based on green chemistry desires [3]. As part of our ongoing program, we are interested in the development of efficient and environmentally benign methods in synthetic organic chemistry. Our aim has been to investigate designing of the catalyst and energy sources to accomplish the desired chemical transformations with minimum by-products or waste generation, as well as to decrease reaction time using ultrasound and porous catalysts Based on our earlier success in the green application of the ultrasonic in organic synthesis [4].

2. Experimental Part

All reagents were obtained from Merck (Germany) and Fluka (Switzerland) and were used without further purification. The IR spectra were determined using a FT-IR Bruker-Vector 22. Progress of reactions was monitored by Thin Layer Chromatography (TLC). ^1H and ^{13}C NMR spectra were measured ($CDCl_3$) with a Bruker DRX-300 AVANCE spectrometer at 300 and 75 MHz, respectively. Synthesis of SBA-15/SO_3H: The

synthesis of SBA-15-PrSO_3H has been achieved using three main steps: first step for preparation of the SBA-15 which known procedure described by Zhao et al. Second, which is thiol functionalization of the SBA-15 and third is oxidation of the SBA-15-Pr-SH to SBA-15-Pr-SO_3H by hydrogen peroxide (Fig. 1).

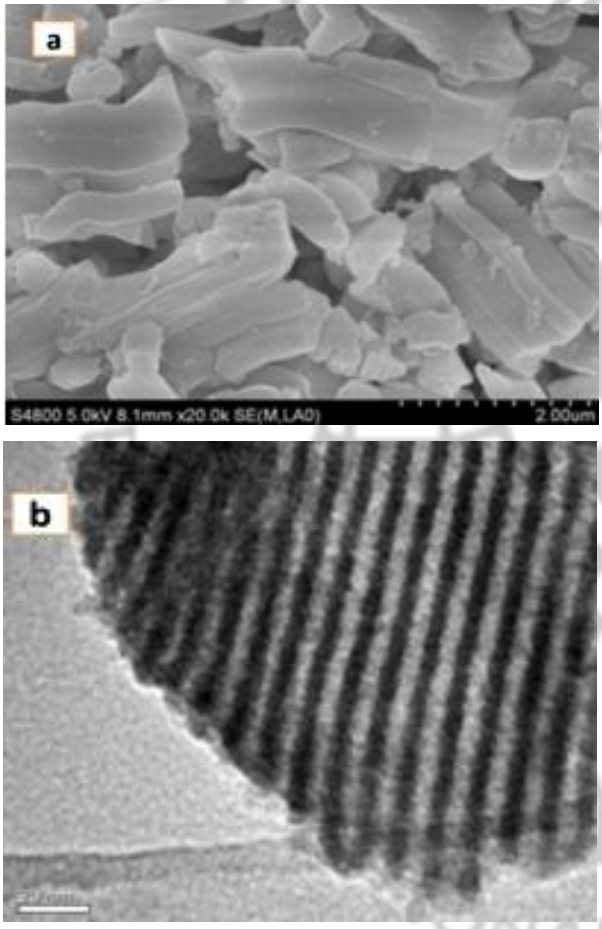

Figure 1. SEM (a) and TEM (b) images of SBA-15/SO_3H nanoreactor.

3. Results and discussion

Based on chemical and biological interests of phosphonates, the catalytic activity of the simultaneously application of SBA-15/SO_3H nanoreactor and ultrasonic irradiation as a combined catalytic system for three-component synthesis of α-amino phosphonates was studied. The reaction was set under the above optimized conditions at room temperature in EtOH medium (Table 1).

Table 1. Optimization of the reaction condition synthesis of α-amino phosphonates

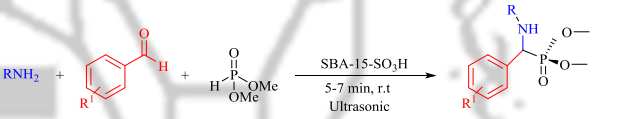

Entry	R^2_2NH	ArCHO	Time (h)	Yield [%]
1	$PhNH_2$	4-Cl-C_6H_4	5	95
2	$PhNH_2$	C_6H_5	5	94
3	$PhNH_2$	3-NO_2-C_6H_4	5	95
4	4-Me-$C_6H_4NH_2$	4-NO_2-C_6H_4	5	94
5	4-Me-$C_6H_4NH_2$	2-MeO-C_6H_4	4	94
6	4-Me-$C_6H_4NH_2$	3-NO_2-C_6H_4	5	95
7	Et_2NH	2-MeO-C_6H_4	4	9.

Reaction condition: aniline (1 mmol), benzaldehyde (1 mmol), dimethyl phosphite (1.2 mmol).

Although we have not established the mechanism of the simultaneously application of SBA-15/SO_3H and ultrasonic irradiation in an experimental manner, a possible explanation is proposed in Fig. 2. In this condition the irradiations of ultrasonic in presence of the SBA-15/SO_3H provide a synergistic means to input

the reactants and also drive out the products for next recycles.

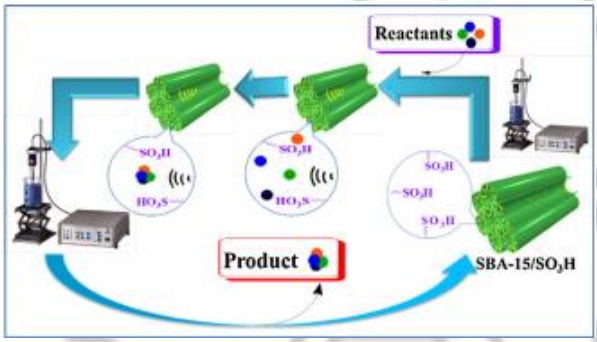

Figure 2. Possible explanation for SBA-15/SO_3H and ultrasonic irradiation catalysis.

4. Conclusions

Simultaneously application of the ultrasonic and nanoreactor as combined catalytic system in preparation of the some biologically interesting organic molecules via multicomponent reaction. In fact, we have developed a green synthetic method for ultrafast and waste-free preparation of the amino phosphonate molecules using SO_3H-functionalized SBA-15 porous nanoreactor in presence of an ultrasound. Undoubtedly, as part of the continuing exploration of ultrasonic/nanoreactor for the green organic synthesis, these reaction methods have great prospects of applications in organic syntheses, pharmacy and industrial processes that which this report opens an important field to the use of green strategy in organic process.

References

[1] D. Choudhary, S. Paul, R. Gupta, and J.H. Clark. *Green Chem*., 8 (2006) 479-482.

[2] J. Liu, Q. Yang, M.P. Kapoor, N. Setoyama, S. Inagaki, J. Yang, and L. Zhang. *J. Phys. Chem. B*, 109 (2005), 12250-12256.

[3] Q. Yang, M.P. Kapoor, N. Shirokura, M. Ohashi, S. Inagaki, J.N. Kondo, and K. Domen. *J. Material. Chem*., 15 (2005) 666-673

[4] S. Rostamnia, E. Doustkhah, A. Nuri, *J. Fluor. Chem*. 153 (2013) 1–6.

5th Iran International Zeolite Conference

University of Tabriz, Tabriz, Iran

26-27 August 2018

The effects of incorporation of silver-zeolite on antibacterial efficacy, setting time and calcium release properties of mineral trioxide aggregate

F. Dabaghi-Tabriz[a], B. Divband[b], M. Rahbar[a]*, A. Bahramian[c], M. Esmailzadeh[d]

[a] *Operative and Esthetic Dentistry Department, Faculty of Dentistry, Tabriz University of Medical Sciences, Tabriz, Iran*

[b] *Department of Inorganic Chemistry, Faculty of Chemistry, University of Tabriz, Tabriz, Iran*

[c] *Oral and Maxillofacial Medicine Department, Faculty of Dentistry, Tabriz University of Medical Sciences, Tabriz, Iran*

[d] *Dentistry Student, Faculty of Dentistry, Tabriz University of Medical Science, Tabriz, Iran*

**Corresponding Author: mahdirhbr@gmail.com*

Keywords: Silver-Zeolite; Antibacterial properties; Mineral Trioxide Aggregate.

1. Introduction

Mineral Trioxide Aggregate (MTA) is a Portland cement and is powder of hydrophilic particles consisting of compounds of tricalcium silicate, tricalcium aluminate, tricalcium oxide and silicate oxide. The biological properties of MTA are attributed to its calcium ion release capacity. The setting time of sealer is important to allow adequate working time and proper consistency to permit complete filling of the root canal system and also a quickly setting after insertion. Among the numerous root end filling materials available MTA is most frequently used and has shown long term clinical but MTA have no effect or to delay the growth of Enterococcus faecalis which is main factor that cause failure of root canal therapy.

Zeolites are biocompatible crystalline aluminosilicates composed of tetrahedral structures, which build open framework consisting of channels and cages of molecular dimension. To make the crystal electrically neutral, metal cations are present in the interstices of the zeolitic framework. Silver zeolite (SZ) has been introduced as a crystalline aluminosilicate material with silver ions possessing antimicrobial effect against almost all microbes, Continuous release of small amounts of silver ions into water results in a long-term antimicrobial effect SZ also acts as an ion pump providing the controlled time release of silver ions in presence of moisture. Thus, the controlled release provides continuous antimicrobial protection for dental products. However, it is very important that physicochemical properties of MTA containing SZ be considered in relation to their use because such filling material should present adequate setting time, Calcium release and antimicrobial activity.

2. Aim

The purpose of this study was to evaluate Calcium release and Setting time of MTA incorporated with antibacterial Silver Zeolite (SZ) and comparing the antibacterial effect of MTA, MTA mixed with silver zeolite and MTA mixed with chlorhexidine against Enterococcus faecalis.

3. Materials and methods

To evaluation of setting time and calcium increase 0%, 0.2% or 2% mass fraction of SZ was added to MTA powder. The amounts of calcium released from the specimen in deionized water were measured with an atomic absorption spectrophotometer. The setting times of the samples were evaluated using Gilmore-type needles.

To compare antibacterial effect, Test materials were divided into three groups namely Group A: MTA, Group B: MTA Silver Zeolite, Group C: MTA + Chlorhexidine. Direct contact test was done by placing a standardized suspension of Enterococcus faecalison the test materials in a 96 well microtiter plate. The bacterial growth was measured spectrophotometrically using ELISA reader.

4. Results

The highest calcium release was detected in 2% SZ MTA at 24 h. The addition of 2% SZ to MTA reduced the setting time statistically ($p<0.05$). All test groups showed antibacterial activity against Enterococcus faecalis. MTA with silver zeolite showed the maximum antibacterial activity followed by MTA with 2% chlorhexidine. The least antibacterial effect was shown by MTA mixed with sterile water.

5. Conclusions

Adding SZ into MTA did not adversely affect the physico-chemical properties of MTA the addition of 2% SZ to MTA reduced the setting time and increased calcium release of it. The ratio of 0.2% is recommended. Silver zeolite and chlorhexidine can be incorporated into MTA to enhance its antibacterial effect against E. Faecalis. Laboratory research on cell cultures are needed before clinical use of SZ MTA.

References

[1] M. Brannstrom, K.J. Nordenvall, *J. Dent. Res*. 57 (1978) 3-10.

[2] H. Horiguchi, Chemistry of Antibacterial and Anti mildew, (1991) Sankyo Press Ltd, 46-59, Tokyo, Japan.

[3] J. Leirskar, *Scand. J. Dent. Res*. 82 (1974) 74-81.

[4] B.M. Hotta, C. Minami, S. Ohashi, D. Taguchi, *Jap. J. Conserv. Dent*. 38 (1995) 23-26.

[5] I.D.J. Bross, *Biometrics* 14 (1958) 18-38.

[6] M. S. L. Yee, P. S Khiew, Y. F Tan, W. S. Chiu, Y. Y. Kok, C. O. Leong. *Microporous Mesoporous Mater*. 218: (2015) 69-78.

[7] M. Samiei, N. Ghasemi, N. Asl-Aminabadi, B. Divband, Y. Golparvar-Dashti, S. Shirazi. *J. Clin. Exp. Dent*. 9.3: (2017) e356.

5th Iran International Zeolite Conference

University of Tabriz, Tabriz, Iran

26-27 August 2018

Stepwise Immobilization of Palladium Complex on to the Metal-organic Framework for Suzuki Cross-coupling Reaction

H. Alamgholiloo, M. Dalili, S. Rostamnia*

Organic and Nano Group (ONG), Department of Chemistry, Faculty of Science, University of Maragheh, PO BOX 55181-83111, Maragheh, Iran.

**Corresponding author: srostamnia@gmail.com*

Abstract: A nanoporous open metal site metal-organic framework OMS-Cu(BDC) was a synthesis by a solvothermal method and used as a high surface area solid support for the multi-step grafting of palladium Schiff-base complex. The palladium ions were coordination onto the Schiff-base (4-Py-SI) decorated Cu(BDC) pore cage. The Pd^{II}@Cu(BDC)/4-Py-SI catalyst was found to be efficient, selective and heterogeneous green catalyst for the suzuki reaction.

Keywords: Metal organic framework; Pd^{II}@Cu(BDC)/4-Py-SI; Suzuki reaction

1. Introduction

Metal-organic frameworks (MOFs) have emerged as an important class of nanoporous solid material owing to their high porosity, surface area and tunability [1]. MOFs are also an ideal platform for post-synthetic modification (PSM) chemistry to achieve multi-purpose materials. A wide range of metal group can be incorporated in to the ligand structure or post synthetically constructed in the pores of the MOF [2-5]. Suzuki-Miaura cross-coupling reaction is one of the most commonly employed transformations for of C-C bond formation in modern organic synthesis [4,5] and because of the availability of regents, and the broad functional group tolerance of this transformation, it has found extensive use in synthetic organic chemistry.

2. Experimental Part

According to the *literature*, in a typical preparation, $Cu(NO_3)_2$ (7.5 mmol) and terephtalic acid (7.5 mmol) in DMF were used. This solution was placed in a teflon-lined autoclave in an oven at 120 ˚C for 36 h.

A solution of 2-aminopyridine or salicylaldehyde was reacted solvent-free condition and added to a suspension in CuBDC.*n*DMF in dry toluene (15 ml) the mixture was heated at 90 ˚C.

A solution of $PdCl_2$ in mixture toluene was added to a suspension of Cu-BDC/4-Py-SI in DCM. The mixture was heated at reflux for 6 h, cooled to ambient temperature. Then the Pd^{II}@Cu(BDC)/4-Py-SI was filtered, washed and dried at 60 ºC under vacuum.

3. Results and discussion

For the use of heterogeneous system, Pd complexes have mainly been immobilized on MOFs (Pd@MOFs). This OMS-MOFs reacted with 4-pyridyl-salicylimine (4-Py-SI) moiety to coordination of 4-Py-SI Schiff-base to unsaturated metal/cluster site of activated Cu(BDC).

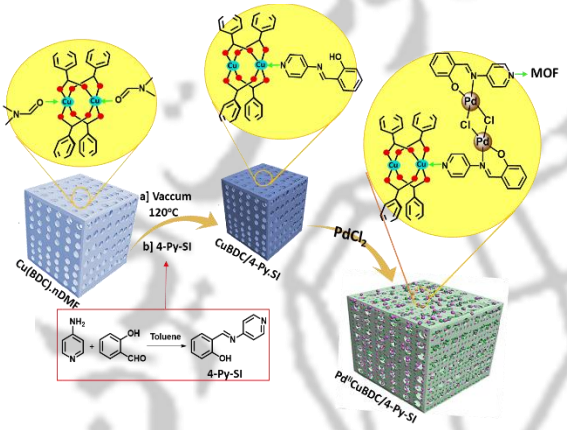

Scheme 1. Immobilization of Pd ions onto the Cu(BDC).

Afterward, $PdCl_2$ was added to a Cu(BDC)/4-Py-SI to produce Pd^{II}@Cu(BDC)/4-Py-SI (Scheme 1).

The crystallinity and purity of as-synthesized Cu(BDC) in DMF and Pd^{II}@Cu(BDC)/4-Py-SI were checked by powder X-ray diffraction (PXRD) measurement. The result demonstrates that the peak positions matched well with that of the simulated diffraction pattern (Figure 1).

SEM image of Cu(BDC) and the modified MOFs sample with the Pd/Py-SI complex revealed the presence of cubic assembled layered microcrystals. The Pd^{II}@Cu(BDC)/4-Py-SI shows its stability of structure and even morphology after multi-step post-modifications (Figure 2).

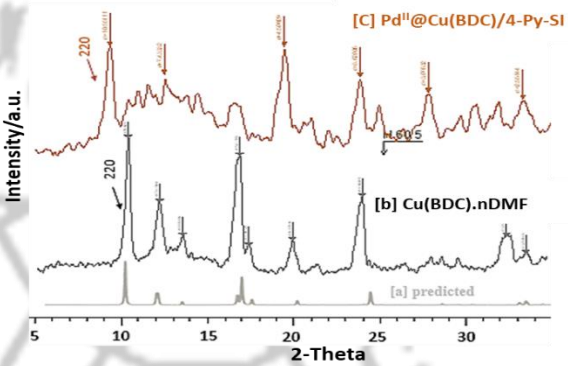

Figure 1. PXRD patterns of the Cu(BDC), as-synthesized Cu(BDC).*n*DMF and Pd^{II}@Cu(BDC)/4-Py-SI.

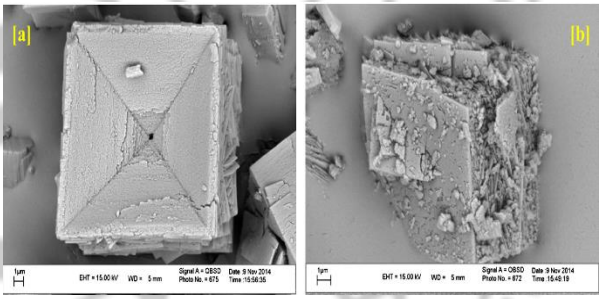

Figure 2. (a) SEM image of Cu(BDC).*n*DMF and (b) Pd^{II}@Cu(BDC)/4-Py-SI.

After sufficient characterization of the catalyst, the catalytic activity of this Pd/MOF was examined for suzuki reaction. Suzuki coupling reaction of aryl halides and aryl bronic acid was examined using different amounts catalyst, base and solvent at 80 ˚C (Scheme 2).

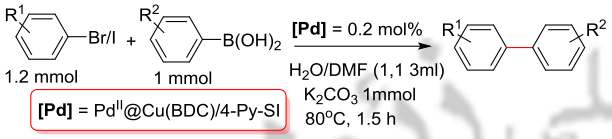

Scheme 2. Suzuki coupling reaction.

After examination of various conditions on the reaction progress, general applicability of the catalyst with aryl halildes and aryl bronic acid containing electron withdrawing or donating substituents, and results are presented in (Table 1). The entire derivatives electron withdrawing or donating were in good to excellent yields. This may be due to higher activity of the catalyst the reaction progress of each derivative.

Table 1. Synthesis of biaryl over suzuki reaction [a].

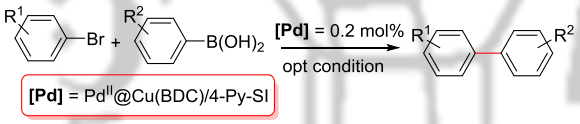

Entry	R^1	R^2	t (min)/Yield[b] (%)
1	H	H	90/ 98
2	H	4-t-Bu	120/ 93
3	OMe	H	120/ 91
4	2-NO_2	3-Me	150/ 89
5	4-CO_2Me	3-Me	180/ 85
6	4-CO_2Me	H	150/ 88

[a] Reaction condition: arylhalide (1.2 mmol), aryl bronic acid (1 mmol), K_2CO_3 (2 mmol), temperature (80 °C).
[b] Isolated yield.

4. Conclusions

The presence of copper (II) open metal sites in Cu(BDC) has been found to provide an intrinsic chelating property with electron-rich functional group, leading to the formation of the thermally stable Pyridyl-salicylimine grafted on the surface MOF. The Pd^{II}@Cu(BDC)/4-Py-SI catalyst was found to be efficient, selective, recyclable and heterogeneous catalyst for the suzuki reaction.

References

[1] Z. Wang, S.M. Cohen, *Chem. Soc. Rev.* 38 (5) (2009) 1315-1329.

[2] S. Rostamnia, H. Alamgholiloo, X. Liu, *J. Colloid Interfac. Sci.* 469 (2016) 310-317.

[3] S. Rostamnia, H. Alamgholiloo, M. Jafari, R. Rookhosh, A.R. Abbasi, *Appl. Organomet. Chem.* 11 (30) (2016) 954-958.

[4] A. Balanta, C. Godard, C. Claver, *Chem. Soc. Rev.* 40 (10) (2011) 4973-4985.

[5] A. Arnanz, M. Pintado-Sierra, A. Corma, M. Iglesias, F. Sánchez, *Adv. Synth. Catal.* 354 (7) (2012) 1347-1355.

5th Iran International Zeolite Conference

University of Tabriz, Tabriz, Iran

26-27 August 2018

Fe_3O_4-encapsulated ZIF-8 as a Novel Catalyst for Oxidative Desulfurization of a Model Fuel

H. Kargar, M. Ghahramaninezhad, M. Niknam Shahrak*

Department of Chemical Engneering, Quchan University of Technology, Quchan, Iran

**Corresponding author: m.niknam.sh@qiet.ac.ir*

Abstract: In this paper, a novel magnetic catalyst is produced through versatile procedure by coating of Zeolitic Imidazolate Framework-8 (ZIF-8) over Fe_3O_4 particles to achieve Fe_3O_4-encapsulated ZIF-8 catalyst. The successful synthesis of the catalyst was also confirmed by various methods such as FT-IR and XRD. Afterward, the produced catalyst was employed for removal of sulfur compounds from a model fuel via oxidative desulfurization process. In particular, Fe_3O_4-encapsulated ZIF-8 showed high catalytic activity for dibenzothiophene (DBT) removal from model fuels where a 90% conversion of process was gained after 11 h only with applying 0.1 g catalyst and at the ratio of O/S = 1 at 80 °C. Furthermore, the effect of temperature and reaction time on the DBT removal efficiency is studied.

Keywords: Oxidative desulfurization; MOFs; Magnetic ZIF-8; Model fuel

1. Introduction

Diesel is the second major transportation fuel and also widely used in the generation of electricity. Nevertheless, a continual problem in using diesel fuel is its high quantity of sulfur and sulfur derivatives [1]. One of the most effective methods for deep removing of sulfur and its derivatives, such dibenzothiophene (DBT), is oxidative desulfurization (ODS) process. In this study, Fe_3O_4-encapsulated ZIF-8 to taking simultaneously advantages of ZIF-8 catalytic activity and Fe_3O_4 magnetic properties used for DBT removal from a model fuel via ODS process.

2. Experimental Part

All chemical agents utilized for the catalyst synthesis were purchased from Merck company and were used as received. In brief, for synthesis of Fe_3O_4 magnetic nanoparticles (MNPs), 100 ml of 3 M $NH_3.H_2O$ was dropwise added into 12.0 ml of 0.01 M $HCl.H_2O$ solution containing 90 g $FeCl_3$ and 19.235 g $FeSO_4$ at 80 °C. The mixture was continuously stirred for several minutes and then NH_3 solution was added to the stirred solution yielding a uniform black suspension. The products were collected and separated by using an

external magnetic field and washed third times with absolute ethanol and distilled water and then dried at 60 °C [2]. After successful synthesis of MNPs, coating of Fe_3O_4 using ZIF-8 was conducted under sonication for 10 min at 60 °C by adding 1 g MNPs to 60 ml methanol solution containing 2.38 g of Zinc nitrate hexahydrate and 60.57 g of 2-MIM and 0.01 ml of HCl. Then the hybrid magnetic ZIF-8 was collected by using magnet and wash twice times with ethanol and the products were dried in vacuum oven at 90 °C [3].

3. Results and discussion

For initial assurance of the correctness synthesis of novel magnetic catalyst as well as investigation of the crystallinity of the structure, the Fourier transform infrared spectroscopy (FT-IR) and x-ray diffraction (XRD) analyses were carried out as they are illustrated in Fig. 1 and Fig. 2, respectively. In Fig. 1, the peak at 569 cm^{-1} shows the Fe-O structure and the other peaks around 1123, 1400 and 1615 cm^{-1} confirm that Fe_3O_4 is correctly synthesized. After encapsulating the Fe_3O_4 inside the ZIF-8, it was again analyzed, and the ZIF-8 salt and linker peaks were respectively detected at 422 cm^{-1} and 3125 cm^{-1} and showed the correctness of the ZIF-8 coating over the Fe_3O_4 structure [2,4]. Furthermore, in Fig. 2, peaks at 18°, 25°, 30°, 35° and 42° are corresponded to the Fe_3O_4. On the other hand, the XRD pattern of produced catalyst Fe_3O_4-encapsulated ZIF-8 reveals the main peaks of both ZIF-8 in the angles of 7°, 11°, 13° and 18° and Fe_3O_4 peaks as mentioned and proved the correctness of the catalyst synthesis [4,5].

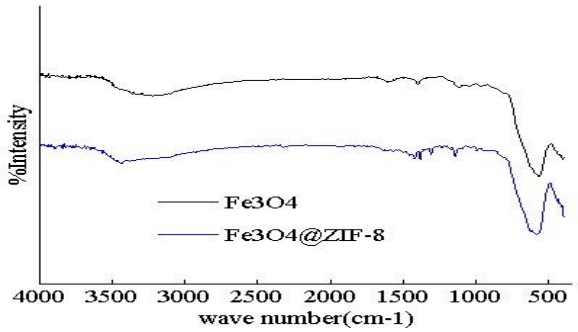

Figure 1. FT-IR spectrum of Fe_3O_4 (top) and Fe_3O_4-encapsulated ZIF-8 (down).

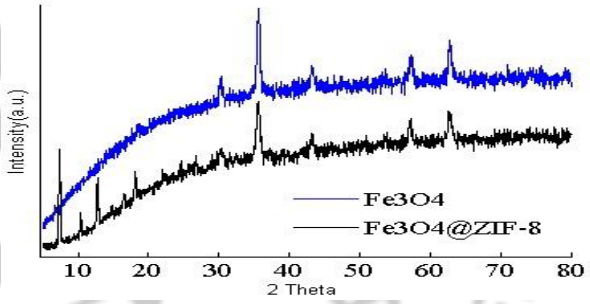

Figure 2. XRD patterns of synthesized Fe_3O_4 (top) and Fe_3O_4-encapsulated ZIF-8 (down).

After successful synthesis of novel Fe_3O_4-encapsulated ZIF-8 catalyst, its application for DBT removal from a model fuel was investigated. To this purpose, at first, the model fuel was prepared by adding various weight of DBT to 20 ml of toluene. After that, a batch ODS reactor equipped with reflux as a condenser containing TBHP as oxidant, catalyst and model fuel was set to study the effect of time and temperature over the

process efficiency. The effect of various reaction temperatures from 20 °C to 80 °C and time from 1 h to 12 h was under investigation in this study. Thin layer chromatography (TLC) for determination of the conversion percentage of DBT was also successfully employed in all experiments. Fig. 3 demonstrates the effect of temperatures (25 °C, 50 °C and 80 °C) and mixing time (1-12 h) over the DBT removal in the presence of Fe_3O_4@ZIF-8 via ODS process. As it is observed in Fig. 3, DBT removal efficiency increases with increasing the temperature and time. Achieve to 90% removal of DBT after 11 h reaction under mild condition of 80 °C presents the produced catalyst as the most promising candidate for practical applications.

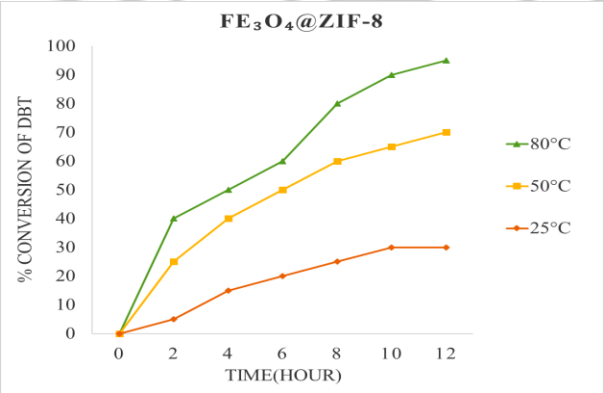

Figure 3. DBT removal efficiency at different temperatures.

4. Conclusions

A novel magnetic catalyst, Fe_3O_4-encapsulated ZIF-8, shows good activity for DBT removal via ODS process. According to the obtained results, with the increase in temperature and time, the removal efficiency increases so that at 80 °C it can be achieved to 90% of conversion after 11 h of reaction.

References

[1] K.M. Nauss, W.F. Jr Busby, A.J. Cohen, 1995, Health Effects Institute, Cambridge, MA, 13-18.

[2] Y.R. Yao, W.Z. Huang, H. Zhou, X. Cui, Y.F. Zheng, X.C. Song, *J. Nanopart. Res.* 16 (2014) 1-10.

[3] C. Yim, H. Lee, S. Lee, S. Jeon, *RSC Adv.* 7 (2017) 1418-1422.

[4] M. Niknam Shahrak, M. Ghahramaninezhad, M. Eydifarash, *Environ. Sci. Pollut. Res.* 24 (2017) 9624-9634.

[5] V. Jabbari, J.M. Veleta, M. Zarei-Chaleshtori, J. Gardea-Torresdey, D. Villagrán, *Chem. Eng. J.* 304 (2016) 774-783.

5th Iran International Zeolite Conference

University of Tabriz, Tabriz, Iran

26-27 August 2018

IRMOF-3 as a heterogeneous nanocatalyst for Kabachnik–Fields three-component reaction

A. Ahadi, H. Mohtasham, S. Rostamnia *

Organic and Nano Group (ONG), Department of Chemistry, Faculty of Science, University of Maragheh, PO BOX 55181-83111, Maragheh, Iran. Email:srostamnia@gmail.com; arefehahadi@yahoo.com

Abstract: IRMOF-3 is found to be an active, selective and stable solid catalyst for three-component, one-pot reaction of amines, aldehydes and dimethyl phosphite to form the corresponding α-amino phosphonates in high yields. The catalyst can be isolated from the reaction mixture and reused at least four times.

Keywords: Metal-organic framework, porous coordination polymer, nanocatalyst, amino phosphonates.

1. Introduction

Metal–organic frameworks (MOFs) have been the focus of increasing attention during the past decade [1]. Recently, unfunctionalized IRMOF-3 has been used as heterogeneous catalyst by Gascon et al. In their investigations, IRMOF-3 catalyst contain non-coordinated amino groups demonstrates that the basicity of the aniline-like amino group is enhanced when incorporated inside the pores of MOF channels [2]. Organic–inorganic hybrid porous IRMOF-3 would make the materials hydrothermal stable and hydrophobic and thus provide the materials with improved catalytic properties during applications for organic small molecules [3]. For these reasons and in our continuing interest in the synthesis and application of the organic-inorganic hybrid nanoporous material in catalyst and multicomponent reactions fields we report herein our results for the application and direct using of the unfunctionalized IRMOF-3 as an suitable, efficient and green catalyst for the three-component condensation of an amine, aldehyde and phosphite without any solvent, salts and additives with excellent yields of biological and medicinal interest α-amino phosphonates [4].

2. Experimental

IRMOF-3 ($Zn_4O(H_2N\text{-}TA)_3$) was synthesized according to the procedure from literature with slight modifications. In a typical catalyst preparation, $Zn(NO_3)_26H_2O$ (12.5 mmol) and H_2ATA (4.1 mmol) were dissolved in 100 ml DMF and stirred for 20 min at room temperature. A mixture of aldehydes (2.2 mmol), amines (2 mmol), dimethyl phosphite (2 mmol) and MOF (0.04 g) under solvent free condition, was stirred at 40° C for 2 h. After completion the reaction, as indicated by TLC, the reaction mixture was cooled to room temperature and CH_2Cl_2 was added.

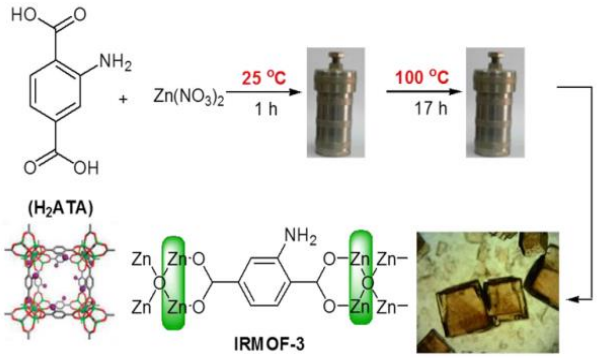

Figure 1. Preparation process of unfunctionalized IRMOF-3.

3. Results and discussion

The nanoporous metal–organic framework IRMOF-3 was prepared by refluxing of 2-aminoterephthalic acid (H_2ATA) and zinc nitrate hexahydrate in DMF by a solvothermal method, according to a literature procedure. The IRMOF-3 structure is made of Zn_4O tetranuclear clusters connected by rigid NH_2-benzenedicarboxylic linkers to generate a cubic framework (Fig. 1)

The IRMOF-3 was then characterized using a variety of different techniques. The IR spectra of IRMOF-3 show two peaks in 3470 and 3359 cm^{-1} due to the existence of the amino groups of the NH2-TA ligand. Diffraction peaks at around 2θ 6.8º and 9.6º are readily recognized from the XRD pattern (Fig. 2d). The nitrogen adsorption–desorption isotherms of the solvothermal synthesized IRMOF-3 are displayed in (Fig. 2b). The optical microscope photograph and SEM images (Fig. 2a and c), together with the XRD patterns showed that the IRMOF-3 was highly crystalline.

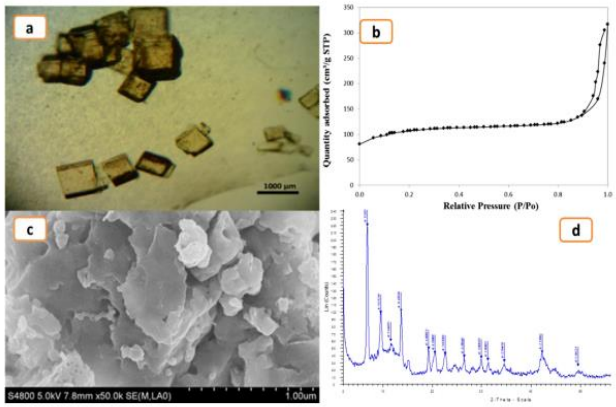

Figure 2. (a) Optical microscope photograph of IRMOF-3, (b) The nitrogen adsorption–desorption isotherms at 77 K of IRMOF-3, (c) SEM images and (d) X-ray diffraction patterns of IRMOF-3.

Table 1: Synthesis of amino phosphonates

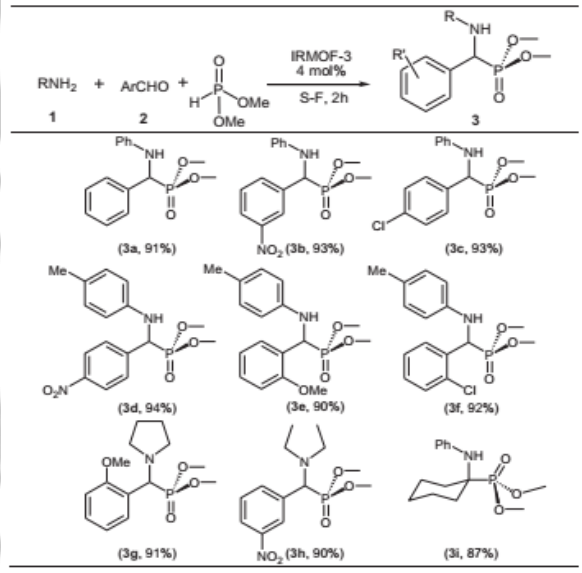

As expected, in which adduct of amines and aldehydes was treated with phosphites under the reaction conditions led to the products α-aminophosphonates **3**, and hydroxy phosphonates **4** (Scheme 1)**.**

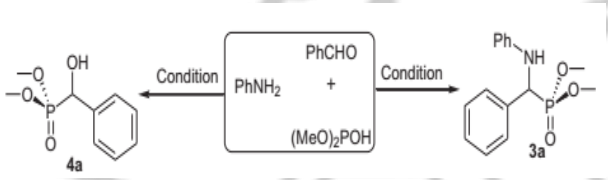

Scheme 1. Expected products from the reaction of dimethyl phosphite, amines and aldehydes.

In order to examine the scope of this process, and to demonstrate the diversity of the IRMOF-3, the optimized conditions were applied to a series of substrate as shown in Table 1.

4. Conclusions

In summary, we reported Kabachnik–Fields three-component coupling of amines, aldehydes, and dimethyl phosphite to produce pharmacy and biological interest a-aminophosphonates catalyzed by IRMOF-3, in high yields under solvent-free
conditions. This method has many advantages such as short reaction time, small amount of catalyst used and facilely recycled, especially the abstaining from toxic organic solvents in the reaction, which provides a green and effective method for synthesis of a-aminophosphonates.

References

[1] H. Li, M. Eddaoudi, M. O'Keeffe, O.M. Yaghi, *Nature* 402 (1999) 276.
[2] J. Gascon, U. Aktay, M.D. Hernandez-Alonso, G.P. van Klink, F. Kapteijn, *J. Catal.* 261 (2009) 75-87.
[3] M.J. Ingleson, J.P. Barrio, J.-B. Guilbaud, Y.Z. Khimyak, M.J. Rosseinsky, *Chem. Commun.* (2008) 2680-2682.
[4] S. Rostamnia, K. Lamei, M. Mohammadquli, M. Sheykhan, A. Heydari, *Tetrahedron Lett.* 53 (2012) 5257-5260.

5th Iran International Zeolite Conference

University of Tabriz, Tabriz, Iran

26-27 August 2018

Synthesis and Characterization of Iron-based Metal-Organic Framework MIL-53

R. Johnny[a], A. Ahmadpour[a]*, M. Ghahramaninezhad[b], T. Rohani Bastami[b]

[a] *Department of Chemical Engineering, Faculty of Engineering, Ferdowsi University of Mashhad, Mashhad, Iran*

[b] *Department of Chemical Engineering, Quchan University of Technology, Quchan, Iran*

**Corresponding author: ahmadpour@um.ac.ir*

Abstract: In this paper, we report series of MIL-53(Fe) materials synthesized by using a solvothermal method under different temperatures and time conditions that used as adsorbents for degradation of wastewater pollutants. Crystalline metal-organic frameworks (MOFs) are formed by reticular synthesis, which creates strong bonds between inorganic and organic units. Careful selection of MOF constituents can yield crystals of ultrahigh porosity and high thermal and chemical stability. Surface area of MIL-53 (Fe) was obtained as 221.65 m^2/g. The adsorbent was characterized by FT-IR, XRD, SEM and N_2 adsorption/desorption measurement.

Keywords: Metal organic framework; MIL-53(Fe); Synthesis; Adsorption

1. Introduction

In the fact that the separation process does not require much chemical and thermal stability, MOFs today have been used extensively in separation processes. The selective separation of molecules according to their shape and size and the separation of pollutants such as sulfur dioxide (SO_2), carbon dioxide and nitrogen oxide by nano-porous materials are well performed as molecular sieves. The series of MIL-53 frameworks was first synthesized in 2005 by Frey and colleagues. Due to their thermal stability and porosity, these materials are very much considered. In this series of MOFs, trivalent cations such as vanadium, chromium and iron, as well as cationic elements that are filled with orbital P, such as aluminum, gallium and indium, are used. For example, MIL-53 (Fe) consists of octopus chains of $FeO_4(OH)_2$, joined by a corner that binds to the terephthalate ligand and forms a three-dimensional structure [1].

In this research, MIL-53 (Fe) has been synthesized using the solvothermal method.

Metal-Organic Frameworks are crystalline compounds that include metal ions or clusters, often attached to organic rigid molecules as linkers. Such connections provide one, two, or three-dimensional structures that can also be porous. Regarding the metallic-organic

frameworks, they consist of two main components: a metal ion or a cluster of metal ions and an organic ligand called a connecting rod [2].

Despite the expansion and innovations, four points were important in expanding the use of MOFs: (I) the octagonal and network structure associated with MOF along with organic ligands that act as connectors. (II) shape and size of MOF adsorbent by the used techniques for characterization of the MOFs. (III) active sites and organic ligands to connect. (IV) MOF adsorbents with different variables, such as changing sizes of cavities [2].

In this study, synthesis of absorbent was performed in the laboratory conditions using special technique and laboratory devices such as autoclave and dryer.

2. Experimental Part

2.1. Chemicals

Terephthalic acid (TPA, 99%), Feric chloride hexahydrate ($FeCl_3.6H_2O$, 99%), N,N-dimethylformamide (DMF, 99.8%), Ethanol (99%), Methanol (99%), and the hydrofluoric acid (HF, 48%) were purchased from MERCK. All the chemicals in this study were used without further purification.

2.2. Synthesis of MIL-53(Fe)

MIL-53(Fe) was prepared from a solution dissolving $FeCl_3 \cdot 6H_2O$ (1.3 mmol) and H_2BDC (1.3 mmol) in DMF (27.1 ml). The mixture was kept under stirring conditions for ~2 h at room temperature to homogenize the synthetic system. Subsequently, the resulting mixture was transferred into a Teflon-lined steel autoclave and kept at 150 °C for 15 h. The obtained solids were then filtered, washed with DMF, and exchanged with dichloromethane.

3. Results and discussion

3.1. Characterization

The prepared MIL-53(Fe) was characterized by means of BET, XRD, SEM, and FT-IR as some of the commonly used techniques for characterization of the MOFs.

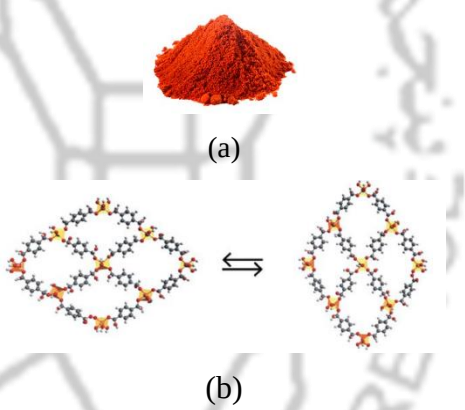

Figure 1. (a) Schematic of MIL-53(Fe) adsorbent (b) structure of MIL-53 (Fe) with open and closed pores.

Figure 1 (a,b) shows schematic and structure of MIL-53(Fe) adsorbent with open and closed pores. FTIR spectroscopy (figure 2) shows the characteristic vibrational bands of the framework −O−C−O− groups around 1510 and 1390 cm^{-1}, confirming the presence of the dicarboxylate within the obtained MIL-53(Fe). Figures 3 and 4 shows simulated PXRD patterns crystal

structure of hydrated MIL-53(Fe). The diffraction peaks matched well with the previous studies [3]. The main peaks of the MIL-53(Fe) are seen at 2θ values of 9.27°, 11.1°, 16.3°, 17.3°, 18.1°, 22.3°, and 27.9°. A main peak at 2θ of 27.9° correspond to the (100) crystalline planes of MIL-53(Fe) [4] (Figure 4).

Comparison of the XRD simulated analysis with that of laboratory indicates good agreement.

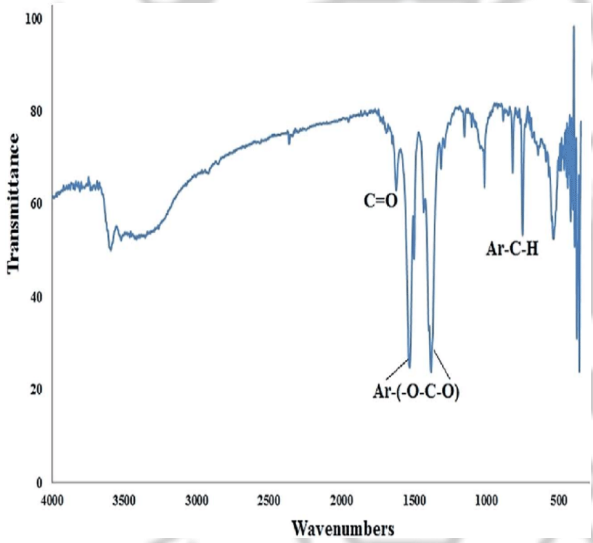

Figure 2. FT-IR patterns of hydrated MIL-53(Fe).

Figure 5 shows the N_2 adsorption/desorption isotherm of the MIL-53(Fe) at 77 K. The specific surface area evaluated with the BET method was 221.65 $m^2.g^{-1}$. The pore volume of the MIL-53(Fe) was found as 0.3632 cm^3/g at a relative pressure of P/P_0 = 0.990. Due to the closed pores for N_2 at 77 K, the flexible MIL-53(Fe) exhibits no accessible porosity [4,5]. The SEM image showed that the synthesized MIL-53(Fe) had octahedron morphology with a dimension of about 250-850 nm (Figure 6).

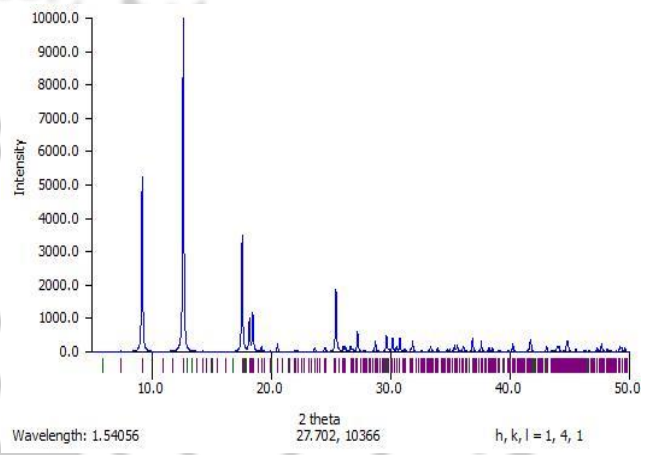

Figure 3. Simulated PXRD patterns of hydrated MIL-53(Fe).

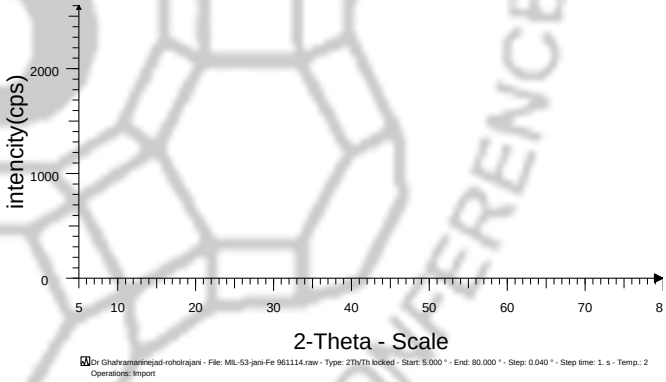

Figure 4. PXRD patterns of hydrated MIL-53(Fe).

The corresponding textual properties were listed in Table 1. The networks of MIL-53(Fe) are made of geometric networks.

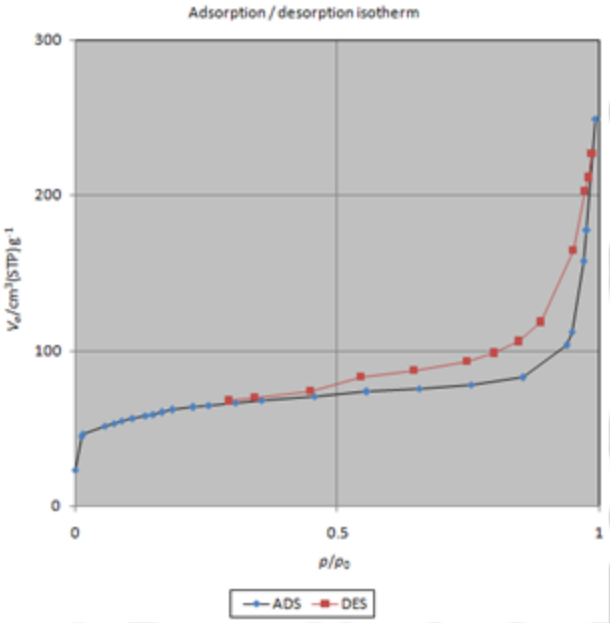

Figure 5. N_2 adsorption-desorption isotherm.

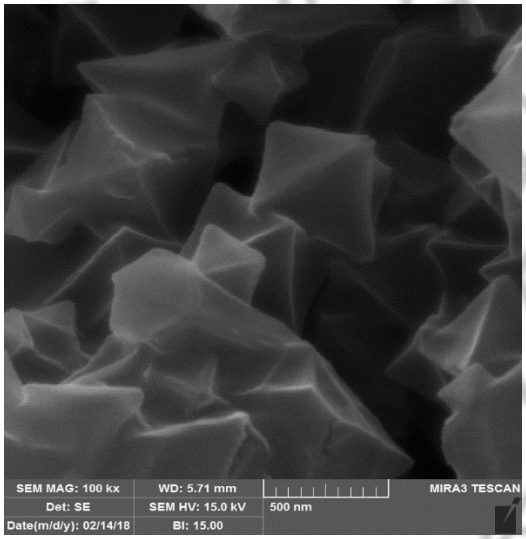

Figure 6. SEM images of MIL-53(Fe).

Table 2. Textual properties for of iron-based metal-organic framework MIL-53.

V_m [$cm^3(STP)g^{-1}$]	50.926
$a_{s,BET}$ [m^2g^{-1}]	221.65
C	660.33
Total pore volume (p/p_0=0.990) [cm^3g^{-1}]	0.3632
Mean pore diameter [nm]	6.5543

4. Conclusions

In this research, using the key techniques of MOF synthesis, we were able to reach a high level of active area i.e. 221.65 m^2/g. The high surface area and flexibility will bring a lot of applications for MOF in the industry. This adsorbent has a low density and a good cavity volume. Characterizations show that the optimal absorbance matches with the present work. The compatibility of the adsorbent with the environment is one of its important features.

References

[1] G. Ferey, C. Draznieks, C. Serre, F. Millange, J. Surble, *Science* 309 (2005) 2040-2042.

[2] O.M. Yaghi, *Nature* 423 (2003) 705-714.

[3] L.-B Sun, J.-R Li, J. Park, H.-C. Zhou, *J. Am. Chem. Soc.* 134 (2012) 126-129.

[4] F. Millange, N. Guillou, M.E. Medina, G. Férey, A. Carlin-Sinclair, K.M. Golden, R.I. Walton, *Chem. Mater.* 22 (14) (2014)237-245.

[5] J. Gordon, H. Kazemian, S. Rohani. *Micropor. Mesopor. Mater.* 162 (2012) 36-43.

5th Iran International Zeolite Conference

University of Tabriz, Tabriz, Iran

26-27 August 2018

Metal Organic Frameworks As an Adsorbent For Water Contaminants

E. Z. Lotfi[a] *, M. R. Fakhri Heravi[a], A. Rostamiiranagh[b]

[a] *East Azerbaijan water & wastewater Company, Tabriz, Iran*

[b] *East Azerbaijan rural water & wastewater company, Tabriz, Iran*

**Corresponding author: elnazzlo@yahoo.com*

Abstract: With two billion people worldwide lacking access to clean and safe drinking water, new research may offer a breakthrough solution. Metal-organic frameworks (MOFs), a next-generation material with the largest internal surface area of any known substance, can be used to capture, store and release chemical compounds. In this paper we try to introduce several methods for preparing MOFs and usage of these materials for water purification.

Keywords: MOFs, Water purification, adsorbent, pollutant.

1. Introduction

Water pollution relating to human beings' health is a universal problem across community society. Highly efficient, economically feasible and easily achievable approaches are long-sought-after for water purification. Adsorption processes with porous materials (e.g. zeolites, activated carbon, silica gel, metal-organic frameworks (MOFs)) have drawn much attention in this field during past decades. In, MOFs with numerous active sites, uniform porosity and tailorable structure diversity are arising to be one of the most promising adsorbents for water purification. During the adsorption processes, influence factors that determine or affect the usability and performances of MOFs are mainly focused on the stability of MOFs, their affinity for contaminants and the conducting conditions (pH, initial concentration of the contaminants). In this review, we will systematically present the performances of MOFs for contaminants purification (inorganic and organic contaminants) in water. The investigations of MOFs for water purifications are mainly focused on the water stability, adsorption capacity, interaction and regeneration. Adsorption capacity (selectivity included) is the key point that shows the major performances of MOFs which are largely affected by the interactions between contaminants and MOFs (active sites or functional groups). And finally, regeneration determines the continuous working possibility of MOFs.

2. Syntheses

A summary of the various approaches for MOF preparation is illustrated in Fig. 1.and Fig2. Most MOF syntheses are liquid-phase syntheses, where separate

metal salt and ligand solutions are mixed together or solvent is added to a mixture of solid salt and ligand in a reaction vial. Selection of a solvent for these liquid-phase reactions can be based on different aspects such as reactivity, solubility, redox potential, stability constant etc. Solvent also plays an important role in determining the thermodynamics and activation energy for a particular reaction. Apart from liquid-phase synthesis, researchers have also attempted solid-phase syntheses of MOFs, because it is quicker and easier, but solid-state synthesis always faces difficulties obtaining single crystals, and thereby determining product structure, which is otherwise quite easy in solution phase reactions.

The slow evaporation method is a regular process of crystallization which has been applied for the last few decades to prepare MOF crystals. Although routine synthesis of MOFs involves solvothermal methods, .other methods such as microwave-assisted synthesis, electrochemical synthesis, mechanochemical synthesis and sonochemical synthesis have been applied as alternatives for MOF synthesis.

3. The removal of inorganic contaminants

The main text of this review will be focused on MOFs for inorganic (arsenic, selenium, fluoride, mercury and chromium) and organics.

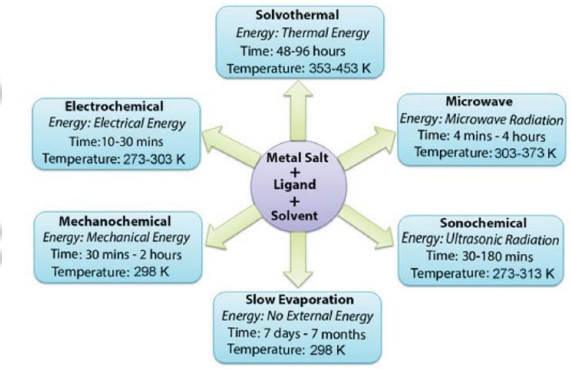

Figure 1. Synthesis conditions commonly used for MOF preparation;

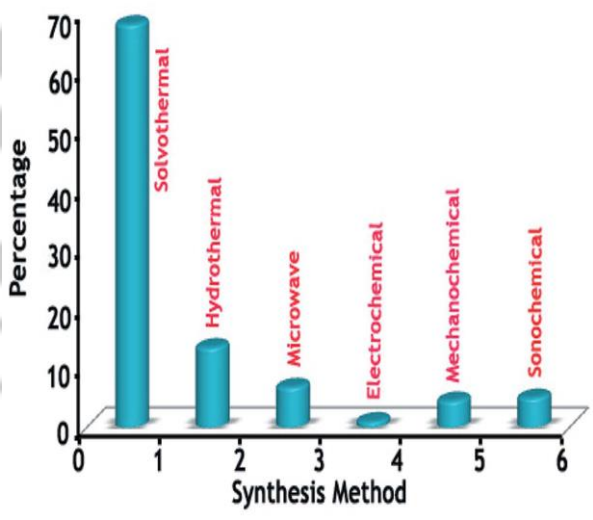

Figure 2. Indicative summary of the percentage of MOFs synthesized using the various preparation routes.

3.1. Removal of arsenic

Arsenic is a naturally occurring element that is tasteless and odorless. As a compound of underground rock and soil, arsenic works its way into groundwater and enters food chains through either drinking water or eating plants and cereals

that have absorbed the mineral. Daily consumption of water with greater than 0.01 mg/L of arsenic, less than 0.2 % of the fatal dose, can lead to problems with the skin and circulatory and nervous systems. If arsenic builds up to higher toxic levels, open lesions, organ damages (such as deafness), neural disorders and organ cancer, often fatal, can result. Adsorption processes can be carried out through porous materials, nano-iron, and transition metal oxides [3]. MOFs such as MIL-96 and ZIF-8 were also reported to be able to work for the removal of arsenic [4-8].

Given that it remains stable in water, MIL-96 (Fe)

was applied in As(V) removal from aqueous solutions by Huang and co-workers.[4] And it proved to be efficient, with relatively high arsenic adsorption capacity (12.287 mg•g-1) which is more than 6 times as large as that of iron oxide nanoparticles with size of 50 nm and 36 times that of commercial iron oxide powders.

3.2. Removal of selenate and selenite

Zr-Based MOFs for adsorption of selenite and selenite were researched on NU-1000, UiO-66, UiO-67 and their derivatives, among which NU-1000 presents the highest adsorption capacity [9-12].

3.3 Removal of fluoride

For using MOFs as adsorbents to remove fluoride, the stability in fluoride solution was firstly considered by Zhong *et al.* based on eleven water-stable MOFs (MIL-53 (Fe, Cr, Al), MIL-68 (Al), CAU-1, CAU-6, UiO-66 (Zr, Hf) and ZIFs-7, -8, -9) [13]. Among the stable ones, UiO-66 (Zr) performs the best in the batch experiments of removing fluoride, with an adsorption capacity of 41.36 mg•g□1 in neutral condition which is higher than most of the reported adsorbents.

3.4. Removal of chromium

removal of Cr(VI) through stand-alone MOF (modified UiO-66-NH2, UiO-66-NH-Met) membranes derived from photoinduced postsynthetic polymerization (PSP) strategy [14].

3.5 Organic dyes

A novel, simple and efficient strategy for fabricating a magnetic metal-organic framework (MOF) as sorbent to remove organic compounds from simulated water samples is presented and tested for removal of methylene blue (MB) as an example. The resulting magnetic MOFs composites (also known as MFCs) have large surface areas (79.52 $m^2\ g^{-1}$), excellent magnetic response (14.89 emu g−1), and large mesopore volume (0.09 $cm^3\ g^{-1}$), as well as good chemical inertness and mechanical stability. Adsorption capacity was 84 mg MB g^{-1} at an initial MB

concentration of 30 mg L^{-1}, which increased to 245 mg g^{-1} when the initial MB concentration was 300 mg L^{-1}.

4. Conclusions

MOFs are currently receiving explosive attention due to their exceptional textural properties and diverse post-synthesis organic modifications feasible. For the practical usage of MOFs in water purification, devices that can keep or enhance performances are desirable. Batch (carried out in test bottles or tubes containing contaminated water, shaking and then filtering to get the final water samples), column, and membranesare three possible solutions.

References

[1] C. Dey, T. Kundu, B. P. Biswal, A. Mallick and R. Banerjee, *Acta Cryst. B.* 70 (2014) 3–10.

[2] Y-R. Lee, J. Kim, W-S. Ahn, *Korean J. Chem. Eng.* 30 (2013) 1667-1680.

[3] B. Daus, R. Wennrich, H. Weiss, *Water Res.* 38 (2004) 2948.

[4] B. J. Zhu, X. Y. Yu, Y. Jia, F. M. Peng, B. Sun, M. Y. Zhang, T. Luo, J. H. Liu, X. J. Huang, *J. Phys. Chem. C*, 116 (2012) 8601.

[5] Y.-n. Wu, M. Zhou, B. Zhang, B. Wu, J. Li, J. Qiao, X. Guan, F. Li, *Nanoscale* 6 (2014) 1105-1112.

[6] M. Jian, B. Liu, G. Zhang, R. Liu, X. Zhang, *Colloid Surf. A*, 465 (2015) 67-76.

[7] Li, J.; Wu, Y. N.; Li, Z. H.; Zhu, M.; Li, F. T. *Water Sci. Technol* 70 (2014) 1391.

[8] Li, J.; Wu, Y. N.; Li, Z. H.; Zhang, B. R.; Zhu, M.; Hu, X.; Zhang, Y. M.; Li, F. T. *J. Phys. Chem., C* 118 (2014) 27382.

[9] Suzuki, T. M.; Bomani, J. O.; Matsunaga, H.; Yokoyama, T. *React. Funct. Polym.* 43 (2000) 165.

[10] Suzuki, T. M.; Tanco, M. L.; Tanaka, D. A. P.; Matsunaga, H.; Yokoyama, T. *Sep. Sci. Technol., 36* (2001) 103.

[11] A. Yuchi, K. Matsuo, *J. Chromatogr.* A. 1082 (2005) 208-213.

[12] A. Heikens, S. Sumarti, M. Van Bergen, B. Widianarko, L. Fokkert, K. Van Leeuwen, W. Seinen, *Sci. Total Environ.* 346 (2005) 56-69.

[13] X. Zhao, D. Liu, H. Huang, W. Zhang, Q. Yang, C. Zhong, *Microporous. Mesoporous. Mater.* 185 (2014) 72-78.

[14] Y. Zhang, X. Feng, H. Li, Y. Chen, J. Zhao, S. Wang, L. Wang, B. Wang, *Angew. Chem., Int. Ed.* 54 (2015) 4259-4263.

5th Iran International Zeolite Conference

University of Tabriz, Tabriz, Iran

26-27 August 2018

Ethylenediamine Grafting on MIL-101(Cr) as an Efficient Catalyst for the Hantzsch Condensation Reaction

H. Alamgholiloo, S. Rostamnia *

Organic and Nano Group (ONG), Department of Chemistry, Faculty of Science, University of Maragheh, PO BOX 55181-83111, Maragheh, Iran. Email:srostamnia@gmail.com; H.alamgholio2013@yahoo.com;

Abstract: Ethylenediamine functionalized MIL-101(Cr) was established to be an efficient organocatalyst for one-pot synthesis of polyhydroquinolines. Ethylenediamine of the parent open metal site MIL-101(Cr) has been carried out through a post-synthetic modification (PSM) technique. Efficient transformation, mild condition, easy product isolation and the potential high recycbility of the organocatalyst are the key feature of this protocol.

Keywords: Metal-organic frameworks, Organocatalyst; Open metal site MIL-101(Cr); Hantzsch reaction.

1. Introduction

Post-synthesis modification (PSM) of metal-organic framework (MOFs) structures has recently emerged as a versatile tool to prepare tailored MOFs in chemical transformation for various applications [1]. Engineering of metal-organic framework structures, to achieve bifunctional MOFs, with strong Lewis acid sites via grafting of coordinated ligands makes them excellent candidates as bifunctional heterogeneous catalysts [2-5].

Multi component Hantzsch reaction are a very important class of heterocyclic compound that attracted much attention because they possess their potential biological and pharmaceutical activities [3]. The heterocyclic ring of polyhydroquinolines are among the most widely used wide range of biological and pharmaceutical activities such as anticancer, antitumor, antidiabetic activity, vasodilator and treatment of Alzheimer's disease [4].

2. Experimental Part

According to the literature [5], MIL-101(Cr) was synthesis by reaction with equimolar quantities of $Cr(NO_3)_2.9H_2O$ (6 mmol) and terephthalic acid 6 mmol) and 5 M HF in 30 ml H_2O were dissolved by sonicate. This solution was placed in a Teflon-lined autoclave and put it in an oven at 220 ºC for 8 h. For synthesis of ED/MIL-101(Cr), 1 g of synthesized dehydrated Cr-MOF was stirred in dry toluene and then 0.3 g of pure ED in toluene was added drop-wise to the mixture at same temperature.

3. Results and discussion

Mesoporous Open metal site MOFs of MIL-101(Cr) with Cr^{3+} clusters and terephthalic acid as a linker, a three-dimensional chromium (III) terephthalate MOF, is outstanding due to its high thermal and chemical stability and its large BET and Langmuir surface area (Scheme 1).

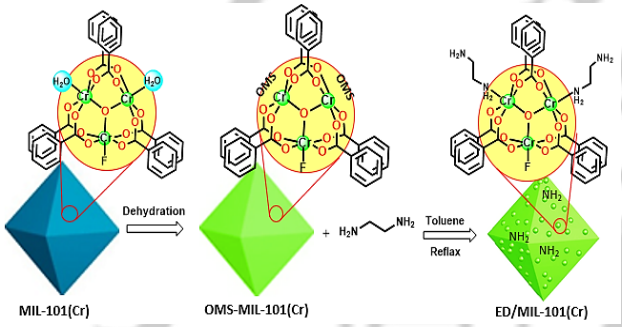

Scheme 1. Schematic illustration for the preparation of ED/MIL-101(Cr).

The crystallinity and purity of OMS-MIL-101(Cr) and ED-MIL-101(Cr) were checked by powder X-ray diffraction (PXRD) measurement. The pattern of the ED grafted MOF materials exhibits a very similar profile with the pattern of the as-synthesized MIL-101(Cr) [5], and is composed of main diffraction peaks of the MOF (Figure 1).

The SEM micrograph of the as-synthesized MIL-101(Cr) and modified MIL-101(Cr) with ED demonstrating a typical octahedral morphology, although the particles are not uniform in size. Moreover, in the TEM images of an individual octahedral shows the clear and regular framework. The SEM and TEM images of the ED/MIL-101(Cr) confirms stability of structure and even morphology after post-modifications ED grafting reaction (Figure 2).

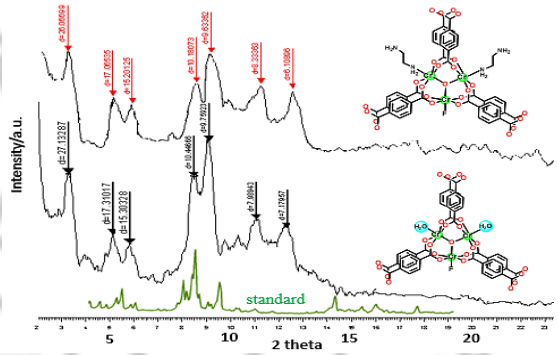

Figure 1. PXRD patterns of the MIL-101(Cr) and ED/MIL-101(Cr).

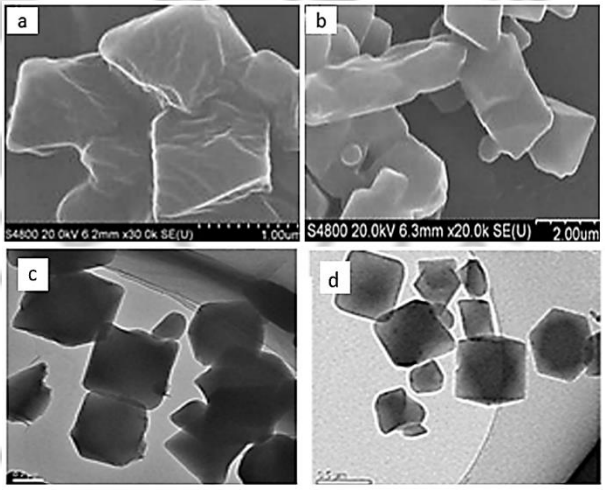

Figure 2. (a,c) SEM and TEM images of MIL-101(Cr) and (b,d) ED/MIL-101(Cr).

After sufficient characterization of the catalyst, the catalytic activity of the synthesized ED/MIL-101(Cr) in

a MCRs condensation between aromatic aldehydes, dimedone, *β*-ketoecters and ammonium acetate was explored. The best yield and selectivity was obtained when the reaction was carried out in the presence of 4 mol% of catalyst in hot ethanol (Table 1).

Table 1. Optimization of the reaction condition in Hantzch coupling reaction. [a]

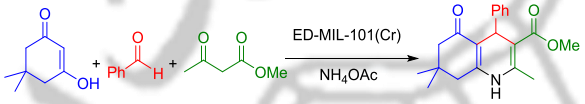

Entry	mol%	Solvent	Time (h)	Temp. (ºC)	Yield (%)[b]
1	-	EtOH	2	80	<5
2	-	EtOH	2	80	55
3	**4**	**EtOH**	**2**	**80**	**>98**
4	4	EtOH	1.5	80	92
5	4	MeOH	2	80	90
6	4	H_2O	2	80	85
7	4	CH_3CN	2	80	80
8	4	DMF	2	80	75
9	4	Toluene	2	80	70
10	4	EtOH	2	25	90

[a] Reaction condition: dimedone (1 mmol), benzaldehyde (1 mmol), methyl acetoacetate (1.2 mmol), NH_4OAc (1.5 mmol) in 3ml of solvents. [b] Isolated yield.

The recyclability and recovery of the ED/MIL-101(Cr) organocatalyst was also monitored by taking the condensation reaction for model reaction. This catalyst could be recycled over five runs without any significant loss of its catalytic activity

4. Conclusions

In summary, ED functionalized MIL-101(Cr) have been synthesized by adopting a post-synthesis modification technique as ligand reagent. The synthesized ED/MIL-101(Cr) exhibits a high surface area and thermal stability and thus can be effectively employed as a organocatalyst for single-pot four-component condensation reaction.

References

[1] J.R. Long, O.M. Yaghi, *Chem. Soc. Rev.* 38 (2009) 1213-1214.

[2] S. Rostamnia, H. Alamgholiloo, X. Liu, *J. Colloid Interface Sci.* 469 (2016) 310-317.

[3] A. Alizadeh, S. Rostamnia, *Synthesis*, 23 (2010) 4057-4060;

[4] L. Saikia, D. Dutta, D.K. Dutta, *Catal. Commun.* 19 (2012) 1-4.

[5] G. Férey, C. Mellot-Draznieks, C. Serre, F. Millange, J. Dutour, S. Surblé, I. Margiolaki, *Science* 309 (2005) 2040-2042.

5th Iran International Zeolite Conference

University of Tabriz, Tabriz, Iran

26-27 August 2018

Combining of Catalytic Properties ZIF-8 and Fluorinated Alcohol Solvents (FAS) for *N*-formylation Reaction

M. Farajzhadeh, H. Alamgholiloo, R. Banaei, S. Rostamnia *

Organic and Nano Group (ONG), Department of Chemistry, Faculty of Science, University of Maragheh, PO BOX 55181-83111, Maragheh, Iran. Email: srostamnia@gmail.com; Mustafa.helix@gmail.com

Abstract: A protocol has been developed for the transmidation of amines with formic acid by using nanoporous zeolitic imidazolate framework of ZIF-8 as a heterogeneous catalyst in vicinity of Fluorinated Alcohol Solvents (FAS) of 2,2,2-trifluoroethanol ($C_2H_3F_3O$). The mild condition, impressive transformation, easy product isolation and the potential high recyclability of the catalyst and TFE are marvelous characteristics in this field.

Keywords: Metal organic framework; Fluorinated Alcohol Solvents (FAS); Zeolitic imidazole framework.

1. Introduction

Metal organic framework (MOFs) because of their high specific surface area, defined pore size and tunability structure are interesting. Notwithstanding the great benefit of MOFs as a heterogeneous catalyst, these types of catalysts have some disadvantages such as deactivation of catalytic sites by chemical reaction, formation of obstructing deposits within the particles, loss of catalyst material because of reactions forming volatile species and [1, 2]. Zeolitic imidazole framework (ZIFs) are subgenus of MOFs which contain of imidazole linker and Zn^{+2} organized by a self-assembly approach [3]. Last few years the use of ZIF-based catalyst has mainly received attention. On the other hand, in organic transformations ZIFs is interesting and nomination for applications as heterogeneous catalyst.

Over the past few years, fluorinated alcohol compounds and Fluorinated Alcohol Solvents (FAS) such as TFE [2,2,2-trifluoroethanol ($C_2H_3F_3O$)] have been made a display of their unique properties to be solvent, co-solvent and additive in the organic synthesis [4].

2. Experimental Part

Synthesis of nanocrystalline ZIF-8 was carried out following the room temperature synthesis method reported in the literature [6] with some minor modification. In typical method, a solution of $Zn(NO_3)_2.6H_2O$ (1 mmol) in 20 ml methanol is added in to solution of 2-methyl imidazole (MeIM) (8 mmol) in 20 ml methanol under stirring for 24 h. Finally, nanocrystalline ZIF-8 was then activated in an oven/vacuum at 100 ^oC for 12 h.

3. Results and discussion

In the structure of ZIF-8, zinc atoms were connected to nitrogen atoms by 2-methylimidazolate (MeIM) as a linker, which created nanoporous formed by four, six, eight and twelve membered ring Zn_4N tetrahedral clusters**.** (Scheme 1)**.**

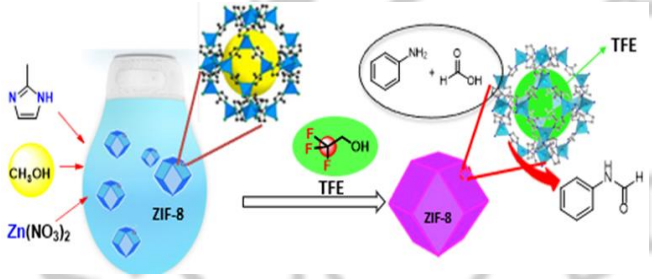

Scheme 1. Synthesis of ZIF-8 and its application in TFE mediate for *N*-formylation reaction**.**

The crystallinity and purity of as-synthesized ZIF-8 were analyzed by powder XRD patterns (Figure 1). The PXRD patterns of ZIF-8/TFE is compromise with ZIF-8. That results, showed picks position in ZIF-8 and ZIF-8/TFE are well matched.

Energy dispersive X-ray spectroscopy (EDX) and Scanning electron microscopy (SEM) were also used to characterize the morphology ZIF-8. Fig. 2a displays octahedral shape and a particle size ranging from 2 to 4 μm. The plot profile of the SEM as active surface in catalysis was measured in Fig. 2b. SEM-EDX analysis were done for the synthesized crystalline ZIF-8. Based on this analysis, Zn, C, O and N atoms exist in the structure.

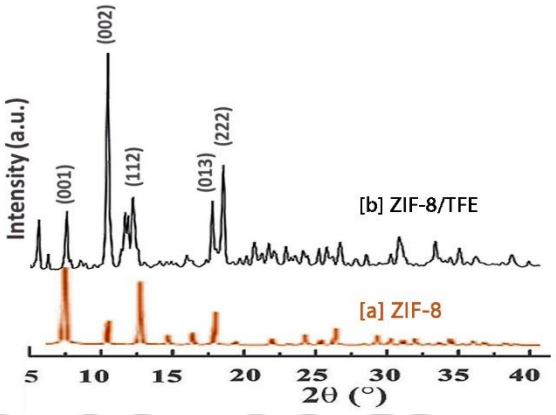

Figure 1. PXRD patterns of ZIF-8 (a) and ZIF-8/TFE (b).

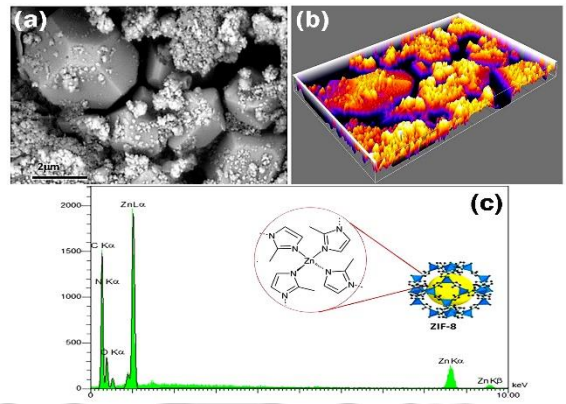

Figure 2. FESEM image (a), plot profile (b), corresponding EDX spectra (c)

The MOFs of ZIF-8 was assessed for its catalytic activity in the *N*-formylation condensation reaction by studying the reaction of aniline with formic acid to form *N*-phenyl formamide as the principal product (Scheme 2)**.**

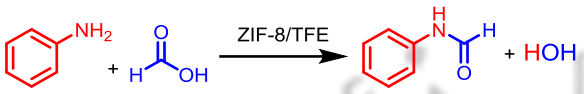

Scheme 2. MOF-catalyst *N*-formylation reaction.

The model reaction was also examined using different amounts of ZIF-8 and solvent at a temperature range of 25-50 ºC (Table 1). The best results were obtained in solvent TFE and in solvent-free condition 88% yield reaction was obtained in 150 min.

Table 1. Optimization of the reaction condition for the *N*-formylation of aniline [a]

Entry	Solvent (3 ml)	Sub. Ratio [b]	ZIF-8 (mg)	Time (min)	Temp. (ºC)	Yield (%)[c]
1	TFE	1/3	-	120	25	<30
2	DMF	1/3	5	120	50	78
3	MeOH	1/3	5	120	50	84
4	TFE	1/2	5	120	25	>92
5	**TFE**	**1/2**	**5**	**90**	**40**	**>99**
6	-	1/2	5	150	50	88

[a] Reaction condition: Set-up in 1 mmol. 3 mL of solvent

[b] Substrate ratio: Aniline/formic acid

[c] Isolated yield.

4. Conclusions

At the end, by reaction of zinc ions and 2-methyl Imidazole as a linker in stirring condition the synthesis of crystalline ZIF-8 was successfully done. This proposed catalyst could be separated from the reaction mixture by common filtration, and could be reused next run a without a significant loss of catalytic activity.

References

[1] R.L. Augustine, S.T. O'Leary, J. Mol. Catal. A: Chem. 95 (1995) 277-285.

[2] E. Cremer, Adv. Catal. Elsevier, (1955) 75-91.

[3] B. Chen, Z. Yang, Y. Zhu, Y. Xia, J. Mater. Chem. A 2 (2014) 16811-16831.

[4] L. Eberson, M.P. Hartshorn, O. Persson, F. Radner, Chem. Commun. (1996) 2105-2112.

[5] J. Cravillon, S. Münzer, S.-J. Lohmeier, A. Feldhoff, K. Huber, M. Wiebcke, Chem. Mater. 21 (2009) 1410-1412.

[6] D. Cai, M. Song, J. Mater. Chem. 17 (2007) 3678-3680.

5th Iran International Zeolite Conference

University of Tabriz, Tabriz, Iran

26-27 August 2018

Efficient adsorption and photocatalytic degradation of Congo Red by Zeolitic Imidazolate Framwork-8-encapsulated POM

F. Akbari Beni [a], M. R. Mozdianfard [a], M. Niknam Shahrak* [b], A. Ayati [b]

[a] *Department of Chemical Engineering, University of Kashan, Kashan, Iran*

[b] *Department of Chemical Engneering, Quchan University of Technology, Quchan, Iran*

**Corresponding author: m.niknam.sh@qiet.ac.ir*

Abstract: In this paper a novel hybrid photocatalyst is synthesized through a convenient procedure by encapsulation of Zeolitic Imidazolate Framework-8 (ZIF-8) inside a polyoxometalate named as phosphotungstic acid (PTA) to achieve ZIF-8-encapsulated PTA photocatalyst. The successful synthesis of the as-synthesized photocatalyst was also confirmed by FT-IR and XRD methods. Afterward, the produced catalyst was utilized for the degradation of Congo Red dye photocatalytically under visible light. In particular, ZIF-8-encapsulated showed acceptable photocatalytic activity for Congo Red removal where a 80% conversion of process was achieved after 1 hr only with applying 0.1 g/L catalyst at room temperature.

Keywords: Photocatalytic degradation; ZIF-8; POM; Congo Red

1. Introduction

Zeolitic imidazolate framework (ZIF) materials are usually prepared via reaction between tetrahedrally coordinated divalent cations such as Zn and Co with various imidazolate ligands [1]. This big family of Metal-Organic Framework (MOF) material is employed in many disciplines including catalytic and photocatalytic processes [2]. Among the big family of ZIF materials, the catalytic application of zeolitic imidazolate framwork-8 (ZF-8) has been rather investigated than other ZIF materials especially for reactions occurring in liquid phase [1] such as photocatalytic degradation owing to its great hydrophobic property [3]. In this paper to enhance the catalytic activity of ZIF-8 we combined it with the phosphotungstic acid (PTA). For this purpose, ZIF-8 crystals were encapsulated in PTA under a convenient procedure to achieve ZIF-8-encapsulated PTA. The produced catalyst was then employed for Congo Red removal under visible light.

2. Experimental Part

All chemical agents including Ammonia solution (25%), ethanol (98%), 2-Methylimidazole (2-MIm) (purity 99%), Zinc nitrate hexahydrate ($Zn(NO_3)_2{\cdot}6H_2O$ purity 99%) were purchased from

Sigma-Aldrich and were used for the ZIF-8 synthesis. Polyoxometalate phosphor tungstic acid (PTA) as well as Congo Red were also taken from Aldrich Company with the purity of 99%. The synthesis process of ZIF-8 was completely followed from available procedures in literature [1]. On the other hand, to fabricate ZIF-8-encapsulated POM, 0.1 g of the as-synthesized ZIF-8 was added to 100 mL fully dispersed solution containing 0.01 g PTA in acetone. Then, the solution was stirred for 1 h at room temperature. Then the mixture was centrifuged and washed with acetone for 3 times to achieve a whitish humid powder. The final product of ZIF-8-encapsulated POM was obtained after 24 h heating in an oven fixed at 160 °C.

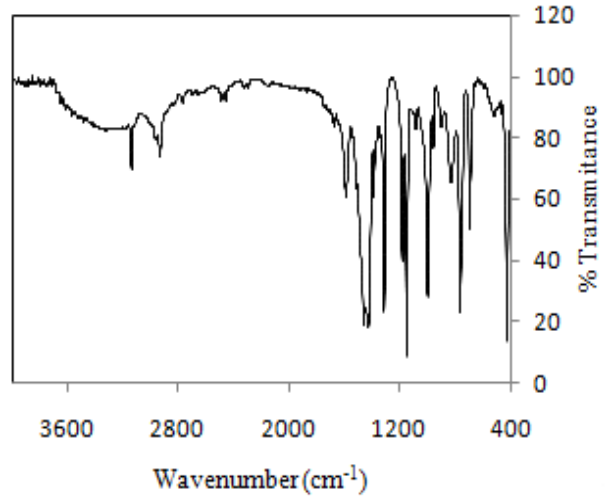

Figure1. FT-IR spectrum of ZIF-8 -encapsulated PTA

3. Results and discussion

For initial assurance of the correctness synthesis of photocatalyst as well as investigation of the crystallinity of the structure, the Fourier transform infrared spectroscopy (FT-IR) and x-ray diffraction (XRD) analyses were fulfilled as shown in Fig. 1 and Fig. 2 respectively.

In Fig. 1, the bands at 3135 and 2929 cm^{-1} are related to the aromatic and the aliphatic C–H stretch of the imidazole ring, respectively [1]. The major band at 1584 cm^{-1} is attributed to the stretching vibration of C=N group. The peaks at 600-1500 cm^{-1} correspond to the entire ring stretching or bending and the band at 421 cm^{-1} is ascribed to Zn-N stretch. These bands are the characteristic of ZIF-8 structure [1]. Furthermore, the absorption band appeared around 800 cm^{-1} to 1050 cm^{-1} is assigned to PTA. The phase structure of the ZIF-8-encapsulated PTA was determined using a X-ray diffractometer as depicted in Fig. 2.

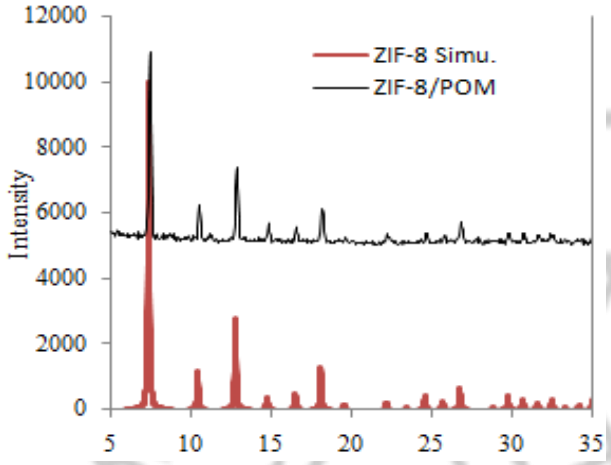

Figure2. XRD patterns of ZIF-8 -encapsulated PTA

As shown in Fig. 2, the peaks observed at 2θ = 7.3, 10.38, 12.74, 14.76, 16.48, 18.1, 22.24, 24.6 and 26.76 are attributed to the (011), (002), (112), (022), (013), (222), (114), (233) and (134) reflection planes of (SOD) topology ZIF-8, respectively [1]. Moreover, the observed peaks around 22.5 and 27.5 are related to PTA structure [4]. After successful synthesis of novel ZIF-8-encapsulated PTA photocatalyst, its application for Congo Red degradation under visible light was evaluated. For this purpose, a simple batch reactor equipped with magnetic stirrer containing dye contaminant solution and specific catalyst was set under UV light. All experiments were firstly stirred in a dark box for 15 min to eliminate any influence of adsorption on the photocatalyst, and then the solution followed under UV irradiation light for specified time. The obtained results for Congo Red degradation using 0.1 g/L catalyst at room temperature after 60 min reaction under visible light with initial concentration of 20 ppm revealed that removal efficiency is around 80%.

4. Conclusions

A novel photocatalyst, ZIF-8-encapsulated PTA, shows good activity for Congo Red degradation via photocatalytic process. According to the obtained results, the removal efficiency of Congo Red at room temperature can be achieved to 80% by using only 0.1 g/L as-synthesized catalyst after 1h reaction.

References

[1] M.N. Shahrak, M. Ghahramaninezhad, M. Eydifarash, *Environ. Sci. Pollut. R.* 24 (2017) 9624-9634.

[2] B. Chen, Z. Yang, Y. Zhu and Y. Xia, *J. Mater. Chem. A*, DOI: 10.1039/c4ta02984d.

[3] A. Ali, N.S. Mahdi, T. Bahareh, S. Mika, *Chemosphere* 160 (2016) 30-44.

[4] M. Prathap Kumar and A. Sivasamy, *Int. J. Innov. Res. Sci. Eng.* (2017) 2347-3207.

5th Iran International Zeolite Conference

University of Tabriz, Tabriz, Iran

26-27 August 2018

Metal-organic Frameworks: Synthesis and Application as a Drug Delivery System

M. Pooresmaeil[a], H. Namazi[a,b*]

[a] *Research Laboratory of Dendrimers and Nanopolymers, Faculty of Chemistry, University of Tabriz, P.O. Box 51666, Tabriz, Iran. Tel.: +98 4133933121, Fax: +98 4133340191,*

[b]*Research Center for Pharmaceutical Nanotechnology (RCPN), Tabriz University of Medical Science, Tabriz, Iran.*

**Corresponding author:* namazi@tabrizu.ac.ir

Abstract: Metal-organic frameworks (MOFs) are a new type of porous solids. Due to some unique properties, MOFs have attracted much attention in the recent years. There are several methods such as microwave, hydro/solvothermal technique, electrochemical and etc for the preparation of MOFs. Compared to conventional porous materials, MOFs have many advantages such as wide surface area, several hollows with particular shape and size, adjustable composition and structure and degradability which enable MOFs to be used in the medicine. Present paper explains some methods for the preparation of MOFs. In addition, MOFs ability to efficiently delivering drugs, as a kind of therapeutic agents is stated.

Keywords: Metal-organic frameworks; Synthesis; Drug carrier.

1. Introduction

Metal-Organic Frameworks or porous coordination networks are new types of advanced materials which prepared through different organic linkers and metal ions. The type of metal ions and the linkers which used in the preparation of MOFs determines the type of obtained network. Recently these materials with high porosity in nature have developed as an extensive class of crystalline materials. Due to some properties such as thermal stability, discrete ordered structure, ultra-low densities, large internal surface area and ease of synthesis MOFs compared to other porous materials like zeolites, activated carbon, and metal-complex hydrides etc. today's MOFs have become one of the most used materials in many areas [1]. Depending on the structural dimensionality, MOFs could be categorized into three groups. Coordination bonds are spread over the polymer in one direction for the one dimensional (1D) MOFs, hence possible voids are accommodated with small sized molecules. In 2D MOFs, the single type layers are superimposed through either edge to edge or staggered type of stacking where

weak interactions exist between the layers. In 3D MOFs, coordination bonds spread in three directions and frameworks are highly porous and stable. The 3D pillared layers and grids exist in the most of MOFs. This article reviews the synthetic method and application of MOFs in the drug delivery systems [1].

2. Synthesis of nanoscale MOFs

Since in the many application fields, especially medicine achieving to the specific size of nanoparticles is required various methods have been developed for the preparation of MOFs. In the below summary of some MOFs preparation methods introduced.

2. 1. Solvothermal synthesis

Solvothermal method is a main method for the synthesis of new MOFs. In this method MOFs have been synthesized via common electric heating in small scale. For example, MIL-101 as a type of MOFs is generally synthesized using a chromium salt and H_2BDC with aid of small amount of HF in an autoclave [2].

2. 2. Microwave-assisted synthesis

This method is the main way for the fast synthesis of nanoporous materials under hydrothermal conditions. Phase selectivity, fast crystallization, narrow particle size distribution potential and facile morphology control are examples of advantages microwave-assisted synthesis of MOFs. In this method, firstly materials are solved in the appropriate solvent and the transferred to the sealed teflon vessel and placed in the microwave. Heating of vessel under microwave for the appropriate time converts the materials to the crystallin MOFs. For the first time, synthesis of Cr-MIL-100 was reported using this synthetic method [3].

2. 3. Sonochemical synthesis of MOFs

This method is a main method for the achieving of MOFs with accelerated nucleation with smaller particles size than MOFs which achieved by the conventional method. By using this method high-quality MOF-5 crystals in the 5-25μm range were synthesized at 30 min [4].

2. 4. Electrochemical method

In the electrochemical synthesis of MOFs, instead of a metal source, ions continuously supplied through the anodic dissolution of metal salts. Then reaction of dissolved linker molecules occurs with ions in the reaction medium by employing protic solvents. Recently, HKUST-1, ZIF-8, Al-MIL-100, Al-MIL-53, and Al-MIL-53-NH2 were synthesized via this method [5].

3. Using of MOFs as drug delivery system

Characteritics such as large surface areas, well-defined structures and highly ordered porosities induces the drug loading and releasing ability to the MOFs. First Férey and co-workers (in 2006) proposed that MOFs have the ability to use in drug delivery [6]. In the one research, porous MIL-100 (Fe) was used as a nanocarrier for delivery of doxorubicin (DOX) [7]. Due to the low toxicity of zinc ion, Wang et al. have reported a chiral Zn-based MOF for the delivery of 5-fluorouracil (5-Fu). In this research adsorption of 5-Fu in the MOF was done by soaking the prepared MOF in

5-Fu solutions. Hydrogen bonding interactions between 5-Fu and the MOF achieved a loading capacity of 0.5 g g^{-1}. By dialyzing the as prepared drug-loaded MOF at phosphate buffered saline, loaded 5-Fu released for a week [8]. To improve the performance of the MOFs, as well as to induce a particular property in them, sometimes MOFs combined with or other compounds or nanoparticles. Guan and co-workers reported in situ pyrolysis method for the fabrication of γ-Fe_2O_3@MOFs. Prepared nanocomposite confirmed its ability for the controllable magnetic IBU releasing [9].

4. Conclusions

Today, significant advances have been made in the synthesis and use of MOFs as a drug delivery system. Due to the excellent properties, MOFs currently received explosive attention. This review offered a short summary to the presently existing MOFs synthesis methods and application of these materials as a drug delivery system.

Acknowledgments

Authors gratefully acknowledge the University of Tabriz and RCPN of the Tabriz University of Medical Science for the financial supports for this research.

References

[1] K.K. Gangu, S. Maddila, S.B. Mukkamala, S.B. Jonnalagadda, *Inorg. Chim. Acta* 446 (2016) 61-74.

[2] G. Férey, C. Mellot-Draznieks, C. Serre, F. Millange, J. Dutour, S. Surblé, I. Margiolaki, *Science* 309 (2005) 2040-2042.

[3] S.-H. Jhung, J.-H. Lee, J.-S. Chang, *Bull. Korean Chem. Soc.* 26 (2005) 880-881.

[4] W.-J. Son, J. Kim, J. Kim, W.-S. Ahn, *Chem. Commun.* (2008) 6336-6338.

[5] A. Martinez Joaristi, J. Juan-Alcañiz, P. Serra-Crespo, F. Kapteijn, J. Gascon, *Cryst. Growth Des.* 12 (2012) 3489-3498.

[6] P. Horcajada, C. Serre, G. Maurin, N.A. Ramsahye, F. Balas, M. Vallet-Regi, M. Sebban, F. Taulelle, G. Férey, *J. Am. Chem. Soc.* 130 (2008) 6774-6780.

[7] P. Horcajada, T. Chalati, C. Serre, B. Gillet, C. Sebrie, T. Baati, J. F. Eubank, D. Heurtaux, P. Clayette, C. Kreuz, J. S. Chang, Y. K. Hwang, V. Marsaud, P. N. Bories, L. Cynober, S. Gil, G. Ferey, P. Couvreur, R. Gref, *Nature Materials*, 9 (2009) 172-178.

[8] S. Chun-Yi, Q. Chao, W. Chun-Gang, S. Zhong-Min, W. Shuang, W. Xin-Long, Y. Guang-Sheng, S. Kui-Zhan, L. Ya-Qian, W. En-Bo, *Advanced Materials*, 23 (2011) 5629-5632.

[9] W. Yi-nan, Z. Meimei, L. Shu, L. Zehua, L. Jie, W. Baozhen, L. Guangtao, L. Fengting, G. Xiaohong, *Small*, 10 (2014) 2927-2936.

5th Iran International Zeolite Conference

University of Tabriz, Tabriz, Iran

26-27 August 2018

Comparison of Congo red removal by a metal-organic framework in the presence of Oxidizing agent & light

M. Rahim Soroush[a], A. Tarlani[a]*, R. Malek mihammadi[a]

[a]*Chemistry and Chemical Engineering Research Center of Iran, Development of Chemical Process Department, Tehran, Iran (CCERCI), Tehran, Iran*

**Tarlani@ccerci.ac.ir*

Abstract: HKUST-1 a metal organic frame work (MOF) has been applied for removing Congo red (Scheme 1) from contaminated water. HKUST-1 [1], contains of Cu(II)-paddlewheel-type node and 1,3,5benzenetricarboxylate struts, features accessible Cu(II) sites to which solvent or other desired molecules can be intentionally coordinated. In this research we discussed the effect of light and oxidizing agent on MOFs mediated removal of Congo red (CR). It was found that the Cu-BTC adsorption capacities of CR are much higher than those of the other types of MOFs and adsorbents.

Keywords: Adsorption performance, Congo red, Cu-BTC

1. Introduction

Todays, dyes are found in wastewaters from various industries such as textile, leather, plastic, food processing, cosmetics, paper, printing, pharmaceutical and dye manufacturing [2]. Presences of synthetic and organic dyes in the environment have a significant effect to the environment and health. Waste water treatment is an important field of study. At present, various techniques and methods can be used to remove organic dyes from aqueous solution, such as physical, chemical, and biological methods. Adsorption as a choice is widely used different methods to remove dyes. Recently, a variety of adsorbents are applied to remove organic dyes.

MOFs have emerged as extensive materials with ultrahigh porosity and enormous internal surface areas. These properties, together with the extraordinary degree of variability for both the organic and inorganic components of their structures, make MOFs of interest for potential applications in gas adsorption, drug delivery and many other applications [3-4].

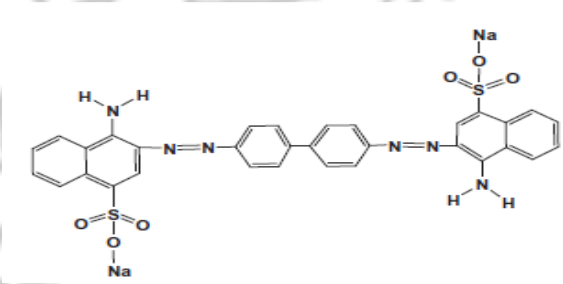

Scheme 1. Chemical structures of CR

In this work we compared the elimination of CR by HKUST-1 and by the mixture HKUST-1 in the presence of oxidants and light.

2. Experimental Part

HKUST-1 was synthesized using hydrothermal method [3]. Experiments took place in 3 parts:

A: An aqueous solution of CR (10M) was prepared .0.005g HKUST-1 added to 15ml solution and stirred without light and oxidant.

B: Two drops of H_2O_2 was added to A suspension and stirred.

C: The solution was stirred under UV light.

3. Results and discussion

HKUST-1 as a porous material has two interesting aspects: First) as an adsorbent due to having large surface area and pore volume. Second) as a catalyst due to having catalytic center of Cu(II). By considering these properties, three experimental protocols were designated (A, B and C). All results are collected in Table 1. As can be seen, when only Congo red and MOF is present in the vessel, after 27 minutes the blue color eliminate completely showing that the HKUST-1 is a good adsorbent toward CR (Table 1, A). By adding two drops of hydrogen peroxide to A, decoloration takes place in a few seconds. It could be concluded that Cu(II) as a catalyst center is activated by hydrogen peroxide as a green oxidant and the removal of CR accelerated by decreasing the time from 27 min to 0.5 min (Table 1, B). In the last experiment, the suspension A illuminated by UV light (11 W). Surprisingly, decoloration did not complete even after 45 min (Table 1, C). As a result, removal of Congo red using HKUST-1 follow the trend of B > A > C. Schematic representation of the process could be found in Scheme 2.

Table 1. Experimental results

Method	Solution volume (mL)	Time (min)	Solution status
A	15	27	Colorless
B	15	0.5	Colorless
C	9	45	Pale pink

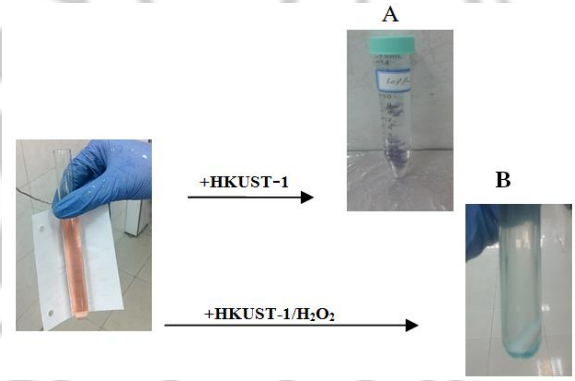

Scheme 2: The effect of oxidant and HKUST-1 on dye removal

Adsorption kinetics

Adsorption kinetics was mainly used to investigate time factor of adsorbed velocity. The adsorption data were fitted to the pseudo-first order and the pseudo-second order model in order to analyze the kinetic data. These models are:

Pseudo-first order model: $\ln(q_e - q_t) = \ln (q_e) - K_1 t$

Pseudo-second order model: $t/q_t = 1/K_2q_e + t/q_e$

Where:

K_1 (1/min) = the adsorption rate constant,

K_2 (g/mg.min) = the rate constant of second-order equation.

q_t and q_c = CR uptake

Calibration equation extracted from plot 1.

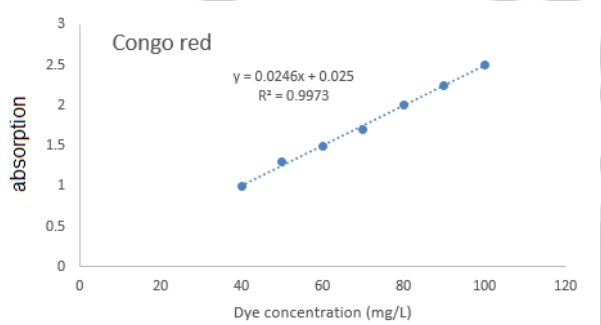

Figure 1: CR absorption standard curve

Between pseudo-first order model (R^2 = 0.9389) and pseudo-second order model (R^2 = 0.9851) our data perfectly matched pseudo-second order model.

4. Conclusions

Congo red dye in contaminated water can be efficiently removed with Cu-BTC. Between three designated conditions by adsorption process (A), catalytic reaction in the presence of H_2O_2 (B) and illumination by UV light (C), it was found that the efficiency of the removal obey the trend of B > A > C.

Acknowledgments

We thank Chemistry & Chemical Engineering Research Center of Iran (CCERCI) for making the conditions to accomplish this study.

References

[1] Jue Hua, Wei Daia & Xiaoyang Yana *a College of Chemistry and Life Science*, Zhejiang Normal University, Zhejiang Province, Jinhua 321004, P.R. China.

[2] J. Hu, H. Yu, W. Dai, X. Yan, X. Hu, H. Huang, *RSC Adv.* 66 (2014) 35124–35130.

[3] K-S. Lin, A. K. Adhikari. C-N. Ku, C.-L. Chiang, H. Kuo, *Int. J. Hydrogen Energy*, 37 (2012), 13865-13871.

[4] S. D. Taherzade, J. Soleimannejad, A. Tarlani, Nanomaterials, 8 (2017) 215-228

5th Iran International Zeolite Conference

University of Tabriz, Tabriz, Iran

26-27 August 2018

Adsorptive Removal of Antibiotic Drugs from Contaminant Water by ZIF-8

R. Malek Mohammadi [a], M. Rahim Soroush,[a] A. Tarlani*[a]

[a]*Chemistry and Chemical Engineering Research Center of Iran, Development of Chemical Process Department, Tehran, Iran (CCERCI), Tehran, Iran*

**Tarlani@ccerci.ac.ir*

Abstract: As environment pollution today is an important subject in human life and nature, in this study Zeolitic Immidazolate Frameworks (ZIFs), as a category of hybrid crystalline materials called 3D Metal Organic Frameworks (MOFs), selected as an adsorbent to remove antibiotic drugs from waste water. This adsorbent has been applied because of its specific features like high surface area about 1300-1900 m^2/g, good pore volume about 1 nm, suitable pore diameter, high adsorption ability and etc. To determine the ability of ZIF-8 in adsorbing antibiotic drugs, the effect of time and adsorption capacity were established. Results showed that ZIF-8 has a good capacity in adsorption of doxycycline (DOX), as an antibiotic drug, from contaminant water and could refine water.

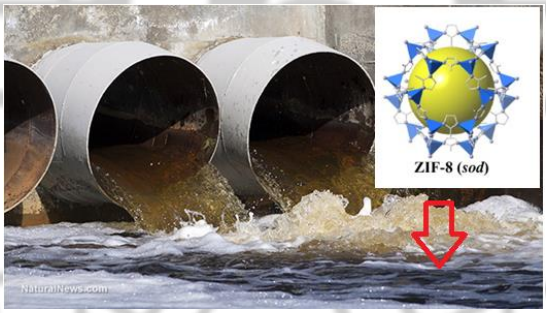

Keywords: Adsorption, ZIFs, Antibiotic, waste water.

1. Introduction

Pharmaceuticals and personal care products (PPCPs), as a new type of emerging pollutant in living environment has drawn great attention owing to the potential hazard [1–5]. Even though, the concentrations of PPCPs in water are generally below the therapeutic dose, there is still enormous risk to the environment and human health. With the heavy use of antibiotics and the increasing antibiotics concentrations in water, bacteria in the water sample form resistance to drug by long-

term exposure. As for the problem of drug contaminant, environmentalists and scientists devote themselves to finding technology to purify contaminated water. Presently, adsorption technology, advanced oxidation processes (AOPs), biological technologies, separation processes, and multiple-treatment processes are used to remove PPCPs from water. Many materials such as mesoporous clay materials, zeolites, carbonaceous materials and biosorbents have been developed as sorbents to remove PPCPs from water. MOFs also known as coordination polymers or coordination networks, are crystalline materials built from metal ions or clusters bridged by organic linkers to form different dimensions. These hybrid materials exhibit various properties, e.g., high relative surface area, order porous structure, magnetism and luminescence, and are hot spot in material field. Doxycycline (DOX) is an antibiotic that is used in the treatment of a number of types of infections caused by bacteria and protozoa. It is useful for bacterial pneumonia, acne, chlamydiainfections, arly lyme disease, cholera and syphilis. It is also useful for the treatment of malaria when used with quinine and for the prevention of malaria. In this study ZIF-8 and DOX selected as adsorbent and drug, respectively.

2. Experimental Part

2.1 Synthesis of ZIF-8

ZIF-8 nanocrystals were synthesized according to this procedure. Briefly, a solution of Zn $(NO_3)_2 \cdot 6H_2O$ (1.173 g) in 80 mL methanol was added into a solution of 2-methylimidazole (2.595 g) in 80 mL methanol under stirring with a magnetic bar. After keeping at room temperature for 1 h, ZIF-8 was formed, and then separated by centrifugation at 10000 rpm for 10 min and washed with methanol three times. The solid was dried at 90 °C for 12 h and ground with an agate mortar for 15 min.

2.2 Adsorption experiments

The adsorption experiments were conducted by adding of 0.02 g of adsorbent to 25 mL of DOX solution in a bottle. The pH of the solution was adjusted to the desired value by adding HCl or NaOH solutions and the mixture was shaken until the equilibrium was attained. After equilibration, the sample was separated by applying external magnetic field and the concentration of DOX in the remaining solution was measured by UV-Vis spectroscopy.

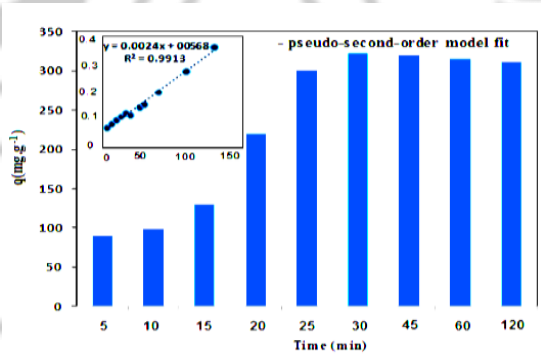

Figure 1. Adsorption of antibiotic by ZIF-8

3. Results and discussion

To study the kinetic of the adsorption process, the removal efficiency was measured for different time interval up to 120 min. By increasing of contact time, initially the adsorption capacity was increased and then remained constant. The adsorption process was kinetically fast and the equilibration was established within 30 min with the adsorption capacity of 320 $mg.g^{-1}$.

4. Conclusions

In summary, we have demonstrated that ZIF-8 showed strong capability toward removal of DOX from the aqueous solutions. The kinetics process over ZIF-8 was fast and can be described by pseudo-second-order equation. The results indicated that the synthesized adsorbent was a suitable adsorbent for elimination of doxycycline from aqueous solutions.

Acknowledgments

We thank Chemistry & Chemical Engineering Research Center of Iran (CCERCI) for making the conditions to accomplish this study.

References

[1] K. Kümmerer, *J. Environ. Manag*. 90 (2009) 2354–2366.

[2] R. L. Oulton, T. Kohn, D. M. Cwiertny, *J. Environ. Monit*. 12 (2010) 1956–1978.

[3] R. H. Lindberg, M. Östman, U. Olofsson, R. Grabic, J. Fick, Water Res. 58 (2014) 221–229.

[4] K. Xia, A. Bhandari, K. Das, G. Pillar, J. Environ. Qual. 34 (2005) 91–104.

[5] L. Arpin-Pont, M. J. M. Bueno, E. Gomez, H. Fenet, Environ. Sci. Pollut. Res. 23 (2016) 4978–4991.

5th Iran International Zeolite Conference

University of Tabriz, Tabriz, Iran

26-27 August 2018

Photodegradation of Methyl Orange Using ZIF-8 from Aqueous Solution

R. Malek Mohammadi[a], M. Rahim Soroush,[a] A. Tarlani[a]*

[a]*Chemistry and Chemical Engineering Research Center of Iran, Development of Chemical Process Department, Tehran, Iran (CCERCI), Tehran, Iran*

**Corresponding author: Tarlani@ccerci.ac.ir*

Abstract: Dyes used in many industries, cause pollution and have danger both for nature and human health. So many different methods used to remove dyes from nature and waste waters. One of these functional methods is adsorptive removal and degradation of dye which is simple, fast and low cost. In this study, Methyl Orang (MO) as an organic dye which behaves as pH indicator frequently in titration and ZIF-8 as adsorbent selected. The ability of ZIF-8 to remove of methyl orang was studied and analyzed by UV spectrophotometry. Results showed that methyl orang could be adsorbed by ZIF-8.

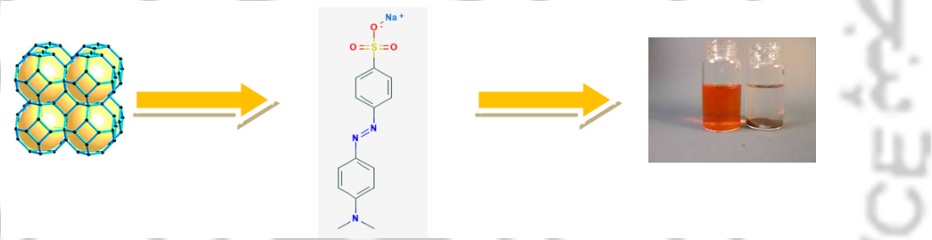

Keywords: Degradation, ZIFs, Methyl Orang, Waste water.

1. Introduction

Removing dyes from wastewater is a necessary problem for water industry. The significant increase in the use of dyes by various industries is causing severe damage to the environment because of their toxicity [1]. Degrading dye materials is difficult because of their stability against light and oxidation reactions [2]. In the process of removal of dye materials from contaminated water, several methods such as physical, chemical and biological ones have been investigated [3,4]. Removal of dyes by physical adsorption technologies is regarded as one of the competitive methods because of high efficiency, economic feasibility and simplicity in design/operation. In this study, metal organic Framework (MOFs) used as adsorbent to remove methyl orang dye. MOFs attracted attentions because of

their ability in various subjects and became popular because of their high surface area, good catalytic activity, good stability and etc.

2. Experimental Part

2.1 ZIF-8 synthesis

A clear solution is prepared by dissolving 30.3 mg (0.22 mmol) of $ZnCl_2$, 36.5 mg (0.44 mmol) of Hmim and 30.3 mg (0.44 mmol) of $NaHCO_2$ in 3 mL of MeOH. The solution with a molar ratio Zn/Hmim/NaHCO2/MeOH 1:2:2:333 is treated without stirring at 130 ^oC for 4 h in a sealed glass tube under homogeneous heating in a convection oven. The crystals are recovered by filtration, washed with MeOH and dried under reduced pressure. Yield is 63% based on Zn. The synthesized ZIF-8 characterized by XRD Fig.1 and Fig. 2.

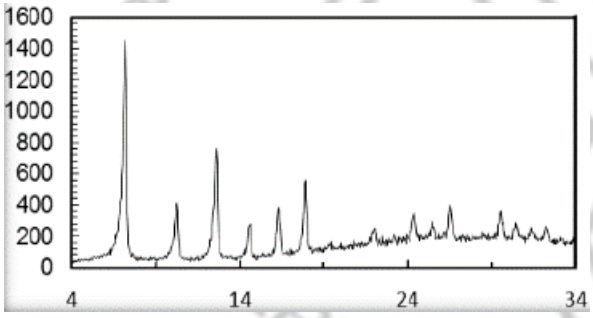

Figure 1. XRD pattern of ZIF-8

2.2 Degradation of MO

50 mg of ZIF-8 was put into 200 mL of MO (10 mg/L) aqueous solution in a 300-mL flask. Prior to irradiation, the suspension was magnetically stirred in dark for 120 min to ensure the establishment of an adsorption/desorption equilibrium. During the photodegradation reaction, stirring was maintained to keep the mixture in suspension. 0.5 mL of sample in different and particular times was extracted and determined by UV-Vis spectrophotometer.

3. Results and discussion

It can be seen that the photocatalytic activities of MO degradation efficiency increased from 24.0% (without ZIF-8) to 91.7% under UV light irradiation within up to 40 min Fig.1 Additionally, the photodegradation reaction of MO in ZIF-8 photocatalyst followed pseudo-first-order kinetics model R^2 = 0.959, as evidenced by the linear plot of $\ln(C/C_0)$ vs. reaction time t. The pseudo-first-order rate constant for the photocatalytic degradation of MO in the presence of ZIF-8 was 0.0605 min^{-1}. As seen from Fig. 3 when the simulated wastewater samples of MO were irradiated under UV light, the maximum absorption peak of MO decreased obviously with the reaction time in the presence of ZIF-8. Furthermore, no other new peak is observed in Fig. 3 indicating that no new pollutants occurred during the process of degradation. Generally, there is an electron transfer from the highest occupied molecular orbital (HOMO) to the lowest unoccupied molecular orbital (LUMO) in the presence of UV light. To understand the photocatalysis mechanisms of MOFs, the terminology of HOMO-LUMO gap rather than traditional semiconductor gap (CB-VB) is suggested to describe the discrete character of the light-

induced transitions. Therefore, a possible mechanism can be proposed to clarify the degradation of organic dyes in the presence of ZIF-8 as photocatalyst as illustrated in Fig. 4.

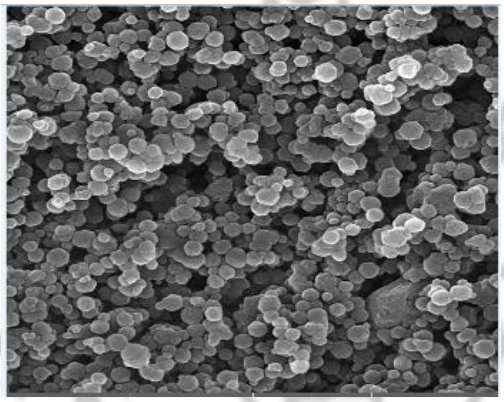

Figure 2. SEM of ZIF-8

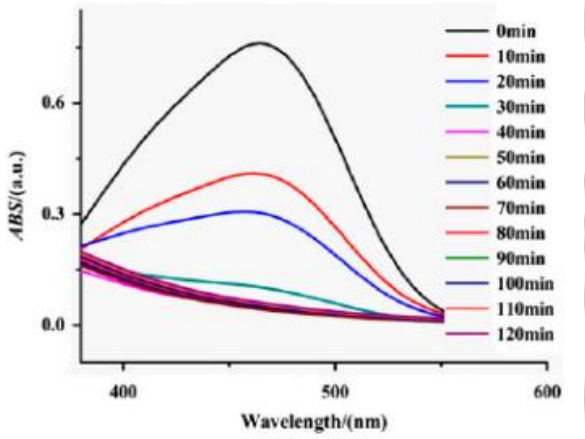

Figure 3. UV–Vis absorption spectra of MO aqueous solution during the photocatalytic degradation under UV lamplight irradiation in the presence of ZIF-8

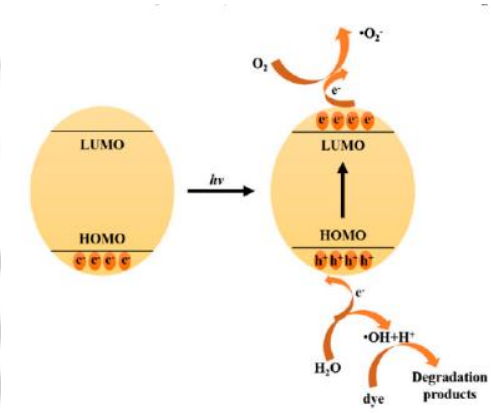

Figure 4. Mechanism of degradation MO under UV light

4. Conclusions

In summary, zif-8 appears to be a photocatalyst to achieve preferential degradation of typical MO, as an organic dye, used in industries. The results showed that ZIF-8 exhibited efficient degradation of MO in short time. Further researches should be carried out to clarify the photocatalytic activities on other organic pollutants.

Acknowledgments

We thank Chemistry & Chemical Engineering Research Center of Iran (CCERCI) for making the conditions to accomplish this study.

References

[1] G. Crini, *Bioresource Technol*. 97 (2006) 1061–1085.

[2] B. H. Hameed, A. A. Rahman, *J. Hazard. Mater*. 160 (2008) 576–581.

[3] P. Vandevivere, R. Bianchi, W. Verstraete, *J. Chem. Technol. Biotechnol*. 72 (1998) 289–302.

[4] Y. Slokar, A. L. Marechal, *Dyes Pigments* 37 (1998) 335–356.

5th Iran International Zeolite Conference

University of Tabriz, Tabriz, Iran

26-27 August 2018

Adsorption Behavior of HKUST-1 for Methylene Blue Decoloration from Contaminated Water

M. Rahim Soroush, A. Tarlani*, R. Malek mohammadi

Chemistry and Chemical Engineering Research Center of Iran, Development of Chemical Process Department, Tehran, Iran (CCERCI), Tehran, Iran

**Corresponding author: Tarlani@ccerci.ac.ir*

Abstract: Metal−Organic frameworks (MOFs) have emerged as an extensive class of crystalline materials with ultrahigh porosity (up to 90% free volume) and enormous internal surface areas, extending beyond 6000 m^2/g. These properties, together with the extraordinary degree of variability for both the organic and inorganic components of their structures, make MOFs to be interested for potential applications. In this work MOF based on copper was applied to the adsorption of methylene blue (MB) from aqueous solution. It was found that the Cu-BTC adsorption capacities of MB are much higher than those of the other types of MOFs and adsorbents. Two simplified kinetic models including pseudo-first-order, pseudo-second-order, were used to investigate the adsorption process. The pseudo-second-order equation was followed for adsorption of MB on Cu-BTC.

Keywords: HKUST-1; Methylene blue; Kinetic model

1. Introduction

About 15% of the total world production of dyes is lost during the dyeing process and is released in the textile effluents [1]. The release of those colored waste waters in the ecosystem is a dramatic source of non-aesthetic pollution, eutrophication and perturbations in the aquatic life [2]. Organic dyes released into the environment have posed a significant threat to the environment and creatures health due to the fact that it has a certain toxicity and even carcinogenic [3]. Adsorption is one of the most attractive approaches among possible dye removal techniques due to its low cost, versatility and ease of operation. A variety of materials capable of removing MB (Scheme 1.) have been reported. Here HKUST-1, a kind of MOFs with surface area 1500 m^2/g and pore volume of 0.57 cm^3/g [3], has been used to remove methylene blue dye. For this purpose, a particular amount of HKUST-1 was added to different concentrations of methylene blue solution and the amount of MB was adsorbed and the kinetic characteristic of dye was analyzed.

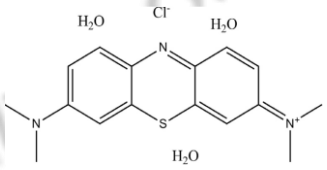

Scheme 1. Chemical structure of MB.

2. Experimental Part

2.1. Synthesis of HKUST-1

HKUST_1 was synthesized using hydrothermal method [4] $Cu(NO_3)_2 \cdot 3H_2O$ (5 g, 0.021 mol) and H_3BTC (2.5 g, 0.012 mol) were dissolved in 300 mL of solvent consisting of equal amounts of DMF, ethanol and deionized water. The solution was placed in an oven and heated to 358 K for 20 h. The blue product was isolated, rinsed with 50 mL DMF for three times, and immersed in absolute ethanol every 24 h for 72 h. Finally, the blue product was heated to 393 K for 24 h in vacuum (Scheme 2).

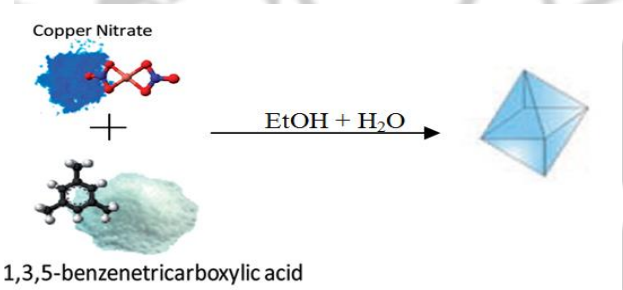

Scheme 2. Schematic representation for the preparation of HKUST-1.

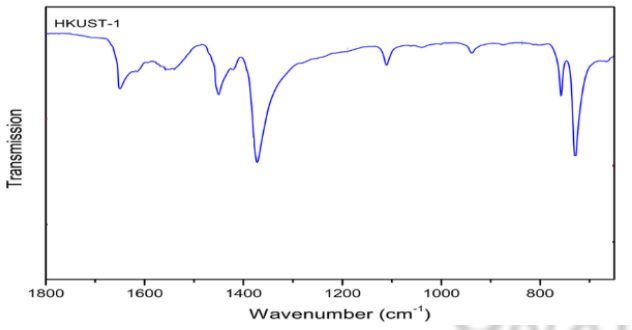

Figure 1. IR spectrum of HKUST-1.

The sample was characterized by IR Spectroscopy (Figure 1). The main peaks are observed between 1300 to 1700 cm^{-1}.

2.2. Adsorption of dye

An aqueous solution of MB (10 M) was prepared. 0.005 of g HKUST-1 was added to 15 mL of the solution and then stirred. Samples were collected in different times. Each time a particular amount of the sample was extracted, centrifuged and the concentrations were determined by UV-Vis spectrophotometer.

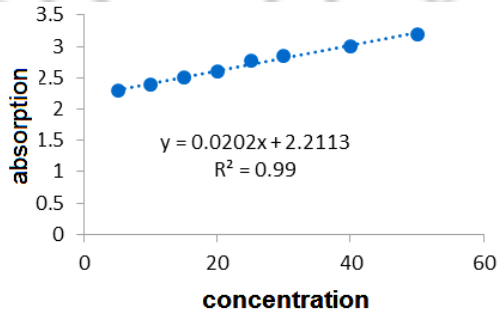

Plot 1. MB absorption standard curve.

3. Results and discussion

3.1. Adsorption kinetics

Adsorption kinetics was mainly used to investigate diffusion mechanism, adsorbed control step and influencing factors of adsorbed velocity. The adsorption data were fitted to the pseudo-first-order kinetic model and the pseudo-second-order kinetic model respectively [5-7]. The procedure used for kinetic tests was identical to that used for equilibrium experiments.

These models can be expressed as:

Pseudo-first order model: $\ln (q_e - qt) = \ln (q_e) - K_1 t$

Pseudo-second order model: $t/qt = 1/K2qe + t/qe$

By considering pseudo-first order model ($R^2 = 0.938$) and pseudo-second order model ($R^2 = 0.9956$) the data could be fitted to pseudo-second order model.

q_e and qt (mg/g) are the uptake of MB at equilibrium and at time t (min), respectively. K_1 (1/min) is the adsorption rate constant, K_2 (g/mg.min) is the rate constant of second-order equation.

4. Conclusions

MB dye in contaminated water can be efficiently removed with Cu-BTC. Batch adsorption tests showed that the adsorption is affected by time. Adsorption kinetics follows the pseudo-second-order model. It can be suggested that Cu-BTC may be applied in the adsorptive removal of dyes in the liquid phase.

Acknowledgments

We thank Chemistry and Chemical Engineering Research Center of Iran (CCERCI) for making the conditions to accomplish this study.

References:

[1] H. Zollinger, *Color Chemistry. Synthesis, Properties and Applications of Organic Dyes and Pigments*, 1991, Wiley-VCH.

[2] S.B. Wang, Y. Boyjoo, A. Choueib, Z.H. Zhu, *Water Res.* 39 (2005) 129-138.

[3] H.-C. Zhou, J.R. Long, O.M. Yaghi, *Am. Chem. Soc.* 112 (2012) 673-674.

[4] K.-S. Lin, A.K. Adhikari. C.-N. Ku, C.-L. Chiang, H. Kuo, *Int. J. Hydrogen Energ.* 37 (2012) 13865-13871.

[5] E. Haque, J.W. Jun, S.H. Jhung, *J. Hazard. Mater.* 185 (2011) 507-511.

[6] J. Yang, K. Qiu, *Chem. Eng. J.* 165 (2010) 209-217.

[7] M. Vinoth, H.Y. Lim, R. Xavier, K. Marimuthu, S. Sreeramanan, H.M.H. Rosemal, S. Kathiresan, *Int. J. Chem. Technol. Res.* 2 (2010)1890-1900.

5th Iran International Zeolite Conference

University of Tabriz, Tabriz, Iran

26-27 August 2018

Application of HKUST-1@GO Nanocomposite for the Removal of Lead from Wastewater

S. Alqaisi[a], A. Ahmadpour[a*], M. Ghahremaninezhad[b], T. Rohani Bastami[b]

[a] *Department of Chemical Engineering, Faculty of Engineering, Ferdowsi University of Mashhad, Mashhad, Iran*

[b] *Department of Chemical Engineering, Quchan University of Technology, Quchan, Iran*

**Corresponding author: ahmadpour@um.ac.ir*

Abstract: Metal organic frameworks (MOFs) and porous hybrid polymer–metal composites at the nanoscale, are recent innovations in the field of chemistry. MOFs are nanoporous materials, consisting of metal ions linked together by organic bridging ligands. In the present study, we report the application of HKUST-1@Graphene Oxide as a novel adsorbent for the fast removal of Pb(II) ions from aqueous solution in view of adsorption isotherms, kinetics, thermodynamics, and adsorbent regeneration. The adsorbent was characterized by FT-IR, XRD, SEM and N_2 adsorption/desorption measurement. The adsorption data follows pseudo-second-order kinetics model and fits the Freundlich adsorption model. The used HKUST-1@GO nanocomposites are regenerated effectively and recycled at least four times without significant loss of adsorption capacity.

Keywords: Metal organic framework, HKUST-1@GO, Lead, Adsorption.

1. Introduction

Heavy metal ions are toxic pollutants existing in wastewater and their presence concerns industries and environmental organizations all over the world. Most of these pollutants are very toxic and dangerous for human health. Among these toxic heavy metals, Lead is one of the most toxic and hazardous elements, because it can cause detrimental effect on metabolic processes of human beings [1].

Up to now, various approaches have been proposed and employed for removing Pb(II) ions in wastewater such as adsorption, ion exchange, and so on [2], in which adsorption is highly recommended due to its simplicity, efficiency and low cost [3]. Traditional adsorbents, such as activated carbons [4], iron oxide nanoparticles [5], bagasse fly ash [6] and pristine yeast have been used for the removal of Pb(II) ions from wastewater.

In the present work, we synthesized a highly porous HKUST-1@GO composite by two facile steps. The application for an efficient adsorption of pollutants from aqueous solution is also discussed.

2. Experimental Part

2.1. Chemicals

The chemicals $Cu(NO_3)_2{\cdot}3H_2O$ (>99.5%), H_3BTC (>98%), Methanol (>99.5%), ethanol (>99.7%), N,N-dimethylformamide (DMF) (>99.5%), and dichloromethane (>99.5%).

2.2 Materials Synthesis

HKUST-1 was prepared as follows: $Cu(NO_3)_2{\cdot}3H_2O$ (3.6 mmol) and H_3BTC (2 mmol) were dissolved in the mixed solvent consisting of ethanol (12 mL) and deionized water (12 mL). Graphene oxide (GO) (10wt% solid input) was dissolved in solvent consisting of ethanol (5 mL) and the mixture was heated at 120°C for 12 h. The obtained solids were filtered, washed with DMF and methanol, and exchanged with dichloromethane.

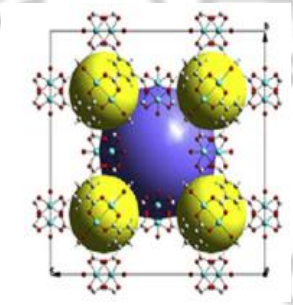

Figure 4: Schematic of HKUST-1 adsorbent

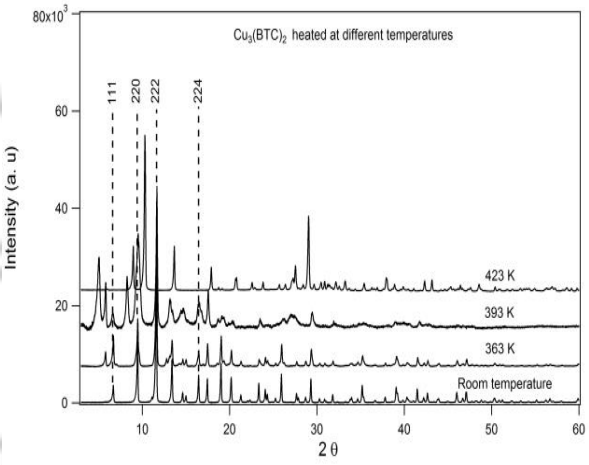

Figure 5: PXRD patterns of hydrated HKUST-1

3. Results and discussion

3.1. Characterization

The prepared GO and HKUST-1@GO were characterized by means of XRD, SEM, and FT-IR.

Surface morphology and composition of the prepared GO and HKUST-1@GO were also characterized by SEM. Figures 1 to 3 shows some characteristics of the adsorbents and its nanocomposites.

3.2. Adsorption isotherms for Pb(II) ions removal from water

The adsorption capacity of Pb(II) ions onto the HKUST-1@GO was calculated by Langmuir equation:

$$\frac{C_e}{q_e} = \frac{1}{q_m K_L} + \frac{C_e}{q_m} \quad (1)$$

where C_e is the equilibrium concentration of the remaining Pb(II) ions in the solution (mg.L^{-1}), qe is the

amount of Pb(II) ions adsorbed on the adsorbent at equilibrium (mg.g^{-1}), q_m is the mono-layer adsorption capacity (mg.g^{-1}), and K_L is the Langmuir constant (L.mg^{-1}).

The Freundlich isotherm can be described by Eq. (2):

$$\ln Q_e = \ln K_f + \frac{1}{n} \ln C_e \quad (2)$$

where K_f (mg.g^{-1}) and n are Freundlich constants incorporating all factors affecting the adsorption process such as adsorption capacity and intensity of adsorption. Table 1 represents adsorption capacities of some adsorbents including the present composites for the Lead ions removal. It is seen that the present composite exhibited very high and excellent adsorption capacity.

Table 1. Comparison of Pb(II) ions removal with other reported systems

Adsorbents	q_m (mg.g^{-1})	Adsorption amount (mg.L^{-1})	Ref.
Iron oxide nanoparticles	36	162	[5]
Bagasse fly ash	2.50	20	[6]
Activated carbon	21.8	50	[4]
Chitosan immobilized on bentonite	26.38	25	[7]
Oxidized MWCNTs	11.2	16	[8]

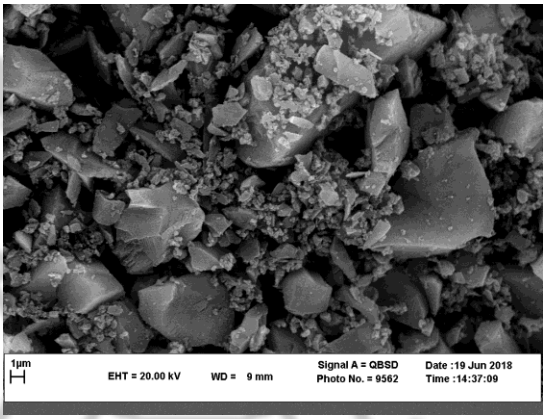

(a)

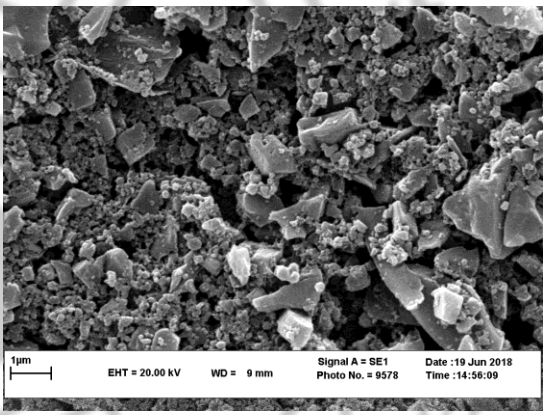

(b)

Figure 3. SEM images of (a) HKUST-1 and (b) HKUST-1@GO

4. Conclusions

In this study, we have successfully demonstrated the use of HKUST-1@GO to remove Pb(II) ions from aqueous solution. The addition of GO nanoparticles makes the hybrid material more attractive for its rapidness

compared with other adsorbents. Moreover, the HKUST-1@GO can be reused many times without obvious decrease in the removal efficiency. The materials exhibited a significant adsorption capacity, good solvent stability and excellent reusability for Pb(II) ions, making them promising as a novel adsorbent for the removal of heavy metal ions from water.

References

[1] E. M. Gama, A. S. Lima, V. A. Lemos, *J. Hazard. Mater. 136* (2006) 735-757.

[2] D. C. Culita, C. M. Simonescu, R. E. Patescu, M. Dragne, N. Stanica, O. Oprea, *J. Solid State Chem.* 238 (2016) 308-311.

[3] X. Jing, F. Liu, X. Yang, P. Ling, L. Li, C. Long, A. Li, *J. Hazard. Mater*. 167 (2009) 550-589.

[4] M. M. Rao, D. Ramana, K. Seshaiah, M. Wang, S. C. Chien, *J. Hazard. Mater*. 166 (2009) 1000-1006.

[5] N. N. Nassar, *J. Hazard. Mater.* 184 (2010) 538.

[6] V. K. Gupta, I. Ali, *J. Colloid Interface Sci.* 271 (2004) 310-321.

[7] C. M. Futalan, C. C. Kan, M. L. Dalida, K. J. Hsien, C. Pascua, M. W. Wan, *Carbohyd. Polym.*, 83 (2011) 512-528.

[8] J. Li, S. Chen, G. Sheng, J. Hu, X. Tan, X. Wang, *Chem. Eng. J.* 166 (2011) 535-551.

5th Iran International Zeolite Conference

University of Tabriz, Tabriz, Iran

26-27 August 2018

Application of graphene quantum dots for drug delivery of anticancer

Z. Kianinejad[a]*

[a] *Department of Inorganic Chemistry, Faculty of Chemistry, University of Tabriz, Tabriz, Iran*

Corresponding author:Zahra.kiani89@gmail.com

Abstract: Cancer is one of the causes of human mortality which has become a public danger all over the world. The primary strategies for healing and treating cancer include surgery, radiation and chemotherapy. The primary treatment in a cancer clinic is usually chemotherapy. However, the effectiveness of chemotherapy is often limited by its side effects. For example, the toxicity of bleeding and cardiac toxicity, as chemotherapeutic agents, can not only break down cancer cells, but also damage healthy cells and tissues in the body [1]. Nanotechnology appears as a promising tool for reducing side effects and effective treatment for cancer chemotherapy. Among the various candidates for nano chemotherapy agents, graphene quantum dots appear to be a striking issue for extensive research. The highlight of this single-atomic layer is with very small horizontal dimensions and oxygen-rich functional groups at the edges. Another feature of graphene quantum dots is their fluorescence origin, graphene quantum dots because of the quantum amplitude and edge effects are the ideal platform for delivering chemicals to cancer cells without using additional fluorescence markers [2-4].

Keywords: graphene quantum dots, chemotherapeutic, fluorescence markers.

1. Introduction

1.1. Synthesis of graphene quantum dots

There are two main methods for the synthesis of graphene quantum dots: the top-down method and the bottom-up method. In the low-up method, nanoparticles are prepared from small organic molecules by pyrolysis, combustion or hydrothermal methods, while in the above method, the nanoparticles of the size desired by crushing small sheets with physical, chemical, or electrochemical methods (Fig. ١). In both methods, the final method is required to purify or modify surface functionalization and increase the efficiency of graphene quantum dots.

1.2. Application of GQD in anticancer therapy

Graphene quantum dots, due to their unique physico-chemical properties, low toxicity and intrinsic fluorescence, have created new opportunities for nanoscience and biotechnology. The researchers also

designed these delivery systems based on graphene quantum dots [5, 6]. Different methods have been proposed for the synthesis of graphene quantum dots with good quantum yields; high purity and controlled size. Anticancer drugs and targeting ligands on the graphene surface have been loaded to improve their therapeutic performance through electrostatic interactions, hydrogen bonding, π-π, or functionalization of the carboxylic groups present on the edges. Therefore, it can be said that the presence of more active groups on the surface of graphene dots makes them suitable for treating and detecting cancer cells (Fig. 2). By modifying the GQD level, not only can their quantum yield improve, but new therapeutic agents Created. Studies have shown that surface reduction or oxidation also improves their luminescence properties. Extensively used to modify the surface of graphene quantum dots, small amounts of amines and polymers (ethylene glycol). The correction of graphene quantum dots by polyethylene glycol increases 10% quantum yield [7]. To synthesize graphene quantum dots functionalized with oligomeric PEG diamine initially carboxyl groups of nanomaterials reacted with thionyl chloride created acyl chloride groups on the surface then the product is created by forming an amide band between the acyl chlorides of surface and the amine groups in the PEG1500N oligomer [8]. The researchers showed that polymer chains with similarity in the distribution of particles, there are differences in quantum yield and emission wavelength range. Researchers have recently investigated the use of modified graphene quantum dots in cancer treatment and reducing the complications of chemotherapy. The important role of surface engineering in improving the in vitro and in vivo compatibility of these nanomaterials is presented.

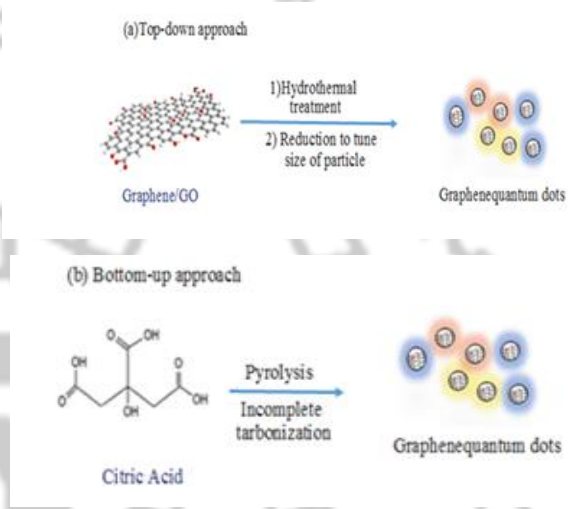

Figure 1. Two general methods of synthesizing graphene quantum dots

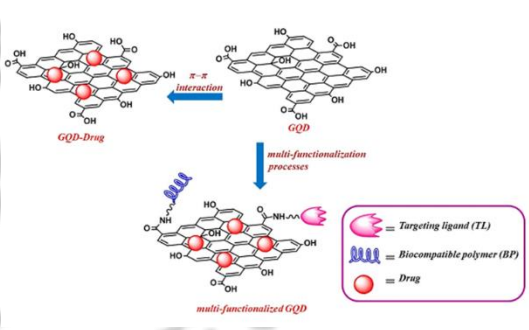

Figure. 2. Chemical routes for the development of GQD as drug delivery systems.

2. Conclusions

In the past decade, the goal of improving the therapeutic efficacy and reducing the toxicity of nanomaterials-based drug delivery systems for cancer treatment has been widely investigated. Many researchers have discovered graphene-based drug delivery systems. Anti-cancer drugs on graphene quantum dots are loaded and selectively transmitted to specific cancerous cells, thereby reducing the side effects of chemotherapy.

References

[1] H. Ding, F. Zhang, C. Zhao, Y. Lv, G. Ma, W. Wei, Z. Tian, *ACS Appl. Mater. Interf.* 9 (2017) 27396-27401.
[2] Z. Fan, S. Zhou, C. Garcia, L. Fan, J. Zhou, *Nanoscale* 9 (2017) 4928-4933.
[3] B. Kong, A. Zhu, C. Ding, X. Zhao, B. Li, Y. Tian, *Adv. Mater.* 24 (2012) 5844-5848.
[4] T. Jing, et al. *Adv. Mater.* 25 (2013) 6569-6574.
[5] P.N. Joshi, S. Kundu, S.K. Sanghi, D. Sarkar, *Graphene quantum dots-from emergence to nanotheranostic applications, Smart Drug Delivery System*, InTech 159–195.
[6] J. Shen, Y. Zhu, X. Yang and C. Li, *Chem. Commun.*, 48 (2012) 3686–3699.
[7] Y. P. Sun, B. Zhou, Y. Lin, W. Wang, K. A. S. Fernando, P. Pathak, M. J. Meziani, B. A. Harruff, X. Wang, H. F. Wang, P. G. Luo, H. Yang, M. E. Kose, B. L. Chen, L. M. Veca and S.-Y. Xie, *J. Am. Chem. Soc.*, 128 (2006) 7756–7757.
[8] X. Wang, L. Cao, S.-T. Yang, F. S. Lu, M. J. Meziani, L. L. Tian, K. W. Su, M. A. Bloodgood and Y.-P. Sun, *Angew. Chem., Int. Ed.*, 49 (2010) 5310–5314.

5th Iran International Zeolite Conference

University of Tabriz, Tabriz, Iran

26-27 August 2018

Potential Application of Graphene Quantum Dots

Z. Kianinejad*, A. Mokhtari

Department of Inorganic Chemistry, Faculty of Chemistry, University of Tabriz, Tabriz, Iran

**Corresponding author: Zahra.kiani89@gmail.com*

Abstract: Graphene quantum dots **(**GQDs**)** have attracted much attention as a new class of fluorescent carbon nanotubes due to its prominent features and potential use in the fields of environment, optoelectronics and energy. GQDs have some unique features like graphene and GO. Functional groups have included oxygen at the surface and wide active surface; have created active sites on the surface, so that drug molecules can be loaded on to the GQD. Recent exciting advances in the use of GQD, such as sensors, bio imaging, pharmaceutical carriers and solar cells, have been highlighted.

Keywords: Graphene quantum dots; Sensors; Bio imaging; Pharmaceutical carriers; Solar cells

1. Introduction

In recent years, nanomaterials have been widely used in medical research, such as diagnosis, prevention, and treatment. GQDs that exhibit a more stable electrical mobility than organic colors and GQD have a more stable electrical mobility than organic colors and show lower cytotoxicity than semiconductor quantum dots. Therefore, the use of GQDs in sensors, delivery of targeted medication, biological imaging, cancer cell imaging, etc. is promising [1,2]. Some of the GQD applications are:

1.1. GQD-based platforms for drug delivery

Research has shown that graphene-based nanomaterials are used to produce targeted materials. GQD has a lower toxicity and greater solubility than graphene. Therefore, multi-purpose GQDs are used for drug-targeted delivery and concurrent imaging of the target cell and increase the effectiveness of chemotherapy. Folic acid is used to delivery targeted anticancer drugs to cancer cells. As folic acid is attached to the GQD, the drug is loaded on to the nano-structure of the FA-GQD and FA-GQD nanostructures detect cancerous cells from healthy cells. These drugs are transmitted to target cells. The intrinsic fluorescence of graphene quantum dots makes possible tracing drug inside the cell without the use of markers. For example, DOX is loaded onto the FA-GQD nanostructure. Then, using the intrinsic fluorescence of the graphene quantum dots, DOX-GQD-FA cell absorption and DOX emission are

controlled at cell surface. Studies have shown that GQD can be used to design delivery targeted drug systems that release drugs in target cells and reduce the side effects of chemotherapy [3].

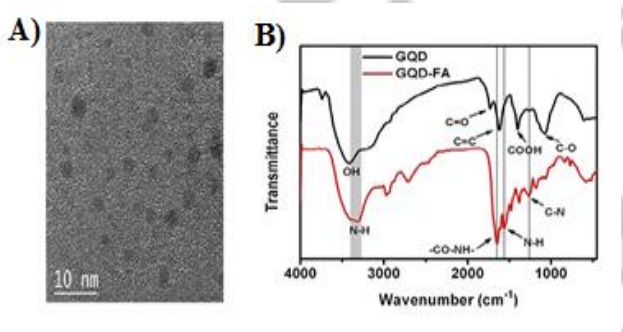

Figure 1. GQDs based nanocomposites in drug delivery. (A) TEM image of GQDs. (B) FTIR spectra of GQDs and GQD–FA.

1.2. Solar cells

One of the most important issues in the field of clean energy is solar cells. The main reason for the use of GQD in solar cells is band gap dependence on particle size. GQDs are more effective in producing solar cells than other materials, such as silicon and pro oxide, due to lower toxicity, better dispersion, adjustable band gap; solar cells based on GQD can be referred to silicon/GQD solar cells Non-harmonic, semiconductor solar cells/GQD. Most research has focused on the use of GQDs as a band gap tanner and as an electron transfer into a hole [4].

1.3. Sensors

Given that the interaction between GQDs and some materials reduces GQD fluorescence intensity, different types of biological and chemical sensors are used to identify inorganic or organic molecules, biological molecules and heavy metal ions, and so on. Fe^{3+} ion can not only be combined with different proteins, it is possible also cause Parkinson's disease, so the detection of Fe^{3+} ions is important [5]. Tam et al. Used N-GQDs as a fluorescent sensor platform to detect Fe^{3+} ions. The interaction between hydroxyl groups on the N-GQDs surface with Fe^{3+} ions reduces the fluorescence intensity of graphene quantum dots When the Fe^{3+} ion concentration in the 80 ppm solution is converted, the GQD fluorescence intensity instantly quench, so metal ions with this concentration have little effect on fluorescence intensity. Li et al., Using fluorescence properties, graphene quantum dots designed a new type of fluorescence electrochemical sensor for the determination of Cd^{2+} ions [6].

1.4. Bio-imaging

GQDs have potential applications due to excellent fluorescence and low toxicity in biological imaging. Dong and colleagues used GQDs to imaging human MCF-7 cancer cells and use the fluorescence properties of GQDs to detect cells, cytoplasmic material, and nuclear membranes [7], and this is the first time that carbon fluorescents for Nuclear imaging is used.

Zhang et al., for imaging of stem cells from GQDs used [8]. Therefore, they cultivated three different types of stem cells with GQD, and the final results showed that GQDs are easily transmitted to stem cells but not seen

in the nucleus, so GQD does not cause genetic disorders in stem cells. Moreover, this indicates low GQDs poisoning, but when the CdS quantum dot is with stem cells, stem cells quickly disappear through the toxicity of heavy metals Cd^{+2}. This demonstrates the advantage of using GQDs to mark stem cells and have many opportunities for medical use.

2. Conclusions

GQDs have attracted much attention due to biocompatibility, low cytotoxicity, high fluorescence, and many biological applications, and are used in biosensors, delivery systems and cell imaging. Of course, there are no convincing explanations for the mechanism of PL in graphene quantum dots, and the effect of crystallization, doping, size, and surface agent in the optics is unknown. In addition, some biological tests have not been performed on mice until now. Despite these challenges, GQDs are encouraging candidates for diagnosis, tracking and treatment in biology and medicine.

References

[1] J. Shen, Y. Zhu, X. Yang, C. Li, *Chem. Comm.* 48 (2012) 3686-3699.

[2] Z. Zhang, J. Zhang, N. Chen, L. Qu, *Energy Environ. Sci.* 5 (2012) 8869-8890.

[3] Y. Lei, C. Yang, J. Hou, F. Wang, S. Min and X. Ma et al., *Appl. Catal. B* 216 (2017) 59-69.

[4] L. Chen, C.X. Guo, Q. Zhang, Y. Lei, J. Xie, S. Ee, *ACS Appl. Mater. Interfaces* 5 (2013) 2047-2052.

[5] A. Ananthanarayanan, X. Wang, P. Routh, B. Sana, S. Lim, D.-H. Kim, K.-H. Lim, *J. Li and P. Chen. Adv. Funct. Mater.* 24 (2014) 3021-3026.

[6] L.L. Li, J. Ji, R. Fei, *Adv. Funct. Mater.* 22 (2012) 2971-2979.

[7] Y. Dong, C. Chen, X. Zheng, *J. Mater. Chem.* 22 (2012) 8764-8766.

[8] M. Zhang, L. Bai, W. Shang, *J. Mater. Chem.* 22 (2012) 7461-7467.

5th Iran International Zeolite Conference

University of Tabriz, Tabriz, Iran

26-27 August 2018

Synthesize of Cu^0/Clinoptilolite and Investigation of Antibacterial properties

Z. Kalateh [a], Z. Mortezaei [a], P. Maleki*[b], M. Zendehdel[a],

[a] *Department of Chemistry, Faculty of Science, Arak University, Arak 38156-8- 8349, Iran*
[b] *Department of Biology, Faculty of Science, Arak University, Arak 38156-8- 8349, Iran*
**Corresponding author: P-Maleki @araku.ac.ir*

Abstract:

In this study Cu^0/Clinoptilolite was prepared and characterized by using FT-IR, XRD, SEM and EDAX techniques. Then, their antibacterial properties against different bacteria (gram-positive and gram negative bacteria) was investigated.

Keywords: Cu, Clinoptilolite, Antibacterial properties, bacteria

1. Introduction

Microorganisms are part of the organic matter in the wastewater. These organic materials can affect human health and are commonly found in wastewater because they are present in fecal material. The removal or inactivation of pathogenic microorganisms is the last step in the treatment of wastewater. Some chemical and physical agents, such as chlorine, ultraviolet light, reverse osmosis, and silver catalyst are well developed [1–3]. Copper is an essential mineral that have antibacterial properties against different bacteria. In the last few years, several investigations were carried out using synthetic and natural zeolites that combined with silver ions to obtain disinfection agents for the treatment by microbiologically polluted water.

2. Experimental Part

Synthesis of Cu^0/ Clinoptilolite

At first, $CuCl_2$.$2H_2O$ solution was added to Clinoptilolite and stirred for 48 h in room temperature and Cu^{2+} introduce on it. Then by adding $NaBH_4$ solution, synthesis the solid compound (Cu^0/Clinoptilolite). The product heated and dried at 120 ºC for 3h in oven.

3. Results and discussion

The Cu^0/Clinoptilolite compound synthesized successfully and characterized using FT-IR, XRD, SEM and EDAX techniques.

The FT-IR spectrum of Cu^0/Clinoptilolite indicate an intense band about ca.1065 cm^{-1} attributable to the asymmetric stretching of Al–O–Si chain of zeolite. The symmetric stretching and bending frequency bands of Al–O–Si framework of zeolite appear at ca.795 and 458 cm^{-1}, respectively.

X-ray diffraction pattern of Cu^0/Clinoptilolite is shown in Fig.1. Some diffraction peaks in the range of 2θ = 0-70˚ can be indexed as the Cu and Clinoptilolite. The result in Fig.2 showed that the synthesized Cu^0/Clinoptilolite powder were particle Shape with the diameter of 13-20 nm and were made.

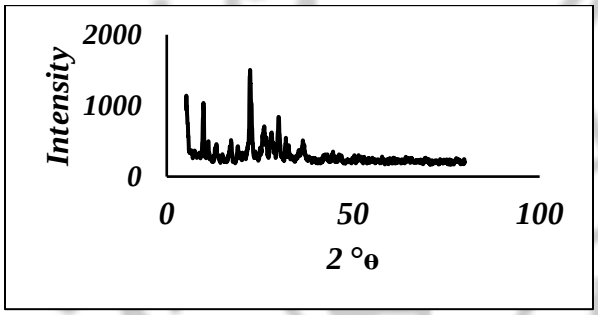

Figure 1. The XRD pattern of Cu^0/Clinoptilolite

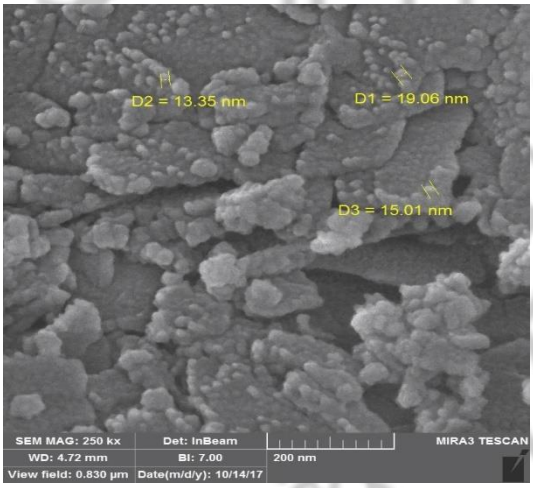

Figure 2. The SEM image of Cu^0/Clinoptilolite

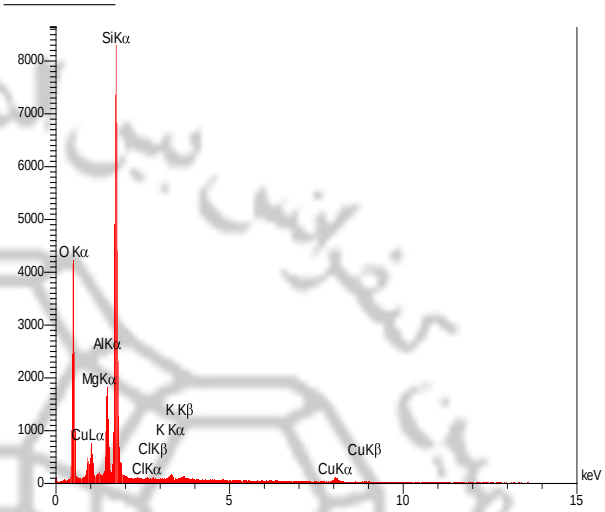

Figure 3. The EDAX of Cu^0/Clinoptilolite

Antibacterial activity study

The in vitro antibacterial activity of the investigated compounds were tested against pathogenic Gram-negative bacteria's (P. aeruginosa and E. coli) and Gram-positive bacteria's (B. subtilis and S. aureus) using the paper disc diffusion method according to the procedure described by Hwang and Ma [4]. The bacteria of interest are swabbed uniformly across a culture plate, while the Petri dishes are cooled over 24 h. Discs of samples were placed on the surface of the medium and finally, all Petri dishes containing bacteria and antibacterial reagents were incubated and maintained at 37 C for 24 h. After this period, the diameters of the inhibition zones formed around each disc were determined and presented in mm (Table 1).

Table 1. The diameters of the inhibition zones formed around each disc.

Sample	Inhibition (mm)			
	Gram-negative bacteria		Gram-positive bacteria	
	E. Coli	*P. aeruginosa*	*S. aureus*	*B. subtilis*
Cu^0/ Clinoptilolite	23	31	32	32
Clinoptilolite	–	–	–	–
Vancomycin	13	-	17	24
Nalidixic acid	24	-	12	23

4. Conclusions

The in vitro antibacterial activity of Cu^0/Clinoptilolite was evaluated against B. subtilis and S. aureus (as Gram-positive bacteria), P. aeruginosa and E. coli (as Gram-negative bacteria), and compared with standard drugs. The results show that Cu^0/Clinoptilolite has excellent inhibition effect on bacterial growth.

References

[1] G. Finch, E. Black, L. Gyurek, *Water quality technology conference, AWWA*, 1994,1303–1309.

[2] W. Gujer, U. Von Gunten, *Water Res,* 37 (2003) 1667–1677.

[3] E. Hassinger, A. D. Thomas, B. B. Paul, *Reverse osmosis units water facts*, 1994.

[4] H. wang JJ, Ma. TW, *Mater. Chem. Phys.* 136 (2012) 613–623.

5th Iran International Zeolite Conference

University of Tabriz, Tabriz, Iran

26-27 August 2018

Removal Efficiency, Kinetic and Isotherms of dyes onto Natural Zeolite, Manisa, Turkey

J. Rahimpour[a]*, D. Lacin[b], F. Esenli[c], A. Z. Aroguz[a]

[a]*Department of Chemistry, Faculty of Engineering, İstanbul University, Avcilar, İstanbul, Turkey*
[b]*Department of Geological Engineering, Faculty of Engineering, İstanbul-Cerrahpaşa University, Avcilar, Turkey*
[c]*Department of Geological Engineering, Faculty of Mines, İstanbul Technical University, İstanbul, Turkey*
**jenipiano76@yahoo.com*

Abstract: In this study, the adsorption capacity and adsorption behavior of zeolite as adsorbent obtained from Gordes region in Manisa province were investigated. Methyl blue (MB) dye was used to investigate the adsorption behavior in a batch system. The adsorption equilibrium of dye was examined using various well-known isotherm models such as Langmuir, Freundlich, Dubinin and Radushkevish and it was observed that the experimental equilibrium data well fitted and found to be in good agreement with Lanmuir isotherm model. This result showed that the multilayer adsorption for methyl blue has been achieved. Adsorption kinetics of this system were studied. The kinetic studies were performed by using pseudo first and second order kinetic equations and it was found that the adsorption processes of both dyes were endothermic and spontaneous.

Keywords: Zeolite, Dye, Adsorption kinetic, Isotherm.

1. Introduction

The dyes have been widely used by many industries for various purpose and their effluents can cause environmental pollution. Many chemical treatments have been used in order to remove dyes from aqueous solution. Among these removal methods, the adsorption process is a foremost method [1,2]. Zeolites are the most popular and widely used adsorbents which have different colors such as greenish, cream and white (Fig. 1).

Zeolites consist of various minerals, hydrated alumino-silicates of alkaline or alkaline earth metals. They are in crystalline and microporous, structure. Their tetrahedral

crystalline lattice are linked together to form cages connected by pores [3]. The negative charge on the lattice is neutralized by the positive charge of cations located within the material's pores. The basic zeolites contain univalent and bivalent metals or their different combinations. The metal cations may be replaced by acidic protons by ion-exchange process. Therefore, due to their exceptional properties, zeolites have been widely used for various applications as catalysts, adsorbents and ion exchangers [3,4]. The general formula of zeolite related to their crystallographic unit cell is given as: $M_{x/n}[(AlO_2)_x (SiO_2)_y] wH_2O$. Here; (M) is an alkali or alkaline earth cation, (n) is the valence of the cation, (w) is the number of water molecules per unit cell. The total number of tetrahedral per unit cell is given as x and y and the ratio of y/x changes from 1 to 5. But, y/x can be ranging from 10 to 100 for the silica zeolite.

In this work, the adsorption capacity and behavior of zeolite from Gordes region in Manisa province were investigated by using methyl blue (MB) dye.

2. Geological Background

As a pyroclastic rock type; the vitric tuffs are widely transform to zeolite−rich rocks in general. In west Turkey, some of the rhyolithic-rhyodacitic pyroclastic rocks within the Miocene sequences contain high amounts of zeolites, particularly heulandite-clinoptilolite.

The basement rock groups in the Gordes are metamorphics of Paleozoic Menderes massif and generally limestone and ophiolite complex of Mesozoic İzmir-Ankara suture zone. Miocene sequence with thickness of about 1000m unconformably overlay the basement. The lower parts of Miocene sequence consist of conglomerates and sandstones. These units are conformably overlain by a volcanic tuff level as zeolite-rich lower tuff unit [5]. The lacustrine sediments having fine−grain and thin−medium layers of clastic and tuffaceous and tuffs conformably overlay this tuff unit.

Figure 1. Gordes zeolite EMD-01

The thickness of the lower tuff unit is around Gordes ranges 5 to 80m from the south to the north of the Gordes city. Glass shards and also pumice fragments of these tuffs were mainly transformed to zeolites and zeolite contents of most of the bulk samples were found higher than 80% [5-7]. Zeolite mineral type is Ca-clinoptilolite in the lower part and K-clinoptilolite in the upper part of the studied tuffs. Clinoptilolites are in the

shape of monoclinic plates with about 10x5x2 mμ size. Clinoptilolites are thermally found stable up to 700 ºC. The mineralogical composition of Gordes zeolite using in this study is as follows:

EMD-01: Clinoptilolite (80-85%) + Opal-CT (10-15%) + Mica (<5%) (Fig. 2). Thin sections made from Gordes zeolite is seen in Fig 3.

The major oxide chemical compositions of the studied sample are given in Table 1. According to their exchangeable cations, the sample of this clinoptilolite can be described as (K-Ca)-clinoptilolite.

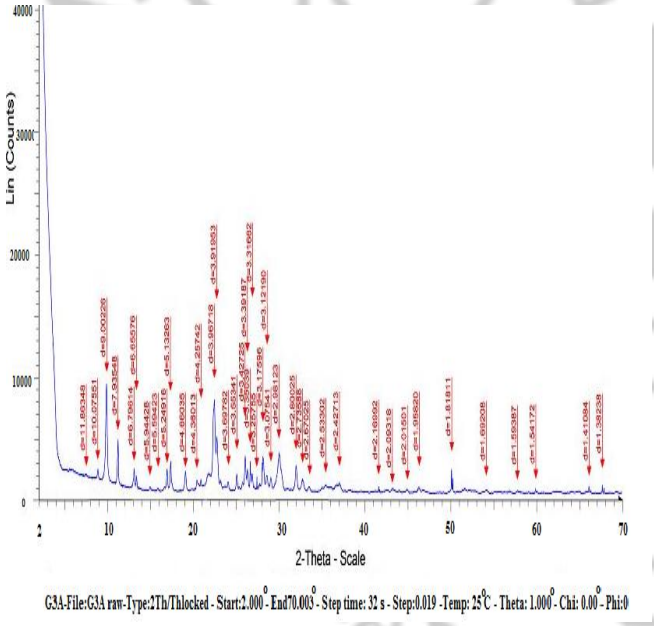

Figure 2: Unoriented XRD graphics of Gordes Zeolite. On the sample, it is seen peaks belong to the Clinoptilolite, Opal-CT and Mica minerals.

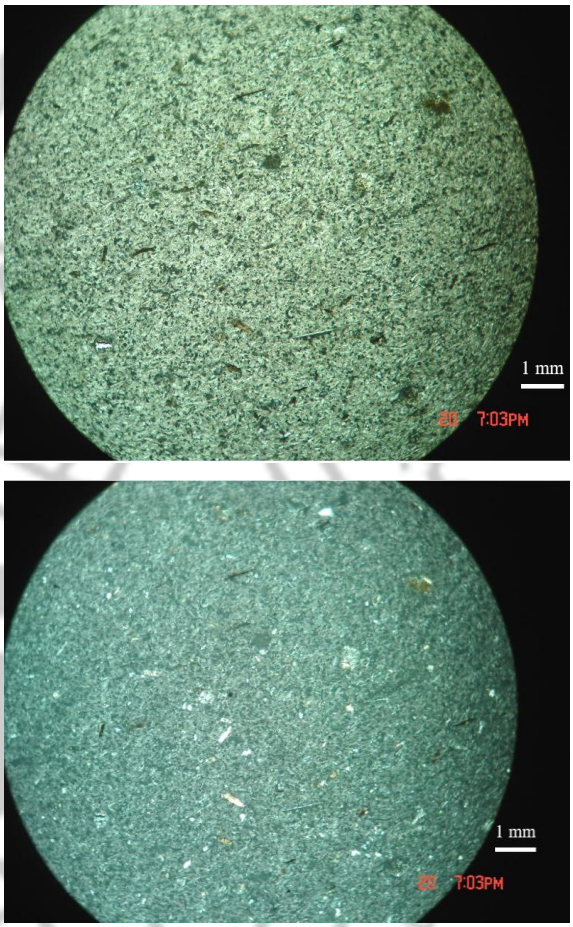

Figure 3: Clinoptilolite, opal-CT and mica minerals are seen in the microscopic appearance of the thin section of Gordes zeolite (A CPL and B PPL).

3. Experimental Part

Batch-adsorption experiments were carried out by stirring 0.1 g zeolite, with 50 ml methyl blue dye solution in different concentrations in an air-tight glassware keeping in a stable water bath at 25 °C. Zeolites used in this study were taken from Western

Anatolia, Manisa-Gordes region of Turkey (Fig.1). The Zeolite samples were grounded and sieved by using an 80 mesh sieved. Zeolites were pre-treated with brine to replace the exchangeable cations in the zeolite with the more easily removable ions as Na+ ions. Thus the effective exchange capacity of zeolite was improved and better performance was obtained. At the predetermined time intervals, samples were drawn out and then centrifuged at 3000 rpm for 5 min.

After filtration the concentration of MB dye remaining in the supernatant before and after adsorption was measured by using a UV-spectrophotometer (PG Instruments T80+), at a wavelength of maximum absorbance at 600 nm, for methyl blue. The adsorption experiments were continued until no change in the concentration of dye solution was observed. The amount of dye adsorbed (mg g^{-1}) on the surface of the adsorbent was determined by the difference between the initial and final concentration of dye.

3. Results and discussion

Various concentrations of dyes ($5x10^{-3}$; $1x10^{-2}$; $1,5x10^{-2}$; $2x10^{-2}$ g/L) were prepared to study kinetic model of the adsorption process. During the adsorption the temperature keeps constant. From the adsorption data it was found that the uptake percentages increase with the increasing of the dye concentration. The adsorption reaches equilibrium almost in 2-3 hours. The adsorption experiments were repeated at different temperatures (30C°, 40C°, 50C°, 60C°). The enthalpy (ΔH°), the entropy (ΔS°) and Gibbs free energy (ΔG°) changes for the adsorption process were estimated. The thermodynamic data indicate that the uptake percentage of dye on zeolite increases with increasing temperature. The results showed that zeolite being natural and eco-friendly adsorbent has high capacity for the adsorption of methyl blue and it might be an alternative adsorbent to remove dyes from aqueous solution.

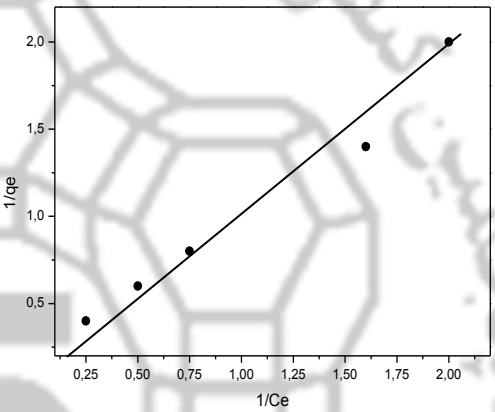

Figure 4: Langmuir isotherm (R=0,9804)

Table 1. Major oxide substances of the studied clinoptilolite - rich samples.

Sample	EMD-01
SiO_2	64.93
Al_2O_3	12.07
Fe_2O_3	1.05
MgO	0.85
CaO	2.33
Na_2O	0.16
K_2O	4.64
TiO_2	0.07
MnO	0.01
P_2O_5	0.02
LOI	13.78
SiO_2/Al_2O_3	5.38
$Na_2O+K_2O/MgO+CaO$	1.51

To find the suitable isotherm model for the adsorption process, Langmuir, Freundlich and Dubinin and Radushkevish isotherms were applied for the resulting data and it was found that the adsorption of methyl blue followed Langmuir adsorption model (Fig. 4).

4. Conclusions

Zeolite obtained from west part of Anatolia and used in this study was found to be an effective adsorbent for the adsorption of methyl blue. The adsorption of methyl blue on zeolite followed first order kinetic model. Langmuir adsorption model known as monolayer adsorption best fits to the adsorption of methyl blue on zeolite. The increasing of the uptake percentage of methyl blue indicates that the adsorption process can be regarded as spontaneous and endothermic process.

Acknowledgments

This research was financially supported by Istanbul University Research Fund (Project number 34003).

References

[1] A. Z. Aroguz, J. Gulen, R. H. Evers, *Bioresource Technol.* 99 (2008) 1503.

[2] A. Z. Aroguz, G. Sayılı, *Polym. Bull.* 73 (2016) 2353-2372.

[3] S. Liakou, U. Zissi, M. Kornaros, G. Lyberatos, *Chem. Eng. Commun.* 190 (2003) 645-661.

[4] A. Sukor, A. Z. A. Azira, M.H.A. Husni. *Malaysian J. Soil Sci.* 21 (2017) 105-112.

[5] F. Esenli, *Türkiye Jeoloji Bülteni*, 36 (1993) 37-44.

[6] F. Esenli, I. Kumbasar, *Clay Clay Miner.* 46 (1998) 679-686.

[7] F. Esenli, A. Sirkecioğlu, *Clay Miner.* 40 (2005) 557-564.

5th Iran International Zeolite Conference

University of Tabriz, Tabriz, Iran

26-27 August 2018

Dehydration of methanol to light olefins upon zeolite/alumina catalysts: Effect of reaction conditions, catalyst support and zeolite modification

Reza Mosayyebi Behbahani [a*], Saeed Hajimirzaee[b], Shahla Azarshin[a]

[a] *Gas Engineering Department, Petroleum University of Technology, Ahwaz, Iran*

[b] *School of Chemical Engineering, University of Birmingham, Birmingham B15 2TT, UK*

[a] *Gas Engineering Department, Petroleum University of Technology, Ahwaz, Iran*

**Corresponding author: behbahani@put.ac.ir*

Abstract: The reaction of methanol to propene was studied in a fixed bed reactor using a pelleted zeolite in alumina matrix support catalyst. The effect of reaction conditions (temperature, pressure, space velocity, feed composition), as well as the effect of support to ZSM-5 zeolite ratio on the conversion of methanol to light olefins (C2 –C4) was studied. The best catalyst and optimum reaction conditions leading to a maximum yield of C2 –C4 were determined. Use of -alumina as support improved the catalyst selectivity to propene and light olefins.

Keywords: Methanol to propene; MTP; ZSM-5; Modification; Wet impregnation

1. Introduction

The formation of hydrocarbons from methanol over zeolite catalysts enables petrochemical and gasoline based products to be obtained from raw materials other than conventional oil based substances. This development is therefore of great importance, as the dependence on resources which are depleting is reduced significantly. Methanol is a key ingredient in the synthesis of many organic molecules. World methanol production has increased from 32 million metric tons annually (MTA) in 2006 to 62 MTA in 2012 an expected to increase to 94 MTA in 2016. Each day more than 100,000 tons of methanol is used as a chemical feedstock or as a transportation fuel. Also, it can be economically converted to ethylene and propene, two of the largest volume petrochemical feed stocks. Using zeolite as catalyst for methanol to olefins (MTO) process has been studied widely while the products are generally the mixed C2–C4 olefins [1]. Extensive research has been devoted to improve the process development and selectivity to light olefins [2, 3, 4, 5, 6, 7]. In this work, firstly, the effect of reaction conditions on the dehydration of methanol to other hydrocarbons over ZSM-5 zeolite with no support was studied and the effects of a number of reaction parameters upon methanol conversion and product selectivity were investigated.

Experimental Part

To convert the ammonium form of ZSM-5 zeolite to hydrogen form, the sample was calcined in flowing air at 773 K for 5 h with a heating rate of 10 K min-1. In order to determine the effect of ZSM-5 to -alumina ratio, powder samples were converted into pellets. Before mixing, ZSM-5 and boehmite were sieved to 100 m. A desired amount of ZSM-5 and boehmite were mixed to make the required amounts of supported ZSM-5
(25, 50, 75 and 85 wt% ZSM-5) with the corresponding finished catalysts named ZSM-5 (25), ZSM-5 (50), ZSM-5 (75) and ZSM-5 (85), respectively. Then 10 ml of distilled water and 0.1 g of nitric acid were added to make it into a paste. The paste was extruded into rods with 3 mm diameters and 5 mm in length using an Instron 4467 Universal Testing Machine with 30 kN uniaxial loading. The samples were dried in an oven at 80 ◦C for 1 h and calcined at 500 ◦C with heating rate of 10 K min-1 for 5 h. The commercial ZSM-5 zeolite named ZSM-5 (100) was used as reference in powder form with no support. The reaction was carried out in a fixed bed reactor charged with 2 g of ZSM-5 (100) catalyst. Glass beads were used above the catalyst bed to ensure a well distributed inlet gas/vapour stream. For a typical run, the feed containing 50 wt% methanol in distilled water was introduced to the top of reactor using a HPLC pump at constant volume flow rate of 1.25 ml min-1. The feed was preheated to reaction temperature before entering the reactor. Fig. 1 shows the schematic diagram of the apparatus.

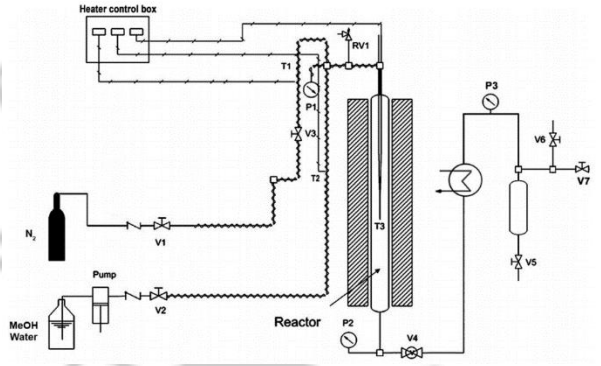

Figure 1: Schematic diagram of the experimental apparatus; pump: HPLC pump for feed mixture. V1, V2, V3, V5, V6 and V7: needle valves. V4: back pressure regulators. T1, T2, and T3: thermocouples. P1, P2 and P3: pressure gauges, and RV1 andRV2: safety pressure relief valves.

3. Results and discussion

The characterisation of catalysts is presented in terms of XRD analysis, acidity strength and distribution, and nitrogen adsorption–desorption measurements**.** Modification of zeolite with Cs and phosphoric acid increased the weak acidic and decreased the strong acidic centres. The decrease in the propene to ethene ratio and increase in the selectivity to C5+ products can be related to the deactivation of the acid sites via coke formation. The methanol conversion and selectivity to olefins at the different temperatures.
Methanol conversion increased from 80% to 94% by increasing the temperature from 340 ◦C to 400 ◦C. However, at higher temperatures the conversion then decreased from 94% to 75%.

By increasing the pressure from 1 bar to 10 bar conversion of methanol was increased from 93% to 98% and declined slightly to 96% at 20 bar after 4 h TOS. The selectivity to propene decreased significantly from 36% to half of this value, whereas the selectivity to ethene increased from 24% to 37%. Also, butane selectivity decreased from 10% to 3%. By decreasing the amount of methanol in feed the conversion was increased from 87% to 97%. The lower conversion at higher concentration of methanol in the feed could be due to the faster coking of zeolite after 4 h and/or dealumination by steam.

4. Conclusions

The results showed that Temperature as high as 400 ◦C is essential to produce light olefins more selectively, although elevated temperatures led to faster deactivation, more selectivity to alkanes and lower selectivity to light olefins. Pressure higher than 1 bar led to production of heavier hydrocarbons (C5+) and lower selectivity to light olefins. High water concentrations in the feed led to higher yields of light olefins. A WHSV higher than 34 h-1 however led to faster deactivation with no improvement in selectivity to propene or other light olefins. Use of -alumina as support improved the catalyst selectivity to propene and light olefins. Zeolite catalyst with 25 wt% ZSM-5 in the catalyst sample led to highest selectivity to propene and light olefins, but faster deactivation was observed on this catalyst

References

[1] Keil, F.J, Microporous Mesoporous Mater. 29(1999)49–66.

[2] Inui, T., Kang, M., Appl. Catal. A: Gen., 164(1997)211–223.

[3] Bjørgen, M., Svelle, S., Joensen, F., Nerlov, J., Kolboe, S., Bonino, F. Palumbo, L., Bordiga, S., Olsbye, U., J. Catal., 249(2007)195–207.

[4] Bibby, D.M., Howe, R.F., McLellan, G.D., Appl. Catal. A: Gen. 93(1992)1–34.

[5] Goto, D., Harada, Y., Furumoto, Y., Takahashi, A., Fujitani, T. Oumi, Y., Sadakane, M., Sano, Appl. Catal. A: Gen. 383(2010)89–95.

[6] Dubois, D.R., Obrzut, D.L., Liu, J., Thundimadathil, J. Adekkanattu, P.M., Guin, J.A., Punnoose, A., Seehra, M.S. Fuel Process. Technol. 83(2003)203–218.

5th Iran International Zeolite Conference

University of Tabriz, Tabriz, Iran

26-27 August 2018

Developing some POMs-templated MOFs: Crystal structure, magnetic and gas adsorption properties

Masoud Mirzaei Shahrabi

Department of Chemistry, Faculty of Science, Ferdowsi University of Mashhad, Mashhad, Iran

E-mail: mirzaeesh@um.ac.ir

Abstract: In the present work, we succeeded in synthesizing inorganic–organic hybrid materials and metal organic frameworks (MOFs) based on dicarboxylate/polyoxometallates (POMs) and dicarboxylate/N-donor bases under mild, hydrothermal, and sonochemical conditions. In continue, the magnetic property and also application of these compounds in the gas storage and separation of CH_4/H_2 and CO_2/N_2 mixtures, were theoretically investigated.

Keywords: Inorganic-organic hybrid, Polyoxometallates, Metal-organic frameworks, Magnetic property, Gas storage.

1. Introduction

In the past decades, great efforts have been devoted to the rational design and synthesis of inorganic-organic hybrid architectures and metal organic frameworks (MOFs). A common feature of such design approaches is to employ poly-functional organic ligands such as dicarboxylic acids and combine them with polyoxometallate (POMs) and N-donor co-ligands to prepare inorganic-organic hybrids and metal organic frameworks, respectively. These crystal structures have high structural stability and infinite variety of unique chemical, physical, and adsorption properties. Due to importance of this field, a series of inorganic-organic hybrid and MOFs architectures based on dicarboxylate/POMs and dicarboxylate/N-donor bases have been synthesized under mild, hydrothermal, and sonochemical conditions [1-5]. The objective of the present speech is to explore the effect of organic ligands, POMs charge density and synthetic conditions in final structures. The magnetic properties of some of these compounds have been investigated. Monte Carlo simulation has been employed for predicting the ability of some of these compounds to capture CH_4 and CO_2 and also to separate CH_4/H_2 and CO_2/N_2 mixtures.

2. Experimental Part

We synthesized hybrid inorganic–organic assemblies generated from Keggin-type polyoxometallates and metal organic frameworks (MOFs) architectures under mild, hydrothermal, and sonochemical conditions.

3. Results and discussion

All of the used compounds in this work, have been characterized by IR spectra, elemental analysis, thermogravimetric analysis (TGA) and single crystal X-ray diffraction. The magnetic properties and also gas storage of some of these compounds have been investigated.

Magnetic Properties: Magnetization measurements in the temperature range of 1.8–300 K were carried out on powdered crystals of compounds at a magnetic field of 0.5 T. Corrections for diamagnetism of the constituting atoms were calculated using Pascal's constant [6]. The effective magnetic moments were calculated from the following expression:

$$\mu_{eff} = 2.83\sqrt{\chi_m^{corr.}T} \text{ (B.M.)}.$$

For example, the temperature variation of the magnetic susceptibility χ_m and of the χ_m T product for two inorganic–organic hybrid assemblies{Na[Ln(pydcOH)$(H_2O)_4]_3$}[$SiW_{12}O_{40}$]·15H_2O [Ln = Nd (**1**) and Ln = Sm, (**2**); pydc-OH =4-hydroxy pyridine-2,6-dicarboxy] is displayed in Figure 1.

The magnetic properties are in agreement with isolated ions in the solid state for **(1)** and **(2)**, and they show the usual temperature dependent

behavior with the gradual depopulation of the Stark levels.

Gas storage: In the adsorption separation processes, selectivity could be a good criterion of the ability of a porous material for separation of different components in a mixture. Evidently, for calculation of selectivity binary equlibrium data of mixture is needed. Because of the difficulty of measuring adsorption equilibrium and process data of gas mixtures, we predicted binary isotherms *via* GCMC. Accordingly, CH_4 selectivities over H_2 were calculated at two above-mentioned levels by resorting to simulated binary isotherms. Figure 2 show the simulated isotherms and calculated selectivities for {Na$(H_2O)_3$[La(HCAM)$(H_2O)_4]_3$}[$SiW_{12}O_{40}$]·15H_2O.

As it can be observed, good agreement between GCMC simulation and IAST calculation indicates that IAST is an efficient allternative for calculations of adsorption selectivities in POMs.

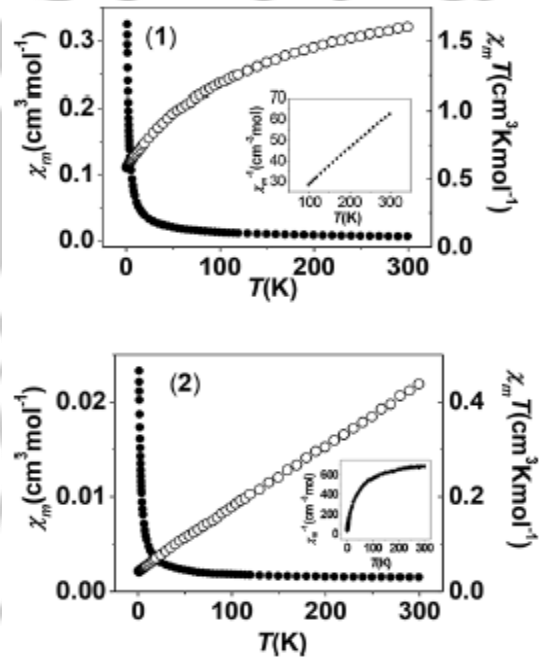

Figure 1. Variable-temperature magnetic susceptibilities of complexes (**1**) and (**2**) in the form of χ_m (●) and $\chi_m T$ (○) versus T (χ_m).

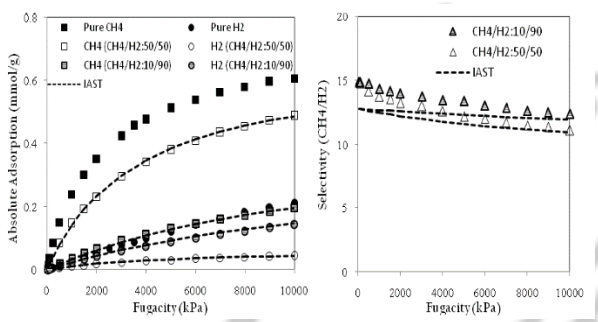

Figure 2. Simulated single and binary isotherms of CH_4 and H_2 at 298K (left), calculated selectivities of CH_4 at different pressures up to 10Mpa (right) for hybrid material.

4. Conclusions

In this work, we synthesized a series of inorganic-organic hybrid and MOFs architectures based on dicarboxylate/POMs and dicarboxylate/N-donor bases. In continue, magnetic property, gas storage, and separation of these novel synthesized species have been investigated.

Acknowledgments

The author would like to thank the Ferdowsi University of Mashhad for financial support of these studies.

References

[1] M. Mirzaei, H. Eshtiagh-Hosseini, M. Alipour, A. Frontera, *Coord. Chem. Rev*. 275 (2014) 1-18.
[2] M. Mirzaei, H. Eshtiagh-Hosseini, N. Lotfian, A. Salimi, A. Bauza, R. Van Deun, R. Decadt, M. Barcelo-Oliver, A. Frontera, *Dalton Trans*. 43 (2014) 1906-1916.
[3] A. Hassanpoor, M. Mirzaei, H. Eshtiagh-Hosseini, A. Majcher, *CrystEngComm*, 20 (2018) 3711-3721.
[4] A. Hassanpoor, M. Mirzaei, H. Eshtiagh-Hosseini, M. Niknam Shahrak, A. Majcher, *Dalton Trans*. (2018), in peer review.
[5] N. Lotfian, M. Mirzaei, H. Eshtiagh-Hosseini, M. Loffler, M. Korabik and A. Salimi, *Eur. J. Inorg. Chem*. (2014) 5908-5915.
[6] G. A. Bain, J. F. Berry, *J. Chem. Educ.* 85 (2008**)** 532.

List of Presenters for Poster Presentation (in alphabetical order)

Name	Num.
	B32
Ahadi , A	B33
Ahadi , A	B37
Akbari, F	B42
Akhgari, Z	B12
Akhgari, Z	B13
Alamgholiloo, H	B35
Alamgholiloo, H	B40
Alqaisi, S	B48
Amani, S	A17
Askari, M	B28
Atashi, N	A1
Atashi, N	A2
Azizi-lalabadi, M	B7
Azizi-lalabadi, M	A11
Bakhtiari Asl, F.	B21
Bakhtiari, A	A30
Barzegar, S	B20
Dabaghi-Tabriz , F	A31
Dalili, M	A49
Dalili, M	A50
Dibazar, M	A22
Ektefa, F	A46
Esmailzadeh, M	A15

Fakhimi, M	A27
Fallah, S	B30
Farajzhadeh, M	B41
Foroughi, M	B19
Froghi, A	A29
Ganji, S	B14
Ghadiri, M	A14
Ghadiri, M	B16
Ghaeini, M	B27
Gharehaghaji, N	A8
Gholinejad, R	B31
Gholizadeh, S	B5
Gorzin, F	A7
Haghighat, M	B23
Hazrati, H	A12
Hazrati, H	A19
Hejazy, M	A20
Hejazy, M	A21
Hossein Nouri, F	B6
Fakhri, M	B24
Fakhri, M	B39
Jafari Foruzin , L	A43
Jafari Foruzin , L	A44
Javani, R	A26
Jodaei, A	A9
Jodaei, A	A10
Johnny, R	B38
Kakili, H	B15
Kamrani, N	B4

Rahimpour, J	B52
Ranjbar Koh Farhadi, A	A28
Rastegar, S	A37
Rastegar, S	A38
Rezaei, A	B9
Rezaie, M	A40
Rezaie, M	A41
Rostamizadeh , M	A3
Safari, S	A5
Sanati, S	A42
Shahi, R	A34
Shahi, R	B2
Sharifi, K	A4
Sharifi, T	A23
Shouhani, S	A24
Taheri, Z	A18
Tahmasebpoor, M	A32
Tavakoli, F	A25
Teymuri, R	A13
Zare Pakzad, F	B17